Oxidative Medicine and Cellular Longevity

Lipid Peroxidation Products in Human Health and Disease

Guest Editors: Kota V. Ramana, Sanjay Srivastava, and Sharad S. Singhal

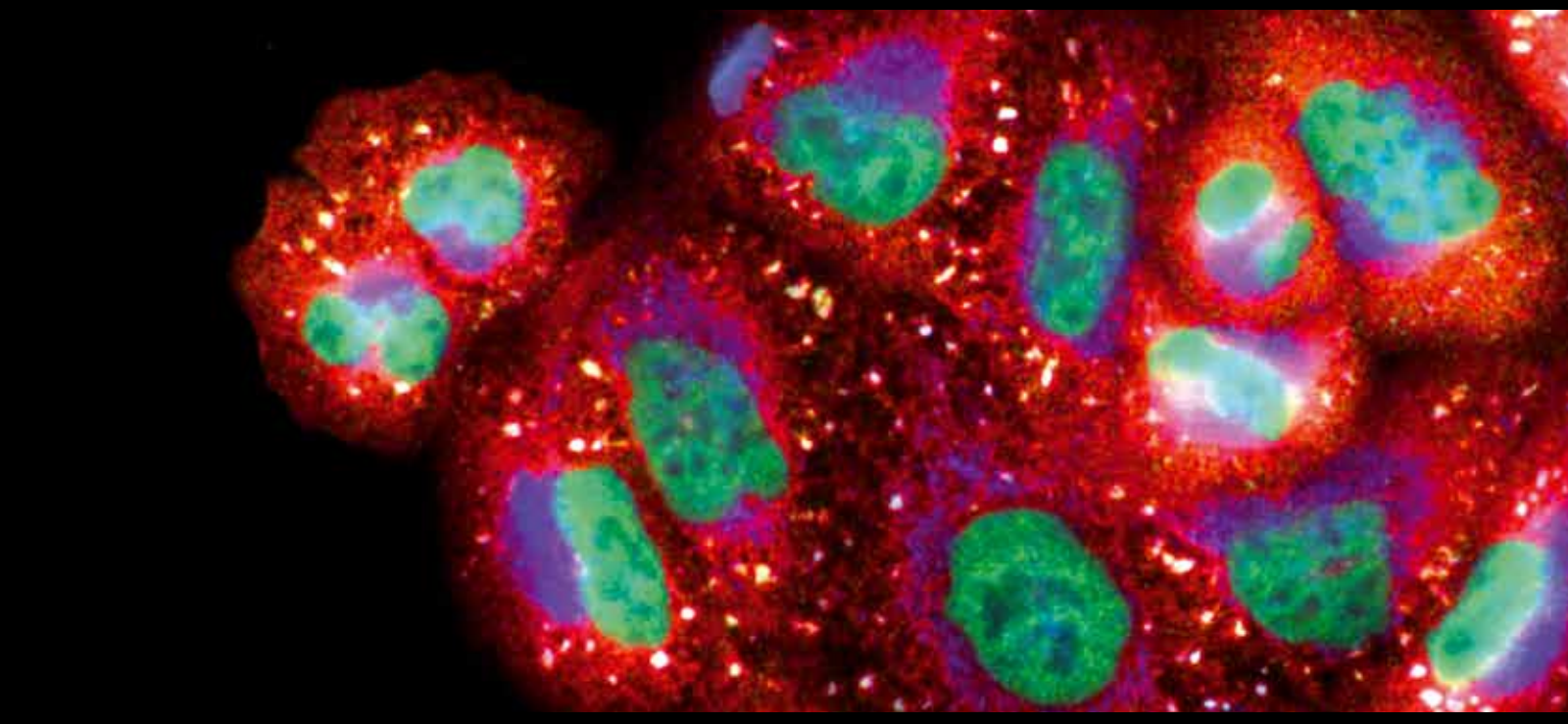

Lipid Peroxidation Products in Human Health and Disease

Oxidative Medicine and Cellular Longevity

Lipid Peroxidation Products in Human Health and Disease

Guest Editors: Kota V. Ramana, Sanjay Srivastava, and Sharad S. Singhal

Editorial Board

Contents

Hindawi Publishing Corporation
Oxidative Medicine and Cellular Longevity
Volume 2013, Article ID 583438, 3 pages
http://dx.doi.org/10.1155/2013/583438

Editorial

Lipid Peroxidation Products in Human Health and Disease

Kota V. Ramana,[1] Sanjay Srivastava,[2] and Sharad S. Singhal[3]

[1] *Department of Biochemistry and Molecular Biology, University of Texas Medical Branch, Galveston, TX 77555, USA*
[2] *Environmental Cardiology, University of Louisville, Louisville, KY 40202, USA*
[3] *Department of Diabetes and Metabolic Diseases Research, Beckman Research Institute, City of Hope National Medical Center, Duarte, CA 91010, USA*

Correspondence should be addressed to Kota V. Ramana; kvramana@utmb.edu

Received 26 September 2013; Accepted 26 September 2013

Enhanced formation of reactive oxygen species (ROS) leads to tissue dysfunction and damage in a number of pathological conditions. ROS oxidize the lipids to generate peroxides and aldehydes. These lipid peroxidation products, especially oxidized lipids-derived aldehydes, are much more stable than the parent ROS and therefore can diffuse from their site of generation and inflict damage at remote locations. Therefore, products of lipid oxidation can extend and propagate the responses and injury initiated by ROS. The lipid peroxidation (LPO) products are highly reactive and display marked biological effects, which, depending upon their concentration, cause selective alterations in cell signaling, protein and DNA damage, and cytotoxicity. Increased formation of lipid peroxides and aldehydes has been observed in atherosclerosis, ischemia-reperfusion, heart failure, Alzheimer's disease, rheumatic arthritis, cancer, and other immunological disorders. Therefore, decreasing the formation of lipid peroxidation products or scavenging them chemically could be beneficial in limiting the deleterious effects of ROS in various pathological conditions. Indeed, recent studies have identified several agents that could interfere with the LPO-mediated cell signaling pathways and could act as potential therapeutic drugs.

This special issue on LPO products in human health and disease compiles 20 excellent manuscripts including clinical studies, research articles, and reviews, which provide comprehensive evidence demonstrating the significance of LPO products in various pathological conditions.

The five review articles of this issue describe current knowledge of oxidative stress induced inflammatory signaling and inflammatory complications. The review article by C. Signorini et al. described the role of specific LPO products in the clinical manifestations and natural history of Rett syndrome, a genetically determined autism spectrum disorder. Specifically, they described how LPO-derived aldehyde products such as 4-hydroxynonenal (4-HNE) and a series of isoprostanes compounds could act as biomarkers of the disease. The review article by S. Joshi et al. described the factors involved in oxalate and calcium-oxalate induced injury in the kidneys and demonstrated how oxidative stress generated ROS via NADPH oxidase could contribute to renal injury. Further, they discussed, in depth, the pathophysiological role of NADPH oxidase in the kidneys and how different antioxidants and NADPH oxidase inhibitors could be used to control hyperoxaluria-induced kidney stone diseases. S. E. Lee and Y. S. Park in their review article discussed how the most potent LPO-derived α, β-unsaturated aldehydes such as acrolein, 4-HNE, and crotanaldehyde were involved in the pathophysiology of vascular complications. Specifically, the authors have nicely described the molecular mechanism by which α, β-unsaturated aldehydes cause vascular inflammation and dysfunction. The review article by P. Filipe et al. discussed how ultraviolet B- (UVB-)induced alterations in the proteins of the interstitial fluid may make consequential contributions to inflammation and degenerative processes of skin under UVB exposure. Further, this article highlights the significance of LPO, high-density lipoprotein (HDL), and low-density lipoprotein (LDL) as important targets of UVB in the interstitial fluid. Final review article by U. C. S. Yadav and K. V. Ramana discussed the significance of

LPO-derived lipid aldehydes in the regulation of nuclear factor-kappa binding protein (NF-κB) -induced inflammatory cell signaling. Specifically, they described how aldose reductase catalyzed lipid aldehydes such as 4-HNE and acrolein and their glutathione-conjugates act as secondary singling molecules to activate redox sensitive transcription factor NF-κB mediated inflammatory signals to contribute to inflammatory pathologies.

The research article by B. A. Leon-Chavez et al. investigates the effect of nitric oxide inhibitor, L-NAME, and zinc on nitrosative stress and cell death in a transient ischemia model by common carotid-artery occlusion in rats. In this study, administration of rats with $ZnCl_2$ reduces accumulation of zinc, level of nitrite and LPO, and cell death in the late phase of the ischemia. Fascinatingly, L-NAME administration in the rats treated with zinc causes time dependent increase in the accumulation of zinc in the early phase and increase in the levels of nitrites, LPO, and cell death by necrosis in the late phase. Based on the results, authors conclude that co-administration of zinc along with L-NAME increased the injury caused by common carotid-artery occlusion when compared to administration of zinc alone. The article by N. S. N. Yusoff et al. examines how antihypertensive drug clonidine regulates oxidative stress in rats. Their study indicates that clonidine in addition to its hypotensive effect enhances the level of antioxidant status and ameliorates the oxidative stress which could reduce the hypertension-induced heart damage in spontaneously hypertensive rats without or with L-NAME administration. Studies by P. Fernández-Robredo et al. demonstrate the effect of lutein and a multivitamin complex with lutein and glutathione on systemic and retinal biochemical and ultrastructural parameters leading to AMD progression in the apoE null mice. These studies indicate that treatment of lutein along with multivitamin complex but not lutein alone substantially reduced VEGF levels and MMP-2 activity and ameliorated the retinal morphological alterations in the apoE null mice.

The research article by S. Sahreen et al. investigates the effect of extracts of Rumex hastatus roots on carbon tetrachloride-induced hapato and testicular oxidative stress and toxicity in the rats. The results provide some evidence that the extracts of Rumex hastatus roots could have beneficial antioxidant properties in preventing free radical-mediated toxicities. In the article by A. Ścibior et al., the protective effects of magnesium against vanadium-induced LPO in rat hepatic tissues were examined. This is an interesting report on how the combination of metal treatments regulates cellular oxidative stress *in vitro* and *in vivo* conditions. I. Sano et al. in their article reported the pathological mechanism of pterygia. Specifically, they have shown the involvement of protein adducts of LPO-derived aldehydes such as 4-HNE and 4-hydroxyhexenal (4-HHE) in human pterygia patient's eyes.

The relation between fluoride intake and oxidative stress in salivary glands of rats was reported by P. M. Yamaguti et al. in their article. Especially, they demonstrate that the single administration of sodium fluoride in rats decreased super oxide dismutase while increased the LPO in the salivary glands as early as in four hours. Interestingly, the oxidative stress induced by sodium fluoride is more in submandibular glands as compared to parotid glands. H.-M. Luo et al. in their research article examined the effects of ulinastatin on burned swine by monitoring the hemodynamic variables by PiCCO system and determining the extent of LPO and tissue edema. Results indicate that LPO regulates ulinastatin diminished burn-induced increase in vascular permeability and net fluid accumulation.

This study suggests a potential small-volume fluid resuscitation strategy in combating with a major burn injury. In the final research article of this issue, Z. Yiran et al. reported involvement of oxidative stress and MAPK in cadmium-induced hepatic cell toxicity and apoptosis. Preincubation of N-acetyl-L_cysteine with BRL3A liver cells decreased cadmium-induced increase in the malondialdehyde level, super oxide dismutase (SOD) and glutathione peroxidase activity and cell viability. The involvement of cadmium-induced hepatotoxicity was confirmed by using inhibitors of p38 MAPK, JNK, and ERK.

The exciting clinical study reported by C. Cipierre et al. indicates malondialdehyde adduct to hemoglobin as a novel biomarker of oxidative stress in the preterm neonates. By using LC-MS/MS methods, this study identified formation of malondialdehyde adducts of hemoglobin from the blood of full-term and preterm neonates and based on these findings authors suggest that the malondialdehyde adduct of hemoglobin might be a useful marker for variety of pathological conditions. In the same issue, C. Cipierre et al. also assessed the influence of the perinatal condition on malondialdehyde-hemoglobin adduct concentrations. In this pilot clinical study, authors found a relationship between blood malondialdehyde-hemoglobin adduct concentrations with neonatal morbidity in very low birth-weight infants. Results from these two manuscripts indicate the significance of early antioxidant treatment to decrease oxidative stress mediated problems in very low birth-weight infants.

Interconnections between the pathological conditions associated with the diabetes and cirrhosis patients were reported by R. Hernández-Muñoz et al. in a clinical study. This study indicates that the levels of oxidative stress markers in the red blood cells of cirrhotic patients were significantly increased, whereas in the patients with coincidence of diabetes and cirrhosis oxidative response was partially reduced. Interestingly, the levels of total phospholipids and cholesterol were enhanced in the patients with both pathologies but not in the patients with the single pathology. In another clinical study, D. Miric et al. have examined the involvement of xanthine oxidase (XOD) in oxidative damage and inflammatory response in end-stage renal disease (ESRD) patients. Results show that patients suffering from ESRD had higher levels of oxidative stress markers such as hydroperoxides, AOPP, SOD, and XOD and a lower level of total SH groups when compared to healthy subjects. Interestingly, XOD activity was only increased in patients with poor nutritional status as indicated by geriatric nutritional risk index (GNRI) score. These findings suggest that increased XOD may contribute to oxidative injury during hemodialysis treatment leading to the pathogenesis of malnutrition-inflammation complex syndrome.

H. Tuzcu et al. have reported the effect of high-dose insulin analog initiation therapy on glycemic variability, LPO, and oxidative stress determined in the plasma and urine samples of type 2 diabetes patients. Especially, treatment with insulin analog along with metformin resulted in a significant reduction in glycemic variability and oxidative stress markers when compared to single oral hypoglycemic agent. Although this study was carried out in 24 patients, the data indicates that the treatment with insulin analogs, regardless of blood glucose changes, exerts inhibitory effects on LPO. In another clinical study, C. Mila-Kierzenkowska et al. have identified the effect of radical nephrectomy on LPO and redox balance in the patients with renal cell carcinoma. The findings suggest that laparoscopy may be used for radical nephrectomy as effectively as open surgery without creating any oxidative stress in the patients of renal cell carcinoma.

In a final note, it is evident from these papers that LPO products play a major role in deregulating key pathways involved in the pathophysiology of a number of pathological disorders. The treatment options that control the production of free radical-mediated generation of LPO products could be potential therapeutic approaches to controlling human diseases.

Acknowledgments

We would like to thank all the editorial staff, authors, and reviewers who took part in the success of this special issue.

Kota V. Ramana
Sanjay Srivastava
Sharad S. Singhal

Hindawi Publishing Corporation
Oxidative Medicine and Cellular Longevity
Volume 2013, Article ID 240560, 10 pages
http://dx.doi.org/10.1155/2013/240560

Research Article

Subacute Zinc Administration and L-NAME Caused an Increase of NO, Zinc, Lipoperoxidation, and Caspase-3 during a Cerebral Hypoxia-Ischemia Process in the Rat

Victor Manuel Blanco-Alvarez,[1] Patricia Lopez-Moreno,[1] Guadalupe Soto-Rodriguez,[1] Daniel Martinez-Fong,[2] Hector Rubio,[3] Juan Antonio Gonzalez-Barrios,[4] Celia Piña-Leyva,[1] Maricela Torres-Soto,[1] María de Jesus Gomez-Villalobos,[5] Daniel Hernandez-Baltazar,[2] Eduardo Brambila,[1] José Ramon Eguibar,[5] Araceli Ugarte,[5] Jorge Cebada,[6] and Bertha Alicia Leon-Chavez[1]

[1] *Facultad de Ciencias Químicas, Benemérita Universidad Autónoma de Puebla, 14 sur y Avenida San Claudio Edif. 105A, CU, Col. San Manuel, 72570 Puebla, PUE, Mexico*
[2] *Departamento de Fisiología, Biofísica y Neurociencias, CINVESTAV, Apartado Postal 14-740, 07000 México, DF, Mexico*
[3] *Facultad de Medicina, Universidad Autónoma de Yucatán, Av. Itzáez No. 498 x 59 y 59-A Col. Centro, C. P. 97000 Mérida, YUC, Mexico*
[4] *Laboratorio de Medicina Genómica del Hospital Regional "1° de Octubre", ISSSTE, Avenida Instituto Politécnico Nacional 1669, 07760 México, DF, Mexico*
[5] *Instituto de Fisiología, Benemérita Universidad Autónoma de Puebla, 14 sur 6301, San Claudio, 72570 Puebla, PUE, Mexico*
[6] *Escuela de Biología, Benemérita Universidad Autónoma de Puebla, Blvd. Valsequillo y Avenida San Claudio Edif. 76, CU, Col. San Manuel, 72570 Puebla, PUE, Mexico*

Correspondence should be addressed to Bertha Alicia Leon-Chavez; alileon04@yahoo.com.mx

Received 8 February 2013; Accepted 4 July 2013

Academic Editor: Kota V. Ramana

Zinc or L-NAME administration has been shown to be protector agents, decreasing oxidative stress and cell death. However, the treatment with zinc and L-NAME by intraperitoneal injection has not been studied. The aim of our work was to study the effect of zinc and L-NAME administration on nitrosative stress and cell death. Male Wistar rats were treated with $ZnCl_2$ (2.5 mg/kg each 24 h, for 4 days) and N-ω-nitro-L-arginine-methyl ester (L-NAME, 10 mg/kg) on the day 5 (1 hour before a common carotid-artery occlusion (CCAO)). The temporoparietal cortex and hippocampus were dissected, and zinc, nitrites, and lipoperoxidation were assayed at different times. Cell death was assayed by histopathology using hematoxylin-eosin staining and caspase-3 active by immunostaining. The subacute administration of zinc before CCAO decreases the levels of zinc, nitrites, lipoperoxidation, and cell death in the late phase of the ischemia. L-NAME administration in the rats treated with zinc showed an increase of zinc levels in the early phase and increase of zinc, nitrites, and lipoperoxidation levels, cell death by necrosis, and the apoptosis in the late phase. These results suggest that the use of these two therapeutic strategies increased the injury caused by the CCAO, unlike the alone administration of zinc.

1. Introduction

A stroke causes disability and death. Extensive studies have shown the participation of oxidative stress as the mechanism underlying a cerebral ischemia injury. Tissue plasminogen activator (tPA) has been the only drug approved by the FDA for treating ischemic stroke, but its use is restricted because to its adverse effects [1]. There is evidence that zinc is a cytoprotector agent [2–4], increasing the antioxidant capacity and decreasing the iron-catalyzed lipid peroxidation, as well as the apoptosis [5].

Zinc has a dual role during the pathological process of stroke. The accumulation of zinc has cytotoxic properties [6–12]. However, the administration of zinc protoporphyrin, zinc ion, or protoporphyrin decreases the focal cerebral ischemia [4] and prevents neuron death [2, 3]. The beneficial action of zinc is caused by its antioxidant properties. The zinc treatment prevents lipid peroxidation and increases glutathione availability in Wilson's disease [13]. Zinc decreases the apoptosis through inhibition of Bax and Bak activation and cytochrome c release [14]. In addition, zinc is a potent inhibitor of the apoptotic proteases, caspase-3 [15, 16], and caspase-8 [17].

Studies have shown the participation of nitric oxide (NO) in zinc accumulation, the increase of cleaved caspase-3 and lipoperoxidation during a process of cerebral hypoxia-ischemia [18], and through release of zinc from presynaptic buttons [19]. Nitric oxide causes the release of zinc from metallothionein by destroying zinc-sulphur clusters without concomitant formation of S-nitrosothiol [20]. However, NO plays a critical role in the protection of the liver from oxidative stress. The mechanisms involved include its role as an antioxidant agent of iron that decreases the oxidative stress in rat hepatocytes [21] or through the pathway of Akt-eNOS-NO-HIF in ischemia postconditioning [22]. The NO has protective properties on the brain during an acute ischemic stroke, but the increase of the NOS activity causes the alteration of microvasculature integrity and edema formation during cerebral ischemia-reperfusion injuries in the rat, without changing arterial blood pressure or blood flow in the ischemic regions [23]. There is evidence that the inhibition of NO by N-ω-nitro-L-arginine methyl ester (L-NAME) decreases the zinc levels and increases cardiac-necrosis marker levels detected in the plasma of rabbits [24]. However, L-NAME administration decreases cell death after the ischemia [18].

These antecedents support the idea that NO and zinc have a dual role during the ischemia process. However, the coadministration of zinc and an NOS inhibitor has not been defined. In this work we study the prophylactic effects of the subacute administration of zinc (2.5 mg/kg, each 24 h for 4 days) and L-NAME (10 mg/kg, one hour before a common carotid-artery occlusion (CCAO)) on nitrite levels, and the production of malonyldialdehyde (MDA) + 4-hydroxialkenals (HAE) at different hours pre- and postreperfusion. Histopathological changes were evaluated through immunoreactivity against cleaved caspase-3 and hematoxylin-eosin staining. Our results support the idea that NO in the early phase is a cytoprotector agent and NO in the later phase acts as a cytotoxic agent. Zinc administration alone has a cytoprotector role against the damage caused by CCAO, but the coadministration of zinc and L-NAME causes more damage compared to the hypoxia-ischemia process.

2. Materials and Methods

2.1. Experimental Animals. Male Wistar rats between 190 g and 240 g were obtained from the vivarium of the CINVESTAV. The animals were maintained in adequate animal rooms with controlled conditions of temperature (22 ± 1°C) and a light-dark cycle (12 h-12 h light-dark; light onset at 0700). Food and water were provided ad libitum. All procedures were in accordance with the Mexican current legislation, the NOM-062-ZOO-1999 (SAGARPA), based on the Guide for the Care and Use of Laboratory Animals, NRC. The Institutional Animal Care and Use Committee (IACUC) approved our animal-use procedures with the protocol number 09-102. All efforts were made to minimize animal suffering.

2.2. Zinc and L-NAME Administration. The rats were grouped into different treatments: (1) control (without treatment), (2) CZn96h; control treated with $ZnCl_2$ (2.5 mg/kg each 24 h for 4 days), from which the brain was obtained at 24 h, 48 h, 72 h, and 96 h postadministration, (3) Zn96h + CCAO; rats treated with a subacute administration of zinc and transient ischemia through a common carotid artery occlusion (CCAO), which was caused for 10 min; the brain was obtained at different hours (4 h, 8 h, 12 h, 24 h, 36 h, 72 h, 96 h, and 168 h postreperfusion), (4) Zn96h + L-NAME control; the rats received a subacute administration of zinc for 4 days plus L-NAME (10 mg/kg), and (5) Zn96h + L-NAME + CCAO; these rats received all treatments, and the brain was obtained at different hours (4 h, 8 h, 12 h, 24 h, 36 h, 72 h, 96 h, and 168 h postreperfusion).

2.3. Nitric Oxide Determination. The temporoparietal cortex and hippocampus of all studied groups ($n = 5$ in each group) were mechanically homogenized in phosphate-buffered saline solution (PBS), pH 7.4, and centrifuged at 12,500 rpm for 30 min at 4°C by using a 17TR microcentrifuge (Hanil Science Industrial Co. Ltd; Inchun, Korea). The NO production was assessed by the accumulation of nitrites (NO_2^-) in the supernatants of homogenates, as described elsewhere [18, 25]. Briefly, the nitrite concentration in 100 μL of supernatant was measured by using a colorimetric reaction generated by the addition of 100 μL of Griess reagent, which was composed of equal volumes of 0.1% N-(1-naphthyl) ethylenediamine dihydrochloride and 1.32% sulfanilamide in 60% acetic acid. The absorbance of the samples was determined at 540 nm with a SmartSpec 3000 spectrophotometer (Bio-Rad; Hercules, CA, USA) and interpolated by using a standard curve of $NaNO_2$ (1 to 10 μM) to calculate the nitrite content.

2.4. Measure of Blood Pressure. The blood pressure was measured in all studied groups ($n = 5$ in each group). Systolic and diastolic blood pressures were measured using the tail-cuff method by using the XBP1000 Blood Pressure System from Kent Scientific Corporation. Systolic and diastolic blood pressures (mean ± SE, mm Hg) were measured in all animals 24-h before and after each treatment as previously described [26].

2.5. Lipoperoxidation. Malonyldialdehyde (MDA) and 4-hydroxyalkanal (HEA) were measured in supernatants of homogenates of the temporoparietal cortex and hippocampus using the method described elsewhere [18, 25]. The colorimetric reaction in 200 μL of the supernatant was produced by the subsequent addition of 0.650 mL of 10.3 mM

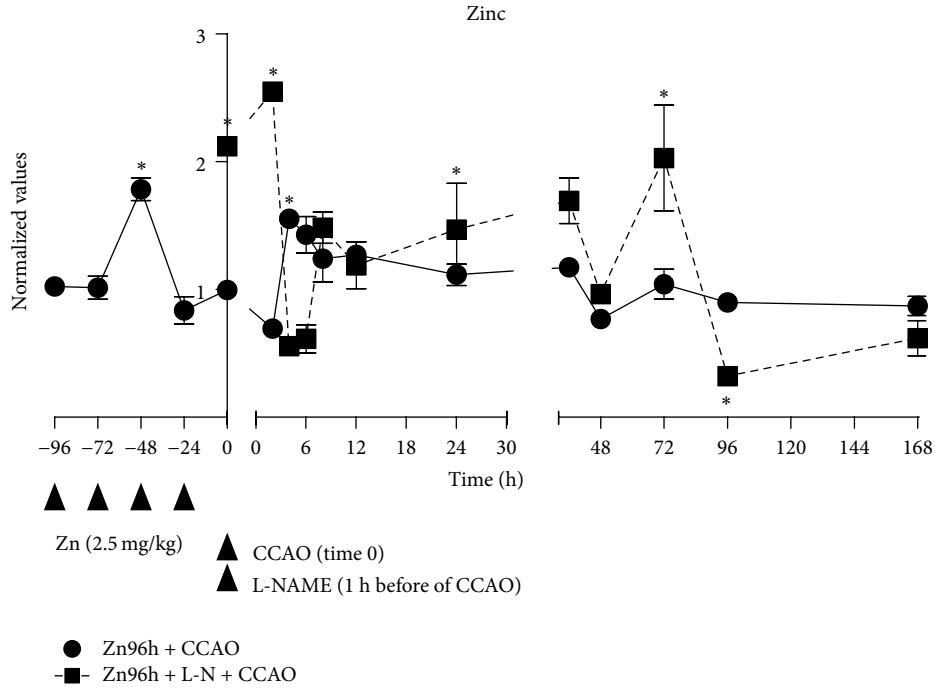

Figure 1: Effect of subacute administration of zinc and L-NAME on zinc levels during a cerebral hypoxia-ischemic process. The zinc levels were assayed by the Johnson method described elsewhere [18, 25]. Each value is the mean ± SE of 5 independent experiments made in triplicate. Zn96h + CCAO: preventive subacute administration of zinc (2.5 mg/kg intraperitoneal each 24 hours during 4 days) and common carotid-artery occlusion (CCAO) for 10 min. Zn96h + L-NM + CCAO: rats treated with zinc in the presence of an inhibitor of nitric oxide synthase (L-NAME) one hour before the CCAO. $^{*}P < 0.05$, an ANOVA test and a post-hoc Dunnet test to compare with the control group, and $^{\dagger}P < 0.05$, unpaired Student's t-test to compare between groups.

N-methyl-2phenyl-indole diluted in a mixture of acetonitrile : methanol (3 : 1). The reaction was started by the addition of 150 μL of methanesulfonic acid. The reaction mixture was strongly vortexed and incubated at 45°C for 1 h and then centrifuged at 3000 rpm for 10 min. The absorbance in the supernatant was read at 586 nm with a SmartSpec 3000 spectrophotometer (Bio-Rad; Hercules, CA, USA). The absorbance values were compared to a standard curve in the concentration range of 0.5 to 5 μM of 1,1,3,3-tetramethoxypropane (10 mM stock) to calculate the malonyldialdehyde and 4-hydroxyalkanal contents in the samples.

2.6. Immunolabeling of Cleaved Caspase-3. The immunoreactivity against cleaved caspase-3 was analyzed by an immunohistochemical method [25]. The fixed brains with 4% paraformaldehyde in PBS were maintained overnight in PBS containing 30% sucrose at 4°C. Then, each brain was frozen and sectioned into 10 μm slices on the coronal plane using a Leica SM100 cryostat (Leica Microsystems, Nussloch, Germany). Slices were individually collected in a 24-well plate containing PBS and used for the immunohistochemistry for cleaved caspase-3. The slices were incubated with PBS-Triton (0.1%) and later with 10% horse serum in PBS-Triton (0.1%) for 60 min at room temperature. The slices were incubated overnight with a rabbit polyclonal antibody against cleaved caspase-3 (1 : 300 dilution; Cell Signaling Technology, Danvers, MA, USA) and then with a 1 : 600 dilution of the secondary biotinylated goat antibody anti-rabbit IgG (H + L) (Vector Laboratories, Burlingame, CA, USA) for 2 hours at room temperature. After rinsing, the slices were incubated with streptavidin-horseradish peroxidase conjugate (BRL Inc., Gaithersburg, MD, USA) and diluted 1 : 400, again for 30 minutes at room temperature. The peroxidase reaction was developed by immersion in a freshly prepared solution of 0.02% 3,3′-diaminobenzidine (DAB, Sigma). The slices were counterstained with cresyl violet. The caspase-3 immunoreactivity was analyzed with a magnification of 5x, 20x, and 40x using a Leica DMIRE2 microscope (Leica Microsystems, Wetzlar, Germany). The images were digitalized with a Leica DC300F camera (Leica Microsystems, Nussloch, Germany) and analyzed with workstation Leica FW4000, version V1.2.1 (Leica Microsystems Vertrieb GmbH; Bensheim, Germany).

The histopathology study of the temporoparietal cortex and hippocampus from the brains of each experimental group was analyzed in coronary brain slices by hematoxylin-eosin staining at 24 h and 7-day postreperfusion ($n = 3$ in each group). The 3 μm paraffin-embedded tissue sections were stained with hematoxylin and eosin and examined at a magnification objective of 40x (Mod BM 1000 Leica, Jenopika Camera, Wetzlar, Germany). Digital micrographs were made from 5 randomly selected fields of each tissue section of each experimental group (Progress capture pro 2.1, Leica).

2.7. Statistical Analysis. All values are the mean ± SE obtained from at least 5 independent experiments. The significance of

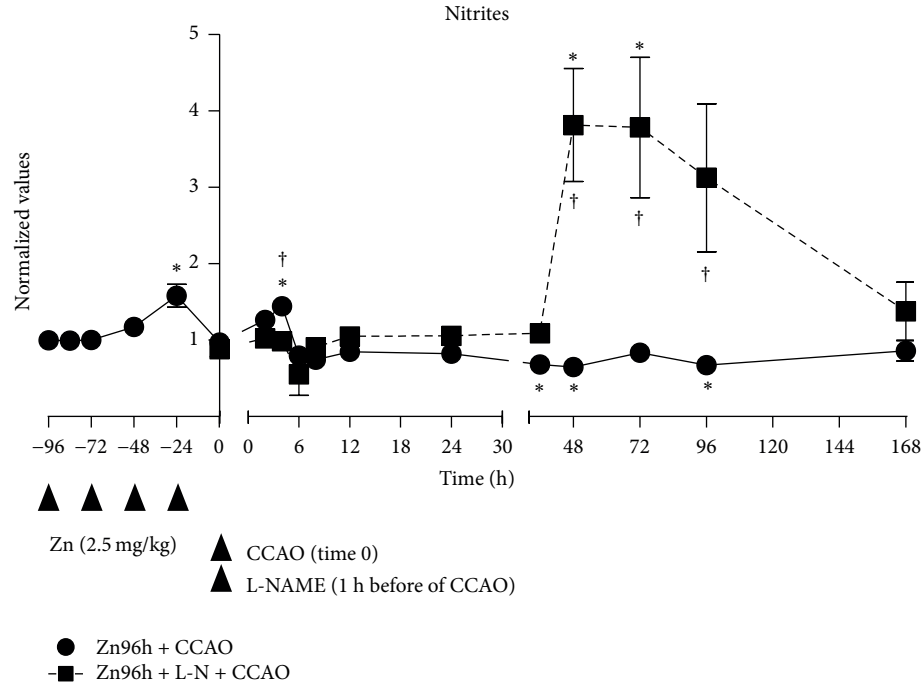

Figure 2: Subacute administration of zinc and L-NAME on nitrite levels during a cerebral hypoxia-ischemic process. The nitrite levels were assayed by the Griess method described elsewhere [18, 25]. Each value is the mean ± SE of 5 independent experiments made in triplicate. Zn96h + CCAO: preventive subacute administration of zinc (2.5 mg/kg each 24 hours during 4 days) and a common carotid-artery occlusion (CCAO) for 10 min. Zn96h + L-NM + CCAO: rats treated with zinc in presence of an inhibitor of nitric oxide synthase (L-NAME) one-hour before CCAO. $^{*}P < 0.05$, an ANOVA test and a post-hoc Dunnet test to compare with control group, and $^{\dagger}P < 0.05$, unpaired Student's t-test to compare between groups.

differences was analyzed by an ANOVA test and a post-hoc Dunnet test to compare with control group and an unpaired Student's t-test to compare between groups. The data were analyzed using the Graph Pad Prism software (version 5.00). A significant value was considered at $P < 0.05$.

3. Results

The zinc levels were determined in homogenized supernatants of the temporoparietal cortex at different hours, before and after the CCAO in rats treated with zinc in the presence or absence of L-NAME (Figure 1). The subacute administration of zinc in control group showed an increase of 79% ± 9% in zinc levels in the temporoparietal cortex on the third day, returning to basal levels on the fourth day of administration (Figure 1). The CCAO in rats treated with zinc caused an increase of 55% ± 5% at 4 h and of 43% ± 14% at 6 h postreperfusion, returning to the baseline at 24 h postreperfusion, maintaining this level in the 168 h (Figure 1). The L-NAME administration before the CCAO in rats treated with zinc caused several increases of zinc levels, from time 0 (CZn96h) of 112% ± 3%, decreasing at 4 h postreperfusion. A second increase of 70% ± 18% was observed at 36 h, a third increase of 103% ± 41% was observed at 72 h postreperfusion, and then decreasing by 68% ± 6% was observed at 96 h, returning again to the baseline at 168 h, after reperfusion (Figure 1).

The subacute administration of zinc in the control group showed an increase of 58% ± 15% in the nitrite levels at the fourth dose of administration (Figure 2). The CCAO caused an increase of 45% ± 8% at 4 h postreperfusion in treated rats with zinc, decreasing at 8 h, but unchanged at the 168 h postreperfusion (Figure 2). However, the L-NAME administration in rats treated with zinc decreased nitrite levels during the firsts 36 h postreperfusion, but caused an increase of 282% ± 74% from 48 h postreperfusion, maintaining this level at 72 h, and then returned to the baseline at the 168 h postreperfusion (Figure 2).

The systolic blood pressure of rats was measured before (P1) and after (P2) each treatment. The subacute administration of zinc in the absence of L-NAME did not change the systolic blood pressure before and after treatment, as compared to the controls without treatment. However, in rats treated with a subacute administration of zinc in the presence of L-NAME showed an increase of systolic blood pressure with ΔP of 25 (P1 was 130 ± 6 mm Hg and P2 was of 155 ± 3 mm Hg).

To evaluate whether the intraperitoneal administration of zinc and L-NAME causes cell damage, several markers of damage (lipid peroxidation and caspase-3) were studied, and cellular death was analyzed by hematoxylin-eosin staining.

The subacute administration of zinc caused an increase of 58% ± 15% in the MDA + HEA levels at the fourth dose, returning to baseline at the 24 h after the last administration

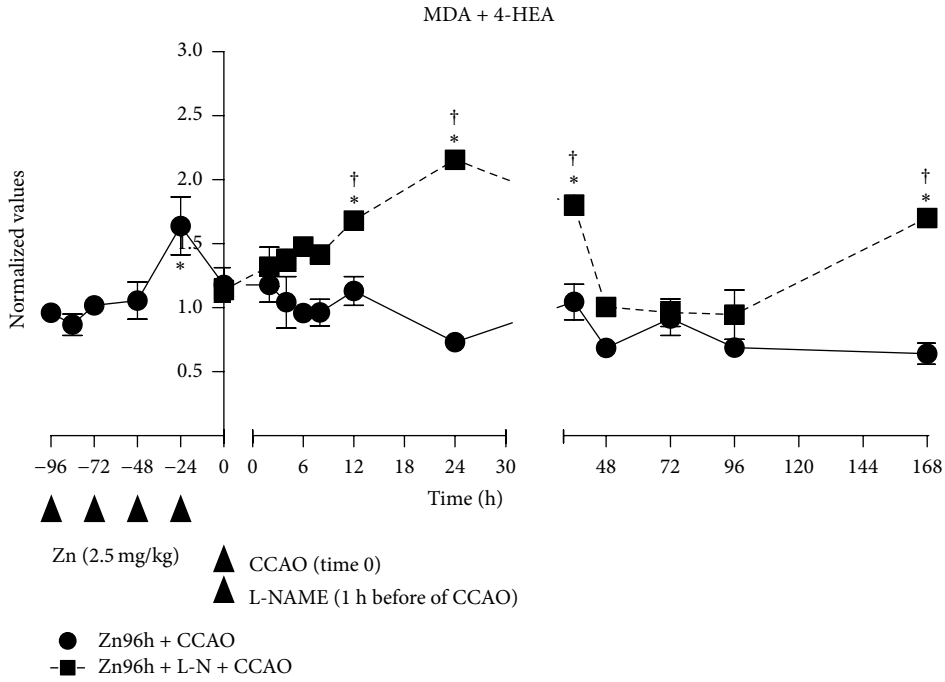

Figure 3: Subacute administration of zinc and L-NAME on lipoperoxidation levels during a cerebral hypoxia-ischemic process. Malonyldialdehyde (MDA) and 4-hydroxyalkanal (4-HEA) concentrations measured by using the method described elsewhere [18, 25] were used as biomarkers of lipoperoxidation. Each value represents the mean ± SE of 5 independent experiments made in triplicate. Zn96h + CCAO: preventive subacute administration of zinc (2.5 mg/kg each 24 hours for 4 days) and common carotid-artery occlusion (CCAO) for 10 min. Zn96h + L-NM + CCAO: rats treated with zinc in the presence of an inhibitor of nitric oxide synthase (L-NAME) one-hour before the CCAO. $^{*}P < 0.05$, an ANOVA test and a post-hoc Dunnet test to compare with the control group, and $^{\dagger}P < 0.05$, unpaired Student's t-test to compare between groups.

(time 0; Figure 3). The CCAO in the rats treated with zinc did not change the MDA + HEA levels over 168 h after reperfusion (Figure 3). However, L-NAME administration before the CCAO in the rats treated with zinc showed an increase of 68% ± 6% at 12 h postreperfusion, with a maximum level of 116% ± 7% at 24 h, returning to baseline and then a second increase of 70% ± 5% was measured at 168 h postreperfusion (Figure 3).

The histopathological study qualitatively showed that zinc administration before the CCAO prevented cell death, whereas the L-NAME in rats treated with zinc caused morphological changes of necrosis and apoptosis (Figure 4) and higher cleaved caspase-3 IR cells from 24 h (data not shown), increasing at day 7 postreperfusion (Figure 5).

The histopathology studies showed that the subacute administration of zinc maintained the cellular structure of the hippocampus in the CA1, CA3, dentate gyrus, and the pyramidal neurons of the cerebral cortex at 24 h postreperfusion but caused changes in the morphology of the granular cells from the CA1 and CA3 at day 7 after reperfusion, showing elongated cells with ramifications, whereas the dentate gyrus showed a change at 24 h, returning to normal morphology at the day 7 postreperfusion. The choroid plexus did not show significant changes in its morphology, but basophilic nuclei were present in the cells (Figure 4). However, the administration of zinc and L-NAME decreased the color intensity in the nuclei of granular cells from CA1, CA3, and dentate gyrus at day 7 postreperfusion, suggesting the presence of cellular necrosis in the hippocampus and basophilic nucleus in the dentate gyrus, possibly due to apoptosis. The choroid plexus showed a decrease in the color intensity of the nucleus at day 7 after reperfusion (Figure 4).

The subacute zinc administration caused a slight increase in the number of immunoreactivity (IR) cells against cleaved caspase-3 in the granular layer of the dentate gyrus (dg) and layer V (LV) of the temporoparietal cortex (arrowhead) at day 7 postreperfusion in control rats (Figure 5). However, the subacute administration of zinc also showed a slight increase of cleaved caspase-3 IR at the day 7 postreperfusion in both regions, whereas the L-NAME administration in the rats treated with zinc increased the caspase-3 IR cells in the granular layer of the dentate gyrus (dg) and layer five (LV) of the temporoparietal cortex at 24 h postreperfusion; however, it was more evident at day 7 postreperfusion. The other regions of hypothalamus also were affected (data not show). In addition, the Nissl staining (blue) showed a decrease in color intensity in the granular layer, it was more evident in the pyramidal cells of the LV of the temporoparietal cortex, with edema cells (arrow), and these results are indicative of cellular necrosis in the rats of the group Zn96h + L-NAME + CCAO (Figure 5).

4. Discussion

Subacute administration of zinc showed a cytoprotector effect leading to a decrease in the lipoperoxidation and

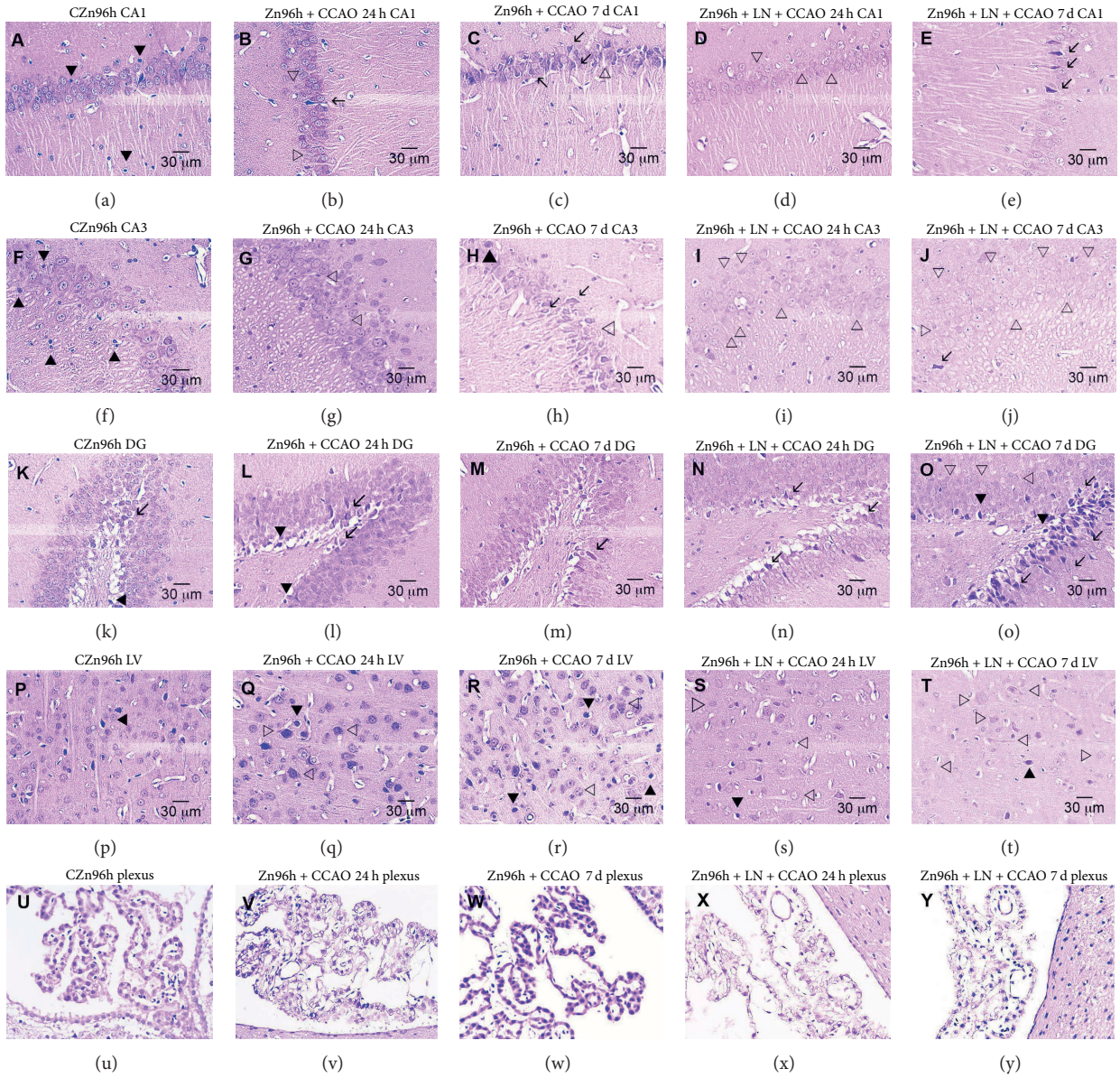

Figure 4: Hematoxylin-eosin staining in slides of the temporoparietal cortex and hippocampus in rats treated with zinc in the presence or absence of L-NAME. Paraffin-embedded tissue sections of 3 μm were stained with hematoxylin and eosin. The Zn96h + CCAO: preventive subacute administration of zinc (2.5 mg/kg each 24 hours for 4 days) and a common carotid-artery occlusion (CCAO) for 10 min. Zn96h + L-NM + CCAO: rats treated with zinc in the presence of an inhibitor of nitric oxide synthase (L-NAME) one hour before a CCAO. CA1 (a–e), CA3 (f–j) regions and dentate gyrus (DG: (k–o)) of hippocampus and LV, layer V of cerebral cortex (p–t). Apoptosis cell (dark arrowhead), necrosis (clear arrowhead), and branched cells (arrow).

immunoreactivity against cleaved caspase-3 by preventing an accumulation of zinc and increase of NO production in the late phase of a hypoxia-ischemia process. However, the coadministration of zinc and L-NAME (two inhibitors of NO production) showed a cytotoxic effect during a cerebral hypoxia ischemia in the rat, increasing the lipoperoxidation and cleaved caspase-3 IR cells from the early phase of a hypoxia-ischemia process, through the zinc accumulation in the early phase and an increase of zinc and the NO production in the late phase.

Prophylactic administration of zinc has a protector effect during hypoxia ischemia; similar results have been reported previously [2, 3, 5]. Other reports have shown neuroprotection when neuronal PC12 cells are preincubated with zinc salts, rather than coincubation [27] or the preventive subacute administration of zinc in rats [2].

Our work shows that a prophylactic subacute administration of zinc prevents the increase of NO caused by a CCAO in the late phase, maintaining the first increase of NO in the early phase of the hypoxia-ischemia process. The beneficial effect of NO in the early phase is related with the production of vasodilation [28] and metallothionein synthesis [29, 30]. In addition, NO acts as an antioxidant in the iron-mediated oxidative stress in rat hepatocytes, by

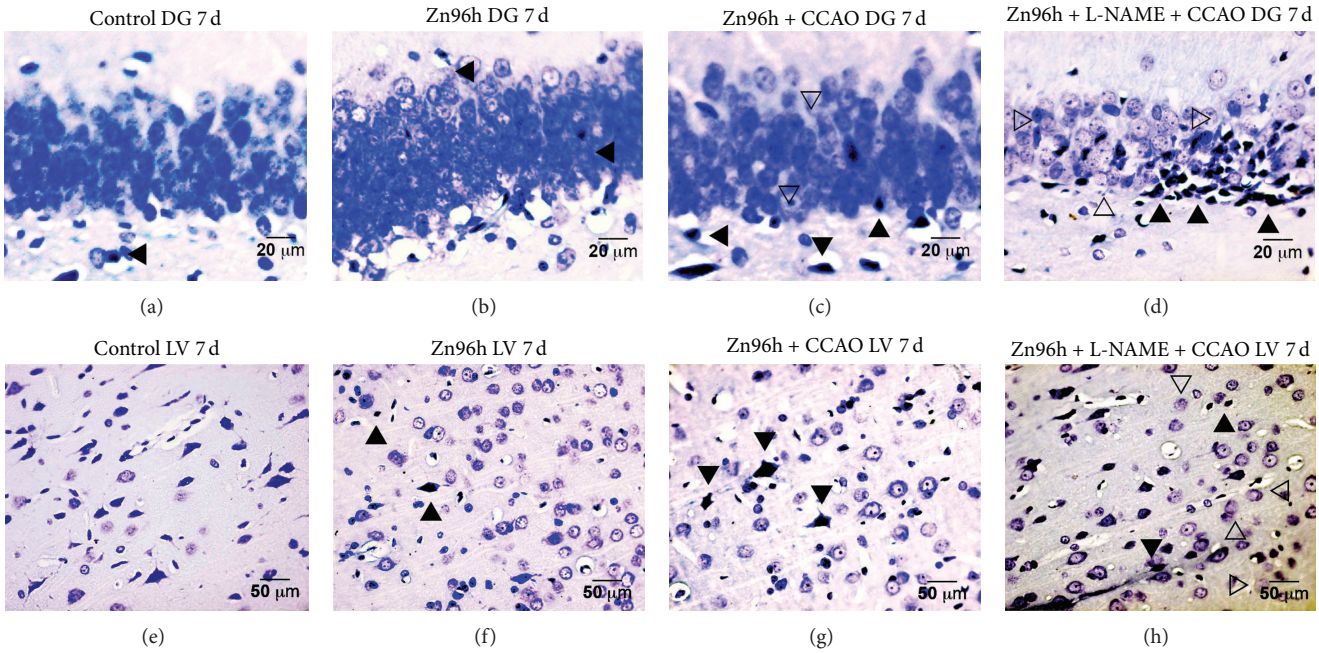

Figure 5: Immunohistochemistry against caspase-3 and Nissl counterstaining in slides of the hippocampus and temporoparietal cortex in zinc-treated rats in the presence or absence of L-NAME. The labels at the left side of the micrographs are cerebral regions. The immunostaining against cleaved caspase-3 is shown by the dark marks (dark arrowhead), and the Nissl stain appears in blue and pale cell (clear arrowhead). Zn96h + CCAO: preventive subacute administration of zinc (2.5 mg/kg each 24 hours for 4 days) and the common carotid-artery occlusion (CCAO) for 10 min. Zn96h + L-NAME + CCAO: rats treated with zinc in presence of an inhibitor of nitric oxide synthase (L-NAME) one-hour before the CCAO. DG: dentate gyrus of hippocampus; LV: layer V of cerebral cortex.

an inhibition of lipoperoxidation [21]. It has been reported that NO participates in ischemic postconditioning process through the increase of NO by the eNOS pathway and attenuating an ischemia-reperfusion injury in liver [22]. Previous reports have shown that the antioxidant enzyme cooper-zinc superoxide dismutase (Cu-Zn SOD) decreases the oxidative stress produced by the NO derived from iNOS in diabetic animals [31] and cardiac embryopathy in maternal diabetes [32].

The stabilization of constitutive NOS (cNOS) by zinc [33, 34] could explain the increase in the NO level in the first hours during a hypoxia-ischemia process, which increases the cNOSs in the first hours of postreperfusion [35]. The zinc administration prevented the second increase of NO at 24 h by a CCAO, as was reported previously [18]. In addition, the zinc inhibits NFκB and the synthesis of the iNOS protein [36], which has been reported at 12 h postreperfusion [35].

The beneficial effect of the zinc supplementation is to regulate the nitrosative stress, inducing antioxidant agents like glutathione [13, 37] and metallothionein [5], increasing the antioxidant capacity through Cu-Zn-SOD, storing the zinc in the intracellular compartment [38], and decreasing catalase and glutathione S-transferase activities [37].

Increased zinc levels found in the rats treated with zinc could cause a preconditioning, where the activation of zinc dependent of caspase-3 could be responsible for the cleavage of poly-ADP ribose polymerase (PARP), contributing to the decrease of the injury upon subsequent toxic exposure [39]. There is evidence that the extracellular zinc accumulation may be protective by preventing overactivation of the NMDA receptors. In addition, subtoxic accumulation intracellular of zinc may trigger a preconditioning effect, diminishing the susceptibility to a subsequent ischemia [39].

The subacute administration of zinc before a CCAO causes a decrease of the apoptosis at 24 h and in the day 7 after reperfusion, this has been reported previously by us [18] and others researchers in the hearts of diabetic mice [32]. The decrease of cleaved caspase-3 by zinc can be explained because zinc is able to directly inhibit the activity of caspase-3 [15, 16] and caspase-8, decreasing the cell death [17], since decrease proapoptotic proteins (Bax and Bak), or inhibits cytocrome c release [14].

It is known that NO participates in zinc accumulation and cell death [18, 40–43], and the administration alone of N-ω-nitro-L-arginine methyl ester (L-NAME) reduces the cerebral infarct [44], NOS activity, the edema [23], and cellular death at 24 h postreperfusion [18]. The administration of two inhibitors of NO production (zinc + L-NAME) causes an increase in systolic blood pressure and cell death in the cerebral cortex of the rat. Some reports found that the chronic inhibition of NO production causes hypertension [45] and decreases the plasma levels of zinc, causing small areas of myocardial coagulative necrosis [24].

The subacute administration of zinc and L-NAME caused an increase of zinc in the first and last hours, in which the increase of zinc could cause oxidative stress in the absence of NO in the first hours, where NO captures free radicals and prevents lipoperoxidation [46]. The increase of zinc in the

late phase caused the increase of NO production and lipoperoxidation. The increase of zinc may trigger the generation of reactive oxygen species (produced by mitochondria, NADPH-oxidase, and other sources), which could cause the intracellular Zn mobilization through a voltage-dependent calcium channel [47] or ZIP transporter, the excessive release of presynaptic zinc (at micromolar concentration) [48, 49], and accumulation of zinc in a postsynaptic neuron [48] and in the mitochondria [50]. These mechanisms could produce damage to neurons (granular cells and pyramidal neurons) and glia, as reported elsewhere [8, 51]. Therefore, excessive zinc accumulation in the early and late phase could be cytotoxic, which is supported by an increase of apoptosis from the early phase and necrosis in the late phase. These findings are in agreement to the cytotoxic effect of zinc [52, 53], where the function of zinc is dependent on the concentration, space, and timing of the cellular response to injury.

5. Conclusions

The treatment with two inhibitors of NO production (zinc and L-NAME) increased the cellular damage by necrosis and apoptosis in the hippocampus and layer V of cerebral cortex after a transient CCAO for 10 min through an increase of the nitrosative stress, zinc accumulation, and lipoperoxidation. This is opposite to that found with the subacute administration of only zinc before CCAO, which caused a cytoprotector effect by a decrease in the nitrosative stress and accumulation of zinc in the late phase.

These results provide evidence to consider the use of two therapeutic strategies that act on NOSs, to minimize damage during a cerebral hypoxic-ischemic process in patients who present a transient ischemia and are at high risk for a stroke or in patients with a disease cerebrovascular.

Conflict of Interests

The authors have no financial, personal, or other relationships with other people or organizations within five years of beginning the submitted work. The authors declare that they have no conflict of interests.

Acknowledgments

This work was supported by J-34143 (BAL-C) Grants VIEP-BUAP G/Nat/2012 (BAL-C). Victor Manuel Blanco Álvarez, Patricia López Moreno, and Guadalupe Soto-Rodriguez were recipient of scholarships from CONACYT. We thank the CINVESTAV for the production and maintenance of rats. Thanks are due to Dr. Ellis Glazier for editing of the English language text.

References

[1] A. Dávalos, "Thrombolysis in acute ischemic stroke: successes, failures, and new hopes," *Cerebrovascular Diseases*, vol. 20, supplement 2, pp. 135–139, 2005.

[2] K. Matsushita, K. Kitagawa, T. Matsuyama et al., "Effect of systemic zinc administration on delayed neuronal death in the gerbil hippocampus," *Brain Research*, vol. 743, no. 1-2, pp. 362–365, 1996.

[3] Y. Kitamura, Y. Iida, J. Abe et al., "Protective effect of zinc against ischemic neuronal injury in a middle cerebral artery occlusion model," *Journal of Pharmacological Sciences*, vol. 100, no. 2, pp. 142–148, 2006.

[4] Y.-J. Zhao, G.-Y. Yang, and E. F. Domino, "Zinc protoporphyrin, zinc ion, and protoporphyrin reduce focal cerebral ischemia," *Stroke*, vol. 27, no. 12, pp. 2299–2303, 1996.

[5] G. K. Helal, "Systemic administration of Zn^{2+} during the reperfusion phase of transient cerebral ischaemia protects rat hippocampus against iron-catalysed postischaemic injury," *Clinical and Experimental Pharmacology and Physiology*, vol. 35, no. 7, pp. 775–781, 2008.

[6] B. Tonder, F. F. Johansen, C. J. Frederickson, J. Zimmer, and N. H. Diemer, "Possible role of zinc in the selective degeneration of dentate hilar neurons after cerebral ischemia in the adult rat," *Neuroscience Letters*, vol. 109, no. 3, pp. 247–252, 1990.

[7] J.-Y. Koh, S. W. Suh, B. J. Gwag, Y. Y. He, C. Y. Hsu, and D. W. Choi, "The role of zinc in selective neuronal death after transient global cerebral ischemia," *Science*, vol. 272, no. 5264, pp. 1013–1016, 1996.

[8] G. J. Lees, A. Lehmann, M. Sandberg, and A. Hamberger, "The neurotoxicity of zinc in the rat hippocampus," *Neuroscience Letters*, vol. 120, no. 2, pp. 155–158, 1990.

[9] A. P. Shabanzadeh, A. Shuaib, T. Yang, A. Salam, and C. X. Wang, "Effect of zinc in ischemic brain injury in an embolic model of stroke in rats," *Neuroscience Letters*, vol. 356, no. 1, pp. 69–71, 2004.

[10] A. Calderone, T. Jover, T. Mashiko et al., "Late calcium EDTA rescues hippocampal CA1 neurons from global ischemia-induced death," *Journal of Neuroscience*, vol. 24, no. 44, pp. 9903–9913, 2004.

[11] J. H. Weiss, S. L. Sensi, and J. Y. Koh, "Zn^{2+}: a novel ionic mediator of neural injury in brain disease," *Trends in Pharmacological Sciences*, vol. 21, no. 10, pp. 395–401, 2000.

[12] J. H. Weiss and S. L. Sensi, "Ca^{2+}-Zn^{2+} permeable AMPA or kainate receptors: possible key factors in selective neurodegeneration," *Trends in Neurosciences*, vol. 23, no. 8, pp. 365–371, 2000.

[13] F. Farinati, R. Cardin, R. D'Inca, R. Naccarato, and G. C. Sturniolo, "Zinc treatment prevents lipid peroxidation and increases glutathione availability in Wilson's disease," *Journal of Laboratory and Clinical Medicine*, vol. 141, no. 6, pp. 372–377, 2003.

[14] N. Ganju and A. Eastman, "Zinc inhibits Bax and Bac activation and cytochrome c release induced by chemical inducers of apoptosis but not by death-receptor-intiated pathways," *Cell Death and Differentiation*, vol. 10, no. 6, pp. 652–661, 2003.

[15] D. K. Perry, M. J. Smyth, H. R. Stennicke et al., "Zinc is a potent inhibitor of the apoptotic protease, caspase-3: a novel target for zinc in the inhibition of apoptosis," *Journal of Biological Chemistry*, vol. 272, no. 30, pp. 18530–18533, 1997.

[16] A. Q. Truong-Tran, J. Carter, R. E. Ruffin, and P. D. Zalewski, "The role of zinc in caspase activation and apoptotic cell death," *BioMetals*, vol. 14, no. 3-4, pp. 315–330, 2001.

[17] A. F. Smith, J. Longpre, and G. Loo, "Inhibition by zinc of deoxycholate-induced apoptosis in HCT-116 cells," *Journal of Cellular Biochemistry*, vol. 113, no. 2, pp. 650–657, 2012.

[18] P. Aguilar-Alonso, D. Martinez-Fong, N. G. Pazos-Salazar et al., "The increase in Zinc levels and upregulation of Zinc transporters are mediated by nitric oxide in the cerebral cortex after transient ischemia in the rat," *Brain Research*, vol. 1200, pp. 89–98, 2008.

[19] C. J. Frederickson, M. P. Cuajungco, C. J. LaBuda, and S. W. Suh, "Nitric oxide causes apparent release of zinc from presynaptic boutons," *Neuroscience*, vol. 115, no. 2, pp. 471–474, 2002.

[20] C. T. Aravindakumar, J. Ceulemans, and M. de Ley, "Nitric oxide induces Zn2+ release from metallothionein by destroying zinc-sulphur clusters without concomitant formation of S-nitrosothiol," *Biochemical Journal*, vol. 344, part 1, pp. 253–258, 1999.

[21] O. Sergent, B. Griffon, I. Morel et al., "Effect of nitric oxide on iron-mediated oxidative stress in primary rat hepatocyte culture," *Hepatology*, vol. 25, no. 1, pp. 122–127, 1997.

[22] J. Y. Guo, T. Yang, X. G. Sun et al., "Ischemic postconditioning attenuates liver warm ischemia-reperfusion injury through Akt-eNOS-NO-HIF pathway," *Journal of Biomedical Science*, vol. 18, no. 1, article 79, 2011.

[23] M. T. Mohammadi, S. M. Shid-Moosavi, and G. A. Dehghani, "Contribution of nitric oxide synthase (NOS) in blood-brain barrier disruption during acute focal cerebral ischemia in normal rat," *Pathophysiology*, vol. 19, no. 1, pp. 13–20, 2012.

[24] A. Pinelli, S. Trivulzio, L. Tomasoni, B. Bertolini, S. Brenna, and E. Bonacina, "Low nitric oxide values associated with low levels of zinc and high levels of cardiac necrosis markers detected in the plasma of rabbits treated with L-NAME," *Journal of Cardiovascular Pharmacology*, vol. 37, no. 3, pp. 310–316, 2001.

[25] G. Soto-Rodriguez, D. Martinez-Fong, R. Arroyo et al., "Nitric oxide production is associated to increased lipoperoxidation and active caspase-3 in demyelinated brain regions of the taiep rat," *Advances in Bioscience and Biotechnology*, vol. 3, no. 6A, pp. 695–704, 2012.

[26] E. Vega, M. de Jésus Gómez-Villalobos, and G. Flores, "Alteration in dendritic morphology of pyramidal neurons from the prefrontal cortex of rats with renovascular hypertension," *Brain Research*, vol. 1021, no. 1, pp. 112–118, 2004.

[27] S. Pavlica and R. Gebhardt, "Comparison of uptake and neuroprotective potential of seven zinc-salts," *Neurochemistry International*, vol. 56, no. 1, pp. 84–93, 2010.

[28] E. Morikawa, M. A. Moskowitz, Z. Huang, T. Yoshida, K. Irikura, and T. Dalkara, "L-Arginine infusion promotes nitric oxide-dependent vasodilation, increases regional cerebral blood flow, and reduces infarction volume in the rat," *Stroke*, vol. 25, no. 2, pp. 429–435, 1994.

[29] K. Katakai, J. Liu, K. Nakajima, L. K. Keefer, and M. P Waalkes, "Nitric oxide induces metallothionein (MT) gene expression apparently by displacing zinc bound to MT," *Toxicology Letters*, vol. 119, no. 2, pp. 103–108, 2001.

[30] B. L. Vallee, "Introduction to metallothionein," *Methods in Enzymology*, vol. 205, pp. 3–7, 1991.

[31] F. C. di Naso, A. S. Dias, M. Porawski, and N. A. P. Marroni, "Exogenous superoxide dismutase: action on liver oxidative stress in animals with streptozotocin-induced diabetes," *Experimental Diabetes Research*, vol. 2011, Article ID 754132, 6 pages, 2011.

[32] S. D. Kumar, M. Vijaya, R. P. Samy, S. T. Dheen, M. Ren, F. Watt et al., "Zinc supplementation prevents cardiomyocyte apoptosis and congenital heart defects in embryos of diabetic mice," *Free Radical Biology*, vol. 53, no. 8, pp. 1595–1606, 2012.

[33] B. Hemmens, W. Goessler, K. Schmidt, and B. Mayer, "Role of bound zinc in dimer stabilization but not enzyme activity of neuronal nitric-oxide synthase," *Journal of Biological Chemistry*, vol. 275, no. 46, pp. 35786–35791, 2000.

[34] H. Li, C. S. Raman, C. B. Glaser et al., "Crystal structures of zinc-free and -bound heme domain of human inducible nitric-oxide synthase. Implications for dimer stability and comparison with endothelial nitric-oxide synthase," *Journal of Biological Chemistry*, vol. 274, no. 30, pp. 21276–21284, 1999.

[35] A. F. Samdani, T. M. Dawson, and V. L. Dawson, "Nitric oxide synthase in models of focal ischemia," *Stroke*, vol. 28, no. 6, pp. 1283–1288, 1997.

[36] E. Ho, N. Quan, Y.-H. Tsai, W. Lai, and T. M. Bray, "Dietary zinc supplementation inhibits NFκB activation and protects against chemically induced diabetes in CD1 mice," *Proceedings of the Society for Experimental Biology and Medicine*, vol. 226, no. 2, pp. 103–111, 2001.

[37] M. S. Farias, P. Budni, C. M. Ribeiro, E. B. Parisotto, C. E. Santos, J. F. Dias et al., "Antioxidant supplementation attenuates oxidative stress in chronic hepatitis C patients," *Gastroenterology and Hepatology*, vol. 35, no. 6, pp. 386–394, 2012.

[38] K. Thambiayya, K. Wasserloos, V. E. Kagan, D. Stoyanovsky, and B. R. Pitt, "A critical role for increased labile zinc in reducing sensitivity of cultured sheep pulmonary artery endothelial cells to LPS-induced apoptosis," *American Journal of Physiology—Lung Cellular and Molecular Physiology*, vol. 302, no. 12, pp. L1287–L1295, 2012.

[39] J.-Y. Lee, Y.-J. Kim, T.-Y. Kim, J.-Y. Koh, and Y.-H. Kim, "Essential role for zinc-triggered p75NTR activation in preconditioning neuroprotection," *Journal of Neuroscience*, vol. 28, no. 43, pp. 10919–10927, 2008.

[40] E. Bossy-Wetzel, M. V. Talantova, W. D. Lee et al., "Crosstalk between nitric oxide and zinc pathways to neuronal cell death involving mitochondrial dysfunction and p38-activated K+ channels," *Neuron*, vol. 41, no. 3, pp. 351–365, 2004.

[41] M. P. Cuajungco and G. J. Lees, "Nitric oxide generators produce accumulation of chelatable zinc in hippocampal neuronal perikarya," *Brain Research*, vol. 799, no. 1, pp. 118–129, 1998.

[42] G. J. Lees, M. P. Cuajungco, and W. Leong, "Effect of metal chelating agents on the direct and seizure-related neuronal death induced by zinc and kainic acid," *Brain Research*, vol. 799, no. 1, pp. 108–117, 1998.

[43] G. Wei, C. J. Hough, Y. Li, and J. M. Sarvey, "Characterization of extracellular accumulation of Zn^{2+} during ischemia and reperfusion of hippocampus slices in rat," *Neuroscience*, vol. 125, no. 4, pp. 867–877, 2004.

[44] L. Ding-Zhou, C. Marchand-Verrecchia, N. Croci, M. Plotkine, and I. Margaill, "L-NAME reduces infarction, neurological deficit and blood-brain barrier disruption following cerebral ischemia in mice," *European Journal of Pharmacology*, vol. 457, no. 2-3, pp. 137–146, 2002.

[45] I. F. Benter, M. H. M. Yousif, F. M. Al-Saleh, R. Raghupathy, M. C. Chappell, and D. I. Diz, "Angiotensin-(1-7) blockade attenuates captopril- or hydralazine-induced cardiovascular protection in spontaneously hypertensive rats treated with NG-nitro-l-arginine methyl ester," *Journal of Cardiovascular Pharmacology*, vol. 57, no. 5, pp. 559–567, 2011.

[46] M. Niziolek, W. Korytowski, and A. W. Girotti, "Nitric oxide inhibition of free radical-mediated lipid peroxidation in photodynamically treated membranes and cells," *Free Radical Biology and Medicine*, vol. 34, no. 8, pp. 997–1005, 2003.

[47] S. L. Sensi, L. M. T. Canzoniero, S. P. Yu et al., "Measurement of intracellular free zinc in living cortical neurons: routes of entry," *Journal of Neuroscience*, vol. 17, no. 24, pp. 9554–9564, 1997.

[48] S. W. Suh, C. J. Frederickson, and G. Danscher, "Neurotoxic zinc translocation into hippocampal neurons is inhibited by hypothermia and is aggravated by hyperthermia after traumatic brain injury in rats," *Journal of Cerebral Blood Flow and Metabolism*, vol. 26, no. 2, pp. 161–169, 2006.

[49] C. J. Frederickson and A. I. Bush, "Synaptically released zinc: physiological functions and pathological effects," *BioMetals*, vol. 14, no. 3-4, pp. 353–366, 2001.

[50] D. Jiang, P. G. Sullivan, S. L. Sensi, O. Steward, and J. H. Weiss, "Zn^{2+} induces permeability transition pore opening and release of pro-apoptotic peptides from neuronal mitochondria," *Journal of Biological Chemistry*, vol. 276, no. 50, pp. 47524–47529, 2001.

[51] H. Manev, E. Kharlamov, T. Uz, R. P. Mason, and C. M. Cagnoli, "Characterization of zinc-induced neuronal death in primary cultures of rat cerebellar granule cells," *Experimental Neurology*, vol. 146, no. 1, pp. 171–178, 1997.

[52] J.-Y. Koh, "Zinc and disease of the brain," *Molecular Neurobiology*, vol. 24, no. 1–3, pp. 99–106, 2001.

[53] S. L. Sensi, P. Paoletti, A. I. Bush, and I. Sekler, "Zinc in the physiology and pathology of the CNS," *Nature Reviews Neuroscience*, vol. 10, no. 11, pp. 780–791, 2009.

Hindawi Publishing Corporation
Oxidative Medicine and Cellular Longevity
Volume 2013, Article ID 343824, 10 pages
http://dx.doi.org/10.1155/2013/343824

Review Article

Isoprostanes and 4-Hydroxy-2-nonenal: Markers or Mediators of Disease? Focus on Rett Syndrome as a Model of Autism Spectrum Disorder

Cinzia Signorini,[1] Claudio De Felice,[2] Thierry Durand,[3] Camille Oger,[3] Jean-Marie Galano,[3] Silvia Leoncini,[1,4] Alessandra Pecorelli,[1,4] Giuseppe Valacchi,[5,6] Lucia Ciccoli,[1] and Joussef Hayek[4]

[1] *Department of Molecular and Developmental Medicine, University of Siena, I-53100 Siena, Italy*
[2] *University General Hospital, Neonatal Intensive Care Unit, Azienda Ospedaliera Universitaria Senese, I-53100 Siena, Italy*
[3] *Institut des Biomolécules Max Mousseron (IBMM), UMR 5247-CNRS-UM I-UM II, BP 14491 34093, Montpellier, Cedex 5, France*
[4] *University General Hospital, Child Neuropsychiatry Unit, Azienda Ospedaliera Universitaria Senese, I-53100 Siena, Italy*
[5] *Department of Life Science and Biotechnologies, University of Ferrara, I-44121 Ferrara, Italy*
[6] *Department of Food and Nutrition, Kyung Hee University, Seoul 130-701, Republic of Korea*

Correspondence should be addressed to Cinzia Signorini; cinzia.signorini@unisi.it

Received 6 February 2013; Revised 23 May 2013; Accepted 24 May 2013

Academic Editor: Kota V. Ramana

Lipid peroxidation, a process known to induce oxidative damage to key cellular components, has been implicated in several diseases. Following three decades of explorations mainly on *in vitro* models reproducible in the laboratories, lipid peroxidation has become increasingly relevant for the interpretation of a wide range of pathophysiological mechanisms in the clinical setting. This cumulative effort has led to the identification of several lipid peroxidation end-products meeting the needs of the *in vivo* evaluation. Among these different molecules, isoprostanes and 4-hydroxy-2-nonenal protein adducts appear to be particularly interesting. This review shows how specific oxidation products, deriving from polyunsaturated fatty acids precursors, are strictly related to the clinical manifestations and the natural history of Rett syndrome, a genetically determined neurodevelopmental pathology, currently classified among the autism spectrum disorders. In our experience, Rett syndrome offers a unique setting for physicians, biologists, and chemists to explore the borders of the lipid mediators concept.

1. Introduction

Oxidative stress (O.S.), a biological condition determined by the imbalance between prooxidant and the antioxidant system, is involved in several conditions, including inflammation, carcinogenesis, neurodegeneration, and development. Lipid peroxidation is a critical component of O.S. In particular, free radicals and specifically reactive oxygen species (ROS) are able to attack polyunsaturated fatty acids (PUFAs) of cell membranes thus generating a family of α,β-unsaturated reactive aldehydes, such as 4-hydroxy-2-nonenal (4-HNE) and prostaglandin-like end-products termed isoprostanes (IsoPs). Emerging knowledge points out the key role of these molecules in generating oxidative-driven damage. Therefore, these compounds, rather than being considered simple biomarkers of disease, are to be considered as mediators. In the present review, we discuss the evidence on the issue by focusing our proof-of-concept reasoning on the unique O.S. model of disease represented by Rett syndrome (RTT), a genetically determined autism spectrum disorder.

2. Role of Oxidative Stress in Human Diseases

O.S., as defined as an imbalance between cellular antioxidant defenses and free radicals production, is implicated in a wide variety of disease processes. To this regard, a role of oxidative damage in cancer [1, 2], neurodegenerative diseases

[3–6], and likely inflammatory bowel disease [7, 8] has been recently reported. In the matter of atherosclerosis, an oxidative damage, especially to lipids, is certain. However, as it concerns the size of its effects and underlying pathogenetic mechanisms there is likely much less certainty than a few years ago [9]. One method to quantify oxidative injury is to measure lipid peroxidation. However, a cause-effect relationship is often difficult, if not impossible, to prove.

3. Oxidative Stress: Shifting from the *In Vitro* to the *In Vivo* Concept

Until the '80s, lipid peroxidation was confined to specialized laboratories in which the phenomenon was mainly evaluated *in vitro*. At this stage, researchers were interested in reproducing lipid peroxidation as a macrophenomenon induced by xenobiotics of such an entity that would be quite unlikely to be present in human physiology and pathology. The meaning of those experiments and tests was mainly to evidence the phenomenon by measuring the products generated in the process. In this particular setting, oxidized aldehydes (chiefly malondialdehyde, MDA, and all the thiobarbituric acid reactive substances, TBARS) were considered to be reliable indicators of lipid peroxidation. Things changed dramatically when a number of laboratories around the world evidenced increased levels of lipid peroxidation markers in tissues and body fluids from patients as compared to those observed in healthy controls. Thus, the setting has progressively moved from *in vitro* to *in vivo* and has allowed to enlighten the role of lipid peroxidation within the mechanisms of several diseases and physiologic signaling pathways.

The entity of the phenomenon became dramatically downscaled so that more sensitive and reliable markers *in vivo* became an urgent necessity. At this further stage, several key markers of lipid peroxidation applicable *in vivo* have been discovered, including IsoPs and 4-HNE protein adducts (4-HNE PAs). The measurement of those markers has allowed a much deeper understanding of the key role of oxidative stress in health and disease. Likely, we are now at the stage in which we are asking whether these end-peroxidation products may have biological activity on their own, thus progressively shifting from markers to mediators.

4. Lipid Peroxidation End-Products: Shifting from Markers to Mediators

Lipid mediators are chemical messengers that are released in response to tissue injury and include prostaglandins, leukotrienes, lipoxins, and neuroprotectins, playing an essential role in the different phases of inflammation. While early in the inflammatory response, arachidonic acid (AA) metabolites (i.e., prostaglandins and leukotrienes) exert proinflammatory actions, by promoting chemotaxis of phagocytic leukocytes and inducing fever; the so-termed "lipid mediator class switching" is responsible for the production of specialized proresolving mediators, such as lipoxins, resolvins, maresins, and protectins, which exert specific roles in counterregulating inflammation and turning on resolution [10, 11]. Thus inflammation can be considered a self-limited process depending on lipid-derived mediators produced in the inflammatory exudates.

Emerging evidence indicates that biomarkers of lipid peroxidation can be interpreted as lipid mediators, acting as key factors in the regulation of the delicate balance between inflammation and the resolution process. One unanswered major question is concerning whether the end-products of peroxidation, such as IsoPs, are to be considered true markers or simple markers of O.S.; in particular whether different lipid mediators would determine different diseases; or whether the time course of production is a critical factor in physiology and disease.

5. Aldehyde Products

As mentioned earlier, the interaction of ROS and lipids can induce the peroxidation process, a chain reaction that produces multiple breakdown molecules, including many highly reactive aldehydes such as malondialdehyde, 4-HNE, 4-hydroxy-2-hexenal, and acrolein [12].

Among them, 4-HNE, a 4-hydroxyalkenal, is the most intensively studied aldehyde and it is one of the best recognized and most studied cytotoxic products derived from the lipid peroxidation processes.

4-HNE derives from the oxidation of ω-6 PUFAs, essentially arachidonic and linoleic acid, that is, the two most represented fatty acids in biomembranes. 4-HNE is an unusual compound containing three functional groups that in many cases act in concert explaining its high reactivity. There is, first of all, a conjugated system consisting of a C=C double bond and a C=O carbonyl group in 4-HNE. The hydroxyl group at carbon four contributes to the reactivity both by polarizing the C=C bond and by facilitating internal cyclisation reactions, such as thioacetal formation [13].

Because of its chemical properties, 4-HNE is an amphiphilic molecule (water soluble while exhibiting strong lipophilic properties). 4-HNE tends to concentrate in biomembranes, where phospholipids, like phosphatidylethanolamine, and proteins, such as transporters, ion channels and receptors, quickly react with it. In addition, since it is a highly electrophilic molecule, it easily reacts with low molecular weight compounds, such as glutathione, and at higher concentration with DNA [12]. Due to its electrophilic nature, 4-HNE can form adducts with cellular protein nucleophiles. Indeed, the reactivity of 4-HNE explains its potential involvement in the modulation of enzymes activity, signal transduction, and gene expression [13].

Adduction to and modification of functional and/or signaling proteins most likely represents one of the main mechanisms by which 4-HNE and also the other α,β-unsaturated aldehydes can influence physiological as well as pathological processes.

Primary reactants for 4-HNE are the amino acids cysteine, histidine, and lysine, which—either free or protein-bound—undergo readily Michael addition reactions to the C=C double bond. Besides this type of reaction, a secondary reaction may occur involving the carbonyl and the hydroxyl groups to form a cyclic hemiacetal derivative. Amino groups

(e.g., Lys) may alternatively react with the carbonyl group of 4-HNE to yield a Schiff base product [14].

Therefore, since proteins play an important role in normal structure and function of the cells, oxidative modifications by increased 4-HNE levels, as in O.S. conditions, may greatly alter their structure. These protein alterations may subsequently lead to loss of normal physiological cell functions and/or may lead to abnormal function of cell and eventually to cell death.

4-HNE adducts contribute to the pool of damaged enzymes, which increases in levels during aging and in several pathological states [15]. Furthermore, impaired protein clearance (i.e., ubiquitin proteosome system dysfunction) and/or the overwhelming production of abnormal proteins play an important role in the pathophysiology of disorders related to O.S., and a lot has been done in the last few decades on their role in neuro-related pathologies [16].

Based on this, 4-HNE represents one of the most useful biomarkers for the occurrence and/or the extent of O.S. [17].

6. Isoprostanes

IsoPs are a unique series of prostaglandin-like compounds generated, via a free radical-catalyzed mechanism, from a number of different PUFAs, including AA, eicosapentaenoic acid (EPA), adrenic acid (AdA), and docosahexaenoic acid (DHA).

Looking at the lipid composition of the tissues of the body [18], AA was found to be localized quite everywhere, whereas PUFAs such as DHA or AdA are mainly localized in nervous tissue and especially in grey and white matters. Thus the clinical relevance of the different classes of IsoPs hinges on the PUFA precursor anatomical distribution.

6.1. F_2-Isoprostanes. The discovery of prostaglandin F_2-like compounds, termed F_2-isoprostanes (F_2-IsoPs), generated by free radical-induced peroxidation of arachidonic acid, was for the first time reported by Morrow et al. [19].

Since F_2-IsoPs, initially formed *in situ* on phospholipids [20], are released into the circulation and because these prostanoids are less reactive than other lipid peroxidation products (i.e., lipoperoxides and aldehydes), they can be detected more easily in plasma. Since the discovery of these molecules, F_2-IsoPs have become the biomarker of choice for assessing endogenous OS, mainly due to their chemical stability and ubiquitousness in tissues and body fluids [21–23]. Elevated levels of plasma or urinary F_2-IsoPs have been reported in several diseases [24–26]. For a correct O.S. damage quantification, Halliwell has suggested to use a combination of blood IsoPs and urinary IsoP metabolites determinations [27]. The 15-F_{2t}-IsoP is the most represented isomer among the F_2-IsoPs and is also referred to as 8-iso-prostaglandin $F_{2\alpha}$ [28].

In addition to F_2-IsoPs with F_2-ring, a variety of IsoPs with different ring structures, E_2-ring and D_2-ring, have been so far identified. Central in the pathway of formation of IsoPs are PGH_2-like endoperoxides. Just as cyclooxygenase-derived PGH_2 are rearranged to PGD_2 and PGE_2, the H_2-IsoP endoperoxides can be reduced to form F_2-ring IsoPs [29] but can also undergo rearrangements to form E_2- and D_2-IsoPs. Biological effects for E_2- and D_2-IsoPs have been described [30]. Subsequent to E_2- and D_2-IsoPs dehydration [29], cyclopentenone IsoPs can be formed [31]; cyclopentenone IsoPs, A_2/J_2-IsoPs, are highly reactive; α,β-unsaturated carbonyl moieties are highly susceptible to Michael addition reactions [32, 33]. In particular, one of the A_2-IsoPs, 15-A_{2t}-IsoP is primarily metabolized by these cells via conjugation to glutathione [34].

6.2. F_4-Neuroprostanes. A series of F_2-IsoP-like molecules named F_4-neuroprostanes (F_4-NeuroPs) originate from the free radical catalyzed peroxidation of DHA, an essential constituent of nervous tissue, highly enriched in neurons, and highly susceptible to oxidation [35]. Quantification of these compounds appears to provide a very sensitive index of oxidative neuronal injury in contrast to the IsoPs, since the amounts of F_4-NeuroPs formed from DHA oxidation exceed the levels of F_2-IsoPs generated from AA by 3.4-fold [36]. Given the well-known role for free radicals in the pathogenesis of a number of neurodegenerative diseases, that is, Alzheimer's disease, Parkinson's disease, Huntington's disease, and amyotrophic lateral sclerosis [20, 29, 37], the quantification of F_4-NeuroPs appears to be a tool to evaluate a brain oxidative injury.

In experimental models of neurodegenerative phenomenon, F_4-NeuroPs appear to be not related to excitotoxicity and epilepsy [38, 39], and a decrease of F_4-NeuroPs levels, subsequent to treatment with antioxidant, was observed [39].

Furthermore, an increase of F_4-NeuroPs has been reported in a neonatal hypoxic-ischemic encephalopathy [40]. The hypoxic-ischemia determines, in association with brain damage, formation of F_4-NeuroPs, as well as F_2-IsoPs. As F_4-NeuroP levels are particularly elevated in ischemic areas, F_4-NeuroPs may represent a specific marker of ischemic damage.

In Alzheimer's or Parkinson's diseases, F_4-NeuroPs, as well as F_2-IsoPs, are markedly increased in brain tissue and cerebrospinal fluid [41]. In particular, the F_4-NeuroP levels were significantly higher as compared to those of F_2-IsoPs, in the brain regions affected by the disease [42, 43]. Increased levels of F_4-NeuroPs have been also reported in the cerebrospinal fluid of patients with subarachnoid hemorrhage from aneurysm. The generation of F_4-NeuroPs in subarachnoid aneurysm hemorrhage and traumatic brain injury [44, 45] appears to be the consequence of a catastrophic central nervous system injury, and it can be considered an useful indicator of the pathological event. Regards to F_4-NeuroPs determination, some researchers have used the chemically synthesized 17-F_{4c}-NeuroP isomer [46], although interference with F_2-dihomo-isoprostanes (F_2-dihomo-IsoPs) cannot be ruled out [44].

6.3. F_2-Dihomo-Isoprostanes. F_2-dihomo-IsoPs are specific markers for free radical-induced AdA peroxidation and have been characterized as potential markers of free radical damage to myelin in human brain [47]. To date, clinical applications for F_2-dihomo-IsoPs are few and studies are reported for white brain matter [47], cerebrospinal fluid [44],

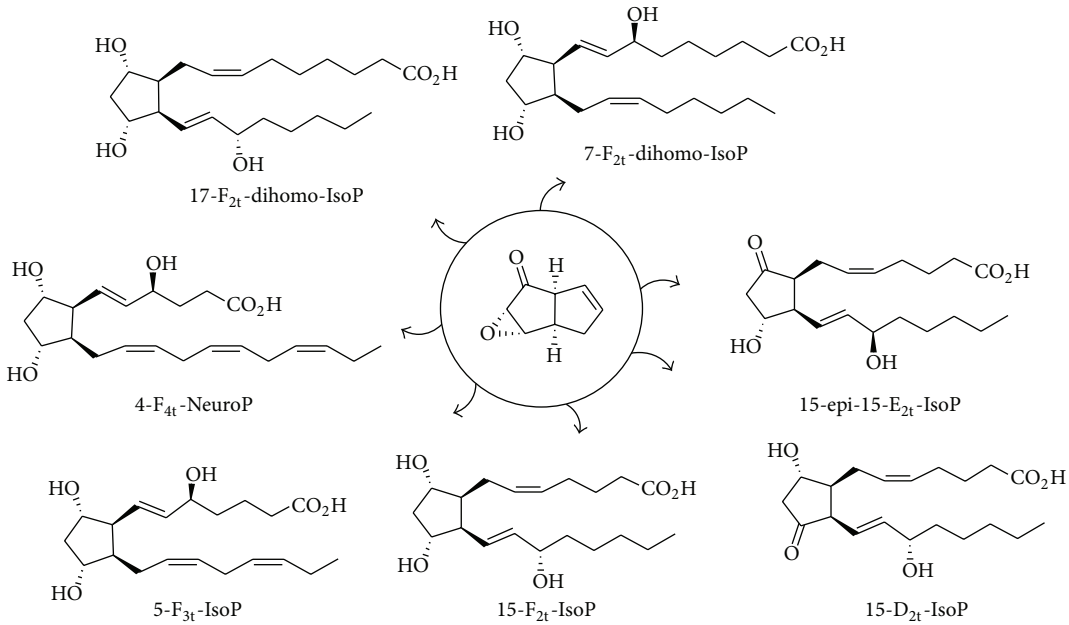

Scheme 1

and plasma [48]. For the first time, our studies have shown the possibility of F_2-dihomo-IsoP evaluation in plasma.

7. IsoPs as Mediators of Disease

15-F_{2t}-IsoP is previously also indicated as 8-epi-PGF2α or 8-iso-PGF2α, as it is one of the most abundantly F_2-IsoP isomer produced *in vivo* and may exhibit biological activity [24].

F_2-IsoPs seem activate receptors analogous or identical to those for the thromboxane A_2 (TxA_2) and induce platelet aggregation [49] and vasoconstriction of renal glomerular arterioles [50, 51]. Via activation of the TxA_2 receptors, IsoPs inhibit angiogenesis [52]. Furthermore, stimulation of DNA synthesis and cell proliferation for F_2-IsoPs on muscle vascular cells [51] and endothelial cells [53] is known, as well as the role of F_2-IsoPs in the pulmonary pathophysiology [54]. In streptozotocin-induced diabetes, F_2-IsoPs appear to mediate an increase of the transforming growth factor-β1 (TGF-β1) [55], while the 5-F_{2t}-IsoPs and 5-epi-5-F_{2t}-IsoPs regulate the [^{3}H]d-aspartate release in isolated bovine retina [56].

The complex F_2-IsoPs bioactivity has been summarized in recent reviews [57–59].

8. The Role of Chemical Synthesis in the Exploration of Lipid Mediators

Oxidative stress is evolved in neurodegeneration of grey matter (Alzheimer's diseases) [60] and white matter (multiple sclerosis or Rett syndrome).

As their isomers F_2-IsoPs are known as the "gold standard" for systemic O.S. [61] and for their biological activities [62, 63], F_4-NeuroPs and F_2-dihomo-IsoPs are potential biomarkers in specific pathologies such as AD or RTT and may as well have biological activities.

In order to demonstrate theses various activities of PUFAs oxygenated metabolites, chemical synthesis is a need and chemists are the link between biochemists and biologists.

Thus, since the discovery of F_2-IsoPs, chemists developed strategies to access to IsoPs [64–66] as well as NeuroPs [67, 68], dihomo-IsoPs [69, 70]. Among them, our laboratory, specialized in total synthesis of lipids metabolites (leukotrienes, isoprostanes, and resolvins), developed during the past twenty years three strategies allowing the access to F-type IsoPs [69, 71, 72] as well as E-type [69, 73, 74], D-type [74], and A-type (Bultel-Poncé et al., unpublished results). Those strategies permitted the syntheses of different series of oxygenated metabolites derived from α-linolenic acid (ALA), AA, DHA, EPA, and AdA (Scheme 1).

With those chemically pure metabolites in hands, biologists and clinicians have shown biomarkers activities [48] as well as biological activities [75, 76] of those oxidative stress-derived metabolites.

9. Rett Syndrome: A Genetic Model of Autism Spectrum Disorder

RTT (OMIM ID: 312750) occurs with a frequency of up to 1/10,000 live female births. Causative mutations in the X-linked methyl-CpG binding protein 2 gene (*MECP2*) are detectable in up to 95% of cases, although a wide genetical and phenotypical heterogeneity is well established [77]. Approximately 80% of RTT clinical cases show the so-called "typical" clinical picture; after an apparently normal development for 6–18 months, RTT girls lose their acquired cognitive, social, and motor skills in a typical 4-stage neurological regression and develop autistic behavior accompanied by stereotypic hand movements [78]. Autistic features are typically transient in RTT.

In addition to typical RTT, it has been recognized that some individuals present with many, but do not necessarily all, of the features of the disorder. New guidelines for the diagnosis of specific "variant" or "atypical" forms of RTT have been developed to identify the preserved speech, early seizure, and the congenital variant [79].

Although the genetic mechanisms of disease have been extraordinary explored in details in RTT, to date the biological mechanisms linking the gene mutation to the phenotypic expression of the disease including its wide heterogeneity are yet to be clarified. Several explanations have been proposed so far, including a key role of *MECP2* in the neuronal maturation [80], maintenance of astroglia, immune dysfunction [81], and neurotransmission pathway abnormality [82]. However, recent discoveries, mainly by our team, concerning the emerging role of alteration of redox homeostasis offer an alternative explanations which is not mutually exclusive with the others previously proposed. Nevertheless, the whole history of RTT is cluttered with several apparently firm points that have been subsequently changed. Interestingly, one of the most firm points to date is that RTT is caused by a single-gene mutation either *MECP2* or other more rarely affected (i.e., *CDKL5* or *FOXG1* genes) [79]. Recently the analysis of the full exome sequencing in two pairs of affected sisters, each with identical *MECP2* gene mutation but discordant phenotype, indicates that several hundreds of gene mutations appear to be associated with the *MECP2* gene mutation and therefore are to be considered previously unknown disease modifier [83].

Currently, no effective pharmacological therapies for RTT exist that can either halt progression, or reverse the neurological and cognitive abnormalities.

10. Lipid Peroxidation and Rett Syndrome

Mounting evidence indicates an emerging role for O.S. in genetically determined diseases [84]. Furthermore, the role of the redox alteration in the pathogenesis of the autism spectrum disorder is under debate [85, 86].

In 2001 indirect evidence for excessive lipid peroxidation, leading to increased plasma malondialdehyde levels, has been reported in RTT patients [87]. However, after that isolated report and before our subsequent series of specific studies in the field, the lipid oxidative damage in RTT had not been further investigated. Our studies were focused on the identification of different classes of IsoPs increased in RTT, thus allowing an inference on the individual oxidized fatty acids precursors relevant to the disease. On the other hand, our reports of increased 4-HNE PAs levels in RTT patients while further supporting the evidence of a lipid damage with formation of the aldehyde 4-HNE also detect the presence of a coexisting protein damage due to the formation of the adducts.

Therefore, our findings in RTT, a rare cause of genetically determined autism spectrum disorder, indicate that this pervasive development disorder can be considered a unique human model for chronic O.S. and could be considered a valuable testing ground for the link between lipid peroxidation byproducts and the mediation of disease processes.

10.1. Isoprostanes and Neuroprostanes in RTT. Our findings [48, 88–90] indicate that typical RTT is characterized by markedly increased levels of IsoPs deriving from the nonenzymatic oxidation of AA, DHA, and AdA at every clinical stage of the disease. IsoPs and NeuroPs levels appear to be closely interrelated to the RTT clinical presentation, suggesting that these lipid oxidation products could mediate the pathogenetic mechanisms underlying the syndrome.

Extremely high (i.e., two orders of magnitude) plasma levels of F_2-dihomo-IsoPs are detectable in RTT girls in stage I of the disease. AdA, whatever the actual origin (brain white matter, adrenal gland, or kidney), is the PUFA that goes through the greatest degree of oxidation during the earliest stage of the typical form of the disease. An insult to AdA and the clinical onset of neuroregression occur at the same time [48]. Thus, during the first two years of the natural evolution of the disease, the peroxidation of AdA, a critical component of myelin [47] in the primate brain, is involved.

Oxidation of the AA appears to be another essential component in the pathogenesis of the first two stages of typical RTT, as can be deduced from the significantly high F_2-IsoPs in the early stages as compared with the late natural progression of classic RTT. Nevertheless, F_2-IsoPs increase not with the same marked raise of the F_2-dihomo-IsoPs. Thus, F_2-dihomo-IsoPs are the prominent lipid peroxidation end-product detectable at this stage of the disease. In RTT girls, plasma F_2-IsoPs are always above the physiological range, and thus, considering the half-life of these prostanoids, lipid peroxidation is continuously carried out in the syndrome. Due to the systemic distribution of AA, free plasma F_2-IsoPs can be considered an index of generalized lipid peroxidation, while in RTT, a specific site of peroxidation events has been identified in the erythrocyte membrane. In fact, esterified F_2-IsoPs are increased in RTT erythrocyte membrane and their levels are correlated to altered red blood cells shape [91].

Patients with typical RTT had significantly higher F_2-IsoPs than those with atypical phenotype and are correlated to RTT clinical severity, as well as F_4-NeuroPs. In particular, F_4-NeuroPs are related to clinical severity markers, including early regression, severe head growth deceleration, major motor impairment, hand use loss, and seizures. In our experience, *MECP2* gene mutations located in critical regions that carry higher phenotype severity usually show a more severely shifted O.S. imbalance [89, 90]. Moreover, the demonstrated link between F_4-NeuroPs and *MECP2* genotype-phenotype correlation suggests that the degree of MeCP2 protein dysfunction is directly proportional to the O.S.-mediated neuronal damage, explaining ~90% of the expressed phenotype variability [90]. Also plasma F_2-IsoPs concentrations are significantly related to *MECP2* genotype; anyway, the strength of the relationship between plasma F_2-IsoPs and MeCP2 phenotype appears to be far weaker than that between plasma F_4-NeuroPs and MeCP2 phenotype [89, 90]. As F_4-NeuroPs plasma levels mirror neurological severity, these molecules may provide evidence on neuronal damage, also considering the specific distribution of DHA in membrane neurons.

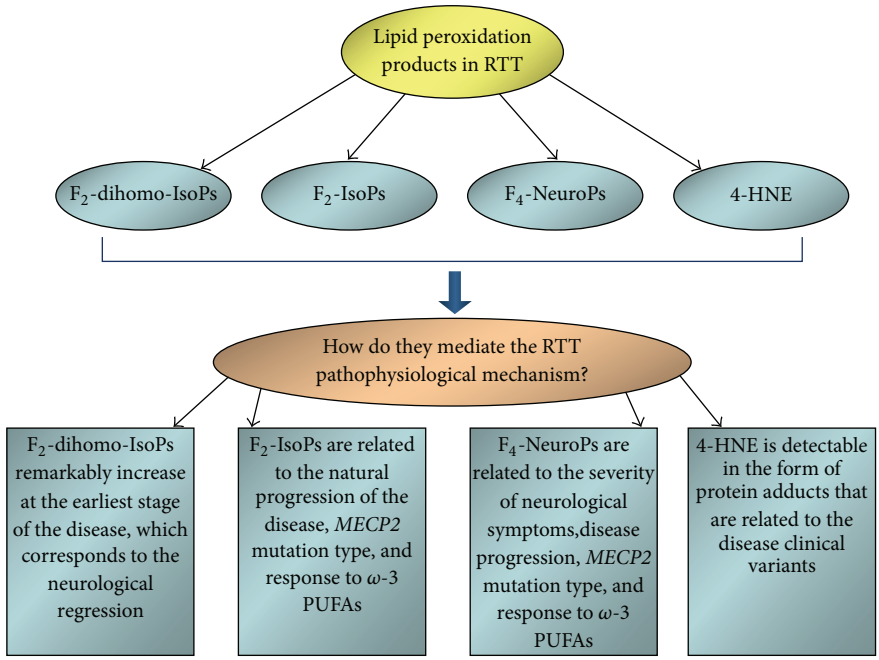

Figure 1: Different classes of isoprostanes (F_2-dihomo-IsoPs, F_2-IsoPs, and F_4-NeuroPs), deriving from polyunsaturated fatty acids precursors (adrenic, arachidonic, and docosahexaenoic acids, resp.), and the 4-hydroxy-2-nonenal protein adducts are strictly related to the clinical manifestations and the natural history of Rett syndrome. The lipid peroxidation events and the disease pathogenic mechanisms are closely interrelated, as demonstrated by the dietary supplementation with ω-3 PUFAs. RTT: Rett syndrome; F_2-dihomo-IsoPs: F_2-dihomo-isoprostanes; F_2-IsoPs: F_2-isoprostanes; F_4-NeuroPs: F_4-neuroprostanes; 4-HNE: 4-hydroxy-2-nonenal; and PUFAs: polyunsaturated fatty acids.

10.2. 4-HNE and RTT. In our recent work, we have shown that the levels of 4-HNE PAs change during the clinical progression of typical RTT [92]. Plasma 4-HNE PAs increase between stage I and stage II and to less extent in the following stages (i.e., III and IV).

Impairment of the GSH system and other detoxification enzymes involved in aldehyde metabolism or defect/dysfunction in the ubiquitin proteasome system, reported in the autism spectrum disorder [93–95], could be involved in the accumulation, in the early stages of RTT, of several 4-HNE plasma protein adducts. This, as a consequence, could play a role in the severe clinical features observed in the later stages of the disease.

As for the IsoPs, a relationship between 4-HNE PAs and phenotypical RTT presentation has been reported. In particular, with reference to the atypical RTT clinical presentation, *CDKL5*-related RTT patients have a significant increase in 4-HNE PAs levels, and on the contrary, *FOXG1*-related RTT patients are not different from the controls [92]. Although the possible cause for the observed difference in *FOXG1*-related RTT is not clear, the 4-HNE PAs, as well as the IsoPs, appear to be directly involved in the RTT pathogenesis. To date, it is not clear how the gene mutations can induce and increase O.S. in RTT patients. It is possible to speculate that it could be an indirect mechanism that might involve mitochondria respiration, modifying therefore the redox state of the cells.

It should be pointed out that the presence of 4-HNE PAs in plasma of RTT patients suggests two events. First, it is indicative of a generalized lipid peroxidation, indicating the occurrence of PUFAs oxidation in various organs and/or tissues. Second, by covalent modification of proteins, 4-HNE is able to cause long-lasting biological consequences. Therefore, plasma proteins can be considered a target of increased O.S. status in RTT. Hence, it is possible to speculate that 4-HNE PAs can contribute to the pathophysiology of RTT, both in the development and in the progression and complications of the disease. We can suggest that 4HNE PAs represent a potential biomarker of RTT as well as disease severity.

In future, to better understand the clinical consequences that the modified plasma proteins have on RTT patients, further studies are needed. It could be of extreme importance to be able to identifying the target proteins modified by 4-HNE in the plasma, as recently shown for mild cognitive impairment and Alzheimer's disease [96, 97].

A close relationship between levels of circulating lipid peroxidation markers in RTT patients and presence of the symptom is not a causative proofs but strongly supports the concept that lipid peroxidation plays a previously unrecognized key role in the pathogenesis of RTT due to the gene mutation. The increase of knowledge on nature of 4-HNE modified proteins in RTT, might lead to better prevention, diagnosis and treatments of the associated physiological processes altered in patients.

Finally, the involvement of lipid peroxidation in RTT was also confirmed in our recent study, where the morphology of erythrocytes in typical RTT patients has been evaluated [91]. Emerging evidence indicates that O.S. imbalance and hypoxemia can lead to erythrocyte shape abnormalities in chronic pulmonary disease [98, 99], and now it has been well proved

that chronic hypoxia, impaired pulmonary gas exchange, and increased O.S. are all present in typical RTT [88]. In fact, our data show the presence of erythrocytes altered shape (mainly leptocytes) and membrane oxidative damage (i.e., 4-HNE PAs) in patients with clinical diagnosis of typical RTT [91]. Consequently, monitoring of erythrocytes morphology can be an important new diagnostic and prognostic tool in this particular form of autism spectrum disorder, in which the lung seems to represent an unexpectedly key organ for the disease pathogenesis.

10.3. Lipid Peroxidation and ω-3 PUFAs Supplementation in RTT. Lipid peroxidation appears to be a peculiar characteristic of RTT, and the relationships between the described lipid peroxidation products and the clinical disease features are summarized in Figure 1.

A better comprehension of the lipid peroxidation involvement in the pathogenetic mechanisms of the disease derives from studies carried out with ω-3 PUFAs supplementation. Interestingly, the supplemented molecules are actually just the same category of molecules that undergo radical damage. Exogenous administration of ω-3 PUFAs, in disease stages I-IV, has been shown to moderately reduce clinical severity and significantly reduce the levels of IsoPs and 4-HNE PAs in RTT patients [89–91, 100]. Following ω-3 PUFAs supplementation, we might have expected an enhanced formation of the lipid oxidation products in plasma. Actually, the assumed fatty acids are not oxidized and the endogenous production is reduced. These results lead us to think that in RTT the lipid-oxidative damage is nonspecific, all fatty acids are not oxidatively damaged, but the oxidative insult regards specific biological targets.

As a consequence, these data, while confirming the involvement of lipid products in the intimate pathogenic mechanisms of the disease, indicate that the fatty acid oxidation is related to the clinical severity of the disease and is a reversible process.

11. Conclusion

Lipid peroxidation end-products appear to be associated with the modulation of RTT disease severity, thus suggesting their likely role as mediators. The identification of the involved classes of molecules (including metabolites) in the disease, the evaluation of their relationship with the disease natural history, and the chance to determine the effects of treatments (i.e., exogenous PUFAs supplementation) and of gene manipulation (i.e., reactivation of *Mecp2* null mice) offer a unique setting for physicians, biologists, and chemists to explore the borders of the lipid mediators concept.

Authors' Contribution

Cinzia Signorini and Claudio De Felice contributed equally to the paper.

References

[1] B. Halliwell, "Oxidative stress and cancer: have we moved forward?" *Biochemical Journal*, vol. 401, no. 1, pp. 1–11, 2007.

[2] L. R. Ferguson, "Chronic inflammation and mutagenesis," *Mutation Research*, vol. 690, no. 1-2, pp. 3–11, 2010.

[3] B. Halliwell, "Free radicals and antioxidants—quo vadis?" *Trends in Pharmacological Sciences*, vol. 32, no. 3, pp. 125–130, 2011.

[4] B. Halliwell, "Oxidative stress and neurodegeneration: where are we now?" *Journal of Neurochemistry*, vol. 97, no. 6, pp. 1634–1658, 2006.

[5] D. Praticò, "The neurobiology of isoprostanes and Alzheimer's disease," *Biochimica et Biophysica Acta*, vol. 1801, no. 8, pp. 930–933, 2010.

[6] C. D. Aluise, R. A. S. Robinson, J. Cai, W. M. Pierce, W. R. Markesbery, and D. A. Butterfield, "Redox proteomics analysis of brains from subjects with amnestic mild cognitive impairment compared to brains from subjects with preclinical alzheimer's disease: insights into memory loss in MCI," *Journal of Alzheimer's Disease*, vol. 23, no. 2, pp. 257–269, 2011.

[7] B. Halliwell, *Free Radicals in Biology and Medicine*, Oxford University Press, Oxford, UK, 4th edition, 2007.

[8] J. C. Brazil, N. A. Louis, and C. A. Parkos, "The role of polymorphonuclear leukocyte trafficking in the perpetuation of inflammation during inflammatory Bowel disease," *Inflammatory Bowel Diseases*, vol. 19, no. 7, pp. 1556–1565, 2013.

[9] B. Halliwell, "Free radicals and antioxidants: updating a personal view," *Nutrition Reviews*, vol. 70, no. 5, pp. 257–265, 2012.

[10] G. L. Bannenberg, "Therapeutic applicability of anti-inflammatory and proresolving polyunsaturated fatty acid-derived lipid mediators," *The Scientific World Journal*, vol. 10, pp. 676–712, 2010.

[11] C. N. Serhan, "Novel lipid mediators and resolution mechanisms in acute inflammation: to resolve or not?" *American Journal of Pathology*, vol. 177, no. 4, pp. 1576–1591, 2010.

[12] H. Esterbauer, R. J. Schaur, and H. Zollner, "Chemistry and Biochemistry of 4-hydroxynonenal, malonaldehyde and related aldehydes," *Free Radical Biology and Medicine*, vol. 11, no. 1, pp. 81–128, 1991.

[13] G. Poli, R. J. Schaur, W. G. Siems, and G. Leonarduzzi, "4-Hydroxynonenal: a membrane lipid oxidation product of medicinal interest," *Medicinal Research Reviews*, vol. 28, no. 4, pp. 569–631, 2008.

[14] D. R. Petersen and J. A. Doorn, "Reactions of 4-hydroxynonenal with proteins and cellular targets," *Free Radical Biology and Medicine*, vol. 37, no. 7, pp. 937–945, 2004.

[15] K. Uchida, "4-Hydroxy-2-nonenal: a product and mediator of oxidative stress," *Progress in Lipid Research*, vol. 42, no. 4, pp. 318–343, 2003.

[16] T. Grune and K. J. A. Davies, "The proteasomal system and HNE-modified proteins," *Molecular Aspects of Medicine*, vol. 24, no. 4-5, pp. 195–204, 2003.

[17] E. E. Dubinina and V. A. Dadali, "Role of 4-hydroxy-trans-2-nonenal in cell functions," *Biochemistry*, vol. 75, no. 9, pp. 1069–1087, 2010.

[18] P. S. Sastry, "Lipids of nervous tissue: composition and metabolism," *Progress in Lipid Research*, vol. 24, no. 2, pp. 69–176, 1985.

[19] J. D. Morrow, K. E. Hill, R. F. Burk, T. M. Nammour, K. F. Badr, and L. J. Roberts II, "A series of prostaglandin F2-like compounds are produced *in vivo* in humans by a non-cyclooxygenase, free radical-catalyzed mechanism," *Proceedings of the National Academy of Sciences of the United States of America*, vol. 87, no. 23, pp. 9383–9387, 1990.

[20] J. D. Morrow, J. A. Awad, H. J. Boss, I. A. Blair, and L. J. Roberts II, "Non-cyclooxygenase-derived prostanoids (F2-isoprostanes) are formed in situ on phospholipids," *Proceedings of the National Academy of Sciences of the United States of America*, vol. 89, no. 22, pp. 10721–10725, 1992.

[21] J. D. Morrow, T. M. Harris, and L. J. Roberts II, "Noncyclooxygenase oxidative formation of a series of novel prostaglandins: analytical ramifications for measurement of eicosanoids," *Analytical Biochemistry*, vol. 184, no. 1, pp. 1–10, 1990.

[22] G. L. Milne, E. S. Musiek, and J. D. Morrow, "F2-isoprostanes as markers of oxidative stress in vivo: an overview," *Biomarkers*, vol. 10, supplement 1, pp. 10–23, 2005.

[23] M. B. Kadiiska, B. C. Gladen, D. D. Baird et al., "Biomarkers of oxidative stress study II. Are oxidation products of lipids, proteins, and DNA markers of CCl_4 poisoning?" *Free Radical Biology and Medicine*, vol. 38, no. 6, pp. 698–710, 2005.

[24] P. Montuschi, P. J. Barnes, and L. J. Roberts II, "Isoprostanes: markers and mediators of oxidative stress," *FASEB Journal*, vol. 18, no. 15, pp. 1791–1800, 2004.

[25] S. Basu, "Fatty acid oxidation and isoprostanes: oxidative strain and oxidative stress," *Prostaglandins Leukotrienes and Essential Fatty Acids*, vol. 82, no. 4–6, pp. 219–225, 2010.

[26] S. Basu, "F2-isoprostanes in human health and diseases: from molecular mechanisms to clinical implications," *Antioxidants and Redox Signaling*, vol. 10, no. 8, pp. 1405–1434, 2008.

[27] B. Halliwell and C. Y. J. Lee, "Using isoprostanes as biomarkers of oxidative stress: some rarely considered issues," *Antioxidants and Redox Signaling*, vol. 13, no. 2, pp. 145–156, 2010.

[28] J. D. Morrow, W. E. Zackert, J. P. Yang et al., "Quantification of the major urinary metabolite of 15-F(2T)-isoprostane (8-iso-PGF(2α)) by a stable isotope dilution mass spectrometric assay," *Analytical Biochemistry*, vol. 269, no. 2, pp. 326–331, 1999.

[29] L. J. Roberts II and J. D. Morrow, "Products of the isoprostane pathway: unique bioactive compounds and markers of lipid peroxidation," *Cellular and Molecular Life Sciences*, vol. 59, no. 5, pp. 808–820, 2002.

[30] J. D. Morrow, T. A. Minton, C. R. Mukundan et al., "Free radical-induced generation of isoprostanes *in vivo*. Evidence for the formation of D-ring and E-ring isoprostanes," *Journal of Biological Chemistry*, vol. 269, no. 6, pp. 4317–4326, 1994.

[31] Y. Chen, J. D. Morrow, and L. J. Roberts II, "Formation of reactive cyclopentenone compounds *in vivo* as products of the isoprostane pathway," *Journal of Biological Chemistry*, vol. 274, no. 16, pp. 10863–10868, 1999.

[32] E. Boyland and L. F. Chasseaud, "Enzymes catalysing conjugations of glutathione with alpha-beta-unsaturated carbonyl compounds," *Biochemical Journal*, vol. 109, no. 4, pp. 651–661, 1968.

[33] J. Atsmon, B. J. Sweetman, S. W. Baertschi, T. M. Harris, and L. J. Roberts II, "Formation of thiol conjugates of 9-deoxy-Δ^9,Δ^{12}(E)-prostaglandin D_2 and Δ^{12}(E)-prostaglandin D_2," *Biochemistry*, vol. 29, no. 15, pp. 3760–3765, 1990.

[34] G. L. Milne, G. Zanoni, A. Porta et al., "The Cyclopentenone Product of Lipid Peroxidation, 15-A 2t-Isoprostane, Is Efficiently Metabolized by HepG2 Cells via Conjugation with Glutathione," *Chemical Research in Toxicology*, vol. 17, no. 1, pp. 17–25, 2004.

[35] J. Nourooz-Zadeh, E. H. C. Liu, B. Yhlen, E. E. Änggård, and B. Halliwell, "F_4-isoprostanes as specific marker of docosahexaenoic acid peroxidation in Alzheimer's disease," *Journal of Neurochemistry*, vol. 72, no. 2, pp. 734–740, 1999.

[36] L. J. Roberts II, T. J. Montine, W. R. Markesbery et al., "Formation of isoprostane-like compounds (neuroprostanes) *in vivo* from docosahexaenoic acid," *Journal of Biological Chemistry*, vol. 273, no. 22, pp. 13605–13612, 1998.

[37] L. J. Roberts II and J. D. Morrow, "Measurement of F2-isoprostanes as an index of oxidative stress *in vivo*," *Free Radical Biology and Medicine*, vol. 28, no. 4, pp. 505–513, 2000.

[38] S. Zaja-Milatovic, R. C. Gupta, M. Aschner, T. J. Montine, and D. Milatovic, "Pharmacologic suppression of oxidative damage and dendritic degeneration following kainic acid-induced excitotoxicity in mouse cerebrum," *NeuroToxicology*, vol. 29, no. 4, pp. 621–627, 2008.

[39] S. Zaja-Milatovic, R. C. Gupta, M. Aschner, and D. Milatovic, "Protection of DFP-induced oxidative damage and neurodegeneration by antioxidants and NMDA receptor antagonist," *Toxicology and Applied Pharmacology*, vol. 240, no. 2, pp. 124–131, 2009.

[40] C. Signorini, L. Ciccoli, S. Leoncini et al., "Free iron, total F2-isoprostanes and total F_4- neuroprostanes in a model of neonatal hypoxic-ischemic encephalopathy: neuroprotective effect of melatonin," *Journal of Pineal Research*, vol. 46, no. 2, pp. 148–154, 2009.

[41] T. J. Montine, J. F. Quinn, D. Milatovic et al., "Peripheral F2-isoprostanes and F_4-neuroprostanes are not increased in Alzheimer's disease," *Annals of Neurology*, vol. 52, no. 2, pp. 175–179, 2002.

[42] K. S. Montine, J. F. Quinn, J. Zhang et al., "Isoprostanes and related products of lipid peroxidation in neurodegenerative diseases," *Chemistry and Physics of Lipids*, vol. 128, no. 1-2, pp. 117–124, 2004.

[43] J. Nourooz-Zadeh, E. H. C. Liu, B. Yhlen, E. E. Änggård, and B. Halliwell, "F_4-isoprostanes as specific marker of docosahexaenoic acid peroxidation in Alzheimer's disease," *Journal of Neurochemistry*, vol. 72, no. 2, pp. 734–740, 1999.

[44] Y.-P. Hsieh, C.-L. Lin, A.-L. Shiue et al., "Correlation of F_4-neuroprostanes levels in cerebrospinal fluid with outcome of aneurysmal subarachnoid hemorrhage in humans," *Free Radical Biology and Medicine*, vol. 47, no. 6, pp. 814–824, 2009.

[45] T. B. Corcoran, E. Mas, A. E. Barden et al., "Are isofurans and neuroprostanes increased after subarachnoid hemorrhage and traumatic brain injury?" *Antioxidants and Redox Signaling*, vol. 15, no. 10, pp. 2663–2667, 2011.

[46] L. G. Quan and J. K. Cha, "Preparation of isoprostanes and neuroprostanes," *Journal of the American Chemical Society*, vol. 124, no. 42, pp. 12424–12425, 2002.

[47] M. Van Rollins, R. L. Woltjer, H. Yin, J. D. Morrow, and T. J. Montine, "F2-Dihomo-isoprostanes arise from free radical attack on adrenic acid," *Journal of Lipid Research*, vol. 49, no. 5, pp. 995–1005, 2008.

[48] C. De Felice, C. Signorini, T. Durand et al., "F2-dihomo-isoprostanes as potential early biomarkers of lipid oxidative damage in Rett syndrome," *Journal of Lipid Research*, vol. 52, no. 12, pp. 2287–2297, 2011.

[49] F. T. Khasawneh, J.-S. Huang, F. Mir, S. Srinivasan, C. Tiruppathi, and G. C. Le Breton, "Characterization of isoprostane signaling: evidence for a unique coordination profile of 8-iso-PGF2α with the thromboxane A_2 receptor, and activation of a separate cAMP-dependent inhibitory pathway in human platelets," *Biochemical Pharmacology*, vol. 75, no. 12, pp. 2301–2315, 2008.

[50] K. Takahashi, T. M. Nammour, M. Fukunaga et al., "Glomerular actions of a free radical-generated novel prostaglandin, 8-epi-

prostaglandin F(2α), in the rat. Evidence for interaction with thromboxane A_2 receptors," *Journal of Clinical Investigation*, vol. 90, no. 1, pp. 136–141, 1992.

[51] M. Fukunaga, N. Makita, L. J. Roberts II, J. D. Morrow, K. Takahashi, and K. F. Badr, "Evidence for the existence of F2-isoprostane receptors on rat vascular smooth muscle cells," *American Journal of Physiology*, vol. 264, no. 6, pp. C1619–C1624, 1993.

[52] R. A. Benndorf, E. Schwedhelm, A. Gnann et al., "Isoprostanes inhibit vascular endothelial growth factor-induced endothelial cell migration, tube formation, and cardiac vessel sprouting in vitro, As well as angiogenesis *in vivo* via activation of the thromboxane A_2 receptor: a potential link between oxidative stress and impaired angiogenesis," *Circulation Research*, vol. 103, no. 9, pp. 1037–1046, 2008.

[53] T. Yura, M. Fukunaga, R. Khan, G. N. Nassar, K. F. Badr, and A. Montero, "Free-radical-generated F2-isoprostane stimulates cell proliferation and endothelin-1 expression on endothelial cells," *Kidney International*, vol. 56, no. 2, pp. 471–478, 1999.

[54] L. J. Janssen, "Isoprostanes: an overview and putative roles in pulmonary pathophysiology," *American Journal of Physiology*, vol. 280, no. 6, pp. L1067–L1082, 2001.

[55] A. Montero, K. A. Munger, R. Z. Khan et al., "F2-isoprostanes mediate high glucose-induced TGF-β synthesis and glomerular proteinuria in experimental type I diabetes," *Kidney International*, vol. 58, no. 5, pp. 1963–1972, 2000.

[56] J. Jamil, A. Wright, N. Harrison et al., "Regulation of [^{3}H]D-aspartate release by the 5-F2t-isoprostane and its 5-epimer in isolated bovine retina," *Neurochemical Research*, vol. 37, no. 3, pp. 574–582, 2012.

[57] S. Basu, "Bioactive eicosanoids: role of prostaglandin F2α and F2-isoprostanes in inflammation and oxidative stress related pathology," *Molecules and Cells*, vol. 30, no. 5, pp. 383–391, 2010.

[58] H. J. Ting and F. T. Khasawneh, "Platelet function and Isoprostane biology. Should Isoprostanes be the newest member of the Orphan-ligand family?" *Journal of Biomedical Science*, vol. 17, no. 1, article 24, 2010.

[59] G. L. Milne, H. Yin, K. D. Hardy, S. S. Davies, and L. J. Roberts, "Isoprostane generation and function," *Chemical Reviews*, vol. 111, no. 10, pp. 5973–5996, 2011.

[60] K. P. Kepp, "Bioinorganic chemistry of Alzheimer's disease," *Chemical Reviews*, vol. 112, pp. 5193–5239, 2012.

[61] M. B. Kadiiska, B. C. Gladen, D. D. Baird et al., "Biomarkers of oxidative stress study III. Effects of the nonsteroidal anti-inflammatory agents indomethacin and meclofenamic acid on measurements of oxidative products of lipids in CCl_4 poisoning," *Free Radical Biology and Medicine*, vol. 38, no. 6, pp. 711–718, 2005.

[62] U. Jahn, J.-M. Galano, and T. Durand, "Beyond prostaglandins—chemistry and biology of cyclic oxygenated metabolites formed by free-radical pathways from polyunsaturated fatty acids," *Angewandte Chemie*, vol. 47, no. 32, pp. 5894–5955, 2008.

[63] J. D. Brooks, E. S. Musiek, T. R. Koestner et al., "The fatty acid oxidation product 15-A3t-Isoprostane is a potent inhibitor of NFκB transcription and macrophage transformation," *Journal of Neurochemistry*, vol. 119, no. 3, pp. 604–616, 2011.

[64] G. Zanoni, A. Porta, and G. Vidari, "First total synthesis of A_2 isoprostane," *Journal of Organic Chemistry*, vol. 67, no. 12, pp. 4346–4351, 2002.

[65] S. W. Hwang, M. Adiyaman, S. Khanapure, L. Schio, and J. Rockach, "Total synthesis of 8-epi-PGF(2α). A novel strategy for the synthesis of isoprostanes," *Journal of the American Chemical Society*, vol. 116, no. 23, pp. 10829–10830, 1994.

[66] T. O. Schrader and M. L. Snapper, "Stereodivergent synthesis of all 15-F2 isoprostanes," *Journal of the American Chemical Society*, vol. 124, no. 37, pp. 10998–11000, 2002.

[67] D. F. Taber, P. G. Reddy, and K. O. Arneson, "A potential route to neuroprostanes and isoprostanes: preparation of the four enantiomerically pure diastereomers of 13-F_{4t}-NeuroP," *Journal of Organic Chemistry*, vol. 73, no. 9, pp. 3467–3474, 2008.

[68] L. G. Quan and J. K. Cha, "Preparation of isoprostanes and neuroprostanes," *Journal of the American Chemical Society*, vol. 124, no. 42, pp. 12424–12425, 2002.

[69] C. Oger, Y. Brinkmann, S. Bouazzaoui, T. Durand, and J.-M. Galano, "Stereocontrolled access to isoprostanes via a bicyclo [3.3.0]octene framework," *Organic Letters*, vol. 10, no. 21, pp. 5087–5090, 2008.

[70] C. Oger, V. Bultel-Poncé, A. Guy, T. Durand, and J.-M. Galano, "Total synthesis of isoprostanes derived from adrenic acid and EPA," *European Journal of Organic Chemistry*, no. 13, pp. 2621–2634, 2012.

[71] B. Rondot, T. Durand, J.-P. Vidal, J.-P. Girard, and J.-C. Rossi, "Synthesis and determination of cis or trans isoprostane precursors by a 1H NMR NOE study," *Journal of the Chemical Society, Perkin Transactions 2*, no. 8, pp. 1589–1594, 1995.

[72] S. El Fangour, A. Guy, J.-P. Vidal, J.-C. Rossi, and T. Durand, "A flexible synthesis of the phytoprostanes B_1 type I and II," *Journal of Organic Chemistry*, vol. 70, no. 3, pp. 989–997, 2005.

[73] E. Pinot, A. Guy, A. Fournial, L. Balas, J.-C. Rossi, and T. Durand, "Total synthesis of the four enantiomerically pure diasteroisomers of the phytoprostanes E1type II and of the 15-E2t-isoprostanes," *Journal of Organic Chemistry*, vol. 73, no. 8, pp. 3063–3069, 2008.

[74] Y. Brinkmann, C. Oger, A. Guy, T. Durand, and J.-M. Galano, "Total synthesis of 15-D_{2t}- and 15-*epi*-15-E_{2t}-isoprostanes," *Journal of Organic Chemistry*, vol. 75, no. 7, pp. 2411–2414, 2010.

[75] J.-Y. Le Guennec, J.-M. Galano, C. Oger et al., "Methods and pharmaceutical composition for the treatment and prevention of cardiac arrhytmias," European Patent, EP12306519. 3, 2012.

[76] J.-M. Galano, E. Mas, A. Barden et al., "Isoprostanes and neuroprostanes: Total synthesis, biological activity and biomarkers of oxidative stress in humans," *Prostaglandins & Other Lipid Mediators*, 2013.

[77] R. E. Amir, I. B. Van Den Veyver, M. Wan, C. Q. Tran, U. Francke, and H. Y. Zoghbi, "Rett syndrome is caused by mutations in X-linked MECP2, encoding methyl- CpG-binding protein 2," *Nature Genetics*, vol. 23, no. 2, pp. 185–188, 1999.

[78] B. Hagberg, J. Aicardi, K. Dias, and O. Ramos, "A progressive syndrome of autism, dementia, ataxia, and loss of purposeful hand use in girls: rett's syndrome. Report of 35 cases," *Annals of Neurology*, vol. 14, no. 4, pp. 471–479, 1983.

[79] J. L. Neul, W. E. Kaufmann, D. G. Glaze et al., "Rett syndrome: revised diagnostic criteria and nomenclature," *Annals of Neurology*, vol. 68, no. 6, pp. 944–950, 2010.

[80] J. Guy, H. Cheval, J. Selfridge, and A. Bird, "The role of MeCP2 in the brain," *Annual Review of Cell and Developmental Biology*, vol. 27, pp. 631–652, 2011.

[81] N. C. Derecki, J. C. Cronk, Z. Lu et al., "Wild-type microglia arrest pathology in a mouse model of Rett syndrome," *Nature*, vol. 484, no. 7392, pp. 105–109, 2012.

[82] H.-T. Chao, H. Chen, R. C. Samaco et al., "Dysfunction in GABA signalling mediates autism-like stereotypies and Rett

syndrome phenotypes," *Nature*, vol. 468, no. 7321, pp. 263–269, 2010.

[83] E. Grillo, C. Lo Rizzo, L. Bianciardi et al., "Revealing the complexity of a monogenic disease: rett syndrome exome sequencing," *PLoS One*, vol. 8, no. 2, Article ID e56599, 2013.

[84] G. Pagano and G. Castello, "Oxidative stress and mitochondrial dysfunction in down syndrome," *Advances in Experimental Medicine and Biology*, vol. 724, pp. 291–299, 2012.

[85] A. Chauhan and V. Chauhan, "Oxidative stress in autism," *Pathophysiology*, vol. 13, no. 3, pp. 171–181, 2006.

[86] N. A. Meguid, A. A. Dardir, E. R. Abdel-Raouf, and A. Hashish, "Evaluation of oxidative stress in autism: defective antioxidant enzymes and increased lipid peroxidation," *Biological Trace Element Research*, vol. 143, no. 1, pp. 58–65, 2011.

[87] C. Sierra, M. A. Vilaseca, N. Brandi et al., "Oxidative stress in Rett syndrome," *Brain and Development*, vol. 23, no. 1, pp. S236–S239, 2001.

[88] C. De Felice, L. Ciccoli, S. Leoncini et al., "Systemic oxidative stress in classic Rett syndrome," *Free Radical Biology and Medicine*, vol. 47, no. 4, pp. 440–448, 2009.

[89] S. Leoncini, C. de Felice, C. Signorini et al., "Oxidative stress in Rett syndrome: natural history, genotype, and variants," *Redox Report*, vol. 16, no. 4, pp. 145–153, 2011.

[90] C. Signorini, C. De Felice, S. Leoncini et al., "F_4-neuroprostanes mediate neurological severity in Rett syndrome," *Clinica Chimica Acta*, vol. 412, no. 15-16, pp. 1399–1406, 2011.

[91] L. Ciccoli, C. De Felice, E. Paccagnini et al., "Morphological changes and oxidative damage in Rett Syndrome erythrocytes," *Biochimica et Biophysica Acta*, vol. 1820, no. 4, pp. 511–520, 2012.

[92] A. Pecorelli, L. Ciccoli, C. Signorini et al., "Increased levels of 4HNE-protein plasma adducts in Rett syndrome," *Clinical Biochemistry*, vol. 44, no. 5-6, pp. 368–371, 2011.

[93] Y. A. Al-Yafee, L. Y. Al- Ayadhi, S. H. Haq, and A. K. El-Ansary, "Novel metabolic biomarkers related to sulfur-dependent detoxification pathways in autistic patients of Saudi Arabia," *BMC Neurology*, vol. 11, article 139, 2011.

[94] K. Bowers, Q. Li, J. Bressler, D. Avramopoulos, C. Newschaffer, and M. D. Fallin, "Glutathione pathway gene variation and risk of autism spectrum disorders," *Journal of Neurodevelopmental Disorders*, vol. 3, no. 2, pp. 132–143, 2011.

[95] N. L. Lehman, "The ubiquitin proteasome system in neuropathology," *Acta Neuropathologica*, vol. 118, no. 3, pp. 329–347, 2009.

[96] T. Reed, M. Perluigi, R. Sultana et al., "Redox proteomic identification of 4-Hydroxy-2-nonenal-modified brain proteins in amnestic mild cognitive impairment: insight into the role of lipid peroxidation in the progression and pathogenesis of Alzheimer's disease," *Neurobiology of Disease*, vol. 30, no. 1, pp. 107–120, 2008.

[97] M. Perluigi, R. Sultana, G. Cenini et al., "Redox proteomics identification of 4-hydroxynonenalmodified brain proteins in Alzheimer's disease: role of lipid peroxidation in Alzheimer's disease pathogenesis," *Proteomics*, vol. 3, no. 6, pp. 682–693, 2009.

[98] G. Lucantoni, D. Pietraforte, P. Matarrese et al., "The red blood cell as a biosensor for monitoring oxidative imbalance in chronic obstructive pulmonary disease: an ex vivo and in vitro study," *Antioxidants and Redox Signaling*, vol. 8, no. 7-8, pp. 1171–1182, 2006.

[99] M. Minetti, T. L. Leto, and W. Malorni, "Radical generation and alterations of erythrocyte integrity as bioindicators of diagnostic or prognostic value in COPD?" *Antioxidants and Redox Signaling*, vol. 10, no. 4, pp. 829–836, 2008.

[100] C. De Felice, C. Signorini, T. Durand et al., "Partial rescue of Rett syndrome by ω-3 polyunsaturated fatty acids (PUFAs) oil," *Genes and Nutrition*, vol. 7, no. 3, pp. 447–458, 2012.

Hindawi Publishing Corporation
Oxidative Medicine and Cellular Longevity
Volume 2013, Article ID 694014, 6 pages
http://dx.doi.org/10.1155/2013/694014

Clinical Study

Malondialdehyde Adduct to Hemoglobin: A New Marker of Oxidative Stress Suitable for Full-Term and Preterm Neonates

Cécile Cipierre,[1,2] Stéphane Haÿs,[2,3] Delphine Maucort-Boulch,[4,5,6] Jean-Paul Steghens,[3,7] and Jean-Charles Picaud[2,3,5]

[1] *Département de Néonatologie, CHU Angers, 4 rue Larrey, 49100 Angers, France*
[2] *Département de Néonatologie, Hôpital de la Croix Rousse, Hospices Civils de Lyon, 69004 Lyon, France*
[3] *Centre de Recherche en Nutrition Humaine Rhône-Alpes, Centre Hospitalier Lyon-Sud, 69310 Pierre Bénite, France*
[4] *Département de Biostatistique, Hospices Civils de Lyon, 69003 Lyon, France*
[5] *Université Claude Bernard Lyon I, 69100 Villeurbanne, France*
[6] *CNRS UMR5558, Laboratoire de Biométrie et Biologie Evolutive, Equipe Biostatistique Santé, 69310 Piere-Bénite, France*
[7] *Centre de Biologie Sud, UF Nutrition et Métabolisme, Centre Hospitalier Lyon-Sud, Hospices Civils de Lyon, 69310 Pierre Bénite, France*

Correspondence should be addressed to Cécile Cipierre; cecile.cipierre@wanadoo.fr

Received 8 February 2013; Revised 13 April 2013; Accepted 16 April 2013

Academic Editor: Kota V. Ramana

Oxidative stress may play a central role in the onset of many diseases during the neonatal period. Malondialdehyde (MDA) is a marker of lipid peroxidation. The aim of this study was to evaluate a new marker, the malondialdehyde adduct to hemoglobin (MDA-Hb), which is measured in red blood cells (RBCs) and thus does not require that an additional blood sample be drawn. In this prospective study, we first adapted the measurement method previously described to Hb solutions obtained from washed RBCs and then evaluated the suitability of the method for use in neonates. MDA-Hb concentrations were measured by liquid chromatography-mass spectrometry. We compared the concentrations of MDA-Hb between preterm and term neonates. Erythrocyte samples were collected at birth from 60 healthy neonates (29 full-term and 31 preterm), as well as from 50 preterm neonates with uncomplicated postnatal evolution during the first months of life. We found a significantly higher MDA-Hb concentration at birth in preterm neonates ($P = 0.002$). During the first months of life, MDA-Hb concentrations were 9.4 nanomol/g Hb in hospitalized preterm neonates. MDA-Hb could be used to assess oxidative stress in preterm neonates. Together with clinical variables, it could be a useful marker for oxidative stress exposition in these higher risk patients.

1. Introduction

Growing evidence indicates that an imbalance between oxidative stress (OS) and antioxidant defense mechanisms plays an important role in the onset of many diseases during the neonatal period [1, 2]. Birth is associated with a strong OS related to the rapid change from a relatively hypoxic intrauterine environment to the extrauterine environment (5-fold increase in alveolar PO_2) and several physiologic processes involved in the delivery [3, 4]. These changes and processes greatly increase the production of free radicals, which must be controlled by the antioxidant defense system that has been maturing over the course of gestation [5, 6].

Free radicals are too short-lived to be detected directly in clinical systems, but oxygen free radicals react with lipids to produce lipid peroxidation products, which when measured serve as indirect biomarkers of *in vivo* oxidative stress status and related diseases. Among these products, malondialdehyde (MDA) is one of the principal and most studied low-molecular-weight end products. It is highly cytotoxic because of its ability to bind proteins or nucleic acids very quickly [7].

The thiobarbituric acid reactive substance method (TBAR test) has been frequently used to assess MDA concentrations, but it lacks specificity as aldehydes other than MDA (formaldehyde, acetaldehyde, etc.) and non lipid substances react with thiobarbituric acid [8, 9]. Other

analytical techniques such as specific derivatization before liquid chromatography with UV or mass spectrometry detection have been proposed to measure MDA more precisely [10]. It should be noted that all these techniques reflect measures only at a specific moment, although peroxidation reactions fluctuate over time.

Determining adducts to proteins, particularly Hb, has proved to be a useful approach for monitoring *in vivo* exposure to genotoxic compounds [11]. An adduct is formed when a low molecular compound binds with a biological molecule [11]. The Hb adducts are stable reaction products derived from electrophilic compounds, by covalent attachment, involving nucleophilic centers in biomolecules that offer possibilities for the sampling and analysis of electrophilic, short-lived compounds [12].

The determination of MDA-Hb obtained with a very complex method has thus been proposed to assess the exposure to lipid peroxidation products [13]. In healthy adults, MDA-Hb values of 0.01 to 10 nanomol/g Hb were reported [14]. Moreover, the method used in these studies was sensitive enough to detect variations in the levels of MDA adducts caused by lipid peroxidation, with a direct correlation between dose and effect [15].

MDA-Hb measurement could provide an assessment of OS in neonates over the middle term because of (i) the stable covalent attachment between MDA and Hb and (ii) MDA-Hb elimination, which is dependent on the relatively well-defined life span of the erythrocyte (120 days in human adults, shorter in neonates) [16]. We tested whether we would be able to determine MDA-Hb in neonates without taking more blood from them, as this is a crucial issue in very low birth weight (VLBW) neonates. We assumed that the erythrocytes remaining from routine blood samples taken for electrolyte determination would be sufficient.

We thus evaluated the feasibility of MDA-Hb measurement in neonates and sought to establish normal MDA-Hb ranges in healthy full-term neonates at birth and uncomplicated premature neonates at birth and during the first months of life.

2. Methods

2.1. Study Populations. To assess MDA-Hb at birth, neonates born on the maternity ward of Croix Rousse University Hospital, Lyon, France, were consecutively enrolled between February and May 2009. They were divided in two groups according to their gestational age (GA). In the first group, inclusion criteria were: healthy neonates born after a full-term gestation (≥37 weeks), delivered vaginally without complications, and presenting good adaptation to extrauterine life (no resuscitation, no evidence of perinatal hypoxia, or respiratory distress), birth weight (BW) appropriate for GA [17], and a normal clinical examination at birth. In the second group, inclusion criteria were: premature neonates (28–36 weeks) who did not require intensive care (no intubation, no chest compression, or drugs for resuscitation), oxygen therapy, or any type of medication at birth. Exclusion criteria were as follows: the need for resuscitation, evidence of perinatal hypoxia (pH $\leq$ 7.20 in cord blood, 5 min Apgar score $<$ 7) or respiratory distress, congenital malformation, sepsis, and small for GA [17], and multiple gestation. Measurements of MDA-Hb at birth were performed in 29 full-term and 31 premature neonates.

To measure MDA-Hb in the first months of life, we collected blood samples from uncomplicated premature neonates, that is, without assisted ventilation, parenteral nutrition, blood transfusion, or anti-inflammatory treatment within the five days before blood sampling. We recorded BW, GA, gender, and postnatal age on the day of sample collection. Measurements of MDA-Hb during the first 8 weeks of life were performed in 50 uncomplicated preterm neonates as previously defined.

The study was completely integrated into the routine care of full-term and preterm neonates and there was no supplementary blood sampling required. All parents signed an informed consent form. The study was approved by the Ethics Committee of the University Hospital Center of Lyon, France, (*CPP Lyon Sud Est IV*).

2.2. Determination of MDA-Hb

2.2.1. Collection of Samples. The assessment of MDA-Hb required the collection of erythrocytes. At the time of birth, arterial cord blood (5 mL) was collected from full-term and preterm neonates who fulfilled the inclusion criteria. As cord blood pH is systematically assessed at birth in our hospital, blood samples for the purpose of our study were also obtained at that time.

During the hospitalization of the preterm neonates who fulfilled the inclusion criteria, erythrocyte samples were collected at the same time as the venous blood sampling usually required for routine assessment of serum electrolytes in these neonates. According to the routine procedure, serum and red blood cells were separated by centrifugation (10 minutes, 4000 G) in the hospital biochemistry laboratory. The tubes were then immediately refrigerated at 4°C until the preparation of samples.

2.2.2. Reagents. Malondialdehyde-bis-dimethylacetal (tetramethoxypropane, TMP) 99% purity and metaphosphoric acid were purchased from sigma- Aldrich Chemie GmbH (Steinheim, Germany). Dideuterated tetraethoxypropane was from CDN Isotopes (88 Leacock Street, Pointe-Claire, QC, Canada). 2,3-Diaminonaphthalene (DAN) was obtained from TCI. Anhydrous potassium dihydrogen phosphate (Suprapur), ethanol, methanol, and acetonitrile gradient grade were from Merck (Darmstadt, Germany). All other chemicals and solvents were of analytical grade. Aqueous solutions were made with pure water (conductivity ≥ 18 MΩ), Elga Pure Lab Option (Elga, France).

Standard stock solution of TMP 608 nM was obtained by seven successive dilutions (1/10) of TMP: three times in ethanol then three times in ethanol/water (40/60, v/v) and finally in water with NH_4OH 90 mM final concentration.

Aliquots of this solution are stable under nitrogen for 3 months at −20°C in the dark. Secondary MDA standards (76,

Table 1: Derivatization of standards and samples.

	Standards (from 76 to 608 nM)	MDA-Hb
Sample volume	100 μL TMP	100 μL
Derivatization	100 μL DAN 5.8 mM in HCl 2.4 N + internal standard	
	Mixing, incubation for 180 min at 37°C	
Hb precipitation	100 μL MPA 10%, mixing, centrifugation 3 min, 15000 × g	
	200 μL supernatant for the next step	
Stabilization at pH 2.0*	100 μL (NaOH 1 N + KH_2PO_4 300 mM pH 2.0)	

* At every new preparation of both reagents, the volumes are adjusted to obtain pH 2.0 with a fixed volume of 300 μL (DAN: diaminonaphthalene; MDA: malondialdehyde; MPA: metaphosphoric acid; TMP: tetramethoxypropane).

152, and 304 nM) were prepared daily by dilution in water of the standard stock solution.

2.2.3. Material. LC-MS analysis was carried out on an Agilent LC 1100 series chromatograph with an Agilent LC-MSD SL single quadrupole as detector. The chromatographic mobile phase was ammonium acetate 5 mmol/L, adjusted at pH 1.8 with formic acid containing 15% (v/v) of a methanol-acetonitrile (1 : 1) mix. Derivatized samples and standards (10 μL) were injected on a 150 ∗ 2 mm Uptishere HDO C18 (3 μm particle size) column (Interchim, Montluçon, France). The flow rate was 0.23 mL/min with the column kept at 50°C in a column oven.

The quantification was carried out with a dideuterated MDA (d2-MDA) internal standard, and the derivatives of MDA and d2-MDA were detected in ESI positive mode $(M + H)^+$ at m/z 195.2 and 197.2, respectively.

2.2.4. Method. The procedure for measuring MDA-Hb consisted of three steps:

(i) isolation of Hb and delipidation in order to avoid any artifactual lipid peroxidation,

(ii) hydrolysis and derivatization of the MDA adduct with DAN to form a diazepinium complex,

(iii) then quantification of the diazepinium by LC-MS.

After a first centrifugation, RBCs (200 μL) were washed two times with four volumes of NaCl (9 g/1000 mL), and centrifuged (5 minutes, 1000 G). 150 μL of washed and packed RBCs were resuspended in distilled water (450 μL) and freeze-dried at −80°C for 5 minutes then thawed in hot water (30 seconds under water at 60°C). After a second cycle of freeze drying-thawing, Hb solution was obtained by centrifugation for 4 min at 8000 G; one aliquot was used to measure Hb concentration and another aliquot (200 μL) was rapidly delipidated by mixing with 100 μL Folch reagent (methanol/chloroform, 1 vol./2 vol.) and centrifuged 5 minutes at 13000 G. The delipidated Hb from the top phase was either hydrolyzed and derivatized with DAN or stored at −20°C until analysis.

Hydrolysis and derivatization, modified from the original method described for free and bound plasmatic MDA, were done according to Table 1. Preliminary experiments showed that to decrease adsorption of the diazepinium (formed between MDA and DAN) to Hb, derivatization had to be done in NaCl (60 g/L).

The adduct of MDA to Hb was expressed in nanomol per gram Hb (nanomol/g Hb).

2.2.5. Reproducibility of Sample Processing. The sample processing (RBCs washing, hemolysis, and delipidation) was checked on two series of measurements with four and six samples, respectively. Each sample was processed four or five times, depending on the available sample volume.

2.2.6. Processed Sample Stability. Twenty-four samples were fully prepared, aliquoted, and stored at −20°C to check the stability of the processed samples. The aliquots were analyzed after 7, 20, and 32 days of storage.

2.3. Statistical Analysis. Categorical variables are expressed as numbers and percentages, whereas continuous variables are expressed as medians and ranges. All variables are described for the whole population and each group: full-term (≥37 weeks) and preterm (<37 weeks) neonates. We compared the characteristics (GA, BW, and gender) of the full-term and preterm neonates. Categorical variables were compared using the χ^2 test, and MDA-Hb concentrations were compared with the Mann-Whitney test. Correlation coefficients between MDA-Hb concentration and GA, BW, and gender were tested with the Spearman test. All tests were considered to be significant for P values less than 5%. Analyses were performed using SPSS, version 15.0 (Statistical Product and Service Solutions 15.0; SPSS Inc., Chicago, Il USA).

3. Results

3.1. Optimization of Derivatization Conditions. The main modification for the sample derivatization, done according to Table 1, was that all the reagents used were prepared in NaCl (60 g/L) to decrease the adsorption of the formed diazepinium to Hb.

3.2. LC-MS Separation and Repeatability. Figure 1 shows a typical chromatogram of the MDA adduct measured as a diazepinium at m/z 195.2 and the corresponding internal standard at m/z 197.2. The method was found to be linear up to 1000 nM. The repeatability of ten successive injections of the same sample was better than 95% (personal data).

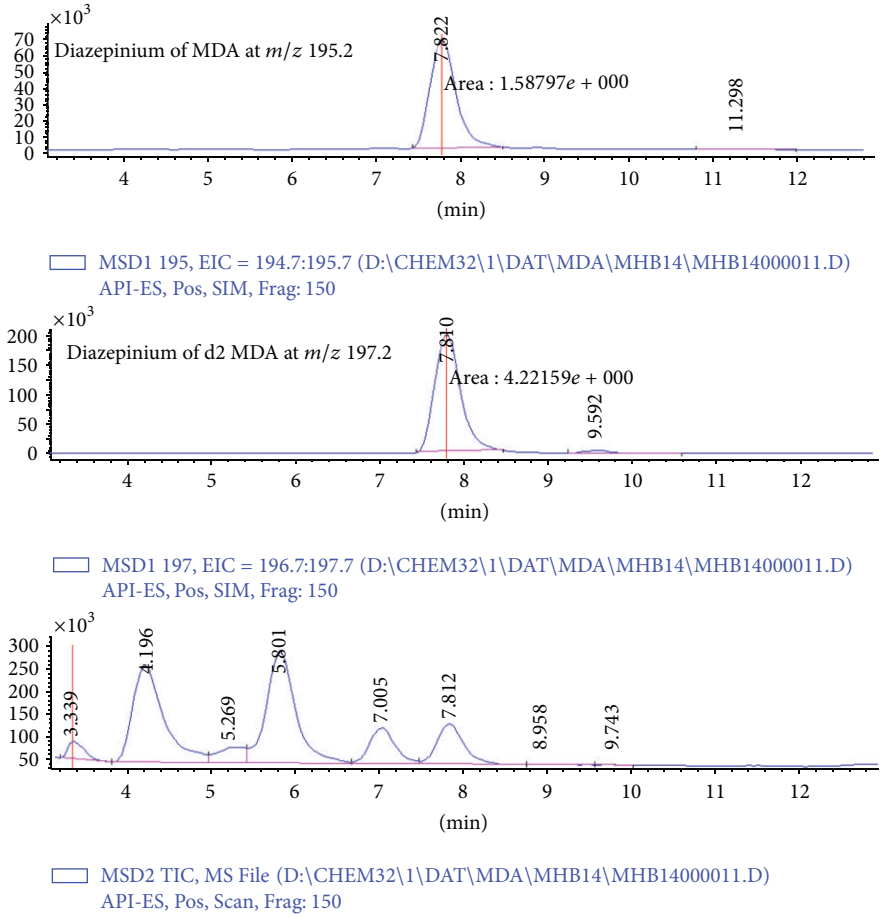

Figure 1: A typical chromatogram for the measurement of malondialdehyde adduct to hemoglobin (MDA-Hb). The upper trace is that of the diazepinium of MDA with its corresponding internal standard in the middle trace. The lower trace is that of the chromatogram in the total ion current (TIC) mode with a scan between m/z 100 and 300.

3.3. Reproducibility of Sample Processing. Even if it is known that handling of packed RBCs is tricky, unexpectedly, first experiments showed that final variation of the results came essentially from sample processing. After optimization and with a good practice, the coefficient of variation (CV) for sample processing evaluated by Hb measurement of delipidated samples (two series with 6 and 4 samples resp., measured four times each) was below 5%, except for one sample (CV = 5.98%).

3.4. Processed Sample Stability. Figure 2 shows the stability of 24 processed samples, aliquoted and stored at −20°C for at least a month. Aliquots were analyzed at day 0 and after 7, 20, and 32 days of storage.

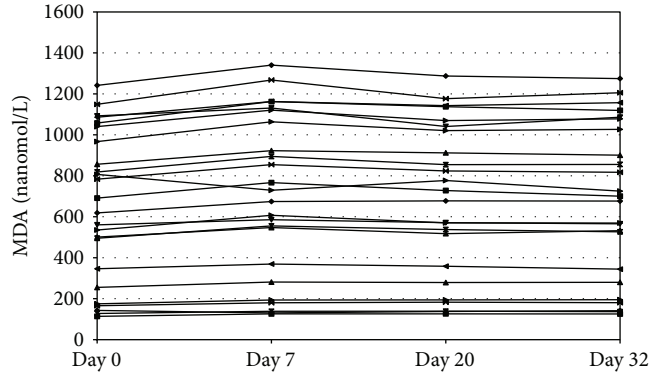

Figure 2: Processed sample stability of MDA: twenty-four different samples prepared, aliquoted, stored at −20°C, and analysed after 7, 20, and 32 days of storage.

3.5. Measurements of MDA-Hb. The characteristics of the studied population are presented in Table 2. The MDA-Hb concentrations at birth were significantly higher in preterm neonates (8.8 (2.6–19.2) nanomol/g Hb) than in full-term neonates (4.6 (2.5–19.3) nanomol/g Hb) (P = 0.002) (Figure 3).

MDA-Hb values during hospitalization were collected in preterm neonates (32.3 (26.5–35.5) weeks) with appropriate GA and BW (1495 (720–2720) g), and measurements were performed at a postnatal age of 12 (2–61) days (Figure 4). During the first 8 weeks of life, 50 samples were analyzed

Table 2: Clinical characteristics (mean (range unless specified *n* (%))) of 60 full-term neonates (GA ≥ 37 weeks, $n = 29$) or preterm (GA < 37 weeks, $n = 31$).

	Full-term neonates	Preterm neonates	*P* value
Gestational age at birth, weeks	39.4 (37.4–41.6)	31.7 (28.1–35.7)	<0.001
Birth weight, grams	3380 (2830–4270)	1580 (730–2580)	<0.001
Male, *n* (%)	14 (48.3)	15 (48.4)	0.993

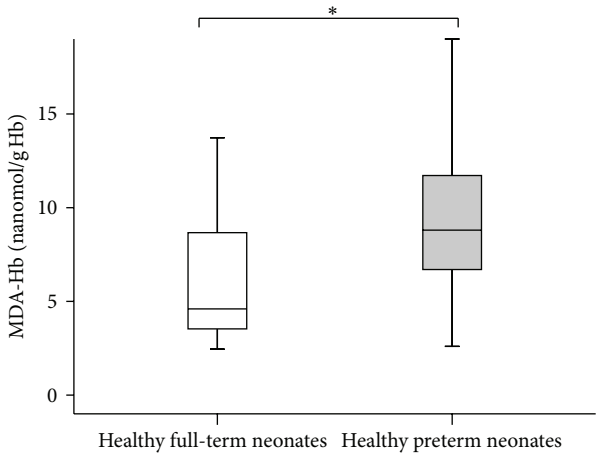

Figure 3: Concentrations of malondialdehyde adduct to hemoglobin (MDA-Hb) at birth in healthy full-term ($n = 29$) and healthy preterm neonates ($n = 31$). Values shown are median levels (25th/75th box; 10th/90th error bars). *Mann-Whitney test: significantly different from full-term neonates ($P = 0.002$).

in 50 uncomplicated preterm neonates (only one sample per preterm neonate) as previously defined. MDA-Hb concentrations were 9.4 (2.4–26.3) nanomol/g Hb. No correlation was found between BW or patient gender and the MDA-Hb concentration.

At birth, GA was significantly and negatively correlated with MDA-Hb concentration ($r = -0.31$, $P = 0.019$).

4. Discussion

We report a convenient method to determine the concentration of MDA adduct to Hb in neonates, which is sensitive enough to detect low concentrations of MDA-Hb and specific enough to assess lipid peroxidation.

The method to assess MDA-Hb is an adaptation of a reliable and validated method [10] used to evaluate the impact of parenteral nutrition composition on lipid peroxidation [18–20]. MDA-Hb was measured by LC-MS using a very specific method based on diaminonaphthalene derivatization [10]. The advantages of the method are its high sensitivity and specificity which rely on the use of DAN. When reacted with MDA, DAN forms a diazepinium with a mass of 194 Dalton higher than that of native MDA (72 Dalton) which makes its detection easier, because of an improved affinity for reverse phase column and this higher mass outside the background

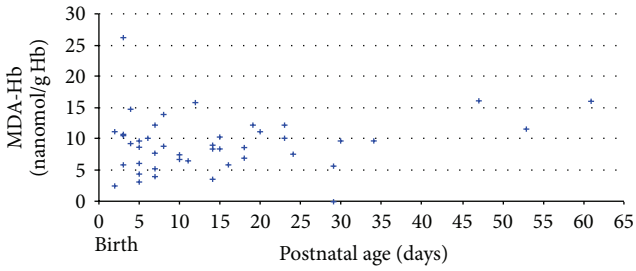

Figure 4: Relationship between concentrations of malondialdehyde adduct to hemoglobin (MDA-Hb) and postnatal age in healthy preterm neonates ($n = 50$).

noise. A direct consequence of this high sensitivity is the low volume of sample needed for measurement (only 200 μL). This is particularly interesting for neonatal care. Typical intra-assay variability is good (5%), and good reproducibility was observed. Although this new method requires rigorous conditions for sample preparation and measurement and may lead to the formation of artifacts, it has the advantage of being relatively simple, which is important for clinical practice. Our results thus suggest that this method is a useful, sensitive, and specific assay for lipid peroxidation in neonates.

Furthermore, this assay has several advantages from a clinical point of view, not the least of them being the simplicity of collecting a component of blood (erythrocytes), that is, usually discarded after serum has been taken for electrolyte assessment from routine blood sampling. The relatively long and well-controlled life span of Hb was an important reason for choosing this protein as a dose monitor for electrolytically reactive compounds. Hb has a predetermined life span equal to that of red blood cells. MDA-Hb could therefore be a long-term indicator of oxidative stress. Moreover, since proteins such as Hb are present in blood in much larger amounts, measurement of protein adducts favors a high capacity of detection [11].

We observed that the method to measure Hb adducts was sensitive enough to detect variations in MDA-Hb concentrations at different GAs at birth. As expected, we observed significantly higher MDA-Hb levels in preterm neonates than in full-term neonates. Indeed, increased oxidative stress in preterm neonates at birth has been described using other oxidative stress markers [4, 6, 21, 22].

Based on these preliminary results, it appears that this marker might be useful in a variety of pathological conditions, such as VLBW neonates, and thus, its clinical relevance should be validated in a larger population. The ability to detect lipid peroxidation noninvasively is of particular importance in preterm neonatal care. A noninvasive technique would be a great aid in improving knowledge about oxidative stress in these patients and evaluating future improvements in neonatal care (assisted ventilation, oxygen therapy, and parenteral nutrition) for diseases related to reactive oxygen species.

In summary, our results suggest that *in vivo* assessment of MDA-Hb in neonates is a feasible, blood-sparing, and simple method to determine oxidative stress, notably in preterm neonates.

Abbreviations

BW: Birth weight
DAN: Diaminonaphthalene
GA: Gestational age
Hb: Hemoglobin
LC-MS: Liquid chromatography-mass spectrometry
MDA: Malondialdehyde
MDA-Hb: Malondialdehyde adduct to hemoglobin
RBCs: Red blood cells
ROS: Reactive oxygen species
TMP: Tetramethoxypropane
OS: Oxidative stress
VLBW: Very low birth weight.

Acknowledgments

The authors thank Brigitte Guy and Blandine Vallet-Sandre for their help in collecting samples, Christine Delore, Catherine Castrichini, and Sophie Vasseur for their help in processing sample analysis, and C. Carmeni for editing the paper.

References

[1] O. D. Saugstad, "Update on oxygen radical disease in neonatology," *Current Opinion in Obstetrics and Gynecology*, vol. 13, pp. 147–153, 2001.

[2] E. Granot and R. Kohen, "Oxidative stress in childhood—in health and disease states," *Clinical Nutrition*, vol. 23, no. 1, pp. 3–11, 2004.

[3] O. D. Saugstad, "Mechanisms of tissue injury by oxygen radicals: implications for neonatal disease," *Acta Paediatrica*, vol. 85, no. 1, pp. 1–4, 1996.

[4] R. Robles, N. Palomino, and A. Robles, "Oxidative stress in the neonate," *Early Human Development*, vol. 65, supplement 2, pp. S75–S81, 2001.

[5] S. Perrone, S. Negro, M. L. Tataranno, and G. Buonocore, "Oxidative stress and antioxidant strategies in newborns," *Journal of Maternal-Fetal and Neonatal Medicine*, vol. 23, no. 3, pp. 63–65, 2010.

[6] J. M. Davis and R. L. Auten, "Maturation of the antioxidant system and the effects on preterm birth," *Seminars in Fetal and Neonatal Medicine*, vol. 15, no. 4, pp. 191–195, 2010.

[7] H. Esterbauer, "Estimation of peroxidative damage. A critical review," *Pathologie Biologie*, vol. 44, no. 1, pp. 25–28, 1996.

[8] D. del Rio, A. J. Stewart, and N. Pellegrini, "A review of recent studies on malondialdehyde as toxic molecule and biological marker of oxidative stress," *Nutrition, Metabolism and Cardiovascular Diseases*, vol. 15, no. 4, pp. 316–328, 2005.

[9] I. F. F. Benzie, "Lipid peroxidation: a review of causes, consequences, measurement and dietary influences," *International Journal of Food Sciences and Nutrition*, vol. 47, no. 3, pp. 233–261, 1996.

[10] J.-P. Steghens, A. L. van Kappel, I. Denis, and C. Collombel, "Diaminonaphtalene, a new highly specific reagent for HPLC-UV measurement of total and free malondialdehyde in human plasma or serum," *Free Radical Biology and Medicine*, vol. 15, no. 31, pp. 242–249, 2001.

[11] M. Törnqvist, C. Fred, J. Haglund, H. Helleberg, B. Paulsson, and P. Rydberg, "Protein adducts: quantitative and qualitative aspects of their formation, analysis and applications," *Journal of Chromatography B*, vol. 778, no. 1-2, pp. 279–308, 2002.

[12] U. Groth and H.-G. Neumann, "The relevance of chemico-biological interactions for the toxic and carcinogenic effects of aromatic amines V. the pharmacokinetics of related aromatic amines in blood," *Chemico-Biological Interactions*, vol. 4, no. 6, pp. 409–419, 1972.

[13] A. Kautiainen, M. Törnqvist, K. Svensson, and S. Osterman-Golkar, "Adducts of malonaldehyde and a few other aldehydes to hemoglobin," *Carcinogenesis*, vol. 10, no. 11, pp. 2123–2130, 1989.

[14] M. Törnqvist and A. Kautiainen, "Adducted proteins for identification of endogenous electrophiles," *Environmental Health Perspectives*, vol. 99, pp. 39–44, 1993.

[15] A. Kautiainen, M. Törnqvist, B. Anderstam, and C. E. Vaca, "In vivo hemoglobin dosimetry of malonaldehyde and ethene in mice after induction of lipid peroxidation. Effects of membrane lipid fatty acid composition," *Carcinogenesis*, vol. 12, no. 6, pp. 1097–1102, 1991.

[16] J. L. Naiman and E. A. Oski, *Hematologic Problems in the Newborn*, WB Saunders, Philadelphia, Pa, USA, 3rd edition, 1982.

[17] R. Usher and F. McLean, "Intrauterine growth of live-born Caucasian infants at sea level: standards obtained from measurements in 7 dimensions of infants born between 25 and 44 weeks," *The Journal of Pediatrics*, vol. 74, no. 6, pp. 901–910, 1969.

[18] J. C. Picaud, J. P. Steghens, C. Auxenfans, A. Barbieux, S. Laborie, and O. Claris, "Lipid peroxidation assessment by malondialdehyde measurement in parenteral nutrition solutions for newborn infants: a pilot study," *Acta Paediatrica*, vol. 93, no. 2, pp. 241–245, 2004.

[19] A. Grand, A. Jalabert, G. Mercier et al., "Influence of vitamins, trace elements, and iron on lipid peroxidation reactions in all-in-one admixtures for neonatal parenteral nutrition," *Journal of Parenteral and Enteral Nutrition*, vol. 35, no. 4, pp. 505–510, 2011.

[20] A. Jalabert, A. Grand, J. P. Steghens, E. Barbotte, C. Pigue, and J. Picaud, "Lipid peroxidation in all-in-one admixtures for preterm neonates: impact of amount of lipid, type of lipid emulsion and delivery condition," *Acta Paediatrica*, vol. 100, no. 9, pp. 1200–1205, 2011.

[21] G. Buonocore, S. Perrone, M. Longini et al., "Oxidative stress in preterm neonates at birth and on the seventh day of life," *Pediatric Research*, vol. 52, no. 1, pp. 46–49, 2002.

[22] J. J. Ochoa, M. C. Ramirez-Tortosa, J. L. Quiles et al., "Oxidative stress in erythrocytes from premature and full-term infants during their first 72 h of life," *Free Radical Research*, vol. 37, no. 3, pp. 317–322, 2003.

Hindawi Publishing Corporation
Oxidative Medicine and Cellular Longevity
Volume 2013, Article ID 657387, 9 pages
http://dx.doi.org/10.1155/2013/657387

Clinical Study

Oxidant Status and Lipid Composition of Erythrocyte Membranes in Patients with Type 2 Diabetes, Chronic Liver Damage, and a Combination of Both Pathologies

Rolando Hernández-Muñoz,[1] Marisela Olguín-Martínez,[1] Irma Aguilar-Delfín,[2] Lourdes Sánchez-Sevilla,[1] Norberto García-García,[1] and Mauricio Díaz-Muñoz[3]

[1] *Departamento de Biología Celular, Instituto de Fisiología Celular, UNAM, 04510 México DF, Mexico*
[2] *Instituto Nacional de Medicina Genómica (INMEGEN), 14610 México DF, Mexico*
[3] *Departamento de Neurobiología Celular y Molecular, Instituto de Neurobiología, Campus UNAM, 76230 Juriquilla QRO, Mexico*

Correspondence should be addressed to Mauricio Díaz-Muñoz; mdiaz@comunidad.unam.mx

Received 1 March 2013; Accepted 22 May 2013

Academic Editor: Kota V. Ramana

There is an important set of cirrhotic and diabetic patients that present both diseases. However, information about metabolic and cellular blood markers that are altered, in conjunction or distinctively, in the 3 pathological conditions is scarce. The aim of this project was to evaluate several indicators of prooxidant reactions and the membrane composition of blood samples (serum and red blood cells (RBCs)) from patients clinically classified as diabetic ($n = 60$), cirrhotic ($n = 70$), and diabetic with liver cirrhosis ($n = 25$) as compared to samples from a similar population of healthy individuals ($n = 60$). The results showed that levels of TBARS, nitrites, cysteine, and conjugated dienes in the RBC of cirrhotic patients were significantly increased. However, the coincidence of diabetes and cirrhosis partially reduced the alterations promoted by the cirrhotic condition. The amount of total phospholipids and cholesterol was greatly enhanced in the patients with both pathologies (between 60 and 200% according to the type of phospholipid) but not in the patients with only one disease. Overall, the data indicate that the cooccurrence of diabetes and cirrhosis elicits a physiopathological equilibrium that is different from the alterations typical of each individual malady.

1. Introduction

Diabetes mellitus (DM) is a worldwide disease frequently associated with a high risk of atherosclerosis and renal, cerebral, and ocular damage [1]. Oxidative damage plays several roles in diabetes and its complications [1–3], and reactive oxygen species (ROS) have been implicated in the pathogenesis of DM [4]. Patients with type 2 DM frequently have vascular endothelium dysfunction associated with hypercholesterolemia. It has been reported that patients with type 2 DM, hypertension, cirrhosis, and malaria show a nitric oxide (NO) deficiency as a major factor contributing to endothelial dysfunction [5].

In the same context, increased production of ROS has been related to protein glycosylation [2] and/or glucose autooxidation in DM patients [6]. Glycosylated proteins differ in their biological half-lives and properties. Glycosylated serum albumin reflects glycemia levels, since hemoglobin undergoes increased glycosylation (Hb A_{1C}) throughout the life span of the red blood cells (RBC) under hyperglycemic conditions [7]. Glycosylation of proteins can lead, in turn, to oxidative stress by direct release of superoxide and H_2O_2 [8]. Glycosylated albumin is a more sensitive index of short-term variations of glycemia than Hb A_{1C} during treatment of diabetic patients [9]. High plasma malondialdehyde (TBARS) and organic hydroxyperoxide concentrations have been observed in patients with ketoacidosis as secondary effects of glycemic disorders [10]. Additionally, increased lipid peroxidation (LP) occurs in RBC membranes due to an excessive production of ROS and decreased levels of GSH. Hematological alterations in plasma and/or blood cells (high serum levels of conjugated dienes and lipid peroxides) have been observed in type 2 DM patients with vascular complications [11].

It is not infrequent to find an association of DM with several modalities of liver disease. Diabetes and liver injury appear to be associated [12]: elevated levels of both alanine and aspartate aminotransferases occur in diabetics more frequently than in the general population [13], even independently of obesity [14], as well as serum γ-glutamyltransferase activity, which has been proposed as a marker of insulin resistance in type 2 DM [15]. Causes of cirrhosis linked to diabetes include nonalcoholic fatty liver disease, hemochromatosis, and hepatitis C infection. Taken together, these data are highly suggestive of a DM effect on liver functions [16].

Nonalcoholic fatty liver disease (NAFLD) represents a spectrum of progressive liver maladies encompassing simple steatosis, nonalcoholic steatohepatitis (NASH), fibrosis, and cirrhosis. NAFLD is strongly associated with glucose intolerance or type 2 DM. Importantly, accumulating evidence indicates that NAFLD is strongly associated with a prothrombotic tendency, which may, at least in part, contribute to the increased risk of atherothrombotic events observed in these patients. NAFLD also exacerbates systemic and hepatic insulin resistance and causes atherogenic dyslipidemia [17]. Also recently, it was reported that interleukin-2R, interleukin-18, and glucagon are higher in DM patients with cirrhosis, suggesting a synergistic effect of both diseases [18]. Moreover, interactions between diabetes and hepatitis C virus exacerbated the liver damage, suggesting that diabetes is a risk factor for the pathological progression of the viral liver disease [19].

Indeed, it has been suggested that the combination of insulin resistance and LP could lead to liver damage, such as those in NASH [20]. Hence, this study was addressed to evaluate the impact of type 2 DM combined with advanced liver damage (diagnosed as cirrhosis) on parameters indicative of oxidative stress and its impact on biological membranes as measured in the patients' RBC.

2. Material and Methods

2.1. Patients and Controls. Subjects with different stages of type 2 DM were recruited from outpatient clinics as coordinated by the Instituto Nacional de Medicina Genómica (INMEGEN). Patients diagnosed with cirrhosis, with or without manifested clinical type 2 DM, were recruited from several outpatient clinics of the Sector Salud (Ministry of Health). The study involved 60 patients with type 2 DM, 70 patients with cirrhosis, 25 patients with both pathologies. Patients were selected based upon the following criteria: all of them were nonalcoholics, nonsmokers, and apparently free from any renal complication. The control group consisted of healthy individuals of similar age, body weight matched, nonsmoking, nonalcoholic, and with no family history of diabetes and/or cirrhosis. Following a 12 h overnight fast, all subjects were blood sampled and clinically evaluated by the same investigators (Norberto García-García and Irma Aguilar-Delfín). This study was carried out in accordance with the Declaration of Helsinki (2000) of the World Medical Association and approved by the Ethics Committees of the Hospital General de México (Ministry of Health) and Instituto de Fisiología Celular (UNAM).

2.2. Clinical Tests. In separate blood samples from healthy subjects and diabetic patients, several clinical parameters were quantified: glucose, glycosylated Hb A_{1C}, cholesterol, triacylglycerols, C-reactive protein (CRP), albumin, bilirubin, coagulation factors, aspartate (GOT) and alanine (GPT) aminotransferase activities, and γ-glutamyltransferase (GGT) activity.

2.3. Blood Samples. Heparin-anticoagulated blood was obtained, and the serum was rapidly separated. Aliquots of serum and RBC were placed in ice cold perchloric acid (8% w/v, final concentration). After centrifugation, acid extracts of plasma as well as of RBC were obtained (dilution: 1 : 3 v/v blood samples/perchloric acid) and stored at −50°C until use.

2.4. Biochemical Measurements. In acid extracts from whole blood, serum, and RBC, thiobarbituric acid reactive substances (TBARS) were determined by the method described by Hernández-Muñoz et al. [21], and free cysteine was colorimetrically assayed with the method described by Gaitonde [22]; in neutralized perchloric acid extracts, nitrites were quantified by the Griess reaction [23]. Cell membrane LP related and conjugated dienes (CD) were assessed as previously described [24], and the protein carbonyl content in the different subcellular fractions was estimated according to Levine et al. [25] as an index of oxidative damage. Total hemoglobin was quantified using Drabkin's reagent.

2.5. Preparation of RBC Membranes (Ghosts). Sets of anticoagulated blood samples were obtained, and the serum was rapidly separated by centrifugation at 900 g for 5 min at 4°C. The buffy coat was removed, and the erythrocyte pellet was washed 4 times with 2 volumes of cold (4°C) 20 mM HEPES (pH 7.4) containing 0.9% NaCl. Thereafter, RBC were gently resuspended in a hypoosmotic solution containing 0.172 M TRIS buffer (pH 7.6) and adjusted to a 50% hematocrit to produce hemolysis. RBCs were then centrifuged at 20,000 g (4°C) for 25 min then washed at least 3 more times to completely remove hemoglobin from the RBC pellet, as described before [26]. Thereafter, membranes were incubated in the same HEPES buffer for 30 min at 37°C, and TBARS was measured [21].

2.6. Calculations and Statistics. Concentration of serum and RBC metabolites were calculated as nmoles/mL and expressed as means ± standard deviation (SD). To compare a continuous variable between groups, the Student's unpaired t-test and the Mann-Whitney test were used; thereafter, these differences were contrasted with a t-test for paired data.

3. Results

3.1. Metabolites Indicating Oxidative Stress and Generation of NO in Patients with Type 2 DM and Cirrhosis. RBC metabolite concentrations clearly differed from those found in serum (Table 1), suggesting that RBCs could act as a biochemical reservoir. In serum from patients with DM, the level of TBARS was not significantly different from that of the control group; however, the RBC content of TBARS was increased in samples obtained from patients with type 2 DM. The ratio

Table 1: TBARS, nitrites, and cysteine levels from serum and red blood cells obtained from control subjects and from patients with type 2 DM and/or cirrhosis.

Parameter	Healthy ($n = 60$)	Diabetes ($n = 60$)	Cirrhosis ($n = 70$)	Diab + Cirrhos ($n = 25$)
Serum TBARS	0.35 ± 0.13	0.40 ± 0.10	0.37 ± 0.09	0.42 ± 0.18
RBC TBARS	0.42 ± 11	0.62 ± 0.08*	1.15 ± 0.35*	0.84 ± 0.35*,***
RBC/serum ratio	1.20 ± 0.34	1.55 ± 0.29*	3.11 ± 0.89*	2.00 ± 0.78*
Serum nitrites	26 ± 3	37 ± 8	63 ± 25*	46 ± 18*
RBC nitrites	32 ± 6	68 ± 7*	150 ± 47*	62 ± 24*
RBC/serum ratio	1.2 ± 0.2	1.8 ± 0.3*	2.3 ± 0.9*	1.4 ± 0.4
Serum cysteine	18 ± 4	44 ± 12*	28 ± 9*	39 ± 15*
RBC cysteine	23 ± 7	37 ± 10	153 ± 52*	87 ± 34*,***
RBC/serum ratio	1.3 ± 0.3	0.8 ± 0.2	5.3 ± 1.8*	2.2 ± 0.9*,***

Results are expressed as mean ± SD of determinations done in blood samples membranes from controls ($n = 60$), patients with type 2 DM ($n = 60$), cirrhotic patients ($n = 70$), and diabetic patients with cirrhosis ($n = 25$). RBC: red blood cells. Statistical significance: $^{*}P < 0.01$, versus control; $^{**}P < 0.01$, versus DM or versus cirrhosis; $^{***}P < 0.01$, versus both the diabetes and cirrhosis groups, separately.

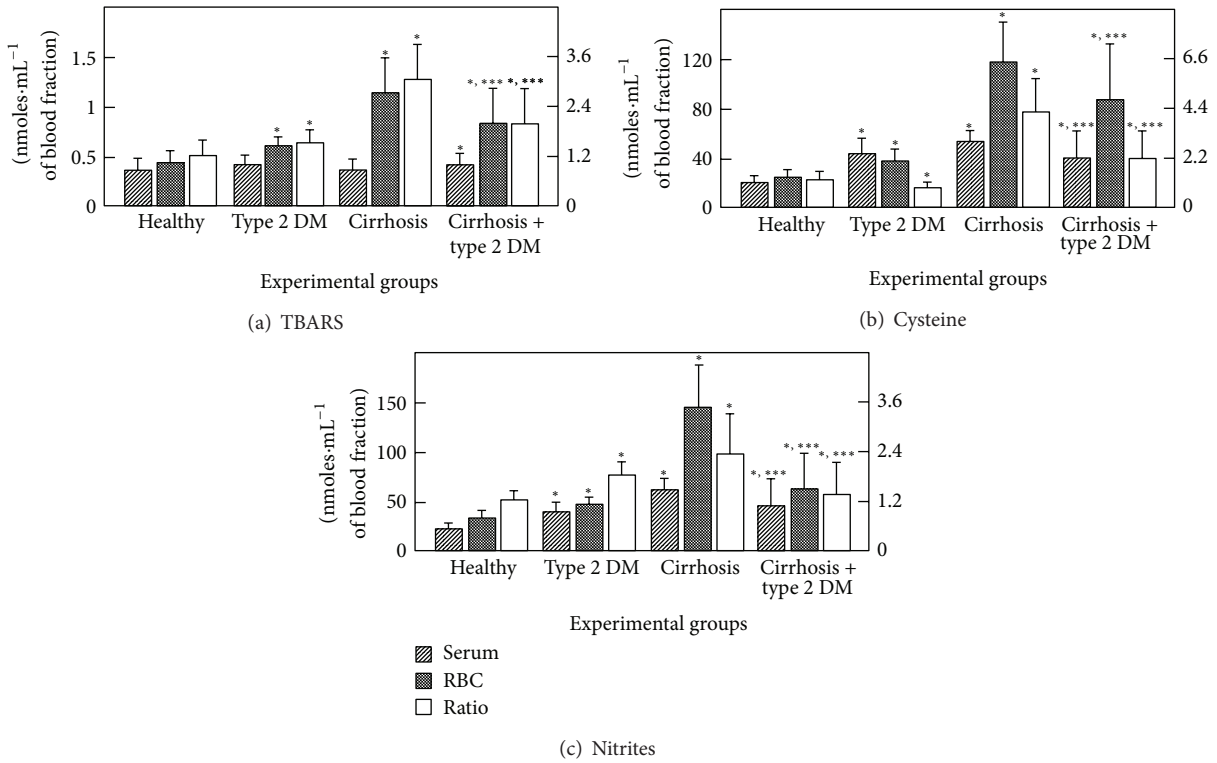

Figure 1: Blood levels of TBARS, cysteine, and of nitrites and its distribution in serum and RBC from patients with type 2 diabetes mellitus and cirrhosis. The results are expressed as the mean ± SD for levels of TBARS (a), free cysteine (b), and for nitrites (c), in serum and RBC samples from control healthy volunteers ($n = 60$), patients with type 2 diabetes mellitus ($n = 60$), patients with cirrhosis ($n = 70$), and those from patients having the combination of both pathologies ($n = 25$). Symbols indicate each blood compartment at the top of the panels. RBC/serum ratio is indicated by the empty bars and assessed by the right scale. Statistical significance: $^{*}P < 0.01$, versus control; $^{**}P < 0.01$, against DM or versus cirrhosis; $^{***}P < 0.01$, against both, the diabetes and cirrhosis groups, separately.

RBC-TBARS/serum TBARS in controls was 1.2, whereas in DM patients it increased significantly ~25% (Figure 1(a)). In the group of cirrhotic patients, RBC-TBARS was drastically increased, while the level of TBARS in serum was practically unchanged, which led to a 3-fold increase in the RBC-TBARS/serum-TBARS ratio (Figure 1(a)). Interestingly, the combination of DM and cirrhosis enhanced serum-TBARS levels, when compared with controls. However, the TBARS level in the RBC was similar to that of the DM patients: the significant increase detected in the cirrhotic patients was not observed (Figure 1(a)).

The levels of free cysteine, which reflect glutathione synthesis and oxidative status, were found to be slightly higher in control RBC than in serum (Figure 1(b)). DM promoted an increased cysteine concentration in both serum and RBC; however, the RBC/serum ratio for this amino acid was

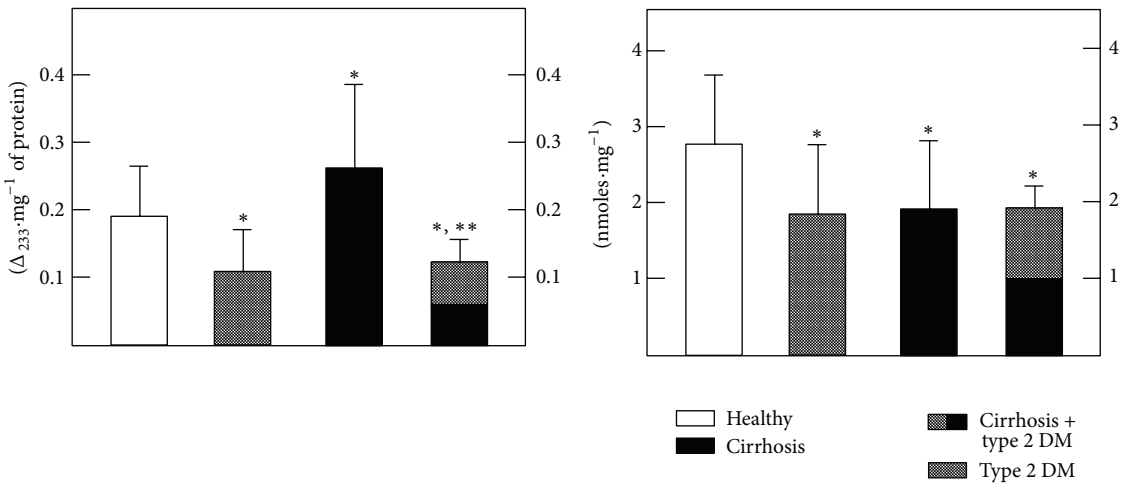

(a) Conjugated dienes (b) Carbonyl groups

Figure 2: Levels of conjugated dienes and of carbonyl groups (oxidized proteins) in RBC membranes obtained from patients with type 2 diabetes mellitus and cirrhosis. The results are expressed as the mean ± SD for levels of conjugated dienes (a) and for nitrites (b), determined in isolated membranes from RBC obtained from control healthy volunteers ($n = 60$), patients with type 2 diabetes mellitus ($n = 60$), patients with cirrhosis ($n = 70$), and those from patients having the combination of both pathologies ($n = 25$). Symbols indicate experimental groups at the top of the figure. Statistics as indicated in Figure 1.

significantly decreased, due a larger increase in serum cysteine (Figure 1(b)). On the other hand, cirrhosis induced the opposite pattern, a drastic increase of cysteine, mainly in the RBC. Again, the cooccurrence of both pathologies partially counteracted the alterations observed in the cirrhotic patients (Figure 1(b)).

The concentration of blood nitrites, as a reflection of NO catabolism, was higher in the RBC than in serum in controls (Figure 1(c)). Patients with type 2 DM clearly showed an increased amount of blood nitrites, particularly in RBC, leading to a significantly higher RBC-nitrite/serum-nitrite ratio. Cirrhosis also promoted NO catabolism mainly in RBC, producing an even more elevated RBC-NO/serum-NO ratio (Figure 1(c)). Interestingly, the combination of the two diseases attenuated their individual effects on nitrites in both blood compartments (Figure 1(c)).

3.2. Oxidative Parameters and TBARS Production by Isolated RBC Membranes from Patients with Type 2 DM and Cirrhosis. The LP rate was evaluated in RBC membranes by measuring conjugated dienes (Figure 2(a), Table 4). Compared to the TBARS generated in whole blood, RBC membranes from patients with DM had a reduced content of conjugated dienes, while those obtained from cirrhotic patients showed a significant increase of these LP by-products (Figure 2(a), Table 4). It was noteworthy that DM completely blocked the cirrhosis-induced enhancement of conjugated dienes in the RBC membranes (Figure 2(a), Table 4). The impact of oxidative stress on proteins, as assessed by the presence of carbonyl groups present in denatured membrane proteins, also changed (Figure 2(b), Table 4). When compared with controls, the RBC ghosts from patients with type 2 DM as well as RBC from cirrhotic patients had significantly lower amounts than that of carbonyl groups (Figure 2(b), Table 4).

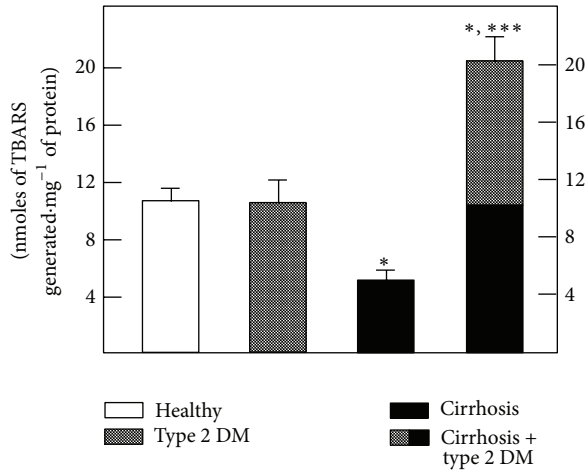

Figure 3: *In vitro* production of TBARS by incubated RBC membranes obtained from patients with type 2 diabetes mellitus and cirrhosis. The results are expressed as the mean ± SD for the amount of TBARS generated by isolated RBC membranes obtained from control healthy volunteers ($n = 60$), patients with type 2 diabetes mellitus ($n = 60$), patients with cirrhosis ($n = 70$), and those from patients having the combination of both pathologies ($n = 25$). Symbols indicate experimental groups at the top of the figure. Statistics as indicated in Figure 1.

In patients with both pathologies, no additional effect was found (Figure 2(b), Table 4).

Since the cooccurrence of type 2 DM in cirrhotic patients seemed to provide some kind of antioxidant effect in the RBC, we assayed *in vitro* for TBARS generation in RBC membranes (Figure 3). TBARS synthesis in samples obtained from the cirrhotic patients was reduced, whereas the samples from DB

Table 2: Levels of phospholipids and cholesterol in RBC membranes obtained from control subjects and from patients with type 2 DM and/or cirrhosis.

Parameter	Healthy ($n = 60$)	Diabetes ($n = 60$)	Cirrhosis ($n = 70$)	Diab + Cirrhos ($n = 25$)
PS (nmoles/mg)	40 ± 14	34 ± 10	30 ± 8*	63 ± 14*,***
PI (nmoles/mg)	46 ± 10	45 ± 11	50 ± 12	126 ± 26*,***
PC (nmoles/mg)	62 ± 14	63 ± 16	77 ± 17*	194 ± 36*,***
PE (nmoles/mg)	23 ± 6	27 ± 6	26 ± 6	70 ± 10*,***
Cholesterol (nmoles/mg)	17 ± 4	18 ± 5	25 ± 6*	41 ± 6*,***

Results are expressed as mean ± SD of determinations done in RBC membranes from controls ($n = 60$), patients with type 2 DM ($n = 60$), cirrhotic patients ($n = 70$), and diabetic patients with cirrhosis ($n = 25$). PC: phosphatidylcholine; PE: phosphatidylethanolamine; PI: phosphatidylinositol; PS: phosphatidylserine; Diab + Cirrhos: diabetes + cirrhosis. Statistical significance: $^{*}P < 0.01$, versus control; $^{**}P < 0.01$, versus DM or versus cirrhosis; $^{***}P < 0.01$, versus both the diabetes and cirrhosis groups, separately.

Table 3: Relations of phospholipids and cholesterol in RBC membranes obtained from control subjects and in patients with type 2 DM and cirrhosis.

Parameter	Healthy ($n = 60$)	Diabetes ($n = 60$)	Cirrhosis ($n = 70$)	Diab + Cirrhos ($n = 25$)
Total phospholipids (nmoles/mg)	171 ± 44	168 ± 42	185 ± 44	453 ± 87*,***
PC/PE ratio	2.72 ± 0.62	2.34 ± 0.54*	2.71 ± 0.58	2.76 ± 0.46**
Cholesterol/T. phospholipids	0.10 ± 0.02	0.11 ± 0.03	0.13 ± 0.03*	0.09 ± 0.02***

Results are expressed as mean ± SD of determinations done in RBC membranes from controls ($n = 60$), patients with type 2 DM ($n = 60$), cirrhotic patients ($n = 70$), and diabetic patients with cirrhosis ($n = 25$). PC: phosphatidylcholine; PE: phosphatidylethanolamine; T: total; Diab + Cirrhos: diabetes + cirrhosis. Statistical significance: $^{*}P < 0.01$, versus control; $^{**}P < 0.01$, versus DM or versus cirrhosis; $^{***}P < 0.01$, versus both the diabetes and cirrhosis groups, separately.

patients did not show significant differences from the control (Figure 3). Moreover, an unexpected potentiation of TBARS production in RBC membranes was detected in samples from patients with both type 2 DM and cirrhosis (Figure 3).

3.3. Changes in Lipid Composition (Phospholipids and Cholesterol) in Isolated RBC Membranes from Patients with Type 2 DM and Cirrhosis. We tested if the changes observed in the oxidative stress parameters could be correlated with alterations in the phospholipid and cholesterol content of the RBC membranes (Tables 2 and 3). The lipid composition of RBC membranes from patients with type 2 DM was practically unmodified when compared to controls (Table 2). In contrast, patients with cirrhosis had a decreased amount of phosphatidylserine (PS), which was accompanied by an elevated concentration of phosphatidylcholine (PC) and cholesterol (Table 2). Again, an unexpected pattern was found in RBC membranes from diabetic patients with cirrhosis, where all phospholipids tested and cholesterol were drastically increased (Table 2).

Two parameters indicative of membrane fluidity were also calculated, namely, the ratio of PC/phosphatidylethanolamine (PE), as well as the total phospholipid/cholesterol ratio. Whereas in patients with DM, the PC/PE ratio was significantly decreased; in the cirrhotic patients, an increase of the membrane cholesterol level was noted, resulting in a significantly higher total phospholipid/cholesterol ratio (Table 3). These effects were completely absent in the DM and cirrhotic patients, since cirrhosis seemed to correct the DM-induced decrease of the PC/PE ratio and type 2 DM normalized the total phospholipid/cholesterol ratio in RBC membranes from cirrhotic patients (Table 3).

4. Discussion

Diabetes is frequently diagnosed in patients with cirrhosis and represents an important risk factor for morbidity and mortality, since pharmacological therapy is limited by hepatotoxicity and the risk of hypoglycemia. Conversely, cirrhosis is a common complication in diabetic patients. Diabetes increases the risk of fatty liver, which can progress to cirrhosis. The interactions of these pathologies are not well understood, but a possible participation of ROS as an underlying mechanism is under robust investigation. In this context, increased adiposity and insulin resistance in obese subjects contribute to the progression of NASH to fibrosis, apparently by augmenting ROS formation and altering adipokine/cytokine production, thereby promoting a profibrotic milieu in the liver [27].

Production of ROS promotes activation of hepatic stellate cells (HSC) and progression to fibrosis. Indeed, in a diabetic state, ROS production is enhanced in association of CYP2E1 induction and activity [28]; the resultant oxidative stress then can directly increase collagen production by activated HSC [29]. This situation confirms that oxidative stress coincides with many pathological conditions and diseases such as chronic obstructive pulmonary disease, cancer, diabetes, ischemia/perfusion, neurological disorders, atherosclerosis, hypertension, idiopathic pulmonary fibrosis, asthma, and liver diseases [30]. Although the negative impact of diabetes on the retinal, renal, nervous, and cardiovascular systems is well recognized [31], little is known about its effect on the liver. Nonetheless, it has recently been reported that hepatic deregulation in the setting of obesity is marked by oxidative stress and steatosis related to insulin resistance [29].

Table 4: Conjugated dienes, carbonyls and TBARS generation in red blood cell membranes obtained from control subjects and in patients with type 2 DM and cirrhosis.

Parameter	Healthy ($n = 60$)	Diabetes ($n = 60$)	Cirrhosis ($n = 70$)	Diab + Cirrhos ($n = 25$)
Conjugated dienes (Δ_{233}/mg)	0.19 ± 0.07	0.11 ± 0.06	0.26 ± 0.12*	0.12 ± 0.03***
Carbonyl groups (nmoles/mg)	2.73 ± 0.90	1.83 ± 0.85*	1.85 ± 0.89*	1.86 ± 0.38*
TBARS generation by RBC membranes	10.9 ± 0.9	10.5 ± 1.4	4.8 ± 1.0*	20.7 ± 1.8*,***

Results are expressed as mean ± SD of determinations done in RBC membranes from controls ($n = 60$), patients with type 2 DM ($n = 60$), cirrhotic patients ($n = 70$), and diabetic patients with cirrhosis ($n = 25$). Statistical significance: $^{*}P < 0.01$, versus control; $^{**}P < 0.01$, versus DM or versus cirrhosis; $^{***}P < 0.01$, versus both the diabetes and cirrhosis groups, separately.

Products of lipid peroxidation, such as TBARS and other unsaturated aldehydes, can inactivate many cellular proteins, such as membrane-bound receptors and enzymes, by forming protein cross-linkages [32] which could alter cell permeability [33]. ROS can also alter the electrical charge and cross-linking of proteins, and by oxidizing specific amino acids such as cysteine and methionine, they increase susceptibility to proteolysis [34]. Moreover, free cysteine is generally the limiting amino acid for the synthesis of reduced glutathione (GSH) [35]. Thus, factors (e.g., insulin and growth factors) that stimulate cysteine (cystine) uptake by cells generally increase intracellular GSH concentrations [36]. In addition, increasing the supply of cysteine or its precursors (e.g., cystine, *N*-acetylcysteine, and L-2-oxothiazolidine-4-carboxylate) prevents GSH deficiency in humans and animals under various nutritional and pathological conditions [37].

The present data indicate that generation of TBARS was higher in RBC from patients with type 2 DM and, to a much larger extent, in the RBC from cirrhotic patients. However, in patients with both pathologies, the enhancement of TBARS was partly counteracted, probably due to the antioxidant status of these cells, since we found only a slight but significant increase in serum TBARS in samples obtained from the diabetic and cirrhotic groups (Figure 1(a)). This condition correlated well with the assessment of membrane conjugated dienes, where it was clear that cirrhosis promoted oxidative stress, which was blunted by the presence of DM (Figure 2(a)). However, the *in vitro* generation of TBARS was significantly diminished in RBC membranes obtained from patients with cirrhosis and largely counteracted by the simultaneous occurrence of DM (Table 4). The latter, which could appear somehow contradictory, might be explained by the antioxidant defense of each population of blood cells. In fact, RBC membranes from patients with type 2 DM and those obtained from cirrhotic patients both showed, separately, an important decrease of oxidized membrane proteins (carbonyl groups); this decrease was not additive when cells obtained from the group with both diseases were assayed (Figure 2(b)).

DM and cirrhosis both induced an enhanced amount of blood cysteine, which was more evident in the RBC, particularly in the patients with cirrhosis. This elevated blood cysteine was also partly attenuated by the combination of both pathologies (Figure 1(b)). It has been demonstrated that acetaldehyde, as a main product of ethanol oxidation, is bound to RBC, possibly due to thiazolidine formation with cysteine, and that the cysteine level was doubled in blood cells from alcoholic patients without severe liver damage [26]. In addition, cirrhotic patients display lower levels of plasma GSH and cysteine; on the contrary, RBC cysteine was found to increase significantly in all cirrhotic patients, particularly in alcoholics [38].

There is evidence that DM patients had altered NO metabolism [39], and in a rat model of cirrhosis that overexpressed caveolin-1, the interaction with eNOS and both the basal and stimulated production of NO are depressed [40]. This interaction may increase portal pressure and contribute to the malady, as occurs in cholestatic disease models where the upregulation of sinusoidal caveolin-1 and a decrease in eNOS activity were seen [41]. Our data agree with this altered NO metabolism, as evaluated by the presence of nitrites; they showed elevated nitrites in serum and RBC in diabetic and cirrhotic patients, a situation that was also partly counteracted when both pathologies occurred together (Figure 1(c)). However, we did not assess the impact of this altered NO production (i.e., production of peroxynitrites or nitrotyrosines) which could give us more insight into the possible mechanism underlying the opposing effects of the two pathologies, when they occur in the same patient.

The lipid composition (phospholipids and cholesterol) of RBC membranes obtained from the experimental groups showed some effects that can be attributed to the level of oxidative stress. PS synthesis and its translocation are ATP-dependent processes [42, 43], while the ratios PC/PE and cholesterol/total phospholipids have been related to the fluidity of a variety of membranes [44, 45]. Indeed, the ratio PS/PE (1.74 in controls; Table 2) was decreased by both pathologies. However, patients with both pathologies exhibited normal PC/PE (decreased by DM) and cholesterol/total phospholipid (increased by cirrhosis) ratios, as shown in Table 2. Both type 2 DM and cirrhosis are complex pathologies involving metabolic disturbances and adaptations, many of which are still unknown. Our data suggest that cooccurrence of both diseases instead of potentiating the severity of metabolic dysfunction somehow allows the achievement of a new metabolic status, whose significance remains to be elucidated.

Recent data support the fact of a complex interplay between the metabolic condition associated with DM and the pathologically defined as nonalcoholic fatty liver disease (NAFLD). NAFLD predicts the development of type 2 diabetes and vice versa, and each condition may serve as a progression factor for the other [46]. Hepatobiliary disease and associated mortality are increased in type 2 diabetes, and factors including fatty infiltration, microangiopathy, and direct

glucotoxicity are likely to contribute to these outcomes [47]. The prevalence of type 2 DM is higher in patients with hepatic deregulation, such as NAFLD, chronic viral hepatitis, hemochromatosis, alcoholic liver disease, and cirrhosis. The development of DM in patients with cirrhosis is well recognized, and it is suggested that DM plays a role in the initiation and progression of liver injury [48]. Patients with chronic hepatitis C virus (HCV) infection have a significantly increased prevalence of type 2 DM compared to controls or hepatitis B virus-infected patients, independent of the presence of cirrhosis [49]. In addition, the levels of Hb A_{1C} and of HOMA-R are increased in DM patients with chronic liver damage and who are undergoing angiopathy [50]. Moreover, since the diabetic condition is associated with a significant increase of mortality in patients with compensated liver cirrhosis [51], there exists a consensus that cirrhosis will negatively impact DM installation and, in turn, DM could shorten the life of patients with the combined pathology. However, the incidence of diabetic retinopathy and cerebrovascular disease was significantly lower in the a diabetic/cirrhotic group compared to the type 2 DM group, probably due to the lower levels of serum lipoprotein A found in the combined group [52]. It has been also postulated a link between the development of fatty liver in which the inflammatory responses lead to the onset of diabetes type 2. In turn, the proinflammatory milieu favors that the diabetic state which in turn becomes a major contributor to progressive liver diseases such as fibrosis and cirrhosis [53]. Taken together, these results suggest that the cooccurrence of the two pathologies elicits a different physiopathological equilibrium between prooxidant reactions and antioxidant activities.

5. Conclusions

Diabetes and cirrhosis are pathological conditions that become interconnected in an important number of patients. Our findings indicate that the oxidative response observed in blood markers in cirrhotic/diabetic patients is ameliorated in some parameters in comparison to the enhanced prooxidant activity promoted by cirrhosis. Another distinctive result was the increased amount of phospholipids content in the red blood cells of the patients with both illnesses. It remains to be elucidated the potential association between the oxidative response in each pathology with structural changes in blood cells.

Acknowledgments

The authors thank Dr. Dorothy Pless for careful corrections in English grammar and style. The present study was partially supported by grants from PAPIIT-DGAPA, UNAM (IN 210611 for Rolando Hernández-Muñoz) and IN IN202412 for Mauricio Díaz-Muñoz), and CONACyT (129-511 for Mauricio Díaz-Muñoz).

References

[1] P. Zimmet, K. Alberti, and J. Shaw, "Global and societal implications of the diabetes epidemic," *Nature*, vol. 414, no. 6865, pp. 782–787, 2001.

[2] J. W. Baynes, "Role of oxidative stress in development of complications in diabetes," *Diabetes*, vol. 40, no. 4, pp. 405–412, 1991.

[3] R. D. Hoeldtke, K. D. Bryner, D. R. McNeill, S. S. Warehime, K. van Dyke, and G. Hobbs, "Oxidative stress and insulin requirements in patients with recent-onset type I diabetes," *Journal of Clinical Endocrinology and Metabolism*, vol. 88, no. 4, pp. 1624–1628, 2003.

[4] S. Taysi, F. Polat, M. Gul, R. Sari, and E. Bakan, "Lipid peroxidation, some extracellular antioxidants, and antioxidant enzymes in serum of patients with rheumatoid arthritis," *Rheumatology International*, vol. 21, no. 5, pp. 200–204, 2002.

[5] G. Wu and C. J. Meininger, "Arginine nutrition and cardiovascular function," *Journal of Nutrition*, vol. 130, no. 11, pp. 2626–2629, 2000.

[6] J. V. Hunt, C. C. T. Smith, and S. P. Wolff, "Autoxidative glycosylation and possible involvement of peroxides and free radicals in LDL modification by glucose," *Diabetes*, vol. 39, no. 11, pp. 1420–1424, 1990.

[7] J. F. Fitzgibbons, R. D. Koler, and R. T. Jones, "Red cell age related changes of hemoglobins A_{Ia+b} and A_{Ic} in normal and diabetic subjects," *Journal of Clinical Investigation*, vol. 58, no. 4, pp. 820–824, 1976.

[8] P. M. Abuja and R. Albertini, "Methods for monitoring oxidative stress, lipid peroxidation and oxidation resistance of lipoproteins," *Clinica Chimica Acta*, vol. 306, no. 1-2, pp. 1–17, 2001.

[9] R. Paroni, F. Ceriotti, R. Galanello et al., "Performance characteristics and clinical utility of an enzymatic method for the measurement of glycated albumin in plasma," *Clinical Biochemistry*, vol. 40, no. 18, pp. 1398–1405, 2007.

[10] P. Faure, P. Corticelli, M. J. Richard et al., "Lipid peroxidation and trace element status in diabetic ketotic patients: influence of insulin therapy," *Clinical Chemistry*, vol. 39, no. 5, pp. 789–793, 1993.

[11] E. Velazquez, P. H. Winocour, P. Kesteven, K. G. M. M. Alberti, and M. F. Laker, "Relation of lipid peroxides to macrovascular disease in type 2 diabetes," *Diabetic Medicine*, vol. 8, no. 8, pp. 752–758, 1991.

[12] A. A. Meltzer and J. E. Everhart, "Association between diabetes and elevated serum alanine aminotransferase activity among Mexican Americans," *American Journal of Epidemiology*, vol. 146, no. 7, pp. 565–571, 1997.

[13] J. E. Everhart, "Digestive diseases and diabetes," in *Diabetes in America*, pp. 631–659, National Institutes of Health. National Institute of Diabetes and Digestive and Kidney Diseases, GPO, Washington, DC, USA, 2nd edition, 1995.

[14] Y. Miyake, H. Eguchi, K. Shinchi, T. Oda, S. Sasazuki, and S. Kono, "Glucose intolerance and serum aminotransferase activities in Japanese men," *Journal of Hepatology*, vol. 38, no. 1, pp. 18–23, 2003.

[15] I. J. Perry, S. G. Wannamethee, and A. G. Shaper, "Prospective study of serum γ-glutamyltransferase and risk of NIDDM," *Diabetes Care*, vol. 21, no. 5, pp. 732–737, 1998.

[16] S. R. Fagiuoli and D. H. van Thiel, "The liver in endocrine disorders," in *The Liver in Systemic Disease*, V. K. Rustgi and D. H. van Thiel, Eds., pp. 285–301, Raven Press, New York, NY, USA, 1993.

[17] G. Targher and C. D. Byrne, "Diagnosis and management of nonalcoholic fatty liver disease and its hemostatic/thrombotic and vascular complications," *Seminars in Thrombosis and Hemostasis*, vol. 39, no. 2, pp. 214–228, 2013.

[18] S. Costantini, F. Capone, E. Guerriero et al., "Cytokinome profile of patients with type 2 diabetes and/or chronic hepatitis C infection," *PLoS One*, vol. 7, no. 6, Article ID e39486, 2012.

[19] L. Cimino, G. Oriani, A. D'Arienzo et al., "Interactions between metabolic disorders [diabetes, gallstones, and dyslipidaemia] and the progression of chronic hepatitis C virus infection to cirrhosis and hepatocellular carcinoma. A cross-sectional multicentre survey," *Digestive and Liver Disease*, vol. 33, no. 3, pp. 240–246, 2001.

[20] W. Youssef and A. J. McCullough, "Diabetes mellitus, obesity, and hepatic steatosis," *Seminars in Gastrointestinal Disease*, vol. 13, no. 1, pp. 17–30, 2002.

[21] R. Hernández-Muñoz, W. Glender, M. Díaz-Muñoz, J. A. García-Sáinz, and V. Chagoya de Sánchez, "Effects of adenosine on liver cell damage induced by carbon tetrachloride," *Biochemical Pharmacology*, vol. 33, no. 16, pp. 2599–2604, 1984.

[22] M. K. Gaitonde, "A spectrophotometric method for the direct determination of cysteine in the presence of other naturally occurring amino acids," *Biochemical Journal*, vol. 104, no. 2, pp. 627–633, 1967.

[23] L. C. Green, D. A. Wagner, J. Glogowski, P. L. Skipper, J. S. Wishnok, and S. R. Tannenbaum, "Analysis of nitrate, nitrite, and [^{15}N]nitrate in biological fluids," *Analytical Biochemistry*, vol. 126, no. 1, pp. 131–138, 1982.

[24] I. Aguilar-Delfín, F. López-Barrera, and R. Hernández-Muñoz, "Selective enhancement of lipid peroxidation in plasma membrane in two experimental models of liver regeneration: partial hepatectomy and acute CCl_4 administration," *Hepatology*, vol. 24, no. 3, pp. 657–662, 1996.

[25] R. L. Levine, D. Garland, C. N. Oliver et al., "Determination of carbonyl content in oxidatively modified proteins," *Methods in Enzymology*, vol. 186, pp. 464–478, 1990.

[26] R. Hernández-Muñoz, E. Baraona, I. Blacksberg, and C. S. Lieber, "Characterization of the increased binding of acetaldehyde to red blood cells in alcoholics," *Alcoholism: Clinical and Experimental Research*, vol. 13, no. 5, pp. 654–659, 1989.

[27] D. J. Chiang, M. T. Pritchard, and L. E. Nagy, "Obesity, diabetes mellitus, and liver fibrosis," *American Journal of Physiology*, vol. 300, no. 5, pp. G697–G702, 2011.

[28] M. Malaguarnera, M. di Rosa, F. Nicoletti, and L. Malaguarnera, "Molecular mechanisms involved in NAFLD progression," *Journal of Molecular Medicine*, vol. 87, no. 7, pp. 679–695, 2009.

[29] J. Jou, S. S. Choi, and A. M. Diehl, "Mechanisms of disease progression in nonalcoholic fatty liver disease," *Seminars in Liver Disease*, vol. 28, no. 4, pp. 370–379, 2008.

[30] E. Birben, U. M. Sahiner, C. Sackesen, S. Erzurum, and O. Kalayci, "Oxidative stress and antioxidant defense," *World Allergy Organization Journal*, vol. 5, no. 1, pp. 9–19, 2012.

[31] G. L. Booth, M. K. Kapral, K. Fung, and J. V. Tu, "Relation between age and cardiovascular disease in men and women with diabetes compared with non-diabetic people: a population-based retrospective cohort study," *The Lancet*, vol. 368, no. 9529, pp. 29–36, 2006.

[32] G. M. Siu and H. H. Draper, "Metabolism of malonaldehyde in vivo and in vitro," *Lipids*, vol. 17, no. 5, pp. 349–355, 1982.

[33] A. W. Girotti, "Mechanisms of lipid peroxidation," *Journal of Free Radicals in Biology and Medicine*, vol. 1, no. 2, pp. 87–95, 1985.

[34] F. J. Kelly and I. S. Mudway, "Protein oxidation at the air-lung interface," *Amino Acids*, vol. 25, no. 3-4, pp. 375–396, 2003.

[35] J. Lyons, A. Rauh-Pfeiffer, Y. M. Yu et al., "Blood glutathione synthesis rates in healthy adults receiving a sulfur amino acid-free diet," *Proceedings of the National Academy of Sciences of the United States of America*, vol. 97, no. 10, pp. 5071–5076, 2000.

[36] S. C. Lu, "Regulation of glutathione synthesis," *Current Topics in Cellular Regulation*, vol. 36, pp. 95–116, 2001.

[37] D. M. Townsend, K. D. Tew, and H. Tapiero, "The importance of glutathione in human disease," *Biomedicine and Pharmacotherapy*, vol. 57, no. 3, pp. 145–155, 2003.

[38] C. Loguercio, C. del Vecchio Blanco, M. Coltorti, and G. Nardi, "Alteration of erythrocyte glutathione, cysteine and glutathione synthetase in alcoholic and non-alcoholic cirrhosis," *Scandinavian Journal of Clinical and Laboratory Investigation*, vol. 52, no. 3, pp. 207–213, 1992.

[39] S. Srinivasan, M. E. Hatley, D. T. Bolick et al., "Hyperglycaemia-induced superoxide production decreases eNOS expression via AP-1 activation in aortic endothelial cells," *Diabetologia*, vol. 47, no. 10, pp. 1727–1734, 2004.

[40] V. Shah, M. Toruner, F. Haddad et al., "Impaired endothelial nitric oxide synthase activity associated with enhanced caveolin binding in experimental cirrhosis in the rat," *Gastroenterology*, vol. 117, no. 5, pp. 1222–1228, 1999.

[41] V. Shah, S. Cao, H. Hendrickson, J. Yao, and Z. S. Katusic, "Regulation of hepatic eNOS by caveolin and calmodulin after bile duct ligation in rats," *American Journal of Physiology*, vol. 280, no. 6, pp. G1209–G1216, 2001.

[42] J. Baranska, "Mechanism of the ATP-dependent phosphatidylserine synthesis in liver subcellular fractions," *FEBS Letters*, vol. 256, no. 1-2, pp. 33–37, 1989.

[43] D. R. Voelker, "Phosphatidylserine translocation to the mitochondrion is an ATP-dependent process in permeabilized animal cells," *Proceedings of the National Academy of Sciences of the United States of America*, vol. 86, no. 24, pp. 9921–9925, 1989.

[44] M. Shinitzky and M. Inbar, "Difference in microviscosity induced by different cholesterol levels in the surface membrane lipid layer of normal lymphocytes and malignant lymphoma cells," *Journal of Molecular Biology*, vol. 85, no. 4, pp. 603–615, 1974.

[45] W. J. van Blitterswijk, R. P. van Hoeven, and B. W. van der Meer, "Lipid structural order parameters (reciprocal of fluidity) in biomembranes derived from steady-state fluorescence polarization measurements," *Biochimica et Biophysica Acta*, vol. 644, no. 2, pp. 323–332, 1981.

[46] K. H. Williams, N. A. Shackel, M. D. Gorrell, S. V. McLennan, and S. M. Twigg, "Diabetes and nonalcoholic fatty liver disease: a pathogenic duo," *Endocrine Reviews*, vol. 34, no. 1, pp. 84–129, 2013.

[47] T. M. Davis, K. E. Peters, D. G. Bruce, and W. A. Davis, "Prevalence, incidence, and prognosis of hepatobiliary disease in community-based patients with type 2 diabetes: the Fremantle Diabetes Study," *The Journal of Clinical Endocrinology & Metabolism*, vol. 97, pp. 1581–1588, 2012.

[48] I. J. Hickman and G. A. Macdonald, "Impact of diabetes on the severity of liver disease," *American Journal of Medicine*, vol. 120, no. 10, pp. 829–834, 2007.

[49] H. Knobler and A. Schattner, "TNF-α, chronic hepatitis C and diabetes: a novel triad," *QJM*, vol. 98, no. 1, pp. 1–6, 2005.

[50] S. Kuriyama, Y. Miwa, H. Fukushima et al., "Prevalence of diabetes and incidence of angiopathy in patients with chronic viral liver disease," *Journal of Clinical Biochemistry and Nutrition*, vol. 40, no. 2, pp. 116–122, 2007.

[51] J. O. Jáquez-Quintana, D. García-Compean, J. A. González-González et al., "The impact of diabetes mellitus in mortality of patients with compensated liver cirrhosis—a prospective study," *Annals of Hepatology*, vol. 10, no. 1, pp. 56–62, 2011.

[52] F. Fujiwara, M. Ishii, H. Taneichi et al., "Low incidence of vascular complications in patients with diabetes mellitus associated with liver cirrhosis as compared with type 2 diabetes mellitus," *Tohoku Journal of Experimental Medicine*, vol. 205, no. 4, pp. 327–334, 2005.

[53] P. Loria, A. Lonardo, and F. Anania, "Liver and diabetes. A vicious circle," *Hepatology Research*, vol. 43, pp. 51–64, 2013.

Hindawi Publishing Corporation
Oxidative Medicine and Cellular Longevity
Volume 2013, Article ID 462361, 18 pages
http://dx.doi.org/10.1155/2013/462361

Review Article

NADPH Oxidase as a Therapeutic Target for Oxalate Induced Injury in Kidneys

Sunil Joshi,[1] Ammon B. Peck,[2] and Saeed R. Khan[1,3]

[1] *Department of Pathology, Immunology & Laboratory Medicine, University of Florida College of Medicine, Gainesville, FL 32610, USA*
[2] *Department of Infectious Diseases & Pathology, University of Florida College of Veterinary Medicine, Gainesville, FL 32610, USA*
[3] *Department of Urology, University of Florida College of Medicine, Gainesville, FL 32610, USA*

Correspondence should be addressed to Saeed R. Khan; khan@pathology.ufl.edu

Received 9 February 2013; Accepted 14 May 2013

Academic Editor: Kota V. Ramana

A major role of the nicotinamide adenine dinucleotide phosphate (NADPH) oxidase family of enzymes is to catalyze the production of superoxides and other reactive oxygen species (ROS). These ROS, in turn, play a key role as messengers in cell signal transduction and cell cycling, but when they are produced in excess they can lead to oxidative stress (OS). Oxidative stress in the kidneys is now considered a major cause of renal injury and inflammation, giving rise to a variety of pathological disorders. In this review, we discuss the putative role of oxalate in producing oxidative stress via the production of reactive oxygen species by isoforms of NADPH oxidases expressed in different cellular locations of the kidneys. Most renal cells produce ROS, and recent data indicate a direct correlation between upregulated gene expressions of NADPH oxidase, ROS, and inflammation. Renal tissue expression of multiple NADPH oxidase isoforms most likely will impact the future use of different antioxidants and NADPH oxidase inhibitors to minimize OS and renal tissue injury in hyperoxaluria-induced kidney stone disease.

1. Introduction

In this review, we aim at focusing on the putative role of oxalate ($C_2O_4^{2-}$) leading to oxidative stress (OS) by production of reactive oxygen species (ROS) via different isoforms of nicotinamide adenine dinucleotide phosphate (NADPH) oxidase present in the kidneys. First, we provide a background of different types of hyperoxaluria and address the factors involved in oxalate and calcium-oxalate (CaOx-) induced injury in the kidneys. Second, we aim at addressing the role and different types of ROS and other free radicals, which when overproduced lead to OS and a brief description of different markers in the kidney which increase during OS. Third, we discuss the different isoforms of NADPH oxidase, their location, function, and expression in different cell types. Fourth, we address the pathophysiological role of NADPH oxidase in the kidneys and the regulation of NADPH oxidase (NOX enzymes). Finally, we discuss the role of antioxidants used for renal treatment and the different NADPH oxidase inhibitors involved in blocking NADPH oxidase from catalyzing production of superoxide with a potential of reducing OS and injury in the kidneys.

Oxalate, the conjugate base of oxalic acid ($C_2H_2O_4$), is a naturally occurring product of metabolism that at high concentrations can cause death in animals and less frequently in humans due to its corrosive effects on cells and tissues [1]. It is a common ingredient in plant foods, such as nuts, fruits, vegetables, grains, and legumes, and is present in the form of salts and esters [2–4]. Oxalate can combine with a variety of cations such as sodium, magnesium, potassium and calcium to form sodium oxalate, magnesium oxalate, potassium oxalate, and calcium oxalate, respectively. Of all the above oxalates, calcium oxalate is the most insoluble in water, whereas all others are reasonably soluble [5]. In normal proportions, it is harmlessly excreted from the body via the kidneys through glomerular filtration and secretion from the tubules [6, 7]. Oxalate, at higher concentrations, leads to various pathological disorders such as hyperoxaluria, nephrolithiasis (formation and accumulation of CaOx crystals in the kidney), and nephrocalcinosis (renal

calcifications) [1, 5, 8, 9]. Hyperoxaluria is considered to be the major risk factor for CaOx type of stones [10] with nearly 75% of all kidney stones composed of CaOx [9]. These CaOx crystals, when formed, can be either excreted in the urine or retained in different parts of the urinary tract, leading to blockage of the renal tubules, injury to different kinds of cells in the glomerular, tubular and intestinal compartments of the kidney, and disruption of cellular functions that result in kidney injury and inflammation, decreased and impaired renal function [11, 12], and end-stage renal disease (ESRD) [13, 14]. Excessive excretion of oxalate in the urine is known as hyperoxaluria and a significant number of individuals with chronic hyperoxaluria often have CaOx kidney stones. Dependent on food intake, a normal healthy individual is expected to have a regular urinary oxalate excretion somewhere between 10–40 mg/24 h (0.1–0.45 mmol/24 h). Anything over 40–45 mg/24 h (0.45–0.5 mmol/24 h) is regarded as clinical hyperoxaluria [15, 16]. Hyperoxaluria can be commonly classified into three types: primary, secondary, and idiopathic. Primary hyperoxaluria in humans is generally due to a genetic defect caused by a mutation in a gene and can be further subdivided into three subgroups, type I–III. It is inherited in an autosomal recessive pattern and results in increased oxalate synthesis due to disorders of glyoxalate metabolism. There is inability to remove glyoxylate. Primary hyperoxaluria type I (PH I) is the most abundant of the three subgroups of primary hyperoxaluria (70–80%) [13], caused by the incorrect sorting of hepatic enzyme alanine-glyoxylate aminotransferase (AGT) to the endosomes instead of the peroxisomes. AGT function is dependent on pyridoxal phosphate protein and converts glyoxalate to glycine. Owing to deficiency of AGT in PH I cases, glyoxalate is alternatively reduced to glycolate and oxidized to oxalate. In some cases of PH I, AGT is present but is misdirected to mitochondria where it remains in an inactive state. The metabolic defect of PH I is restricted to liver peroxisomes and the AGT fails to detoxify glyoxalate in the peroxisomes. Primary hyperoxaluria type II (PH II) results from the scarcity of hepatic enzyme glyoxylate reductase/hydroxypyruvate reductase (GRHPR) activity normally found in the cytosol. In studies, different cohorts have shown concentrations of urinary oxalate excretion between 88–352 mg/24 h (1–4 mmol/24 h) for PH I and 88–176 mg/24 h (1-2 mmol/24 h) for PH II [13, 17, 18]. In some cases, there is natural occurrence of AGT and GRHPR activities, but still there may be PH type III due to anion exchanger SLC26A6 and mutations in DHDPSL [13, 19–21]. All three types of PH show symptoms from infant to adolescence stages, with a majority showing clinical symptoms at 5 years in PH I to 15 years in PH II, and during the neonatal years in PH III [18]. Approximately, 35% of patients with PH I may be unnoticed due to misinterpretation, lack or subtlety of the symptoms, until the onset of renal failure [13].

In contrast to primary hyperoxaluria, secondary hyperoxaluria appears to result from eating foods rich in high-oxalate levels or exposure to large amounts of oxalate/oxalate precursors. Regular daily oxalate consumption by Western populations varies highly from 44 to 351 mg/day (0.5–4 mmol/day) but may exceed 1000 mg/day (11.4 mmol/day) when oxalate rich foods (e.g., spinach or rhubarb) are eaten in excess [3, 22–24]. Exceedingly high values of up to 2045 mg/day have also been reported due to consumption of seasonal foods consisting of purslane, pigweed, amaranth, and spinach [25]. There are different factors that affect dietary oxalate absorption such as oxalate bioavailability in the gut after it is consumed, number and accessibility of cations that attach to oxalate, such as calcium (Ca^{2+}) and magnesium (Mg^{2+}) in the gut, oxalate precursors and their effect on dietary oxalate, inherited absorption capacity, emptying of the gastrointestinal fluids, time taken for transit in the intestine, and the accessibility of oxalate degrading microorganisms such as *Oxalobacter formigenes* [15, 22–26]. A further subtype of hyperoxaluria is idiopathic hyperoxaluria which is spontaneous with unknown causes. Previous research has shown that idiopathic CaOx stone patients have the ability to absorb a greater quantity of oxalate as compared to normal individuals [27–29]. This may be true for why some autistic children have a high state of hyperoxaluria.

Previous studies have shown that dietary oxalate usually contributes just 10–20% of the urinary oxalate [9] but can be as high as ~50%, as oxalate is neither stored nor further metabolized inside the body [2]. Different studies have shown that foods rich in oxalate cause a transient state of hyperoxaluria, therefore difficult sometimes to detect in 24 h urinary samples [4, 30] Another mechanism for hyperoxaluria is fat malabsorption, also known as enteric hyperoxaluria. It can arise for two different reasons: (a) greater access of the mucous membrane in the intestine to oxalate caused by greater numbers of dihydroxy bile acids such as taurocholic and glycocholic acid and (b) interaction of fatty acids with calcium present in the lumen, augmenting the quantity of soluble oxalate when few insoluble CaOx complexes are formed [31]. This condition has been shown to be linked with bypass surgeries of small distal bowel or resections and other pathophysiological disorders in which grave steatorrhea occurs, for example, in pancreatic insufficiency and celiac spruce in both children and adults. Furthermore, patients who have had jejunoileal bypass surgery also tend to have higher rate of occurrence of enteric hyperoxaluria. Additional reasons for malabsorption include biliary obstruction, overgrowth of bacteria, and blind loop syndrome [31].

2. Oxalate and Calcium Oxalate Induced Injury

Studies have shown that oxalate and calcium oxalate cause renal injury leading to inflammation and other pathophysiological conditions in the kidneys [32–35]. Oxalate levels in the urine crosses the supersaturation limits, causing crystallization of CaOx, calcium oxalate monohydrate (COM) deposition in the renal cells and tissues that leads to damage that ultimately results in end-stage renal failure [35]. Many studies have shown that oxalate and CaOx crystals lead to death of cells in *in vitro* analyses [32, 36, 37].

Oxalate ions are generated in the liver by glyoxalate metabolism, but due to low solubility they are carried at low concentrations in the plasma membrane [38]. Previous

studies have shown that oxalate is quickly taken up by proximal tubule cells and high concentration of oxalate can be excreted in urine by the secretary pathway [39, 40]. The major pathway of oxalate excretion from the body is via urinary excretion; however, a study in rats has shown that large quantities of oxalate can also be removed by the gastrointestinal system when there is kidney failure [41].

It is now well known that CaOx crystals cause injury to cells and tissues by causing damage to cell membranes, production of lipid mediators (prostaglandins, leukotrienes), and excessive production of reactive oxygen species, all of which lead to an imbalance between oxidants and antioxidants, with malfunctioning of mitochondria [42, 43]. Studies have shown that CaOx crystals induce the phosphatidylserine imbalance in the membrane and greater production of ceramide, signals of cell death [42–44]. CaOx also causes hemolysis of red blood cells [45] and CaOx crystal injury may also be due to abundant release of ROS and other free radicals produced from molecular oxygen which ultimately lead to oxidative stress. Our review provides an insight on oxalate- and CaOX-induced renal injury due to different types of ROS produced by numerous enzyme complexes and mitochondria with special focus on NADPH oxidases leading to oxidative stress.

3. Reactive Oxygen Species (ROS) and Oxidative Stress

Reactive oxygen species are chemically reactive molecules and free radicals generated from molecular oxygen that, if produced in excess, cause damage to tissues and different components of the cells. Yet, if produced in physiological balance, ROS have been shown to play a principle role in normal cell signal transduction pathways, including apoptosis, gene expression, and activation of different cell signaling cascades. They are produced by different constitutively active oxidases such as NADPH oxidase, xanthine oxidase, lipoxygenase, cyclooxygenase, hemeoxygenase, and in the electron transport chain of mitochondria during cellular respiration [1, 46]. Major cellular ROS include the superoxide anion ($O_2^{-\bullet}$), nitric oxide radical ($NO^{\bullet}$), hydroxyl radical ($OH^{\bullet}$), and hydrogen peroxide (H_2O_2), all of which are produced by different signaling pathways [1, 46]. The superoxide anion, precursor of the more powerful and complex oxidants, is mainly produced by the respiratory burst of phagocytes which is regarded as the most significant free-radical generator *in vivo* [47]. These ROS may react with chemicals and enzymes to generate additional oxidative species or become ineffective by nonenzymatic and enzymatic intercellular and intracellular reactions [48]. $O_2^{-\bullet}$ reacts with nitric oxide (NO) to produce peroxynitrite ($ONOO^-$) which is a highly reactive and toxic nitrogen-containing species which nitrates proteins causing nitrative stress, augment platelet aggregation and vasoconstriction of the blood vessels [49]. Due to this reaction, there is diminished bioavailability of NO, a cell-to-cell messenger, and this causes beneficial effects such as decreasing blood pressure [50]. Superoxide is highly reactive, has a short half-life, cannot cross the cell membrane, and is therefore acted on by the scavenging enzyme, superoxide dismutase (SOD), which converts it to hydrogen peroxide (H_2O_2). Hydrogen peroxide is more stable as compared to superoxide and it diffuses though the lipid bilayer. Hydrogen peroxide (H_2O_2) is further acted on by another scavenging enzyme, catalase (CAT), which neutralizes it to water and oxygen (Figure 1). In a metal catalyzed reaction, called the Haber-Weiss reaction, hydrogen peroxide yields a short-lived, short-ranged, and more reactive hydroxyl radical. Also, in the presence of Fe^{2+}, a highly reactive hydroxyl radical ($OH^{\bullet}$), is formed (Fenton reaction). Hydrogen peroxide, after oxidation by myeloperoxidase, gives rise to another extremely reactive oxygen species, hypochlorous acid (HOCl). Hypochlorous acid is a powerful oxidizing agent which is known to alter lipid structure and function, other membranous components of the cells and proteoglycans. It acts on thiol groups of membranous proteins and is known to cause chlorinative stress [49]. Studies have shown that hypochlorous acid, along with hypobromous acid (HOBr), and hypothiocyanous acids (HOSCN) have a role in antimicrobial defense by neutrophils [48, 51]. These reactive oxygen species under normal conditions function as mediators in different cell signaling and regulatory pathways involving growth and proliferation, activation or inhibition of different molecules and in regulating different transcriptional activities. Signaling molecules that are controlled by these ROS include phosphatases, Ras, phospholipases, calcium signals, serine/theonine kinases and protein tyrosine kinases. ROS also regulate different nuclear factors such as nuclear factor-κB (NFκB), transcription factor activation protein-1 (AP-1), and different genes such as *c-myc, c-fos*, and *c-jun* (1). ROS are also involved in initiation and implementation of programmed cell death (apoptosis). Under normal conditions, these ROS and reactive nitrogen species (RNS) are present at equilibrium with other antioxidants and are only generated when required and then vigorously removed by various scavenging enzymes and antioxidants. They play significant regulatory roles in various physiological processes, including innate immunity, modulation of redox-dependant signaling pathways, and as cofactors in the production of hormones.

ROS, when overproduced, can lead to oxidative stress. The majority of cells respond by increasing the levels of intracellular levels of antioxidants, but an excess of oxidants within a biological system leads to a change in the redox state, towards one that is more oxidizing [52, 53]. Oxidative stress or abundance of ROS causes permanent damage to macromolecules and also causes interference in the important redox-dependant signaling processes [54]. Oxidative stress causes disruption of the nitric oxide (NO) signaling pathway [55]. NO has anti-inflammatory and vasodilator functions, but under excessive ROS, gets converted to peroxynitrite [56, 57], a powerful oxidant that causes oxidation of small-molecule antioxidants such as glutathione, cysteine, and tetrahydrobiopterin [58]. Limited presence of tetrahydrobiopterin leads to uncoupling of endothelial nitric oxide synthase (eNOS), which in turn changes this enzyme from an NO-producing, vasoprotective enzyme to a superoxide-producing, oxidative stress enzyme [59, 60]. Peroxynitrite is

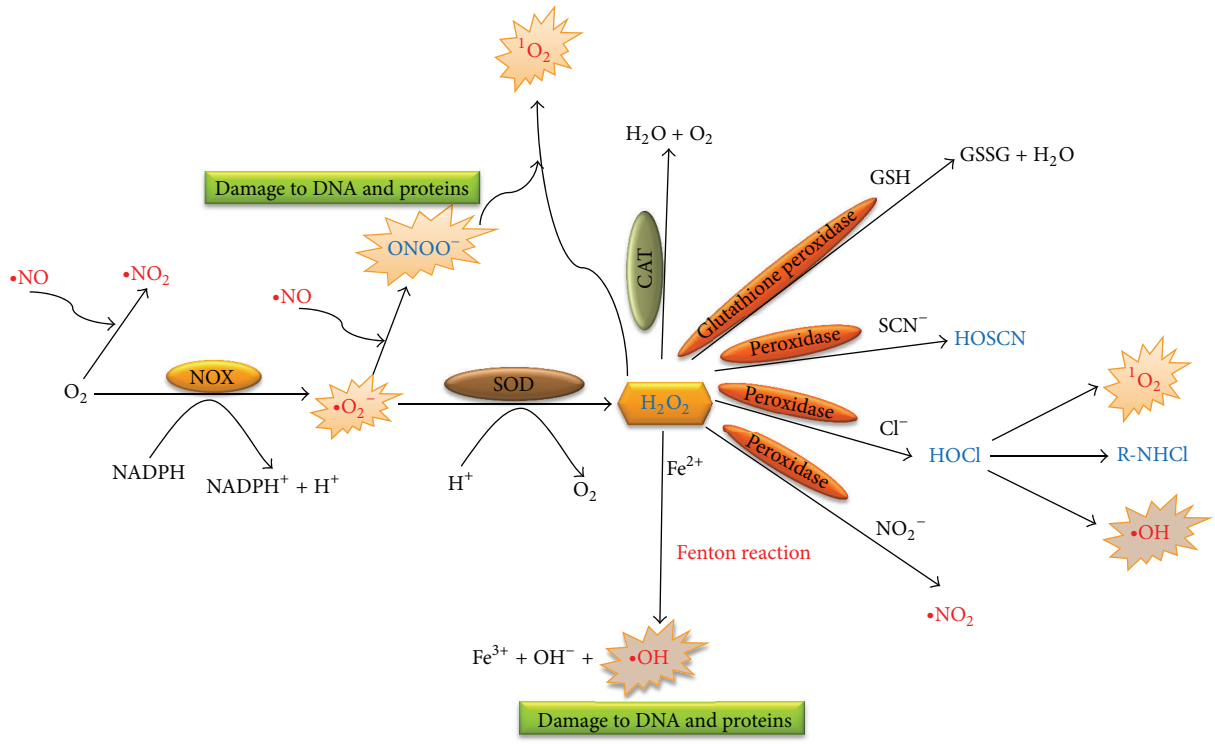

Figure 1: Production of ROS and different reactions. ROS with 1 free electron are shown in red and 2 free electrons are shown in blue. ROS, when produced in excess, cause damage to different components of the cell. Excess production of hydrogen peroxide (H_2O_2) and peroxynitrite ($ONOO^-$) leads to the production of singlet oxygen ($^1O_2$). The other radicals shown in the figure are superoxide ($\bullet O_2^-$), nitric oxide (•NO), nitrogen dioxide ($\bullet NO_2$), hydroxyl radical (•OH), glutathione (GSH), glutathione disulphide (GSSG), thiocyanate (SCN^-), hypothiocyanous acid (HOSCN), hypochlorous acid (HOCl), and chroramine (R-NHCl). Figure modified from [1, 46].

very harmful and can hinder the activity or totally deactivate useful antioxidant enzymes such as superoxide dismutase, glutaredoxin, and glutathione reductase [58]. Peroxynitrite causes oxidation of the zinc thiolate center of NO synthase resulting in decreased formation of NO [61]. Decrease in NO can lead to increase in inflammation and remodeling of different biomolecules. Research has shown that ROS cause change in confirmation due to oxidation of proteins, such as kinases and phosphatases, and activation of nuclear factor-κB (NFκB) which play important roles in the regulation of immune response to infection [62]. NFκB is mainly involved in transcription where incorrect regulation can lead to inflammation, cancer, and autoimmune diseases. Activation of NFκB also leads to expression of adhesion molecules such as ICAM-1 (intercellular cell adhesion molecule-1), VCAM-1 (vascular cell adhesion molecule-1), and E selectin on the endothelium [63]. NFκB activation also leads to proliferation and migration of vascular smooth muscle cells [64]. In this regard, ROS are also known to excite different cytosolic molecular complexes known as inflammasomes that have enzymatic activity mediated by the activation of caspase-1. Inflamasomes are involved in maturation and cleavage of cytokines such as IL-1β which is involved in inflammatory response [65].

There are a variety of markers in the kidneys which increase during oxidative stress. These include an increase in renal excretion of lipid peroxidation markers, but this increase in renal excretion is not a proof of increased ROS. Research has shown that there is greater excretion of 8-Isoprostane, $PGF_{2\alpha}$, and malondialdehyde (MDA) by long-time infusion of ANG II in rats [66, 67]. Also one study has shown that animals secrete significantly higher amounts of thiobarbituric acid reactive substances (TBARS) in the urine, generated as a byproduct of lipid peroxidation and an indication of oxidative stress in the kidneys [68]. The presence of α-glutathione S-transferase (α-GST) in the urine of animals was also shown to be an indication of oxidative stress in the kidneys [68]. Oxidative stress is due to excessive production of ROS or reduction in antioxidants leading to production of free radicals that are injurious to all components of the cell including proteins, lipids, and DNA. Oxidative stress also leads to interruption in the normal signaling processes. *β-galactosidase* (GAL) and N-*acetyl-β-glucosaminidase* (NAG), both markers of renal epithelial injury, also showed increased excretion in the urine [69]. Previous research has also shown greater urinary MDA, plasma MDA, and urinary NAG activity but diminished glutathione (GSH), cellular glutathione peroxidase (cGPx), protein thiol, and vitamin E activity observed in patients diagnosed with kidney stones which showed decreased urinary MDA, plasma MDA, and increased vitamin E after supplementation with potassium citrate (60 mEq/day for 1 month) [1]. There is also an increase

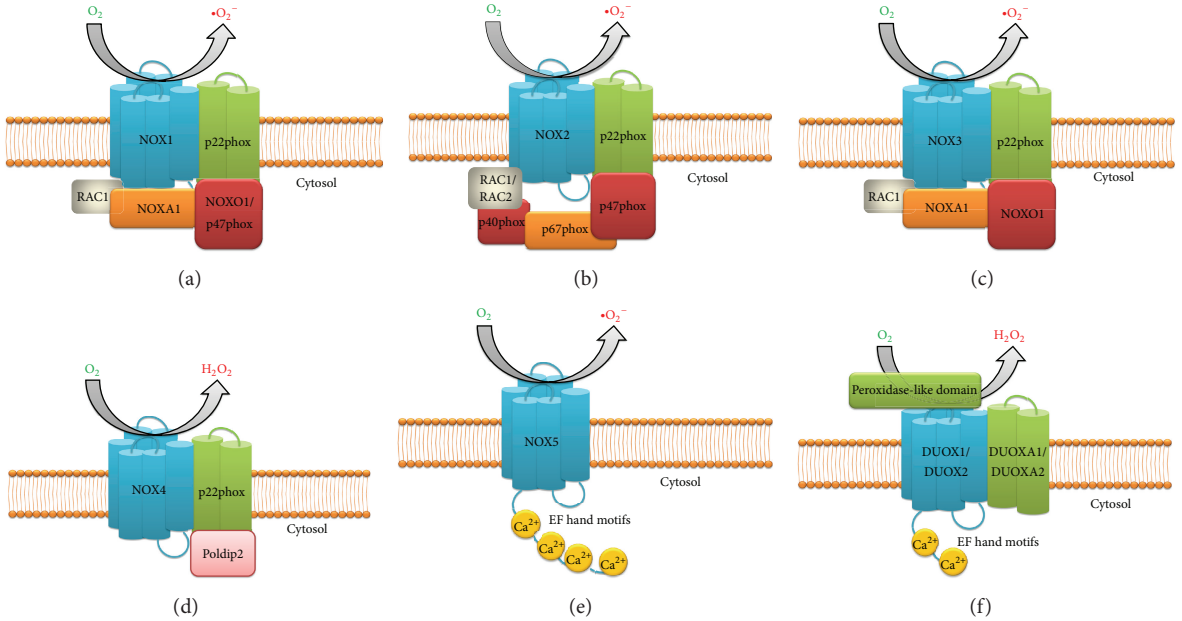

FIGURE 2: Seven different NOX isoforms-NADPH oxidase complexes. NOX isoform expression is relatively regulated at different transcriptional, post-transcriptional and translational levels under certain pathophysiological conditions. Most of the NOX isoforms have structural similarities to NOX2, with maximum in NOX3. NOX4 is most abundant in the kidneys in various kinds of cells. NOX4 is known to be constitutively active and do not require any subunits. NOX5 is directly activated by calcium. The core subunits of all the complexes (NOX1-NOX5, DUOX1/DUOX2) are shown in blue; their membrane bound subunits (p22phox, DUOXA1 and DUOXA2) are shown in green; the cytosolic subunits which acts as organizers (p40phox, NOXO1 and p47phox) are shown in red; activator subunits of NADPH oxidase complexes present in the cytosol (p67phox and NOXA1) are shown in orange; small GTPases (RAC1 and RAC2) are shown in grey; EF hand motifs are shown in yellow which bind with calcium to regulate the activity of NOX5, DUOX1 and DUOX2 (see text for details).

in the ROS-dependant products such as an increase in the renal nitrotyrosine immunoreactivity in kidneys of SHR [70], 2k, 1C rats [71]. Also, it is possible to take direct measurements of ROS such as superoxide production in the medulla [72] and the production of H_2O_2 by an ANG type 1 receptor-dependant mechanism in rats which helps us estimate the degree of oxidative imbalance in the kidneys [73]. These abovementioned markers provide an estimate of OS and renal injury but further studies and validation of all markers of OS would greatly augment our understanding of the role OS plays in causing renal injury.

4. Isoforms of NADPH Oxidase

To date, seven different isoforms of NADPH oxidase have been described. These are NADPH oxidase 1 (NOX1), NADPH oxidase 2 (NOX2), NADPH oxidase 3 (NOX3), NADPH oxidase 4 (NOX4), NADPH oxidase 5 (NOX5), Dual oxidase 1 (DUOX1), and Dual oxidase 2 (DUOX2). These isoforms are comprised of different core catalytic subunits: p22phox, p47phox, p67phox, p40phox, DUOX activator 1 (DUOXA1), DUOX activator 2 (DUOXA2), NOX activator 1 (NOXA1), and NOX organizer 1 (NOXO1) (Figure 2). These regulatory subunits are involved in different functions. While p22phox, DUOXA1, and DUOXA2 are responsible for the growth and expression of the NOX and DUOX core units in biological membranes, P67phox, and NOXA1 are involved in enzyme activation and p40phox, p47phox, and NOXO1 in the spatial organization of different subunits of the enzyme [74]. RAC1 and RAC2 (small GTPases) may also be involved in the activation in some isoforms of NADPH oxidase, *per se*. Most of the isoforms generate superoxide except NOX4, DUOX1, and DUOX2 oxidases which directly generate H_2O_2 [75, 76]. NOX2 or gp91phox (91-kDa glycoprotein), previously known as mitogenic oxidase 1 (mox-1), along with p22phox (22-kDa protein) forms the two components of flavocytochrome b_{558}, a heterodimeric integral membrane protein [77]. NOX2 is a catalytic subunit which produces superoxide and is a protein which consists of six transmembrane domains with cytosolic C- and N-terminus [78]. Studies have shown that NOX2 has highest structural similarity with NOX3 (58%), followed by NOX1 (56%). NOX4 and NOX5 are remotely associated with NOX2 showing around 37% and 30% resemblance, respectively [77]. NOX5 has more structural similarity with the DUOX's subunits as they all have EF hand motifs (calcium-binding motifs) [77]. NOX1 isoform has been shown to be concerned with redox-dependent cell signaling and regulation of gene expression [79] and is mainly expressed in the colon epithelial cells [80]. However, other studies have shown NOX1 to be present in vascular smooth muscle cells (VSMC), sinusoidal endothelial cells, uterus, prostate, osteoclasts, placenta, retinal pericytes, and microglia [78]. NOX2 expression is well established in the phagocytes [81–83] but has also been observed in nonphagocytic cells such as neurons, hematopoietic stem cells, smooth muscle cells, endothelium, cardiomyocytes,

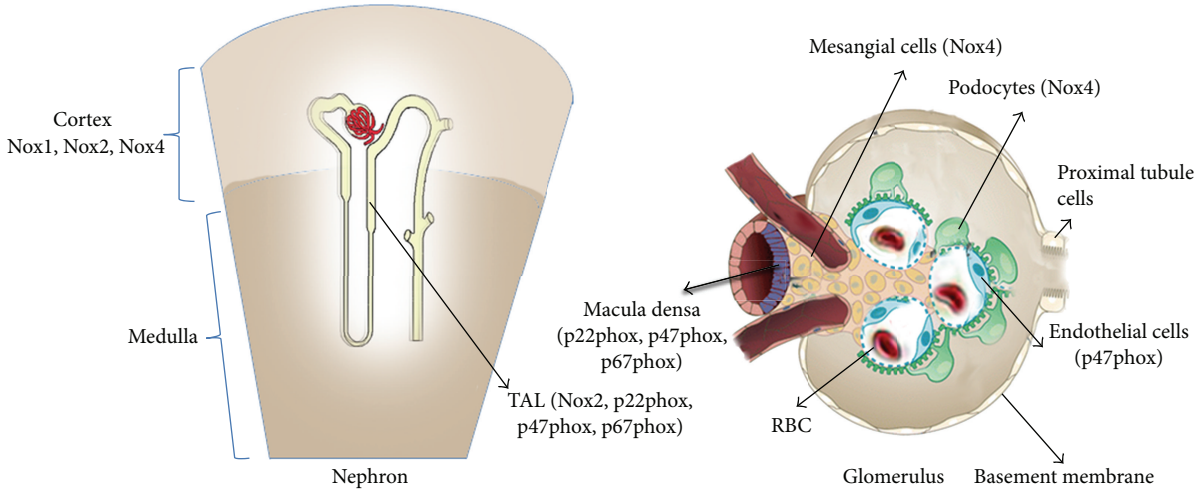

FIGURE 3: Different isoforms of NADPH oxidase complex present in different parts of the kidneys. The Nox isoforms expressed in the cortex and medulla as shown in the nephron and different cellular populations in the glomerulus (see text for details).

skeletal muscle cells, hepatocytes, and neutrophils [78, 81]. NOX3 isoform is known to be significantly expressed in the inner ear, fetal kidney, brain, and skull [84], while NOX3 has been shown to be favorably localized in cochlear and vestibular epithelial cells as well as spiral ganglion [78]. NOX4 isoform or renal NADPH oxidase (RENOX) is known to be highly expressed in the kidneys and is found in different cell types including neurons, smooth muscle cells, adipocytes, keratinocytes, hematopoietic stem cells, melanoma cells, fibroblasts, osteoclasts, and endothelial cells. NOX4 is the predominant isoform in the endothelial cells [85–88]. NOX5 isoform has been found in different parts of the body such as testis, vascular smooth muscles, ovaries, lymph nodes, myometrium, pancreas, spleen, and prostrate [89–91]. NOX5 has been involved in cell growth and thus far 5 subtypes, namely, NOX5α, β, δ, γ, and ε, have been found [89–92]. The other isoforms of NOX, DOUX1, and DOUX2 originally identified as thyroid oxidases have been extensively found in the thyroid [93], but also in prostate gland and airway epithelial cells. DUOX1 is expressed in bronchial and tracheal airway epithelial cells, whereas DUOX2 is found in epithelial cells of salivary glands, stomach, and brush border cells of various rectal glands such as caecum and sigmoidal colon [94]. All of these NOX isoforms play a significant role in the generation of ROS and oxidative stress. These enzymes are involved in many pathophysiological processes that are very crucial for different functions such as cellular signaling, regulation of gene expression, and cell differentiation.

5. NADPH Oxidases in the Kidney

Research has shown that NADPH oxidase in the kidneys may have a specific pathophysiological role; thus, it is present in different cellular compartments of the kidneys (Figure 3). The mammalian kidney consists of different cellular populations including mesangial cells, fenestrated endothelial cells, tubular epithelial cells of the proximal and distal nephron segments, glomerular podocytes, dendritic cells, and the cortical fibroblasts [95, 96]. Previous research has shown that the main supplier of ROS in the form of superoxide $O_2^{-\bullet}$ in the renal cortex is NADPH oxidase, whereas in the renal medulla xanthine oxidase also makes similar contribution to $O_2^{-\bullet}$ generation along with NADPH oxidase [97]. Different subunits of the NADPH oxidase have also been shown to be abundantly present in the macula densa (MD), thick ascending loop of henle (TAL), interstitial cells, blood vessels, glomeruli, and tubules in the kidneys of spontaneously hypertensive rats (SHR) [98]. Previous studies in the human glomerular mesangial cells (HMC) have recognized α and β subunits of cytochrome b_{558} and the 45-kDa flavoprotein [99]. Human glomerular mesangial cells produce ROS such as superoxide and express different NADPH oxidase subunits like p22phox, p67phox, and p47phox [100] and Nox4 [101, 102]. Studies have shown that the thick ascending loop of henle (TAL) in the outer medullary region expresses different NADPH oxidase subunits such as p40phox, p47phox, p22phox, and Nox2 [103]. Podocytes or visceral epithelial cells present around the capillaries of the glomerulus in the kidneys play a significant role in the functioning of the glomerular capillary wall. Research has shown the production of ROS in the cultured human podocytes and ROS was generated by NADPH oxidase and different subunits of NADPH oxidase such as p67phox, p47phox, Nox2, and p22phox were expressed in the podocytes, present in the glomerulus of the kidneys [104]. Nox4 has been shown as the most common Nox isoform to be expressed in the kidney epithelial cells [105, 106] and is distributed in the microvasculature, glomeruli, mesangial cells, and nephron segments [102, 105, 107]. Nox1, Nox2, and Nox4 have also been shown to be expressed in the renal cortex [66, 108]. Chabrashvili et al. have shown the expression of p67phox, p22phox, and p47phox in the renal cortex [66, 98]. The same group compartmentalized the NADPH oxidase subunits in the renal cortex to macula densa, specific nephron segments in the

TAL, cortical and medullary ducts, distal convoluted tubule, renal microvasculature and glomeruli [66, 98]. P47phox which is also known as neutrophil cytosol factor-1 (Ncf-1) was found to be present in the endothelium and glomerular podocytes and p22phox subunit in the renal interstitial fibroblasts [98]. These studies give us an insight on the role of different NADPH oxidase subunits found and expressed in various subcompartments of the kidneys, making NADPH oxidase complex as one of the most important contributor of oxidative stress in the kidneys.

6. Regulation of NADPH Oxidase (NOX Enzymes) Expression in the Kidney

It is now well accepted that a significant amount of ROS production in mammalian cells is derived from the NADPH oxidase (NOX) of phagocytes (Phox), especially neutrophils and macrophages that catalyze the respiratory burst (i.e., the production of large number of ROS and utilization of large amounts of O_2) [109]. Normally, the NADPH oxidase is nonfunctional but can be activated quickly when a cell comes in contact with different inflammatory biomolecules or microorganisms resulting in generation of ROS apart from mitochondrial production. Cytosolic NADPH oxidase is the electron donor for all the NADPH oxidase isoforms with molecular oxygen acting as the final electron acceptor. The electron transfer to molecular oxygen results in the release of superoxide from the oxidase enzyme in NOX1, NOX2, and NOX5 isoforms [110]. The other NOX isoforms such as NOX4, DUOX1, and DUOX2 oxidases do not directly release superoxide anion as their primary ROS; instead, they release hydrogen peroxide [75, 76]. The NADPH oxidase complex consists of the membrane subunits Nox2 (gp91phox) and p22phox along with the regulatory cytosolic subunits p67phox, p47phox, p40phox, and the small GTPases protein, RAC [111].

Research has shown that NADPH oxidase is activated by Ang II infusion in the rat kidneys leading to increased expression of p22phox and Nox1 in the renal cortex with concomitant reduction in the presence of Nox4 and SOD [66]. Also, high salt intake increased oxidative stress by increasing the expression of NOX2 and p47phox subunits and decreased SOD expression [108]. The prolonged effect of Angiotensin in the kidney has been shown to cause the activation of NADPH oxidase, enhanced expression of p22phox, and decrease in the scavenging enzyme SOD leading to renal cortical hypoxia, renal vasoconstriction, and hypertension [67]. The Nox1 subunit has been shown to be upregulated in the rat-cultured vascular smooth muscle cells (VSMC) by PDGF, Ang II, and serum [112], whereas research has shown downregulation of Nox4 in the kidney cortex by the infusion of Ang II [108]. Ang II has been shown to upregulate p67phox expression in rabbit periadventitial fibroblasts [113] and the mouse aorta [114]. These research findings provide a brief insight on the role of angiotensin on the different subunits of NADPH oxidase and the regulation of expression of NADPH oxidase in the kidneys.

7. Antioxidants for Renal Treatment

Antioxidants have been shown to reduce oxidative stress. Treating the kidneys with vitamin E (α-tocopherol) along with mannitol removed the chances of deposition of CaOx crystals in rat kidneys injected with sodium oxalate [115]. Furthermore, antioxidants such as methionine, combination of vitamin E plus selenium, and glutathione monoester subdued CaOx crystals in the hyperoxaluric rat kidneys [116–118]. However, recent studies have shown that it is not easy to remove oxidative stress with increased levels of antioxidants such as vitamin E in clinical trials [119–121]. These disparate observations cannot be regarded as proof against antioxidants as several clinical trials involved high risk patients in which the end-stage renal disease was quite advanced and doses of vitamin E differed greatly between trials. Antioxidant concentration is very critical in controlling oxidative stress because of the very high rate constants of the reactions between ROS and other molecules such as NO, certain amino acids, and nucleic acids. The reaction between NO and ROS happens at a rate of $1.9 \times 10^{10}\,M^{-1}\,S^{-1}$ which is 6 times faster in magnitude than the reaction between superoxide and vitamin E [122, 123]. Vitamin E in the body also faces a highly oxidizing environment one that can lead to rapid removal of reduced forms of antioxidants. It would seem that the best approach for reducing oxidative stress is by targeting the enzyme responsible for the generation of ROS, perhaps targeting NADPH oxidase by use of inhibitors of NADPH oxidase.

8. NADPH Oxidase Inhibitors

Identification of NADPH oxidase inhibitors is an ongoing active field, focused primarily on substances that obstruct a specific NADPH oxidase from catalyzing production of superoxide. NADPH oxidase inhibitors act through interference in the assembly of the NADPH oxidase complex by interacting with their subunits, blocking electron transfer decreasing production of ROS [124]. Table 1 lists a number of chemicals that alleviate oxidative stress through inhibiting ROS production by NADPH oxidases. In addition, Table 1 also describes the mode of action and pharmacologic effects of different peptide and nonpeptide inhibitors. These chemicals include, but are not limited to, Apocynin, diphenyleneiodonium chloride (DPI), pefabloc, proline-arginine rich antimicrobial peptide (PR-39), and new peptide inhibitors that have been developed to particularly target NADPH oxidases, such as gp91 ds-tat and novel nonpeptide VAS2870 [125]. The two most studied NADPH oxidase inhibitors are Apocynin and DPI. Apocynin, also known as 4-hydroxy-3-methoxy acetophenone or acetovanillone, is the best known inhibitor of NADPH oxidase to date. It was extracted from the roots of *Apocynum cannabinum* by Schmiedeberg in 1883 [126] and found to block the association of p47phox with membrane-bound p22phox subunit of the NADPH oxidase complex in leukocytes, monocytes, and endothelial cells and is also a scavenger of H_2O_2 [127]. At high concentration, it was shown to block Nox4, and Nox5 [128], making it more

Table 1: Inhibitors of NADPH oxidase.

Name	Mode of action	Pharmacological effects	References
Apocynin	NADPH oxidase complex assembly inhibitor: inhibits binding of p47phox with membrane bound p22phox	Scavenger of H_2O_2	[130–132]
DPI	Inhibitor of flavoprotein, takes electrons from FAD and prevents electron flow through the flavocytochrome channel	Inhibitor of NADH-ubiquinone oxidoreductase, NADH dehydrogenase, xanthine oxidase, cytochrome p450 oxidoreductase, NOS, and bacterial nicotine oxidase	[133–139]
AEBSF	Inhibits association of NOX2 subunit with p47phox. Prevents binding of p47phox and p67phox with cytochrome b559	Irreversible serine protease inhibitor	[140]
Plumbagin	Inhibits $O_2^{-\bullet}$ production in various cell lines expressing NOX4 oxidase; unknown mechanism	Naphthoquinone structure may confer ROS-scavenging effects	[141, 142]
PR-39	Inhibits p47phox from binding to p22phox subunit by cohering to SH3 domains of p47pphox	Non selective for NADPH oxidase	[143]
S17834	Flavonoid derivative proposed to directly inhibit NADPH oxidase activity, although the mechanism is undefined	None	[144]
VAS2870	Undefined mechanism: inhibits NADPH oxidase activity in NOX2 oxidase-containing HL-60 cell line and in vascular endothelial cells containing NOX2 and NOX4 oxidases; does not scavenge $O_2^{-\bullet}$	None	[145, 146]
Gp91dstat	Oxidase assembly inhibitor: inhibits association of Nox2 with p47phox. Does not scavenge superoxide generated by cell-free systems	None	[147, 148]
Statins	Decrease superoxide production by inhibiting synthesis of farnesylpyrophosphate and geranylgeranylpyrophosphate which are crucial for membrane attachment of Rac and NADPH oxidase assembly. May also decrease p22phox and Nox1 expression. Likely to influence Nox1 and Nox2 activities	HMG-CoA reductase inhibitor. Decreases AT1 receptor expression; increases eNOS expression, most effective for treating cardiovascular disease with questionable benefit in those without previous CVD but with elevated cholesterol levels	[149, 150]
AT1 receptor antagonists	Decrease Ang II-dependent activation of NADPH oxidase via AT1 receptors. Unlikely to display Nox selectivity as Ang II stimulates Nox1 and Nox4 oxidases	None. Controlling high blood pressure	[151]
Nebivolol	Inhibits membrane association and also interaction of p67phox and Rac and decreases oxidase expression. Inhibits Nox1-dependent superoxide production	β-adrenoceptor blocker, used in treatment of hypertension	[152–155]
Gliotoxin	A fungal metabolite, thiol-modifying toxin thought to inhibit phosphorylation of p47phox by preventing PKC colocalization with p47phox. Also, inhibits electron transport through the flavocytochrome before oxidase activation. Low potency for blocking Nox4	Stimulation of cGMP release. Cytoskeletal reorganization. Disrupts the mitochondrial membrane potential, possesses immunosuppressive properties, anti-inflammatory activity.	[75, 156–160]

Table 1: Continued.

Name	Mode of action	Pharmacological effects	References
Clostridium difficile toxin B	Glycosylation of threonine-35 on Rac, which modifies GTPases activity	Likely to inhibit all Rac-dependent protein activity. High toxicity, vascular permeability and inflammation	[161]
Nordihydroguaiaretic acid	Blocks H_2O_2 production in macrophages in response to phorbol esters and in endothelial cells in response to thrombin	Lipooxigenase inhibitor. Blocks arachidonic acid metabolism	[162–164]
SKF525A	Decreases superoxide and H_2O_2 production in endothelial cells	Cytochrome P450 inhibitor	[162, 165]
Metformin	Scavenges hydroxyl radicals but not superoxide. Could also inhibit PMA and Ang II-dependent ROS production from NADPH oxidase. However, this is likely to be due to inhibition of PKC activity	Antihyperglycemic agent. PKC inhibitor	[166–168]
Sildenafil-citrate	Inhibitor of endothelial superoxide production and gp91phox expression	Inhibits phosphodiesterase type 5. Nonselective and in direct inhibitor for NADPH oxidase isoforms. Have been shown to influence immune system due to changes in gp91phox expression	[169–172]
Bilirubin	Inhibitor of superoxide production. No effect on Nox2, p22phox and p47phox but may reduce p47phox phosphorylation	ROS scavenger	[173–175]
Minocycline	Downregulates p67phox expression. Inhibitor of superoxide generation in microglia and dopaminergic neurons in response to stimuli such as thrombin	Antibiotic	[176, 177]
Perhexiline	Inhibits superoxide production in intact neutrophils stimulated by fMLP or PMA. Mechanism unknown	Efficient antianginal agent that blocks carnitine-palmitoyl-transferase	[178, 179]
Roxithromycin	Inhibits superoxide generated by intact neutrophils activated by fMPL or PMA but not by cell lysates. No effect on PKC-dependent phosphorylation. May inhibit translocation of p47phox and/or p67phox	Macrolide antibiotic. Inhibit RNA-dependent protein synthesis. Efficient in blocking cytochrome P450	[180–182]
Taurine chloramines	Inhibits translocation of p47phox and p67phox to the membrane. Also inhibits phosphorylation of p47phox. Reversible inhibition of PMA-dependent superoxide anion production in human neutrophils	Blocks inducible NOS in alveolar macrophages	[183, 184]
Resveratrol	Reduces superoxide generation in intact macrophages and homogenates. Does not scavenge superoxide in cell-free systems	Inhibitor of PKC	[185–187]
Curcurmin	Reduces superoxide production in intact macrophages and homogenates. Does not scavenge superoxide in cell-free systems	Irreversible inhibitor of thioredoxin reductase via alkylation of cysteine residues	[185, 188]
Nitrolinoleate	Nitrated lipid which blocks PMA- and FMLP-dependent superoxide generation and degranulation in human neutrophils by enhancing cAMP but not cGMP levels	Also linked with increasing cAMP vasorelaxation	[189, 190]
Mycophenolate acid	Fungal derivative that blocks endothelial and neutrophil-derived superoxide by reducing Rac levels. Does not alter mRNA levels of Nox2, Nox4, and p47phox	Efficient inhibitor of inosine monophosphate dehydrogenase associated with purine synthesis in B and T lymphocytes	[191, 192]
GK-136901	Well known NOX1 and NOX4 oxidase inhibitor. Unknown mechanism, but structural similarity with NADPH suggests that it may act as a competitive substrate inhibitor of this enzyme	None	[193, 194]

Table 1: Continued.

Name	Mode of action	Pharmacological effects	References
ML171	Phenothiazine compound with selectivity for NOX1 oxidase (IC_{50} of 0.25 μM) over other NADPH oxidases (IC_{50} > 3 μM). Does not scavenge oxygen radicals generated by xanthine oxidase activity	None	[195]
Mastoparan	Inhibits superoxide production by neutrophil lysates most likely via interaction with N-terminal of p67phox	An amphiphilic cationic tetradecapeptide isolated from wasp venom. Has affinity towards SH3 domains. Also interact with G-proteins	[196–199]
Ghrelin	Blocks superoxide production by thoracic aorta most probably via release of NO. Does not scavenge superoxide	Capable of releasing growth hormone releasing peptide. Stimulates gastric acid secretion	[200–202]
Alpha tocopherol	Inhibitor of p67phox-p47phox translocation and p47phox phosphorylation in monocytes, neutrophils and microglial cells. This effect is likely to be due to PKC inhibition	ROS scavenger	[203–206]
Benzylisothiocyanate	Concentration-dependent. Inhibits TPA-induced superoxide production in a human leukemia cell line. Does not affect PKC activity and p47phox translocation. Mechanism may involve covalent cysteine modification of the NADPH oxidase	May inhibit NO, PGE2 and TNF-α production. Also known to cause apoptosis via induction of Bak and Bax proteins	[207–209]
Probucol	Known to reduce superoxide production in rabbit aorta, by down-regulation of p22phox	Free radical scavenger	[54, 210–213]
Nox2ds-tat	Oxidase assembly inhibitor: inhibits association of NOX2 subunit with p47phox. Does not scavenge $O_2^{-\bullet}$ generated by cell-free systems	None	[148, 214]
VAS3947	Triazolopyrimidine that decreased ROS production in several cell lines with low micro molar efficiency, irrespective of the specific isoforms expressed; showed no inhibitory effects against xanthine oxidase-derived ROS or eNOS activity	None	[215]

Adapted from [125, 216].
eNOS: endothelial nitric oxide synthase; IC_{50}: half-maximal inhibitory concentration; Nox: NADPH oxidase; $O_2^{-\bullet}$: superoxide; ROS: reactive oxygen species; SH3: Src homology 3; DPI: diphenyleneiodonium chloride; AEBSF: 4-(2-aminoethyl)-benzenesulfonyl fluoride; S178341: 4-dimethyl-2,3,5,6-triiodobenzene; VAS-2870: 3-benzyl-7-(2-benzoxazolyl) thio-1,2,3-triazolo (4,5-d) pyrimidine; SKF 525A: 2-diethylaminoethyl 2:2–diphenylvalerate hydrochloride.

effective against Nox2, Nox4, and Nox5 dependant NADPH oxidase-dependant activity. Apocynin has been shown to reverse activation of the NADPH oxidase system in rat kidneys induced by hydroxyl-l-proline (HLP) treatment even in the face of high levels of hyperoxaluria, revealing the role of Apocynin as an inhibitor as well as having antioxidant inductive activities [129].

The most frequently used inhibitor of NADPH oxidase is diphenyleneiodonium chloride (DPI), also known as dibenziodolium chloride. Its mode of action is by taking electrons from electron transporter and creating a radical which blocks the appropriate transporter of electrons through a covalent binding step [124]. Regarding NOX isoforms, the action of DPI appears to be nonspecific towards any isoform and it partially or completely inhibits different types of enzymes such as iNOS, xanthine oxidase, and NADPH oxidase [124].

9. Summary

In this review, we talk about renal injury caused by oxalate and calcium oxalate crystals due to hyperoxaluria. Oxalate and calcium oxalate can lead to renal injury due to disruption of membranes, ROS-induced oxidative stress, and mitochondrial dysfunction. We put the main emphasis on oxidative stress caused by ROS produced by different isoforms of NADPH oxidase as it has been found that these different isoforms of NADPH oxidase are one of the most important contributors of ROS and oxidative stress produced in the different subcellular localizations of the kidneys. These NADPH oxidase complexes play a crucial role in host defense, various signaling pathways leading to regulation of gene expression, and protein functions under normal conditions of oxidative balance. When this oxidative balance is disturbed

due to environmental and/or physiological processes, the potential of the NADPH oxidases in inducing injury to both microorganisms and cells makes regulation essential, not only through normal physiological activities, but also exogenous inhibitors. Chemicals that inhibit generation of ROS provide considerable benefits over general antioxidants such as vitamin E, which appears to be less efficient due to various properties, including decreased bioavailability. It would seem, therefore, that in order to reduce the function and downstream effects of NADPH oxidase, a main focus should be on blocking the assembly of NADPH oxidase subunits. Various peptide and non-peptide inhibitors are known which mainly operate by disrupting the association of NADPH oxidase complex assembly. Special focus should be on targeting the organizer subunit, that is, p47phox or the NOXO1 subunits. Other molecular subunits for therapy may be the activator subunits such as p67phox and NOXA1 along with Rac. Thus, the main focus should be to develop an inhibitor with increased efficiency and specificity of binding with the protein subunit. Comprehensive studies are needed on the molecular subunit structures to be targeted and their effects on interactions with other subunits present downstream in the NADPH oxidase complex.

Acknowledgments

This research was supported by National Institutes of Health Grant no. RO1-DK078602 and the University of Florida Center for the Study of Lithiasis.

References

[1] S. R. Khan, "Hyperoxaluria-induced oxidative stress and antioxidants for renal protection," *Urological Research*, vol. 33, no. 5, pp. 349–357, 2005.

[2] R. P. Holmes, H. O. Goodman, and D. G. Assimos, "Contribution of dietary oxalate to urinary oxalate excretion," *Kidney International*, vol. 59, no. 1, pp. 270–276, 2001.

[3] R. P. Holmes and D. G. Assimos, "The impact of dietary oxalate on kidney stone formation," *Urological Research*, vol. 32, no. 5, pp. 311–316, 2004.

[4] R. P. Holmes, W. T. Ambrosius, and D. G. Assimos, "Dietary oxalate loads and renal oxalate handling," *Journal of Urology*, vol. 174, no. 3, pp. 943–947, 2005.

[5] J. Streit, L. C. Tran-Ho, and E. Königsberger, "Solubility of the three calcium oxalate hydrates in sodium chloride solutions and urine-like liquors," *Monatshefte fur Chemie*, vol. 129, no. 12, pp. 1225–1236, 1998.

[6] T. F. Knight, S. C. Sansom, H. O. Senekjian, and E. J. Weinman, "Oxalate secretion in the rat proximal tubule," *The American Journal of Physiology*, vol. 240, no. 4, pp. F295–F298, 1981.

[7] E. J. Weinman, S. J. Frankfurt, A. Ince, and S. Sansom, "Renal tubular transport of organic acids. Studies with oxalate and para-aminohippurate in the rat," *The Journal of Clinical Investigation*, vol. 61, no. 3, pp. 801–806, 1978.

[8] L. F. James, "Oxalate toxicosis," *Clinical Toxicology*, vol. 5, no. 2, pp. 231–243, 1972.

[9] H. E. Williams and T. R. Wandzilak, "Oxalate synthesis, transport and the hyperoxaluric syndromes," *Journal of Urology*, vol. 141, no. 3, pp. 742–749, 1989.

[10] W. G. Robertson and H. Hughes, "Importance of mild hyperoxaluria in the pathogenesis of urolithiasis—new evidence from studies in the Arabian Peninsula," *Scanning Microscopy*, vol. 7, no. 1, pp. 391–402, 1993.

[11] E. M. Worcester, J. H. Parks, A. P. Evan et al., "Renal function in patients with nephrolithiasis," *Journal of Urology*, vol. 176, no. 2, pp. 600–603, 2006.

[12] A. D. Rule, E. J. Bergstralh, L. J. Melton III et al., "Kidney stones and the risk for chronic kidney disease," *Clinical Journal of the American Society of Nephrology*, vol. 4, no. 4, pp. 804–811, 2009.

[13] B. Hoppe, B. B. Beck, and D. S. Milliner, "The primary hyperoxalurias," *Kidney International*, vol. 75, no. 12, pp. 1264–1271, 2009.

[14] B. A. Vervaet, A. Verhulst, P. C. D'Haese, and M. E. De Broe, "Nephrocalcinosis: new insights into mechanisms and consequences," *Nephrology Dialysis Transplantation*, vol. 24, no. 7, pp. 2030–2035, 2009.

[15] J. R. Asplin, "Hyperoxaluric calcium nephrolithiasis," *Endocrinology and Metabolism Clinics of North America*, vol. 31, no. 4, pp. 927–949, 2002.

[16] S. R. Marengo and A. M. P. Romani, "Oxalate in renal stone disease: the terminal metabolite that just won't go away," *Nature Clinical Practice Nephrology*, vol. 4, no. 7, pp. 368–377, 2008.

[17] A. E. Bobrowski and C. B. Langman, "The primary hyperoxalurias," *Seminars in Nephrology*, vol. 28, no. 2, pp. 152–162, 2008.

[18] E. Leumann and B. Hoppe, "The primary hyperoxalurias," *Journal of the American Society of Nephrology*, vol. 12, no. 9, pp. 1986–1993, 2001.

[19] C. G. Monico, M. Persson, G. C. Ford, G. Rumsby, and D. S. Milliner, "Potential mechanisms of marked hyperoxaluria not due to primary hyperoxaluria I or II," *Kidney International*, vol. 62, no. 2, pp. 392–400, 2002.

[20] C. G. Monico, A. Weinstein, Z. Jiang et al., "Phenotypic and functional analysis of human SLC26A6 variants in patients with familial hyperoxaluria and calcium oxalate nephrolithiasis," *American Journal of Kidney Diseases*, vol. 52, no. 6, pp. 1096–1103, 2008.

[21] R. Belostotsky, E. Seboun, G. H. Idelson et al., "Mutations in DHDPSL are responsible for primary hyperoxaluria type III," *American Journal of Human Genetics*, vol. 87, no. 3, pp. 392–399, 2010.

[22] R. P. Holmes and M. Kennedy, "Estimation of the oxalate content of foods and daily oxalate intake," *Kidney International*, vol. 57, no. 4, pp. 1662–1667, 2000.

[23] B. Hoppe, G. von Unruh, N. Laube, A. Hesse, and H. Sidhu, "Oxalate degrading bacteria: new treatment option for patients with primary and secondary hyperoxaluria?" *Urological Research*, vol. 33, no. 5, pp. 372–375, 2005.

[24] R. Siener, D. Ebert, C. Nicolay, and A. Hesse, "Dietary risk factors for hyperoxaluria in calcium oxalate stone formers," *Kidney International*, vol. 63, no. 3, pp. 1037–1043, 2003.

[25] P. P. Singh, L. K. Kothari, D. C. Sharma, and S. N. Saxena, "Nutritional value of foods in relation to their oxalic acid content," *American Journal of Clinical Nutrition*, vol. 25, no. 11, pp. 1147–1152, 1972.

[26] G. E. von Unruh, S. Voss, T. Sauerbruch, and A. Hesse, "Dependence of oxalate absorption on the daily calcium intake," *Journal of the American Society of Nephrology*, vol. 15, no. 6, pp. 1567–1573, 2004.

[27] A. Hesse, W. Schneeberger, S. Engfeed, G. E. von Unruh, and T. Sauerbruch, "Intestinal hyperabsorption of oxalate in

calcium oxalate stone formers: application of a new test with [13C2]oxalate," *Journal of the American Society of Nephrology*, vol. 10, supplement 14, pp. S329–S333, 1999.

[28] S. Voss, A. Hesse, D. J. Zimmermann, T. Sauerbruch, and G. E. von Unruh, "Intestinal oxalate absorption is higher in idiopathic calcium oxalate stone formers than in healthy controls: measurements with the [(13)C2]oxalate absorption test," *Journal of Urology*, vol. 175, no. 5, pp. 1711–1715, 2006.

[29] M. Lindsjo, B. G. Danielson, B. Fellstrom, and S. Ljunghall, "Intestinal oxalate and calcium absorption in recurrent renal stone formers and healthy subjects," *Scandinavian Journal of Urology and Nephrology*, vol. 23, no. 1, pp. 55–59, 1989.

[30] J. Knight, R. P. Holmes, and D. G. Assimos, "Intestinal and renal handling of oxalate loads in normal individuals and stone formers," *Urological Research*, vol. 35, no. 3, pp. 111–117, 2007.

[31] E. M. Worcester, "Stones from bowel disease," *Endocrinology and Metabolism Clinics of North America*, vol. 31, no. 4, pp. 979–999, 2002.

[32] S. Thamilselvan and S. R. Khan, "Oxalate and calcium oxalate crystals are injurious to renal epithelial cells: results of in vivo and in vitro studies," *Journal of Nephrology*, vol. 11, supplement 1, pp. 66–69, 1998.

[33] S. R. Khan, J. M. Johnson, A. B. Peck, J. G. Cornelius, and P. A. Glenton, "Expression of osteopontin in rat kidneys: induction during ethylene glycol induced calcium oxalate nephrolithiasis," *Journal of Urology*, vol. 168, no. 3, pp. 1173–1181, 2002.

[34] S. Thamilselvan, S. R. Khan, and M. Menon, "Oxalate and calcium oxalate mediated free radical toxicity in renal epithelial cells: effect of antioxidants," *Urological Research*, vol. 31, no. 1, pp. 3–9, 2003.

[35] K. McMartin, "Are calcium oxalate crystals involved in the mechanism of acute renal failure in ethylene glycol poisoning Ethylene glycol renal toxicity mechanism," *Clinical Toxicology*, vol. 47, no. 9, pp. 859–869, 2009.

[36] C. Miller, L. Kennington, R. Cooney et al., "Oxalate toxicity in renal epithelial cells: characteristics of apoptosis and necrosis," *Toxicology and Applied Pharmacology*, vol. 162, no. 2, pp. 132–141, 2000.

[37] A. Bhandari, S. Koul, A. Sekhon et al., "Effects of oxalate on HK-2 cells, a line of proximal tubular epithelial cells from normal human kidney," *Journal of Urology*, vol. 168, no. 1, pp. 253–259, 2002.

[38] J. Burgess and D. N. Drasdo, "Solubilities of calcium salts of dicarboxylic acids in methanol-water mixtures; transfer chemical potentials of dicarboxylate anions," *Polyhedron*, vol. 12, no. 24, pp. 2905–2911, 1993.

[39] S. Ebisuno, H. Koul, M. Menon, and C. Scheid, "Oxalate transport in a line of porcine renal epithelial cells-LLC-PK1 cells," *Journal of Urology*, vol. 152, no. 1, pp. 237–242, 1994.

[40] H. Koul, S. Ebisuno, L. Renzulli, M. Yanagawa, M. Menon, and C. Scheid, "Polarized distribution of oxalate transport systems in LLC-PK1 cells, a line of renal epithelial cells," *American Journal of Physiology*, vol. 266, no. 2, pp. F266–F274, 1994.

[41] M. Hatch, R. W. Freel, and N. D. Vaziri, "Intestinal excretion of oxalate in chronic renal failure," *Journal of the American Society of Nephrology*, vol. 5, no. 6, pp. 1339–1343, 1994.

[42] M. W. Bigelow, J. H. Wiessner, J. G. Kleinman, and N. S. Mandel, "Surface exposure of phosphatidylserine increases calcium oxalate crystal attachment to IMCD cells," *American Journal of Physiology*, vol. 272, no. 1, pp. F55–F62, 1997.

[43] L. C. Cao, T. Honeyman, J. Jonassen, and C. Scheid, "Oxalate-induced ceramide accumulation in Madin-Darby canine kidney and LLC-PK1 cells," *Kidney International*, vol. 57, no. 6, pp. 2403–2411, 2000.

[44] L. C. Cao, J. Jonassen, T. W. Honeyman, and C. Scheid, "Oxalate-induced redistribution of phosphatidylserine in renal epithelial cells: implications for kidney stone disease," *American Journal of Nephrology*, vol. 21, no. 1, pp. 69–77, 2001.

[45] C. Guo, T. A. Cenac, Y. Li, and K. E. McMartin, "Calcium oxalate, and not other metabolites, is responsible for the renal toxicity of ethylene glycol," *Toxicology Letters*, vol. 173, no. 1, pp. 8–16, 2007.

[46] O. Sareila, T. Kelkka, A. Pizzolla et al., "NOX2 complex-derived ROS as immune regulators," *Antioxidants & Redox Signaling*, vol. 15, no. 8, pp. 2197–2208, 2011.

[47] B. Descamps-Latscha, T. Drüeke, and V. Witko-Sarsat, "Dialysis-induced oxidative stress: biological aspects, clinical consequences, and therapy," *Seminars in Dialysis*, vol. 14, no. 3, pp. 193–199, 2001.

[48] C. C. Winterbourn, "Reconciling the chemistry and biology of reactive oxygen species," *Nature Chemical Biology*, vol. 4, no. 5, pp. 278–286, 2008.

[49] M. P. Kao, D. S. Ang, A. Pall, and A. D. Struthers, "Oxidative stress in renal dysfunction: mechanisms, clinical sequelae and therapeutic options," *Journal of Human Hypertension*, vol. 24, no. 1, pp. 1–8, 2010.

[50] Y. C. Hou, A. Janczuk, and P. G. Wang, "Current trends in the development of nitric oxide donors," *Current Pharmaceutical Design*, vol. 5, no. 6, pp. 417–441, 1999.

[51] S. J. Klebanoff, "Myeloperoxidase: friend and foe," *Journal of Leukocyte Biology*, vol. 77, no. 5, pp. 598–625, 2005.

[52] D. P. Jones, "Radical-free biology of oxidative stress," *American Journal of Physiology*, vol. 295, no. 4, pp. 849–868, 2008.

[53] S. R. Thomas, P. K. Witting, and G. R. Drummond, "Redox control of endothelial function and dysfunction: molecular mechanisms and therapeutic opportunities," *Antioxidants & Redox Signaling*, vol. 10, no. 10, pp. 1713–1765, 2008.

[54] R. Stocker and J. F. Keaney, "Role of oxidative modifications in atherosclerosis," *Physiological Reviews*, vol. 84, no. 4, pp. 1381–1478, 2004.

[55] U. Forstermann, "Nitric oxide and oxidative stress in vascular disease," *Pflügers Archiv*, vol. 459, no. 6, pp. 923–939, 2010.

[56] N. V. Blough and O. C. Zafiriou, "Reaction of superoxide with nitric oxide to form peroxonitrite in alkaline aqueous solution," *Inorganic Chemistry*, vol. 24, no. 22, pp. 3502–3504, 1985.

[57] R. J. Gryglewski, R. M. J. Palmer, and S. Moncada, "Superoxide anion is involved in the breakdown of endothelium-derived vascular relaxing factor," *Nature*, vol. 320, no. 6061, pp. 454–456, 1986.

[58] C. Szabo, H. Ischiropoulos, and R. Radi, "Peroxynitrite: biochemistry, pathophysiology and development of therapeutics," *Nature Reviews Drug Discovery*, vol. 6, no. 8, pp. 662–680, 2007.

[59] D. G. Harrison, W. Chen, S. Dikalov, and L. Li, "Regulation of endothelial cell tetrahydrobiopterin. Pathophysiological and therapeutic implications," *Advances in Pharmacology*, vol. 60, pp. 116–132, 2010.

[60] J. B. Laursen, M. Somers, S. Kurz et al., "Endothelial regulation of vasomotion in ApoE-deficient mice: implications for interactions between peroxynitrite and tetrahydrobiopterin," *Circulation*, vol. 103, no. 9, pp. 1282–1288, 2001.

[61] W. Droge, "Free radicals in the physiological control of cell function," *Physiological Reviews*, vol. 82, no. 1, pp. 47–95, 2002.

[62] J. Anrather, G. Racchumi, and C. Iadecola, "NF-κB regulates phagocytic NADPH oxidase by inducing the expression of gp91phox," *The Journal of Biological Chemistry*, vol. 281, no. 9, pp. 5657–5667, 2006.

[63] R. Dworakowski, S. P. Alom-Ruiz, and A. M. Shah, "NADPH oxidase-derived reactive oxygen species in the regulation of endothelial phenotype," *Pharmacological Reports*, vol. 60, no. 1, pp. 21–28, 2008.

[64] B. Lassegue and K. K. Griendling, "NADPH oxidases: functions and pathologies in the vasculature," *Arteriosclerosis, Thrombosis, and Vascular Biology*, vol. 30, no. 4, pp. 653–661, 2001.

[65] F. Martinon, "Signaling by ROS drives inflammasome activation," *European Journal of Immunology*, vol. 40, no. 3, pp. 616–619, 2010.

[66] T. Chabrashvili, C. Kitiyakara, J. Blau et al., "Effects of ANG II type 1 and 2 receptors on oxidative stress, renal NADPH oxidase, and SOD expression," *American Journal of Physiology*, vol. 285, no. 1, pp. R117–R124, 2003.

[67] W. J. Welch, J. Blau, H. Xie et al., "Angiotensin-induced defects in renal oxygenation: role of oxidative stress," *American Journal of Physiology*, vol. 288, no. 1, pp. 22–28, 2005.

[68] H. S. Huang, M. C. Ma, C. F. Chen, and J. Chen, "Lipid peroxidation and its correlations with urinary levels of oxalate, citric acid, and osteopontin in patients with renal calcium oxalate stones," *Urology*, vol. 62, no. 6, pp. 1123–1128, 2003.

[69] K. Tungsanga, P. Sriboonlue, P. Futrakul, C. Yachantha, and P. Tosukhowong, "Renal tubular cell damage and oxidative stress in renal stone patients and the effect of potassium citrate treatment," *Urological Research*, vol. 33, no. 1, pp. 65–69, 2005.

[70] W. J. Welch, A. Tojo, and C. S. Wilcox, "Roles of NO and oxygen radicals in tubuloglomerular feedback in SHR," *American Journal of Physiology*, vol. 278, no. 5, pp. F769–F776, 2000.

[71] H. M. Bosse and S. Bachmann, "Immunohistochemically detected protein nitration indicates sites of renal nitric oxide release in Goldblatt hypertension," *Hypertension*, vol. 30, no. 4, pp. 948–952, 1997.

[72] A. P. Zou, N. Li, and A. W. Cowley Jr., "Production and actions of superoxide in the renal medulla," *Hypertension*, vol. 37, no. 2, pp. 547–553, 2001.

[73] M. L. Onozato, A. Tojo, A. Goto, T. Fujita, and C. S. Wilcox, "Oxidative stress and nitric oxide synthase in rat diabetic nephropathy: effects of ACEI and ARB," *Kidney International*, vol. 61, no. 1, pp. 186–194, 2002.

[74] T. L. Leto, S. Morand, D. Hurt, and T. Ueyama, "Targeting and regulation of reactive oxygen species generation by Nox family NADPH oxidases," *Antioxidants & Redox Signaling*, vol. 11, no. 10, pp. 2607–2619, 2009.

[75] L. Serrander, L. Cartier, K. Bedard et al., "NOX4 activity is determined by mRNA levels and reveals a unique pattern of ROS generation," *Biochemical Journal*, vol. 406, no. 1, pp. 105–114, 2007.

[76] S. I. Dikalov, A. E. Dikalova, A. T. Bikineyeva, H. H. H. W. Schmidt, D. G. Harrison, and K. K. Griendling, "Distinct roles of Nox1 and Nox4 in basal and angiotensin II-stimulated superoxide and hydrogen peroxide production," *Free Radical Biology and Medicine*, vol. 45, no. 9, pp. 1340–1351, 2008.

[77] B. T. Kawahara, M. T. Quinn, and J. D. Lambeth, "Molecular evolution of the reactive oxygen-generating NADPH oxidase (Nox/Duox) family of enzymes," *BMC Evolutionary Biology*, vol. 7, article 109, 2007.

[78] K. Bedard and K. H. Krause, "The NOX family of ROS-generating NADPH oxidases: physiology and pathophysiology," *Physiological Reviews*, vol. 87, no. 1, pp. 245–313, 2007.

[79] W. Chamulitrat, R. Schmidt, P. Tomakidi et al., "Association of gp91phox homolog Nox1 with anchorage-independent growth and MAP kinase-activation of transformed human keratinocytes," *Oncogene*, vol. 22, no. 38, pp. 6045–6053, 2003.

[80] N. Coant, S. B. Mkaddem, E. Pedruzzi et al., "NADPH oxidase 1 modulates WNT and NOTCH1 signaling to control the fate of proliferative progenitor cells in the colon," *Molecular and Cellular Biology*, vol. 30, no. 11, pp. 2636–2650, 2010.

[81] W. M. Nauseef, "Nox enzymes in immune cells," *Seminars in Immunopathology*, vol. 30, no. 3, pp. 195–208, 2008.

[82] S. F. Moore and A. B. MacKenzie, "NADPH oxidase NOX2 mediates rapid cellular oxidation following ATP stimulation of endotoxin-primed macrophages," *Journal of Immunology*, vol. 183, no. 5, pp. 3302–3308, 2009.

[83] R. L. McCaffrey, J. T. Schwartz, S. R. Lindemann et al., "Multiple mechanisms of NADPH oxidase inhibition by type A and type B Francisella tularensis," *Journal of Leukocyte Biology*, vol. 88, no. 4, pp. 791–805, 2010.

[84] D. Mukherjea, S. Jajoo, K. Sheehan et al., "NOX3 NADPH oxidase couples transient receptor potential vanilloid 1 to signal transducer and activator of transcription 1-mediated inflammation and hearing loss," *Antioxidants & Redox Signaling*, vol. 14, no. 6, pp. 999–1010, 2011.

[85] K. Schroder, K. Wandzioch, I. Helmcke et al., "Nox4 acts as a switch between differentiation and proliferation in preadipocytes," *Arteriosclerosis, Thrombosis, and Vascular Biology*, vol. 29, no. 2, pp. 239–245, 2009.

[86] S. Pendyala, I. A. Gorshkova, P. V. Usatyuk et al., "Role of Nox4 and Nox2 in hyperoxia-induced reactive oxygen species generation and migration of human lung endothelial cells," *Antioxidants & Redox Signaling*, vol. 11, no. 4, pp. 747–764, 2009.

[87] A. N. Lyle, N. N. Deshpande, Y. Taniyama et al., "Poldip2, a novel regulator of Nox4 and cytoskeletal integrity in vascular smooth muscle cells," *Circulation Research*, vol. 105, no. 3, pp. 249–259, 2009.

[88] J. I. Jun and L. F. Lau, "The matricellular protein CCN1 induces fibroblast senescence and restricts fibrosis in cutaneous wound healing," *Nature Cell Biology*, vol. 12, no. 7, pp. 676–685, 2010.

[89] J. Si, J. Behar, J. Wands et al., "STAT5 mediates PAF-induced NADPH oxidase NOX5-S expression in Barrett's esophageal adenocarcinoma cells," *American Journal of Physiology*, vol. 294, no. 1, pp. 174–183, 2008.

[90] D. B. Jay, C. A. Papaharalambus, B. Seidel-Rogol, A. E. Dikalova, B. Lassègue, and K. K. Griendling, "Nox5 mediates PDGF-induced proliferation in human aortic smooth muscle cells," *Free Radical Biology and Medicine*, vol. 45, no. 3, pp. 329–335, 2008.

[91] A. S. Kamiguti, L. Serrander, K. Lin et al., "Expression and activity of NOX5 in the circulating malignant B cells of hairy cell leukemia," *Journal of Immunology*, vol. 175, no. 12, pp. 8424–8430, 2005.

[92] J. Si, X. Fu, J. Behar et al., "NADPH oxidase NOX5-S mediates acid-induced cyclooxygenase-2 expression via activation of NF-κB in Barrett's esophageal adenocarcinoma cells," *The Journal of Biological Chemistry*, vol. 282, no. 22, pp. 16244–16255, 2007.

[93] H. Fischer, "Mechanisms and function of DUOX in epithelia of the lung," *Antioxidants & Redox Signaling*, vol. 11, no. 10, pp. 2453–2465, 2009.

[94] A. Allaoui, A. Botteaux, J. E. Dumont, C. Hoste, and X. De Deken, "Dual oxidases and hydrogen peroxide in a complex dialogue between host mucosae and bacteria," *Trends in Molecular Medicine*, vol. 15, no. 12, pp. 571–579, 2009.

[95] P. S. Gill and C. S. Wilcox, "NADPH oxidases in the kidney," *Antioxidants & Redox Signaling*, vol. 8, no. 9-10, pp. 1597–1607, 2006.

[96] J. K. Guo and L. G. Cantley, "Cellular maintenance and repair of the kidney," *Annual Review of Physiology*, vol. 72, pp. 357–376, 2010.

[97] D. Wang, Y. Chen, T. Chabrashvili et al., "Role of oxidative stress in endothelial dysfunction and enhanced responses to angiotensin II of afferent arterioles from rabbits infused with angiotensin II," *Journal of the American Society of Nephrology*, vol. 14, no. 11, pp. 2783–2789, 2003.

[98] T. Chabrashvili, A. Tojo, M. L. Onozato et al., "Expression and cellular localization of classic NADPH oxidase subunits in the spontaneously hypertensive rat kidney," *Hypertension*, vol. 39, no. 2, pp. 269–274, 2002.

[99] H. H. Radeke, A. R. Cross, J. T. Hancock et al., "Functional expression of NADPH oxidase components (α- and β-subunits of cytochrome b558 and 45-kDa flavoprotein) by intrinsic human glomerular mesangial cells," *The Journal of Biological Chemistry*, vol. 266, no. 31, pp. 21025–21029, 1991.

[100] S. A. Jones, J. T. Hancock, O. T. G. Jones, A. Neubauer, and N. Topley, "The expression of NADPH oxidase components in human glomerular mesangial cells: detection of protein and mRNA for p47phox, p67phox, and p22phox," *Journal of the American Society of Nephrology*, vol. 5, no. 7, pp. 1483–1491, 1995.

[101] Y. Gorin, K. Block, J. Hernandez et al., "Nox4 NAD(P)H oxidase mediates hypertrophy and fibronectin expression in the diabetic kidney," *The Journal of Biological Chemistry*, vol. 280, no. 47, pp. 39616–39626, 2005.

[102] Y. Gorin, J. M. Ricono, N. H. Kim, B. Bhandari, G. G. Choudhury, and H. E. Abboud, "Nox4 mediates angiotensin II-induced activation of Akt/protein kinase B in mesangial cells," *American Journal of Physiology*, vol. 285, no. 2, pp. F219–F229, 2003.

[103] N. Li, F. X. Yi, J. L. Spurrier, C. A. Bobrowitz, and A. P. Zou, "Production of superoxide through NADH oxidase in thick ascending limb of Henle's loop in rat kidney," *American Journal of Physiology*, vol. 282, no. 6, pp. F1111–F1119, 2002.

[104] S. Greiber, T. Munzel, S. Kastner et al., "NAD(P)H oxidase activity in cultured human podocytes: effects of adenosine triphosphate," *Kidney International*, vol. 53, no. 3, pp. 654–663, 1998.

[105] M. Geiszt, J. B. Kopp, P. Varnai et al., "Identification of renox, an NAD(P)H oxidase in kidney," *Proceedings of the National Academy of Sciences of the United States of America*, vol. 97, no. 14, pp. 8010–8014, 2000.

[106] A. Shiose, J. Kuroda, K. Tsuruya et al., "A novel superoxide-producing NAD(P)H oxidase in kidney," *The Journal of Biological Chemistry*, vol. 276, no. 2, pp. 1417–1423, 2001.

[107] P. Modlinger, T. Chabrashvili, P. S. Gill et al., "RNA silencing in vivo reveals role of p22phox in rat angiotensin slow pressor response," *Hypertension*, vol. 47, no. 2, pp. 238–244, 2006.

[108] C. Kitiyakara, T. Chabrashvili, Y. Chen et al., "Salt intake, oxidative stress, and renal expression of NADPH oxidase and superoxide dismutase," *Journal of the American Society of Nephrology*, vol. 14, no. 11, pp. 2775–2782, 2003.

[109] B. M. Babior, J. D. Lambeth, and W. Nauseef, "The neutrophil NADPH oxidase," *Archives of Biochemistry and Biophysics*, vol. 397, no. 2, pp. 342–344, 2002.

[110] F. J. Miller, M. Filali, G. J. Huss et al., "Cytokine activation of nuclear factor κB in vascular smooth muscle cells requires signaling endosomes containing Nox1 and ClC-3," *Circulation Research*, vol. 101, no. 7, pp. 663–671, 2007.

[111] J. D. Lambeth, "NOX enzymes and the biology of reactive oxygen," *Nature Reviews Immunology*, vol. 4, no. 3, pp. 181–189, 2004.

[112] B. Lassègue, D. Sorescu, K. Szöcs et al., "Novel gp91phox homologues in vascular smooth muscle cells: Nox1 mediates angiotensin II-induced superoxide formation and redox-sensitive signaling pathways," *Circulation Research*, vol. 88, no. 9, pp. 888–894, 2001.

[113] P. J. Pagano, S. J. Chanock, D. A. Siwik, W. S. Colucci, and J. K. Clark, "Angiotensin II induces p67(phox) mRNA expression and NADPH oxidase superoxide generation in rabbit aortic adventitial fibroblasts," *Hypertension*, vol. 32, no. 2, pp. 331–337, 1998.

[114] M. E. Cifuentes, F. E. Rey, O. A. Carretero, and P. J. Pagano, "Upregulation of p67(phox) and gp91(phox) in aortas from angiotensin II-infused mice," *American Journal of Physiology*, vol. 279, no. 5, pp. H2234–H2240, 2000.

[115] S. Thamilselvan and R. Selvam, "Effect of vitamin E and mannitol on renal calcium oxalate retention in experimental nephrolithiasis," *Indian Journal of Biochemistry and Biophysics*, vol. 34, no. 3, pp. 319–323, 1997.

[116] M. Santhosh Kumar and R. Selvam, "Supplementation of vitamin E and selenium prevents hyperoxaluria in experimental urolithic rats," *Journal of Nutritional Biochemistry*, vol. 14, no. 6, pp. 306–313, 2003.

[117] R. Selvam and V. Ravichandran, "Restoration of tissue antioxidants and prevention of renal stone deposition in vitamin B6 deficient rats fed with vitamin E or methionine," *Indian Journal of Experimental Biology*, vol. 31, no. 11, pp. 882–887, 1993.

[118] A. Muthukumar and R. Selvam, "Role of glutathione on renal mitochondrial status in hyperoxaluria," *Molecular and Cellular Biochemistry*, vol. 185, no. 1-2, pp. 77–84, 1998.

[119] J. Bleys, E. R. Miller III, R. Pastor-Barriuso et al., "Vitamin-mineral supplementation and the progression of atherosclerosis: a meta-analysis of randomized controlled trials," *American Journal of Clinical Nutrition*, vol. 84, no. 4, pp. 880–887, 2006.

[120] D. P. Vivekananthan, M. S. Penn, S. K. Sapp, A. Hsu, and E. J. Topol, "Use of antioxidant vitamins for the prevention of cardiovascular disease: meta-analysis of randomised trials," *The Lancet*, vol. 361, no. 9374, pp. 2017–2023, 2003.

[121] E. L. Schiffrin, "Antioxidants in hypertension and cardiovascular disease," *Molecular Interventions*, vol. 10, no. 6, pp. 354–362, 2010.

[122] R. Kissner, T. Nauser, P. Bugnon, P. G. Lye, and W. H. Koppenol, "Formation and properties of peroxynitrite as studied by laser flash photolysis, high-pressure stopped-flow technique, pulse radiolysis," *Chemical Research in Toxicology*, vol. 10, no. 11, pp. 1285–1292, 1997.

[123] N. Gotoh and E. Niki, "Rates of interactions of superoxide with vitamin E, vitamin C and related compounds as measured by chemiluminescence," *Biochimica et Biophysica Acta*, vol. 1115, no. 3, pp. 201–207, 1992.

[124] S. Selemidis, C. G. Sobey, K. Wingler, H. H. H. W. Schmidt, and G. R. Drummond, "NADPH oxidases in the vasculature:

molecular features, roles in disease and pharmacological inhibition," *Pharmacology and Therapeutics*, vol. 120, no. 3, pp. 254–291, 2008.

[125] P. Kleniewska, A. Piechota, B. Skibska et al., "The NADPH oxidase family and its inhibitors," *Archivum Immunologiae et Therapiae Experimentalis*, vol. 60, no. 4, pp. 277–294, 2012.

[126] J. Stefanska and R. Pawliczak, "Apocynin: molecular aptitudes," *Mediators of Inflammation*, vol. 2008, Article ID 106507, 10 pages, 2008.

[127] D. K. Johnson, K. J. Schillinger, D. M. Kwait et al., "Inhibition of NADPH oxidase activation in endothelial cells by ortho-methoxy-substituted catechols," *Endothelium*, vol. 9, no. 3, pp. 191–203, 2002.

[128] S. H. M. Ellmark, G. J. Dusting, M. N. Tang Fui, N. Guzzo-Pernell, and G. R. Drummond, "The contribution of Nox4 to NADPH oxidase activity in mouse vascular smooth muscle," *Cardiovascular Research*, vol. 65, no. 2, pp. 495–504, 2005.

[129] S. Joshi, B. T. Saylor, W. Wang et al., "Apocynin-treatment reverses hyperoxaluria induced changes in NADPH oxidase system expression in rat kidneys: a transcriptional study," *PLoS One*, vol. 7, no. 10, Article ID e47738, 2012.

[130] J. M. Simons, L. A. Hart, H. van Dijk, F. C. Fischer, K. T. D. De Silva, and R. P. Labadie, "Immunodulatory compounds from Picrorhiza kurroa: isolation and characterization of two anti-complementary polymeric fractions from an aqueous root extract," *Journal of Ethnopharmacology*, vol. 26, no. 2, pp. 169–182, 1989.

[131] J. Stolk, T. J. Hiltermann, J. H. Dijkman, and A. J. Verhoeven, "Characteristics of the inhibition of NADPH oxidase activation in neutrophils by apocynin, a methoxy-substituted catechol," *American Journal of Respiratory Cell and Molecular Biology*, vol. 11, no. 1, pp. 95–102, 1994.

[132] B. A. Hart, J. M. Simons, S. Knaan-Shanzer, N. P. M. Bakker, and R. P. Labadie, "Antiarthritic activity of the newly developed neutrophil oxidative burst antagonist apocynin," *Free Radical Biology and Medicine*, vol. 9, no. 2, pp. 127–131, 1990.

[133] V. B. O'Donnell, D. G. Tew, O. T. G. Jones, and P. J. England, "Studies on the inhibitory mechanism of iodonium compounds with special reference to neutrophil NADPH oxidase," *Biochemical Journal*, vol. 290, no. 1, pp. 41–49, 1993.

[134] V. B. O'Donnell, G. C. M. Smith, and O. T. G. Jones, "Involvement of phenyl radicals in iodonium compound inhibition of flavoenzymes," *Molecular Pharmacology*, vol. 46, no. 4, pp. 778–785, 1994.

[135] D. J. Stuehr, O. A. Fasehun, N. S. Kwon et al., "Inhibition of macrophage and endothelial cell nitric oxide synthase by diphenyleneiodonium and its analogs," *FASEB Journal*, vol. 5, no. 1, pp. 98–103, 1991.

[136] S. J. Gatley and H. S. A. Sherratt, "The effects of diphenyleneiodonium on mitochondrial reactions. Relation of binding of diphenylene[125I]iodonium to mitochondria to the extent of inhibition of oxygen uptake," *Biochemical Journal*, vol. 158, no. 2, pp. 307–315, 1976.

[137] A. R. Cross, J. F. Parkinson, and O. T. G. Jones, "The superoxide-generating oxidase of leucocytes. NADPH-dependent reduction of flavin and cytochrome b in solubilized preparations," *Biochemical Journal*, vol. 223, no. 2, pp. 337–344, 1984.

[138] A. R. Cross and O. T. G. Jones, "The effect of the inhibitor diphenylene iodonium on the superoxide-generating system of neutrophils. Specific labelling of a component polypeptide of the oxidase," *Biochemical Journal*, vol. 237, no. 1, pp. 111–116, 1986.

[139] R. Brandsch and V. Bichler, "Studies in vitro on the flavinylation of 6-hydroxy-D-nicotine oxidase," *European Journal of Biochemistry*, vol. 160, no. 2, pp. 285–289, 1986.

[140] V. Diatchuk, O. Lotan, V. Koshkin, P. Wikstroem, and E. Pick, "Inhibition of NADPH oxidase activation by 4-(2-aminoethyl)-benzenesulfonyl fluoride and related compounds," *The Journal of Biological Chemistry*, vol. 272, no. 20, pp. 13292–13301, 1997.

[141] A. Rossary, K. Arab, and J. P. Steghens, "Polyunsaturated fatty acids modulate NOX 4 anion superoxide production in human fibroblasts," *Biochemical Journal*, vol. 406, no. 1, pp. 77–83, 2007.

[142] C. Fan, M. Katsuyama, T. Nishinaka, and C. Yabe-Nishimura, "Transactivation of the EGF receptor and a PI3 kinase-ATF-1 pathway is involved in the upregulation of NOX1, a catalytic subunit of NADPH oxidase," *FEBS Letters*, vol. 579, no. 5, pp. 1301–1305, 2005.

[143] J. Shi, C. R. Ross, T. L. Leto, and F. Blecha, "PR-39, a proline-rich antibacterial peptide that inhibits phagocyte NADPH oxidase activity by binding to Src homology 3 domains of p47phox," *Proceedings of the National Academy of Sciences of the United States of America*, vol. 93, no. 12, pp. 6014–6018, 1996.

[144] A. J. Cayatte, A. Rupin, J. Oliver-Krasinski et al., "S17834, a new inhibitor of cell adhesion and atherosclerosis that targets nadph oxidase," *Arteriosclerosis, Thrombosis, and Vascular Biology*, vol. 21, no. 10, pp. 1577–1584, 2001.

[145] C. Stielow, R. A. Catar, G. Muller et al., "Novel Nox inhibitor of oxLDL-induced reactive oxygen species formation in human endothelial cells," *Biochemical and Biophysical Research Communications*, vol. 344, no. 1, pp. 200–205, 2006.

[146] H. ten Freyhaus, M. Huntgeburth, K. Wingler et al., "Novel Nox inhibitor VAS2870 attenuates PDGF-dependent smooth muscle cell chemotaxis, but not proliferation," *Cardiovascular Research*, vol. 71, no. 2, pp. 331–341, 2006.

[147] F. R. DeLeo, L. Yu, J. B. Burritt et al., "Mapping sites of interaction of p47-phox and flavocytochrome b with random-sequence peptide phage display libraries," *Proceedings of the National Academy of Sciences of the United States of America*, vol. 92, no. 15, pp. 7110–7114, 1995.

[148] F. E. Rey, M. E. Cifuentes, A. Kiarash, M. T. Quinn, and P. J. Pagano, "Novel competitive inhibitor of NAD(P)H oxidase assembly attenuates vascular O2- and systolic blood pressure in mice," *Circulation Research*, vol. 89, no. 5, pp. 408–414, 2001.

[149] G. M. Bokoch and V. Prossnitz, "Isoprenoid metabolism is required for stimulation of the respiratory burst oxidase of HL-60 cells," *The Journal of Clinical Investigation*, vol. 89, no. 2, pp. 402–408, 1992.

[150] S. Wassmann, U. Laufs, K. Muller et al., "Cellular antioxidant effects of atorvastatin in vitro and in vivo," *Arteriosclerosis, Thrombosis, and Vascular Biology*, vol. 22, no. 2, pp. 300–305, 2002.

[151] S. Rajagopalan, S. Kurz, T. Münzel et al., "Angiotensin II-mediated hypertension in the rat increases vascular superoxide production via membrane NADH/NADPH oxidase activation: contribution to alterations of vasomotor tone," *The Journal of Clinical Investigation*, vol. 97, no. 8, pp. 1916–1923, 1996.

[152] R. P. Mason, L. Kalinowski, R. F. Jacob, A. M. Jacoby, and T. Malinski, "Nebivolol reduces nitroxidative stress and restores nitric oxide bioavailability in endothelium of black Americans," *Circulation*, vol. 112, no. 24, pp. 3795–3801, 2005.

[153] H. Mollnau, E. Schulz, A. Daiber et al., "Nebivolol prevents vascular NOS III uncoupling in experimental hyperlipidemia and inhibits NADPH oxidase activity in inflammatory cells,"

Arteriosclerosis, Thrombosis, and Vascular Biology, vol. 23, no. 4, pp. 615–621, 2003.

[154] M. Oelze, A. Daiber, R. P. Brandes et al., "Nebivolol inhibits superoxide formation by NADPH oxidase and endothelial dysfunction in angiotensin II-treated rats," *Hypertension*, vol. 48, no. 4, pp. 677–684, 2006.

[155] R. Troost, E. Schwedhelm, S. Rojczyk, D. Tsikas, and J. C. Frolich, "Nebivolol decreases systemic oxidative stress in healthy volunteers," *British Journal of Clinical Pharmacology*, vol. 50, no. 4, pp. 377–379, 2000.

[156] C. Coméra, K. André, J. Laffitte, X. Collet, P. Galtier, and I. Maridonneau-Parini, "Gliotoxin from Aspergillus fumigatus affects phagocytosis and the organization of the actin cytoskeleton by distinct signalling pathways in human neutrophils," *Microbes and Infection*, vol. 9, no. 1, pp. 47–54, 2007.

[157] T. Kawahara, Y. Kuwano, S. Teshima-Kondo et al., "Role of nicotinamide adenine dinucleotide phosphate oxidase 1 in oxidative burst response to Toll-like receptor 5 signaling in large intestinal epithelial cells," *Journal of Immunology*, vol. 172, no. 5, pp. 3051–3058, 2004.

[158] Y. O. Kweon, Y. H. Paik, B. Schnabl, T. Qian, J. J. Lemasters, and D. A. Brenner, "Gliotoxin-mediated apoptosis of activated human hepatic stellate cells," *Journal of Hepatology*, vol. 39, no. 1, pp. 38–46, 2003.

[159] S. Tsunawaki, L. S. Yoshida, S. Nishida, T. Kobayashi, and T. Shimoyama, "Fungal metabolite gliotoxin inhibits assembly of the human respiratory burst NADPH oxidase," *Infection and Immunity*, vol. 72, no. 6, pp. 3373–3382, 2004.

[160] L. S. Yoshida, S. Abe, and S. Tsunawaki, "Fungal gliotoxin targets the onset of superoxide-generating NADPH oxidase of human neutrophils," *Biochemical and Biophysical Research Communications*, vol. 268, no. 3, pp. 716–723, 2000.

[161] P. Sehr, G. Joseph, H. Genth, I. Just, E. Pick, and K. Aktories, "Glucosylation and ADP ribosylation of Rho proteins: effects on nucleotide binding, GTPase activity, and effector coupling," *Biochemistry*, vol. 37, no. 15, pp. 5296–5304, 1998.

[162] J. A. Holland, J. W. Meyer, M. M. Chang, R. W. O'Donnell, D. K. Johnson, and L. M. Ziegler, "Thrombin stimulated reactive oxygen species production in cultured human endothelial cells," *Endothelium*, vol. 6, no. 2, pp. 113–121, 1998.

[163] Y. Ozaki, T. Ohashi, and Y. Niwa, "A comparative study on the effects of inhibitors of the lipoxygenase pathway on neutrophil function. Inhibitory effects on neutrophil function may not be attributed to inhibition of the lipoxygenase pathway," *Biochemical Pharmacology*, vol. 35, no. 20, pp. 3481–3488, 1986.

[164] S. Tsunawaki and C. F. Nathan, "Release of arachidonate and reduction of oxygen. Independent metabolic bursts of the mouse peritoneal macrophage," *The Journal of Biological Chemistry*, vol. 261, no. 25, pp. 11563–11570, 1986.

[165] J. A. Holland, J. W. Meyer, M. E. Schmitt et al., "Low-density lipoprotein stimulated peroxide production and endocytosis in cultured human endothelial cells: mechanisms of action," *Endothelium*, vol. 5, no. 3, pp. 191–207, 1997.

[166] D. Bonnefont-Rousselot, B. Raji, S. Walrand et al., "An intracellular modulation of free radical production could contribute to the beneficial effects of metformin towards oxidative stress," *Metabolism*, vol. 52, no. 5, pp. 586–589, 2003.

[167] M. Mahrouf, N. Ouslimani, J. Peynet et al., "Metformin reduces angiotensin-mediated intracellular production of reactive oxygen species in endothelial cells through the inhibition of protein kinase C," *Biochemical Pharmacology*, vol. 72, no. 2, pp. 176–183, 2006.

[168] N. Ouslimani, J. Peynet, D. Bonnefont-Rousselot, P. Thérond, A. Legrand, and J. L. Beaudeux, "Metformin decreases intracellular production of reactive oxygen species in aortic endothelial cells," *Metabolism*, vol. 54, no. 6, pp. 829–834, 2005.

[169] A. J. Koupparis, J. Y. Jeremy, S. Muzaffar, R. Persad, and N. Shukla, "Sildenafil inhibits the formation of superoxide and the expression of gp47phox NAD[P]H oxidase induced by the thromboxane A2 mimetic, U46619, in corpus cavernosal smooth muscle cells," *British Journal of Urology International*, vol. 96, no. 3, pp. 423–427, 2005.

[170] M. Guazzi and M. Samaja, "The role of PDE5-inhibitors in cardiopulmonary disorders: from basic evidence to clinical development," *Current Medicinal Chemistry*, vol. 14, no. 20, pp. 2181–2192, 2007.

[171] S. Muzaffar, N. Shukla, A. Srivastava, G. D. Angelini, and J. Y. Jeremy, "Sildenafil citrate and sildenafil nitrate (NCX 911) are potent inhibitors of superoxide formation and gp91phox expression in porcine pulmonary artery endothelial cells," *British Journal of Pharmacology*, vol. 146, no. 1, pp. 109–117, 2005.

[172] N. Shukla, R. Jones, R. Persad, G. D. Angelini, and J. Y. Jeremy, "Effect of sildenafil citrate and a nitric oxide donating sildenafil derivative, NCX 911, on cavernosal relaxation and superoxide formation in hypercholesterolaemic rabbits," *European Journal of Pharmacology*, vol. 517, no. 3, pp. 224–231, 2005.

[173] J. Y. Kwak, K. Takeshige, B. S. Cheung, and S. Minakami, "Bilirubin inhibits the activation of superoxide-producing NADPH oxidase in a neutrophil cell-free system," *Biochimica et Biophysica Acta*, vol. 1076, no. 3, pp. 369–373, 1991.

[174] S. Lanone, S. Bloc, R. Foresti et al., "Bilirubin decreases nos2 expression via inhibition of NAD(P)H oxidase: implications for protection against endotoxic shock in rats," *FASEB Journal*, vol. 19, no. 13, pp. 1890–1892, 2005.

[175] A. Pflueger, A. J. Croatt, T. E. Peterson et al., "The hyperbilirubinemic Gunn rat is resistant to the pressor effects of angiotensin II," *American Journal of Physiology*, vol. 288, no. 3, pp. F552–F558, 2005.

[176] K. N. Agwuh and A. MacGowan, "Pharmacokinetics and pharmacodynamics of the tetracyclines including glycylcyclines," *Journal of Antimicrobial Chemotherapy*, vol. 58, no. 2, pp. 256–265, 2006.

[177] S. H. Choi, D. Y. Lee, E. S. Chung, Y. B. Hong, S. U. Kim, and B. K. Jin, "Inhibition of thrombin-induced microglial activation and NADPH oxidase by minocycline protects dopaminergic neurons in the substantia nigra in vivo," *Journal of Neurochemistry*, vol. 95, no. 6, pp. 1755–1765, 2005.

[178] H. Ashrafian, J. D. Horowitz, and M. P. Frenneaux, "Perhexiline," *Cardiovascular Drug Reviews*, vol. 25, no. 1, pp. 76–97, 2007.

[179] J. A. Kennedy, K. Beck-Oldach, K. McFadden-Lewis et al., "Effect of the anti-anginal agent, perhexiline, on neutrophil, valvular and vascular superoxide formation," *European Journal of Pharmacology*, vol. 531, no. 1–3, pp. 13–19, 2006.

[180] H. Abdelghaffar, C. Babin-Chevaye, and M. T. Labro, "The macrolide roxithromycin impairs NADPH oxidase activation and alters translocation of its cytosolic components to the neutrophil membrane in vitro," *Antimicrobial Agents and Chemotherapy*, vol. 49, no. 7, pp. 2986–2989, 2005.

[181] R. Anderson, "Erythromycin and roxithromycin potentiate human neutrophil locomotion in vitro by inhibition of leukoattractant-activated superoxide generation and autooxidation," *Journal of Infectious Diseases*, vol. 159, no. 5, pp. 966–973, 1989.

[182] D. K. Perry, W. L. Hand, D. E. Edmondson, and J. D. Lambeth, "Role of phospholipase D-derived diradylglycerol in the activation of the human neutrophil respiratory burst oxidase: inhibition by phosphatidic acid phosphohydrolase inhibitors," *Journal of Immunology*, vol. 149, no. 8, pp. 2749–2758, 1992.

[183] M. Barua, Y. Liu, and M. R. Quinn, "Taurine chloramine inhibits inducible nitric oxide synthase and TNF-α gene expression in activated alveolar macrophages: decreased NF-κB activation and IκB kinase activity," *Journal of Immunology*, vol. 167, no. 4, pp. 2275–2281, 2001.

[184] C. Kim, E. Park, M. R. Quinn, and G. Schuller-Levis, "The production of superoxide anion and nitric oxide by cultured murine leukocytes and the accumulation of TNF-α in the conditioned media is inhibited by taurine chloramine," *Immunopharmacology*, vol. 34, no. 2-3, pp. 89–95, 1996.

[185] G. Deby-Dupont, A. Mouithys-Mickalad, D. Serteyn, M. Lamy, and C. Deby, "Resveratrol and curcumin reduce the respiratory burst of Chlamydia-primed THP-1 cells," *Biochemical and Biophysical Research Communications*, vol. 333, no. 1, pp. 21–27, 2005.

[186] J. Leiro, E. Álvarez, J. A. Arranz, R. Laguna, E. Uriarte, and F. Orallo, "Effects of cis-resveratrol on inflammatory murine macrophages: antioxidant activity and down-regulation of inflammatory genes," *Journal of Leukocyte Biology*, vol. 75, no. 6, pp. 1156–1165, 2004.

[187] T. M. Poolman, L. L. Ng, P. B. Farmer, and M. M. Manson, "Inhibition of the respiratory burst by resveratrol in human monocytes: correlation with inhibition of PI3K signaling," *Free Radical Biology and Medicine*, vol. 39, no. 1, pp. 118–132, 2005.

[188] J. Fang, J. Lu, and A. Holmgren, "Thioredoxin reductase is irreversibly modified by curcumin: a novel molecular mechanism for its anticancer activity," *The Journal of Biological Chemistry*, vol. 280, no. 26, pp. 25284–25290, 2005.

[189] B. Coles, A. Bloodsworth, S. R. Clark et al., "Nitrolinoleate inhibits superoxide generation, degranulation, and integrin expression by human neutrophils: novel antiinflammatory properties of nitric oxide-derived reactive species in vascular cells," *Circulation Research*, vol. 91, no. 5, pp. 375–381, 2002.

[190] E. S. Lima, M. G. Bonini, O. Augusto, H. V. Barbeiro, H. P. Souza, and D. S. P. Abdalla, "Nitrated lipids decompose to nitric oxide and lipid radicals and cause vasorelaxation," *Free Radical Biology and Medicine*, vol. 39, no. 4, pp. 532–539, 2005.

[191] A. C. Allison and E. M. Eugui, "Mycophenolate mofetil and its mechanisms of action," *Immunopharmacology*, vol. 47, no. 2-3, pp. 85–118, 2000.

[192] F. Krötz, M. Keller, S. Derflinger et al., "Mycophenolate acid inhibits endothelial NAD(P)H oxidase activity and superoxide formation by a Rac1-dependent mechanism," *Hypertension*, vol. 49, no. 1, pp. 201–208, 2007.

[193] B. Laleu, F. Gaggini, M. Orchard et al., "First in class, potent, and orally bioavailable NADPH oxidase isoform 4 (Nox4) inhibitors for the treatment of idiopathic pulmonary fibrosis," *Journal of Medicinal Chemistry*, vol. 53, no. 21, pp. 7715–7730, 2010.

[194] M. Sedeek, G. Callera, A. Montezano et al., "Critical role of Nox4-based NADPH oxidase in glucose-induced oxidative stress in the kidney: implications in type 2 diabetic nephropathy," *American Journal of Physiology*, vol. 299, no. 6, pp. F1348–F1358, 2010.

[195] D. Gianni, N. Taulet, H. Zhang et al., "A novel and specific NADPH oxidase-1 (Nox1) small-molecule inhibitor blocks the formation of functional invadopodia in human colon cancer cells," *ACS Chemical Biology*, vol. 5, no. 10, pp. 981–993, 2010.

[196] S. Jones and J. Howl, "Biological applications of the receptor mimetic peptide mastoparan," *Current Protein and Peptide Science*, vol. 7, no. 6, pp. 501–508, 2006.

[197] D. Tisch, Y. Sharoni, M. Danilenko, and I. Aviram, "The assembly of neutrophil NADPH oxidase: effects of mastoparan and its synthetic analogues," *Biochemical Journal*, vol. 310, no. 2, pp. 715–719, 1995.

[198] D. Tisch-Idelson, M. Fridkin, F. Wientjes, and I. Aviram, "Structure-function relationship in the interaction of mastoparan analogs with neutrophil NADPH oxidase," *Biochemical Pharmacology*, vol. 61, no. 9, pp. 1063–1071, 2001.

[199] G. Yibin, Z. Jiang, Z. Hong et al., "A synthesized cationic tetradecapeptide from hornet venom kills bacteria and neutralizes lipopolysaccharide in vivo and in vitro," *Biochemical Pharmacology*, vol. 70, no. 2, pp. 209–219, 2005.

[200] A. Kawczynska-Drozdz, R. Olszanecki, J. Jawien et al., "Ghrelin inhibits vascular superoxide production in spontaneously hypertensive rats," *American Journal of Hypertension*, vol. 19, no. 7, pp. 764–767, 2006.

[201] M. L. Schubert, "Gastric secretion," *Current Opinion in Gastroenterology*, vol. 23, no. 6, pp. 595–601, 2007.

[202] Y. Sun, M. Asnicar, and R. G. Smith, "Central and peripheral roles of ghrelin on glucose homeostasis," *Neuroendocrinology*, vol. 86, no. 3, pp. 215–228, 2007.

[203] O. Cachia, J. El Benna, E. Pedruzzi, B. Descomps, M. A. Gougerot-Pocidalo, and C. L. Leger, "α-Tocopherol inhibits the respiratory burst in human monocytes: attenuation of p47(phox) membrane translocation and phosphorylation," *The Journal of Biological Chemistry*, vol. 273, no. 49, pp. 32801–32805, 1998.

[204] T. Egger, A. Hammer, A. Wintersperger, D. Goti, E. Malle, and W. Sattler, "Modulation of microglial superoxide production by α-tocopherol in vitro: attenuation of p67phox translocation by a protein phosphatase-dependent pathway," *Journal of Neurochemistry*, vol. 79, no. 6, pp. 1169–1182, 2001.

[205] T. Kanno, T. Utsumi, Y. Takehara et al., "Inhibition of neutrophil-superoxide generation by α-tocopherol and coenzyme Q," *Free Radical Research*, vol. 24, no. 4, pp. 281–289, 1996.

[206] S. K. Venugopal, S. Devaraj, T. Yang, and I. Jialal, "Alpha-tocopherol decreases superoxide anion release in human monocytes under hyperglycemic conditions via inhibition of protein kinase C-α," *Diabetes*, vol. 51, no. 10, pp. 3049–3054, 2002.

[207] K. Ippoushi, H. Itou, K. Azuma, and H. Higashio, "Effect of naturally occurring organosulfur compounds on nitric oxide production in lipopolysaccharide-activated macrophages," *Life Sciences*, vol. 71, no. 4, pp. 411–419, 2002.

[208] N. Miyoshi, S. Takabayashi, T. Osawa, and Y. Nakamura, "Benzyl isothiocyanate inhibits excessive superoxide generation in inflammatory leukocytes: implication for prevention against inflammation-related carcinogenesis," *Carcinogenesis*, vol. 25, no. 4, pp. 567–575, 2004.

[209] D. Xiao, V. Vogel, and S. V. Singh, "Benzyl isothiocyanate-induced apoptosis in human breast cancer cells is initiated by reactive oxygen species and regulated by Bax and Bak," *Molecular Cancer Therapeutics*, vol. 5, no. 11, pp. 2931–2945, 2006.

[210] N. Inoue, Y. Ohara, T. Fukai, D. G. Harrison, and K. Nishida, "Probucol improves endothelial-dependent relaxation and decreases vascular superoxide production in cholesterol-fed rabbits," *American Journal of the Medical Sciences*, vol. 315, no. 4, pp. 242–247, 1998.

[211] H. Itoh, K. Komori, J. Okazaki et al., "The effect of probucol on intimal thickening of autologous vein grafts in hyperlipidemic rabbit," *Cardiovascular Surgery*, vol. 5, no. 5, pp. 497–503, 1997.

[212] S. Itoh, S. Umemoto, M. Hiromoto et al., "Importance of NAD(P)H oxidase-mediated oxidative stress and contractile type smooth muscle myosin heavy chain SM2 at the early stage of atherosclerosis," *Circulation*, vol. 105, no. 19, pp. 2288–2295, 2002.

[213] J. F. Keaney Jr., A. Xu, D. Cunningham, T. Jackson, B. Frei, and J. A. Vita, "Dietary probucol preserves endothelial function in cholesterol-fed rabbits by limiting vascular oxidative stress and superoxide generation," *The Journal of Clinical Investigation*, vol. 95, no. 6, pp. 2520–2529, 1995.

[214] F. R. DeLeo, W. M. Nauseef, A. J. Jesaitis, J. B. Burritt, R. A. Clark, and M. T. Quinn, "A domain of p47(phox) that interacts with human neutrophil flavocytochrome b558," *The Journal of Biological Chemistry*, vol. 270, no. 44, pp. 26246–26251, 1995.

[215] S. Wind, K. Beuerlein, T. Eucker et al., "Comparative pharmacology of chemically distinct NADPH oxidase inhibitors," *British Journal of Pharmacology*, vol. 161, no. 4, pp. 885–898, 2010.

[216] G. R. Drummond, S. Selemidis, K. K. Griendling, and C. G. Sobey, "Combating oxidative stress in vascular disease: NADPH oxidases as therapeutic targets," *Nature Reviews Drug Discovery*, vol. 10, no. 6, pp. 453–471, 2011.

Hindawi Publishing Corporation
Oxidative Medicine and Cellular Longevity
Volume 2013, Article ID 245253, 8 pages
http://dx.doi.org/10.1155/2013/245253

Clinical Study

The Role of Xanthine Oxidase in Hemodialysis-Induced Oxidative Injury: Relationship with Nutritional Status

Dijana Miric,[1] Bojana Kisic,[1] Radojica Stolic,[2] Bratislav Miric,[3] Radoslav Mitic,[4] and Snezana Janicijevic-Hudomal[4]

[1] *Institute of Biochemistry, Medical Faculty Pristina, 38220 Kosovska Mitrovica, Serbia*
[2] *Internal Clinic, Medical Faculty Pristina, 38220 Kosovska Mitrovica, Serbia*
[3] *Department of Informatics, State University of Novi Pazar, 36300 Novi Pazar, Serbia*
[4] *Institute of Pharmacology, Medical Faculty Pristina, 38220 Kosovska Mitrovica, Serbia*

Correspondence should be addressed to Dijana Miric; miric.dijana@gmail.com

Received 31 January 2013; Accepted 17 May 2013

Academic Editor: Kota V. Ramana

The role of xanthine oxidase (XOD) in patients undergoing chronic hemodialysis treatment (HD) is poorly understood. Geriatric nutritional risk index (GNRI) ≤ 90 could be linked with malnutrition-inflammation complex syndrome. This study measured XOD, myeloperoxidase (MPO), superoxide dismutase (SOD), lipid hydroperoxides, total free thiol groups, and advanced oxidation protein products (AOPP) in 50 HD patients before commencing (pre-HD) and immediately after completion of HD session (post-HD) and in 22 healthy controls. Pre-HD serum hydroperoxides, AOPP, XOD, and SOD were higher and total thiol groups were lower in patients than in controls ($P < 0.05$, resp.). Compared to baseline values, serum MPO activity was increased irrespective of GNRI status. Serum XOD activity was increasing during HD treatment in the group with GNRI ≤ 90 ($P = 0.030$) whilst decreasing in the group with GNRI > 90 ($P = 0.002$). In a multiple regression analysis, post-HD serum XOD activity was independently associated with GNRI ≤ 90 ($\beta \pm$ SE: 0.398 ± 0.151; $P = 0.012$) and HD vintage ($\beta \pm$ SE: -0.349 ± 0.139; $P = 0.016$). These results indicate that an upregulated XOD may be implicated in HD-induced oxidative injury contributing to accelerated protein damage in patients with GNRI ≤ 90.

1. Introduction

Oxidative stress and malnutrition-inflammation complex syndrome often coexist in critically ill patients and have recently came into a focus as nontraditional risk factors of cardiovascular morbidity and overall mortality in patients with end-stage renal disease (ESRD) [1–5]. The reasons underlying chronically disturbed oxidant homeostasis in ESRD may include various factors, such as progressive deterioration of renal metabolic activities, inflammation, uremic toxins, and restrictive diets [1, 6, 7]. It has been previously shown that even a single hemodialysis (HD) treatment can provoke the formation of oxidants, which was largely attributed to activation of leukocytes by bio-incompatible dialysis membrane and release of myeloperoxidase (MPO) into the blood [2]. Extracellular MPO is well known to catalyze the peroxidation of the blood low-density lipoproteins (LDL) and albumin, leading to the formation of oxidized LDL and advanced oxidation protein products (AOPP), thereby contributing to augmentation of prooxidant and proinflammatory state in the vascular compartment [2, 4, 5].

Xanthine dehydrogenase (XDH) is a cytoplasmic enzyme implicated in hydroxylation of hypoxanthine to xanthine and its oxidation to uric acid and a relevant source of oxidants in vasculature [8–10]. XDH may undergo limited proteolysis or oxidation of critical cysteine residues to yield the xanthine oxidase (XOD) form. Unlike XDH that generates mostly superoxide anion radicals, XOD more efficiently catalyzes the formation of hydrogen peroxide, which is less reactive but long-lived oxidant. Previous studies have revealed systematically upregulated XOD in inflammation, diabetes, and cardiovascular diseases [11, 12]. Moreover, serum XOD activity was found to be markedly elevated in HD and peritoneal dialysis patients, independently of dialysis modality [13].

Patients undergoing HD treatment have high prevalence of malnutrition-inflammation syndrome, clinically presented as muscle and fat tissue wasting, loss of visceral proteins, and higher inflammatory and oxidative state [1, 4, 5]. There is currently no clear explanation about mechanisms underlying enhanced oxidative stress in HD patients with low nutritional status. However, recent experimental studies suggest that targeting XOD by allopurinol may protect against oxidative stress, inflammatory cytokine signaling, proteolytic activity, and tissue wasting [14]. Geriatric nutritional risk index (GNRI) is a useful tool for nutritional screening, based on simple anthropometric measures and serum albumin concentration. In a cohort of 490 chronic HD patients, the predialytic GNRI values below 90 have been recently linked with increased inflammatory CRP levels and mortality rates [3]. Given that prooxidant enzymes can play significant roles in oxidative stress, this study assessed serum MPO and XOD activities and oxidative stress markers in relation to nutritional status in ESRD patients on chronic HD treatment.

2. Subjects and Methods

2.1. Study Participants. Fifty adults, clinically stabile nonsmoker ESRD patients (23 males, 27 females, mean age 57.4 ± 12.6 years) were enrolled in the study after written informed consent was provided. Patients were routinely dialyzed 12 hours per week in two local dialysis centers using commercially available dialysers in the bicarbonate hemodialysis and hemodiafiltration (Fresenius Medical Care, Bad Homburg, Germany). The causes of ESRD were diabetic nephropathy (28%), polycystic kidney disease (22%), chronic glomerulonephritis (16%), nephrosclerosis (12%) chronic pyelonephritis (8%), and nephropathy of unknown etiology (14%). Excluded were patients with known malignant, hepatic or autoimmune diseases, acute infections, or recent cardiovascular events. The control group was consisted of 22 age- and sex-matched healthy subjects (9 males, 13 females, mean age 58.4 ± 9.3 years). This study was conducted following the tenets of Declaration of Helsinki. Ethical clearance for the study was obtained from the Ethics Committee of Medical Faculty Pristina, Kosovska Mitrovica.

2.2. Sample Collection. At the middle of dialysis week, 10 mL of blood was taken into tubes with or without EDTA, prior to anticoagulation and start of HD (pre-HD) and immediately after completion of HD treatment (post-HD).

2.3. Biochemical Methods

2.3.1. Measurement of Serum Xanthine Oxidase Activity. Serum XOD activity was determined by UV method, using xanthine as a substrate, as described in [15]. The formation of uric acid was continuously monitored at $\lambda = 293$ nm on an UV/VIS spectrophotometer equipped with a constant temperature cuvette compartment (SAFAS 2, Monaco). XOD activity was calculated after correction for preexisting uric acid using molar absorbance of $\varepsilon = 1.26 \times 10^4\ \mathrm{L} \times \mathrm{M}^{-1} \times \mathrm{cm}^{-1}$. One unit of XOD activity was defined as 1 μmol uric acid formed per minute at 37°C.

2.3.2. Assessment of Extracellular Myeloperoxidase Activity. Serum MPO activity was measured in the system of 4-aminoantipyrine and phenol with hydrogen peroxide as a substrate, by monitoring the formation of pinkish colored quinoneimine at $\lambda = 505$ nm [16]. MPO activity was calculated using molar absorbance of $\varepsilon = 1.3 \times 10^4\ \mathrm{L} \times \mathrm{M}^{-1} \times \mathrm{cm}^{-1}$. One unit of MPO activity was defined as amount of enzyme degrading 1 μmol of hydrogen peroxide per minute, at 25°C.

2.3.3. Assessment of Extracellular Superoxide Dismutase Activity. Superoxide dismutase (SOD) is an antioxidant enzyme that catalyzes the conversion of superoxide anion radicals to hydrogen peroxide and molecular oxygen. Serum SOD activity was determined by the rate of inhibition of adrenaline autooxidation to adrenochrome, continuously monitored at 25°C for 3 minutes at $\lambda = 480$ nm and calculated using the molar absorbance of $\varepsilon = 4.02 \times 10^3\ \mathrm{L} \times \mathrm{M}^{-1} \times \mathrm{cm}^{-1}$ [17]. One unit of SOD activity was defined as the quantity of enzyme that inhibits autooxidation of 5 mmol adrenaline by 50%.

2.3.4. Determination of Total Free Thiol Groups. Serum free thiol groups (SH) are implicated in nonenzymatic antioxidant defense and can serve as a marker of acute oxidative protein injury. Concentration of serum SH groups was determined with Ellman's reagent and calculated using molar absorbance of $\varepsilon = 1.36 \times 10^4\ \mathrm{L} \times \mathrm{mol}^{-1} \times \mathrm{cm}^{-1}$ [18].

2.3.5. Measurement of Blood Oxidative Stress Markers. We measured two oxidative stress markers: total hydroperoxides, indicating an ongoing lipid peroxidation (LPO) and advanced oxidation protein products (AOPP) representing a marker of protein oxidative injury. Concentration of total serum hydroperoxides was measured by the ferrous-oxidation xylenol-orange method (FOX), following reduction of preexisting peroxides with triphenylphosphine [19]. Plasma AOPP was measured by the method of Anderstam et al. [20]. The absorbance readings were taken at $\lambda = 340$ nm against reagent blank. Concentration of AOPP was calculated respective to chloramine-T standard, corrected for dilution factor.

2.3.6. Other Hematological and Blood Biochemical Measurements and Calculations. Blood cell count and differential were measured in EDTA blood samples with the Onyx hematology analyzer (Beckman Coulter, Krefeld, Germany). Total proteins, albumin, urea, total cholesterol, HDL-cholesterol, triglyceride, uric acid, and C-reactive protein (CRP) were routinely measured on Hitachi 902 chemistry analyzer (Roche Diagnostics GmbH, Mannheim, Germany), according to manufacturer's instructions. LDL cholesterol was calculated using Friedewald's formula. Plasma atherogenic index was calculated as Log (triglycerides/HDL cholesterol) [21].

Post-HD values of biochemical variables were corrected for intradialytic decrease of plasma volume, according to Leypoldt et al. [22]. The following formula was applied: $X_{\text{POST-corrected}} = X_{\text{POST}} \times [1 - (\text{TP}_{\text{POST}} - \text{TP}_{\text{PRE}})/\text{TP}_{\text{POST}}]$, where X and TP denote the particular biochemical variable and total serum protein concentrations in post-HD (TP_{POST}) and pre-HD samples (TP_{PRE}), respectively. The quality of dialysis was assessed as urea-based Kt/V formula.

2.4. Anthropometric and Nutritional Indices. Body mass index (BMI) was calculated respective to predialytic body weight by the formula: BMI (kg/m^2) = present body weight/height^2. Geriatric nutritional risk index (GNRI) was applied to assess nutritional status, calculated as follows using predialytic values of variables: GNRI = (1.489 × serum albumin (g/L)) + (41.7 × present/ideal body weight) [3]. The GNRI ≤ 90 was considered to be low [3].

2.5. Statistical Methods. Statistical analyses were accomplished with statistical software package MedCalc, version 8.0, (MedCalc Software, Ostend, Belgium). Data distribution and homogeneity of variance were tested by Kolmogorov-Smirnov test. Data were presented as mean value ± SD, geometric mean and 95% confidence interval (CI) of the mean or frequencies. Differences between groups were tested by one-way ANOVA and Student's t-test for independent or paired samples, where appropriate; chi-square test was used to compare nonparametric data. Correlation analysis was accomplished by calculating the Pearson's correlation coefficient (r). Multiple regression analysis was used to examine the influence of multiple clinical and biochemical variables on XOD activity. The significance level was set at $P < 0.05$.

3. Results

A total of 50 ESRD patients and 22 controls were included in the study. Basic clinical and biochemical data of patients and controls are summarized in Table 1. In comparison to controls, patients with ESRD had higher neutrophil leukocyte count, ferritin, and CRP, while lower blood hemoglobin levels (Table 1).

Baseline levels of oxidative stress markers, prooxidant enzymes, and SOD activity in ESRD patients and control subjects are presented in Table 2. In comparison to control values, serum total hydroperoxides and AOPP were significantly higher, and total SH groups were lower in patients. Also, extracellular SOD and XOD activities were at the baseline higher in patients than in controls, while MPO activity was comparable to control values (Table 2).

According to adopted criterion [3], ESRD patients were further divided into group with GNRI ≤ 90 ($n = 15$) and group with GNRI > 90 ($n = 35$). Seven patients in each group had diabetic nephropathy (chi-square = 2.499; $P = 0.114$). There was also no significant difference between GNRI > 90 and GNRI ≤ 90 groups regarding baseline concentrations of serum hydroperoxides and AOPP, as well as XOD and MPO activities (Table 3, Figure 1). However, baseline serum total SH groups were significantly lower, whilst SOD activity was higher in GNRI ≤ 90 than in GNRI > 90 group (Table 3).

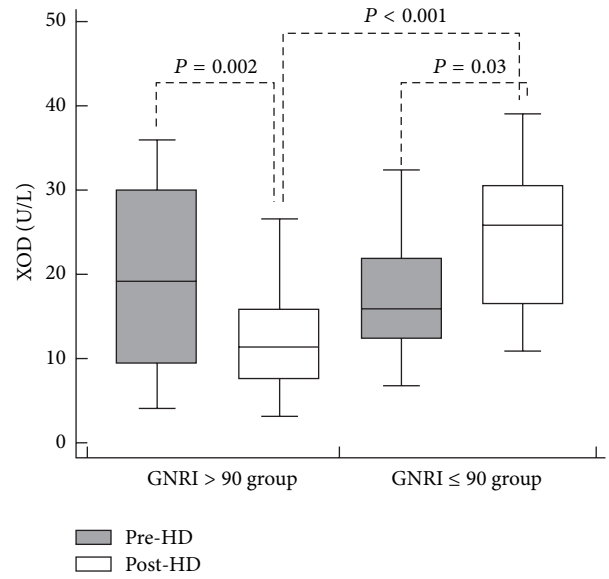

Figure 1: The impact of a single hemodialysis session on serum XOD activity. Serum xanthine oxidase activity (XOD) was determined prior to (pre-HD) and immediately after completion of hemodialysis session (post-HD) in patients with normal geriatric nutritional risk index (GNRI > 90) and with GNRI ≤ 90. In contrast to GNRI > 90 group, where a single HD session induced the fall of serum XOD activity from 19.3 ± 10.6 U/L to 12.1 ± 6.0 U/L ($P = 0.002$, paired samples t-test), in the group with GNRI ≤ 90, there was an elevation of serum XOD activity from 18.4 ± 7.8 U/L to 24.8 ± 7.3 U/L ($P = 0.030$, paired samples t-test), contributing to significant post-HD differences between GNRI groups ($P < 0.001$, independent samples t-test).

To evaluate the impact of a single HD session on blood oxidants and antioxidants, all post-HD values were corrected for intradialytic decrease of blood plasma volume [22]. In comparison to baseline values, post-HD serum hydroperoxides and total SH groups were lower, while AOPP levels were unchanged. Relative to pre-HD values, serum SOD and MPO activities were higher in post-HD samples. The post-HD serum MPO activity was correlated with AOPP ($r = 0.355$; $P = 0.011$).

In comparison to group with GNRI > 90, post-HD serum hydroperoxides were higher and total SH groups were lower than in the group with GNRI ≤ 90 (Table 3). Post-HD XOD activity also differed between groups (Figure 1), in such way that in GNRI > 90 group baseline serum XOD activity declined during HD from 19.3 ± 10.6 U/L to 12.1 ± 6.0 U/L ($P = 0.002$, paired samples t-test) while increased after HD treatment in GNRI ≤ 90 group from 18.4 ± 7.8 U/L to 24.8 ± 7.3 U/L ($P = 0.030$, paired samples t-test). Post-HD serum XOD activity was correlated with hydroperoxides ($r = 0.540$; $P < 0.001$), AOPP ($r = 0.324$; $P = 0.022$), and total SH groups ($r = -0.578$; $P < 0.001$).

We also modeled a multiple regression analysis to examine the influence of age, gender (male versus female), HD

Table 1: Basic clinical and biochemical data of ESRD patients and controls.

	Control group ($n = 22$)	ESRD patients ($n = 50$)
Age (years)	58.9 ± 13.3	61.7 ± 10.7
Gender (male/female, n)	9/13	14/14
Hypertension (yes/no, n)	8/14	8/14
Hemodialysis vintage (months)	NA	46.3 ± 36.6
Kt/V urea	NA	1.10 ± 0.37
Neutrophil leukocytes (10^9/L)	4.10 ± 1.92	4.89 ± 2.07
Lymphocytes (10^9/L)	2.21 ± 0.55	2.39 ± 0.92
Log CRP (mg/L)	0.114 ± 0.335	0.534 ± 0.633*
Albumin (g/L)	45.6 ± 5.1	40.6 ± 7.3*
Hemoglobin (g/L)	133.7 ± 20.2	118.6 ± 24.1*
Ferritin (μg/L)	85 ± 62	511 ± 647*
Body mass index (kg/m^2)	22.9 ± 5.3	21.4 ± 4.4
GNRI	114.3 ± 16.0	105.9 ± 13.4
Total cholesterol (mmol/L)	4.65 ± 1.14	4.90 ± 0.96
HDL cholesterol (mmol/L)	1.76 ± 0.54	1.54 ± 0.51
LDL cholesterol (mmol/L)	2.75 ± 0.65	3.09 ± 0.62
Triglycerides (mmol/L)	1.92 ± 0.91	2.13 ± 0.77
Plasma atherogenic index	0.152 ± 0.175	0.196 ± 0.172

* $P < 0.05$ versus controls; NA: not applicable.

Table 2: Blood oxidative stress markers and antioxidants in ESRD patients and controls.

	Control group ($n = 22$)	ESRD patients ($n = 50$)
Hydroperoxides (μmol/L)	6.1 ± 1.5	12.5 ± 4.1*
AOPP (μmol/L)	40.1 ± 11.1	91.3 ± 24.9*
Total SH groups (μmol/L)	462 ± 73	371 ± 59*
SOD (kU/L)	43.6 ± 12.5	61.3 ± 17.1*
MPO (U/L)	16.9 ± 6.5	18.1 ± 5.4
XOD (U/L)	3.7 ± 1.0	18.5 ± 10.6*

* $P < 0.05$ versus controls.

vintage, the quality of HD, presence of hypertension or diabetes (yes versus no, resp.), inflammatory CRP levels, plasma atherogenic index, and GNRI status (GNRI ≤ 90 versus GNRI > 90) on post-HD serum XOD activity. Univariate analysis (Table 4) showed that post-HD serum XOD activity was significantly correlated with HD vintage ($P = 0.016$), serum CRP ($P = 0.028$), and GNRI status ($P = 0.001$). In a multivariate regression with stepwise elimination mode, HD vintage ($P = 0.016$) and GNRI status ($P = 0.012$) were retained as independent predictors of post-HD serum XOD activity (Table 4).

4. Discussion

In the present study, we evaluated the relationship between serum XOD activity, oxidative stress markers, and nutritional status in HD patients. The major finding was that elevation of XOD activity during a single HD session was positively correlated with serum hydroperoxides and AOPP and independently associated with GNRI ≤ 90, as an indicator of poor nutritional status. These results suggest that an upregulated XOD may exacerbate oxidative injury during HD treatment contributing to pathogenesis of malnutrition-inflammation complex syndrome.

Chronic uremia is known to induce a large-scale oxidative modifications of blood lipids and proteins, leading to increased hydroperoxides and AOPP and loss of free SH groups [2, 6, 7], as was also observed in the current study. The majority of serum free SH groups are provided by albumin, whose single free SH group at cysteine 34 is exposed at the surface of the molecule. Acting as a sacrificial antioxidant albumin can prevent oxidative damage of practically all blood constituents, which is particularly important in cases when other antioxidants, such as vitamin C, are present at chronically low levels or at highly oxidized state. However, the oxidation of free SH and other critical groups may facilitate albumin fragmentation and subsequent breakdown [23, 24] and further deteriorate the blood protein, nutritional and antioxidant status. Moreover, some blood antioxidant and anti-inflammatory proteins, such as α_1-antitrypsin and HDL apolipoprotein A, were found to be extensively oxidized in ESRD patients with malnutrition-inflammation complex syndrome [4, 5].

Table 3: Comparisons of blood oxidative stress markers, MPO and SOD, activities before and after completion of hemodialysis session.

	GNRI > 90 group ($n = 35$)		GNRI ≤ 90 group ($n = 15$)	
	Pre-HD	Post-HD	Pre-HD	Post-HD
Hydroperoxides (μmol/L)	12.9 ± 3.7	5.8 ± 1.7*	11.9 ± 3.0	7.9 ±2.8*,¶
AOPP (μmol/L)	94.6 ± 30.6	95.3 ± 28.7	82.2 ± 29.4	90.4 ± 27.5
Total thiol groups (μmol/L)	371 ± 59	292 ± 60*	296 ±67¶	193 ±62*,¶
MPO (U/L)	18.2 ± 6.9	71.3 ± 22.1*	19.6 ± 9.1	68.5 ± 25.9*
SOD (kU/L)	53.4 ± 20.4	101.3 ± 12.7*	75.6 ± 25.2*	107.1 ± 17.2*

Data are mean value ± SD. Differences between GNRI groups or between pre-HD and post-HD values were tested by independent samples t-test or paired samples t-test, respectively.
* $P < 0.05$ post-HD versus correspondent pre-HD value: ¶ $P < 0.05$ GNRI ≤ 90 versus GNRI > 90 group, at the same sampling time.

Table 4: Univariate and multivariate regression modeling predicting postdialytic serum XOD activity in ESRD patients.

Independent predictors	Univariate correlations			Multivariate model		
	β	SEM	P value	β	SEM	P value
Age (years)	0.008	0.144	0.953	−0.039	0.138	0.778
Gender (male versus female)	0.220	0.141	0.125	0.151	0.137	0.277
Hypertension (yes versus no)	−0.159	0.142	0.269	−0.044	0.135	0.742
Hemodialysis vintage (months)	−0.337	0.136	0.016	−0.349	0.139	0.016
Diabetes (yes versus no)	0.192	0.142	0.183	0.082	0.129	0.526
Kt/V urea	0.052	0.144	0.722	0.085	0.155	0.586
Log CRP (mg/L)	0.310	0.137	0.028	0.247	0.143	0.091
Plasma atherogenic index	0.116	0.143	0.424	0.175	0.128	0.225
GNRI ≤ 90 versus GNRI > 90	0.453	0.129	0.001	0.398	0.151	0.012

Multivariate R^2-adjusted = 0.278; $P = 0.006$.

Despite of the fact that the maintenance HD is currently the major treatment modality in ESRD, there are many controversies of whether and how it influences the burden of oxidatively modified molecules. Previous studies have demonstrated both the fall of serum hydroperoxides, as early as the first hour of HD session, and a significant increase of LPO adducts and AOPP in post-HD samples [6, 7]. In the current study serum hydroperoxides were markedly reduced during HD, while AOPP remained virtually unchanged (Table 3). Such findings could reflect different diffusion rates of hydroperoxides and macromolecular AOPP into dialytic fluid or faster decomposition of hydroperoxides to other LPO adducts that could not be detected with xylenol orange test. We observed that in comparison to the group with normal GNRI, those with low GNRI values had higher serum hydroperoxides and lower total SH groups after completion of HD treatment, which may indicate a higher degree of oxidative damage imposed during HD associated with worse blood nutritional status.

Aside from chronic uremia-induced oxidative stress, ESRD patients usually endure an intermittent oxidative injury during each HD treatment. It is generally believed that the major reason is activation of leukocytes upon contact with bio-incompatible dialysis membrane or impurity in dialysis fluid and release of MPO into the blood [1, 2]. Extracellular MPO is a powerful catalyst of the LPO process and induce chlorination and nitrosylation of various blood compounds, giving rise to dysfunctional molecules, toxic mediators, atherogenic lipids and protein oxidation products, such as AOPP [2]. Accordingly, serum MPO activity was by 300% increased after completion of HD and positively correlated with AOPP ($r = 0.355$; $P = 0.011$), which is consistent with evidence that dityrosine-containing oxidized albumin is the main constituent of AOPP [2, 25]. However, in agreement to some previous studies [4, 26], baseline serum MPO activity was in ESRD patients similar to that in healthy controls and comparable between GNRI groups (Table 2), and the post-HD MPO activities do not differ between patients' groups (Table 3).

On the other side, the baseline serum XOD activity was in ESRD patients far over the values in healthy subjects (Table 2) and in agreement with Choi et al. [13]. However, this finding may be rather expected having in mind that a variety of stimuli usually present in ESRD, like endotoxemia or hypoxia, can enhance the transcriptional activity of the XOD gene [9]. Beside controlling purine catabolic pathway, the XOD can induce the expression of cyclooxygenase-2 [27], translocation of nuclear factor-κB, synthesis of TNF-α, activation of neutrophils, and phagocytic killing [8, 12], being therefore a potent modulator of innate immune response. In turn, inflammatory cytokines may be responsible for upregulated synthesis of both CRP and XOD [28], and a positive correlation between these parameters in the current study (Table 4) further supports the idea that XOD has a putative role in inflammatory signal transduction [8].

XDH/XOD is constitutively expressed in endothelial and many other cells. Still, the majority of vascular enzyme are most probably of hepatic origin [9] and are reversibly

attached to endothelial cell surface via glycosaminoglycan-rich receptors. The release of extracellular XOD into circulation occurs upon competitive binding of heparin, proportionally to the content of vascular wall enzyme [10]. This was used for determination of endothelial XOD *in vivo*, particularly in pathologies associated with endothelial dysfunction. For example, a bolus injection of heparin (5000 IU) has been shown to induce an increase of serum XOD activity by 200% within a few minutes in patients with chronic heart failure but not in healthy controls [23]. In the current study all ESRD patients were routinely anticoagulated with unfractionated heparin solution, in accordance to European best practice guidelines. Taking into account the results of previous studies [10, 23], we may speculate that the post-HD elevation of serum XOD activity in the group with low GNRI status could reflect the basically higher content of endothelium-bound XOD.

Endothelial cells also contain some SOD enzyme bound to the cell surface, which probably serves to counterbalance the local formation of oxidants and is also released into the blood after bolus injection of heparin [23]. In the current study, there were differences regarding absolute values and the direction in which serum XOD activities have changed during HD, although the rise of SOD activity was almost equal in both GNRI groups. These results suggest that a poor nutritional status in ESRD could be associated with an imbalanced presence of prooxidant and antioxidant enzymes in the vascular compartment.

Patients undergoing HD treatment often experience some degree of intradialytic hypoxia associated with volume overload that may extend between two HD sessions [22]. During hypoxic periods, there is a decrease of intracellular pH leading to facilitated conversion of XDH to XOD form [9], while breakdown products, inosine and hypoxanthine, may accumulate due to poor regeneration of ATP. Hypoxanthine is normally present in plasma at only 1-2 μM but is several fold increased in HD patients [13] and can serve as a substrate for XOD-catalyzed formation of oxidants in the blood. *Ex vivo* incubation of human plasma with 5 mU/mL XOD and 500 μM hypoxanthine has been shown to oxidize up to 50% of total SH groups, mostly within the first 20 minutes [24]. According to our results, one of the reasons of enhanced oxidative damage in patients with low GNRI status could be increased presence of vascular XOD and/or the conversion of enzyme to oxidase form due to more severe hypoxia.

XOD is present in the blood almost entirely at oxidase form but has a relatively short half-life of 2-3 hours [9]. However, in circulation, this enzyme retains the ability to prime naïve phagocytic cells [4] and produce oxidants [10, 12], especially at loci exposed to mechanical forces, such as oscillatory shear stress [29], causing activation of inflammatory cascade, deprivation of nitric oxide, and vascular dysfunction. In addition, the circulating XOD can be distributed to remote tissues, and after internalization into vascular and other cells, it may further exert pathological effects [30]. Moreover, targeting XOD with allopurinol has been shown to attenuate oxidative stress, cytokine signaling, and muscle wasting in a rat model of cancer cachexia [14] and inhibit MAPKinase signaling and ubiquitin-proteosome pathway thereby preventing atrophy and proteolysis in disused muscles [31]. The second major source of serum XOD in humans is gastrointestinal tract. The gut hypoperfusion or ischemic/reperfusion injury, prolonged parenteral nutrition, or poor nutritional status may upregulate XOD, which increases the permeability of intestinal barrier and mediates transmigration of bacteria (and endotoxin) into the blood, contributing to sustained microinflammatory state in ESRD [32]. Inflammation is highly prevalent in HD patients, and although its sources are not fully elucidated, it may lead to accelerated atherosclerosis. Moreover, murine macrophages overexpressing XOD have been shown to differentiate to foam cells [12], implicated in atherosclerotic plaque development.

The results from experimental studies imply that hyper- and dyslipidemia and cholesterol-rich diets can create a positive feedback loop and profoundly affect XOD activity, thereby linking lipid abnormalities with high expression of XOD [11, 12]. The present study found no significant relationship between serum XOD activity and atherogenic index of plasma, as a surrogate marker of atherogenic dyslipidemia [21]. Instead, the post-HD serum XOD activity was independently associated with low GNRI status ($\beta \pm$ SE: 0.398 ± 0.151; $P = 0.012$). Given that concentration of serum albumin is included in calculation of GNRI score, these results suggest that XOD can be implicated in protein oxidative injury during HD treatment. Due to chronic inflammation, uremia, loss of amino acids, restrictive diets or anorexia, and albumin synthesis may be insufficient to compensate for enhanced catabolic rate, and damage imposed by XOD-derived oxidants would probably enhance its breakdown, leading overtime to evident hypoalbuminemia.

5. Conclusions

Taken together, these results indicate that an upregulated XOD can be implicated in protein oxidative damage and inflammatory cascade in ESRD patients. Repetitive liberation of XOD into the blood during each HD treatment could contribute to augmented oxidative damage and pathogenesis of inflammation-malnutrition complex syndrome. In ageing world population, there is increasing number of patients requiring maintenance HD treatment, and targeting factors associated with oxidative injury in ESRD may have medical, social, and economic aspects. Therefore, further studies are needed to evaluate the long-term relationships between XOD, oxidative stress, and nutritional status in patients on chronic HD treatment.

Conflict of Interests

Authors declare no financial or other conflict of interests regarding this paper.

References

[1] K. Kalantar-Zadeh and V. S. Balakrishnan, "The kidney disease wasting: inflammation, oxidative stress, and diet-gene interaction," *Hemodialysis International*, vol. 10, no. 4, pp. 315–325, 2006.

[2] C. Capeillère-Blandin, V. Gausson, A. T. Nguyen, B. Descamps-Latscha, T. Drüeke, and V. Witko-Sarsat, "Respective role of uraemic toxins and myeloperoxidase in the uraemic state," *Nephrology Dialysis Transplantation*, vol. 21, no. 6, pp. 1555–1563, 2006.

[3] I. Kobayashi, E. Ishimura, Y. Kato et al., "Geriatric Nutritional Risk Index, a simplified nutritional screening index, is a significant predictor of mortality in chronic dialysis patients," *Nephrology Dialysis Transplantation*, vol. 25, no. 10, pp. 3361–3365, 2010.

[4] H. Honda, M. Ueda, S. Kojima et al., "Assessment of myeloperoxidase and oxidative a1-antitrypsin in patients on hemodialysis," *Clinical Journal of the American Society of Nephrology*, vol. 4, pp. 142–151, 2009.

[5] H. Honda, M. Ueda, S. Kojima et al., "Oxidized high-density lipoprotein is associated with protein-energy wasting in maintenance hemodialysis patients," *Clinical Journal of the American Society of Nephrology*, vol. 5, pp. 1021–1028, 2010.

[6] U. R. Kuppusamy, M. Indran, T. Ahmad, S. W. Wong, S. Y. Tan, and A. A. Mahmood, "Comparison of oxidative damage in Malaysian end-stage renal disease patients with or without non-insulin-dependent diabetes mellitus," *Clinica Chimica Acta*, vol. 351, no. 1-2, pp. 197–201, 2005.

[7] M. Obara, A. Hirayama, M. Gotoh et al., "Elimination of lipid peroxide during hemodialysis," *Nephron Clinical Practice*, vol. 106, pp. c162–c168, 2007.

[8] S. Gibbings, N. D. Elkins, H. Fitzgerald et al., "Xanthine oxidoreductase promotes the inflammatory state of mononuclear phagocytes through effects on chemokine expression, peroxisome proliferator-activated receptor-γ sumoylation, and HIF-1α," *Journal of Biological Chemistry*, vol. 286, no. 2, pp. 961–975, 2011.

[9] P. Pacher, A. Nivorozhkin, and C. Szabó, "Therapeutic effects of xanthine oxidase inhibitors: renaissance half a century after the discovery of allopurinol," *Pharmacological Reviews*, vol. 58, no. 1, pp. 87–114, 2006.

[10] M. Houston, A. Estevez, P. Chumley et al., "Binding of xanthine oxidase to vascular endothelium: kinetic characterization and oxidative impairment of nitric oxide-dependent signaling," *Journal of Biological Chemistry*, vol. 274, no. 8, pp. 4985–4994, 1999.

[11] W. Gwinner, H. Scheuer, H. Haller, R. P. Brandes, and H. Groene, "Pivotal role of xanthine oxidase in the initiation of tubulointerstitial renal injury in rats with hyperlipidemia," *Kidney International*, vol. 69, no. 3, pp. 481–487, 2006.

[12] A. Kushiyama, H. Okubo, H. Sakoda et al., "Xanthine oxidoreductase is involved in macrophage foam cell formation and atherosclerosis development," *Arteriosclerosis, Thrombosis, and Vascular Biology*, vol. 32, pp. 291–298, 2012.

[13] J. Y. Choi, Y. J. Yoon, H. J. Choi et al., "Dialysis modality-dependent changes in serum metabolites: accumulation of inosine and hypoxanthine in patients undergoing hemodialysis," *Nephrology Dialysis Transplantation*, vol. 26, pp. 1304–1313, 2011.

[14] J. Springer, A. Tschimer, K. Hartman et al., "Inhibition of xanthine oxidase reduces wasting and improves outcome in a rat model of cancer cachexia," *International Journal of Cancer*, vol. 131, pp. 2187–2196, 2012.

[15] G. G. Roussos, "Xanthine oxidase from bovine small intestine," *Methods in Enzymology*, vol. 12, pp. 5–16, 1967.

[16] J. A. Metcalf, J. I. Gallin, W. M. Nauseef, and R. K. Root, "Myeloperoxidase functional assays," in *Laboratory Manual of Neutrophil Function*, pp. 150–151, Raven Press, New York, NY, USA, 1986.

[17] H. P. Misra and I. Fridovich, "The role of superoxide anion in the autoxidation of epinephrine and a simple assay for superoxide dismutase," *Journal of Biological Chemistry*, vol. 247, no. 10, pp. 3170–3175, 1972.

[18] E. Beutler, O. Duron, and B. M. Kelly, "Improved method for the determination of blood glutathione," *The Journal of Laboratory and Clinical Medicine*, vol. 61, pp. 882–888, 1963.

[19] J. Nourooz-Zadeh, J. Tajaddini-Sarmadi, K. L. E. Ling, and S. P. Wolff, "Low-density lipoprotein is the major carrier of lipid hydroperoxides in plasma: relevance to determination of total plasma lipid hydroperoxide concentrations," *Biochemical Journal*, vol. 313, no. 3, pp. 781–786, 1996.

[20] B. Anderstam, B. Ann-Christin, A. Valli, P. Stenvinkel, B. Lindholm, and M. E. Suliman, "Modification of the oxidative stress biomarker AOPP assay: application in uremic samples," *Clinica Chimica Acta*, vol. 393, no. 2, pp. 114–118, 2008.

[21] M. Dobiášová and J. Frohlich, "The plasma parameter log (TG/HDL-C) as an atherogenic index: correlation with lipoprotein particle size and esterification rate inapob-lipoprotein-depleted plasma (FER_{HDL})," *Clinical Biochemistry*, vol. 34, no. 7, pp. 583–588, 2001.

[22] J. K. Leypoldt, A. K. Cheung, J. A. Delmez et al., "Relationship between volume status and blood pressure during chronic hemodialysis," *Kidney International*, vol. 61, no. 1, pp. 266–275, 2002.

[23] U. Landmesser, S. Spiekermann, S. Dikalov et al., "Vascular oxidative stress and endothelial dysfunction in patients with chronic heart failure: role of xanthine-oxidase and extracellular superoxide dismutase," *Circulation*, vol. 106, no. 24, pp. 3073–3078, 2002.

[24] R. Radi, K. M. Bush, T. P. Cosgrove, and B. A. Freeman, "Reaction of xanthine oxidase-derived oxidants with lipid and protein of human plasma," *Archives of Biochemistry and Biophysics*, vol. 286, no. 1, pp. 117–125, 1991.

[25] V. Witko-Sarsat, M. Friedlander, N. T. Khoa et al., "Advanced oxidation protein products as novel mediators of inflammation and monocyte activation in chronic renal failure," *Journal of Immunology*, vol. 161, pp. 2524–2532, 1998.

[26] Ş. Demirci, M. R. Şekeroğlu, T. Noyan et al., "The importance of oxidative stress in patients with chronic renal failure whose hypertension is treated with peritoneal dialysis," *Cell Biochemistry and Function*, vol. 29, no. 3, pp. 249–254, 2011.

[27] T. Ohtsubo, I. I. Rovira, M. F. Starost, C. Liu, and T. Finkel, "Xanthine oxidoreductase is an endogenous regulator of cyclooxygenase-2," *Circulation Research*, vol. 95, no. 11, pp. 1118–1124, 2004.

[28] H. J. Moshage, J. A. M. Janssen, and J. H. Franssen, "Study of the molecular mechanism of decreased liver synthesis of albumin in inflammation," *Journal of Clinical Investigation*, vol. 79, no. 6, pp. 1635–1641, 1987.

[29] J. S. McNally, M. E. Davis, D. P. Giddens et al., "Role of xanthine oxidoreductase and NAD(P)H oxidase in endothelial superoxide production in response to oscillatory shear stress," *American Journal of Physiology*, vol. 285, no. 6, pp. H2290–H2297, 2003.

[30] W. L. Biffl and E. E. Moore, "Splanchnic ischaemia/reperfusion and multiple organ failure," *British Journal of Anaesthesia*, vol. 77, no. 1, pp. 59–70, 1996.

[31] F. Derbre, B. Ferrando, M. C. Gomez-Cabrera et al., "Inhibition of xanthine oxidase by allopurinol prevents skeletal muscle atrophy: role of p38 MAPKinase and E3 ubiquitin ligases," *PloS ONE*, vol. 7, Article ID e46668, 2012.

[32] F. Wang, H. Jiang, K. Shi, Y. Ren, P. Zhang, and S. Cheng, "Gut bacterial translocation is associated with microinflammation in end-stage renal disease patients," *Nephrology*, vol. 17, pp. 733–738, 2012.

Hindawi Publishing Corporation
Oxidative Medicine and Cellular Longevity
Volume 2013, Article ID 629028, 7 pages
http://dx.doi.org/10.1155/2013/629028

Review Article

Role of Lipid Peroxidation-Derived α, β-Unsaturated Aldehydes in Vascular Dysfunction

Seung Eun Lee and Yong Seek Park

Department of Microbiology, School of Medicine, Kyung Hee University, No.1 Hoegi-dong, Dongdaemun-gu, Seoul 130-701, Republic of Korea

Correspondence should be addressed to Yong Seek Park; yongseek@khu.ac.kr

Received 28 January 2013; Revised 30 April 2013; Accepted 7 May 2013

Academic Editor: Kota V. Ramana

Vascular diseases are the most prominent cause of death, and inflammation and vascular dysfunction are key initiators of the pathophysiology of vascular disease. Lipid peroxidation products, such as acrolein and other α, β-unsaturated aldehydes, have been implicated as mediators of inflammation and vascular dysfunction. α, β-Unsaturated aldehydes are toxic because of their high reactivity with nucleophiles and their ability to form protein and DNA adducts without prior metabolic activation. This strong reactivity leads to electrophilic stress that disrupts normal cellular function. Furthermore, α, β-unsaturated aldehydes are reported to cause endothelial dysfunction by induction of oxidative stress, redox-sensitive mechanisms, and inflammatory changes such as induction of cyclooxygenase-2 and cytokines. This review provides an overview of the effects of lipid peroxidation products, α, β-unsaturated aldehydes, on inflammation and vascular dysfunction.

1. Introduction

Vascular disease, a chronic inflammatory disorder associated with vascular injury due to lipid and protein oxidation [1], is the most prevalent cause of mortality and morbidity in almost all parts of the world [2]. Its etiological factors include an interplay between multiple factors such as hyperlipidemia, hypertension, diabetes, obesity, infection, and smoking [3]. Most of these risk factors cause oxidative stress by increasing the level of reactive oxygen species (ROS) [4].

Numerous studies have revealed that lipid peroxidation (LPO) products are associated with the development of inflammation-related diseases, such as chronic obstructive pulmonary disease (COPD) and vascular diseases, (including atherosclerosis, Alzheimer's disease and stroke) [5–8]. The accumulation of LPO products in human tissues is a major cause of cellular and tissue dysfunction that may act as physiological mediators in oxidative stress-related diseases [5, 9]. Among LPO products, reactive α, β-unsaturated aldehydes are thought to contribute to vascular disease and other oxidative stress-related pathologies by covalently modifying proteins and affecting critical protein functions [10]. These products may also promote atherosclerosis by modifying lipoproteins and can cause cardiac cell damage by impairing metabolic enzymes [11]. In this review, we focus on the molecular evidence supporting the role of α, β-unsaturated aldehydes generated during the lipid peroxidation in inflammation and vascular dysfunction.

2. α, β-Unsaturated Aldehydes

In this review, we concentrate on the role of α, β-unsaturated aldehydes in vascular disease from exogenous (e.g., cigarette smoke) and/or endogenous (e.g., LPO) sources. α, β-Unsaturated aldehydes can be generated during inflammation because of LPO which is accelerated by diverse oxidative stressors, such as cigarette smoke-generated ROS, reactive nitrogen species (RNS), and free radicals [12]. During LPO, various ROS/RNS oxidize membrane lipids, particularly the polyunsaturated fatty acids, lead to free radical chain reactions and subsequent formation of byproducts, such as α, β-unsaturated aldehydes. α, β-Unsaturated aldehydes are highly

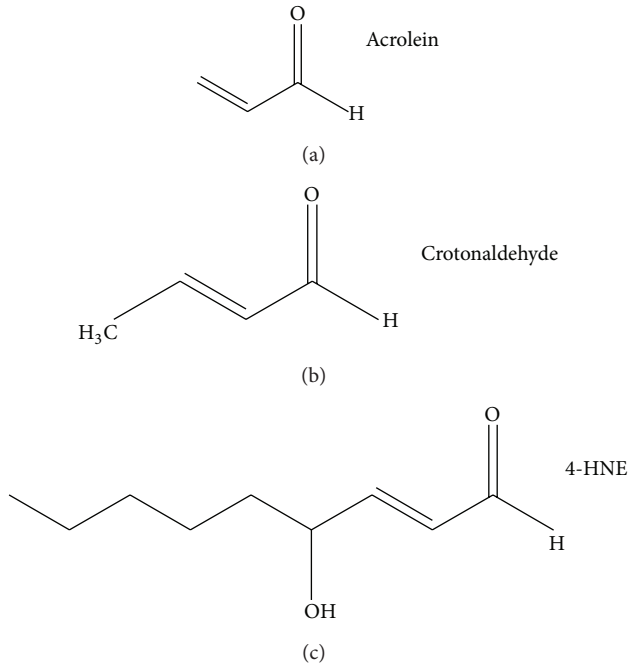

Figure 1: Structures of α, β-unsaturated aldehydes.

reactive and can cause atherogenic and carcinogenic effects by injuring blood vessel walls and by forming DNA adducts, respectively.

Acrolein (ACR), 4-hydroxy-2-nonenal (4-HNE), and crotonaldehyde (CRA) are the most reactive and toxic α, β-unsaturated aldehydes (Figure 1). These LPO products can modify nucleophilic side chains on amino acid residues, such as the sulfhydryl groups of cysteine, the imidazole groups of histidine, and the amino acid groups of lysine [13]. Recent studies are reported to the detailed chemistry and the relative electrophilicities of these aldehydes using quantum mechanical parameters [14, 15]. The generation of these strong electrophilic aldehydes and the subsequent adduction of protein nucleophiles may have pathophysiological implications. These aldehydes are associated with elevated tissue levels of their respective protein adducts in disease processes that involve oxidative damage [16, 17]. In addition, the formation of adducts by these reactive aldehydes has been linked to the disruption of cell signaling and mitochondrial dysfunction [14].

2.1. Acrolein (ACR). ACR is present in relatively large amounts (10–140 μg/cigarette) in cigarette smoke and has been implicated in the pathogenesis of vascular disease [18]. ACR is also produced during the incomplete combustion of wood, plastics, gasoline, and diesel fuel; the heating of animal and vegetable fats; and endogenous LPO that is caused by oxidative stress [19]. ACR has a strong electrophilic reactivity towards nucleophiles; therefore, it disrupts the redox control of protein function and causes cytotoxicity via irreversible adduction. In addition, ACR may play a role in the pathogenesis of cardiovascular and neurodegenerative disorders [17]. It is an important oxidative stress biomarker for LPO, and ACR levels increase during aging and in disease, such as atherosclerosis and Alzheimer's disease [20, 21]. Several recent studies have linked ACR exposure to atherosclerosis [22], hypertension [23], dyslipidemia [24], and infarction [25].

2.2. Crotonaldehyde (CRA). CRA is abundant in the environment and is also produced endogenously during lipid metabolism [26]. CRA is reported to be present in many foods, such as fish, meat, fruit, and vegetables, and in various liquors [27]. It is formed as a product of LPO and is also produced during the combustion of carbon-containing fuels and other materials [28]; cigarette smoke is another important source of CRA (31–169 μg/kg body weight) [29]. CRA is mutagenic without metabolic activation in numerous cell systems [30] and induces hepatic tumors in rodents [29]. The toxicity of CRA is caused by its strongly reactive electrophilic carbonyl group [31]. Many studies have indicated that CRA directly or enzymatically conjugates with glutathione (GSH), thereby reducing the GSH levels [32]. Previous studies showed that CRA can modulate biological reactions through various downstream signaling pathways and cause cellular oxidative stress [33].

2.3. 4-Hydroxy-2-Nonenal (4-HNE). 4-HNE, a strongly reactive α, β-unsaturated aldehyde, is a diffusible end product of endogenous LPO and is a known marker of oxidative stress. 4-HNE is a potent alkylating agent that reacts with DNA and proteins, thereby generating various types of adducts [31, 34]. These adducts can induce stress signaling pathways and apoptosis [34]. It has been reported that cigarette smoke extract (CSE) causes 4-HNE production either directly or indirectly via LPO in various cell types. In another study by Kode et al. [35], CSE caused a dose-dependent increase in oxidative stress in various cell lines and in 4-HNE levels in small airway epithelial cells (SAECs). CSE-induced cytotoxicity in different cell lines has been attributed to an increase in the endogenous production of 4-HNE.

Kumagai et al. showed that 4-HNE may be a major inflammatory mediator in the development and progression of atherogenesis [36]. 4-HNE is reported to be producing nerve terminal toxicity by forming adducts that play a critical role in Alzheimer's disease [37]. In addition, studies have revealed that 4-HNE is associated with several other pathological conditions, such as COPD [38], acute respiratory distress syndrome (ARDS) [39], and atherosclerosis [40].

3. α, β-Unsaturated Aldehydes in the Pathogenesis of Vascular Diseases

Vascular disease is a complex inflammatory disease that involves several types of inflammatory cells, multiple inflammatory mediators, and oxidative stress. α, β-Unsaturated aldehydes cause inflammation and damage cells by inducing oxidative stress, redox-sensitive mechanisms, and proinflammatory mediators. The results of many studies have implicated α, β-unsaturated aldehydes in the pathogenesis of vascular disease (Table 1).

Table 1: α, β-unsaturated aldehydes and vascular diseases.

α, β-Unsaturated aldehydes	Diseases	References
Acrolein (endogenous/exogenous)	Alzheimer's	Lovell et al., 2001 [41], Bradley et al., 2010 [42]
	Diabetes	Uesugi et al., 2004 [43], Grigsby et al., 2012 [44]
	Atherosclerosis	Uchida et al., 1998 [19], Srivastava et al., 2011 [45]
	COPD	Wang et al., 2009 [46]
Crotonaldehyde (endogenous/exogenous)	Alzheimer's	Kawaguchi-Niida et al., 2006 [28]
	COPD	Volpi et al., 2011 [47]
4-HNE (endogenous/exogenous)	Alzheimer's	Tsirulnikov et al., 2012 [48], Butterfield et al., 2010 [37]
	Ischemia	Eaton et al., 1999 [49]
	Atherosclerosis	Leonarduzzi et al., 2005 [50], Kumagai et al., 2004 [36]
	COPD	Rahman et al., 2002 [38], Halliwell and Poulsen 2006 [51]

3.1. α, β-Unsaturated Aldehydes and Oxidative Stress. Oxidative stress induced by α, β-unsaturated aldehydes plays an important role in the pathogenesis of vascular disease through direct injury to the endothelium, as well as through redox-sensitive mechanisms. α, β-Unsaturated aldehydes increase oxidative stress in endothelial, macrophage, and smooth muscle cells which in turn induces a proinflammatory vascular phenotype by stimulating the transcription of various genes. Cellular oxidative stress and inflammation are implicated in the pathogenesis of many diseases, including stroke, myocardial infarction, and atherosclerosis. Reactive α, β-unsaturated aldehydes have been shown to induce intracellular peroxide production in endothelial cells [52]. α, β-Unsaturated aldehydes tend to trigger the formation of ROS or act as oxidants and potentiate oxidative stress in cells [53]. Adams Jr. and Klaidman reported that ACR was oxidized by xanthine oxidase to produce oxygen radicals and that the GSH adduct of ACR also induced oxygen radical formation [54]. ACR depletes endogenous GSH which itself is a critical component of the endogenous antioxidant defense system, thereby increasing the ROS levels [55]. In addition, it has been shown that 4-HNE mediates endothelial nitric oxide synthase (eNOS) uncoupling and superoxide generation by altering tetrahydrobiopterin (BH_4) homeostasis [56] and that it induces ROS generation by activating nicotinamide adenine dinucleotide phosphate (NADPH) oxidase which is dependent on the activity of 5-lipoxygenase (5-LO) [57].

Maintaining the redox balance in the vascular system is of paramount importance since uncompensated oxidative stress contributes to endothelial dysfunction and vascular disease. Oxidative stress is increasingly seen as a major upstream component in the signaling cascade involved in many cellular functions, such as cell proliferation, inflammatory responses, adhesion molecule stimulation, and chemoattractant production. The mechanisms by which endothelial oxidative stress leads to vascular inflammation and the development of atherosclerosis have been reported [58].

3.2. α, β-Unsaturated Aldehydes and Antioxidant Enzymes. Oxidative (electrophilic) stress induces NF-E2-related factor 2 (Nrf2)/antioxidant response element (ARE)-mediated expression of phase II detoxifying and antioxidant enzymes and activates other stress-inducible genes [59]. α, β-Unsaturated aldehydes are attracted to electrons and can inactivate the nucleophilic active sites of thiolate or selenocysteine enzymes, such as glutathione peroxidase (GPx) through covalent bonding [31]. The inactivation of GPx by α, β-unsaturated aldehydes is involved in imbalance of the redox state in cell [60]. The thioredoxin (Trx)/thioredoxin reductase (TR) system plays a crucial role in many biological functions, such as redox regulation, apoptosis, and immunomodulation in diverse organisms. Endothelial cells exposed to ACR show rapidly inactivation of TR, resulting in an increase in oxidative cellular damage [52]. In ACR-stimulated human umbilical vein endothelial cells (HUVECs), the induction of heat shock protein 72 (Hsp72) is considered to be a defense system unique to HUVECs [61]. The results of some studies indicate that a highly electrophilic compound, such as ACR, would have the potential to increase Nrf2-mediated gene expression, including that of the cytoprotective antioxidant heme oxygenase-1 (HO-1) in macrophages [62] and endothelial cells [63]. Furthermore, 4-HNE and CRA induces HO-1 expression in endothelial cells [53, 64]. HO-1, a rate-limiting enzyme in heme metabolism, has been recognized as an important factor that protects vascular tissue against atherosclerosis by exerting antioxidative, anti-inflammatory, antiproliferative, anti-apoptotic, and vasodilatory effects on the vasculature. Therefore, increased HO-1 expression in various cells treated with α, β-unsaturated aldehydes may serve as an adaptive response to oxidative damage.

3.3. α, β-Unsaturated Aldehydes and Inflammation. α, β-Unsaturated aldehyde-induced toxicity is reported to occur because of depletion of cellular GSH, which subsequently induces ROS production that leads to cell malfunction [55, 65]. ROS was also shown to induce the production of various atherogenic factors, including inflammatory mediators.

3.3.1. α, β-Unsaturated Aldehydes and Nuclear Factor Kappa-Light-Chain-Enhancer of Activated B Cells. The nuclear factor kappa-light-chain-enhancer of activated B cells (NF-κB)/Rel family complex is a redox-sensitive transcription factor that plays a role in the expression of various rapid-response genes

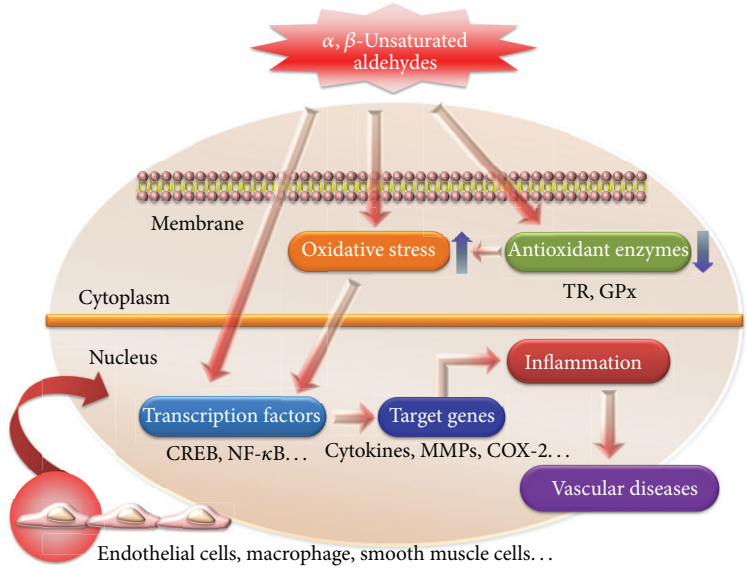

Figure 2: Schematic representation of α, β-unsaturated aldehydes stimulated leading to inflammation and vascular disease. α, β-Unsaturated aldehyde reacts directly or indirectly with various genes and transcription factors and induces oxidative stress which may play an important role in inflammation and vascular diseases.

associated with the inflammatory and immune responses. In addition, NF-κB activation may play a role in the development of chronic inflammatory diseases, such as rheumatoid arthritis, Alzheimer's disease, and atherosclerosis.

The results of many studies suggest that α, β-unsaturated aldehydes can regulate inflammation by modulating NF-κB signaling [55]. ACR may affect NF-κB activation, either indirectly by decreasing cellular reduced GSH content or directly by binding to the reactive cysteine on the subunit of IκB kinase (IKK) [55]. The effect of ACR on NF-κB may be cell-type specific and other regulatory mechanisms may also be involved. Li et al. reported that ACR induced IκB expression in rat alveolar macrophage cells, an effect that led to the inhibition of NF-κB activation [66]. However, Haberzettl et al. showed that the ACR-induced increase in cytokine production was accompanied by NF-κB activation [67]. The other α, β-unsaturated aldehyde, 4-HNE, may also play a role in modulating NF-κB activation through a mechanism similar to that of ACR. It has been suggested that 4-HNE induces 5-LO expression via epidermal growth factor receptor (EGFR)-mediated activation of the NF-κB/extracellular-regulated kinase (ERK) pathways in murine macrophages [68].

3.3.2. α, β-Unsaturated Aldehydes and Proinflammatory Mediators. Cyclooxygenase (COX)-2 is an inducible isoform of COX, which is the key enzyme that regulates the amount of and the duration for which proinflammatory prostaglandins (PG) are produced and also plays a crucial role in inflammation. Under normal conditions, COX-2 expression is tightly regulated, but it is dramatically induced during inflammation by various stimulants. Burleigh et al. suggested that COX-2 expression promotes atherosclerotic inflammation [69]. Since chronic inflammation plays a significant role in atherosclerosis, COX-2 may participate in the development of atherosclerosis.

The endothelium is a vulnerable target for ACR and related aldehydes. Several studies have reported that exposure to ACR causes endothelial damage [18]. Endothelial cells exposed to ACR exhibit a time-and dose-dependent stimulation of COX-2 expression and enhancement of PG synthesis [21]. The increased PG synthesis in endothelial cells after treatment with ACR reflects an increase in the levels of functional COX-2 protein. In addition, the induction of COX-2 by ACR occurs through activation of the protein kinase C (PKC), p38 mitogen-activated protein kinase (MAPK), and cAMP response element-binding protein (CREB) pathways; it has been suggested that ACR plays an important role in the progression of atherosclerosis via an inflammatory response involving COX-2 expression. 4-HNE is reported to strongly induce COX-2 expression in macrophages [36]. These data suggest that the 4-HNE accumulated in macrophages/foam cells functions as an inflammatory mediator that plays a role in stimulating the inflammatory response and contributes to the progression of atherogenesis.

In addition, Haberzettl et al. showed that ACR treatment increased the production of interleukin-6 (IL-6), tumor necrosis factor-α (TNF-α), and interleukin-8 (IL-8) in endothelial cells [67]. These findings suggest new proinflammatory and atherogenic aspects of ACR toxicity and the possibility that endogenously produced ACR can contribute toward endothelial injury and inflammation. Because the induction of cytokines, such as TNF-α, IL-6, and IL-8, plays a crucial role in atherosclerosis, production of these cytokines may be a significant feature of atherogenesis. Furthermore, ACR treatment induced endoplasmic reticulum (ER) stress and triggered the unfolded protein response [67].

Activated macrophages are reported to generate and secrete matrix metalloproteinase (MMP)-9 which degrades atherosclerotic plaque constituents. A recent study by O'Toole et al. reported that secretion of MMP-9 increases in ACR-stimulated human macrophages [70]. In addition, murine macrophages exposed to ACR exhibited 5-LO overexpression, subsequent proinflammatory leukotriene (LT) accumulation, and enhanced MMP-9 biosynthesis [71]. These data support the possibility that exposure to oxidants or acute inflammatory events can trigger plaque rupture. Akiba et al. showed that 4-HNE accelerates MMP-1 production in human coronary smooth muscle cells (hCSMCs) [72]. MMP-1 (collagenases) cleave native collagen types I and III, which are predominant structural components of atherosclerotic lesions, indicating that increase in the levels of collagenases is a critical event in the progression of atherosclerosis.

4. Conclusions

Lipid peroxidation-derived α, β-unsaturated aldehydes have been shown to play an important pathophysiological role in vascular diseases. α, β-Unsaturated aldehydes from exogenous and/or endogenous sources, being highly reactive electrophilic molecules, react and modify both proteins and DNA resulting in toxicity. These aldehydes have been implicated in oxidative stress-induced vascular pathologies which act as redox signaling mediators leading to cellular and tissue injury. Furthermore, α, β-unsaturated aldehydes were reported to induce inactivation of antioxidant enzyme such as GPx and TR, activation of NF-κB signaling pathway, and stimulation of inflammatory response through activation of the proinflammatory signaling pathway (Figure 2). Together, results of these studies provide a better understanding of the involvement of LPO-derived α, β-unsaturated aldehydes in vascular dysfunction and their possible role in vascular disease. Understanding the mechanism of inflammation-related vascular dysfunction mediated by LPO-derived α, β-unsaturated aldehydes may help in revealing the pathological factors responsible for vascular diseases and in developing effective therapeutic strategies for these diseases.

Acknowledgment

This study was supported by a grant from the Korean Health Technology R&D Project, Ministry of Health & Welfare, Republic of Korea (A111834).

References

[1] R. Stocker and J. F. Keaney Jr., "Role of oxidative modifications in atherosclerosis," *Physiological Reviews*, vol. 84, no. 4, pp. 1381–1478, 2004.

[2] A. D. Lopez, C. D. Mathers, M. Ezzati, D. T. Jamison, and C. J. Murray, "Global and regional burden of disease and risk factors, 2001: systematic analysis of population health data," *The Lancet*, vol. 367, no. 9524, pp. 1747–1757, 2006.

[3] S. Sevinç and A. D. Akyol, "Cardiac risk factors and quality of life in patients with coronary artery disease," *Journal of Clinical Nursing*, vol. 19, no. 9-10, pp. 1315–1325, 2010.

[4] T. Sonta, T. Inoguchi, H. Tsubouchi et al., "Evidence for contribution of vascular NAD(P)H oxidase to increased oxidative stress in animal models of diabetes and obesity," *Free Radical Biology and Medicine*, vol. 37, no. 1, pp. 115–123, 2004.

[5] A. Negre-Salvayre, C. Coatrieux, C. Ingueneau, and R. Salvayre, "Advanced lipid peroxidation end products in oxidative damage to proteins. Potential role in diseases and therapeutic prospects for the inhibitors," *British Journal of Pharmacology*, vol. 153, no. 1, pp. 6–20, 2008.

[6] K. Uchida, "Role of reactive aldehyde in cardiovascular diseases," *Free Radical Biology and Medicine*, vol. 28, no. 12, pp. 1685–1696, 2000.

[7] L. Chen, R. Na, M. Gu, A. Richardson, and Q. Ran, "Lipid peroxidation up-regulates BACE1 expression in vivo: a possible early event of amyloidogenesis in Alzheimer's disease," *Journal of Neurochemistry*, vol. 107, no. 1, pp. 197–207, 2008.

[8] I. Rahman, "Oxidative stress in pathogenesis of chronic obstructive pulmonary disease: cellular and molecular mechanisms," *Cell Biochemistry and Biophysics*, vol. 43, no. 1, pp. 167–188, 2005.

[9] A. Negre-Salvayre, N. Auge, V. Ayala et al., "Pathological aspects of lipid peroxidation," *Free Radical Research*, vol. 44, no. 10, pp. 1125–1171, 2010.

[10] M. E. Szapacs, H. H. Kim, N. A. Porter, and D. C. Liebler, "Identification of proteins adducted by lipid peroxidation products in plasma and modifications of apolipoprotein A1 with a novel biotinylated phospholipid probe," *Journal of Proteome Research*, vol. 7, no. 10, pp. 4237–4246, 2008.

[11] M. P. Mattson, "Roles of the lipid peroxidation product 4-hydroxynonenal in obesity, the metabolic syndrome, and associated vascular and neurodegenerative disorders," *Experimental Gerontology*, vol. 44, no. 10, pp. 625–633, 2009.

[12] E. I. Finkelstein, J. Ruben, C. W. Koot, M. Hristova, and A. Van Der Vliet, "Regulation of constitutive neutrophil apoptosis by the α,β- unsaturated aldehydes acrolein and 4-hydroxynonenal," *American Journal of Physiology*, vol. 289, no. 6, pp. L1019–L1028, 2005.

[13] L. J. Marnett, J. N. Riggins, and J. D. West, "Endogenous generation of reactive oxidants and electrophiles and their reactions with DNA and protein," *Journal of Clinical Investigation*, vol. 111, no. 5, pp. 583–593, 2003.

[14] R. M. LoPachin, T. Gavin, D. R. Petersen, and D. S. Barber, "Molecular mechanisms of 4-hydroxy-2-nonenal and acrolein toxicity: nucleophilic targets and adduct formation," *Chemical Research in Toxicology*, vol. 22, no. 9, pp. 1499–1508, 2009.

[15] I. G. Minko, I. D. Kozekov, T. M. Harris, C. J. Rizzo, R. S. Lloyd, and M. P. Stone, "Chemistry and biology of DNA containing 1,N2-deoxyguanosine adducts of the α,β-unsaturated aldehydes acrolein, crotonaldehyde, and 4-hydroxynonenal," *Chemical Research in Toxicology*, vol. 22, no. 5, pp. 759–778, 2009.

[16] R. M. Lopachin, D. S. Barber, and T. Gavin, "Molecular mechanisms of the conjugated α,β-unsaturated carbonyl derivatives: relevance to neurotoxicity and neurodegenerative diseases," *Toxicological Sciences*, vol. 104, no. 2, pp. 235–249, 2008.

[17] N. Y. Calingasan, K. Uchida, and G. E. Gibson, "Protein-bound acrolein: a novel marker of oxidative stress in Alzheimer's disease," *Journal of Neurochemistry*, vol. 72, no. 2, pp. 751–756, 1999.

[18] N. L. Tsakadze, S. Srivastava, S. O. Awe, A. S. O. Adeagbo, A. Bhatnagar, and S. E. D'Souza, "Acrolein-induced vasomotor responses of rat aorta," *American Journal of Physiology*, vol. 285, no. 2, pp. H727–H734, 2003.

[19] K. Uchida, M. Kanematsu, Y. Morimitsu, T. Osawa, N. Noguchi, and E. Niki, "Acrolein is a product of lipid peroxidation reaction: formation of free acrolein and its conjugate with lysine residues in oxidized low density lipoproteins," *Journal of Biological Chemistry*, vol. 273, no. 26, pp. 16058–16066, 1998.

[20] K. Hamann, A. Durkes, H. Ouyang, K. Uchida, A. Pond, and R. Shi, "Critical role of acrolein in secondary injury following ex vivo spinal cord trauma," *Journal of Neurochemistry*, vol. 107, no. 3, pp. 712–721, 2008.

[21] Y. S. Park, J. Kim, Y. Misonou et al., "Acrolein induces cyclooxygenase-2 and prostaglandin production in human umbilical vein endothelial cells: roles of p38 MAP kinase," *Arteriosclerosis, Thrombosis, and Vascular Biology*, vol. 27, no. 6, pp. 1319–1325, 2007.

[22] S. E. Lee, S. H. Lee, D. S. Ryu, C. Park, K. Park, and Y. S. Park, "Differentially-expressed genes related to atherosclerosis in acrolein-stimulated human umbilical vein endothelial cells," *Biochip Journal*, vol. 4, no. 4, pp. 264–271, 2010.

[23] D. J. Conklin, A. Bhatnagar, H. R. Cowley et al., "Acrolein generation stimulates hypercontraction in isolated human blood vessels," *Toxicology and Applied Pharmacology*, vol. 217, no. 3, pp. 277–288, 2006.

[24] M. R. McCall, J. Y. Tang, J. K. Bielicki, and T. M. Forte, "Inhibition of lecithin-cholesterol acyltransferase and modification of HDL apolipoproteins by aldehydes," *Arteriosclerosis, Thrombosis, and Vascular Biology*, vol. 15, no. 10, pp. 1599–1606, 1995.

[25] L. Alfredsson, N. Hammar, and C. Hogstedt, "Incidence of myocardial infarction and mortality from specific causes among bus drivers in Sweden," *International Journal of Epidemiology*, vol. 22, no. 1, pp. 57–61, 1993.

[26] M. P. Stonez, Y. Cho, H. Huang et al., "Interstrand DNA cross-links induced by α,β-unsaturated aldehydes derived from lipid peroxidation and environmental sources," *Accounts of Chemical Research*, vol. 41, no. 7, pp. 793–804, 2008.

[27] E. Eder and B. Budiawan, "Cancer risk assessment for the environmental mutagen and carcinogen crotonaldehyde on the basis of TD50 and comparison with 1,N2-propanodeoxyguanosine adduct levels," *Cancer Epidemiology Biomarkers and Prevention*, vol. 10, no. 8, pp. 883–888, 2001.

[28] M. Kawaguchi-Niida, N. Shibata, S. Morikawa et al., "Crotonaldehyde accumulates in glial cells of Alzheimer's disease brain," *Acta Neuropathologica*, vol. 111, no. 5, pp. 422–429, 2006.

[29] E. Eder, D. Schuler, and B. Budiawan, "Cancer risk assessment for crotonaldehyde and 2-hexenal: an approach," *IARC Scientific Publications*, no. 150, pp. 219–232, 1999.

[30] T. Neudecker, E. Eder, C. Deininger, and D. Henschler, "Crotonaldehyde is mutagenic in Salmonella typhimurium TA100," *Environmental and Molecular Mutagenesis*, vol. 14, no. 3, pp. 146–148, 1989.

[31] H. Esterbauer, R. J. Schaur, and H. Zollner, "Chemistry and Biochemistry of 4-hydroxynonenal, malonaldehyde and related aldehydes," *Free Radical Biology and Medicine*, vol. 11, no. 1, pp. 81–128, 1991.

[32] M. Van Der Toorn, M. P. Smit-de Vries, D. Slebos et al., "Cigarette smoke irreversibly modifies glutathione in airway epithelial cells," *American Journal of Physiology*, vol. 293, no. 5, pp. L1156–L1162, 2007.

[33] X. Liu, Z. Yang, X. Pan, M. Zhu, and J. Xie, "Crotonaldehyde induces oxidative stress and caspase-dependent apoptosis in human bronchial epithelial cells," *Toxicology Letters*, vol. 195, no. 1, pp. 90–98, 2010.

[34] K. Uchida, M. Shiraishi, Y. Naito, Y. Torii, Y. Nakamura, and T. Osawa, "Activation of stress signaling pathways by the end product of lipid peroxidation: 4-Hydroxy-2-nonenal is a potential inducer of intracellular peroxide production," *Journal of Biological Chemistry*, vol. 274, no. 4, pp. 2234–2242, 1999.

[35] A. Kode, S. Yang, and I. Rahman, "Differential effects of cigarette smoke on oxidative stress and proinflammatory cytokine release in primary human airway epithelial cells and in a variety of transformed alveolar epithelial cells," *Respiratory Research*, vol. 7, article 132, 2006.

[36] T. Kumagai, N. Matsukawa, Y. Kaneko, Y. Kusumi, M. Mitsumata, and K. Uchida, "A lipid peroxidation-derived inflammatory mediator: identification of 4-hydroxy-2-nonenal as a potential inducer of cyclooxygenase-2 in macrophages," *Journal of Biological Chemistry*, vol. 279, no. 46, pp. 48389–48396, 2004.

[37] D. A. Butterfield, M. L. Bader Lange, and R. Sultana, "Involvements of the lipid peroxidation product, HNE, in the pathogenesis and progression of Alzheimer's disease," *Biochimica et Biophysica Acta*, vol. 1801, no. 8, pp. 924–929, 2010.

[38] I. Rahman, A. A. M. Van Schadewijk, A. J. L. Crowther et al., "4-Hydroxy-2-nonenal, a specific lipid peroxidation product, is elevated in lungs of patients with chronic obstructive pulmonary disease," *American Journal of Respiratory and Critical Care Medicine*, vol. 166, no. 4, pp. 490–495, 2002.

[39] G. J. Quinlan, T. W. Evans, and J. M. C. Gutteridge, "4-Hydroxy-2-nonenal levels increase in the plasma of patients with adult respiratory distress syndrome as linoleic acid appears to fall," *Free Radical Research*, vol. 21, no. 2, pp. 95–106, 1994.

[40] C. Napoli, F. P. D'Armiento, F. P. Mancini et al., "Fatty streak formation occurs in human fetal aortas and is greatly enhanced maternal, hypercholesterolemia. Intimal accumulation of low density lipoprotein and its oxidation precede monocyte recruitment into early atheroeclerotic lesions," *Journal of Clinical Investigation*, vol. 100, no. 11, pp. 2680–2690, 1997.

[41] M. A. Lovell, C. Xie, and W. R. Markesbery, "Acrolein is increased in Alzheimer's disease brain and is toxic to primary hippocampal cultures," *Neurobiology of Aging*, vol. 22, no. 2, pp. 187–194, 2001.

[42] M. A. Bradley, W. R. Markesbery, and M. A. Lovell, "Increased levels of 4-hydroxynonenal and acrolein in the brain in preclinical Alzheimer disease," *Free Radical Biology and Medicine*, vol. 48, no. 12, pp. 1570–1576, 2010.

[43] N. Uesugi, N. Sakata, M. Nangaku et al., "Possible mechanism for medial smooth muscle cell injury in diabetic nephropathy: glycoxidation-mediated local complement activation," *American Journal of Kidney Diseases*, vol. 44, no. 2, pp. 224–238, 2004.

[44] J. Grigsby, B. Betts, E. Vidro-Kotchan, R. Culbert, and A. Tsin, "A possible role of acrolein in diabetic retinopathy: involvement of a VEGF/TGFbeta signaling pathway of the retinal pigment epithelium in hyperglycemia," *Current Eye Research*, vol. 37, no. 11, pp. 1045–1053, 2012.

[45] S. Srivastava, S. D. Sithu, E. Vladykovskaya et al., "Oral exposure to acrolein exacerbates atherosclerosis in apoE-null mice," *Atherosclerosis*, vol. 215, no. 2, pp. 301–308, 2011.

[46] T. Wang, Y. Liu, L. Chen et al., "Effect of sildenafil on acrolein-induced airway inflammation and mucus production in rats," *European Respiratory Journal*, vol. 33, no. 5, pp. 1122–1132, 2009.

[47] G. Volpi, F. Facchinetti, N. Moretto, M. Civelli, and R. Patacchini, "Cigarette smoke and α,β-unsaturated aldehydes elicit VEGF release through the p38 MAPK pathway in human airway smooth muscle cells and lung fibroblasts," *British Journal of Pharmacology*, vol. 163, no. 3, pp. 649–661, 2011.

[48] K. Tsirulnikov, N. Abuladze, A. Bragin et al., "Inhibition of aminoacylase 3 protects rat brain cortex neuronal cells from the toxicity of 4-hydroxy-2-nonenal mercapturate and 4-hydroxy-2-nonenal," *Toxicology and Applied Pharmacology*, vol. 263, no. 3, pp. 303–314, 2012.

[49] P. Eaton, J. Li, D. J. Hearse, and M. J. Shattock, "Formation of 4-hydroxy-2-nonenal-modified proteins in ischemic rat heart," *American Journal of Physiology*, vol. 276, no. 3, pp. H935–H943, 1999.

[50] G. Leonarduzzi, E. Chiarpotto, F. Biasi, and G. Poli, "4-Hydroxynonenal and cholesterol oxidation products in atherosclerosis," *Molecular Nutrition and Food Research*, vol. 49, no. 11, pp. 1044–1049, 2005.

[51] B. Halliwell and H. E. Poulsen, *Cigarette Smoke and Oxidative Stress*, Springer, Berlin, Germany, 2006.

[52] Y. S. Park, Y. Misonou, N. Fujiwara et al., "Induction of thioredoxin reductase as an adaptive response to acrolein in human umbilical vein endothelial cells," *Biochemical and Biophysical Research Communications*, vol. 327, no. 4, pp. 1058–1065, 2005.

[53] S. E. Lee, S. I. Jeong, G. Kim et al., "Upregulation of heme oxygenase-1 as an adaptive mechanism for protection against crotonaldehyde in human umbilical vein endothelial cells," *Toxicology Letters*, vol. 201, no. 3, pp. 240–248, 2011.

[54] J. D. Adams Jr. and L. K. Klaidman, "Acrolein-induced oxygen radical formation," *Free Radical Biology and Medicine*, vol. 15, no. 2, pp. 187–193, 1993.

[55] J. P. Kehrer and S. S. Biswal, "The molecular effects of acrolein," *Toxicological Sciences*, vol. 57, no. 1, pp. 6–15, 2000.

[56] J. Whitsett, M. J. Picklo Sr., and J. Vasquez-Vivar, "4-Hydroxy-2-nonenal increases superoxide anion radical in endothelial cells via stimulated GTP cyclohydrolase proteasomal degradation," *Arteriosclerosis, Thrombosis, and Vascular Biology*, vol. 27, no. 11, pp. 2340–2347, 2007.

[57] M. R. Yun, H. M. Park, K. W. Seo, S. J. Lee, D. S. Im, and C. D. Kim, "5-Lipoxygenase plays an essential role in 4-HNE-enhanced ROS production in murine macrophages via activation of NADPH oxidase," *Free Radical Research*, vol. 44, no. 7, pp. 742–750, 2010.

[58] R. Foncea, C. Carvajal, C. Almarza, and F. Leighton, "Endothelial cell oxidative stress and signal transduction," *Biological Research*, vol. 33, no. 2, pp. 89–96, 2000.

[59] T. Nguyen, C. S. Yang, and C. B. Pickett, "The pathways and molecular mechanisms regulating Nrf2 activation in response to chemical stress," *Free Radical Biology and Medicine*, vol. 37, no. 4, pp. 433–441, 2004.

[60] Y. Miyamoto, Y. H. Koh, Y. S. Park et al., "Oxidative stress caused by inactivation of glutathione peroxidase and adaptive responses," *Biological Chemistry*, vol. 384, no. 4, pp. 567–574, 2003.

[61] Y. Misonou, M. Takahashi, Y. S. Park et al., "Acrolein induces Hsp72 via both PKCδ/JNK and calcium signaling pathways in human umbilical vein endothelial cells," *Free Radical Research*, vol. 39, no. 5, pp. 507–512, 2005.

[62] N. J. Lee, S. E. Lee, S. H. Lee, D. S. Ryu, and Y. S. Park, "Acrolein induces adaptive response through upregulate of HO-1 via activation of Nrf2 in RAW 264. 7 macrophage," *Molecular & Cellular Toxicology*, vol. 5, no. 3, p. 77, 2009.

[63] C. C. Wu, C. W. Hsieh, P. H. Lai, J. B. Lin, Y. C. Liu, and B. S. Wung, "Upregulation of endothelial heme oxygenase-1 expression through the activation of the JNK pathway by sublethal concentrations of acrolein," *Toxicology and Applied Pharmacology*, vol. 214, no. 3, pp. 244–252, 2006.

[64] A. Ishikado, Y. Nishio, K. Morino et al., "Low concentration of 4-hydroxy hexenal increases heme oxygenase-1 expression through activation of Nrf2 and antioxidative activity in vascular endothelial cells," *Biochemical and Biophysical Research Communications*, vol. 402, no. 1, pp. 99–104, 2010.

[65] Y. S. Park and N. Taniguchi, "Acrolein induces inflammatory response underlying endothelial dysfunction: a risk factor for atherosclerosis," *Annals of the New York Academy of Sciences*, vol. 1126, pp. 185–189, 2008.

[66] L. Li, R. F. Hamilton Jr., and A. Holian, "Effect of acrolein on human alveolar macrophage NF-κB activity," *American Journal of Physiology*, vol. 277, no. 3, pp. L550–L557, 1999.

[67] P. Haberzettl, E. Vladykovskaya, S. Srivastava, and A. Bhatnagar, "Role of endoplasmic reticulum stress in acrolein-induced endothelial activation," *Toxicology and Applied Pharmacology*, vol. 234, no. 1, pp. 14–24, 2009.

[68] S. J. Lee, C. E. Kim, K. W. Seo, and C. D. Kim, "HNE-induced 5-LO expression is regulated by NF-κB/ERK and Sp1/p38 MAPK pathways via EGF receptor in murine macrophages," *Cardiovascular Research*, vol. 88, no. 2, pp. 352–359, 2010.

[69] M. E. Burleigh, V. R. Babaev, J. A. Oates et al., "Cyclooxygenase-2 promotes early atherosclerotic lesion formation in LDL receptor-deficient mice," *Circulation*, vol. 105, no. 15, pp. 1816–1823, 2002.

[70] T. E. O'Toole, Y. Zheng, J. Hellmann, D. J. Conklin, O. Barski, and A. Bhatnagar, "Acrolein activates matrix metalloproteinases by increasing reactive oxygen species in macrophages," *Toxicology and Applied Pharmacology*, vol. 236, no. 2, pp. 194–201, 2009.

[71] C. E. Kim, S. J. Lee, K. W. Seo et al., "Acrolein increases 5-lipoxygenase expression in murine macrophages through activation of ERK pathway," *Toxicology and Applied Pharmacology*, vol. 245, no. 1, pp. 76–82, 2010.

[72] S. Akiba, S. Kumazawa, H. Yamaguchi et al., "Acceleration of matrix metalloproteinase-1 production and activation of platelet-derived growth factor receptor β in human coronary smooth muscle cells by oxidized LDL and 4-hydroxynonenal," *Biochimica et Biophysica Acta*, vol. 1763, no. 8, pp. 797–804, 2006.

Hindawi Publishing Corporation
Oxidative Medicine and Cellular Longevity
Volume 2013, Article ID 927214, 7 pages
http://dx.doi.org/10.1155/2013/927214

Research Article

Effect of Clonidine (an Antihypertensive Drug) Treatment on Oxidative Stress Markers in the Heart of Spontaneously Hypertensive Rats

Nik Syamimi Nik Yusoff, Zulkarnain Mustapha, Chandran Govindasamy, and K. N. S. Sirajudeen

Department of Chemical Pathology, School of Medical Sciences, Universiti Sains Malaysia, Health Campus, 16150 Kubang Kerian, Kelantan, Malaysia

Correspondence should be addressed to K. N. S. Sirajudeen; sirajuden@kb.usm.my

Received 9 February 2013; Accepted 4 April 2013

Academic Editor: Kota V. Ramana

Hypertension is a risk factor for several cardiovascular diseases and oxidative stress suggested to be involved in the pathophysiology. Antihypertensive drug Clonidine action in ameliorating oxidative stress was not well studied. Therefore, this study investigate the effect of Clonidine on oxidative stress markers and nitric oxide (NO) in SHR and nitric oxide synthase inhibitor, N-nitro-L-arginine methyl ester (L-NAME) administered SHR. Male rats were divided into four groups [SHR, SHR+Clonidine (SHR-C), SHR+L-NAME, SHR+Clonidine+L-NAME(SHRC+L-NAME)]. Rats (SHRC) were administered with Clonidine (0.5 mg kg^{-1} day^{-1}) from 4 weeks to 28 weeks in drinking water and L-NAME (25 mg kg^{-1} day^{-1}) from 16 weeks to 28 weeks to SHRC+L-NAME. Systolic blood pressure (SBP) was measured. At the end of 28 weeks, all rats were sacrificed and in their heart homogenate, oxidative stress parameters and NO was assessed. Clonidine treatment significantly enhanced the total antioxidant status (TAS) ($P < 0.001$) and reduced the thibarbituric acid reactive substances (TBARS) ($P < 0.001$) and protein carbonyl content (PCO) ($P < 0.05$). These data suggest that oxidative stress is involved in the hypertensive organ damage and Clonidine not only lowers the SBP but also ameliorated the oxidative stress in the heart of SHR and SHR+L-NAME.

1. Introduction

Globally, near one billion people have hypertension; of these, two-thirds are in developing countries, killing nearly 8 million people worldwide every year and nearly 1.5 million people each year in South-East Asia region approximately one-third of the adult population in this region has high blood pressure [1]. The Sixth Reports of the Joint National Committee on Prevention, Detection, Evaluation, and Treatment of High Blood Pressure (JNC VI) define hypertension or high blood pressure to be present if it is persistently at or above 140/90 mmHg.

Hypertension is a risk factor for several cardiovascular diseases such as atherosclerosis or myocardial infarction [2], kidney failure [3], stroke, and death [4].

Growing evidence indicated that oxidative stress plays an important role in the pathophysiology of hypertension [5]. Hypertension is associated with imbalance of oxidant antioxidant status which causes alteration in lipid peroxidation [6] superoxide dismutase and glutathione peroxidase [7] and higher production in hydrogen peroxide [8].

Nitric oxide (NO) (endothelium-derived relaxing factor) is synthesised in biological system by nitric oxide synthase (NOS) and has a strong vasodilatory effect [9]. NOS inhibitor such as N-nitro-L-arginine methyl ester (L-NAME) has a causal role in oxidative stress [10–12] as well as promotes persistent hypertension and progressive cardiovascular damage [13]. Zhou and Frohlich [13] developed and established the L-NAME/SHR model that mimics the pathophysiological alterations associated with naturally-occurring progressive impairment of cardiac and renal functions and structure. They have reviewed series of studies designed using the L-NAME/SHR to investigate the effect of antihypertensive agents on prevention, development, progression, and even

reversal of hypertensive nephrosclerosis. Each report documented the pathophysiological actions by the intervention of an antihypertensive agent either concomitantly with or subsequently following L-NAME. However, the studies were focusing on pathophysiological effect of calcium antagonists, angiotensine converting enzyme inhibitors and aldosterone antagonist. Therefore, using the L-NAME/SHR model, we would like to determine the effects of Clonidine, an a-adrenoceptor agonists, another class of antihypertensive drug on oxidative stress markers [thiobarbituric acid reactive substances (TBARS), protein carbonyl (PCO), total antioxidant status (TAS)] and nitric oxide level in the heart of SHR and SHR+L-NAME.

2. Methods

This study was approved by the Animal Ethics and Welfare Committee of Universiti Sains Malaysia. Male SHR aged 4 weeks were obtained from the Animal Research and Service Centre (ARASC), Health Campus Universiti Sains Malaysia, and housed in individual cages in standard environment (25–27°C) room temperature under 12 hours light and 12 hours dark cycle (lights on 0700–1900 hours). The animals were fed with commercial rat food pellet and Clonidine (Sigma, USA) was given through drinking water. Rats were divided into 4 groups: (1) SHR (untreated), (2) SHR treated with Clonidine ($0.5\,mg\,kg^{-1}\,day^{-1}$; 4–28 weeks) (SHRC), (3) SHR administered L-NAME ($25\,mg\,kg^{-1}\,day^{-1}$) (untreated)(SHR/L-NAME), and (4) SHR administered L-NAME ($25\,mg\,kg^{-1}\,day^{-1}$) treated with Clonidine ($0.5\,mg\,kg^{-1}\,day^{-1}$; 4–28 weeks) (SHRC/L-NAME) of which each group consists of 6 animals ($n = 6$). Chronic administration of L-NAME started in rats aged 16 weeks until 28 weeks in group 3 and group 4. The normotensive Wistar-Kyoto (WKY) rats were divided and treated with clonidine in a similar manner with SHR groups.

Systolic blood pressure (SBP) was taken during the experimental period for every two weeks using the tail plethysmography blood pressure analyzer (IITC Life Science, USA). Rats were weighed and sacrificed at the end of 28th weeks. The heart was collected and homogenized (Glas-Col, USA) in 0.05 M sodium phosphate buffer (pH 7.4). Supernatant of heart homogenate was stored at −70°C until use for biochemical analysis.

Lipid peroxidation was determined as thiobarbituric acid reactive substances (TBARS) according to the method of Chatterjee et al. [14]. MDA, an end product of fatty acid peroxidation, react with TBA to form coloured complex which has maximum absorbance at 532 nm. 1,1,3,3-Tetraethoxypropane (TEP); a form of MDA was used as standard in this assay. 0.1% of heart homogenate or MDA standard (2 μM, 4 μM, 6 μM, and 8 μM) were pipette into each test tubes. The test tubes were vortexed and then kept in boiling water bath at 95°C for 60 minutes. After cooling, the tubes were centrifuged at 3000 ×g for 10 minutes. One mL of each supernatant was transferred to semimicrocuvette and absorbance was read at 532 nm on a spectrophotometer.

Protein carbonyl (PCO) levels were determined using Protein Carbonyl Assay Kit (Cayman, USA) according to the method of Rohrbach et al. [15]. DNHP react with protein carbonyl, forming a Schiff base to produce corresponding hydrazone. The amount of protein-hydrazone produced was quantified spectrophotometrically at an absorbance between 360 and 385 nm.

Total antioxidant status (TAS) was assessed according to the method of Koracevic et al. [16]. It was based on the principle that a standardized solution of Fe-EDTA complex reacted with hydrogen peroxide by a Fenton-type reaction, leading to the formation of hydroxyl radicals. These reactive oxygen species degraded benzoate, resulting in the release of TBARS. Antioxidants from the added sample of heart homogenate caused suppression of the production of TBARS that was proportional to their concentration. This reaction was measured spectrophotometrically at 532 nm and the inhibition of colour development was defined as the TAS.

Nitric Oxide (NO) was determined using Nitrate/Nitrite Colorimetric Assay Kit according to the method Yui et al. [17]. Nitrate reductase utilizes NADPH in the enzymatic reduction of nitrate to nitrite. Nitrite produced reacts with Griess Reagent 1 followed by Griess Reagent 2 to produce Azo product. The concentration of the Azo product in the sample was obtained by measuring the absorbance at 540 nm.

3. Statistical Analysis

Data were analyzed using One-Way ANOVA with post hoc Tukey test. Data were analyzed using Statistical Package for the Social Science (SPSS) software version 20. Significant level was set at ($P < 0.05$). Data are expressed as mean and standard error mean (mean ± SEM) for six animals in each group.

4. Results

4.1. SBP, Oxidative Stress Parameters, and NO of Clonidine Treated and Untreated SHR and SHR+L-NAME. The SBP of Clonidine treated and untreated SHR and SHR+L-NAME were presented in Figure 1. SBP of SHR treated with Clonidine (SHRC) were significantly lower from age of 8 weeks until 28 weeks when compared to untreated SHR ($P < 0.001$, a^{***}). L-NAME was administered to rats at age of 16 weeks. Therefore, SHR+L-NAME treated with Clonidine (SHRC+L-NAME) showed significant increase compared to untreated SHR+L-NAME (c^{***}, $P < 0.001$), before L-NAME was administered as these still represent the SHRC compared to SHR. After administration of L-NAME, SHR+L-NAME showed significant increase in SBP in weeks 26 ($P < 0.01$, b^{**}) and in weeks 28 ($P < 0.001$, b^{***}) compared to SHR. There was also significant decrease of SBP in Clonidine treated SHR administered L-NAME (SHRC+L-NAME) when compared to untreated SHR+L-NAME from weeks 20 until weeks 28 (week 20: $P < 0.05$, d^{*}, week 22 and 24: $P < 0.01$, d^{**}, and week 26 & 28: $P < 0.001$, d^{***}).

4.2. TAS. Figure 2 represents the level of TAS in Clonidine treated and untreated SHR and SHR+L-NAME. The level of TAS was significantly increased with Clonidine treatment in SHR ($P < 0.001$, a^{***}). However, no significant difference in TAS level in L-NAME administered SHR when compared to

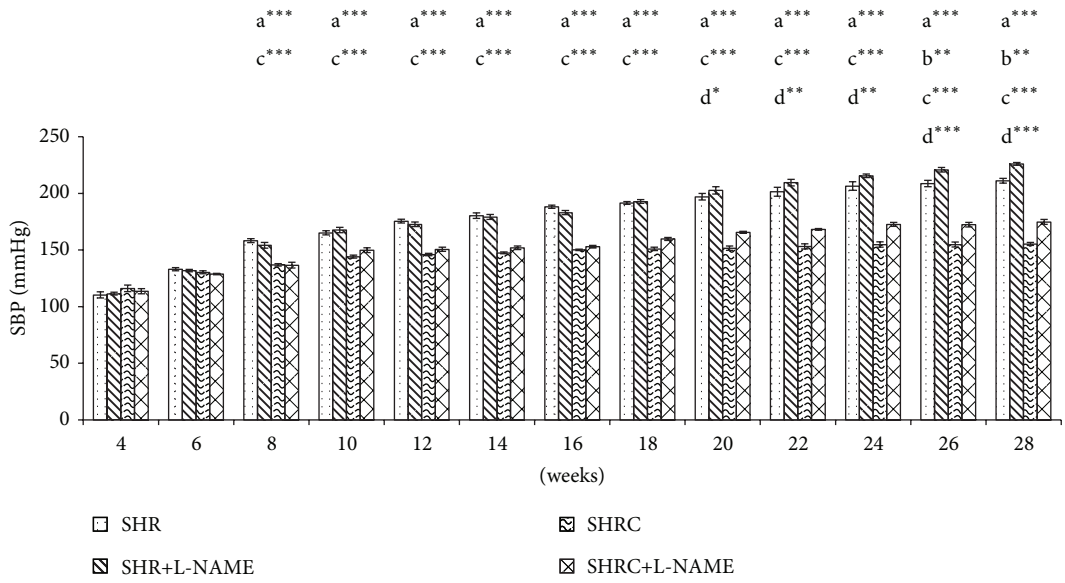

Figure 1: SBP of Clonidine treated and untreated SHR administered with L-NAME. a^{***} $P < 0.001$ SHR compared to SHRC, b^{**} $P < 0.01$ SHR+L-NAME compared to SHR, c^{***} $P < 0.001$ SHRC+L-NAME compared to SHR+L-NAME and d^{*} $P < 0.05$, d^{**} $P < 0.01$, and d^{***} $P < 0.001$ SHRC+L-NAME compared to SHRC.

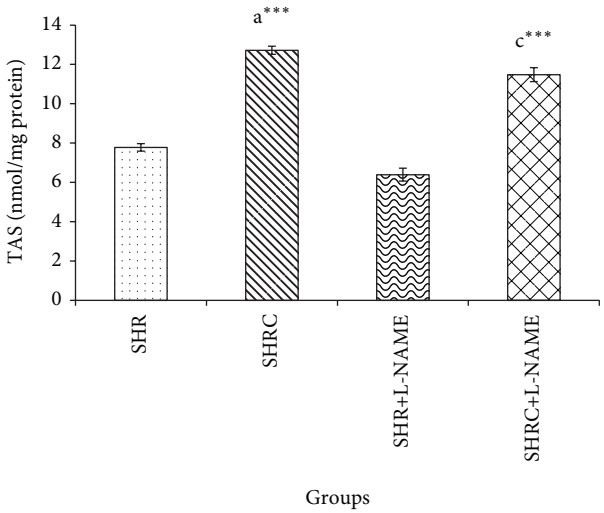

Figure 2: TAS levels in Clonidine treated and untreated SHR administered with L-NAME. a^{***} $P < 0.001$ SHR compared to SHRC, c^{***} $P < 0.001$ SHRC+L-NAME compared to SHR+L-NAME.

SHR. Significant increase was evident in TAS level in Clonidine treated SHR administered with L-NAME (SHRC+L-NAME) when compared to untreated SHR administered L-NAME (SHR+L-NAME) ($P < 0.001$, c^{***}). No significant difference was observed in SHRC+L-NAME when compared to Clonidine treated SHR without L-NAME (SHRC).

4.3. TBARS. The TBARS levels of Clonidine treated and untreated SHR and SHR+L-NAME were provided in Figure 3. TBARS level in Clonidine treated SHR was significantly lower compared to untreated SHR ($P < 0.001$, a^{***}). The levels of TBARS in SHR administered with L-NAME (SHR+L-NAME) were significantly higher when compared to SHR ($P < 0.001$, b^{***}). Significant decrease was evident in TBARS level in Clonidine treated SHR administered with L-NAME (SHRC+L-NAME) when compared to untreated SHR administered L-NAME (SHR+L-NAME) ($P < 0.001$, c^{***}). No significant difference was observed in SHRC+L-NAME when compared to Clonidine treated SHR without L-NAME (SHRC).

4.4. PCO. Figure 4 represents the PCO level of Clonidine treated and untreated SHR and SHR+L-NAME. PCO level in Clonidine treated SHR was significantly lower compared to untreated SHR ($P < 0.05$, a^{*}). Significant increase was observed in PCO levels of SHR administered L-NAME (SHR+L-NAME) when compared to SHR ($P < 0.001$, b^{***}). Significant decrease was evident in PCO level in Clonidine treated SHR administered with L-NAME (SHRC+L-NAME) when compared to untreated SHR administered L-NAME (SHR+L-NAME) ($P < 0.05$, c^{*}). Significant increase also was observed in SHRC+L-NAME when compared to Clonidine treated SHR without L-NAME (SHRC) ($P < 0.001$, d^{***}).

4.5. NO. The NO levels of Clonidine treated and untreated SHR and SHR+L-NAME were given in Figure 5. NO level in Clonidine treated SHR and SHR+L-NAME was increased but not statistically significant compared to untreated SHR. Significant decrease was observed in NO levels of SHR administered L-NAME (SHR+L-NAME) when compared to SHR ($P < 0.001$, b^{***}). No significant difference was evident in NO level in Clonidine treated SHR administered with L-NAME (SHRC+L-NAME) when compared to untreated

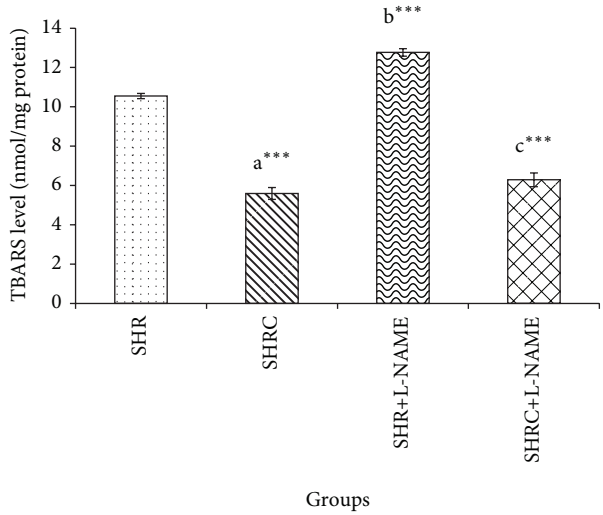

Figure 3: TBARS levels in Clonidine treated and untreated SHR administered with L-NAME. a*** $P < 0.001$ SHR compared to SHRC, b*** $P < 0.001$ SHR+L-NAME compared to SHR, and c*** $P < 0.001$ SHRC+L-NAME compared to SHR+L-NAME.

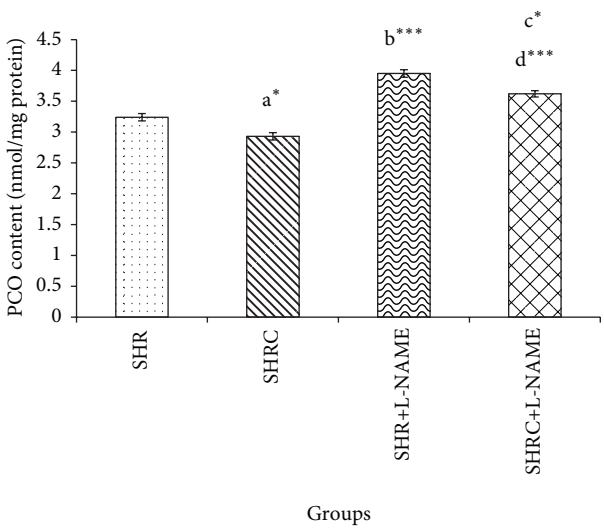

Figure 4: PCO levels in Clonidine treated and untreated SHR administered with L-NAME. a* $P < 0.05$ SHR compared to SHRC, b*** $P < 0.001$ SHR+L-NAME compared to SHR, c* $P < 0.05$ SHRC+L-NAME compared to SHR+L-NAME, and d*** $P < 0.001$ SHRC+L-NAME compared to SHRC.

SHR administered L-NAME (SHR+L-NAME). Significant decrease also was observed in SHRC+L-NAME when compared to Clonidine treated SHR without L-NAME (SHRC) ($P < 0.001$, d***).

4.6. SBP, Oxidative Stress Parameters, and NO of Clonidine Treated and Untreated WKY and WKY+L-NAME. WKY rats showed normal SBP. As expected, L-NAME administration in WKY significantly increases the SBP at 18 weeks ($P < 0.05$) and 20 weeks onward ($P < 0.001$) when

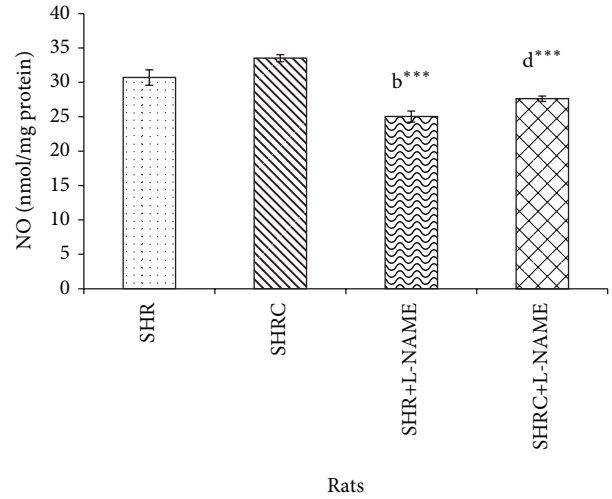

Figure 5: NO levels in Clonidine treated and untreated SHR administered with L-NAME. b*** $P < 0.001$ SHR+L-NAME compared to SHR and d*** $P < 0.001$ SHRC+L-NAME compared to SHRC.

compared to WKY. Clonidine treatment significantly reduced the SBP in WKY+L-NAME when compared to WKY+L-NAME untreated (data not shown).

Table 1 showed the oxidative stress parameters and NO of normotensive WKY rats. Significant increase (b***, $P < 0.001$) was evident in TBARS and PCO levels of WKY+L-NAME when compared to WKY. However, no significant difference was evident in TAS levels of WKY+L-NAME when compared to WKY. Clonidine treatment significantly elevated the TAS level in WKY when compared to untreated WKY (a***, $P < 0.001$), but no significant difference was seen in PCO levels. TBARS level showed significant increase in Clonidine treated WKY (a*, $P < 0.05$) and WKY+L-NAME (c*, $P < 0.05$) when compared to their matched untreated groups. Significant decrease (b*** and d***, $P < 0.001$) in NO level was evident in L-NAME administered groups. However, no significant difference was evident in NO level in Clonidine treated WKY and WKY+L-NAME when compared to their matched untreated groups.

5. Discussions

The results of this study showed that SBP was significantly elevated in SHR as demonstrated in previous studies [18, 19]. Administration of L-NAME at 16 weeks initially did not elevate SBP in SHR. However, at weeks 26 and 28, SBP was elevated in SHR+L-NAME. Gerová et al. [20] showed that the use of L-NAME as NOS inhibitor alters the regulation of blood pressure and is accompanied by development of cardiovascular disorders. It has been shown that chronic reduction of NO synthesis resulted in hypertension [20, 21] and reduced endothelial vasorelaxation [22–24] and myocardial hypertrophy [25]. The results of this study demonstrated that Clonidine can attenuate development of high blood pressure and end-organ damage in SHR and SHR+L-NAME with significant endothelial dysfunction produced by inhibition of NO synthesis. Since 1960, Clonidine is believed to

Table 1: Effect of Clonidine treatment on TBARS, PCO, TAS, and NO level of Clonidine treated and untreated WKY and WKY administered L-NAME.

Parameters	Groups			
	WKY	WKY+L-NAME	WKYC	WKYC+L-NAME
TAS	7.64 ± 0.17	6.91 ± 0.05	10.54 ± 0.93 a***	8.53 ± 0.18
TBARS	5.59 ± 0.32	7.49 ± 0.20 b***	7.80 ± 0.49 a*	8.98 ± 0.25 c*
PCO	2.69 ± 0.07	3.12 ± 0.05 b***	2.94 ± 0.18	3.11 ± 0.19 c*
NO	37.65 ± 0.56	27.92 ± 0.79 b***	39.25 ± 0.65	30.71 ± 0.69 d***

Values are expressed as mean ± S.E.M. ($n = 6$ per group).
WKY: WKY no treatment, WKY+L-NAME: WKY no treatment+L-NAME, WKYC: WKY+Clonidine, and WKYC+L-NAME: WKY+Clonidine+L-NAME.
a* $P < 0.05$, a*** $P < 0.001$ WKY compared to WKYC, b*** $P < 0.001$ WKY+L-NAME compared to WKY, c* $P < 0.05$ WKYC+L-NAME compared to WKY+L-NAME, and d*** $P < 0.001$ WKYC+L-NAME compared to WKYC.

lower blood pressure through several modes of action such as stimulating a-adrenoceptors in the cardiovascular centers with a reduction of sympathetic nerve activity and noradrenaline release [26, 27] producing suppressant effect on adrenal medullary function, and decreasing adrenal sympathetic nerve activity [28–30], and activation of nonadrenergic depressor pathways, and activation of baroreflex [31, 32].

Clonidine treatment also delayed the onset and attenuated the severity of hypertension produced by L-NAME inhibition. Rizzoni et al. reported that SHR are normotensive at 4 weeks of age and develop hypertension, cardiac hypertrophy and vascular dysfunction by 8–12 weeks [33].

The increase in the systolic blood pressure in SHR was accompanied by changes in the marker of oxidative stress, such as lower heart total antioxidant status, higher thiobarbituric acid reactive substance, and elevation of protein carbonyl content. This implies, as previously demonstrated, an increase in the production of reactive oxygen species, which in turn produce a higher systemic and heart oxidative stress in SHR [5]. Alteration in oxidant-antioxidant balance in SHR demonstrated in this study may contribute to the generation and/or maintenance of hypertension via promoting vascular smooth muscle cell proliferation and hypertrophy as well as collagen deposition, leading to thickening of vascular media and narrowing of the vascular lumen as reviewed by Grossman [34]. In addition, increase oxidative stress may damage the endothelium, impair endothelium-dependent vascular relaxation, and increase vascular contractile activity [35].

The present study demonstrates that nitric oxide synthase inhibition by L-NAME reduced the nitric oxide level in SHR. By contrast, administration of L-NAME was not affecting the TAS. L-NAME inhibits the production of vasodilator nitric oxide.

Regarding Clonidine treatment, data from the study herein revealed that Clonidine treatment elevated total antioxidant status in SHR. To further evaluate the effect of Clonidine against hypertension-associated oxidative stress, the lipid peroxidation product (TBARS) and protein oxidation product (PCO) in heart were examined. Clonidine treatment decreases the level of lipid peroxidation product and protein oxidation product in heart of SHR and SHR administered L-NAME in comparison to untreated groups.

The protective effect of clonidine may have multiple components in its action. Clonidine, an α2-adrenergic receptor agonist, is thought to decrease blood pressure by causing a reduced sympathetic nerve firing rate with the locus of its action within the CNS [36]. The same report also demonstrated that Clonidine treatment results in hypotensive in SHR through action of sympathetic vasoconstrictor fibers. α2-Adrenoceptor agonists, such as clonidine, attenuate hypoxia-induced damage to brain and retinal neurones by a mechanism of action which likely involves stimulation of a-adrenoceptors. When compared to Clonidine administered WKY and WKY+L-NAME (Table 1), Clonidine administered SHR and SHR+L-NAME showed a significant reduction in oxidative stress parameters which clearly indicate that Clonidine is reducing oxidative stress in SHR and SHR+L-NAME.

From this study, therefore, it concluded that some evident was found to support the idea that, in addition to the hypotensive effect of Clonidine, this antihypertensive drug enhance the level of antioxidant status and ameliorate the oxidative stress which might reduce the hypertension induced heart damage in SHR and SHR+L-NAME. A better understanding of the complexity of oxidative stress and hypertension, role of nitric oxide, and development of new class of antihypertensive drug which ameliorates oxidative stress will likely be the avenues for future research to prevent hypertension and hypertension induced cardiovascular complications.

Conflict of Interests

No conflict of interests, financial or otherwise, is declared by the authors.

Acknowledgments

This study was supported by the Research University Grant Scheme (RU 1001/PPSP/811167) provided by Universiti Sains Malaysia. The first author thanked the Universiti Sains Malaysia for providing fellowship under USM Fellowship Scheme.

References

[1] 2012, http://www.searo.who.int/entity/noncommunicable_diseases/media/non_communicable_diseases_hypertension_fs.pdf.

[2] D. Binda, L. Nicod, C. Viollon-Abadie et al., "Strain difference (WKY, SPRD) in the hepatic antioxidant status in rat and effect of hypertension (SHR, DOCA). Ex vivo and in vitro data,"

Molecular and Cellular Biochemistry, vol. 218, no. 1-2, pp. 139–146, 2001.

[3] D. Tian, S. Ling, G. Chen et al., "Hypertensive nephropathy treatment by heart-protecting musk pill: a study of anti-inflammatory therapy for target organ damage of hypertension," *International Journal of General Medicine*, vol. 4, pp. 131–139, 2011.

[4] A. V. Chobanian, G. L. Bakris, H. R. Black et al., "The seventh report of the joint national committee on prevention, detection, evaluation, and treatment of high blood pressure: the JNC 7 report," *Journal of the American Medical Association*, vol. 289, no. 19, pp. 2560–2572, 2003.

[5] G. Zalba, G. San Jose, M. U. Moreno et al., "Oxidative stress in arterial hypertension role of NAD(P)H oxidase," *Hypertension*, vol. 38, no. 6, pp. 1395–1399, 2001.

[6] C. Russo, O. Olivieri, D. Girelli et al., "Antioxidant status and lipid peroxidation in patients with essential hypertension," *Journal of Hypertension*, vol. 16, no. 9, pp. 1267–1271, 1998.

[7] J. Pedro-Botet, M. I. Covas, S. Martín, and J. Rubiés-Prat, "Decreased endogenous antioxidant enzymatic status in essential hypertension," *Journal of Human Hypertension*, vol. 14, no. 6, pp. 343–345, 2000.

[8] F. Lacy, M. T. Kailasam, D. T. O'Connor, G. W. Schmid-Schönbein, and R. J. Parmer, "Plasma hydrogen peroxide production in human essential hypertension: role of heredity, gender, and ethnicity," *Hypertension*, vol. 36, no. 5, pp. 878–884, 2000.

[9] S. Mokuno, T. Ito, Y. Numaguchi et al., "Impaired nitric oxide production and enhanced autoregulation of coronary circulation in young spontaneously hypertensive rats at prehypertensive stage," *Hypertension Research*, vol. 24, no. 4, pp. 395–401, 2001.

[10] S. M. Gardiner, P. A. Kemp, T. Bennett, C. Bose, R. Foulkes, and B. Hughes, "Involvement of β_2-adrenoceptors in the regional haemodynamic responses to bradykinin in conscious rats," *British Journal of Pharmacology*, vol. 105, no. 4, pp. 839–848, 1992.

[11] C. F. Küng, P. Moreau, H. Takase, and T. F. Luscher, "L-NAME hypertension alters endothelial and smooth muscle function in rat aorta: prevention by trandolapril and verapamil," *Hypertension*, vol. 26, no. 5, pp. 744–751, 1995.

[12] T. Tsuchihashi, S. Kagiyama, K. Matsumura, Y. Lin, I. Abe, and M. Fujishima, "Cardiovascular responses to glutamate and angiotensin II in ventrolateral medulla of hypertension induced by chronic inhibition of nitric oxide," *Hypertension Research*, vol. 23, no. 4, pp. 359–364, 2000.

[13] X. Zhou and E. D. Frohlich, "Analogy of cardiac and renal complications in essential hypertension and aged SHR or L-NAME/SHR," *Medicinal Chemistry*, vol. 3, no. 1, pp. 61–65, 2007.

[14] P. K. Chatterjee, S. Cuzzocrea, P. A. J. Brown et al., "Tempol, a membrane-permeable radical scavenger, reduces oxidant stress-mediated renal dysfunction and injury in the rat," *Kidney International*, vol. 58, no. 2, pp. 658–673, 2000.

[15] S. Rohrbach, A. Martin, B. Niemann, and A. Cherubini, "Enhanced myocardial vitamin C accumulation in left ventricular hypertrophy in rats is not attenuated with transition to heart failure," *European Journal of Heart Failure*, vol. 10, no. 3, pp. 226–232, 2008.

[16] D. Koracevic, G. Koracevic, V. Djordjevic, S. Andrejevic, and V. Cosic, "Method for the measurement of antioxidant activity in human fluids," *Journal of Clinical Pathology*, vol. 54, no. 5, pp. 356–361, 2001.

[17] Y. Yui, R. Hattori, K. Kosuga et al., "Calmodulin-independent nitric oxide synthase from rat polymorphonuclear neutrophils," *The Journal of Biological Chemistry*, vol. 266, no. 6, pp. 3369–3371, 1991.

[18] O. O. Erajuwa, S. A. Sulaiman, M. S. Ab Wahab, K. N. S. Sirajudeen, S. Salleh, and S. Gurtu, "Honey supplemention in spontaneously hypertensive rats elicits antihypertensive effect via amelioration of renal oxidative stress," *Oxidative Medicine and Cellular Longevity*, vol. 2012, Article ID 374037, 14 pages, 2012.

[19] S. K. Lee, S. Arunkumar, K. N. S. Sirajudeen, and H. J. Singh, "Glutathione system in young spontaneously hypertensive rats," *Journal of Physiology and Biochemistry*, vol. 66, no. 4, pp. 321–327, 2010.

[20] M. Gerová, J. Török, O. Pecháòová, and J. Matušková, "Rilmenidine prevents blood pressure increase in rats with compromised nitric oxide production," *Acta Pharmacologica Sinica*, vol. 25, no. 12, pp. 1640–1646, 2004.

[21] R. Zatz and C. Baylis, "Chronic nitric oxide inhibition model six years on," *Hypertension*, vol. 32, no. 6, pp. 958–964, 1998.

[22] J. Török and F. Kristek, "Beneficial effect of pentaerythrityl tetranitrate on functional and morphological changes in the rat thoracic aorta evoked by long-term nitric oxide synthase inhibition," *Vascular Pharmacology*, vol. 38, no. 3, pp. 177–182, 2002.

[23] I. Bernátová, O. Pechanova, V. Pelouch, and F. Šimko, "Regression of chronic L-NAME-treatment-induced left ventricular hypertrophy: effect of captopril," *Journal of Molecular and Cellular Cardiology*, vol. 32, no. 2, pp. 177–185, 2000.

[24] L. Paulis, J. Zicha, J. Kunes et al., "Regression of L-NAME-induced hypertension: the role of nitric oxide and endothelium-derived constricting factor," *Hypertension Research*, vol. 31, no. 4, pp. 793–803, 2008.

[25] F. Simko, A. Potacova, V. Pelouch et al., "Spontaneous, L-arginine-induced and spironolactone induced regression of protein remodeling of the left ventricle in L-NAME-induced hypertension," *Physiological Research*, vol. 56, supplement 2, pp. S55–S62, 2007.

[26] S. Berthelsen and W. A. Pettinger, "A functional basis for classification of α-adrenergic receptors," *Life Sciences*, vol. 21, no. 5, pp. 595–606, 1977.

[27] K. Starke and J. Docherty, "Recent developments in [alpha]-adrenoceptor research," *Journal of Cardiovascular Pharmacology*, vol. 2, pp. S269–S286, 1980.

[28] K. Shimamura, H. Togashi, and H. Saito, "Effect of clonidine on the function of the adrenal medulla in rats," *Research Communications in Chemical Pathology and Pharmacology*, vol. 31, no. 1, pp. 189–192, 1981.

[29] H. Togashi, "Central and peripheral effects of clonidine on the adrenal medullary function in spontaneously hypertensive rats," *Journal of Pharmacology and Experimental Therapeutics*, vol. 225, no. 1, pp. 191–197, 1983.

[30] M. Kurosawa, M. Minami, H. Togashi, and H. Saito, "The effect of clonidine on adrenal sympathetic nerve responses to mechanical, noxious and innocuous stimulation of the skin in rats," *Neuroscience Letters*, vol. 53, no. 3, pp. 253–258, 1985.

[31] A. Mitchell, S. Bührmann, A. Opazo et al., "Clonidine lowers blood pressure by reducing vascular resistance and cardiac output in young, healthy males," *Cardiovascular Drugs and Therapy*, vol. 19, no. 1, pp. 49–55, 2005.

[32] M. Frisk-Holmberg, "Evidence for a histamine H_2-receptor involvement in clonidine's antihypertensive effects during multiple dosing," *Acta Physiologica Scandinavica*, vol. 108, no. 2, pp. 191–193, 1980.

[33] D. Rizzoni, M. Castellano, E. Porteri, G. Bettoni, M. L. Muiesan, and E. Agabiti-Rosei, "Vascular structural and functional alterations before and after the development of hypertension in SHR," *American Journal of Hypertension*, vol. 7, no. 2, pp. 193–200, 1994.

[34] E. Grossman, "Does increased oxidative stress cause hypertension?" *Diabetes Care*, vol. 31, pp. S185–S189, 2008.

[35] M. McIntyre, D. F. Bohr, and A. F. Dominiczak, "Endothelial function in hypertension: the role of superoxide anion," *Hypertension*, vol. 34, no. 4, pp. 539–545, 1999.

[36] J. Iriuchijima, "Why is the hypotensive effect of Clonidine greater in hypertensive rats?" *Tohoku Journal of Experimental Medicine*, vol. 182, no. 4, pp. 271–276, 1997.

Hindawi Publishing Corporation
Oxidative Medicine and Cellular Longevity
Volume 2013, Article ID 325406, 11 pages
http://dx.doi.org/10.1155/2013/325406

Research Article

Ameliorating Effect of Various Fractions of *Rumex hastatus* Roots against Hepato- and Testicular Toxicity Caused by CCl_4

Sumaira Sahreen,[1] Muhammad Rashid Khan,[2] and Rahmat Ali Khan[3]

[1] *Botanical Sciences Division, Pakistan Museum of Natural History, Garden Avenue, Shakarparian, Islamabad, Pakistan*
[2] *Department of Biochemistry, Faculty of Biological Sciences, Quaid-i-Azam University, Islamabad 45320, Pakistan*
[3] *Department of Biotechnology, Faculty of Biological Sciences, University of Science and Technology, Bannu, Khyber Pakhtunkhwa 28100, Pakistan*

Correspondence should be addressed to Rahmat Ali Khan; rahmatgul_81@yahoo.com

Received 14 February 2013; Revised 4 April 2013; Accepted 4 April 2013

Academic Editor: Kota V. Ramana

Effect of methanolic extract of *Rumex hastatus* roots (MRR) and its derived fractions, n-hexane (HRR), ethyl acetate (ERR), chloroform (CRR), butanol (BRR), and aqueous extract (ARR), was studied against carbon tetrachloride (CCl_4) induced hepato and testicular toxicity in rats. Intraperitoneal dose of 20 percent CCl_4 (0.5 ml/kg bw) was administered twice a week for eight weeks to a group of rats. Other groups were given CCl_4 and various fractions of *R. hastatus* roots (200 mg/kg bw). CCl_4 treatment depleted glutathione contents and activities of antioxidant enzymes while increased the concentration of lipid peroxides (TBARS) along with corresponding DNA injuries and histopathological damages. Supplementation with various fractions of *R. hastatus* roots (200 mg/kg body weight) attenuated the toxicity of CCl_4 in liver and testis tissues through improvement in the serological, enzymatic, and histological parameters towards the normal. Posttreatment of *R. hastatus* roots (200 mg/kg body weight) also reversed the alteration in reproductive hormonal secretions and DNA damages in CCl_4 treated rats. The results clearly demonstrated that *R. hastatus* treatment augments the antioxidants defense mechanism and provides the evidence that it may have a therapeutic role in free radical mediated diseases.

1. Introduction

Reactive oxygen species (ROS), like hydroxyl, peroxyl, and superoxide radicals, are very transient and highly reactive causes of the pathogenesis of atherosclerosis, neurodegeneration, inflammation, cardiovascular diseases, diabetes, and cataracts [1, 2]. CCl_4 is a toxic chemical, commonly used to induce hepatic cirrhosis [3] and testicular injuries in experimental animals [4]. Metabolic activation of CCl_4 by cytochrome P_{450} resulted in the production of trichloromethyl radical ($^{\bullet}CCl_3$) and peroxy trichloromethyl radical ($^{\bullet}OOCCl_3$) that in turn initiate lipid peroxidation, responsible for injuries in various organs like liver and testis [5]. These free radicals combine with polyunsaturated fatty acids of hepatic and testicular cell membranes, cause elevation of thiobarbituric acid reactive substances (TBARSs) concentration with subsequent necrosis [6], and increase lysosomal enzymes activities [7]. The health promoting effects of antioxidants on oxidative damage are mostly examined through cellular antioxidants enzymes in addition to TBARS and GSH concentration [5, 8]. It is also reported that increase in oxidative damage to sperm membranes, proteins, and DNA is associated with alterations in signal transduction mechanisms that affect fertility [9] and cause degeneration of somniferous tubules showing a relationship between hypogonadism and liver cirrhosis [5]. *Rumex hastatus* D. Don belongs to the Polygonaceae family and is popularly known as "khatimal." It is distributed in northern Pakistan, northeast Afghanistan, and southwest China, growing between 700 and 2500 m, and sometimes grows as a pure population. It is reported that the whole plant is used as medicine. It is laxative, alterative, tonic, and is used in rheumatism [10] and sexually transmitted diseases including AIDS [11]. Our previous studies substantiated the *R. hastatus* leaves as a good

antioxidant source with sufficient amount of phenolics [12]. Zhang et al. [13] by referring the use in Chinese herbal system reported seven phenolic compounds from *R. hastatus* roots. Thus, regarding the cultural/ethnic use present toxicological studies in rat models have been planned to evaluate the protective effect of various fractions of *R. hastatus* roots against hepato- and testicular toxicity caused by CCl_4.

2. Materials and Methods

2.1. Extract Preparation. R. hastatus District roots were collected from Havelian, Abbottabad, Pakistan. Shade dried roots were powdered in a Willy Mill to 60-mesh size and used for solvent extraction. Five kg powder was extracted twice with 10 liters of 95 percent methanol at 25°C for 48 h and filtered. The methanolic solution was dried in a rotary evaporator (Panchun Scientific Co., Kaohsiung, Taiwan) to obtain methanolic crude extract of *R. hastatus* roots (MRR). In order to resolve the compounds with escalating polarity, a part of the extract was suspended in distilled water and subjected to liquid-liquid partition by using solvents in a sequence of *n*-hexane (HRR), ethyl acetate (ERR), chloroform (CRR), and butanol (BRR), while the remaining soluble portion was filtered and used as aqueous fraction (ARR). After fractioning, the solvent of the respective fraction was evaporated by rotary evaporator [14].

2.2. In Vivo Evaluation of Fractions. For *in vivo* studies six-week-old male Sprague-Dawley rats weighting 180±10 g were provided with food and water *ad libitum* and kept at 20–22°C on a 12 h light-dark cycle. All experimental procedures involving animals were conducted in accordance with the guidelines of National Institutes of Health, Islamabad, Pakistan. The study protocol was approved by Ethical Committee of Quaid-i-Azam University, Islamabad Pakistan. The rats were acclimatized to laboratory condition for 7 days before commencement of experiments.

2.3. Experimental Plan. For subchronic toxicity, eight-week experiment was designed according to Shyu et al. [3]. Ninety-six rats were randomly divided into sixteen groups (6 rats of each group). Group I animals remained untreated, while Group II animals received olive oil and DMSO twice a week for eight weeks. Animals of Groups III, IV, V, VI, VII, VIII, IX, and X received intraperitoneally 0.5 mL of CCl_4, (20 percent in olive oil) twice a week for eight weeks. Group III received only CCl_4, while Group IV administered silymarin at a dose of 50 mg/kg bw after 48 h of CCl_4 treatment. Groups V, VI, VII, VIII, IX, and X received different fractions at a dose of 200 mg/kg bw, HFC, EFC, CFC, BFC, MFC, and AFC, twice a week for eight weeks orally. However, Groups XI, XII, XIII, XIV, XV, and XVI received fractions (200 mg/kg bw) alone twice a week for eight weeks after 48 hr of CCl_4 treatment orally. At the end of eight weeks, after 24 h of the last treatment, animals were given chloroform anesthesia and dissected from ventral side. Blood was drawn and centrifuged at 1500 ×g for 10 min, at 4°C to collect the serum. Liver and testis tissues were perfused with ice cold saline and excised. Subsequently, half of both tissue portions were treated with liquid nitrogen and stored at −80°C for further enzymatic and DNA damage analysis, while other portions were processed for histology.

2.4. Analysis of Serum. For estimation of liver function tests serum samples were assayed for ALT, AST, ALP,-γ-GT, total cholesterol, triglycerides, LDL, and HDL by using standard AMP diagnostic kits (Graz, Austria).

Serum analysis of testicular hormones like FSH, LH, testosterone, prolactin, and estradiol was radioimmunoassayed by using Marseille Cedex 9 France Kits and Czech Republic Kits from Immunotech Company.

2.5. Assessment of Antioxidant Enzymes. Ten percent of homogenates of liver and testis tissues were prepared separately in 100 mM KH_2PO_4 buffer containing 1 mM EDTA (pH 7.4) and centrifuged at 12,000 ×g for 30 min at 4°C. The supernatant was collected and used for the following experiments as described below. Protein concentration of the supernatant was determined by the method of Lowry et al. [15] using crystalline bovine serum albumin as standard.

2.5.1. Catalase Assay (CAT). CAT activities were determined by using H_2O_2 as a substrate [16]. 0.1 mL of the supernatant was mixed with 2.5 mL of 50 mM phosphate buffer (pH 5.0) and 0.4 mL of 5.9 mM H_2O_2, and change in absorbance was recorded at 240 nm after one min. One unit of CAT activity was defined as an absorbance change of 0.01 as units/min.

2.5.2. Peroxidase Assay (POD). In this method guaiacol was used as the substrate [16]. For the POD activity determination 0.1 mL of the supernatant was added to the reaction mixture having 2.5 mL of 50 mM phosphate buffer (pH 5.0), 0.1 mL of 20 mM guaiacol, and 0.3 mL of 40 mM H_2O_2. Changes in absorbance of the reaction solution at 470 nm were determined after one min. One unit of POD activity was defined as an absorbance change of 0.01 units/min.

2.5.3. Superoxide Dismutase Assay (SOD). In this method NADH was used as the substrate [17]. Reaction mixture of this method contained 0.1 mL of phenazine methosulphate (186 μM), 1.2 mL of sodium pyrophosphate buffer (0.052 mM; pH 7.0), and 0.3 mL of supernatant after centrifugation (1500 ×g for 10 min followed by 10000 ×g for 15 min) of tissue homogenate was added to the reaction mixture. Enzyme reaction was initiated by adding 0.2 mL of NADH (780 μM) and stopped after 1 min by adding 1 mL of glacial acetic acid. Amount of chromogen formed was measured by recording color intensity at 560 nm. Results are expressed in units/mg protein.

2.5.4. Glutathione-S-Transferase Assay (GST). Glutathione-S-transferase activity was assayed by the method of Habig et al. [18]. The reaction mixture consisted of 1.475 mL phosphate buffer (0.1 mol, pH 6.5), 0.2 mL reduced glutathione (1 mM), 0.025 mL of 1-chloro-2,4-dinitrobenzene (CDNB) (1 mM), and 0.3 mL of supernatant in a total volume of 2.0 mL. The changes in the absorbance were recorded at 340 nm, and

enzymes activity was calculated as nM CDNB conjugate formed/min/mg protein using a molar extinction coefficient of $9.6 \times 10^3\ M^{-1}\ cm^{-1}$.

2.5.5. Glutathione Reductase Assay (GSR). Glutathione reductase activity was determined by the method of Carlberg and Mannervik [19]. The reaction mixture consisted of 1.65 mL phosphate buffer (0.1 mol; pH 7.6), 0.1 mL EDTA (0.5 mM), 0.05 mL oxidized glutathione (1 mM), 0.1 mL NADPH (0.1 mmol), and 0.1 mL of supernatant in a total volume of 2 mL. Enzyme activity was quantitated at 25°C by measuring disappearance of NADPH at 340 nm and was calculated as nM NADPH oxidized/min/mg protein using molar extinction coefficient of $6.22 \times 10^3\ M^{-1}\ cm^{-1}$.

2.5.6. Glutathione Peroxidase Assay (GSH-Px). Glutathione peroxidase activity was assayed by the method of Mohandas et al. [20]. The reaction mixture consisted of 1.49 mL phosphate buffer (0.1 M; pH 7.4), 0.1 mL EDTA (1 mM), 0.1 mL sodium azide (1 mM), 0.05 mL glutathione reductase (1 IU/mL), 0.05 mL GSH (1 mM), 0.1 mL NADPH (0.2 mM), 0.01 mL H_2O_2 (0.25 mM), and 0.1 mL of supernatant in a total volume of 2 mL. The disappearance of NADPH at 340 nm was recorded at 25°C. Enzyme activity was calculated as nM NADPH oxidized/min/mg protein using molar extinction coefficient of $6.22 \times 10^3\ M^{-1}\ cm^{-1}$.

2.5.7. Quinone Reductase Assay (QR). The activity of quinone reductase was determined by the method of Benson et al. [21]. The 3.0 mL reaction mixture consisted of 2.13 mL Tris-HCl buffer (25 mM; pH 7.4), 0.7 mL BSA, 0.1 mL FAD, 0.02 mL NADPH (0.1 mM), and 0.1 mL of supernatant. The reduction of dichlorophenolindophenol (DCPIP) was recorded at 600 nm, and enzyme activity was calculated as nM of DCPIP reduced/min/mg protein using molar extinction coefficient of $2.1 \times 10^4\ M^{-1}\ cm^{-1}$.

2.6. Reduced Glutathione Assay (GSH). Reduced glutathione was estimated by the method of Jollow et al. [22]. 1.0 mL sample of supernatant was precipitated with 1.0 mL of (4 percent) sulfosalicylic acid. The samples were kept at 4°C for 1 h and then centrifuged at 1200 ×g for 20 min at 4°C. The total volume of 3.0 mL assay mixture contained 0.1 mL filtered aliquot, 2.7 mL phosphate buffer (0.1 M; pH 7.4), and 0.2 mL of 1,2-dithio-bis-nitrobenzoic acid DTNB (100 mM). The yellow color developed was read immediately at 412 nm on a SmartSpec Plus Spectrophotometer. It was expressed as μM GSH/g tissue.

2.7. Estimation of Lipid Peroxidation (TBARS). The assay for lipid peroxidation was carried out following the modified method of Iqbal et al. [23]. One milliliter of 20 percent TCA aqueous solution and 1.0 mL of 0.67 percent TBA aqueous solution was added to 0.6 mL of phosphate buffer (0.1 M; pH 7.4) and 0.4 mL of homogenate sample. The reaction mixture was heated in a boiling water bath for 20 min and then shifted to crushed ice-bath before centrifuging at 2500 ×g for 10 min. The amount of TBARS formed in each of the samples was assessed by measuring optical density of the supernatant at 535 nm using spectrophotometer against a reagent blank. The results were expressed as nM TBARS/min/mg tissue at 37°C using molar extinction coefficient of $1.56 \times 10^5\ M^{-1}\ cm^{-1}$.

2.8. Hydrogen Peroxide Assay (H_2O_2). Hydrogen peroxide (H_2O_2) was assayed by H_2O_2-mediated horseradish peroxidase-dependent oxidation of phenol red by the method of Pick and Keisari [24]. 2.0 mL of homogenate sample was suspended in 1.0 mL of solution containing phenol red (0.28 nM), horse radish peroxidase (8.5 units), dextrose (5.5 nM), and phosphate buffer (0.05 M; pH 7.0) and was incubated at 37°C for 60 min. The reaction was stopped by the addition of 0.01 mL of NaOH (10 N) and then centrifuged at 800 ×g for 5 min. The absorbance of the supernatant was recorded at 610 nm against a reagent blank. The quantity of H_2O_2 produced was expressed as nM H_2O_2/min/mg tissue based on the standard curve of H_2O_2 oxidized phenol red.

2.9. DNA Fragmentation Assay. DNA fragmentation assay was conducted using the procedure of Wu et al. [25]. Tissue samples (50 mg) were homogenized in 10 volumes of a TE solution pH 8.0 (5 mM Tris-HCl, 20 mmol EDTA) and 0.2 percent triton X-100. 1.0 mL aliquot of each sample was centrifuged at 27,000 ×g for 20 min to separate the intact chromatin (pellet, B) from the fragmented DNA (supernatant, T). The pellet and supernatant fractions were assayed for DNA content using a freshly prepared DPA (Diphenylamine) solution for reaction. Optical density was read at 620 nm at (SmartSpec Plus Spectrophotometer catalog no. 170-2525) spectrophotometer. The results were expressed as an amount of percent fragmented DNA by the following formula:

$$\text{percent fragmented DNA} = \text{T} \times \frac{100}{\text{T} + \text{B}}. \quad (1)$$

2.10. DNA Ladder Assay. DNA was isolated from tissue samples by using the method of Wu et al. [25] to estimate DNA damages. 5 μg of DNA of rats separately was loaded in 1.5 percent agarose gel containing 1.0 μg/mL ethidium bromide including DNA standards (0.5 μg per well). After electrophoresis gel was studied under gel doc system and was photographed through digital camera.

2.11. Histopathological Studies. For microscopic evaluation tissues were fixed in a fixative (absolute alcohol 60 percent, formaldehyde 30 percent, glacial acetic acid 10 percent) and embedded in paraffin, sectioned at 4 μm, and subsequently stained with hematoxylin and eosin. Sections were studied under light microscope (DIALUX 20 EB) at 10x magnifications. Slides of all the treated groups were studied and photographed.

2.12. Statistical Analysis. Data are expressed as means ± SD ($n = 6$), and significant differences between the groups were statistically analyzed by Duncan's multiple range test (Statistica Software, 1990). Concentration of significance among the various treatments was determined at $P < 0.05$.

Table 1: Effects of various fractions of *R. hastatus* roots on liver function tests.

Group	AST (U/L)	ALT (U/L)	ALP (U/L)	γ-GT (U/L)
Control	$78.25 \pm 2.09^{++}$	$65.23 \pm 1.78^{++}$	$121.65 \pm 2.19^{++}$	$1.94 \pm 0.07^{++}$
Oil + DMSO	$76.46 \pm 2.94^{++}$	$64.74 \pm 2.02^{++}$	$123.29 \pm 2.55^{++}$	$1.95 \pm 0.16^{++}$
CCl_4	$240.15 \pm 4.19^{**}$	$198.93 \pm 4.27^{**}$	$350.79 \pm 5.31^{**}$	$5.11 \pm 0.53^{**}$
Silymarin + CCl_4	$104.23 \pm 3.24^{++}$	$89.28 \pm 2.19^{++}$	$171.54 \pm 2.63^{++}$	$2.27 \pm 0.13^{++}$
HRR + CCl_4	$213.23 \pm 4.21^{+}$	$130.94 \pm 4.18^{++}$	$235.67 \pm 4.86^{++}$	$3.15 \pm 0.48^{++}$
ERR + CCl_4	$202.18 \pm 5.23^{+}$	$128.32 \pm 3.15^{++}$	$229.92 \pm 5.95^{++}$	$3.01 \pm 0.36^{++}$
CRR + CCl_4	$176.33 \pm 3.09^{++}$	$106.23 \pm 2.56^{++}$	$207.11 \pm 4.23^{++}$	$2.79 \pm 0.11^{++}$
BRR + CCl_4	$142.01 \pm 3.29^{++}$	$94.28 \pm 2.66^{++}$	$189.61 \pm 2.16^{++}$	$2.72 \pm 0.13^{++}$
MRR + CCl_4	$139.28 \pm 4.13^{++}$	$99.91 \pm 2.73^{++}$	$193.26 \pm 3.42^{++}$	$2.57 \pm 0.32^{++}$
ARR + CCl_4	$170.45 \pm 4.27^{++}$	$90.34 \pm 3.11^{++}$	$175.24 \pm 3.18^{++}$	$2.33 \pm 0.12^{++}$
HRR alone	$78.45 \pm 1.29^{++}$	$63.26 \pm 1.45^{++}$	$124.65 \pm 1.27^{++}$	$1.93 \pm 0.10^{++}$
ERR alone	$75.37 \pm 1.55^{++}$	$65.34 \pm 1.34^{++}$	$122.15 \pm 2.67^{++}$	$1.90 \pm 0.09^{++}$
CRR alone	$79.43 \pm 0.95^{++}$	$68.86 \pm 0.93^{++}$	$123.15 \pm 1.23^{++}$	$1.92 \pm 0.17^{++}$
BRR alone	$76.76 \pm 1.56^{++}$	$66.56 \pm 2.20^{++}$	$120.55 \pm 2.32^{++}$	$1.99 \pm 0.04^{++}$
MRR alone	$74.51 \pm 1.34^{++}$	$62.02 \pm 0.74^{++}$	$125.34 \pm 1.22^{++}$	$1.97 \pm 0.07^{++}$
ARR alone	$77.45 \pm 1.75^{++}$	$63.36 \pm 1.34^{++}$	$122.20 \pm 2.85^{++}$	$2.01 \pm 0.07^{++}$

Mean ± SE ($n = 6$ number).
**indicate significance from the control group at $P < 0.01$ probability level.
$^{++}$indicate significance from the CCl_4 group at $P < 0.01$ probability level.

Table 2: Effects of various fractions of *R. hastatus* roots on lipid profile.

Group	Triglycerides (mg/dL)	Total cholesterol (mg/dL)	HDL (mg/dL)	LDL (mg/dL)
Control	140.00 ± 3.57^{e}	29.14 ± 1.59^{d}	41.23 ± 1.44^{d}	23.25 ± 1.01^{d}
Oil + DMSO	139.89 ± 4.73^{e}	30.00 ± 1.34^{d}	40.92 ± 1.71^{d}	23.98 ± 1.26^{d}
CCl_4	263.67 ± 2.62^{a}	72.09 ± 1.99^{a}	60.80 ± 2.89^{a}	37.21 ± 1.98^{a}
Sily + CCl_4	182.14 ± 2.36^{d}	40.80 ± 2.18^{c}	47.29 ± 1.70^{c}	27.83 ± 1.71^{c}
HRR + CCl_4	205.23 ± 3.17^{c}	64.30 ± 1.79^{b}	56.36 ± 0.77^{b}	34.38 ± 0.16^{b}
ERR + CCl_4	213.85 ± 3.25^{b}	60.96 ± 2.64^{b}	54.50 ± 1.24^{b}	33.65 ± 0.84^{b}
CRR + CCl_4	199.13 ± 4.44^{c}	56.36 ± 3.60^{b}	50.97 ± 1.12^{c}	30.35 ± 1.14^{c}
BRR + CCl_4	189.16 ± 3.82^{c}	42.51 ± 2.84^{c}	46.54 ± 1.56^{c}	27.93 ± 1.28^{c}
MRR + CCl_4	194.83 ± 2.92^{c}	44.89 ± 2.06^{c}	45.27 ± 1.46^{c}	29.51 ± 2.08^{c}
ARR + CCl_4	190.65 ± 3.54^{c}	54.57 ± 2.35^{b}	49.35 ± 0.43^{c}	31.23 ± 0.66^{c}
HRR alone	138.45 ± 1.35^{e}	31.55 ± 1.44^{d}	40.56 ± 1.33^{d}	24.78 ± 0.15^{d}
ERR alone	137.96 ± 2.50^{e}	32.14 ± 1.32^{d}	41.66 ± 1.45^{d}	23.25 ± 1.35^{d}
CRR alone	140.26 ± 1.64^{e}	30.23 ± 1.74^{d}	42.55 ± 1.56^{d}	22.98 ± 1.01^{d}
BRR alone	138.76 ± 1.41^{e}	28.15 ± 1.46^{d}	40.12 ± 1.68^{d}	24.98 ± 0.23^{d}
MRR alone	141.01 ± 1.62^{e}	33.10 ± 2.81^{d}	42.20 ± 0.72^{d}	22.25 ± 0.95^{d}
ARR alone	139.78 ± 3.84^{e}	29.14 ± 1.36^{d}	39.23 ± 1.45^{d}	23.25 ± 0.16^{d}

Values are mean ± SD (06 number). Sily: Silymarin.
$^{a-d}$(means with different letters) indicate significance at $P < 0.05$.

3. Result

3.1. Effects of R. hastatus Roots on Liver Function Test and Biochemical Markers. The serological concentrations of AST, ALT, ALP, and γ-GT are highly susceptible to oxidative stress in liver tissue as shown in Table 1. Chronic CCl_4 treatment considerably ($P < 0.05$) augmented the concentrations of serum marker enzymes of liver which was attenuated significantly ($P < 0.05$) by oral administration of various fraction of *R. hastatus* roots. However, various fractions of *R. hastatus* roots alone showed the same serum enzyme concentration like that of control group. Hepatotoxin also reacts with polyunsaturated fatty acids to cause lipid peroxidation by disturbing lipid profile as summarized in Table 2. These parameters were significantly restored ($P < 0.05$) by various fractions of *R. hastatus* roots near to control. For serological investigations fractions can be ordered as BRR > MRR > ARR > CRR > ERR > HRR.

3.2. Effects of R. hastatus Roots on Male Reproductive Hormones of Rats. To estimate the testicular toxicity, reproductive hormones act as effective biomarkers. CCl_4 intoxication alters the secretion of pituitary and reproductive hormonal concentration. The effects of various fractions of

Table 3: Effects of various fractions of *R. hastatus* roots on male reproductive hormonal concentration.

Group	Testosterone (ng/mL)	Luteinizing hormone (ng/mL)	Follicle stimulating hormone (ng/mL)	Prolactin (ng/mL)	Estradiol (ng/mL)
Control	2.87 ± 0.09^{h}	3.08 ± 0.06^{d}	45.63 ± 0.27^{h}	10.23 ± 1.41^{f}	15.23 ± 0.78^{g}
Oil + DMSO	2.82 ± 0.05^{h}	2.98 ± 0.09^{d}	45.28 ± 0.37^{h}	12.26 ± 1.45^{f}	16.74 ± 0.45^{g}
CCl_4	1.12 ± 0.06^{a}	1.21 ± 0.10^{a}	20.69 ± 0.39^{a}	25.61 ± 0.32^{a}	32.45 ± 0.19^{a}
Sily + CCl_4	2.55 ± 0.08^{g}	2.67 ± 0.14^{c}	38.96 ± 0.60^{g}	15.45 ± 0.74^{e}	19.48 ± 0.90^{f}
HRR + CCl_4	1.40 ± 0.04^{b}	1.34 ± 0.06^{a}	22.34 ± 0.42^{b}	22.05 ± 0.80^{b}	29.04 ± 0.45^{b}
ERR + CCl_4	1.45 ± 0.10^{b}	1.33 ± 0.09^{a}	22.31 ± 0.38^{b}	23.14 ± 0.62^{b}	28.92 ± 0.36^{b}
CRR + CCl_4	1.75 ± 0.11^{c}	1.64 ± 0.10^{b}	25.62 ± 0.71^{c}	20.55 ± 0.70^{c}	25.24 ± 0.74^{c}
BRR + CCl_4	2.30 ± 0.07^{f}	2.26 ± 0.11^{c}	33.61 ± 0.32^{e}	17.90 ± 0.63^{d}	23.51 ± 0.17^{d}
MRR + CCl_4	2.25 ± 0.06^{e}	2.44 ± 0.12^{c}	34.37 ± 0.25^{f}	18.26 ± 0.56^{d}	21.35 ± 0.78^{e}
ARR + CCl_4	2.02 ± 0.05^{d}	2.04 ± 0.13^{c}	28.55 ± 0.65^{d}	20.31 ± 0.38^{c}	25.37 ± 0.28^{c}
HRR alone	2.80 ± 0.08^{h}	2.93 ± 0.11^{d}	45.22 ± 0.47^{h}	12.11 ± 0.65^{f}	16.73 ± 0.47^{g}
ERR alone	2.78 ± 0.16^{h}	2.88 ± 0.18^{d}	45.53 ± 0.60^{h}	10.53 ± 0.71^{f}	17.03 ± 0.80^{g}
CRR alone	2.99 ± 0.09^{h}	3.00 ± 0.10^{d}	45.48 ± 0.49^{h}	13.06 ± 1.06^{f}	16.61 ± 0.35^{g}
BRR alone	2.75 ± 0.05^{h}	3.18 ± 0.09^{d}	45.78 ± 0.46^{h}	9.76 ± 1.93^{f}	16.74 ± 0.65^{g}
MRR alone	2.98 ± 0.09^{h}	3.11 ± 0.06^{d}	46.05 ± 0.26^{h}	10.45 ± 1.48^{f}	14.63 ± 0.97^{g}
ARR alone	2.93 ± 0.10^{h}	3.08 ± 0.07^{d}	46.13 ± 0.58^{h}	12.17 ± 1.42^{f}	15.47 ± 0.87^{g}

Values are mean ± SD (06 number). Sily: Silymarin.
$^{a-h}$(means with different letters) indicate significance at $P < 0.05$.

Table 4: Effects of various fractions of *R. hastatus* roots on tissue proteins and antioxidant enzyme concentrations.

Group	Protein (μg/mg tissue)	CAT (U/min)	POD (U/min)	SOD (U/mg protein)	TBARS (nM/min/mg protein)	H_2O_2 (μM/mL)
Control	2.27 ± 0.020^{f}	4.80 ± 0.10^{d}	14.31 ± 0.25^{d}	4.33 ± 0.46^{d}	2.30 ± 0.41^{c}	1.89 ± 0.10^{c}
Oil + DMSO	2.30 ± 0.010^{f}	4.75 ± 0.15^{d}	13.90 ± 0.20^{d}	4.10 ± 0.28^{d}	2.08 ± 0.33^{c}	1.78 ± 0.12^{c}
CCl_4	1.05 ± 0.021^{a}	2.10 ± 0.07^{a}	6.67 ± 0.17^{a}	1.23 ± 0.54^{a}	6.52 ± 0.58^{a}	3.54 ± 0.26^{a}
Sily + CCl_4	1.91 ± 0.023^{e}	3.97 ± 0.06^{c}	11.67 ± 0.44^{c}	3.14 ± 0.43^{c}	3.11 ± 0.80^{b}	2.18 ± 0.31^{b}
HRR + CCl_4	1.42 ± 0.009^{b}	2.92 ± 0.32^{b}	9.09 ± 0.34^{b}	1.96 ± 0.16^{b}	6.00 ± 0.54^{a}	3.40 ± 0.17^{a}
ERR + CCl_4	1.43 ± 0.010^{b}	3.07 ± 0.20^{b}	9.57 ± 0.21^{b}	2.05 ± 0.21^{b}	6.18 ± 0.33^{a}	3.29 ± 0.11^{a}
CRR + CCl_4	1.50 ± 0.013^{c}	3.63 ± 0.17^{c}	10.13 ± 0.64^{c}	2.38 ± 0.31^{b}	5.03 ± 0.26^{b}	2.89 ± 0.20^{b}
BRR + CCl_4	1.82 ± 0.085^{e}	3.99 ± 0.15^{c}	11.01 ± 0.24^{c}	2.90 ± 0.15^{c}	4.18 ± 0.92^{b}	2.69 ± 0.31^{b}
MRR + CCl_4	1.78 ± 0.060^{e}	4.00 ± 0.26^{c}	11.61 ± 0.75^{c}	3.32 ± 0.43^{c}	3.65 ± 0.75^{b}	2.27 ± 0.42^{b}
ARR + CCl_4	1.65 ± 0.014^{d}	3.80 ± 0.10^{c}	10.60 ± 0.55^{c}	2.96 ± 0.18^{c}	4.62 ± 0.71^{b}	2.77 ± 0.25^{b}
HRR alone	2.30 ± 0.011^{f}	4.71 ± 0.12^{d}	14.68 ± 0.62^{d}	4.21 ± 0.50^{d}	2.19 ± 0.74^{c}	1.82 ± 0.34^{c}
ERR alone	2.33 ± 0.019^{f}	4.65 ± 0.24^{d}	14.71 ± 0.71^{d}	4.78 ± 0.36^{d}	2.34 ± 0.82^{c}	1.84 ± 0.57^{c}
CRR alone	2.44 ± 0.010^{f}	4.91 ± 0.27^{d}	14.99 ± 0.53^{d}	4.64 ± 0.45^{d}	2.52 ± 0.67^{c}	1.96 ± 0.77^{c}
BRR alone	2.26 ± 0.009^{f}	4.96 ± 0.41^{d}	14.66 ± 0.45^{d}	4.71 ± 0.33^{d}	2.24 ± 0.63^{c}	1.93 ± 0.61^{c}
MRR alone	2.38 ± 0.028^{f}	4.86 ± 0.21^{d}	15.07 ± 0.23^{d}	4.73 ± 0.21^{d}	2.18 ± 0.64^{c}	2.01 ± 0.49^{c}
ARR alone	2.35 ± 0.012^{f}	4.84 ± 0.15^{d}	15.01 ± 0.10^{d}	4.58 ± 0.26^{d}	2.39 ± 0.45^{c}	1.92 ± 0.70^{c}

Values are mean ± SD (06 number). Sily: Silymarin.
$^{a-f}$(means with different letters) indicate significance at $P < 0.05$.

R. hastatus roots against CCl_4 toxicity on hormonal concentration of testosterone, luteinizing hormone (LH), follicle stimulating hormone (FSH), prolactin, and estradiol are summarized in Table 3. CCl_4 intoxicated rats considerably ($P < 0.05$) decreased the testosterone, FSH, and LH concentration of serum while significantly ($P < 0.05$) raised the prolactin and estradiol concentration. The serum concentrations of LH, testosterone, prolactin, and estradiol were restored ($P < 0.05$) by oral administration of various fractions of *R. hastatus* roots near to control group except HRR and ERR that showed no significance for luteinizing hormone.

3.3. Effects of R. hastatus Roots on Testis Enzymatic Antioxidant Concentrations. In the present study scavenging effects of various antioxidant enzymes were assessed. The effects of various fractions of *R. hastatus* roots against CCl_4 intoxication on tissue soluble protein and antioxidant enzyme system such as CAT, POD, SOD, TBARS, and H_2O_2 testis are reported in Table 4. Free radicals generated by CCl_4 injection,

Table 5: Effects of various fractions of *R. hastatus* roots on phase II antioxidant enzymes and DNA fragmentation.

Group	GST (nM/mg protein)	GPx (nM/mg protein)	GR (nM/mg protein)	GSH (μM/g tissue)	QR (nM/mg protein)	Percent DNA injuries
Control	150.21 ± 4.11^{g}	110.71 ± 3.23^{e}	198.47 ± 4.72^{h}	17.69 ± 1.11^{e}	105.33 ± 1.34^{g}	9.21 ± 1.30^{e}
Oil + DMSO	146.34 ± 4.10^{g}	104.56 ± 3.10^{e}	190.69 ± 4.39^{h}	15.40 ± 1.30^{e}	107.12 ± 1.46^{g}	8.38 ± 1.63^{e}
CCl_4	87.48 ± 3.45^{a}	57.86 ± 2.67^{a}	120.76 ± 3.02^{a}	7.63 ± 0.75^{a}	63.34 ± 1.01^{a}	51.11 ± 2.02^{a}
Sily + CCl_4	122.22 ± 3.18^{e}	94.62 ± 2.47^{d}	158.61 ± 2.35^{g}	13.73 ± 0.73^{d}	91.54 ± 2.11^{f}	22.43 ± 1.57^{d}
HRR + CCl_4	94.05 ± 2.56^{b}	68.44 ± 2.37^{b}	127.11 ± 2.34^{b}	10.08 ± 0.39^{b}	69.69 ± 1.72^{b}	42.22 ± 1.27^{b}
ERR + CCl_4	95.67 ± 2.48^{b}	70.37 ± 2.42^{b}	127.51 ± 2.55^{b}	10.25 ± 0.36^{b}	71.47 ± 1.95^{b}	35.33 ± 2.15^{c}
CRR + CCl_4	100.28 ± 2.27^{c}	76.22 ± 2.71^{c}	132.17 ± 2.33^{c}	11.17 ± 0.28^{c}	75.56 ± 1.38^{c}	26.44 ± 1.73^{d}
BRR + CCl_4	119.16 ± 3.15^{e}	80.51 ± 2.33^{c}	144.43 ± 2.26^{e}	12.19 ± 0.43^{d}	83.24 ± 2.82^{e}	25.53 ± 2.15^{d}
MRR + CCl_4	130.53 ± 2.34^{f}	88.61 ± 2.20^{c}	150.39 ± 2.41^{f}	12.36 ± 0.15^{d}	90.97 ± 2.61^{f}	23.78 ± 1.23^{d}
ARR + CCl_4	108.26 ± 3.68^{d}	85.47 ± 2.62^{c}	139.40 ± 2.16^{d}	11.53 ± 0.32^{c}	79.87 ± 2.28^{d}	25.73 ± 1.56^{d}
HRR alone	149.67 ± 3.63^{g}	107.34 ± 3.57^{e}	192.22 ± 2.23^{h}	16.22 ± 0.50^{e}	108.34 ± 1.41^{g}	7.66 ± 1.27^{e}
ERR alone	155.87 ± 4.58^{g}	106.48 ± 4.53^{e}	201.47 ± 3.50^{h}	18.37 ± 0.38^{e}	100.44 ± 1.70^{g}	7.22 ± 1.43^{e}
CRR alone	148.51 ± 3.45^{g}	109.38 ± 3.22^{e}	191.71 ± 3.00^{h}	15.30 ± 0.38^{e}	109.34 ± 1.24^{g}	7.80 ± 1.28^{e}
BRR alone	156.63 ± 4.43^{g}	107.68 ± 4.34^{e}	195.45 ± 3.45^{h}	17.04 ± 0.38^{e}	108.45 ± 1.89^{g}	8.34 ± 0.28^{e}
MRR alone	156.52 ± 3.23^{g}	111.51 ± 3.38^{e}	200.10 ± 2.69^{h}	18.10 ± 0.23^{e}	110.71 ± 1.57^{g}	8.23 ± 0.93^{e}
ARR alone	157.77 ± 3.76^{g}	102.57 ± 3.43^{e}	197.53 ± 4.02^{h}	15.37 ± 0.20^{e}	109.34 ± 1.45^{g}	6.78 ± 1.73^{e}

Values are mean ± SD (06 number). Sily: Silymarin.

$^{a-h}$(means with different letters) indicate significance at $P < 0.05$.

disturbing the cell membrane by reacting with phospholipids, leading to lipid peroxidation, caused significant elevation of TBARS and H_2O_2 content. Our results point to the ability of CCl_4 on tissue to cause significant damage by decreasing the tissue protein as well as CAT, POD, and SOD activities in addition to increasing the lipid peroxidation and hydrogen peroxide contents versus control group. Posttreatment of various fractions of *R. hastatus* roots with CCl_4 improved the activity of reduced enzymes and the soluble protein whereas reduced the concentration of TBARS and H_2O_2. The effects of various fractions of *R. hastatus* roots on phase II antioxidant enzymes like GST, GPx, GR, GSH, QR, and DNA fragmentation percent of testicular tissue are presented in Table 5. Administration of CCl_4 significantly ($P < 0.05$) decreased the glutathione status of GST, GPx, GR, GSH, and QR while amplifying the percent fragmentation of DNA. Posttreatment of various fractions of *R. hastatus* roots along with CCl_4 treatment markedly improved the activities of GST, GPx, GR, GSH, QR, and percent DNA fragmentation.

3.4. Effects of R. hastatus Roots on DNA Damages (Ladder Assay). CCl_4 induces DNA damages in the testicular tissues of rats. DNA ladder assay showed that intact genomic DNA was found in control as well as DMSO treated group. Conversely, CCl_4 group showed severe DNA damages. Postadministration of silymarin and different fractions of *R. hastatus* roots showed reduction in DNA damages as DNA band patterns of these groups were more similar to control group (Figure 1).

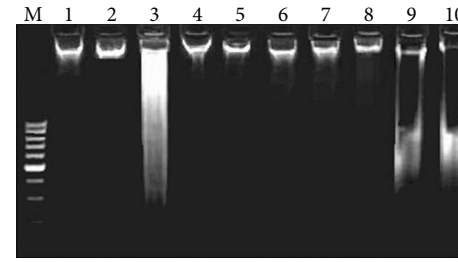

Figure 1: Agarose gel showing DNA damage by CCl_4 and protective effects of various fractions of *R. hastatus* leaves in testicular tissue. Lanes from left (M) low molecular weight marker, (1) control, (2) DMSO + olive oil group, (3) CCl_4 group, (4) silymarin + CCl_4 group, (5) MRR + CCl_4 group, (6) BRR + CCl_4 group, (7) ARR + CCl_4 group, (8) CRR + CCl_4 group, (9) ERR + CCl_4 group, and (10) HRR + CCl_4 group.

3.5. Effects of R. hastatus Roots on Testis Histoarchitecture. Figure 2 illustrates the histological examination of testicular tissues of different treatment groups. Microscopic assessment of male reproductive system revealed the normal seminiferous tubules, sperms with normal morphology, and concentration in control as shown in Figure 2(a). Histological structure of germ cells was found to be normal in appearance. Figure 2(b) demonstrates that CCl_4 intoxication caused degenerative changes such as loss of germ cells, abnormality of germinative epithelium, interruption in meiosis, sperm with abnormal shape and concentration, and delocalization of seminiferous tubules. These changes were markedly

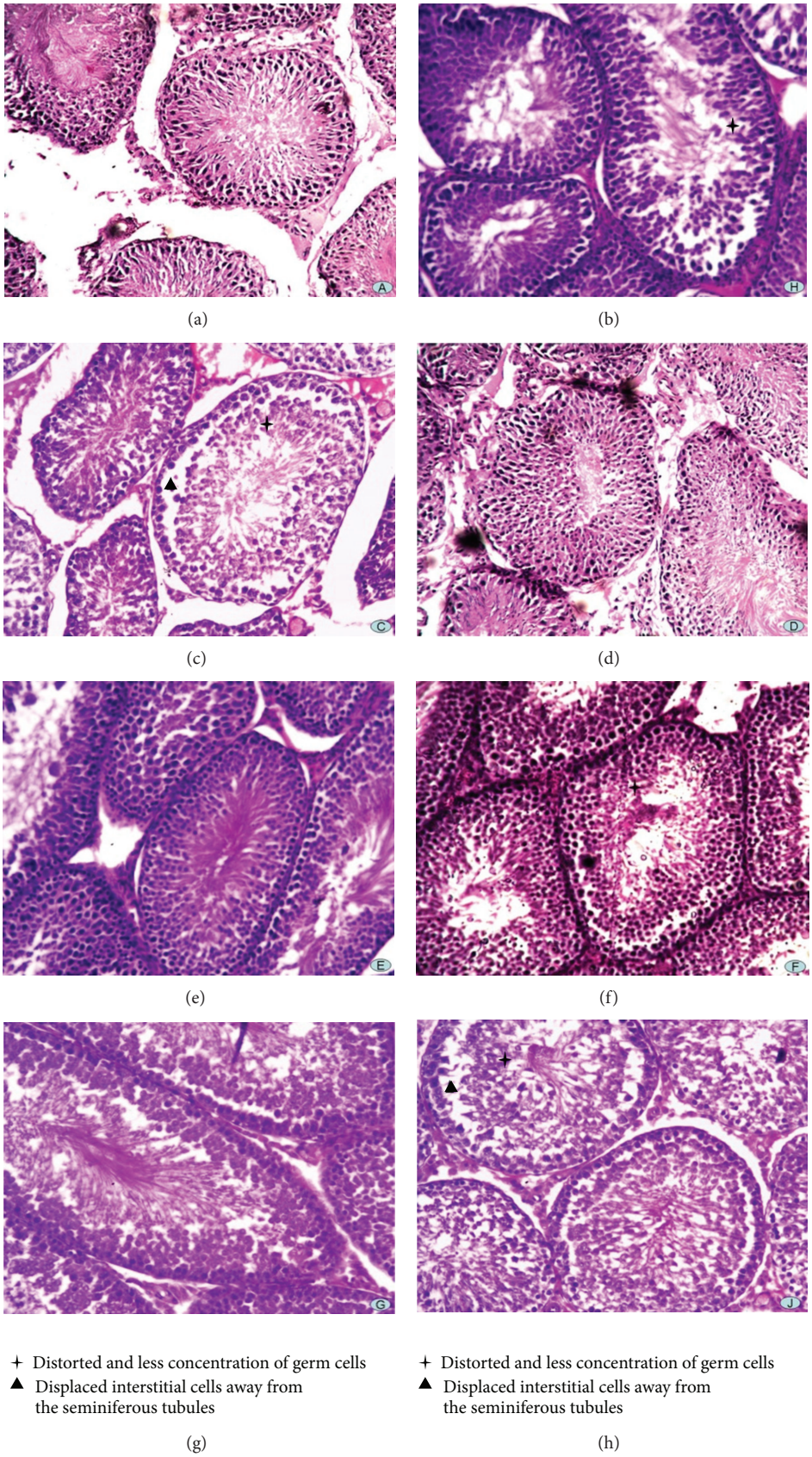

Figure 2: Microphotograph of rat testis (H&E stain). (a) Representative section of testis from the control group showing normal histology, (b) CCl_4 group, (c) MRR + CCl_4 group, (d) BRR + CCl_4 group, (e) ARR + CCl_4 group, (f) CRR + CCl_4 group, (g) ERR + CCl_4 group, and (h) HRR + CCl_4 group.

reduced with oral administration of various fractions of *R. hastatus* roots or silymarin revealing a marked repairing of testicular abnormalities. Among all the tested samples of *R. hastatus* roots, MRR and BRR as shown in Figures 2(c) and 2(d) demonstrated maximum antioxidant and healing effects against CCl_4 induced damage showing sperm with normal morphology and concentration near to control group. Histopathological findings are in accord with the results of above studied parameters for testicular toxicity.

3.6. Effects of R. hastatus Roots on Histopathology of Liver. Slides of liver tissues were prepared for histopathological study and stained with hematoxylin and eosins as shown in Figure 3. Figure 3(c) depicts that administration of CCl_4 causes fatty changes like ballooning of cells, inflammatory cells infiltrations, dilation of central vein, cellular hypertrophy, necrosis, and degeneration of the lobular architecture. CCl_4 administration for eight weeks resulted in chronic injury in the form of hepatic cirrhosis. Postadministration of various fractions of *R. hastatus* roots attenuated the hepatic injuries and percent them such as with very less or no fatty changes, no dilation of blood vessel, and uniform morphology of hepatocytes near to control group as shown in Figures 3(c)–3(h). Abnormal changes were not found in the morphology of control group (Figure 3(a)).

4. Discussion

Medicinal plants extracts and their bioactive metabolites play important role in the prevention of oxidative damages especially CCl_4 induced hepatic and testicular injuries in experimental animals [7, 26]. In the present investigations administration of various fractions of *R. hastatus* revealed reduction in elevated concentrations of AST, ALT, ALP, and γGT to maintain the structural consistency of the hepatocellular structure. Our findings are in agreement with Singh et al. [6] who reported that rise in serum markers has association with immense centrilobular necrosis, cellular infiltration, and ballooning of liver. CCl_4 treatment caused alteration in cholesterol profile which was significantly reversed with postadministration of various fractions of *R. hastatus*. Similar investigations were reported by Wang et al. [27] while working on female rats to assess hepatic protection of Noni fruit juice against CCl_4 induced chronic liver damage. Like testicular histology, serum gonadotropin releasing hormone (GnRH) including LH and FSH concentrations may facilitate in discovering conclusion about toxicosis. The reduction in serum testosterone concentrations indicates either a direct effect of chemical (CCl_4) at Leydig cell concentration or an indirect effect by disturbing the hormonal environment at hypothalamopituitary axis [28] due to oxidative trauma in CCl_4 treated rats. Tohda et al. [29] also reported that abnormal concentration of intratesticular testosterones inhibits spermatogenesis. The production of testosterone in Leydig cells is stimulated by LH, which activates FSH to bind with Sertoli cells to stimulate spermatogenesis [30]. CCl_4 insults revealed the suppression in FSH concentration of serum that was in consistency with Khan and Ahmed [5] who reported significant reduction in serum FSH concentration. CCl_4 intoxicated rats show the malfunctioning of pituitary to secrete FSH and LH indicating that testicular dysfunction leads to infertility. Estradiol directly stimulates the pituitary by determining prolactinemia, with hypothalamic dysfunction in case of hypogonadism. Thus, increased concentration of estradiol and prolactin may also be liable for the origin of hypogonadism in the present study. GSH concentrations are dependent upon the activities of glutathione reductase (GR) and NADH [31]. Glutathione system including GPx, GR, GST, as well as SOD and CAT represents a mutually loyal team of defense against ROS [32]. Enhanced lipid peroxidations expressed in terms of TBARS determine structural and functional alterations of cellular membranes [33]. In the present study, administration of various fractions of *R. hastatus* improved the activities of antioxidant enzymatic (SOD, CAT, POD, GPx, GST, GR, and QR) as well as nonenzymatic (GSH, TBARS, and H_2O_2). Hence, the present results regarding chronic toxicity of CCl_4 are in accordance with previous reports of Khan and Ahmed [5] while studying the protective effects of *Digera muricata* (L.) Mart on testis against CCl_4 oxidative stress. It was reported that CCl_4 resulted in the oxidative damage to testicular proteins and DNA in rats [4, 34]. From the present study, it can be assumed that various fractions of *R. hastatus* ameliorated the toxic effects on DNA as revealed by percent DNA fragmentation and ladder assay. The present study clearly augments the defensive mechanism of various samples against oxidative stress induced by CCl_4 and provides confirmation about its therapeutic use in reproductive abnormalities. Hepatohistology of CCl_4 intoxicated rats revealed necrosis, fatty changes, cellular hypertrophy, infiltrated kupffer cells and lymphocyte, cirrhosis, and nuclear degeneration in some areas, which was markedly diminished by induction of various fractions of *R. hastatus*. Our study revealed similar investigation which is in agreement with earlier findings [3], while evaluating the medicinal activity of plants against CCl_4 stimulated hepatotoxicity in rats. The CCl_4 challenge revealed testicular destruction [35] and degeneration in histological architecture like that of profenofos that was recorded by Moustafa et al. [36]. Data of the present study revealed that CCl_4 may cause proliferative behavior of testicular cells and obstruct reproduction. However, groups administered various fractions of *R. hastatus* demonstrated a quality active spermatogenesis, thin basement membranes, and normal seminiferous tubules in most of the part of testis. Same histopathology was noticed by Manjrekar et al. [37] while evaluating the protective effects of *Phyllanthus niruri* Linn. on testis against CCl_4 intoxication.

5. Conclusions

It can be concluded from the current study that various fractions of *R. hastatus* roots have the ability to recover the metabolic enzymatic activities and repair cellular injuries, thus providing scientific evidence in favour of its pharmacological use in hepatic and testicular dysfunctioning.

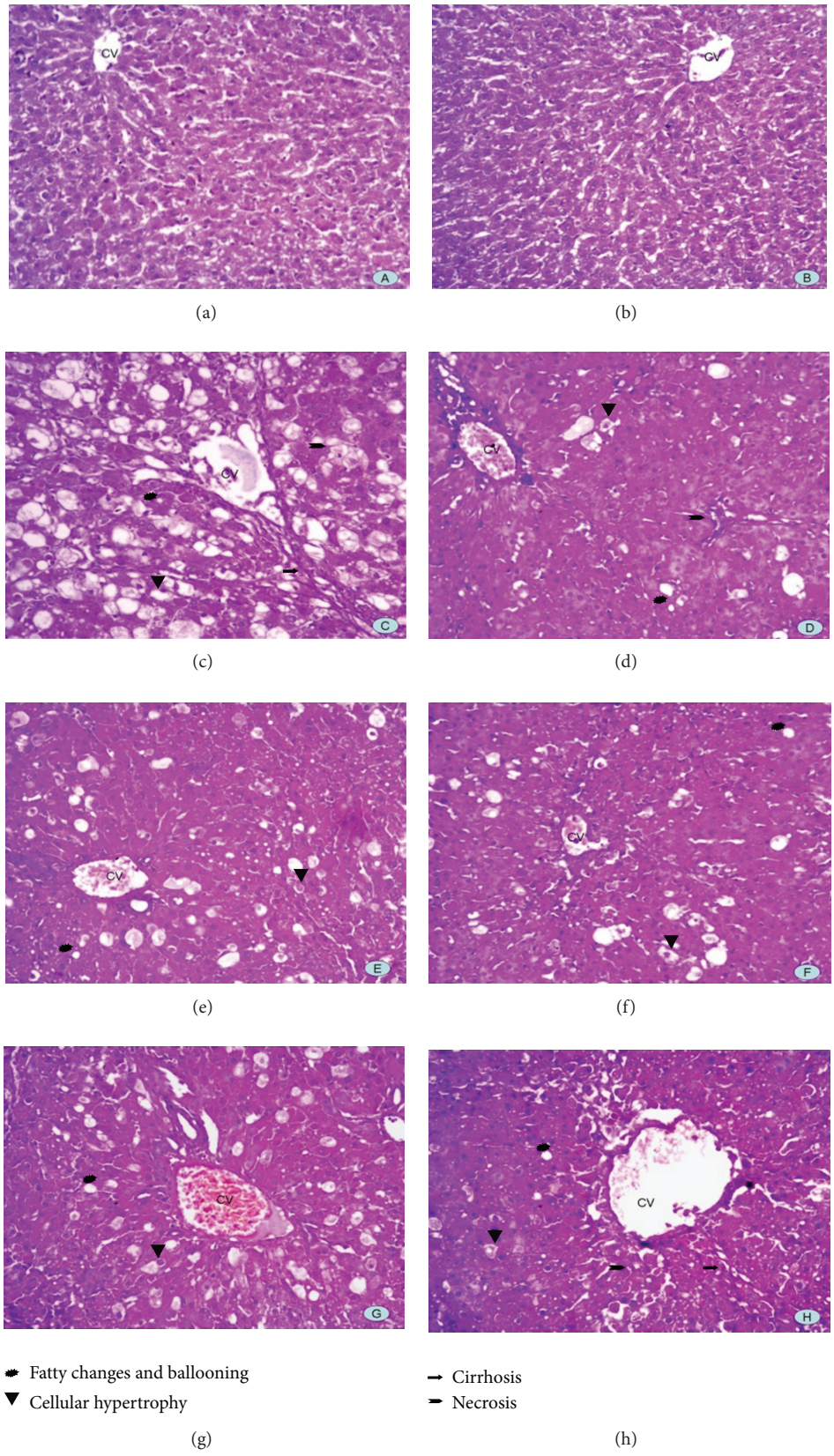

Figure 3: Microphotograph of rat liver (H&E stain). (a) Representative section of liver from the control group showing normal histology, (b) CCl4 group, (c) MRR + CCl_4 group, (d) BRR + CCl_4 group, (e) ARR + CCl_4 group, (f) CRR + CCl_4 group, (g) ERR + CCl_4 group, and (h) HRR + CCl_4 group.

References

[1] O. I. Aruoma, "Free radicals, oxidative stress, and antioxidants in human health and disease," *Journal of the American Oil Chemists' Society*, vol. 75, no. 2, pp. 199–212, 1998.

[2] B. Halliwell and J. M. C. Gutteridge, *Free Radicals in Biology and Medicine*, Oxford University Press, Oxford, UK, 1999.

[3] M. H. Shyu, T. C. Kao, and G. C. Yen, "Hsian-tsao (*Mesona procumbens* Heml.) prevents against rat liver fibrosis induced by CCl_4 via inhibition of hepatic stellate cells activation," *Food and Chemical Toxicology*, vol. 46, no. 12, pp. 3707–3713, 2008.

[4] P. Abraham, G. Wilfred, and S. P. Cathrine, "Oxidative damage to the lipids and proteins of the lungs, testis and kidney of rats during carbon tetrachloride intoxication," *Clinica Chimica Acta*, vol. 289, no. 1-2, pp. 177–179, 1999.

[5] M. R. Khan and D. Ahmed, "Protective effects of *Digera muricata* (L.) Mart. on testis against oxidative stress of carbon tetrachloride in rat," *Food and Chemical Toxicology*, vol. 47, no. 6, pp. 1393–1399, 2009.

[6] N. Singh, V. Kamath, K. Narasimhamurthy, and P. S. Rajini, "Protective effect of potato peel extract against carbon tetrachloride-induced liver injury in rats," *Environmental Toxicology and Pharmacology*, vol. 26, no. 2, pp. 241–246, 2008.

[7] P. Abraham and G. Wilfred, "Lysosomal enzymes in the pathogenesis of carbontetrachloride induced injury to the kidney and testis in the rat," *Indian Journal of Pharmacology*, vol. 32, no. 3, pp. 250–251, 2000.

[8] S. Sahreen, M. R. Khan, and R. A. Khan, "Hepatoprotective effects of methanol extract of Carissa opaca leaves on CCl_4-induced damage in rat," *BMC Complementary and Alternative Medicine*, vol. 11, article 48, 2011.

[9] S. C. Sikka, M. Rajasekaran, and W. J. G. Hellstrom, "Role of oxidative stress and antioxidants in male infertility," *Journal of Andrology*, vol. 16, no. 6, pp. 464–468, 1995.

[10] Z. K. Shinwari and S. S. Gilani, "Sustainable harvest of medicinal plants at Bulashbar Nullah, Astore (Northern Pakistan)," *Journal of Ethnopharmacology*, vol. 84, no. 2-3, pp. 289–298, 2003.

[11] K. Vermani and S. Garg, "Herbal medicines for sexually transmitted diseases and AIDS," *Journal of Ethnopharmacology*, vol. 80, no. 1, pp. 49–66, 2002.

[12] S. Sahreen, M. R. Khan, and R. A. Khan, "Phenolic compounds and antioxidant activities of *Rumex hastatus* D. Don. leaves," *Journal of Medicinal Plant Research*, vol. 5, no. 13, pp. 2755–2765, 2011.

[13] L. S. Zhang, Z. Li, R. Q. Mei et al., "Hastatusides A and B: two new phenolic glucosides from *Rumex hastatus*," *Helvetica Chimica Acta*, vol. 92, no. 4, pp. 774–778, 2009.

[14] H. Y. Kil, E. S. Seong, B. K. Ghimire et al., "Antioxidant and antimicrobial activities of crude sorghum extract," *Food Chemistry*, vol. 115, no. 4, pp. 1234–1239, 2009.

[15] O. H. Lowry, N. J. Rosebrough, A. L. Farr, and R. J. Randall, "Protein measurement with the Folin phenol reagent," *The Journal of Biological Chemistry*, vol. 193, no. 1, pp. 265–275, 1951.

[16] B. Chance and A. C. Maehly, "Assay of catalases and peroxidases," *Methods in Enzymology*, vol. 2, pp. 764–775, 1955.

[17] P. Kakkar, B. Das, and P. N. Viswanathan, "A modified spectrophotometric assay of superoxide dismutase," *Indian Journal of Biochemistry and Biophysics*, vol. 21, no. 2, pp. 130–132, 1984.

[18] W. H. Habig, M. J. Pabst, and W. B. Jakoby, "Glutathione S transferases. The first enzymatic step in mercapturic acid formation," *Journal of Biological Chemistry*, vol. 249, no. 22, pp. 7130–7139, 1974.

[19] I. Carlberg and E. B. Mannervik, "Glutathione concentration in rat brain," *Journal of Biological Chemistry*, vol. 250, pp. 4475–4480, 1975.

[20] J. Mohandas, J. J. Marshall, and G. G. Duggin, "Differential distribution of glutathione and glutathione-related enzymes in rabbit kidney. Possible implications in analgesic nephropathy," *Biochemical Pharmacology*, vol. 33, no. 11, pp. 1801–1807, 1984.

[21] A. M. Benson, M. J. Hunkeler, and P. Talalay, "Increase of NAD(P)H:quinone reductase by dietary antioxidants: possible role in protection against carcinogenesis and toxicity," *Proceedings of the National Academy of Sciences of the United States of America*, vol. 77, no. 9, pp. 5216–5220, 1980.

[22] D. J. Jollow, J. R. Mitchell, N. Zampaglione, and J. R. Gillette, "Bromobenzene induced liver necrosis. Protective role of glutathione and evidence for 3,4 bromobenzene oxide as the hepatotoxic metabolite," *Pharmacology*, vol. 11, no. 3, pp. 151–169, 1974.

[23] M. Iqbal, S. D. Sharma, H. R. Zadeh, N. Hasan, M. Abdulla, and M. Athar, "Glutathione metabolizing enzymes and oxidative stress in ferric nitrilotriacetate (Fe-NTA) mediated hepatic injury," *Redox Report*, vol. 2, pp. 385–391, 1996.

[24] E. Pick and Y. Keisari, "Superoxide anion and hydrogen peroxide production by chemically elicited peritoneal macrophages—induction by multiple nonphagocytic stimuli," *Cellular Immunology*, vol. 59, no. 2, pp. 301–318, 1981.

[25] B. Wu, A. Ootani, R. Iwakiri et al., "T cell deficiency leads to liver carcinogenesis in azoxymethane-treated rats," *Experimental Biology and Medicine*, vol. 231, no. 1, pp. 91–98, 2006.

[26] A. Tombolini and M. Cingolani, "Fatal accidental ingestion of carbon tetrachloride: a postmortem distribution study," *Journal of Forensic Sciences*, vol. 41, no. 1, pp. 166–168, 1996.

[27] M. Y. Wang, G. Anderson, D. Nowicki, and J. Jensen, "Hepatic protection by noni fruit juice against CCl_4-induced chronic liver damage in female SD rats," *Plant Foods for Human Nutrition*, vol. 63, no. 3, pp. 141–145, 2008.

[28] R. Latif, G. M. Lodhi, and M. Aslam, "Effects of amlodipine on serum testosterone, testicular weight and gonado-somatic index in adult rats," *Journal of Ayub Medical College, Abbottabad*, vol. 20, no. 4, pp. 8–10, 2008.

[29] A. Tohda, K. Matsumiya, Y. Tadokoro et al., "Testosterone suppresses spermatogenesis in juvenile spermatogonial depletion (jsd) mice," *Biology of Reproduction*, vol. 65, no. 2, pp. 532–537, 2001.

[30] P. M. Conn, "The molecular basis of gonadotropin-releasing hormone action," *Endocrine Reviews*, vol. 7, no. 1, pp. 3–10, 1986.

[31] A. Meister and M. E. Anderson, "Glutathione," *Annual Review of Biochemistry*, vol. 52, pp. 711–760, 1983.

[32] U. Bandyopadhyay, D. Das, and R. K. Banerjee, "Reactive oxygen species: oxidative damage and pathogenesis," *Current Science*, vol. 77, no. 5, pp. 658–666, 1999.

[33] B. Halliwell, R. Aeschbach, J. Löliger, and O. I. Aruoma, "The characterization of antioxidants," *Food and Chemical Toxicology*, vol. 33, no. 7, pp. 601–617, 1995.

[34] I. Manierea, T. Godardb, D. R. Doergec et al., "DNA damage and DNA adduct formation in rat tissues following oral administration of acrylamide," *Mutation Research*, vol. 580, pp. 119–129, 2005.

[35] D. Debnath and T. K. Mandal, "Study of quinalphos (an environmental oestrogenic insecticide) formulation (Ekalux 25 E.C.)-induced damage of the testicular tissues and antioxidant defence systems in Sprague-Dawley albino rats," *Journal of Applied Toxicology*, vol. 20, pp. 197–204, 2000.

[36] G. G. Moustafa, Z. S. Ibrahim, Y. Hashimoto et al., "Testicular toxicity of profenofos in matured male rats," *Archives of Toxicology*, vol. 81, no. 12, pp. 875–881, 2007.

[37] A. P. Manjrekar, V. Jisha, P. P. Bag et al., "Effect of *Phyllanthus niruri* Linn. treatment on liver, kidney and testes in CCl_4 induced hepatotoxic rats," *Indian Journal of Experimental Biology*, vol. 46, no. 7, pp. 514–520, 2008.

Hindawi Publishing Corporation
Oxidative Medicine and Cellular Longevity
Volume 2013, Article ID 802734, 11 pages
http://dx.doi.org/10.1155/2013/802734

Research Article

Magnesium Can Protect against Vanadium-Induced Lipid Peroxidation in the Hepatic Tissue

Agnieszka Ścibior,[1,2] Dorota Gołębiowska,[1] and Irmina Niedźwiecka[1]

[1] *Department of Zoology and Invertebrate Ecology, Laboratory of Physiology and Animal Biochemistry, The John Paul II Catholic University of Lublin, 102 Kraśnicka Avenue, 20-718 Lublin, Poland*
[2] *Centre of Interdisciplinary Research, Laboratory of Oxidative Stress, The John Paul II Catholic University of Lublin, 102 Kraśnicka Avenue, 20-718 Lublin, Poland*

Correspondence should be addressed to Agnieszka Ścibior; cellbiol@kul.lublin.pl

Received 3 February 2013; Revised 7 April 2013; Accepted 8 April 2013

Academic Editor: Kota V. Ramana

The protective effect of magnesium as magnesium sulfate (MS) on sodium-metavanadate- (SMV-) induced lipid peroxidation (LPO) under *in vivo* and *in vitro* conditions was studied. The 18-week SMV intoxication (Group II, 0.125 V_{end}/mL) enhanced spontaneous malondialdehyde (MDA) generation in rat liver, compared with the control (Group I) and MS-supplemented animals (Group III, 0.06 Mg_{end}/mL). Coadministration of SMV with MS (Group IV, SMV-MS) caused a return of the MDA level to the control value range. The effect seems to result from the Mg_{end}-independent action and its antagonistic interaction with V_{end}. The *in vitro* treatment of liver supernatants (LS) obtained from all the tested animals groups with selected exogenous concentrations of Fe_{exg} or V_{exg} exhibited enhanced MDA production, compared with spontaneously formed MDA. It also showed Mg_{exg}-stimulating effect on LPO (LS I, Group I) and revealed that the changes in the MDA generation in LS IV (Group IV) might have resulted from the synergistic interactions of V_{end} with Fe_{exg} and V_{exg} and from the antagonistic interactions of Mg_{end} with Fe_{exg} and V_{exg}. The findings allow a suggestion that adequate Mg intake for a specific period in the conditions of SMV exposure may prevent V-induced LPO in the liver.

1. Introduction

Lipid peroxidation (LPO) is a well-known free-radical process defined as oxidative deterioration of lipids. It is used as an indicator of oxidative stress (OS), which occurs when the balance between the production of reactive oxygen species (ROS) and free radicals (FR) overrides the antioxidant capability of the cells or tissues [1–3]. It may be one of the possible mechanisms underlying oxidative cellular damage caused by ROS, and it can be implicated in the pathogenesis of a number of diseases [2, 4]. The products formed during LPO such as aldehydes, inter alia, and malondialdehyde (MDA) are well known to have deleterious effects. They can alter biological membrane organization and modify proteins and DNA. On the other hand, they can also modulate signal transduction pathways, induce adaptive response, as well as increase tolerance against forthcoming OS by upregulating defense capacity [5, 6].

Vanadium (V), which is a widely distributed element, has a wide range of industrial use. It interplays environmentally, occupationally, and biologically with human life [7]. Its toxicity depends, inter alia, on the route of administration, chemical form, and oxidation state, which determines the extensive biological effects of this element [8]. Due to its harmful health effects [9], our particular interest has been focused on searching factors which might prevent the deleterious action of V and attenuate its prooxidant activity.

As a redox-active metal, V may modulate the cellular redox potential and be involved in oxidative injury mechanisms. In certain conditions, it may enhance the generation of oxygen-derived reactive species and stimulate LPO [10]. Its prooxidant properties have been revealed in *in vivo* and

in vitro conditions both by us [11, 12] and by some other researchers [10, 13–21]. On the other hand, antioxidant action of V [22], its insulin-like effects [23], and anticarcinogenic activity [24–26] have also been reported.

In turn, the relatively non-toxic and nonredox reactive magnesium (Mg) cannot participate in redox reactions that yield FR. It may effectively protect against FR and peroxidative damage. Its inhibitory effects on LPO have been demonstrated *in vitro* [27, 28] and *in vivo* in various animal models, including rats, [29–32] as well as in human studies [33, 34]. The limitation of LPO by this element has also been revealed under the conditions of cadmium and mercury exposure in a rat model [35, 35]. However, in some conditions Mg may stimulate LPO causing OS. Its ability to elevate LPO has been revealed by us [11, 12] and by some other investigators [27].

The antioxidant potential of Mg and its beneficial role in limiting LPO and the strong prooxidant potential of V and its well-known toxicological impact as well as insufficient information about the possible protective influence of Mg on V-induced LPO prompted us to perform an experiment in a rat model to explore the hypothesis whether an 18-week administration of Mg as magnesium sulfate ($MgSO_4$, MS, 0.06 mg Mg/mL) in combination with sodium metavanadate ($NaVO_3$, SMV) will be able to effectively limit V-stimulated LPO in the liver. This organ is one of the sites of V accumulation and plays a major role in the storage, secretion and production of many important substances as well as in maintenance of homeostasis and detoxification allowing the body to function and live. The influence of exogenous Mg, V and Fe on LPO in liver supernatants (LS) and the effects of interactions between them, recognition of which may help in elucidation of the cellular mechanisms of the response to combinations of metals, have also been examined.

2. Material and Methods

2.1. Chemicals and Reagents. $NaVO_3$ (SMV), ($MgSO_4$, MS), iron sulfate ($FeSO_4$), and thiobarbituric acid (TBA) were obtained from Sigma Chemicals (St. Louis, MO, USA). All the other chemicals and reagents used were of analytical grade.

2.2. Experimental Design. The experiment was conducted on 40 adult outbred albino male Wistar rats with average initial body weight about 267 g, which, following an adaptation period of 7 days in a room in controlled conventional conditions, were randomly divided into 4 groups (10 rats per group). All the rats were individually housed in stainless steel cages (one rat per cage) when the experiment was started. Every day over a 18-week period, all the rats had unlimited access to the rodent laboratory chow (Labofeed B; Fodder and Concentrate Factory, Kcynia, Poland) in the shape of pellets of 12 mm diameter and they received to drink: Group I (untreated control)—deionized water; Group II (SMV)—a water solution of $NaVO_3$ at a concentration of 0.125 mg V/mL; Group III (MS) a water solution of $MgSO_4$ at a concentration of 0.06 mg Mg/mL; Group IV (SMV-MS)— a water solution of $NaVO_3$ and $MgSO_4$ at the same concentrations as in Group II for $NaVO_3$ and in Group III for $MgSO_4$. Food, fluids, and deionized water were offered *ad libitum*. Throughout the 18-weeks period, body weight was obtained weekly and at the time of slaughter. Animals' behavior was also observed.

The stock solutions of $NaVO_3$ and $MgSO_4$ were replaced by freshly prepared solutions every 2 days. The daily intake of water and the solutions of SMV, MS, and SMV-MS were measured with a measuring cylinder and the water and fluid intake was expressed as mL/rat/24 h. In turn, the daily intake of V and Mg in the SMV- or/and MS-administered animals was estimated on the basis of the 24 h consumption of the SMV, MS, and SMV-MS solutions and expressed as mg/kg b.wt./24 h. However, the food intake was calculated on the basis of the 24 h consumption of food by the rats from all the groups (the remainder of food together with additional spillage was weighed and subtracted from the whole food that the rats received to eat) and expressed as g/rat/24 h. The V and Mg concentrations in drinking water were selected on the basis of our previous experiments conducted in a rat model [11, 12, 36] and studies of other researchers [37, 38]. The concentration of V was chosen to reveal its prooxidant potential, which was meant to be attenuated by the administration of this element in combination with Mg. The concentration of Mg was chosen to be not too high since Mg (as $MgSO_4$) has been reported to induce diarrhea [39, 40].

After 18 weeks, all the rats were sectioned between 8:00 and 11:00 am and livers, which were used to prepare LS for determination of the MDA level, and other organs were dissected, directly washed in ice-cold physiological saline solution (0.9% NaCl), and weighed. The biological material that was not used immediately was stored frozen at –20°C or –80°C in a deep-freezer HFU 486 basic (bought as part of the Project entitled "Building of the Centre of Interdisciplinary Research" realized within the frame of the Operating Programme "Development of Eastern Poland" 2007–2013, Priority I: Modern Economy, Action I.3. The Advancement of Innovation, cofinanced by the European Regional Development Fund) (Thermo Fisher Scientific, Germany) until further analysis. The experiment was conducted according to the experimental protocol approved by the 1st Local Ethical Committee for Animal Studies in Lublin, Poland.

2.3. Analytical Procedure. LSs, in which the MDA level was determined using TBA, were obtained from 40 outbred 6.5-month-old albino male Wistar rats. More details concerning the preparation of LS for measurement of MDA and the methodology of determination of this LPO marker have been described by us previously [11]. LSs obtained from all the groups of rats: LS I (from Group I, Control), LS II (from Group II, SMV), LS III (from Group III, MS), and LS IV (from Group IV, SMV-MS) were divided into a few parts and subsequently incubated (a) without an inductor: LPO spontaneous ($LPO_{spont.}$), (b) with 30 μM $FeSO_4$ ($Fe_{exg\ 30\,\mu M}$), (c) with 100, 200, or 400 μM SMV ($V_{exg\ 100,\ 200,\ 400\,\mu M}$), or (d) with 100, 200, or 400 μM MS ($Mg_{exg\ 100,\ 200,\ 400\,\mu M}$). The MDA formed was calculated using the molar extinction coefficient $1.56 \times 10^5\ M^{-1}\ cm^{-1}$ and the results were expressed in nmoles per gram of wet tissue (nmol/g wet tissue).

Table 1: Main and interactive effects of V_{end} and Mg_{end} on the measured variables in male Wistar rats after 18-week administration of both elements as SMV and MS in combination.

Variables[a]	Two-way ANOVA analysis[b]			Character of interaction revealed[c]
	Main effect of V_{end}	Main effect of Mg_{end}	Interactive effect of $V_{end} \times Mg_{end}$	
Fluid I	$F = 61.263$, $P = 0.000$	NS	NS	—
Food I	$F = 45.645$, $P = 0.000$	NS	NS	—
BWG	$F = 46.591$, $P = 0.000$	NS	NS	—
$LPO_{spontaneous}$	$F = 22.678$, $P = 0.000$	$F = 21.722$, $P = 0.000$	$F = 9.091$, $P = 0.005$	Antagonistic

[a] Fluid I and Food I: fluid and food intake expressed as mL and g/rat/24 h, respectively; BWG: body weight gain expressed as g/18 week.

[b] Data are presented as F values and the levels of significance (P). NS: no significant effect.

[c] The effect of V_{end} and Mg_{end} in combination (V_{end} + Mg_{end} effect) < or > sum of the effects of V_{end} and Mg_{end} alone (V_{end} effect + Mg_{end} effect) (antagonistic or synergistic interaction, resp.).

2.4. Statistical Analysis. The results were processed with the Statistica and SPSS, version 9.0 and 14.0 PL for Windows, respectively. The distribution patterns in the data were evaluated using the Shapiro-Wilk's normality test. The homogeneity of variances was verified employing Levene's test and sometimes also Hartley's Fmax, Cochran's C and Bartlett's tests. The two-way analysis of variance (2-way ANOVA) with the vanadium (V_{end}) and magnesium (Mg_{end}) factors and the F test were employed to indicate the significant effects of V_{end}, Mg_{end}, or the $V_{end} \times Mg_{end}$ interaction. In addition, the three-way ANOVA analysis of variance (3-way ANOVA) with exogenous iron ($Fe_{exg\ 30\,\mu M}$), exogenous vanadium ($V_{exg\ 100,\ 200,\ 400\,\mu M}$), and exogenous magnesium ($Mg_{exg\ 100,\ 200,\ 400\,\mu M}$) factors as well as the F test were also employed to reveal significant effects of $Fe_{exg\ 30\,\mu M}$, $V_{exg\ 100,\ 200,\ 400\,\mu M}$, or $Mg_{exg\ 100,\ 200,\ 400\,\mu M}$. F values which had P values smaller than 0.05 were considered statistically significant. If the 2- or 3-way ANOVA tests demonstrated interactive effects between the elements used or trends toward those effects, subsequent calculations were done in order to describe the character of the interactions revealed (antagonistic or synergistic) [41]. The *post hoc* comparisons between the four individual groups were performed using Tukey's or T3 Dunnett's tests. Comparisons between spontaneous LPO and LPO modified exogenously by Fe_{exg}, V_{exg} and Mg_{exg} were assessed by the t-test or Wilcoxon test for dependent samples. The Student's "t"-test for independent samples was also applied for the detection of significant differences in the consumed V doses between the rats in Groups II and IV and Mg doses between the rats in Groups III and IV. The differences were considered significant if the P values were smaller than 0.05. All the results are expressed as mean ± SEM.

3. Results

3.1. General Observation. No distinct differences in the physical appearance and motor behavior were observed during the 18 experimental weeks in most of the rats receiving the SMV or/and MS solutions to drink, compared with the control. Some of the rats which drank the SMV and MS solutions separately (Groups II and III, resp.) and in combination (Group IV) had gastrointestinal disturbances, which were probably caused by the ingestion of V or/and Mg. Only one rat from Group IV had one-day diarrhea in the third and eight week of the experiment. In turn, loose stool was observed in one rat in Group II and in three rats in Groups III and IV in the first or/and second week of the experiment. However, in two rats in Group II and in one in Group III loose stool was observed at the turn of fifth and sixth week of the experiment and at the turn of second and fifth week of the study, respectively.

3.2. Basic Parameters. The fluid and food intakes as well as body weight gain in the rats of Groups II and IV were lower, compared with those found in the animals in Groups I and III (Figures 1(a), 1(c), and 1(d)). As the two-way ANOVA revealed, the decrease in the abovementioned parameters observed in the rats of Group IV was due to the independent action of V only (Table 1). It was also observed that the rats in Group IV took up slightly less V (by 8%), in comparison with the animals in Group II, but this difference did not turn out to be statistically significant. In turn, the consumption of Mg by the rats in Group IV was significantly lowered (by 21%), compared with that found in the animals in Group III (Figure 1(b)), which might be an effect of reduced fluid intake due to the SMV administration (Figure 1(a)).

3.3. Spontaneously Formed Hepatic MDA. As presented in Figure 2(a), the exposure to SMV alone (Group II) significantly enhanced the level of spontaneously generated MDA, compared with the control (Group I), the MS-supplemented (Group III) and the SMV-MS-applicated (Group IV) rats. Supplementation of the rats with MS alone did not change markedly the MDA formation, compared with the control, whereas the administration of MS in combination with SMV reduced its level by 62%, compared with the SMV-intoxicated rats. It was also observed that the level of the examined LPO marker was within the same value range that was found in the control animals. The two-way ANOVA revealed that the decrease in the spontaneously formed MDA in the rats of Group IV was influenced by the independent action of Mg and by its interaction with V (Table 1).

3.4. MDA Level Modified by Fe_{exg}, V_{exg}, and Mg_{exg}. In LS II, the MDA level modified by $Fe_{exg\ 30\,\mu M}$ (Figure 2(b)), $V_{exg\ 100,\ 200,\ 400\,\mu M}$ (Figures 2(c), 2(d), and 2(e)) or $Mg_{exg\ 100,\ 200,\ 400\,\mu M}$ (Figures 2(f), 2(g), and 2(h)) increased

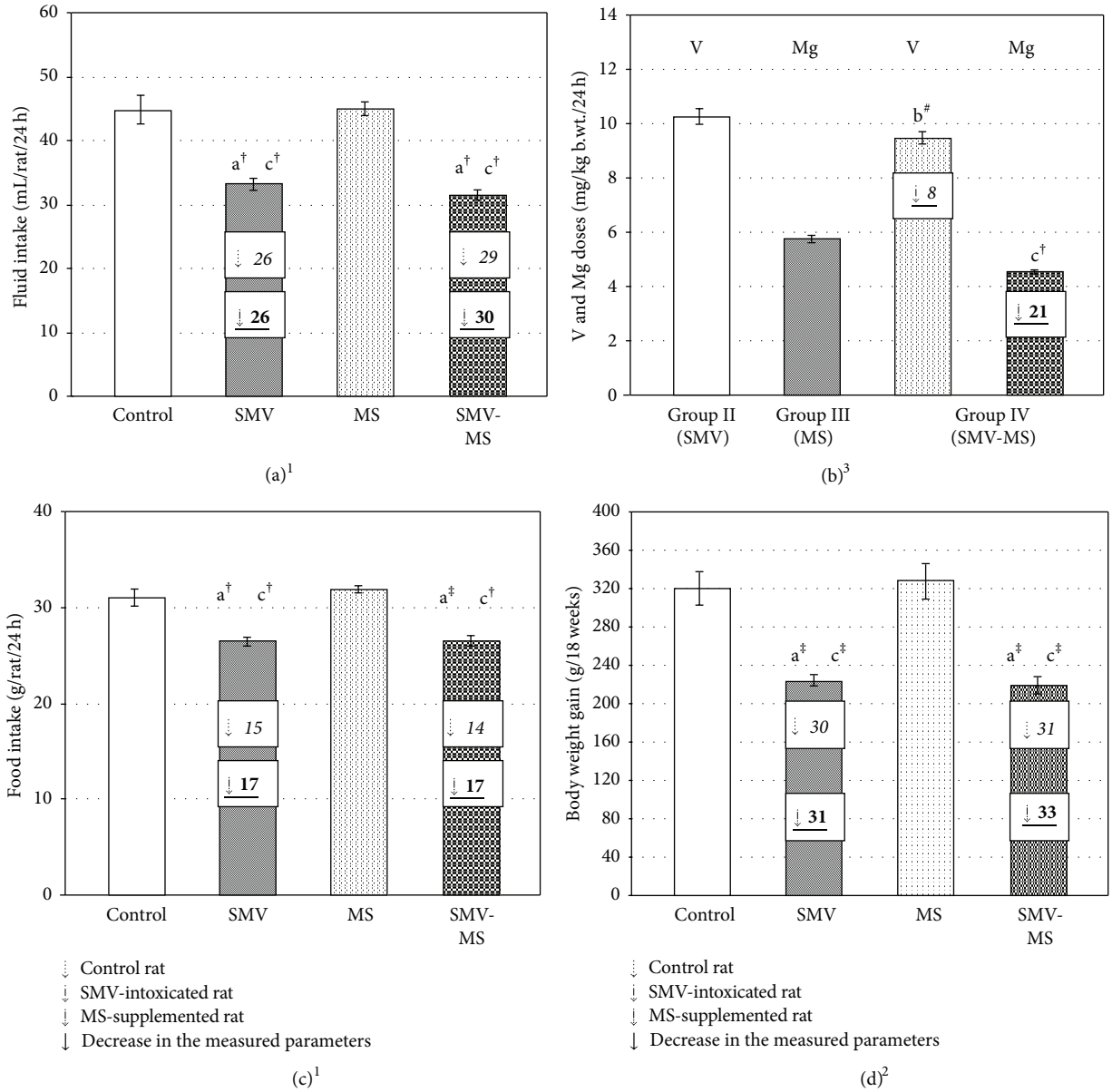

Figure 1: Fluid intake (a), V and Mg doses consumed by the rats through drinking water (b), food intake (c) and body weight gain (d) in the tested animals groups. Differences are indicated by ^{a,b,c}versus control, SMV-intoxicated and MS-supplemented rats, respectively (^{1,2,3}Tukey's, T3 Dunnett's and t test, resp.). $^{*}P < 0.05$, $^{\ddagger}P < 0.01$, $^{\dagger}P < 0.001$, $^{\#}P = 0.09$. Numerical values in the bars indicate the percentage of the decrease in the measured parameters (↓), compared with the control (italic alone), the SMV-intoxicated (italic underline bold), and the MS-supplemented (underline bold) rats.

markedly, compared with that found in LS I, III, and IV incubated in the same *in vitro* conditions. Further, in LS IV incubated with the concentrations of $Fe_{exg\ 30\,\mu M}$, $V_{exg\ 100,\ 200,\ 400\,\mu M}$, or $Mg_{exg\ 100,\ 200,\ 400\,\mu M}$, the level of MDA was markedly decreased by 76%, 38.5%, 29%, 22%, 53%, 51%, and 48%, respectively, in comparison with that found in LS II incubated in the same manner (Figures 2(b)–2(h)). Moreover, in LS IV incubated with $Fe_{exg\ 30\,\mu M}$ (Figure 2(b)) or with $Mg_{exg\ 100,\ 200,\ 400\,\mu M}$ (Figures 2(f)–2(h)), the MDA level returned to the range of values obtained for LS I incubated with the same concentrations of Fe_{exg} and Mg_{exg}. In the presence of $V_{exg\ 100\,\mu M}$ or $V_{exg\ 200\,\mu M}$ (Figures 2(c) and 2(d)), the level of this LPO marker was not significantly elevated, compared with that demonstrated in LS I. Only in the presence of the highest V concentration ($V_{exg\ 400\,\mu M}$), its level was significantly higher, compared with LS I (Figure 2(e)). Furthermore, in LS IV incubated with $V_{exg\ 100,\ 200,\ 400\,\mu M}$ (Figures 2(c), 2(d) and 2(e)), the MDA level was also significantly higher, compared with that found in LS III incubated in the presence of the abovementioned V_{exg} concentrations.

It was also shown that in LS III incubated in the presence of $Fe_{exg\ 30\,\mu M}$ (Figure 2(b)), $V_{exg\ 100\,\mu M}$ (Figure 2(c)), or $Mg_{exg\ 100,\ 400\,\mu M}$ (Figures 2(f) and 2(h)), the level of MDA

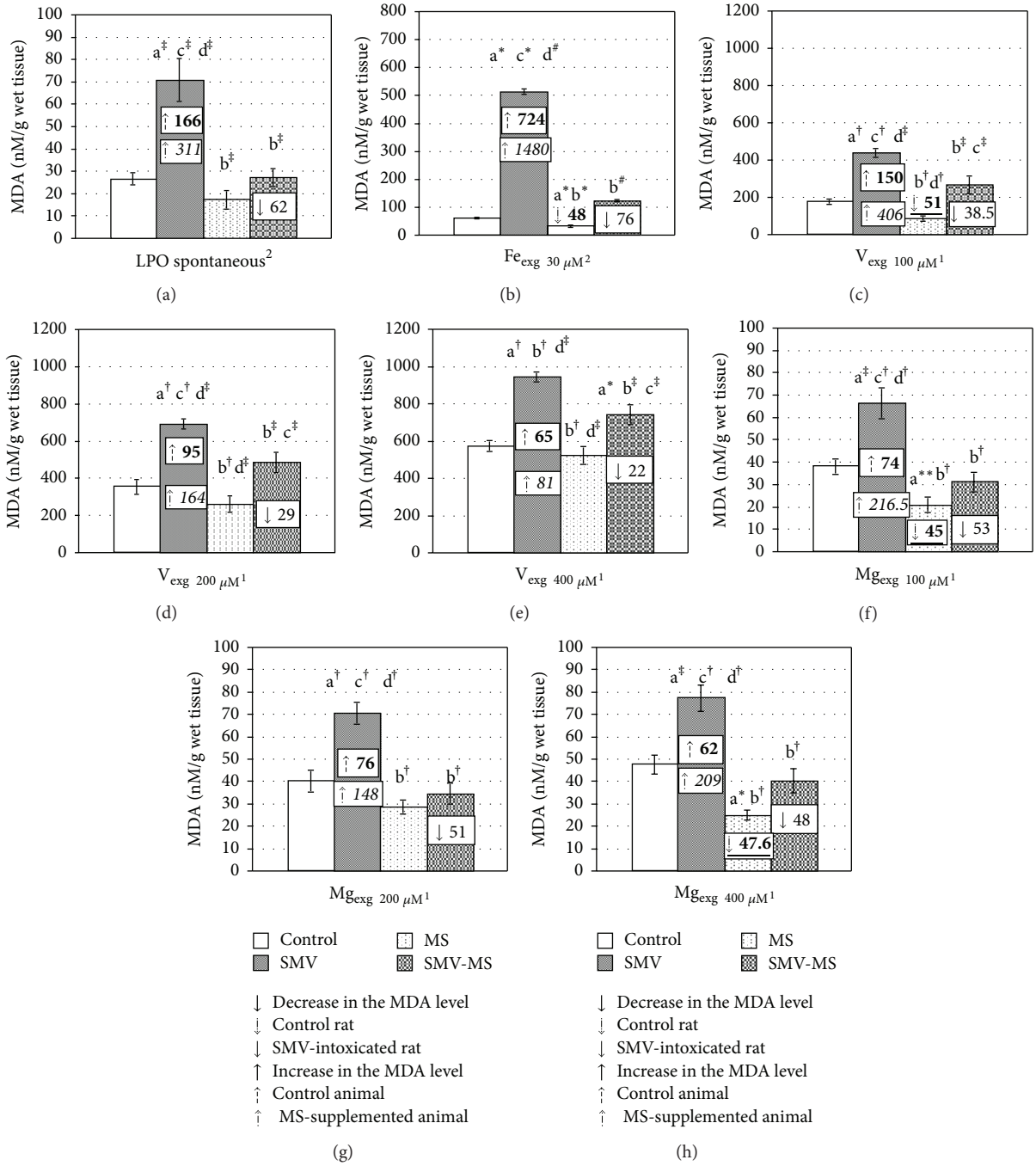

Figure 2: MDA level in LS obtained from the control, SMV-, MS- and SMV-MS-administered rats incubated without an oxidation inductor (LPO spontaneous) (a) or with $Fe_{exg\ 30\,\mu M}$ ($FeSO_4$) (b), $V_{exg\ 100,\ 200,\ 400\,\mu M}$ ($NaVO_3$) (c, d, e), or $Mg_{exg\ 100,\ 200,\ 400\,\mu M}$ ($MgSO_4$) (f, g, h). Differences are indicated by ^{a,b,c,d}versus control, SMV-intoxicated, MS-supplemented, and SMV-MS-administered rats, respectively ([1]Tukey's and [2]T3 Dunnett's test). $^{*}P < 0.05$, $^{\ddagger}P < 0.01$, $^{\dagger}P < 0.001$, $^{**}P = 0.07$, $^{\#}P = 0.09$, $^{\#\#}P = 0.13$. Numerical values in the bars or above them indicate the percentage of the decrease in the MDA level (↓), compared with the control (underline bold) and the SMV-intoxicated (normal alone) rats; other numerical values in the bars indicate the percentage of the increase in the MDA level (↑), compared with the control (bold alone) and the MS-supplemented (bold italic) animals.

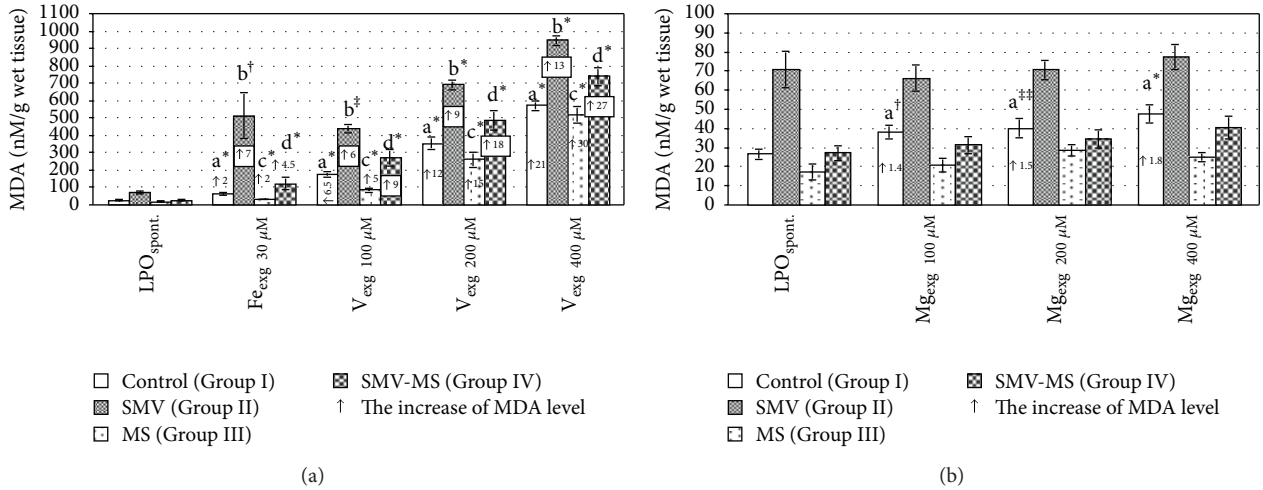

Figure 3: MDA level in LS obtained from the control, SMV-, MS- and SMV-MS-administered rats incubated without an oxidation inductor (LPO spontaneous) or with different exogenously added concentrations of $Fe_{exg\ 30\,\mu M}$ or $V_{exg\ 100,\ 200,\ 400\,\mu M}$ (a) or $Mg_{exg\ 100,\ 200,\ 400\,\mu M}$ (b) as $FeSO_4$, $NaVO_3$ and $MgSO_4$, respectively. Differences are indicated by ^{a,b,c,d}versus $Control_{LPO\ spont.}$, $SMV_{LPO\ spont.}$, $MS_{LPO\ spont.}$ and $SMV\text{-}MS_{LPO\ spont.}$, respectively, (Wilcoxon or t test). $^{*}P < 0.05$, $^{\ddagger}P < 0.01$, $^{\dagger}P < 0.001$, $^{\ddagger\ddagger}P = 0.07$. Numerical values in the bars or above them indicate how many times the MDA level increased (↑).

was lowered by 48%, 51%, 45%, and 47.6%, respectively, in comparison with that in LS I incubated with the same concentrations of Fe_{exg}, V_{exg}, or Mg_{exg}. The level of MDA in LS III incubated with $V_{exg\ 200\,\mu M}$, $V_{exg\ 400\,\mu M}$ (Figures 2(d) and 2(e)), or $Mg_{exg\ 200\,\mu M}$ (Figure 2(g)) was also lower, compared with that observed in LS I, but these differences were not so clear.

In addition, LS I, obtained from the control rats, which were incubated with $Fe_{exg\ 30\,\mu M}$, $V_{exg\ 100,\ 200,\ 400\,\mu M}$ or $Mg_{exg\ 100,\ 200,\ 400\,\mu M}$ exhibited higher MDA production, compared with that observed in LS I incubated without ($Control_{LPO\ spont.}$) the abovementioned concentrations of Fe_{exg} or V_{exg} (Figure 3(a)) or Mg_{exg} (Figure 3(b)). Higher MDA production was also demonstrated in LS II, III, and IV obtained from the SMV-intoxicated, MS-supplemented, and SMV-MS-administered rats, respectively, incubated in the presence of $Fe_{exg\ 30\,\mu M}$ or $V_{exg\ 100,\ 200,\ 400\,\mu M}$, in comparison with the spontaneously formed MDA in those LSs (Figure 3(a)). In turn, the incubation of LS II, III, and IV in the presence of $Mg_{exg\ 100,\ 200,\ 400\,\mu M}$ did not significantly change the level of MDA, compared with $SMV_{LPO\ spont.}$, $MS_{LPO\ spont.}$, and $SMV\text{-}MS_{LPO\ spont.}$, respectively (Figure 3(b)).

The three-way analysis of variance revealed that the changes in the MDA level in LS IV (obtained from the rats supplemented with MS during the SMV exposure) modified by exogenous $Fe_{exg\ 30\,\mu M}$, $V_{exg\ 100,\ 200,\ 400\,\mu M}$, or $Mg_{exg\ 100,\ 200,\ 400\,\mu M}$ resulted from the independent action of V_{end} and Mg_{end} as well as from their interaction or a distinct trend toward the $V_{end} \times Mg_{end}$ interaction (Table 2). In addition, the three-way ANOVA indicated that, beside the effects revealed between V_{end} and Mg_{end}, the alterations in the MDA production in LS IV incubated with $Fe_{exg\ 30\,\mu M}$ were also a consequence of the independent action of Fe_{exg} and its interaction with V_{end} and Mg_{end} as well as an effect of the interaction between three elements: Fe_{exg}, V_{end}, and Mg_{end}. In turn, the changes in the MDA generation in LS IV incubated with $V_{exg\ 100\,\mu M}$, $V_{exg\ 200\,\mu M}$, or $V_{exg\ 400\,\mu M}$ additionally resulted from the independent action of $V_{exg\ 100\,\mu M}$, $V_{exg\ 200\,\mu M}$, and $V_{exg\ 400\,\mu M}$ and from their interaction with V_{end} and Mg_{end} (Table 2). In the case of incubation of LS IV with $Mg_{exg\ 200\,\mu M}$ or $Mg_{exg\ 400\,\mu M}$, the three-way analysis of variance revealed that the alterations in the level of MDA in LS IV in the presence of $Mg_{exg\ 200\,\mu M}$ or $Mg_{exg\ 400\,\mu M}$ were also an effect of independent action of $Mg_{exg\ 200\,\mu M}$ and $Mg_{exg\ 400\,\mu M}$. In turn, any significant effect of $Mg_{exg\ 100\,\mu M}$ on the MDA production in LS IV was revealed by the performed analysis (Table 2).

4. Discussion

The current report demonstrates the influence of the 18-week V and Mg administration (as SMV and MS, resp.), separately and in combination, on changes in such basic parameters as fluid and food intakes, and body weight gain in male Wistar rats. It also presents (a) the protective impact of Mg on the *in vivo* SMV-stimulated LPO in the rat liver, (b) the modulating effects of the exogenously used Mg, V, and Fe on LPO in *in vitro* conditions, (c) the main and interactive effects of the abovementioned elements, and (d) the character of their interactions with respect to changes in the explored free radical process.

On the basis of the data obtained, we may state that the supplementation of the rats with MS during the 18-week SMV exposure did not limit the decrease in the fluid and food intake and body weight gain (Figures 1(a), 1(c) and 1(d)). Similar effects had also been observed by us previously in rats supplemented with MS during the 12-week SMV exposure

Table 2: Main and interactive effects of V_{end}, Mg_{end}, Fe_{exg}, V_{exg} and Mg_{exg} on the MDA level measured in liver supernatants obtained from the SMV-MS coapplied rats incubated in *in vitro* conditions with $Fe_{exg\ 30\ \mu M}$, $V_{exg\ 100, 200, 400\ \mu M}$ or $Mg_{exg\ 100, 200, 400\ \mu M}$.

Three-way ANOVA analysis[a]		Character of interaction revealed or character of a trend toward interaction
LPO modified by $Fe_{exg\ 30\ \mu M}$		
Main effect of V_{end}	$F = 18.412$, $P = 0.000$	—
Main effect of Mg_{end}	$F = 11.626$, $P = 0.001$	—
Interactive effect of $V_{end} \times Mg_{end}$	$F = 8.097$, $P = 0.006$	Antagonistic[b]
Main effect of $Fe_{exg\ 30\ \mu M}$	$F = 17.994$, $P = 0.000$	—
Interactive effect of $Fe_{exg\ 30\ \mu M} \times V_{end}$	$F = 12.317$, $P = 0.001$	Synergistic[c]
Interactive effect of $Fe_{exg\ 30\ \mu M} \times Mg_{end}$	$F = 6.995$, $P = 0.010$	Antagonistic[d]
Interactive effect of $Fe_{exg\ 30\ \mu M} \times V_{end} \times Mg_{end}$	$F = 5.526$, $P = 0.021$	
LPO modified by $V_{exg\ 100\ \mu M}$		
Main effect of V_{end}	$F = 75.402$, $P = 0.000$	—
Main effect of Mg_{end}	$F = 29.066$, $P = 0.000$	—
Interactive effect of $V_{end} \times Mg_{end}$	$F = 6.950$, $P = 0.051$	Antagonistic[b]
Main effect of $V_{exg\ 100\ \mu M}$	$F = 206.252$, $P = 0.000$	—
Interactive effect of $V_{exg\ 100\ \mu M} \times V_{end}$	$F = 46.205$, $P = 0.000$	Synergistic[e]
Interactive effect of $V_{exg\ 100\ \mu M} \times Mg_{end}$	$F = 12.570$, $P = 0.001$	Antagonistic[f]
Interactive effect of $V_{exg\ 100\ \mu M} \times V_{end} \times Mg_{end}$	NS	—
LPO modified by $V_{exg\ 200\ \mu M}$		
Main effect of V_{end}	$F = 51.672$, $P = 0.000$	—
Main effect of Mg_{end}	$F = 16.998$, $P = 0.000$	—
Interactive effect of $V_{end} \times Mg_{end}$	$F = 2.999$, $P = 0.088$	Antagonistic[b]
Main effect of $V_{exg\ 200\ \mu M}$	$F = 372.550$, $P = 0.000$	—
Interactive effect of $V_{exg\ 200\ \mu M} \times V_{end}$	$F = 35.037$, $P = 0.000$	Synergistic[e]
Interactive effect of $V_{exg\ 200\ \mu M} \times Mg_{end}$	$F = 8.299$, $P = 0.005$	Antagonistic[f]
Interactive effect of $V_{exg\ 200\ \mu M} \times V_{end} \times Mg_{end}$	NS	—
LPO modified by $V_{exg\ 400\ \mu M}$		
Main effect of V_{end}	$F = 61.594$, $P = 0.000$	—
Main effect of Mg_{end}	$F = 14.220$, $P = 0.000$	—
Interactive effect of $V_{end} \times Mg_{end}$	$F = 5.271$, $P = 0.025$	Antagonistic[b]
Main effect of $V_{exg\ 400\ \mu M}$	$F = 1026.907$, $P = 0.000$	—
Interactive effect of $V_{exg\ 400\ \mu M} \times V_{end}$	$F = 42.650$, $P = 0.000$	Synergistic[e]
Interactive effect of $V_{exg\ 400\ \mu M} \times Mg_{end}$	$F = 6.158$, $P = 0.015$	Antagonistic[f]
Interactive effect of $V_{exg\ 400\ \mu M} \times V_{end} \times Mg_{end}$	NS	—
LPO modified by $Mg_{exg\ 100\ \mu M}$		
Main effect of V_{end}	$F = 38.869$, $P = 0.000$	—
Main effect of Mg_{end}	$F = 49.991$, $P = 0.000$	—
Interactive effect of $V_{end} \times Mg_{end}$	$F = 12.331$, $P = 0.001$	Antagonistic[b]
Main effect of $Mg_{exg\ 100\ \mu M}$	NS	—
Interactive effect of $Mg_{exg\ 100\ \mu M} \times V_{end}$	NS	—
Interactive effect of $Mg_{exg\ 100\ \mu M} \times Mg_{end}$	NS	—
Interactive effect of $Mg_{exg\ 100\ \mu M} \times V_{end} \times Mg_{end}$	NS	—
LPO modified by $Mg_{exg\ 200\ \mu M}$		—
Main effect of V_{end}	$F = 39.615$, $P = 0.000$	—
Main effect of Mg_{end}	$F = 48.829$, $P = 0.000$	—
Interactive effect of $V_{end} \times Mg_{end}$	$F = 16.616$, $P = 0.000$	Antagonistic[b]
Main effect of $Mg_{exg\ 200\ \mu M}$	$F = 4.838$, $P = 0.031$	—
Interactive effect of $Mg_{exg\ 200\ \mu M} \times V_{end}$	NS	—
Interactive effect of $Mg_{exg\ 200\ \mu M} \times Mg_{end}$	NS	—
Interactive effect of $Mg_{exg\ 200\ \mu M} \times V_{end} \times Mg_{end}$	NS	—

Table 2: Continued.

Three-way ANOVA analysis[a]		Character of interaction revealed or character of a trend toward interaction
LPO modified by $Mg_{exg\,400\,\mu M}$		
Main effect of V_{end}	$F = 41.824$, $P = 0.000$	—
Main effect of Mg_{end}	$F = 53.944$, $P = 0.000$	—
Interactive effect of $V_{end} \times Mg_{end}$	$F = 10.024$, $P = 0.002$	Antagonistic[b]
Main effect of $Mg_{exg\,400\,\mu M}$	$F = 10.024$, $P = 0.002$	—
Interactive effect of $Mg_{exg\,400\,\mu M} \times V_{end}$	NS	—
Interactive effect of $Mg_{exg\,400\,\mu M} \times Mg_{end}$	NS	—
Interactive effect of $Mg_{exg\,400\,\mu M} \times V_{end} \times Mg_{end}$	NS	—

V_{end} and Mg_{end}: endogenous V ($NaVO_3$, SMV) and Mg ($MgSO_4$, MS) which were received in combination for 18 weeks; Fe_{exg}, V_{exg}, Mg_{exg}: exogenous Fe ($FeSO_4$), V ($NaVO_3$) and Mg ($MgSO_4$) added to liver supernatants obtained from the SMV-MS-coadministered rats.

[a]Data are presented as F values and the levels of significance (P). NS: no significant effect.

[b]The effect of V_{end} and Mg_{end} in combination in the presence of $Fe_{exg\,30\,\mu M}$ or $V_{exg\,100,\,200,\,400\,\mu M}$ or $Mg_{exg\,100,\,200,\,400\,\mu M}$ < sum of the effects of V_{end} and Mg_{end} alone in the presence of $Fe_{exg\,30\,\mu M}$ or $V_{exg\,100,\,200,\,400\,\mu M}$ or $Mg_{exg\,100,\,200,\,400\,\mu M}$ (antagonistic interaction).

[c]The effect of V_{end} and $Fe_{exg\,30\,\mu M}$ in combination in the presence of Mg_{end} > sum of the effects of V_{end} and $Fe_{exg\,30\,\mu M}$ alone in the presence of Mg_{end} (synergistic interaction).

[d]The effect of Mg_{end} and $Fe_{exg\,30\,\mu M}$ in combination in the presence of V_{end} < sum of the effects of Mg_{end} and $Fe_{exg\,30\,\mu M}$ alone in the presence of V_{end} (antagonistic interaction).

[e]The effect of V_{end} and $V_{exg\,100,\,200,\,400\,\mu M}$ in combination in the presence of Mg_{end} > sum of the effects of V_{end} and $V_{exg\,100,\,200,\,400\,\mu M}$ alone in the presence of Mg_{end} (synergistic interaction).

[f]The effect of Mg_{end} and $V_{exg\,100,\,200,\,400\,\mu M}$ in combination in the presence of V_{end} < sum of the effects of Mg_{end} and $V_{exg\,100,\,200,\,400\,\mu M}$ alone in the presence of V_{end} (antagonistic interaction).

[36, 42]. The changes in the fluid and food intake and in the body weight gain in rats after SMV intoxication had already been discussed [43].

As we expected, V (as SMV) enhanced LPO (Figures 1(a) and 3(a)). The elevated level of LPO in the liver of rats after intoxication with SMV or ammonium metavanadate (AMV) and in LS incubated with sodium vanadate in the *in vitro* system was also reported by other investigators [44–46]. A strong correlation between the induction of LPO and hepatotoxicity and the inhibition of both processes in parallel by antioxidants, suggesting a causative role for LPO in V-induced hepatotoxicity, was observed as well [47].

The performed analysis allowed us to conclude that the increase in the MDA production observed in LS IV (Group IV) in the presence of $Fe_{exg\,30\,\mu M}$ or $V_{exg\,100,\,200,\,400\,\mu M}$ (Figure 3(a)) was not only a consequence of the independent action of both elements but it also resulted from the synergistic interactions between Fe_{exg} and V_{end} and between V_{end} and V_{exg} (Table 2). The same interactive effects were found by us previously [11]. This is not surprising, as both elements may intensify LPO [48].

In turn, the incubation of LS II, III, and IV with $Mg_{exg\,100,\,200,\,400\,\mu M}$ did not significantly alter the MDA level, compared with spontaneously generated MDA, and only in LS I was a stimulating action of Mg on the hepatic MDA formation demonstrated (Figure 3(b)). The stimulating effect of Mg on the hepatic MDA production was also observed by us previously [11].

On the other hand, the present findings clearly demonstrated that the male Wistar rats receiving SMV in combination with MS (Group IV) for 18 weeks had a significantly lowered spontaneous MDA level than those exposed to SMV (Group II), in which the hepatic spontaneous MDA generation was markedly higher, compared with that found in the control (Group I) and MS-supplemented animals (Group III) (Figure 2(a)). The results obtained from the two-way ANOVA analysis allowed us to conclude that the protective impact of Mg on reduction of the SMV-stimulated hepatic MDA generation during the 18-week combined SMV and MS administration resulted from the independent action of Mg_{end} and from its antagonistic interaction with V_{end} (Table 1). Unfortunately, when the rats were supplemented with MS during the shorter 12-week SMV exposure, we did not demonstrate any significant fall in the spontaneously generated MDA in the liver, compared with that found in SMV-intoxicated rats [11]. We may suppose that the differences in the duration of the experimental period might be, at least partly, the cause of the discrepancies observed.

In addition, the results of the three-way ANOVA analysis also allowed us to state that the limitation in the increase in the MDA production in LS IV incubated with $Fe_{exg\,30\,\mu M}$ or $V_{exg\,100,\,200,\,400\,\mu M}$, compared with LS II (Figures 2(b)–2(e)), might be associated with the antagonistic interaction of Mg_{end} with Fe_{exg} and V_{exg} (Table 2). Neither the antagonistic $V_{end} \times Mg_{end}$, $Fe_{exg} \times Mg_{end}$, and $Mg_{end} \times V_{exg}$ interactions nor the three-way interaction (Fe × V × Mg) (Table 2) had been observed by us previously [11].

An important new finding of the study is that the independent action of Mg_{end} was a major effect responsible for suppression of the spontaneously formed MDA in the liver of rats supplemented with MS during the SMV exposure (Table 1). We cannot exclude that the antiradical activity of Mg might underlie, at least in part, its beneficial effect [28, 49–51]. The effect of Mg on some antioxidants appears

also worthy of inquiry [31, 52]. Therefore, further work is necessary to explain precisely the mechanism(s) responsible for the beneficial action of Mg in the 18-week conditions of the SMV-MS coadministration.

The $V_{end} \times Mg_{end}$ antagonistic interaction also played a significant role in the reduction of the SMV-induced spontaneous LPO in the liver of the SMV-MS-coadministered rats (Table 1). The V × Mg interactions investigated in *in vivo* and *in vitro* conditions are still little known, and only single reports about this issue have appeared in the literature [38, 53, 54]. Recently Sánchez et al. [55] showed that the interactions between V and Mg might occur in the rats' digestive and renal systems. The antagonistic character of the interaction revealed between V_{end} and Mg_{end} in our experimental conditions requires additional analyses. This seems to be important especially for extending the knowledge of the mechanism of the vanadate effect on organisms and the potential role of Mg in prevention of V toxicity.

5. Conclusion

To the best of our knowledge, the current report is the first demonstration of the protective action of Mg against the prooxidant potential of V revealed in a rat model. The study has clearly demonstrated that the 18-week supplementation of male Wistar rats with Mg (as MS) during the exposure to V (as SMV) may protect against V-induced hepatic LPO. The study provides evidence that the beneficial influence of Mg on limitation of the increase in the hepatic MDA generation during the 18-week SMV intoxication may result from the independent action of Mg and from its antagonistic interaction with V. However, further studies are needed to explain the exact mechanism(s) accounting for the protective effect of Mg against the SMV-induced OS in our experimental conditions. The results obtained seem to suggest that a proper Mg intake for a specific time period in the conditions of SMV exposure may prevent V-stimulated LPO in the liver.

The present study has also shown the degree to which the independent action of the elements used (V, Mg, and Fe) and their mutual interactions may modify the hepatic MDA production. Simultaneously, it has confirmed that Mg is able to promote LPO in certain conditions by revealing its stimulating action on the explored free radical process in the *in vitro* system.

Abbreviations

Mg_{end}: Mg (as MS) administered to rats endogenously
V_{end}: V (as SMV) administered to rats endogenously
Mg_{exg}: Mg (as $MgSO_4$) added exogenously to liver supernatants (LS)
V_{exg}: V (as $NaVO_3$) added exogenously to liver supernatants (LS)
Fe_{exg}: Fe (as $FeSO_4$) added exogenously to liver supernatants (LS).

Conflict of Interests

The authors declare that they have no conflict of interests.

References

[1] J. E. Klaunig, Y. Xu, J. S. Isenberg et al., "The role of oxidative stress in chemical carcinogenesis," *Environmental Health Perspectives*, vol. 106, supplement 1, pp. 289–295, 1998.

[2] G. Bartosz, *Druga Twarz Tlenu. Wolne Rodniki w Przyrodzie*, Wydawnictwo Naukowe PWN, Warszawa, Poland, 2004.

[3] E. Niki, "Lipid peroxidation: physiological levels and dual biological effects," *Free Radical Biology and Medicine*, vol. 47, no. 5, pp. 469–484, 2009.

[4] E. Niki, Y. Yoshida, Y. Saito, and N. Noguchi, "Lipid peroxidation: mechanisms, inhibition, and biological effects," *Biochemical and Biophysical Research Communications*, vol. 338, no. 1, pp. 668–676, 2005.

[5] S. Srivastava, B. Chandrasekar, A. Bhatnagar, and S. D. Prabhu, "Lipid peroxidation-derived aldehydes and oxidative stress in the failing heart: role of aldose reductase," *American Journal of Physiology*, vol. 283, no. 6, pp. H2612–H2619, 2002.

[6] Z. H. Chen and E. Niki, "Two faces of lipid peroxidation products: the "Yin and Yang" principles of oxidative stress," *Journal of Experimental and Integrative Medicine*, vol. 1, no. 4, pp. 215–219, 2011.

[7] M. A. Altamirano-Lozano and M. E. Roldán-Reyes, "Genetic toxicology of vanadium compounds," in *Vanadium in the Environment Part II: Health Effects*, J. O. Nriagu, Ed., vol. 31, pp. 159–179, John Wiley & Sons, New York, NY, USA, 1998.

[8] A. Goc, "Biological activity of vanadium compounds," *Central European Journal of Biology*, vol. 1, no. 3, pp. 314–332, 2006.

[9] J. O. Nriagu, *Vanadium in the Environment. Health Effects*, vol. 31, part 2, John Wiley & Sons, New York, NY, USA, 1998.

[10] J. Z. Byczkowski and A. P. Kulkarni, "Oxidative stress and prooxidant biological effects of vanadium," in *Vanadium in the Environment Part II: Health Effects*, J. O. Nriagu, Ed., vol. 31, pp. 235–264, John Wiley & Sons, New York, NY, USA, 1998.

[11] A. Ścibior, H. Zaporowska, and I. Niedźwiecka, "Lipid peroxidation in the liver of rats treated with V and/or Mg in drinking water," *Journal of Applied Toxicology*, vol. 29, no. 7, pp. 619–628, 2009.

[12] A. Ścibior, H. Zaporowska, and I. Niedźwiecka, "Lipid peroxidation in the kidney of rats treated with V and/or Mg in drinking water," *Journal of Applied Toxiology*, vol. 30, no. 5, pp. 487–496, 2010.

[13] N. H. Stacey and C. D. Klaassen, "Comparison of the effects of metals on cellular injury and lipid peroxidation in isolated rat hepatocytes," *Journal of Toxicology and Environmental Health*, vol. 7, no. 1, pp. 139–147, 1981.

[14] J. Donaldson and F. LaBella, "Prooxidant properties of vanadate *in vitro* on catecholamines and on lipid peroxidation by mouse and rat tissues," *Journal of Toxicology and Environmental Health*, vol. 12, no. 1, pp. 119–126, 1983.

[15] J. Donaldson, R. Hemming, and F. LaBella, "Vanadium exposure enhances lipid peroxidation in the kidney of rats and mice," *Canadian Journal of Physiology and Pharmacology*, vol. 63, no. 3, pp. 196–199, 1985.

[16] M. H. Oster, J. M. Llobet, J. L. Domingo, J. B. German, and C. L. Keen, "Vanadium treatment of diabetic Sprague-Dawley rats results in tissue vanadium accumulation and pro-oxidant effects," *Toxicology*, vol. 83, no. 1–3, pp. 115–130, 1993.

[17] K. Furuno, T. Suetsugu, and N. Sugihara, "Effects of metal ions on lipid peroxidation in cultured rat hepatocytes loaded with α-linolenic acid," *Journal of Toxicology and Environmental Health A*, vol. 48, no. 2, pp. 121–129, 1996.

[18] A. Soussi, F. Croute, J. P. Soleilhavoup, A. Kammoun, and A. El Feki, "Impact of green tea on oxidative stress induced by ammonium metavanadate exposure in male rats," *Comptes Rendus*, vol. 329, no. 10, pp. 775–784, 2006.

[19] S. S. Soares, H. Martins, R. O. Duarte et al., "Vanadium distribution, lipid peroxidation and oxidative stress markers upon decavanadate *in vivo* administration," *Journal of Inorganic Biochemistry*, vol. 101, no. 1, pp. 80–88, 2007.

[20] Y. Deng, H. Cui, X. Peng et al., "Dietary vanadium induces oxidative stress in the intestine of broilers," *Biological Trace Element Research*, vol. 145, pp. 52–58, 2012.

[21] J. Liu, H. Cui, X. Liu et al., "Dietary vanadium causes oxidative damage-induced renal and hepatic toxicity in broilers," *Biological Trace Element Research*, vol. 145, no. 2, pp. 189–200, 2012.

[22] T. Matsubara, S. Musat-Marcu, H. P. Misra, and N. S. Dhalla, "Protective effect of vanadate on oxyradical-induced changes in isolated perfused heart," *Molecular and Cellular Biochemistry*, vol. 153, no. 1-2, pp. 79–85, 1995.

[23] M. C. Cam, R. W. Brownsey, and J. H. McNeill, "Mechanisms of vanadium action: insulin-mimetic or insulin-enhancing agent?" *Canadian Journal of Physiology and Pharmacology*, vol. 78, no. 10, pp. 829–847, 2000.

[24] A. Bishayee, R. Karmakar, A. Mandal, S. N. Kundu, and M. Chatterjee, "Vanadium-mediated chemoprotection against chemical hepatocarcinogenesis in rats: haematological and histological characteristics," *European Journal of Cancer Prevention*, vol. 6, no. 1, pp. 58–70, 1997.

[25] P. S. Kanna, C. B. Mahendrakumar, B. N. Indira et al., "Chemopreventive effects of vanadium toward 1,2-dimethylhydrazine-induced genotoxicity and preneoplastic lesions in rat colon," *Environmental and Molecular Mutagenesis*, vol. 44, no. 2, pp. 113–118, 2004.

[26] T. Chakraborty, A. Chatterjee, M. G. Saralaya, D. Dhachinamoorthi, and M. Chatterjee, "Vanadium inhibits the development of 2-acetylaminofluorene-induced premalignant phenotype in a two-stage chemical rat hepatocarcinogenesis model," *Life Sciences*, vol. 78, no. 24, pp. 2839–2851, 2006.

[27] E. Niedworok, M. Wardas, M. Stec, and M. Dołowy, "Ocena procesu peroksydacji lipidów modyfikowanego jonami magnezu i etanolem w izolowanych hepatocytach szczura," *Nowiny Lekarskie*, vol. 71, no. 6, pp. 295–298, 2002.

[28] R. F. Regan, E. Jasper, Y. Guo, and S. S. Panter, "The effect of magnesium on oxidative neuronal injury *in vitro*," *Journal of Neurochemistry*, vol. 70, no. 1, pp. 77–85, 1998.

[29] Y. Yamaguchi, S. Kitagawa, M. Kunitomo, and M. Fujiwara, "Preventive effects of magnesium on raised serum lipid peroxide levels and aortic cholesterol deposition in mice fed an atherogenic diet," *Magnesium Research*, vol. 7, no. 1, pp. 31–37, 1994.

[30] H. Bariskaner, M. E. Ustun, A. Ak, A. Yosunkaya, H. B. Ulusoy, and M. Gurbilek, "Effects of magnesium sulfate on tissue lactate and malondialdehyde levels after cerebral ischemia," *Pharmacology*, vol. 68, no. 3, pp. 162–168, 2003.

[31] C. P. Hans, D. P. Chaudhary, and D. D. Bansal, "Effect of magnesium supplementation on oxidative stress in alloxanic diabetic rats," *Magnesium Research*, vol. 16, no. 1, pp. 13–19, 2003.

[32] N. Sahin, M. Onderci, K. Sahin, G. Cikim, and O. Kucuk, "Magnesium proteinate is more protective than magnesium oxide in heat-stressed quail," *Journal of Nutrition*, vol. 135, no. 7, pp. 1732–1737, 2005.

[33] C. Abad, A. Teppa-Garrán, T. Proverbio, S. Piñero, F. Proverbio, and R. Marín, "Effect of magnesium sulfate on the calcium-stimulated adenosine triphosphatase activity and lipid peroxidation of red blood cell membranes from preeclamptic women," *Biochemical Pharmacology*, vol. 70, no. 11, pp. 1634–1641, 2005.

[34] A. C. Ariza, N. Bobadilla, C. Fernández, R. M. Muñoz-Fuentes, F. Larrea, and A. Halhali, "Effects of magnesium sulfate on lipid peroxidation and blood pressure regulators in preeclampsia," *Clinical Biochemistry*, vol. 38, no. 2, pp. 128–133, 2005.

[35] S. Shukla, V. Singh, and D. Joshi, "Modulation of toxic effects of organic mercury by different antioxidants," *Toxicology International*, vol. 14, no. 1, pp. 67–71, 2007.

[36] A. Ścibior, A. Adamczyk, D. Gołłębiowska, and I. Niedźwiecka, "Effect of 12-week vanadate and magnesium co-administration on chosen haematological parameters as well as on some indices of iron and copper metabolism and biomarkers of oxidative stress in rats," *Environmental Toxicology and Pharmacology*, vol. 34, no. 2, pp. 235–252, 2012.

[37] J. L. Domingo, "Vanadium: a review of the reproductive and developmental toxicity," *Reproductive Toxicology*, vol. 10, no. 3, pp. 175–182, 1996.

[38] M. Matsuda, L. Mandarino, and R. A. DeFronzo, "Synergistic interaction of magnesium and vanadate on glucose metabolism in diabetic rats," *Metabolism*, vol. 48, no. 6, pp. 725–731, 1999.

[39] U.S. EPA (United States Environmental Protection Agency), "Drinking water advisory: consumer acceptability advice and health effects analysis on sulphate," EPA 822-R-03-007, February 2003.

[40] WHO (World Health Organization), "Sulfate in drinking water," Background Document For Development of WHO Guidelines For Drinking-Water Quality WHO/SDE/WSH/03.04/114, 2004.

[41] A. A. Gołubiew, E. I. Lublina, N. A. Tołokncew, and W. A. Fiłow, *Toksykologia Ilościowa*, Wydawnictwo Lekarskie PZWL, Warszawa, Poland, 1978.

[42] A. Ścibior and H. Zaporowska, "Effects of combined vanadate and magnesium treatment on erythrocyte antioxidant defence system in rats," *Environmental Toxicology and Pharmacology*, vol. 30, no. 2, pp. 153–161, 2010.

[43] A. Ścibior, H. Zaporowska, A. Wolińska, and J. Ostrowski, "Antioxidant enzyme activity and lipid peroxidation in the blood of rats co-treated with vanadium (V^{+5}) and chromium (Cr^{+3})," *Cell Biology and Toxicology*, vol. 26, no. 6, pp. 509–526, 2010.

[44] M. Younes, M. Albrecht, and C. F. Siegers, "Lipid peroxidation and lysosomal enzyme release induced by vanadate *in vitro*," *Research Communications in Chemical Pathology and Pharmacology*, vol. 43, no. 3, pp. 487–495, 1984.

[45] M. Elfant and C. L. Keen, "Sodium vanadate toxicity in adult and developing rats. Role of peroxidative damage," *Biological Trace Element Research*, vol. 14, no. 3, pp. 193–208, 1987.

[46] E. Russanov, H. Zaporowska, E. Ivancheva, M. Kirkova, and S. Konstantinova, "Lipid peroxidation and antioxidant enzymes in vanadate-treated rats," *Comparative Biochemistry and Physiology C*, vol. 107, no. 3, pp. 415–421, 1994.

[47] M. Younes and O. Strubelt, "Vanadate-induced toxicity towards isolated perfused rat livers: the role of lipid peroxidation," *Toxicology*, vol. 66, no. 1, pp. 63–74, 1991.

[48] N. H. Stacey and H. Kappus, "Comparison of methods of assessment of metal-induced lipid peroxidation in isolated rat hepatocytes," *Journal of Toxicology and Environmental Health*, vol. 9, no. 2, pp. 277–285, 1982.

[49] L. A. Garcia, S. C. Dejong, S. M. Martin, R. S. Smith, G. R. Buettner, and R. E. Kerber, "Magnesium reduces free radicals in an *in vivo* coronary occlusion- reperfusion model," *Journal of the American College of Cardiology*, vol. 32, no. 2, pp. 536–539, 1998.

[50] I. T. Mak, A. M. Komarov, J. H. Kramer, and W. B. Weglicki, "Protective mechanisms of Mg-gluconate against oxidative endothelial cytotoxicity," *Cellular and Molecular Biology*, vol. 46, no. 8, pp. 1337–1344, 2000.

[51] S. B. Murthi, R. M. Wise, W. B. Weglicki, A. M. Komarov, and J. H. Kramer, "Mg-gluconate provides superior protection against postischemic dysfunction and oxidative injury compared to Mg-sulfate," *Molecular and Cellular Biochemistry*, vol. 245, no. 1-2, pp. 141–148, 2003.

[52] B. Matkovics, I. Kiss, and S. A. Kiss, "The activation by magnesium treatment of anti-oxidants eliminating the oxygen free radicals in drosophila melanogaster *in vivo*," *Magnesium Research*, vol. 10, no. 1, pp. 33–38, 1997.

[53] P. J. Romero, "Synergistic activation of the human red cell calcium ATPase by magnesium and vanadate," *Biochimica et Biophysica Acta*, vol. 1143, no. 1, pp. 45–50, 1993.

[54] P. J. Romero and A. F. Rega, "Effects of magnesium plus vanadate on partial reactions of the Ca^{2+}-ATPase from human red cell membranes," *Biochimica et Biophysica Acta*, vol. 1235, no. 1, pp. 155–157, 1995.

[55] C. Sánchez, M. Torres, M. C. Bermúdez-Peña et al., "Bioavailability, tissue distribution and hypoglycaemic effect of vanadium in magnesium-deficient rats," *Magnesium Research*, vol. 24, no. 4, pp. 196–208, 2011.

Hindawi Publishing Corporation
Oxidative Medicine and Cellular Longevity
Volume 2013, Article ID 602029, 7 pages
http://dx.doi.org/10.1155/2013/602029

Research Article

4-Hydroxyhexenal- and 4-Hydroxynonenal-Modified Proteins in Pterygia

Ichiya Sano,[1] Sachiko Kaidzu,[1] Masaki Tanito,[1] Katsunori Hara,[1] Tsutomu Okuno,[2] and Akihiro Ohira[1]

[1] *Department of Ophthalmology, Shimane University Faculty of Medicine, Enya 89-1, Izumo, Shimane 693-8501, Japan*
[2] *National Institute of Occupational Safety and Health, Kawasaki, Japan*

Correspondence should be addressed to Masaki Tanito; tanito-oph@umin.ac.jp

Received 6 February 2013; Revised 15 April 2013; Accepted 16 April 2013

Academic Editor: Kota V. Ramana

Oxidative stress has been suspected of contributing to the pathogenesis of pterygia. We evaluated the immunohistochemical localization of the markers of oxidative stress, that is, the proteins modified by 4-hydroxyhexenal (4-HHE) and 4-hydroxynonenal (4-HNE), which are reactive aldehydes derived from nonenzymatic oxidation of n-3 and n-6 polyunsaturated fatty acids, respectively. In the pterygial head, labeling of 4-HHE- and 4-HNE-modified proteins was prominent in the nuclei and cytosol of the epithelium. In the pterygial body, strong labeling was observed in the nuclei and cytosol of the epithelium and proliferating subepithelial connective tissue. In normal conjunctival specimens, only trace immunoreactivity of both proteins was observed in the epithelial and stromal layers. Exposures of ultraviolet (330 nm, 48.32 ± 0.55 J/cm^2) or blue light (400 nm, 293.0 ± 2.0 J/cm^2) to rat eyes enhanced labeling of 4-HHE- and 4-HNE-modified proteins in the nuclei of conjunctival epithelium. Protein modifications by biologically active aldehydes are a molecular event involved in the development of pterygia.

1. Introduction

Pterygium, a common ocular surface disease only observed in humans [1, 2], is a chronic condition characterized by encroachment of a fleshy, triangular portion of the bulbar conjunctiva into the cornea. Pterygia develop more often on the nasal side of the eye and are often bilateral [2–6]. Progression of lesions with central migration into the visual axis results in severe visual impairment [7, 8]; thus, surgical excision needs to be considered when progression occurs.

Histologically, pterygia are comprised of a superficial growth of a highly vascularized elastoid and basophilic degenerated connective tissue; that is, covered by an alternately thickened or thinned epithelium [9]. Although the pathogenesis of pterygia is not fully understood, it has been proposed that their typical location can be explained by the corneal focusing of incident sunlight on the medial limbus [10–12]. Epidemiologic studies also have indicated a possible association between chronic sunlight exposure, especially ultraviolet light (UV), and development of pterygia [2, 13–15]. The detrimental effects of ultraviolet irradiation could be due either directly to an ultraviolet phototoxic effect or indirectly to formation of radial oxygen species that cause oxidative stress [16].

The current thinking suggests that free radicals that form during oxidative stress can directly attack critical biomolecules including polyunsaturated fatty acids (PUFAs) and initiate free radical chain reactions that result in lipid peroxidation in cellular membranes. This chain reaction amplifies generation of lipid radical species, causing PUFA degeneration in a variety of oxidized products, including aldehydes [17]. 4-Hydroxyhexenal (4-HHE) and 4-hydroxynonenal (4-HNE) are α, β-unsaturated aldehydes that are end products of nonenzymatic oxidation of n-3 and n-6 polyunsaturated fatty acids, respectively [18]. These highly reactive aldehydes can react readily with histidine, cysteine, or lysine residues of proteins, leading to formation of stable Michael adducts with a hemiacetal structure [19]. Formation of these adducts leads to a variety of cytopathological effects, that is, inhibition of enzyme activity; inhibition

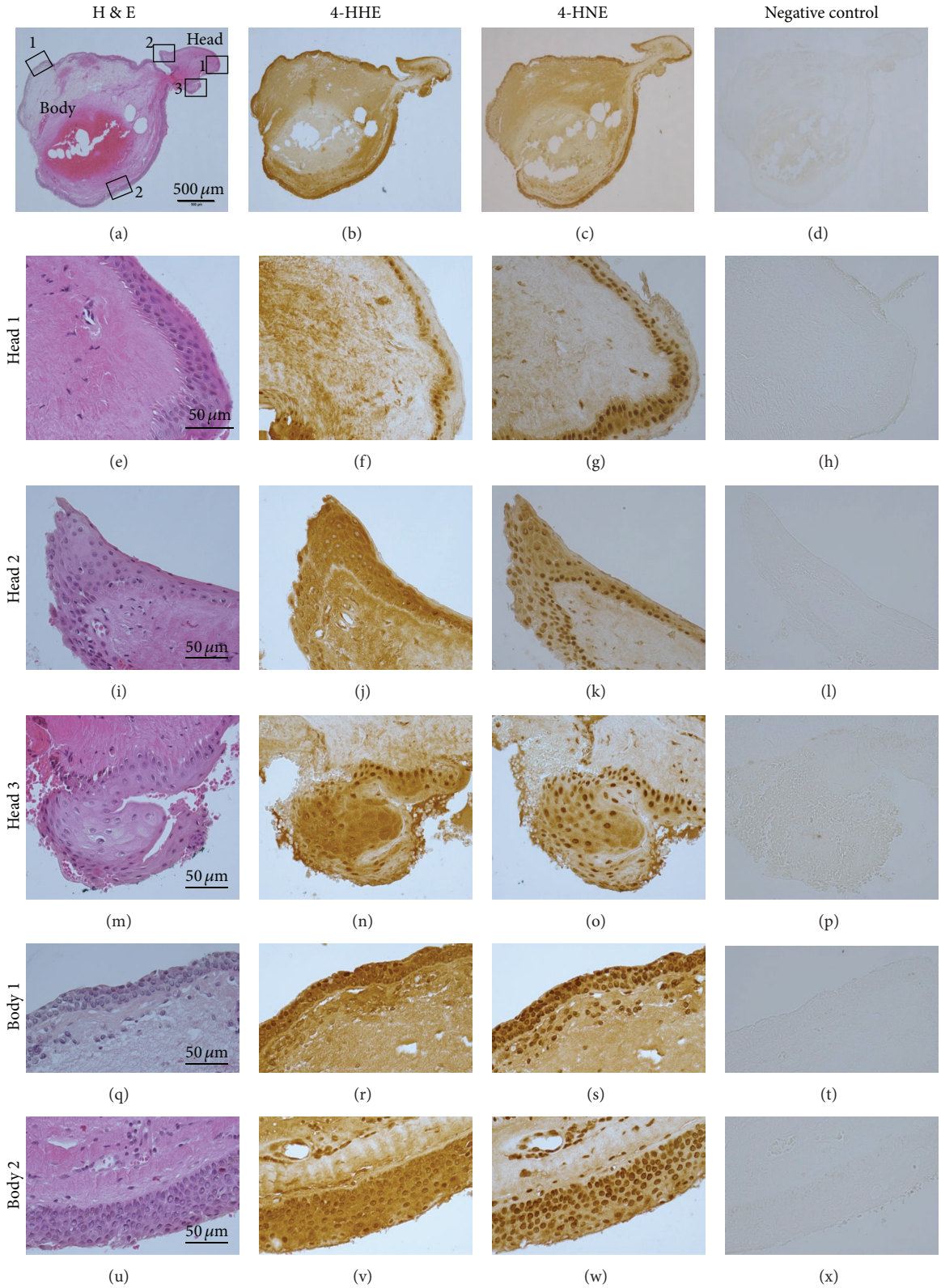

Figure 1: Expressions of aldehyde-modified proteins in pterygia. Representative images of H&E staining (a, e, i, m, q, and u), 4-HHE (b, f, j, n, r, and v) and 4-HNE (c, g, k, o, s, and w) immunohistochemistry, and negative control staining (d, h, l, p, t, and x) are shown. Three specimens from the pterygial head (head 1, 2, and 3) and two specimens from the pterygial body (body 1 and 2) are shown at higher magnifications. H&E: hematoxylin and eosin; 4-HHE: 4-hydroxyhexenal; 4-HNE: 4-hydroxynonenal.

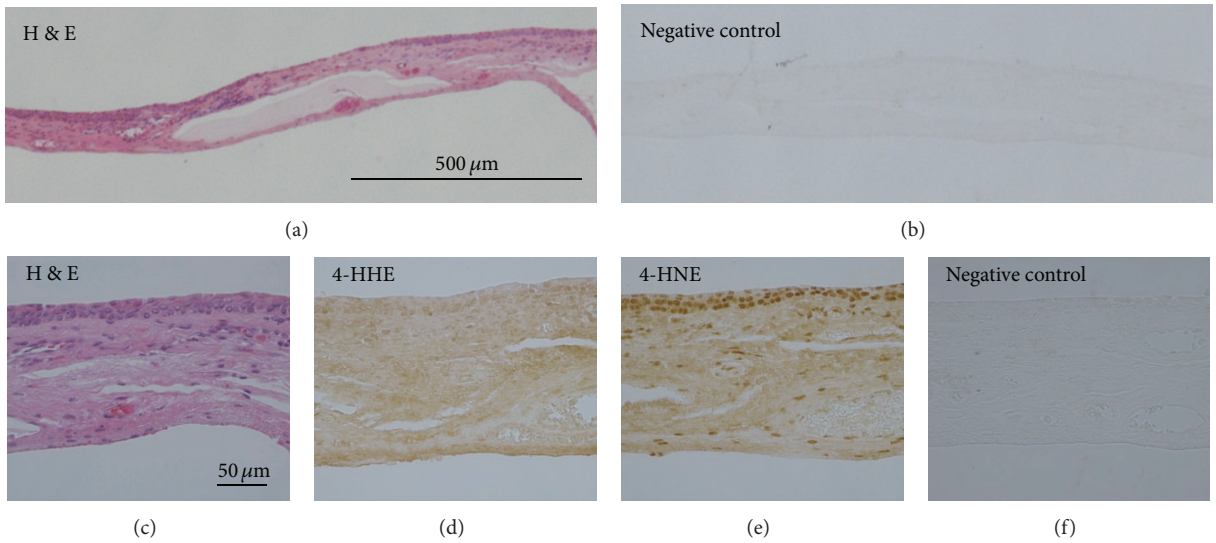

Figure 2: Expressions of aldehyde-modified proteins in normal conjunctiva. Representative images of H&E (a, c) staining, 4-HHE (d) and 4-HNE (e) immunohistochemistry, and negative control staining (b, f) are shown. (a, b) Lower magnification. (c–f) Higher magnification. H&E: hematoxylin and eosin; 4-HHE: 4-hydroxyhexenal; 4-HNE: 4-hydroxynonenal.

of protein, RNA, and DNA synthesis; cell cycle arrest, and apoptosis [20, 21]. The use of specific antibodies to recognize the hemiacetal structure of the Michael adducts enables their detection in tissues [22].

Increasing evidence suggests that protein modifications by reactive aldehydes are involved in various diseases. We evaluated the immunohistochemical localization of proteins modified by these aldehydes in pterygial specimens from patients and conjunctivae from rats that were exposed to the short wavelength lights. The aims of the current study were to evaluate the expression of the two aldehyde-modified proteins in the epithelial and stromal layers of human pterygia and normal conjunctiva to determine if they participate in the development of pterygia, and to test the possible relationship between short-wavelength light radiation and the development of pterygia.

2. Subjects and Methods

Human biopsy study was conducted as a part of the study protocol "Establishment of a Library of Ocular Tissues and Cells Obtained during Various Ophthalmic Surgeries," that the institutional review board of Shimane University Hospital reviewed and approved. All subjects provided written informed consent. The human biopsy specimens of pterygia and adjacent normal conjunctiva were obtained intraoperatively during pterygial excision from four eyes of three patients (1 man, 2 women; age range, 63–80 years).

The specimens were fixed in 4% paraformaldehyde containing 20% isopropanol, 2% trichloroacetic acid, and 2% zinc chloride, for 24 hours at room temperature, processed for paraffin embedding, and morphologically analyzed using hematoxylin and eosin (H&E) staining and immunohistochemistry for 4-HHE and 4-HNE, as described previously [23, 24]. Briefly, the sections were deparaffinized and endogenous peroxidase activity was inactivated with 3% H_2O_2 for 10 minutes. After blocking with a serum-free blocking reagent (Dako, Carpinteria, CA, USA) for 30 minutes at room temperature, the sections were incubated with the anti-4-HHE (1 : 100) or anti-4-HNE (1 : 100) antibody diluted with antibody diluent (Dako) for 2 hours at 37°C and then with the peroxidase-linked anti-mouse IgG polymer (EnVision+ System, Dako) for 1 hour at 37°C. For negative control experiments, sections were incubated with antibody diluent without a primary antibody for 2 hours at 37°C and then with the peroxidase-linked anti-mouse IgG polymer for 1 hour at 37°C. Signals were developed with 3′,3′-diaminobenzidine (Dako) in chromogen solution. Monoclonal anti-4-HHE- and anti-4-HNE-modified protein antibodies were purchased from NOF Corporation (Tokyo, Japan).

For animals, all procedures were performed according to the ARVO Statement for the Use of Animals in Ophthalmic and Vision Research and The Shimane University Guidelines for Animals in Research. Male Sprague-Dawley rats (4-week-old) were obtained from Charles River Laboratories Japan Inc. (Kanagawa, Japan) and maintained in our colony room for 7–10 days before the experiments. The light intensity in the cages was 10–20 lux. All rats were kept in a 12-hour (7 AM to 7 PM) light-dark cycle.

After anesthesia was induced by the intramuscular injection of a mixture of ketamine (120 mg/kg) and xylazine (6 mg/kg), light exposure was performed to the left eyes, and the opposite eyes left unexposed to light were served as controls. Rats were exposed to 330 or 400 nm lights with 10 nm in bandwidth, using a xenon lamp light source with bandpass filters (Asahi Spectra Co., Ltd., Tokyo, Japan) for an estimated period as described later. Light was exposed at a right angle to the center of the cornea. During exposure, diluted saline (×2) was adequately dropped to the surface of

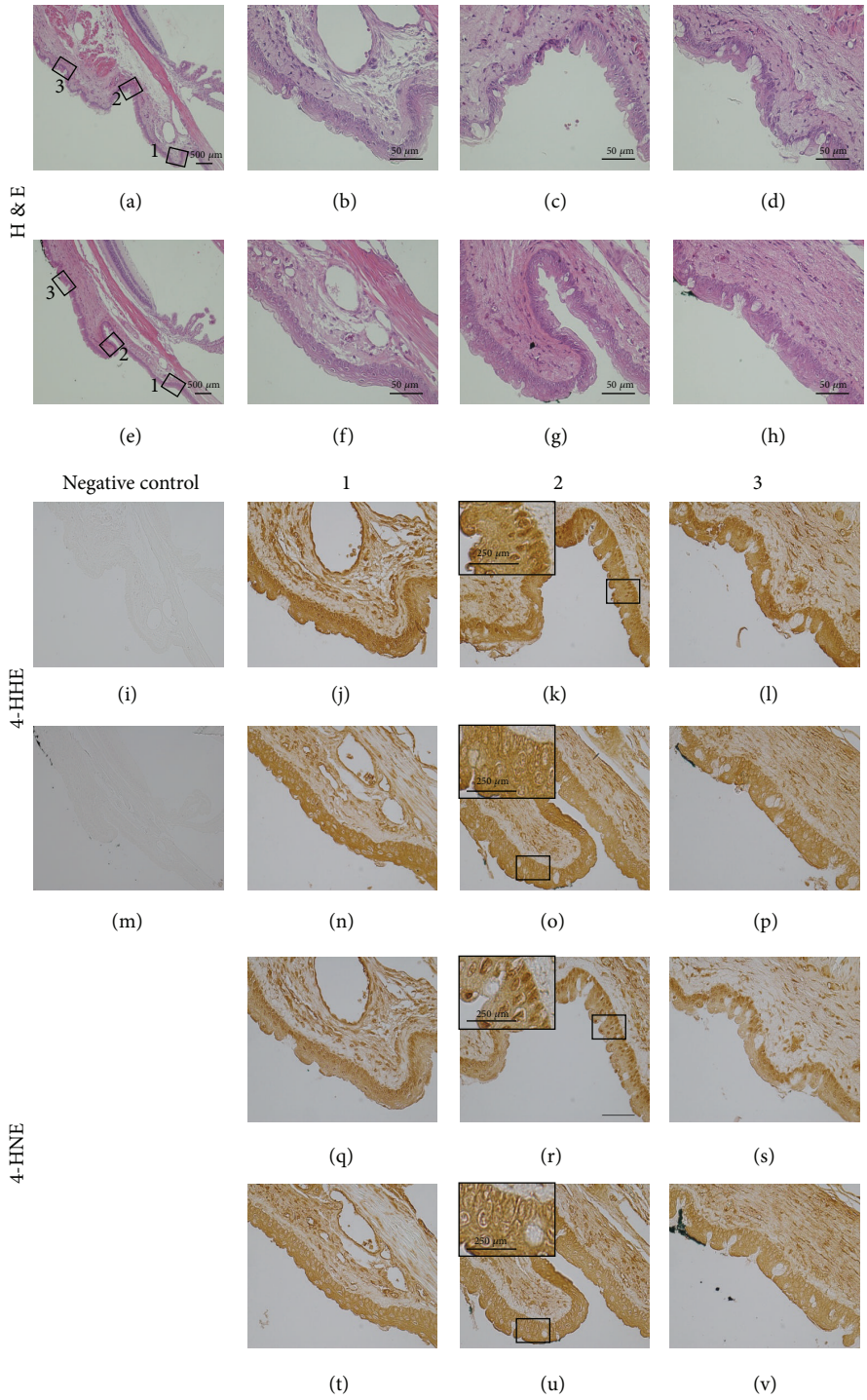

Figure 3: Expressions of aldehyde-modified proteins in conjunctiva from rats exposed to 330 nm wavelength light. The eyes were exposed (a–d, i–l, and q–s) or unexposed (e–h, m–p, and t–v) to the light. Representative images of H&E staining (a–h) 4-HHE (j–l, n–p) and 4-HNE (q–v) immunohistochemistry, and negative control staining (i, m) are shown. Three specimens from the conjunctiva (1, 2, and 3) are shown at high magnifications. Insertions are higher magnifications of squares (k, o, r, and u). H&E: hematoxylin and eosin; 4-HHE: 4-hydroxyhexenal; 4-HNE: 4-hydroxynonenal.

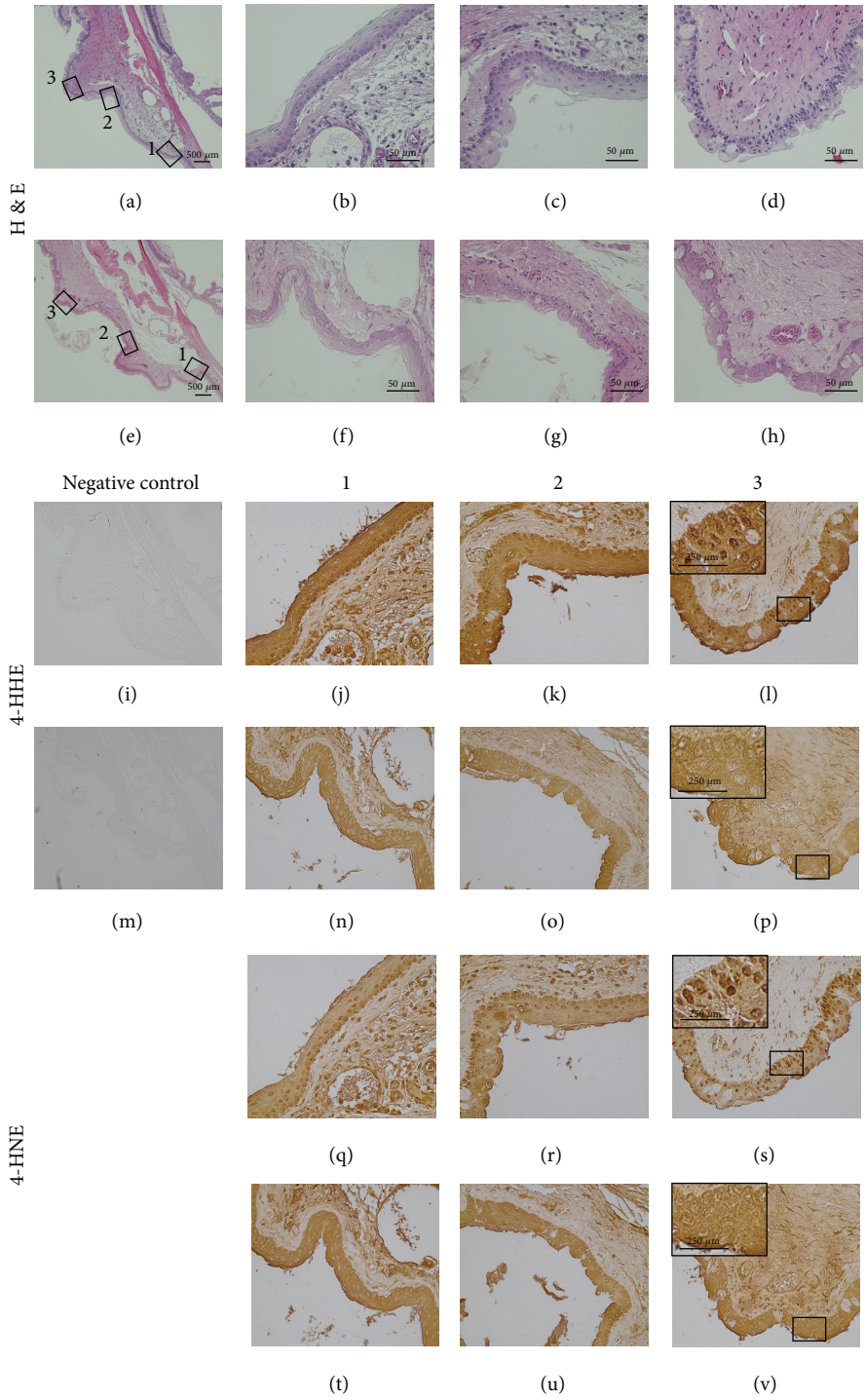

Figure 4: Expressions of aldehyde-modified proteins in conjunctiva from rat exposed to 400 nm wavelength light. The eyes were exposed (a–d, i–l, and q–s) or unexposed (e–h, m–p, and t–v) to the light. Representative images of H&E staining (a–h), 4-HHE (j–l, n–p) and 4-HNE (q–v) immunohistochemistry, and negative control staining (i, m) are shown. Three specimens from the conjunctiva (1, 2, and 3) are shown at high magnifications. Insertions are higher magnifications of squares (l, p, s, and v). H&E: hematoxylin and eosin; 4-HHE: 4-hydroxyhexenal; 4-HNE: 4-hydroxynonenal.

the cornea to prevent drying, and intramuscular injection of anesthetic drug was added to keep the anesthesia. After exposure, rats were kept in the cyclic light (10–20 lux, 12-hour light-dark cycle) for 7 days until enucleation. The number of animals was 6 (12 eyes) in each light wavelength.

Before the start of each exposure, irradiance was measured at the position of the cornea with a radiometer (IL 1400A, International Light Technologies, Peabody, MA, USA) connected to a silicon photodiode detector (SEL033, International Light Technologies), and exposure duration was determined by dividing the target corneal radiant exposure. The radiometer was calibrated prior to each light exposure. After the light exposure, corneal irradiance measured again, and with the initial measurement value was recalculated to secure the radiant exposure to the cornea was around 48.32 ± 0.55 J/cm^2 for 330 nm and 293.0 ± 2.0 J/cm^2 for 400 nm light.

The eyes enucleated were analyzed by H&E and immunohistochemical procedures as described in human specimen analysis.

3. Results and Discussion

At lower magnifications (Figures 1(a)–1(d)), the 4-HHE- and 4-HNE-modified proteins were seen throughout the pterygial specimens including the head, where the corneal-migration front of the pterygium, and the body, where active proliferation of subepithelial connective tissues occurred. At higher magnifications, in the head of the pterygium (Figures 1(e)–1(p)), prominent immunoreactivity of both 4-HHE- and 4-HNE-modificed proteins was observed in the nuclei and cytosol of the epithelium; the immunoreactivity of both aldehyde-modified proteins was moderate in the subepithelial stroma. In the body (Figures 1(q)–1(x)), strong immunoreactivity of the aldehyde-modified proteins was observed in the nuclei and cytosol of the epithelium and in the subepithelial stromal layer. The expression patterns of both aldehyde-modified proteins were consistent in three other pterygial specimens analyzed (data not shown). In the normal conjunctival specimen, only trace immunoreactivity was observed in the epithelial and stromal layers (Figures 2(a)–2(f)).

The results clearly showed marked upregulation of reactive aldehydes-modified proteins in pterygial tissue compared with trace expression in normal conjunctiva; in the pterygial stromal layer, immunoreactivity was more prominent in the proliferating body than in the head. Since 4-HNE modulates cellular proliferation and differentiation including proto-oncogene expression [25], reactive aldehyde might alter the proliferative regulation in the pathogenesis of pterygium. Previously, reduced enzymatic activity of antioxidant enzymes including catalase, superoxide dismutase (SOD), and glutathione peroxidase (GPX) was reported in human pterygial tissue [16]. Protein modification by incubation with reactive aldehydes including 4-HHE and 4-HNE effectively diminishes the enzymatic activities of SOD, GPX, and glutathione S-transferase [26]. Protein modification of thioredoxin, another antioxidant enzyme, by 4-HNE initiates tissue inflammation [27]. Thus, a compromised antioxidative defense system and initiation of inflammation due to oxidative modification of antioxidant enzymes may be involved in the proliferative mechanisms of pterygia.

We also tested a possible association between light exposure and levels of protein modifications by 4-HNE and 4-HHE in rats' conjunctival samples. Compared to eyes unexposed to the light (Figures 3(n)–3(p), 3(t)–3(v), 4(n)–4(p), and 4(t)–4(v)), exposures of UV (Figure 3) or blue light (Figure 4) clearly enhanced the nuclear labeling of both 4-HHE-(Figures 3(j)–3(l) and 4(j)–4(l)) and 4-HNE-(Figures 3(q)–3(s) and 4(q)–4(s)) modified proteins in conjunctivae. The expression patterns of both aldehyde-modified proteins were consistent in 5 other animals analyzed (data not shown).

Although other factors may contribute to pterygial development, intracellular damage accruing from short wavelength light including UV exposure has been suggested to be the most important likely etiology [15, 28, 29]. UV radiation acts directly by phototoxicity or indirectly through free radicals. Intracellularly, the free radicals cause oxidative damage by acting on macromolecules such as proteins, lipids, and nucleic acids [30]. Previous investigators have demonstrated the formation of 8-hydroxydeoxyguanosine, an established marker of oxidized damage in nucleic acids [31, 32] in pterygia [33, 34]. The current study found evidence that oxidation of lipids and proteins also is involved in the pathogenesis of pterygial formation and progression; the results suggest the possible causative relationships between UV or short-wavelength visible light radiation and the oxidation of lipids and proteins in pterygia.

4. Conclusions

Oxidative stress has been suspected of contributing to the pathogenesis of pterygia. We assessed the possible relationship between abnormal protein oxidation and modification by reactive aldehydes in pterygia. The results suggested that protein modifications by 4-HNE and 4-HHE are molecular events involved in the development of pterygia and that short-wavelength light radiations to ocular surface are involved in these aldehyde-modified protein formations.

Conflict of Interests

None of the authors has any financial interests to disclose.

References

[1] M. T. Coroneo, N. di Girolamo, and D. Wakefield, "The pathogenesis of pterygia," *Current Opinion in Ophthalmology*, vol. 10, no. 4, pp. 282–288, 1999.

[2] F. D. Mackenzie, L. W. Hirst, D. Battistutta, and A. Green, "Risk analysis in the development of pterygia," *Ophthalmology*, vol. 99, no. 7, pp. 1056–1061, 1992.

[3] S. M. Saw and D. Tan, "Pterygium: prevalence, demography and risk factors," *Ophthalmic Epidemiology*, vol. 6, no. 3, pp. 219–228, 1999.

[4] A. J. Maloof, A. Ho, and M. T. Coroneo, "Influence of corneal shape on limbal light focusing," *Investigative Ophthalmology and Visual Science*, vol. 35, no. 5, pp. 2592–2598, 1994.

[5] M. T. Coroneo, N. W. Muller-Stolzenburg, and A. Ho, "Peripheral light focusing by the anterior eye and the ophthalmohelioses," *Ophthalmic Surgery*, vol. 22, no. 12, pp. 705–711, 1991.

[6] L. Kria, A. Ohira, and T. Amemiya, "Immunohistochemical localization of basic fibroblast growth factor, platelet derived growth factor, transforming growth factor-β and tumor necrosis factor-α in the pterygium," *Acta Histochemica*, vol. 98, no. 2, pp. 195–201, 1996.

[7] S. Moncada, R. M. J. Palmer, and E. A. Higgs, "Nitric oxide: physiology, pathophysiology, and pharmacology," *Pharmacological Reviews*, vol. 43, no. 2, pp. 109–142, 1991.

[8] A. L. Marcovich, Y. Morad, J. Sandbank et al., "Angiogenesis in pterygium: morphometric and immunohistochemical study," *Current Eye Research*, vol. 25, no. 1, pp. 17–22, 2002.

[9] A. Papapetropoulos, G. García-Cardeña, J. A. Madri, and W. C. Sessa, "Nitric oxide production contributes to the angiogenic properties of vascular endothelial growth factor in human endothelial cells," *Journal of Clinical Investigation*, vol. 100, no. 12, pp. 3131–3139, 1997.

[10] H. R. Taylor, S. K. West, F. S. Rosenthal, B. Munoz, H. S. Newland, and E. A. Emmett, "Corneal changes associated with chronic UV irradiation," *Archives of Ophthalmology*, vol. 107, no. 10, pp. 1481–1484, 1989.

[11] O. D. Schein, "Phototoxicity and the cornea," *Journal of the National Medical Association*, vol. 84, no. 7, pp. 579–583, 1992.

[12] J. Cejkova and Z. Lojda, "The damaging effect of UV rays below 320 mm on the rabbit anterior eye segment, II. Enzyme histochemical changes and plasmin activity after prolonged irradiation," *Acta Histochemica*, vol. 97, no. 2, pp. 183–188, 1995.

[13] D. J. Moran and F. C. Hollows, "Pterygium and ultraviolet radiation: a positive correlation," *British Journal of Ophthalmology*, vol. 68, no. 5, pp. 343–346, 1984.

[14] A. P. Cullen, "Photokeratitis and other phototoxic effects on the cornea and conjunctiva," *International Journal of Toxicology*, vol. 21, no. 6, pp. 455–464, 2002.

[15] H. C. Kau, C. C. Tsai, C. F. Lee et al., "Increased oxidative DNA damage, 8-hydroxydeoxy-guanosine, in human pterygium," *Eye*, vol. 20, no. 7, pp. 826–831, 2006.

[16] M. Balci, S. Şahin, F. M. Mutlu, R. Yağci, P. Karanci, and M. Yildiz, "Investigation of oxidative stress in pterygium tissue," *Molecular Vision*, vol. 17, pp. 443–447, 2011.

[17] M. Tanito, H. Haniu, M. H. Elliott, A. K. Singh, H. Matsumoto, and R. E. Anderson, "Identification of 4-hydroxynonenal-modified retinal proteins induced by photooxidative stress prior to retinal degeneration," *Free Radical Biology and Medicine*, vol. 41, no. 12, pp. 1847–1859, 2006.

[18] H. Esterbauer, "Cytotoxicity and genotoxicity of lipid-oxidation products," *The American Journal of Clinical Nutrition*, vol. 57, pp. 779S–786S, 1993.

[19] K. Uchida and E. R. Stadtman, "Modification of histidine residues in proteins by reaction with 4-hydroxynonenal," *Proceedings of the National Academy of Sciences of the United States of America*, vol. 89, no. 10, pp. 4544–4548, 1992.

[20] Y. C. Awasthi, Y. Yang, N. K. Tiwari et al., "Regulation of 4-hydroxynonenal-mediated signaling by glutathione S-transferases," *Free Radical Biology and Medicine*, vol. 37, no. 5, pp. 607–619, 2004.

[21] M. Tanito, M. P. Agbaga, and R. E. Anderson, "Upregulation of thioredoxin system via Nrf2-antioxidant responsive element pathway in adaptive-retinal neuroprotection in vivo and in vitro," *Free Radical Biology and Medicine*, vol. 42, no. 12, pp. 1838–1850, 2007.

[22] K. Uchida, L. I. Szweda, H. Z. Chae, and E. R. Stadtman, "Immunochemical detection of 4-hydroxynonenal protein adducts in oxidized hepatocytes," *Proceedings of the National Academy of Sciences of the United States of America*, vol. 90, no. 18, pp. 8742–8746, 1993.

[23] S. Kaidzu, M. Tanito, A. Ohira et al., "Immunohistochemical analysis of aldehyde-modified proteins in drusen in cynomolgus monkeys (Macaca fascicularis)," *Experimental Eye Research*, vol. 86, no. 5, pp. 856–859, 2008.

[24] M. Tanito, M. H. Elliott, Y. Kotake, and R. E. Anderson, "Protein modifications by 4-hydroxynonenal and 4-hydroxyhexenal in light-exposed rat retina," *Investigative Ophthalmology and Visual Science*, vol. 46, no. 10, pp. 3859–3868, 2005.

[25] F. Guéraud, M. Atalay, N. Bresgen et al., "Chemistry and biochemistry of lipid peroxidation products," *Free Radical Research*, vol. 44, no. 10, pp. 1098–1124, 2010.

[26] J. F. Lesgards, C. Gauthier, J. Iovanna, N. Vidal, A. Dolla, and P. Stocker, "Effect of reactive oxygen and carbonyl species on crucial cellular antioxidant enzymes," *Chemico-Biological Interactions*, vol. 190, no. 1, pp. 28–34, 2011.

[27] Y. M. Go, P. J. Halvey, J. M. Hansen, M. Reed, J. Pohl, and D. P. Jones, "Reactive aldehyde modification of thioredoxin-1 activates early steps of inflammation and cell adhesion," *The American Journal of Pathology*, vol. 171, no. 5, pp. 1670–1681, 2007.

[28] D. Reisman, J. W. McFadden, and G. Lu, "Loss of heterozygosity and p53 expression in Pterygium," *Cancer Letters*, vol. 206, no. 1, pp. 77–83, 2004.

[29] L. Wang, W. Dai, and L. Lu, "Ultraviolet irradiation-induced K^+ channel activity involving p53 activation in corneal epithelial cells," *Oncogene*, vol. 24, no. 18, pp. 3020–3027, 2005.

[30] M. Tanito and R. E. Anderson, "Dual roles of polyunsaturated fatty acids in retinal physiology and pathophysiology associated with retinal degeneration," *Clinical Lipidology*, vol. 4, no. 6, pp. 821–827, 2009.

[31] S. D. Bruner, D. P. G. Norman, and G. L. Verdine, "Structural basis for recognition and repair of the endogenous mutagen 8-oxoguanine in DNA," *Nature*, vol. 403, no. 6772, pp. 859–866, 2000.

[32] M. Ichihashi, M. Ueda, A. Budiyanto et al., "UV-induced skin damage," *Toxicology*, vol. 189, no. 1-2, pp. 21–39, 2003.

[33] Y. Y. Tsai, Y. W. Cheng, H. Lee et al., "Oxidative DNA damage in pterygium," *Molecular Vision*, vol. 11, pp. 71–75, 2005.

[34] M. T. Perra, C. Maxia, A. Corbu et al., "Oxidative stress in pterygium: relationship between p53 and 8-hydroxydeoxyguanosine," *Molecular Vision*, vol. 12, pp. 1136–1142, 2006.

Hindawi Publishing Corporation
Oxidative Medicine and Cellular Longevity
Volume 2013, Article ID 213505, 11 pages
http://dx.doi.org/10.1155/2013/213505

Research Article

Effect of Lutein and Antioxidant Supplementation on VEGF Expression, MMP-2 Activity, and Ultrastructural Alterations in Apolipoprotein E-Deficient Mouse

Patricia Fernández-Robredo,[1] Luis M. Sádaba,[2] Angel Salinas-Alamán,[2] Sergio Recalde,[1] José A. Rodríguez,[3] and Alfredo García-Layana[1,2]

[1] *Experimental Ophthalmology Laboratory, Clínica Universidad de Navarra, School of Medicine, University of Navarra, ES-31008 Pamplona, Spain*
[2] *Department of Ophthalmology, Clínica Universidad de Navarra, School of Medicine, University of Navarra, Pio XII 36, ES-31008 Pamplona, Spain*
[3] *Atherothrombosis Research Laboratory, Division of Cardiovascular Sciences, Center for Applied Medical Research (CIMA), University of Navarra, ES-31008 Pamplona, Spain*

Correspondence should be addressed to Alfredo García-Layana; aglayana@unav.es

Received 7 February 2013; Revised 5 April 2013; Accepted 8 April 2013

Academic Editor: Kota V. Ramana

Oxidative stress is involved in the pathogenesis of several diseases such as atherosclerosis and age-related macular degeneration (AMD). ApoE-deficient mice (apoE$^{-/-}$) are a well-established model of genetic hypercholesterolemia and develop retinal alterations similar to those found in humans with AMD. Thus supplementation with lutein or multivitamin plus lutein and glutathione complex (MV) could prevent the onset of these alterations. ApoE$^{-/-}$ mice (n = 40, 3 months old) were treated daily for 3 months with lutein (AE-LUT) or MV (two doses): AE-MV15 (15 mg/kg/day) and AE-MV50 (50 mg/kg/day) and were compared to controls with vehicle (AE-C). Wild-type mice (n = 10) were also used as control (WT-C). ApoE$^{-/-}$ mice showed higher retinal lipid peroxidation and increased VEGF expression and MMP-2 activity, associated with ultrastructural alterations such as basal laminar deposits, vacuoles, and an increase in Bruch's membrane thickness. While lutein alone partially prevented the alterations observed in apoE$^{-/-}$ mice, MV treatment substantially reduced VEGF levels and MMP-2 activity and ameliorated the retinal morphological alterations. These results suggest that oxidative stress in addition to an increased expression and activity of proangiogenic factors could participate in the onset or development of retinal alterations of apoE$^{-/-}$ mice. Moreover, these changes could be prevented by efficient antioxidant treatments.

1. Introduction

Oxidative and nitrosative stress can induce alterations in DNA, proteins, and lipids, and extensive data suggest that oxidative damage may play a major causal role in a number of human diseases such as atherosclerosis, cancer, and cataracts as well as retinal pathologies such as age-related macular degeneration (AMD) [1, 2]. Currently, AMD is the most common cause of severe and irreversible blindness in Europe and the United States in people older than 65 years, and its prevalence is expected to increase as the population ages [3, 4]. The pathogenesis of AMD is unclear; however, several mechanisms influenced by genetic, systemic health, and environmental risk factors have been proposed. Numerous studies have also shown a relationship between cardiovascular disease and AMD, although others have not been able to verify this correlation. Dietary fat, in particular, cholesterol, is positively linked to increased incidence of coronary heart disease (CHD), and evidence suggests that abnormal lipid levels may contribute to the development of AMD, either directly or through the promotion of vascular disease [1, 2, 5].

Animal models attempting to recreate AMD through phototoxicity, senescence acceleration, candidate gene manipulation, and high-fat diets do not fully replicate the clinical, histologic, and angiographic features of the human condition, probably because of the multifactorial aspect of the disease [6]. The histopathology of early AMD reveals accumulation of specific lipid-rich deposits under the retinal pigment epithelium (RPE) [7]. Moreover, as it has been postulated on the hypothetical model of RPE oxidant injury, matrix metalloproteinases could participate in extracellular matrix (ECM) turnover in Bruch's membrane (BM) [8]. Degenerative changes of the RPE and photoreceptor cells are early events in AMD [9], and it has been demonstrated that apoE deficiency predisposes to ultrastructural changes in BM [10]. Apolipoprotein E-deficient mice (apoE$^{-/-}$) develop spontaneous hypercholesterolemia in a few weeks [11] and also display morphological and ultrastructural alterations in RPE [10, 12, 13] similar to those in human AMD. Based on functional and structural analyses, the apoE$^{-/-}$ mouse constitutes a valuable tool in elucidating the underlying mechanism of retinal degeneration [13].

Lutein and zeaxanthin are essential carotenoids that need to be obtained from certain vegetables, such as spinach, corn, pumpkin, and egg yolk [14]. They accumulate in the retina, where they play an important role in maintaining visual sensitivity and protecting against light-induced retinal damage [15, 16]. In the retina, lutein and zeaxanthin coexist with large amounts of polyunsaturated fatty acids that are highly susceptible to oxidation suggesting that antioxidants could prevent degenerative pathologies in which oxidative stress is of high importance such as AMD [17–20]. Our group previously showed an increase in oxidative processes related to the retinal morphological alterations observed in apoE$^{-/-}$ mice and other models of hypercholesterolemia. Furthermore, we have reported the protective effect of antioxidants, such as vitamins C and E, lutein, egg yolk, and a multivitamin-mineral complex on retinal oxidative stress and hypercholesterolemia-derived ultrastructural alterations in apoE$^{-/-}$ mice [21–24].

The aim of the present study was to investigate the effect of lutein and a multivitamin complex with lutein and glutathione on systemic and retinal biochemical and ultrastructural parameters in apoE$^{-/-}$ mice.

2. Material and Methods

2.1. Experimental Design. Ten 3-month-old male mice C57BL/6 and forty apoE$^{-/-}$ mice were used for this study. Progenitor couples were obtained from "Center for Transgene Technology and Gene Therapy," Flanders Interuniversity Institute for Biotechnology, Leuven (Belgium). All experimental procedures followed the Guidelines for the Use of Animals in Association for Research in Vision and Ophthalmology (ARVO) and were approved by the Animal Research Ethics Committee of the Universidad de Navarra. Animal welfare was applied during all experimental process and animals were euthanized by CO_2 inhalation according to ethics guidelines.

Animals were randomly divided into five experimental groups ($n = 10$), fed a standard rodent chow (9605/8, Harlan Teklad TRM, Madison, WI, USA) water ad libitum for 90 days, and housed in cages in a temperature-controlled room (20–22°C) with a 12-hour light/dark cycle. The five study groups were as follows: wild type (WT-C) and apoE$^{-/-}$ (AE-C) receiving vehicle; apoE$^{-/-}$ (AE-MV15) mice receiving 15 mg/kg/d of multivitamin-mineral, glutathione and lutein complex (providing 0.027 mg/kg/day of lutein) (composition in Table 1); apoE$^{-/-}$ (AE-MV50) mice receiving 50 mg/kg/d of multivitamin-mineral, glutathione and lutein complex (providing 0.086 mg/kg/day of lutein); and apoE$^{-/-}$ (AE-LUT) mice receiving 0.093 mg/kg/d lutein. Multivitamin treatment was administered according to the approved regimen for humans.

The treatments were emulsified in a mixture of water : soybean oil : Tween-80 (1 : 1 : 0.02; v : v : v) and administered daily by gastroesophageal cannula for 3 months (100 μL). Purified lutein was kindly provided by Dr. Christine Gartner (Cognis, Germany), and multivitamin complex, Nutrof, was a kind gift by Laboratorios Thea (Barcelona, Spain).

At the beginning and end of the treatment, eyes were examined by indirect fundoscopy with a 78-diopter lens and 0.5% cycloplegic eye drops. No retinal alterations were found in any group.

2.2. Lipid Plasma Analysis. Blood samples were collected after mice were killed and plasma obtained after separating the red blood cells by centrifugation (2,600 g, 10 min, 4°C) and were immediately frozen in liquid nitrogen and stored at −80°C. Concentrations of plasma total cholesterol (TC) and triglycerides (TG) were measured following the manufacturers' instructions (Sigma Chemical Co., St. Louis, MO), using a microplate ELISA reader and calculated from the linear range of standards.

2.3. Retinal and RPE-Choroid Homogenates Preparation. Immediately after blood collection, eyes were enucleated and transferred to a saline solution (pH 7.4). Retinas were rapidly dissected by making a small incision with a scalpel 1 mm behind the limbus and extending the incision through 360° using fine ophthalmic scissors. Anterior segment structures (cornea, iris, and lens) were removed. RPE-choroid samples were homogenized with a Teflon pestle in lysis buffer (RIPA buffer) and centrifuged for 20 minutes at 13,000 rpm at 4°C. Supernatant was collected and protein concentration was determined by Bradford assay with slight modification [21, 24].

2.4. Lipid Peroxidation in Plasma and Retinal Homogenates Based on Measurement of Thiobarbituric Acid Reactive Substances. Thiobarbituric acid reactive substances (TBARS) were measured in plasma and retinal homogenates as an index of oxidative stress, increasing the sensitivity by using a fluorometric modification of the method of Conti et al. as described [25]. Values were corrected by total protein content.

Table 1: Daily dose per body weight of substances in the multivitamin-mineral complex.

	100 g	15 mg/kg/day (μg)	50 mg/kg/day (μg)
Vitamins			
Vitamin A	71.7 mg	0.32	1.08
β-carotene	0.4 g	1.8	6
Vitamin C (ascorbic acid)	10.7 g	48.15	160.5
Vitamin E (d-α-tocopherol)	1.8 g	8.1	27
Vitamin B_1 (thiamin)	250.8 mg	1.13	3.78
Vitamin B_2 (riboflavin)	286.6 mg	1.3	4.33
Vitamin B_3 (niacin)	3.2 g	14.4	48
Vitamin B_6 (pyridoxine)	358.3 mg	1.61	5.37
Vitamin B_9 (folic acid)	35.8 mg	0.16	0.54
Vitamin B_{12} (cyanocobalamin)	179.2 μg	0.00081	0.00269
Oligoelements			
Zinc (Zn)	1.3 g	5.85	19.5
Magnesium (Mg)	1.8 g	8.1	26.9
Manganese (Mn)	179.2 mg	0.81	2.69
Selenium (Se)	4.5 mg	0.02	0.066
Others			
Glutathione	179.2 mg	0.81	2.69
Lutein	179.2 mg	0.81	2.69

Data per 100 g of product are shown as mg and for daily dose in μg. Calculation based on a 30 g mouse.

2.5. Measurement of Total Nitrites and Nitrates as an Indirect Indicator of NO Synthesis. Nitric oxide (NO) is oxidized rapidly in biological tissues, firstly to nitrites and secondly to nitrates. Determination of nitrites (NO_2^-) and nitrates (NO_3^-) is an indirect indicator of NO synthesis. Methodology employed for nitrites and nitrates measurement was adapted from Archer and Marzinzig [26, 27] with slight modifications. Briefly, samples were deproteinized with sulfosalicilic acid (25%), mixed with 5 μL NaOH 1 M to arise pH 7,6, and centrifuged for 10 minutes (10,000 g). Standard curve was prepared with $NaNO_3$ and ranged between 0 and 30 μM. Fourteen mU of nitrate reductase (NADPH 40 μM and FAD 1 μM in Tris 20 mM; pH 7,6) were added to 10 μL of supernatant. Samples were developed by adding diaminonaphthalene (DAN) 0.1 mg/mL and reaction was stopped with NaOH 2.8 mM. Fluorescence at 410 nm was read in a microplate reader (POLARstar Galaxy, BMG LABTECH GmbH) after excitation at 380 nm.

2.6. Western Blotting for Vascular Endothelial Growth Factor (VEGF). Equal amounts of RPE-choroid homogenates (5 μg) were mixed with Laemmli buffer (62.5 mM Tris-HCl, pH 6.8; 2% SDS; 10% glycerol; 0.1% bromophenol blue) and boiled for 5 min. Samples were separated on 12% SDS-PAGE gels and transferred to a nitrocellulose membrane. After blocking with 5% skimmed milk (w/v), 0.1% Tween-20 (w/v) in TBS for 1 hour at room temperature, membranes were exposed to the primary antibody (0.2 μg/μL, monoclonal anti-VEGF, sc7269, Santa Cruz Biotechnology Inc., Santa Cruz, CA) at room temperature for 1 hour followed by incubation with a horseradish peroxidase-conjugated goat antimouse antibody (sc2005; 0.4 μg/μL, Santa Cruz Biotechnology Inc.). Signals were detected with an enhanced chemoluminescence (ECL) kit (ECL western blotting detection kit, GE Healthcare, Fairfield, CT) and exposure to autoradiographic film (Hyperfilm ECL, GE Healthcare). The relative intensities of the immunoreactive bands were analyzed with Quantity One software (version 4.2.2, Bio-Rad Laboratories, Hercules, CA). The loading was verified by Ponceau S red, and the same blot was stripped and reblotted with an anti-β-actin monoclonal antibody (Sigma-Aldrich) to normalize the VEGF level.

2.7. Gelatin Zymography Assay for Matrix Metalloproteinase-2 (MMP-2) Activity. MMP-2 activity was quantified by gelatin zymography on RPE-choroid homogenates [28]. Eight μg of total protein from homogenate supernatants were mixed with nonreducing sample buffer (62.5 mM Tris-HCl, pH 6.8; 10% glycerol; 0.1% bromophenol blue) and electrophoresed directly on 9% SDS-polyacrylamide gels (SDS-PAGE) containing 0.1% gelatin (w/v). After electrophoresis, gels were washed 4 times for 20 minutes at room temperature in a 2.5% (v/v) Triton X-100 solution to remove excess of SDS, transferred to a solution (zymogram development buffer, Bio-Rad), and incubated for at least 18 hr at 37°C. Protein fixation was developed by incubating gels for 15 minutes with 50% methanol/7% acetic acid and then washing for 30 minutes (6 times of 5 minutes each) with distilled water. After that, gels were stained for 1 hour with GelCode Blue Stain Reagent (Pierce, Rockford, USA) counterstained with distilled water and then analyzed with Quantity One software (version 4.2.2, Bio-Rad) after densitometric scanning of the gels. The active MMP-2/(active MMP-2 + proMMP-2) intensity ratio was designated as the MMP-2 activation ratio. Each zymography assay was repeated at least three times to ensure accuracy.

2.8. Electron Microscopy. Three or four eyes from each group were processed for histological examination. The whole enucleated murine eyes were fixed in 2.5% glutaraldehyde, 0.1 mol/L cacodylate, 0.2 mol/L PBS. The posterior pole was dissected as described above and postfixed in 1% osmium tetroxide, stained with 1% uranyl acetate, and embedded in Epon Araldite resin. One-micrometer sections were cut with an ultramicrotome, stained with 2% toluidine blue O, and examined under a light microscope to determine the areas of interest. Thin sections (approximately 50–90 nm) were cut, collected on copper grids, and stained with 4% uranyl acetate and lead citrate. Subsequently, three sections from each animal were evaluated by transmission electron microscopy (TEM) (EM10, Carl Zeiss, Thornwood, NY) and photographed for posterior analysis. For semiquantitative scoring, 2-3 representative high-power micrographs were made of each low-power section. The high-power micrographs were graded by two independent examiners unaware of the experimental procedures. The variables evaluated were as follows: frequency of BLamD, BM thickness, presence of vacuoles in RPE, presence of vacuoles and lucent areas in BM, and presence of deposits of amorphous material in the RPE. BM thickness was directly measured in three different standardized locations in each image and averaged to provide a mean score for that micrograph. The mean of high-power micrographs was used to assign an average BM thickness for an individual specimen (μm). The remaining variables were graded following previous score grading method [24, 29] with slight modification: absence (−), any (+), moderate (++), and severe presence (+++). In addition, the frequency of BLamD was classified as follows. "Any BLamD" was defined as the presence of any discrete focal nodule of homogenous material of intermediate electron density between the RPE cell membrane and BM in at least one micrograph. "Severe BLamD" was defined as the presence, in at least three micrographs, of the following: continuous BLamD extending under two or more cells, deposit thickness equal to or greater than 20% of RPE cell cross-sectional thickness.

2.9. Statistical Analysis. Values are reported throughout as the mean ± the standard error of the mean (SEM). Statistical significance for biochemical parameters and BM thickness was determined applying analysis of variance (ANOVA) or Kruskal Wallis test to assess differences among groups. After a significant ANOVA or Kruskal Wallis, comparisons between groups were made with Bonferroni posthoc or Mann Whitney test, respectively. Statistical significance was accepted at the 95% confidence level ($P < 0.05$), and analysis was performed by using the computer program SPSS (v. 15.0, SPSS Inc. Chicago, USA).

3. Results

3.1. ApoE$^{-/-}$ Mouse Weight and Lipid Profile. Table 2 summarizes the general characteristics of the different animal groups. AE-C weight was higher than WT-C weight ($P < 0.05$), and apoE$^{-/-}$ phenotype was confirmed by measuring plasma TC. Plasma TC and TG in the AE-C were significantly higher ($P < 0.001$ and $P < 0.05$, resp.) than in WT-C mice (Table 2).

Table 2: Body weight, TC, and TG of the different animal groups at the time of sacrifice.

	Body weight	TC	TG
WT-C	28.3 ± 3.3	69.9 ± 9.5	83.2 ± 11.6
AE-C	35.6 ± 3.7*	624.7 ± 169.0***	123.4 ± 15.0*
AE-MV15	34.3 ± 2.8*	675.7 ± 142.6***	104.7 ± 21.1
AE-MV50	34.4 ± 2.4*	663.1 ± 161.4***	86.4 ± 30.7†
AE-LUT	35.6 ± 2.3*	675.7 ± 189.9***	137.6 ± 53.3

Data are expressed as g (body weight) and mg/dL (TC and TG) ± S.D. Statistically significant differences from WT-C are marked as $^{*}P < 0.05$ and $^{***}P < 0.001$ and from AE-C as $^{\dagger}P < 0.05$. (n = 8–10).

Table 3: Plasma and retinal lipid peroxidation of the different animal groups at the time of sacrifice.

	TBARS plasma	TBARS retina	NO retina
WT-C	1.22 ± 0.06	3.02 ± 0.33	11.03 ± 1.18
AE-C	1.66 ± 0.10**	8.72 ± 0.78**	5.91 ± 0.85**
AE-MV15	1.32 ± 0.08†	4.77 ± 0.43††	2.13 ± 0.27†
AE-MV50	1.25 ± 0.11†	6.58 ± 0.67†	3.64 ± 0.48†
AE-LUT	1.57 ± 0.08	7.83 ± 0.36	2.21 ± 0.90†

Data are expressed as μM malondialdehyde (MDA; TBARS plasma), nmol MDA/mg protein (TBARS retina), and nmol nitrates/mg protein (NO retina) media ± S.E.M. Statistically significant differences from WT-C are marked as $^{*}P < 0.05$ and $^{**}P < 0.01$ and from AE-C as $^{\dagger}P < 0.05$ and $^{\dagger\dagger}P < 0.01$ (n = 8–10).

All mice had similar weight evolution during treatment, and treatments did not modify mice weight. Also, diet supplementation with nutritional supplement or lutein did not modify TC in apoE$^{-/-}$ mice, showing that the effects observed in this study were independent of cholesterol concentration modifications. Nutritional supplementation in diet, in addition to not increasing plasma TC concentration, induces a decrease in TG concentration in apoE$^{-/-}$ mice ($P < 0.05$). Lutein supplementation did not significantly modify TG levels (Table 2).

3.2. Plasma and Retinal Lipid Peroxidation. AE-C animals showed an increase in plasma and retinal lipid peroxidation ($P < 0.01$), as assessed by TBARS production, compared with WT-C (Table 3).

Both doses of nutritional complex (MV) induced a reduction in systemic and retinal lipid peroxidation ($P < 0.05$ and $P < 0.01$) to values similar to control group (Table 3). AE-LUT animals did not show statistical differences regarding lipid peroxidation when compared to AE-C group (Table 3).

3.3. NO in Retina. Retinal NO synthesis was lower in AE-C compared with WT-C animals ($P < 0.01$, Table 3). All treatments administered were able to significantly ($P < 0.05$, Table 3) reduce NO synthesis compared to AE-C group.

Table 4: The effect of the different treatments on RPE and BM deposit severity, vacuolization, and BM thickness.

	WT-C	AE-C	AE-MV15	AE-MV50	AE-LUT
BM thickness	$0.45 \pm 0.03^{**}$	1.08 ± 0.05	0.78 ± 0.07	$0.58 \pm 0.04^{*}$	0.75 ± 0.06
Frequency of images with evidence of BLamD	−	+++	++	+	++
Presence of lucent areas in BM	−	++	+	−	+
Vacuolization in RPE	−	+++	+	+	+

Absence (−), any (+), moderate (++), and severe (+++) presence. BM thickness shown in μm (mean ± SD). $^{*}P < 0.05$ and $^{**}P < 0.001$ versus AE-C (n = 3-4 for each group).

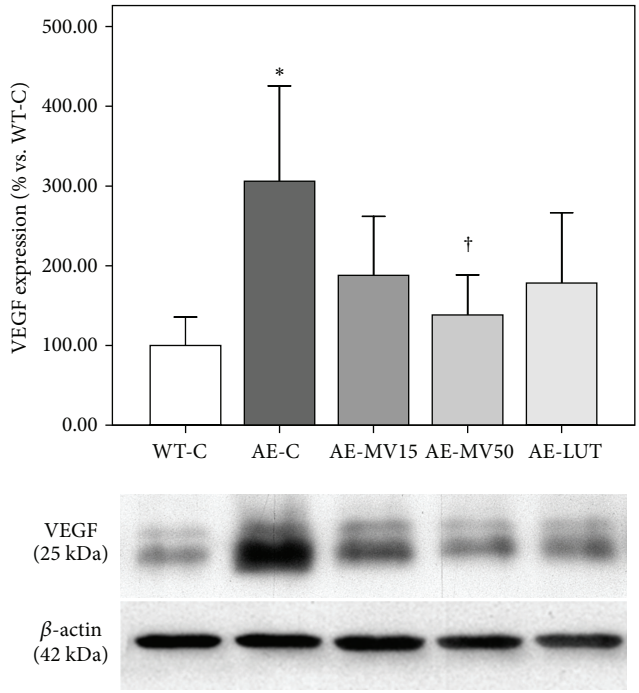

Figure 1: Changes in VEGF protein expression in RPE-choroid homogenates, reported as percentage increase with respect to untreated wt mice. Augmented VEGF protein in apoE$^{-/-}$, assessed by western blot (densitometric analysis and representative blot showing the 25 kDa VEGF monomer), is reduced in apoE$^{-/-}$ MV-50. β-actin was used as load control. Differences from WT-C are marked as $^{*}P < 0.05$ and from AE-C as $^{\dagger}P < 0.05$ (n = 6-7).

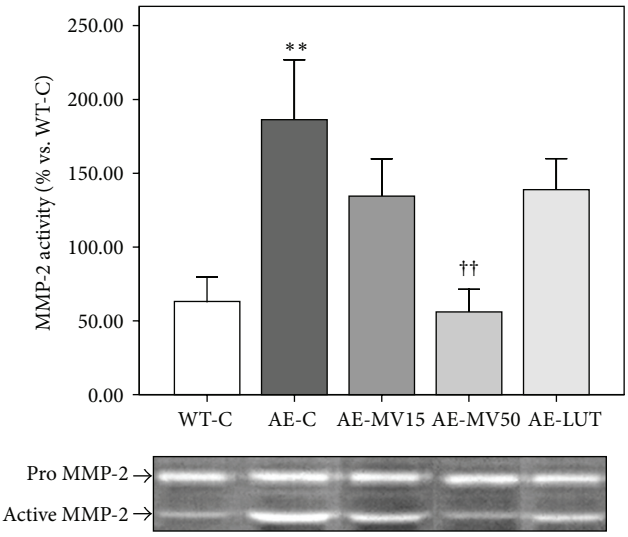

Figure 2: Zymogram analysis of MMP-2 activity in RPE-choroid, reported as percentage increase with respect to untreated wt mice. Eyecups homogenates of apoE$^{-/-}$ mice showed an increase in gelatinase activity in comparison to WT-C mice. Mutivitamin treatment (AE-MV50) reduced MMP-2 activity back to control levels. AE-LUT and AE-MV15 groups exhibited a little but no significant reduction. Differences from WT-C are marked as $^{**}P < 0.01$ and from AE-C as $^{\dagger\dagger}P < 0.01$ (n = 6-7).

3.4. VEGF Expression in ApoE$^{-/-}$ Mouse and the Effect of Supplementation. Western blot with anti-VEGF antibody revealed an almost 3-fold increase in the AE-C group in comparison to WT-C ($P < 0.05$, Figure 1).

AE-MV50 mice showed VEGF protein levels similar to WT-C ($P < 0.05$ versus AE-C, Figure 1). AE-LUT and AE-MV15 had a marginal reduction when compared to AE-C animals, but this difference did not reach statistical significance.

3.5. MMP-2 Activity in ApoE$^{-/-}$ Mouse and the Effect of Supplementation. Zymography analysis of total RPE-choroid homogenates showed that MMP-2 activity increased in AE-C groups when compared to WT-C tissues ($P < 0.01$, Figure 2). Gelatinase activity was significantly ($P < 0.01$) reduced in the AE-MV50 group compared with AE-C. AE-MV15 ($P = 0.062$) and AE-LUT ($P = 0.072$) animals did not show statistically significant MMP-2 activity modification, although a reduction was observed (Figure 2).

3.6. Ultrastructural Alterations in ApoE$^{-/-}$ Mice and the Effect of Supplementation with Lutein and Multivitamin Complex. None of the eyes examined microscopically showed any type of drusen or neovascularization, but some alterations were observed in apoE$^{-/-}$ mice (see below). ApoE$^{-/-}$ mice showed basal laminar deposits, vacuoles, and an increase in BM thickness. While lutein alone partially prevented the alterations observed in apoE$^{-/-}$ mice, MV treatment substantially ameliorated the retinal morphological alterations. Figure 3 depicts photomicrographs of retinal cross sections from representative mice of WT-C and AE-C groups, Figure 4 shows representative images of the AE-treated groups, and Table 4 summarized the score grading for microscopic parameters analyzed.

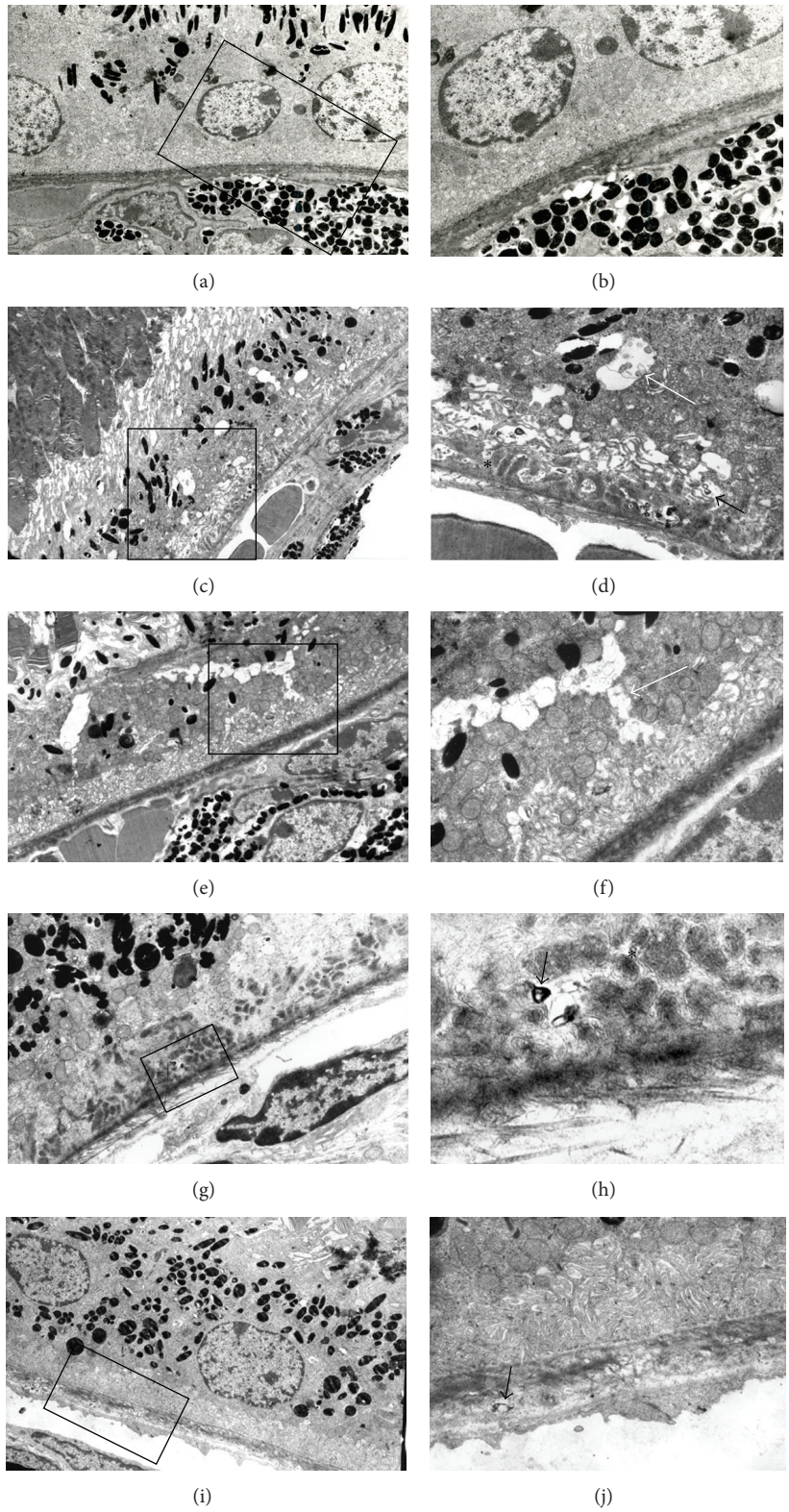

Figure 3: Transmission electron micrographs of the outer retina and choroid of WT-C (a, b) and AE-C (c–j) groups (n = 3-4). Photographs of wt mice reveal no accumulation of sub-RPE deposits, with normal RPE basal infoldings and BM ((a) ×2, 250 and detail in (b) ×4, 250). In contrast, apoE$^{-/-}$ control mice show some ultrastructural alterations like vacuolization in RPE (white arrow), swelling of basal infoldings (black arrow), subRPE electrodense deposits (black asterisk) ((c) ×1, 200 and detail in (d) ×5, 250), and opening of intercellular junctions ((e) ×2, 500 and detail in (f), ×5, 250; white arrow). Also, electrodense material, seeming BLamD (black asterisk) is observed in RPE ((g) ×2, 500 and details in (h) ×10, 000) combined with some amorphous electro-dense material (black arrow). BM thickening is evident compared with WT-C animals, and non-membrane-bound lucent vacuoles inside BM were present ((i) ×3, 975 and (j) ×7, 725; black arrow).

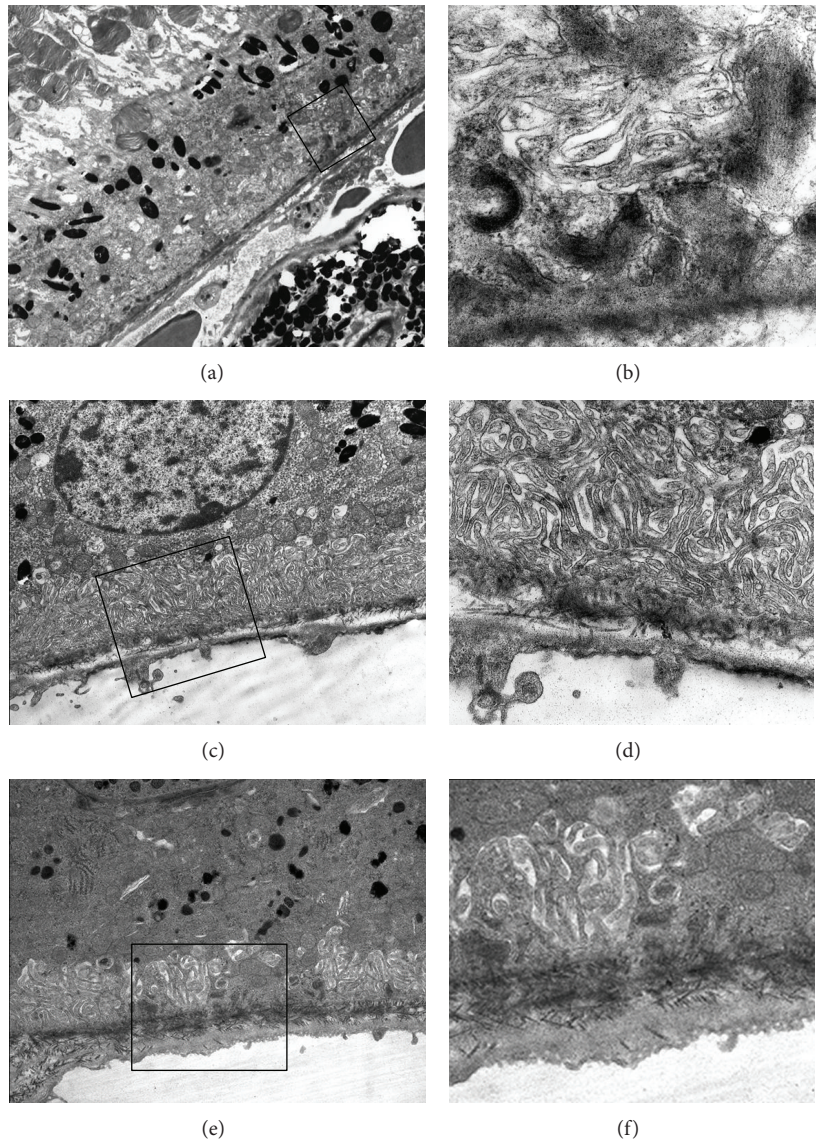

Figure 4: TEM from apoE$^{-/-}$ animals supplemented with the different treatments. AE-MV15 ((a) ×2, 500 and (b) ×10, 000) and AE-LUT ((e) ×5, 250 and (f) ×7, 725) animals showed less confluent and more diffuse BLamD and less lucent areas in BM, whereas those alterations were almost absent in AE-MV50 mice ((c) ×5, 250 and (d) ×7, 725).

WT-C mice showed normal RPE and BM features. RPE nuclei were rounded and displayed straight borders. The BM structure was conserved. TEM of the outer retina and choroid revealed no accumulation of sub-RPE deposits with normal basal infoldings, BM, and choriocapillaris (Figures 3(a) and 3(b)).

Compared with WT-C, AE-C mice showed ultrastructural changes (Figures 3(c)–3(j)). Low-power microphotographs revealed a disruption of cellular components and disorganized structure (Figures 3(c) and 3(e)). Also, eyes from AE-C mice had an increase in the number and size of empty and autophagocytic cytoplasmic vacuoles (Figure 3(d)) and, as previously reported [10, 13, 30, 31], basal laminar deposits-like (BLamD-like) structures located in the extracellular space between the basal lamina of the RPE and the inner collagenous layer of BM (Figures 3(c), 3(d), 3(g), and 3(h)). Moreover, most of RPE cells analyzed exhibited swelling of basal infoldings and opening of intercellular space junctions between RPE cells (Figures 3(e) and 3(f)). We also observed abnormal deposits of electrodense amorphous material in the subRPE space confined to a small area located to the RPE side of BM (Figures 3(d), 3(f), and 3(h)), as well as areas of increased thickness in BM (Figures 3(i) and 3(j)). The thickness of BM was statistically significantly higher in AE-C group than in WT-C (Table 4, $P < 0.001$). The BM of AE-C exhibited lucent non-membrane-bounded vacuoles dispersed through both collagenous layers (Figures 3(i) and 3(j)).

In contrast with the apoE$^{-/-}$ untreated animals, mice fed with the MV complex exhibited less severe structural

alterations in RPE and BM, with less swelling of basal infoldings and less cytoplasm vacuoles in the RPE and in BM. Mice supplemented with the low dose of multivitamin complex (AE-MV15; Figures 4(a) and 4(b)) and lutein (AE-LUT; Figures 4(e) and 4(f)) still showed moderate presence of BLamD in RPE, which were absent in AE-MV50 animals (Table 4, Figures 4(c) and 4(d)). BM thickening in all groups supplemented was less pronounced compared to AE-C animals. However, only in AE-MV50 group a statistically significant reduction was observed (Table 4, $P < 0.05$).

4. Discussion

In this study we examined the utility of apoE$^{-/-}$ mice as a model for AMD-like retinal degeneration and the effects of antioxidant treatments on the phenotypical and biochemical changes observed in this model. The most important findings are the increased VEGF expression and MMP-2 activity in the RPE-choroid of apoE$^{-/-}$ mice and the corresponding decrease in VEGF levels and MMP-2 activity after high doses of a multivitamin complex with lutein and glutathione. In addition, multivitamin supplementation reduced systemic and retinal oxidation and ameliorated the pathological AMD-like changes in apoE$^{-/-}$ mice. The fact that lutein and the multivitamin complex prevented biochemical and morphologic changes strongly suggests that hypercholesterolemia-derived oxidative stress is at least partly responsible for the alterations.

Based on biochemical and structural analyses, the apoE$^{-/-}$ mouse is a valuable tool in elucidating the underlying mechanism of retinal degeneration. ApoE$^{-/-}$ mice accrued marked increases in plasma TG and TC that were associated with increased systemic oxidative status. TG levels were reduced in animals supplemented with high-dose multivitamin complex, and this reduction may contribute, at least in part, to systemic oxidative stress decrease. We and others have reported evidence of systemic oxidative stress in apoE$^{-/-}$ mice [22–24], and our group has previously demonstrated that systemic and retinal oxidative stress in apoE$^{-/-}$ mice is reduced by dietary antioxidants present in egg yolk [23] and zeaxanthin [22]. Moreover, vitamins C and E were effective in reducing oxidative and nitrative stress in apoE$^{-/-}$ mice [24] and in a model of porcine dietary hypercholesterolemia [21]. VEGF can be regulated by hypoxia, oxidative stress, and nitric oxide [32]. Matrix metalloproteinases (MMPs) are involved in extracellular matrix remodelling. Both VEGF and MMPs are regulated, at least in part, by oxidative stress [33, 34]; thus, it is relevant to study their activation and expression in pathologies where oxidative stress seems to play an important role.

In the present work we observed a reduction in total NO production in the retinas of apoE$^{-/-}$ mice compared to wild-type animals which could be a consequence of a reduced nNOS activity and, subsequently, reduced NO production [35]. In our study, the treatments groups showed NO reduction compared to apoE$^{-/-}$ controls. It is possible that the decrease or increase in reduced glutathione (GSH) concentration (as a consequence of supplement administration) is able to alter the effects of NO (GSH forms adducts with NO: S-nitrosoglutathione) without affecting the expression of NOS [36]. It has been demonstrated that GSNO and NO protect neurons from hydroxyl radical-induced oxidative stress *in vivo* by terminating lipid peroxidation and augmenting the antioxidative potency of GSH, among other effects [37]. Therefore, restoring GSH levels can help NO to exert its beneficial effects, whereas the decrease in GSH levels could enhance the neurotoxic effects of free NO. Alterations in NO synthesis and bioavailability not only activate growth factors as VEGF but also induce physiological changes such as vasoconstriction and decreased choroidal flux. Increased oxidative stress in apoE$^{-/-}$ mice could result in an excess of $O_2^{\bullet -}$, which would react with NO to form $ONOO^-$, decreasing NO bioavailability. However, the methodology employed in the present study did not permit us to evaluate NO bioavailability in genetic hypercholesterolemia.

ApoE$^{-/-}$ mice showed an increase in VEGF expression and MMP-2 activity in the RPE compared to wild-type-animals, probably produced in response to high oxidative stress environment. VEGF expression is regulated partly by oxidative stress or NO and hypoxia in RPE cells [38]. Our results agree with those obtained in apoE$^{-/-}$ mice aortas showing an increase in gelatinase activity, VEGF, and VEGFR2 compared to controls [39, 40]. VEGF and MMPs can positively regulate each other [41]. An increase in VEGF expression in RPE has been previously reported by us; however, to our knowledge this study is the first showing an increased MMP-2 activity in posterior eyecups of apoE$^{-/-}$ mice. It is possible that the augmented VEGF expression and MMP-2 activity in apoE$^{-/-}$ mice could be derived, at least partly, from the increased oxidation observed in the retinal environment, where the presence of free radicals could stimulate cytokine or growth factors production.

GSH and its related enzymes are part of the antioxidant defense against oxidative stress elevation. GSH depletion occurs in several forms of cell death, including in the retina [42, 43]. In *rd*1 mice it has been demonstrated that antioxidant supplementation (lutein, zeaxanthin, α-lipoic acid, and GSH) prevents photoreceptor apoptosis and DNA oxidative damage. When administered individually, none of the antioxidants produced a significant decrease in the number of apoptotic cells or DNA damage level in photoreceptors [44]. These results agree with ours in showing a decrease in retinal lipid peroxidation, VEGF, and MMP-2 activity in animals supplemented with the mixture of antioxidants with lutein and GSH but no significant modifications in animals supplemented with lutein alone. Our group demonstrated the decrease of superoxide anion as well as retinal lipid peroxidation by vitamins C and E oral administration in hypercholesterolemic porcine RPEs [21]. That result confirmed the association of retinal lipid peroxidation and changes in reactive oxygen species synthesis and could be the same mechanism in apoE$^{-/-}$ mice and the multivitamin complex.

This is the first study showing a decrease in VEGF expression and MMP-2 activity in the retina after nutritional

supplementation in the apoE-deficient mouse. According to the most recent review on lutein [45], there is only one study that demonstrated a reduction in VEGF after lutein supplementation where Izumi-Nagai et al. [46] showed a reduction of VEGF in RPE protein extracts from a murine model of choroidal neovascularization. Their experimental setting is completely different from our model; lutein was administered only during 6 days (3 days before laser photocoagulation and 3 days afterwards), while our treatment lasted for 3 months. Moreover, to the best of our knowledge, there is only one paper showing a decrease in VEGF expression in ARPE-19 cells after TNF-alpha stimulation [47].

To determine whether the biochemical changes are accompanied by retinal ultrastructural alterations, we performed limited electron microscopy analyses. In the future, extensive examination of several eye cross sections will render a more accurate depiction of eye-wide morphological changes. Nevertheless, our electron microscopy evaluation shows that apoE$^{-/-}$ mice develop several ultrastructural alterations. BLamDs, defined as amorphous electron-dense material among the basal infoldings on the RPE side of BM, were present as previously reported [10, 22–24]. We observed ultrastructural changes in the BM of apoE$^{-/-}$ similar to those reported by Dithmar et al. [10]. BLamD was more dispersed, and the sub-RPE layer contained far less electron-dense material in animals supplemented with multivitamin complex than in the controls or the untreated groups. The impact of dietary antioxidants on BLamD is consistent with reports that increased exposure to oxidation (e.g., inhalation of cigarette smoke and exposure to photooxidative stress) induces increased formation of BM deposits [29, 48]. Lipid peroxidation is likely one of many potential stimuli of injury, and it is possible that BLamD formation reflects a final common pathway of reparative processes shared by many cellular types in response to injury [49]. Our results strongly suggest that the reduced quantity of BLamD in the 6-month-old AE-MV50 retinas resulted from increased turnover or reduced formation of BLamD. Furthermore, we demonstrate an increase in BM thickness in apoE$^{-/-}$ mice, that is, reduced by supplementation with antioxidants, lutein and GSH. The results obtained in this animal model agree with those showed in a porcine model of dietetic hypercholesterolemia [21] and with the observations in other models of retinal degeneration such as *rd*1 mice [44]. Our hypothesis is that the hypercholesterolemic status of apoE$^{-/-}$ mice may have contributed significantly to the retinal abnormalities, probably mediated by an increase in oxidative stress.

Moreover, this hypothesis is supported by the fact that those mice supplemented with multivitamin complex did not show these characteristic features. Therefore, these compounds could play a role in protection of oxidative stress-derived damage in the retina. This could be considered in preventive therapy for ocular degenerative pathologies, as a mean to improve life quality in patients. The reduction of VEGF expression and MMP-2 activity, accompanied by oxidative stress reduction, could be one of the mechanisms underlying the reduction in ultrastructural alterations. When lutein is combined with other antioxidant substances, beneficial effects are observed in hypercholesterolemia oxidative stress-derived changes. Although our study did not establish a causal relationship between phenotypical and biochemical findings, the latter can be associated with cytoplasmic and BM ultrastructural alterations. The increase in VEGF expression could be responsible for the increased permeability in choroid and BM, and MMP-2 activity could degrade BM, leading to the observed thickening and vacuolization. MMPs are enzymes involved in synthesis and degradation of extracellular matrix and have specific substrates such as collagen and elastin, both of them BM components. RPE cells are subsequently stimulated to increase synthesis of MMPs and other molecules responsible for ECM turnover. Increased matrix turnover is characterized by increased MMPs and decreased collagens [8]. As these morphological changes are ameliorated with supplementation with antioxidants, it is probable that oxidative stress increase is the initiating factor for the molecular and morphological changes in apoE$^{-/-}$ mice.

5. Conclusions

This study provides data suggesting an evolving role for hypercholesterolemia in the development of retinal oxidative stress and the influence of dietary fat in ultrastructural RPE changes. Furthermore, VEGF and MMP-2 are responsible, at least in part, for some of the changes caused by hypercholesterolemia-derived oxidative stress. Additionally, supplementation with lutein, glutathione, and a complex of vitamins appears to be effective in reducing these retinal changes. However, further experimental, epidemiological and clinical studies are required to confirm these findings.

Abbreviations

AE-C:	ApoE$^{-/-}$ mice treated with vehicle
AE-LUT:	ApoE$^{-/-}$ mice treated with lutein
AE-MV15:	ApoE$^{-/-}$ mice treated with MV (15 mg/kg/day)
AE-MV50:	ApoE$^{-/-}$ mice treated with MV (50 mg/kg/day)
AMD:	Age-related macular degeneration
ANOVA:	Analysis of variance
APOE$^{-/-}$:	ApoE-deficient mice
ARVO:	Association for research in vision and ophthalmology
BLamD:	Basal laminar deposits
BM:	Bruch's membrane
CHD:	Coronary heart disease
DAN:	Diaminonaphthalene
ECL:	Enhanced chemoluminescence
GSH:	Reduced glutathione
GSNO:	S-nitrosoglutathione
MMP-2:	Matrix metalloproteinase-2
MV:	Multivitamin complex
NADPH:	Reduced nicotinamide adenine dinucleotide phosphate

nNOS: Neuronal NOS
NO: Nitric oxide
NO_2^-: Nitrites
NO_3^-: Nitrates
NOS: Nitric oxide synthase
$O_2^{\bullet-}$: Superoxide anion
$ONOO^-$: Peroxynitrite
RPE: Retinal pigment epithelium
TBARS: Thiobarbituric acid reactive substances
TC: Total cholesterol
TEM: Transmission electron microscopy
TG: Triglycerides
VEGF: Vascular endothelial growth factor
WT-C: Control mice.

Conflict of Interest

The authors declare that they have no conflict of interests.

Acknowledgments

The authors are grateful to the staff of the Department of Histology and Pathology (Universidad de Navarra), especially Laura Guembe, Ph.D., for help with electron microscopy interpretation and to Blanca Irigoyen for technical assistance; to the personnel at the Atherosclerosis Research Laboratory, Division of Cardiovascular Sciences (CIMA-Universidad de Navarra); and to Javier Guillén and Juan Percaz for excellent animal care. P. Fernández-Robredo received a grant from Departamento de Educación, Gobierno de Navarra and from Fundación Jesús de Gangoiti Barrera. Parts of the study were funded by Thea Laboratoires (France) and with the structure of RETICS RD07/0062.

References

[1] C. A. Curcio, M. Johnson, J. D. Huang, and M. Rudolf, "Aging, age-related macular degeneration, and the response-to-retention of apolipoprotein B-containing lipoproteins," *Progress in Retinal and Eye Research*, vol. 28, no. 6, pp. 393–422, 2009.

[2] X. Ding, M. Patel, and C. C. Chan, "Molecular pathology of age-related macular degeneration," *Progress in Retinal and Eye Research*, vol. 28, no. 1, pp. 1–18, 2009.

[3] G. S. Hageman, K. Gehrs, S. Lejnine et al., "Clinical validation of a genetic model to estimate the risk of developing choroidal neovascular age-related macular degeneration," *Human Genomics*, vol. 5, no. 5, pp. 420–440, 2011.

[4] G. J. McKay, C. C. Patterson, U. Chakravarthy et al., "Evidence of association of APOE with age-related macular degeneration-a pooled analysis of 15 studies," *Human Mutation*, vol. 32, no. 12, pp. 1407–1416, 2011.

[5] R. H. Guymer and E. W. T. Chong, "Modifiable risk factors for age-related macular degeneration," *Medical Journal of Australia*, vol. 184, no. 9, pp. 455–458, 2006.

[6] J. Ambati, B. K. Ambati, S. H. Yoo, S. Ianchulev, and A. P. Adamis, "Age-related macular degeneration: etiology, pathogenesis, and therapeutic strategies," *Survey of Ophthalmology*, vol. 48, no. 3, pp. 257–293, 2003.

[7] W. R. Green, "Histopathology of age-related macular degeneration," *Molecular Vision*, vol. 5, p. 27, 1999.

[8] P. S. Mettu, A. R. Wielgus, S. S. Ong, and S. W. Cousins, "Retinal pigment epithelium response to oxidant injury in the pathogenesis of early age-related macular degeneration," *Molecular Aspects of Medicine*, vol. 33, no. 4, pp. 376–398, 2012.

[9] B. Falsini, M. Piccardi, G. Iarossi, A. Fadda, E. Merendino, and P. Valentini, "Influence of short-term antioxidant supplementation on macular function in age-related maculopathy: a pilot study including electrophysiologic assessment," *Ophthalmology*, vol. 110, no. 1, pp. 51–60, 2003.

[10] S. Dithmar, C. A. Curcio, N. A. Le, S. Brown, and H. E. Grossniklaus, "Ultrastructural changes in Bruch's membrane of apolipoprotein E- deficient mice," *Investigative Ophthalmology and Visual Science*, vol. 41, no. 8, pp. 2035–2042, 2000.

[11] D. Praticò, R. K. Tangirala, D. J. Rader, J. Rokach, and G. A. Fitzgerald, "Vitamin E suppresses isoprostane generation in vivo and reduces atherosclerosis in ApoE-deficient mice," *Nature Medicine*, vol. 4, no. 10, pp. 1189–1192, 1998.

[12] M. Kliffen, E. Lutgens, M. J. A. P. Daemen, E. D. De Muinck, C. M. Mooy, and P. T. V. M. De Jong, "The APO*E3-Leiden mouse as an animal model for basal laminar deposit," *British Journal of Ophthalmology*, vol. 84, no. 12, pp. 1415–1419, 2000.

[13] J. M. Ong, N. C. Zorapapel, K. A. Rich et al., "Effects of cholesterol and apolipoprotein E on retinal abnormalities in ApoE-deficient mice," *Investigative Ophthalmology and Visual Science*, vol. 42, no. 8, pp. 1891–1900, 2001.

[14] E. Applegate, "Introduction: nutritional and functional roles of eggs in the diet," *Journal of the American College of Nutrition*, vol. 19, supplement 5, pp. 495S–498S, 2000.

[15] E. W. T. Chong, T. Y. Wong, A. J. Kreis, J. A. Simpson, and R. H. Guymer, "Dietary antioxidants and primary prevention of age related macular degeneration: systematic review and meta-analysis," *British Medical Journal*, vol. 335, no. 7623, pp. 755–759, 2007.

[16] E. Loane, J. M. Nolan, O. O'Donovan, P. Bhosale, P. S. Bernstein, and S. Beatty, "Transport and retinal capture of lutein and zeaxanthin with reference to age-related macular degeneration," *Survey of Ophthalmology*, vol. 53, no. 1, pp. 68–81, 2008.

[17] J. T. Landrum, R. A. Bone, H. Joa, M. D. Kilburn, L. L. Moore, and K. E. Sprague, "A one year study of the macular pigment: the effect of 140 days of a lutein supplement," *Experimental Eye Research*, vol. 65, no. 1, pp. 57–62, 1997.

[18] S. Pratt, "Dietary prevention of age-related macular degeneration," *Optometry*, vol. 70, no. 1, pp. 39–47, 1999.

[19] D. M. Snodderly, "Evidence for protection against age-related macular degeneration by carotenoids and antioxidant vitamins," *American Journal of Clinical Nutrition*, vol. 62, supplement 6, pp. 1448S–1461S, 1995.

[20] L. M. Rapp, S. S. Maple, and J. H. Choi, "Lutein and zeaxanthin concentrations in rod outer segment membranes from perifoveal and peripheral human retina," *Investigative Ophthalmology and Visual Science*, vol. 41, no. 5, pp. 1200–1209, 2000.

[21] P. Fernandez-Robredo, D. Moya, J. A. Rodriguez, and A. Garcia-Layana, "Vitamins C and E reduce retinal oxidative stress and nitric oxide metabolites and prevent ultrastructural alterations in porcine hypercholesterolemia," *Investigative Ophthalmology and Visual Science*, vol. 46, no. 4, pp. 1140–1146, 2005.

[22] P. Fernández-Robredo, S. Recalde, G. Arnáiz et al., "Effect of zeaxanthin and antioxidant supplementation on vascular endothelial growth factor (VEGF) expression in apolipoprotein-e deficient mice," *Current Eye Research*, vol. 34, no. 7, pp. 543–552, 2009.

[23] P. Fernandez-Robredo, S. R. Maestre, J. Zarranz-Ventura, H. H. Mulero, A. Salinas-Alaman, and A. Garcia-Layana, "Myopic choroidal neovascularization genetics," *Ophthalmology*, vol. 115, no. 9, pp. 1632–e1, 2008.

[24] P. Fernández-Robredo, J. A. Rodríguez, L. M. Sádaba, S. Recalde, and A. García-Layana, "Egg yolk improves lipid profile, lipid peroxidation and retinal abnormalities in a murine model of genetic hypercholesterolemia," *Journal of Nutritional Biochemistry*, vol. 19, no. 1, pp. 40–48, 2008.

[25] M. Conti, P. C. Morand, P. Levillain, and A. Lemonnier, "Improved fluorometric determination of malonaldehyde," *Clinical Chemistry*, vol. 37, no. 7, pp. 1273–1275, 1991.

[26] S. Archer, "Measurement of nitric oxide in biological models," *FASEB Journal*, vol. 7, no. 2, pp. 349–360, 1993.

[27] M. Marzinzig, A. K. Nussler, J. Stadler et al., "Improved methods to measure end products of nitric oxide in biological fluids: nitrite, nitrate, and S-nitrosothiols," *Nitric Oxide*, vol. 1, no. 2, pp. 177–189, 1997.

[28] P. A. M. Snoek-van Beurden and J. W. Von Den Hoff, "Zymographic techniques for the analysis of matrix metalloproteinases and their inhibitors," *BioTechniques*, vol. 38, no. 1, pp. 73–83, 2005.

[29] D. G. Espinosa-Heidmann, J. Sall, E. P. Hernandez, and S. W. Cousins, "Basal laminar deposit formation in APO B100 transgenic mice: complex interactions between dietary fat, blue light, and vitamin E," *Investigative Ophthalmology and Visual Science*, vol. 45, no. 1, pp. 260–266, 2004.

[30] M. V. Miceli, D. A. Newsome, D. J. Tate, and T. G. Sarphie, "Pathologic changes in the retinal pigment epithelium and Bruch's membrane of fat-fed atherogenic mice," *Current Eye Research*, vol. 20, no. 1, pp. 8–16, 2000.

[31] S. Dithmar, N. A. Sharara, C. A. Curcio et al., "Murine high-fat diet and laser photochemical model of basal deposits in bruch membrane," *Archives of Ophthalmology*, vol. 119, no. 11, pp. 1643–1649, 2001.

[32] A. N. Witmer, G. F. J. M. Vrensen, C. J. F. Van Noorden, and R. O. Schlingemann, "Vascular endothelial growth factors and angiogenesis in eye disease," *Progress in Retinal and Eye Research*, vol. 22, no. 1, pp. 1–29, 2003.

[33] T. T. L. Wong, C. Sethi, J. T. Daniels, G. A. Limb, G. Murphy, and P. T. Khaw, "Matrix metalloproteinases in disease and repair processes in the anterior segment," *Survey of Ophthalmology*, vol. 47, no. 3, pp. 239–256, 2002.

[34] H. Nagaset and J. F. Woessner, "Matrix metalloproteinases," *Journal of Biological Chemistry*, vol. 274, no. 31, pp. 21491–21494, 1999.

[35] I. A. Bhutto, T. Baba, C. Merges, D. S. McLeod, and G. A. Lutty, "Low nitric oxide synthases (NOSs) in eyes with age-related macular degeneration (AMD)," *Experimental Eye Research*, vol. 90, no. 1, pp. 155–167, 2010.

[36] J. M. Seddon, U. A. Ajani, R. D. Sperduto et al., "Dietary carotenoids, vitamins A, C, and E, and advanced age-related macular degeneration," *Journal of the American Medical Association*, vol. 272, no. 18, pp. 1413–1420, 1994.

[37] C. R. Gale, N. F. Hall, D. I. W. Phillips, and C. N. Martyn, "Lutein and zeaxanthin status and risk of age-related macular degeneration," *Investigative Ophthalmology and Visual Science*, vol. 44, no. 6, pp. 2461–2465, 2003.

[38] R. Kannan, N. Zhang, P. G. Sreekumar et al., "Stimulation of apical and basolateral vascular endothelial growth factor-A and vascular endothelial growth factor-C secretion by oxidative stress in polarized retinal pigment epithelial cells," *Molecular Vision*, vol. 12, pp. 1649–1659, 2006.

[39] R. Arias, *Efecto de la homocisteína sobre la expresión vascular del TIMP-1 y la Metaloproteinasa-2. Implicaciones en la aterosclerosis [Ph.D. thesis]*, Universidad de Navarra, Pamplona, Spain, 2002.

[40] B. Nespereira, M. Pérez-Ilzarbe, P. Fernández, A. M. Fuentes, J. A. Páramo, and J. A. Rodríguez, "Vitamins C and E downregulate vascular VEGF and VEGFR-2 expression in apolipoprotein-E-deficient mice," *Atherosclerosis*, vol. 171, no. 1, pp. 67–73, 2003.

[41] G. Hashimoto, I. Inoki, Y. Fujii, T. Aoki, E. Ikeda, and Y. Okada, "Matrix metalloproteinases cleave connective tissue growth factor and reactivate angiogenic activity of vascular endothelial growth factor 165," *Journal of Biological Chemistry*, vol. 277, no. 39, pp. 36288–36295, 2002.

[42] Y. J. Roh, C. Moon, S. Y. Kim et al., "Glutathione depletion induces differential apoptosis in cells of mouse retina, in vivo," *Neuroscience Letters*, vol. 417, no. 3, pp. 266–270, 2007.

[43] P. Maher and A. Hanneken, "Flavonoids protect retinal ganglion cells from oxidative stress-induced death," *Investigative Ophthalmology and Visual Science*, vol. 46, no. 12, pp. 4796–4803, 2005.

[44] M. Miranda, E. Arnal, S. Ahuja et al., "Antioxidants rescue photoreceptors in rd1 mice: relationship with thiol metabolism," *Free Radical Biology and Medicine*, vol. 48, no. 2, pp. 216–222, 2010.

[45] A. Kijlstra, Y. Tian, E. R. Kelly, and T. T. Berendschot, "Lutein: more than just a filter for blue light," *Progress in Retinal and Eye Research*, vol. 31, no. 4, pp. 303–315, 2012.

[46] K. Izumi-Nagai, N. Nagai, K. Ohgami et al., "Macular pigment lutein is antiinflammatory in preventing choroidal neovascularization," *Arteriosclerosis, Thrombosis, and Vascular Biology*, vol. 27, no. 12, pp. 2555–2562, 2007.

[47] Z. Sun, J. Liu, X. Zeng et al., "Protective actions of microalgae against endogenous and exogenous advanced glycation end-products (AGEs) in human retinal pigment epithelial cells," *Food and Function*, vol. 2, no. 5, pp. 251–258, 2011.

[48] D. G. Espinosa-Heidmann, I. J. Suner, P. Catanuto, E. P. Hernandez, M. E. Marin-Castano, and S. W. Cousins, "Cigarette smoke-related oxidants and the development of sub-RPE deposits in an experimental animal model of dry AMD," *Investigative Ophthalmology and Visual Science*, vol. 47, no. 2, pp. 729–737, 2006.

[49] S. W. Cousins, D. G. Espinosa-Heidmann, A. Alexandridou, J. Sall, S. Dubovy, and K. Csaky, "The role of aging, high fat diet and blue light exposure in an experimental mouse model for basal laminar deposit formation," *Experimental Eye Research*, vol. 75, no. 5, pp. 543–553, 2002.

Hindawi Publishing Corporation
Oxidative Medicine and Cellular Longevity
Volume 2013, Article ID 901253, 8 pages
http://dx.doi.org/10.1155/2013/901253

Clinical Study

Adduct of Malondialdehyde to Hemoglobin: A New Marker of Oxidative Stress That Is Associated with Significant Morbidity in Preterm Infants

Cécile Cipierre,[1,2] Stéphane Haÿs,[2,3] Delphine Maucort-Boulch,[4,5,6] Jean-Paul Steghens,[3,7] and Jean-Charles Picaud[2,3,5]

[1] *Département de Néonatologie, CHU Angers, 49100 Angers, France*
[2] *Département de Néonatologie, Hôpital de la Croix Rousse, Hospices Civils de Lyon, 69004 Lyon, France*
[3] *Centre de Recherche en Nutrition Humaine Rhône-Alpes, Centre hospitalier Lyon-Sud, 69310 Pierrre Bénite, France*
[4] *Département de Biostatistique, Hospices Civils de Lyon, 69003 Lyon, France*
[5] *Université Claude Bernard Lyon I, 69100 Villeurbanne, France*
[6] *CNRS UMR5558, Laboratoire de Biométrie et Biologie Evolutive, Equipe Biostatistique Santé, 69310 Pierre-Bénite, France*
[7] *Centre de Biologie Sud, UF Nutrition et Métabolisme, Centre hospitalier Lyon-Sud, Hospices Civils de Lyon, 69310 Pierrre Bénite, France*

Correspondence should be addressed to Cécile Cipierre; cecile.cipierre@wanadoo.fr

Received 8 February 2013; Revised 28 March 2013; Accepted 29 March 2013

Academic Editor: Kota V. Ramana

Preterm infants (PT) are particularly exposed to oxidative stress (OS), and a blood-sparing marker, the malondialdehyde adduct to hemoglobin (MDA-Hb), may be useful to accurately assess OS-related neonatal morbidity. In a prospective study, MDA-Hb concentrations were assessed in two groups of PT, one with and one without severe neonatal morbidity as estimated by a composite index of severe morbidity (ISM). All PT born in a single tertiary care NICU (<32 weeks and birth weight < 1500 g) were consecutively included. MDA-Hb and blood glutathione (GSH) concentrations were measured by liquid chromatography-mass spectrometry during the first 6 weeks of life. Linear regressions and a multilevel model were fitted to study the relationship between MDA-Hb or GSH and ISM. Of the 83 PT (mean ± SD: 28.3 ± 2 weeks, 1089 ± 288 g), 21% presented severe neonatal morbidity. In the multivariate model, MDA-Hb concentrations were significantly higher in the ISM+ group than in the ISM– group during the first 6 weeks of life ($P = 0.009$). No significant difference in GSH concentrations was observed between groups ($P = 0.180$). MDA-Hb is a marker of interest for estimating oxidative stress in PT and could be useful to evaluate the impact of strategies to improve perinatal outcomes.

1. Introduction

As very low birth weight (VLBW) infants present an imbalance between the prooxidant and antioxidant systems [1–3], they are at high risk for oxidative-stress- (OS-) related damage. Antioxidant enzymes mature in late gestation, and the maternal-fetal transfer of antioxidant molecules like alpha-tocopherol and ascorbic acid is not complete in premature neonates [4]. Yet, these infants also often require oxygen therapy and a parenteral nutrition. Although parenteral nutrition solutions contain antioxidant molecules like vitamins A, C, and E, they also contain polyunsaturated fatty acids that are particularly sensitive to peroxidation, which generates toxic byproducts of the reactive oxygen species [5, 6]. The lipid peroxidation in these solutions depends on their composition and is increased by light exposure [7–9]. A relationship has been suggested between lipid peroxidation and several common morbidities of prematurity, including bronchopulmonary dysplasia (BPD), retinopathy of prematurity, periventricular leukomalacia, and necrotizing enterocolitis (NEC) [10–13]. However, the studies show discrepancies because of differences in peroxidation assessment.

Malondialdehyde (MDA) is the most studied product of polyunsaturated fatty acid peroxidation, but most assays have been developed on the basis of its derivatization with thiobarbituric acid (TBA), which has poor specificity [14, 15]. Other methods, such as liquid chromatography coupled with mass spectrometry, have been proposed to improve MDA assessment [16, 17]. We recently validated a new sensitive and specific method to measure MDA adduct to hemoglobin (MDA-Hb) in neonates [18]. This method would facilitate OS evaluation over several weeks or months based on the stability of MDA-Hb, as its elimination depends on the lifespan of the erythrocyte [19]. As MDA-Hb is measured in erythrocytes, additional blood despoliation is avoided, which makes the method well suited to VLBW infants.

This pilot study sought to determine the relationship between blood MDA-Hb concentrations and neonatal morbidity in VLBW infants. A secondary objective was to assess the influence of the perinatal condition on MDA-Hb concentrations.

2. Methods

2.1. Population. All PT born at a gestational age (GA) of 24 to 31 weeks, with a birth weight (BW) below 1500 g, and admitted before the first 6 hours of life to our tertiary care neonatal unit at Croix Rousse University Hospital, Lyon, France, were consecutively enrolled in this prospective study. Infants with major congenital abnormalities (including cardiac, neurological, renal, and digestive malformation) or metabolic disease, and those requiring surgery, were excluded. The study was totally integrated into the usual care of PT hospitalized in the unit. No additional blood sampling was needed for the present study, and the protocols of respiratory and nutritional care did not change during the study. The international recommendations for nutrition were followed for all infants. All parents signed an informed consent form. The study was approved by the ethics committee of the University Hospital Center of Lyon, France (*CPP Lyon Sud Est IV*).

2.2. Study Design. The patients were included at birth and the study lasted for the first 6 weeks of life or infant transfer/death. The clinical data were collected by a single person (C. Cipierre). We prospectively recorded variables concerning the antenatal context in four categories: fetal growth restriction (FGR) (estimated fetal weight <10th percentile), preeclampsia (characterized by hypertension and proteinuria), suspicion of maternal antenatal infection (positive blood culture, maternal fever $\geq 38.5^{\circ}$C, and C-reactive protein > 20 mg/L), and other causes (metrorrhagia and placental abnormalities). We also collected data at birth: GA, BW, Apgar score at 5 min, and the need for specific intensive resuscitation (intubation, chest compression, or drugs for resuscitation). The infants were considered as growth restricted when BW was < -2 SD [20]. We also collected data concerning respiratory care (assisted ventilation, oxygen supply, and surfactant administration), hemodynamics (vasoactive amine, ibuprofen administration), nutrition (total parenteral supply), and complications during hospitalization (early onset sepsis, late onset sepsis, BPD, NEC, intraventricular haemorrhage, and periventricular leukomalacia).

A composite index of severe morbidity (ISM) was considered as present (ISM+) within the first 6 weeks of life when the patients presented severe respiratory, neurological, or digestive morbidity. The composite index of severe morbidity (ISM) was considered when at least one of the three morbidities was present. Severe respiratory morbidity was defined by the presence of at least one of the following: oxygen dependency at 36 weeks postconceptional age or median duration of assisted ventilation >+2 SD compared with the median duration of ventilation in the same population of GA infants hospitalized in the service between 2005 and 2007 (109 infants born at GA < 28 weeks: median = 249 hours (IC 95%: 288–417) and 202 infants born at GA $\geq$ 28 weeks: median = 321 hours (IC 95%: 57–844)) (personal data). Severe neurological morbidity was defined as the existence of at least one of the following abnormalities: severe intraventricular haemorrhage (grade 3 or 4) or periventricular leukomalacia. Severe digestive morbidity was defined as NEC of grade 3 or 4 [21].

2.3. Measurement of Oxidative Stress Markers. MDA-Hb and reduced glutathione (GSH), a key antioxidant, were measured once a week in the first 6 weeks of life and it did not require an additional blood sample to be drawn. We assumed that the erythrocytes remaining from routine blood samples taken for electrolyte determination would be sufficient for MDA-Hb assessment.

At birth, MDA-Hb and GSH concentrations were assessed at the time of admission in the neonatal unit, that is, before the first hour of life for inborn infants and before the first 6 hours of life for outborn infants.

All samples were stored at -80°C until analysis. These markers were measured by a unique laboratory, as previously described [18].

The procedure for measuring MDA-Hb consisted of three steps: isolation of Hb and delipidation for avoiding any artifactual lipid peroxidation, hydrolysis and derivatization of the adduct, and then measurement of the adduct. In brief, after a first centrifugation, RBCs (one volume) were washed two times with four volumes of NaCl (9 g/1000 mL), centrifuged (5 minutes, 1000 G). 150 μL of washed and packed RBCs was resuspended in distilled water (450 μL) and freeze-dried at -80°C for 5 minutes then thawed in hot water (30 seconds under water at 60°C). After a second cycle of freeze drying—thawing, Hb solution was obtained by centrifugation for 4 min at 8000 G; one aliquot was used to measure Hb concentration and another aliquot (200 μL) was rapidly delipidated by mixing with 100 μL Folch reagent (methanol/chloroform, 1 vol./2 vol.) and centrifuged for 5 minutes at 13000 G. The delipidated Hb from the top phase was stored at -80°C until analysis. The original method to derivatize plasmatic MDA with diaminonaphthalene (DAN) was previously described [22]. Preliminary experiments showed that to decrease adsorption of the diazepinium (formed between MDA and DAN) to Hb, derivatization had to be done in saline. The quantification was carried out by

LC-MS with a dideurated internal standard; the derivatives of MDA and dideuterated MDA were detected at m/z 195.2 and 197.2, respectively, as described by Steghens et al. [16]. The adduct of MDA to Hb was expressed in nanomol per gram Hb (nanomol/g Hb).

For GSH assessment, we used whole blood (25 μl) kept into the guarding of the needle at the end of venipuncture. As described in [23], GSH was measured after derivatization with *N-ethylmaleimide* (NEM) to avoid any artifactual production of oxidized glutathione (GSSG) due to protein acid precipitation. The method used for GSH measurement by LC-MS discriminates GSNEM detected at m/z = 433.7 with a retention time at 2.9 min and GSSG detected at m/z = 614.1 with a retention time at 4.4 min. The results are expressed in micromole per liter (μmol/L) of whole blood.

To consider the possible contribution of blood transfusions, we measured the MDA-Hb and whole blood GSH concentrations in five randomly selected packed red cells used in preterm infants included in our study.

2.4. Statistical Analysis. All the collected variables are described in the studied population and within both groups defined by the outcome. Categorical variables are presented as numbers and percentages, and continuous variables are presented as median and extreme values. Percentages were compared using the Fisher exact test, and medians were compared using the Wilcoxon test. Differences were considered significant for P values < 5%. We compared the concentrations of MDA-Hb and GSH at birth in the two ISM groups (absent/present) with regard to the four antenatal contexts previously described. Linear regressions were fitted to study the relationship between MDA-Hb and ISM (absent/present) in the first 6 weeks of life. Because the MDA-Hb measures were repeated weekly in each infant, a multilevel model with random effects, or frailties, was used to account for correlations between measures in the same infant due to unobserved factors. MDA-Hb values were log-transformed to normalize their distribution. To study the trend over time of the repeated MDA-Hb measurements, time in weeks was introduced into the model as a continuous variable in addition to ISM. Similar models were fitted for GSH. Analyses were performed using R software (R Development Core Team; R: a language for environmental and statistical computing, Vienna: R Foundation, 2008) and SPSS version 15.0 software (Statistical Product and Service Solutions 15.0; SPSS, Inc, Chicago, IL, USA).

3. Results

Between February and July, 2009, 83 VLBW infants were consecutively enrolled in this study, 40% of whom were very immature (GA ≤ 28 wks). Seventeen of them (21%) presented a composite index of severe morbidity (ISM+), and 3 of these infants died. The first one died after 4 days from septic shock. Two others died from severe neurological complications (HIV stage 4, status) after 2 and 10 days of life.

As expected, the characteristics of infants with severe neonatal morbidity (ISM+) were significantly different from those of infants without morbidity (ISM−) (Table 1). The ISM+ group comprised more immature and sicker children who had assisted ventilation, oxygen supply, and parenteral nutrition for longer periods than in the ISM− group. They also more frequently presented patent ductus arteriosus requiring ibuprofen and late onset sepsis, and they received more blood transfusions: 14 of the 17 infants in the ISM+ group had at least one transfusion, and 10 of these had received more than 2 transfusions. The median postnatal age at the first and second transfusions was, respectively, 7 and 12 days for the ISM+ group and 7 and 13 days for the ISM− group. Antenatal factors did not differ significantly between the ISM+ and ISM− groups.

MDA-Hb concentrations at birth differed according to the antenatal context (Figure 1). Significantly higher MDA-Hb concentrations were observed in infants with maternal antenatal infection compared with infants without infection (P = 0.023). In contrast, GSH concentrations at birth were similar regardless of the prenatal environment (infants with suspicion of maternal antenatal infection compared with infants without, P = 0.931).

MDA-Hb concentrations at birth were significantly higher in the ISM+ group than in the ISM− group, but GSH concentrations were similar in the two groups (Table 2). The maximal MDA-Hb value ISM− group was related to only one infant, which can be considered as an outlier. It was a neonate born at 30 weeks by C-section after a 9h ROM in a mother with subnormal PCR (30 mg/L). There was no neonatal infection.

Thereafter, in the first 6 weeks of life, the concentrations of these markers were significantly different between the ISM+ and ISM− groups (Figure 2). Median MDA-Hb concentrations were significantly higher in the ISM+ group during this period (P = 0.009), and, at 6 weeks, they were approximately 3-fold higher in ISM+ (25.5 nanomol/g Hb) than in ISM− (9.3 nanomol/g Hb) (P = 0.01). Conversely, no significant difference in the GSH concentrations was observed between the groups in the first 6 weeks of life (P = 0.18) (Figure 2).

As the increment of MDA-Hb could be associated to hyperbilirubinemia or phototherapy, we adjusted for presence or absence of phototherapy and for the maximal serum bilirubin concentration, using a multivariate analysis. The difference in MDA-Hb remained statistically significant (resp., P = 0.02 and P = 0.03).

The median MDA-Hb and whole blood GSH concentrations in 5 packed red cells were, respectively, 8.4 nanomol/g Hb and 1568 μM/L.

4. Discussion

To our knowledge, this is the first report in neonates on the malondialdehyde adduct to hemoglobin (MDA-Hb), a marker of OS measured in red blood cells, that is, without requiring an additional blood sample. We observed that MDA-Hb concentrations were influenced by the clinical context, as described in studies with MDA [11].

Table 1: Characteristics of 83 very preterm infants with (ISM+) or without (ISM−) composite index of severe morbidity (ISM).

	All $N = 83$	ISM+ $n = 17$	ISM− $n = 66$	P value*
Singleton, *n* (%)	62 (74.7)	14 (82.3)	48 (72.7)	0.07
Antenatal steroids, *n* (%)	74 (89.1)	14 (88.3)	60 (90.9)	0.38
Fetal growth restriction, *n* (%)	11 (13.3)	1 (5.9)	10 (15.2)	0.45
Preeclampsia, *n* (%)	10 (12)	0 (0)	10 (15.2)	0.11
Maternal antenatal infection, *n* (%)	5 (6.0)	1 (5.9)	4 (6.1)	1.00
Others causes, *n* (%)	57 (68.7)	15 (88.2)	42 (63.6)	0.08
Cesarean section, *n* (%)	50 (62.6)	7 (41.2)	45 (68.2)	0.05
Gestational age at birth, weeks	28.7 (24.0–31.6)	26.0 (24.0–30.4)	29.0 (24.5–31.6)	<0.01
Birth weight, grams	1085 (570–1500)	765 (570–1500)	1120 (690–1500)	<0.01
Male, *n* (%)	39 (47.0)	11 (64.7)	28 (44.4)	0.10
Apgar score at 5 min, value	9 (2–10)	8 (6–10)	9 (2–10)	0.09
Resuscitation in DR, *n* (%)	49 (59.0)	14 (82.4)	35 (53.0)	0.08
RDS, *n* (%)	80 (96.4)	17 (100.0)	63 (95.5)	0.37
Surfactant, *n* (%)	51 (61.4)	14 (82.3)	37 (56.0)	0.03
Oxygen therapy, hours	37 (1–1661)	276 (1–1661)	68 (1–948)	<0.01
Assisted ventilation, hours	64 (1–1107)	427 (5–1107)	27 (1–764)	<0.01
Early onset sepsis, *n* (%)	6 (7.2)	4 (23.5)	2 (3.0)	0.01
Late onset sepsis, *n* (%)	22 (26.5)	10 (58.8)	12 (18.2)	<0.01
Persistent ductus arteriosus, *n* (%)	22 (26.5)	8 (47.0)	14 (21.2)	0.03
Blood transfusions, *n* (%)	34 (41.0)	14 (82.3)	20 (30.3)	<0.01
Parenteral nutrition, *n* (%)	63 (75.9)	15 (88.2)	48 (72.7)	<0.01
Parenteral nutrition duration, d	8 (1–35)	13 (1–35)	9 (1–28)	<0.01

Categorical variables are presented as number (%) and continuous variables as median (min–max).
*Comparison between the 2 groups (ISM+ versus ISM−, Mann-Whitney or Chi2 test).

Table 2: Concentrations of malondialdehyde (MDA-Hb) and reduced glutathione (GSH) at birth in 83 very preterm infants with (ISM+) or without (ISM−) composite index of severe morbidity (ISM).

	All $N = 83$	ISM+ $n = 17$	ISM− $n = 66$	P value*
MDA-Hb (nanomol/g Hb)	11.3 (2.2–134.3)	19.9 (6.6–117.5)	9.3 (2.2–134.3)	0.03
GSH (μM/L)	1310 (301–2168)	1295 (301–2168)	1324 (989–2042)	0.50

*Comparison between the 2 groups (ISM+ versus ISM−, Mann-Whitney or Chi2 test).

Published data about background levels of MDA-Hb in humans are scarce. Kautiainen et al. [24] assessed MDA-Hb concentrations in one healthy adult and in mice. They reported lower values (0.2 and 3.8 nanomol/g Hb) which are not comparable to ours because they used a very different and complex method: using a 4 ml sample volume, the final measurement of the 3 OH Pr Val was obtained after reduction with sodium borohydride (NaBH4), dialysis, and globin precipitation, derivatization with PFPITC, proteolysis with trypsin and pronase, and a last Dowex chromatography. This is not usable in human neonates (blood volume, complex assay). Furthermore, these values were obtained in a very small number of subjects (1 human adult and some mice) and cannot be compared to values obtained in a significant number of newborn infants.

For the purpose of monitoring, Hb can be preferred to DNA because of its better-defined lifespan and more facile chemical identification of adducts. In particular, the estimated half-live of the adduct to N-terminal valine in Hb is about six days [25]; thus, it is possible that this type of adduct may accumulate in the blood of newborn.

The present study has several limitations which need to be addressed. First, this was our definition of the composite index of severe morbidity. The composite index of severe morbidity included several types of neonatal morbidity with different time courses. For example, respiratory morbidity develops over a few weeks, whereas the onset of NEC is quite rapid. Our global approach might be considered as less precise than if we had considered each type of morbidity individually, but a global approach was essential to our

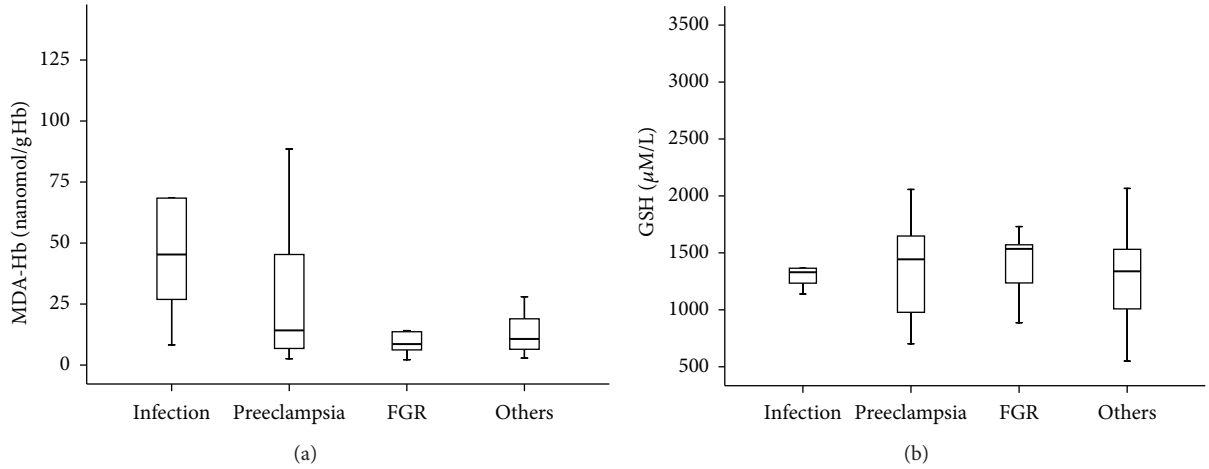

Figure 1: Box plot of the concentrations of malondialdehyde (MDA-Hb) (a) and reduced glutathione (GSH) (b) at birth, in 83 very low birth weight infants, depending on the antenatal context. FGR: fetal growth restriction. Values shown are median levels (25th/75th box; 10th/90th error bars).

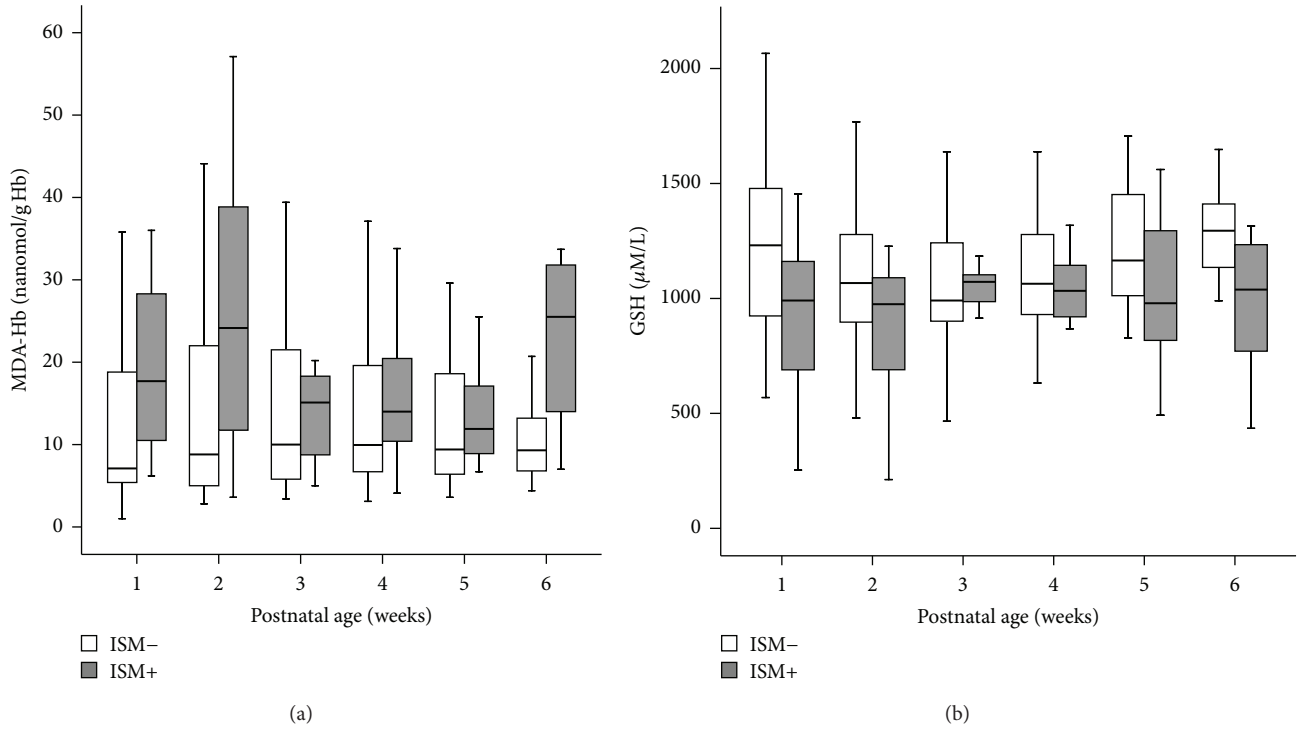

Figure 2: Box plot of the concentrations of malondialdehyde (MDA-Hb) (a) and reduced glutathione (GSH) (b) in the first 6 weeks of life, in 83 very low birth weight infants with (n = 17) or without (n = 66) a composite index of severe morbidity (ISM). Values shown are median levels (25th/75th box; 10th/90th error bars).

study as we aimed to include all the situations carrying significant morbidity. Although the number of patients was not very large, the population was rather homogeneous and representative of the population of PT from 24 to 31 weeks. Moreover, the population was large enough to reveal a relationship between the level of OS and both the antenatal context and the neonatal morbidity. In our population, we found maximal MDA-Hb value in one infant of the control (ISM−) group. It could be considered as an outlier. It could be also a false-positive result. There was no neonatal infection. We do not have any explanation for that high value. However, as we aimed to evaluate whether MDA-Hb could be used as a marker of oxidative stress in a population of preterm infants, we could not expect a 100% specificity.

Our population represented the four classes of etiology in preterm delivery: maternal antenatal infection, preeclampsia,

fetal growth restriction (FGR), and other causes (metrorrhagia, placental abnormalities). The first three are associated with inflammation, which is known to affect redox balance [26]. We found the significantly highest MDA-Hb concentration at birth in the cases of maternal antenatal infection, which is characterized by the release of inflammatory cytokines by decidua and fetal membranes, leading to preterm labor and the generation of free radicals and ROS in fetal and maternal circulation [27]. In contrast, GSH concentrations at birth were similar regardless of the prenatal environment and similar to GSH concentrations in healthy adults [23]. Lower GSH concentrations were observed in VLBW infants compared with full-term infants [28], but GSH at birth has not been studied in VLBW infants in relation to the perinatal context, to our knowledge.

Various fundamental and clinical data have underlined the central role of OS in the physiopathology of current neonatal diseases related to prematurity [29–33]. Therefore, higher concentrations of oxidant markers were expected in the sicker infants, and we indeed found an association between MDA-Hb, an index of lipid peroxidation, and neonatal morbidity. This finding agrees with previous findings using other oxidative markers [1, 29, 30, 34].

The MDA-Hb concentration at birth could be useful in identifying neonates at high risk for severe morbidity, as we found higher values in the ISM+ group than in the ISM− group. This fits quite well with the results recently published by Perrone et al. [35], reporting significantly higher levels of oxidant markers in the cord blood of preterm infants with NEC than in preterm infants without NEC [29, 34–36]. Higher MDA-Hb concentrations were found in the ISM+ group not only during the first postnatal week, as often described [29, 34, 37], but also over the first 6 weeks of life.

The evidence of OS persisting for at least a month strongly suggests a long-lasting imbalance between antioxidant and oxidant-generating systems, which causes oxidative damage in preterm infants.

Depletion of whole blood GSH is known to occur in preterm infants, and GSH correlates with gestational age [38, 39]. Therefore, the GSH concentrations should have been lower in the less mature infants (ISM+ group) than in the ISM− group. This was not the case, suggesting the absence of a clear relationship between GSH concentrations and severe neonatal morbidity. Two explanations for our finding may be the small size of our study population and the influence of blood transfusions (more frequent in the ISM+ group). However, one should note that the GSH concentrations in both the ISM+ and ISM− groups were similar to those of healthy adults, as measured by Steghens et al. using the same dosage method [23]. Very few studies have reported reduced glutathione measurement, and most of these studies concerned cord blood samples from neonates not yet exposed to true OS and compared preterm infants with healthy full-term infants. To our knowledge, this study is the first to evaluate the relationship between severe morbidity in preterm infants at birth and over 6 weeks of age and the GSH concentration.

In the studies performed several days after birth, lower GSH concentrations (in erythrocytes and cells from tracheal aspirates) were observed in preterm infants with respiratory distress syndrome [39, 40]. In the present study, no difference in GSH concentrations in the ISM+ and ISM− groups was observed in the first 6 weeks of life. The lowest concentration of GSH in the ISM+ group was observed at the time of the MDA-Hb peak, during the second week of life. This could be explained by an abnormality in the antioxidant system in the ISM+ infants, who were exposed to higher levels of OS related to excessive consumption and/or reduced capacities of GSH synthesis due to hepatic immaturity or a deficit in cysteine, the main acid amine regulator of GSH synthesis [41–43].

The infants in the ISM+ group had more blood transfusions, which may have had an impact on the MDA-Hb and GSH concentrations. For example, the MDA-Hb concentrations may have been underestimated due to the influence of blood transfusions. This would explain the MDA-Hb decrease in the third week of life in the ISM+ group. Moreover, the cumulative effect of MDA-Hb over time may also have been affected. On the other hand, the GSH concentrations may have been overestimated in this group, but no conclusions can be drawn regarding our GSH results, which did not differentiate the groups but nevertheless remain interesting from a clinical point of view. To estimate the impact of transfusions, we had to measure the MDA and GSH concentrations in five randomly selected packed red cells used in preterm infants included in our study. Both MDA-Hb and whole blood GSH concentrations in packed red cells were neither very low nor very high. As they were close to those measured in healthy full-term neonates at birth [18], the contribution of blood transfusions to MDA-Hb and GSH levels in preterm infants is unlikely.

It appears that the OS level in the ISM+ group was such that oxygen-free radical production, as reflected by the MDA adduct to hemoglobin, exceeded the antioxidant defense system. The evidence of a strong pro/antioxidant imbalance raises many questions about the involvement of OS in the physiopathology of neonatal complications, without being able to establish a causal link.

In conclusion, the present study is the first step in the validating technique to evaluate postnatal OS without the need of additional blood sampling. The higher MDA-Hb concentrations in the sicker infants suggest that MDA-Hb is a marker of interest for estimating and quantifying OS in VLBW infants. This noninvasive method may help to enhance our understanding of OS, thereby improving the accuracy of modifications in therapeutics (assisted ventilation, oxygen therapy, and parenteral nutrition) to reduce free radical generation and providing guidelines for developing future applications of antioxidant therapy in premature infants. Although these findings require confirmation in a larger population, the results of our study provide insight into the relationship between MDA-Hb and neonatal morbidity.

Abbreviations

BPD: Bronchopulmonary dysplasia
BW: Birth weight
ISM: Index of severe morbidity
DAN: Diaminonaphthalene

FGR: Fetal growth restriction
GA: Gestational age
GSH: Reduced Glutathione
Hb: Hemoglobin
LC-MS: Liquid chromatography-mass spectrometry
MDA: Malondialdehyde
MDA-Hb: Malondialdehyde adduct to hemoglobin
NEC: Necrotizing enterocolitis
OS: Oxidative stress
PT: Preterm infants
RBC: Red blood cell
ROS: Reactive oxygen species
VLBW: Very low birth weight.

Acknowledgments

The authors thank Brigitte Guy and Blandine Vallet-Sandre for their help in collecting the samples; Christine Delore, Catherine Castrichini, and Sophie Vasseur for their help in processing the analysis; and C. Carmeni for editing the paper.

References

[1] O. M. Pitkanen, M. Hallman, and S. M. Andersson, "Correlation of free oxygen radical-induced lipid peroxidation with outcome in very low birth weight infants," *Journal of Pediatrics*, vol. 116, no. 5, pp. 760–764, 1990.

[2] J. H. N. Lindeman, D. van Zoeren-Grobben, J. Schrijver, A. J. Speek, B. J. H. M. Poorthuis, and H. M. Berger, "The total free radical trapping ability of cord blood plasma in preterm and term babies," *Pediatric Research*, vol. 26, no. 1, pp. 20–24, 1989.

[3] J. L. Sullivan and R. B. Newton, "Serum antioxidant activity in neonates," *Archives of Disease in Childhood*, vol. 63, no. 7, pp. 748–750, 1988.

[4] R. Robles, N. Palomino, and A. Robles, "Oxidative stress in the neonate," *Early Human Development*, vol. 65, no. 2, pp. S75–S81, 2001.

[5] H. J. Helbock, P. A. Motchnik, and B. N. Ames, "Toxic hydroperoxides in intravenous lipid emulsions used in preterm infants," *Pediatrics*, vol. 91, no. 1, pp. 83–87, 1993.

[6] L. Pironi, M. Guidetti, C. Zolezzi et al., "Peroxidation potential of lipid emulsions after compounding in all-in-one solutions," *Nutrition*, vol. 19, no. 9, pp. 784–788, 2003.

[7] J. C. Picaud, J. P. Steghens, C. Auxenfans, A. Barbieux, S. Laborie, and O. Claris, "Lipid peroxidation assessment by malondialdehyde measurement in parenteral nutrition solutions for newborn infants: a pilot study," *Acta Paediatrica*, vol. 93, no. 2, pp. 241–245, 2004.

[8] S. Laborie, J. C. Lavoie, and P. Chessex, "Increased urinary peroxides in newborn infants receiving parenteral nutrition exposed to light," *Journal of Pediatrics*, vol. 136, no. 5, pp. 628–632, 2000.

[9] A. Jalabert, A. Grand, J. P. Steghens, E. Barbotte, C. Pigue, and J. C. Picaud, "Lipid peroxidation in all-in-one admixtures for preterm neonates: impact of amount of lipid, type of lipid emulsion and delivery condition," *Acta Paediatrica*, vol. 9, pp. 1200–1205, 2011.

[10] O. D. Saugstad, "Bronchopulmonary dysplasia and oxidative stress: are we closer to an understanding of the pathogenesis of BPD?" *Acta Paediatrica*, vol. 86, no. 12, pp. 1277–1282, 1997.

[11] T. E. Inder, B. A. Darlow, K. B. Sluis et al., "The correlation of elevated levels of an index of lipid peroxidation (MDA-TBA) with adverse outcome in the very low birthweight infant," *Acta Paediatrica*, vol. 85, no. 9, pp. 1116–1122, 1996.

[12] F. J. Kelly, "Free radical disorders of preterm infants," *British Medical Bulletin*, vol. 49, no. 3, pp. 668–678, 1993.

[13] D. W. Thibeault, "The precarious antioxidant defenses of the preterm infant," *American Journal of Perinatology*, vol. 17, no. 4, pp. 167–181, 2000.

[14] D. Del Rio, A. J. Stewart, and N. Pellegrini, "A review of recent studies on malondialdehyde as toxic molecule and biological marker of oxidative stress," *Nutrition, Metabolism and Cardiovascular Diseases*, vol. 15, no. 4, pp. 316–328, 2005.

[15] I. F. F. Benzie, "Lipid peroxidation: a review of causes, consequences, measurement and dietary influences," *International Journal of Food Sciences and Nutrition*, vol. 47, no. 3, pp. 233–261, 1996.

[16] J. P. Steghens, K. Arab, A. Rossary, and L. Soulère, "Conjugated linoleic acid, unlike other unsaturated fatty acids, strongly induces glutathione synthesis without any lipoperoxidation," *British Journal of Nutrition*, vol. 96, no. 5, pp. 811–819, 2006.

[17] A. Grand, A. Jalabert, G. Mercier et al., "Influence of vitamins, trace-elements and iron on lipid peroxidation reactions in all-in-one admixtures for parenteral nutrition in neonates," *Journal of Parenteral and Enteral Nutrition*, vol. 35, pp. 505–510, 2011.

[18] C. Cipierre, S. Haÿs, D. Maucort-Boulch, J.-P. Steghens, and J.-C. Picaud, "Malondialdehyde adducts to hemoglobin: a new marker of oxidative stress suitable for full-term and preterm neonates," *Oxidative Medicine and Cellular Longevity*. In press.

[19] M. Tornqvist and A. Kautiainen, "Adducted proteins for identification of endogenous electrophiles," *Environmental Health Perspectives*, vol. 99, pp. 39–44, 1993.

[20] R. Usher and F. McLean, "Intrauterine growth of live-born Caucasian infants at sea level: standards obtained from measurements in 7 dimensions of infants born between 25 and 44 weeks," *The Journal of Pediatrics*, vol. 74, no. 6, pp. 901–910, 1969.

[21] M. C. Walsh and R. M. Kliegman, "Necrotizing enterocolitis: treatment based on staging criteria," *Pediatric Clinics of North America*, vol. 33, no. 1, pp. 179–201, 1986.

[22] J. P. Steghens, A. L. Van Kappel, I. Denis, and C. Collombel, "Diaminonaphtalene, a new highly specific reagent for HPLC-UV measurement of total and free malondialdehyde in human plasma or serum," *Free Radical Biology and Medicine*, vol. 31, no. 2, pp. 242–249, 2001.

[23] J. P. Steghens, F. Flourié, K. Arab, and C. Collombel, "Fast liquid chromatography-mass spectrometry glutathione measurement in whole blood: micromolar GSSG is a sample preparation artifact," *Journal of Chromatography B*, vol. 798, no. 2, pp. 343–349, 2003.

[24] A. Kautiainen, M. Tornqvist, K. Svensson, and S. Osterman-Golkar, "Adducts of malonaldehyde and a few other aldehydes to hemoglobin," *Carcinogenesis*, vol. 10, no. 11, pp. 2123–2130, 1989.

[25] A. Kautiainen, C. E. Vaca, and F. Granath, "Studies on the relationship between hemoglobin and DNA adducts of malonaldehyde and their stability in vivo," *Carcinogenesis*, vol. 14, no. 4, pp. 705–708, 1993.

[26] M. Valko, D. Leibfritz, J. Moncol, M. T. D. Cronin, M. Mazur, and J. Telser, "Free radicals and antioxidants in normal physiological functions and human disease," *International Journal of Biochemistry and Cell Biology*, vol. 39, no. 1, pp. 44–84, 2007.

[27] J. R. Woods Jr., "Reactive oxygen species and preterm premature rupture of membranes—a review," *Placenta*, vol. 22, no. 1, pp. S38–S44, 2001.

[28] A. Küster, I. Tea, V. Ferchaud-Roucher et al., "Cord blood glutathione depletion in preterm infants: correlation with maternal cysteine depletion," *PLoS ONE*, vol. 6, no. 11, Article ID e27626, 2011.

[29] T. E. Inder, P. Graham, P. G. K. Sanderson, and B. J. Taylor, "Lipid peroxidation as a measure of oxygen free radical damage in the very low birthweight infant," *Archives of Disease in Childhood*, vol. 70, no. 2, pp. F107–F111, 1994.

[30] E. Varsila, O. Pitkanen, M. Hallman, and S. Andersson, "Immaturity-dependent free radical activity in premature infants," *Pediatric Research*, vol. 36, no. 1, pp. 55–59, 1994.

[31] B. Weinberger, S. Nisar, M. Anwar, B. Ostfeld, and T. Hegyi, "Lipid peroxidation in cord blood and neonatal outcome," *Pediatrics International*, vol. 48, no. 5, pp. 479–483, 2006.

[32] M. Vento, M. Moro, R. Escrig et al., "Preterm resuscitation with low oxygen causes less oxidative stress, inflammation, and chronic lung disease," *Pediatrics*, vol. 124, pp. 439–449, 2009.

[33] D. J. O'Donovan and C. J. Fernandes, "Free radicals and diseases in premature infants," *Antioxidants and Redox Signaling*, vol. 6, no. 1, pp. 169–176, 2004.

[34] G. Buonocore, S. Perrone, M. Longini et al., "Oxidative stress in preterm neonates at birth and on the seventh day of life," *Pediatric Research*, vol. 52, no. 1, pp. 46–49, 2002.

[35] S. Perrone, M. L. Tataranno, S. Negro et al., "May oxidative stress biomarkers in cord blood predict the occurrence of necrotizing enterocolitis in preterm infants?" *Journal of Maternal-Fetal and Neonatal Medicine*, vol. 15, pp. 128–131, 2012.

[36] S. Perrone, M. L. Tataranno, S. Negro et al., "Early identification of the risk for free radical-related diseases in preterm newborns," *Early Human Development*, vol. 86, no. 4, pp. 241–244, 2010.

[37] G. Buonocore, S. Perrone, M. Longini, L. Terzuoli, and R. Bracci, "Total hydroperoxide and advanced oxidation protein products in preterm hypoxic babies," *Pediatric Research*, vol. 47, no. 2, pp. 221–224, 2000.

[38] A. Jain, T. Mehta, P. A. Auld et al., "Glutathione metabolism in newborns: evidence for glutathione deficiency in plasma, bronchoalveolar lavage fluid, and lymphocytes in prematures," *Pediatric Pulmonology*, vol. 20, no. 3, pp. 160–166, 1995.

[39] I. Németh and D. Boda, "Blood glutathione redox ratio as a parameter of oxidative stress in premature infants with IRDS," *Free Radical Biology and Medicine*, vol. 16, no. 3, pp. 347–353, 1994.

[40] J. C. Lavoie and P. Chessex, "Gender and maturation affect glutathione status in human neonatal tissues," *Free Radical Biology and Medicine*, vol. 23, no. 4, pp. 648–657, 1997.

[41] J. Vina, M. Vento, F. Garcia-Sala et al., "L-cysteine and glutathione metabolism are impaired in premature infants due to cystathionase deficiency," *American Journal of Clinical Nutrition*, vol. 61, no. 5, pp. 1067–1069, 1995.

[42] G. Wu, Y. Z. Fang, S. Yang, J. R. Lupton, and N. D. Turner, "Glutathione metabolism and its implications for health," *Journal of Nutrition*, vol. 134, no. 3, pp. 489–492, 2004.

[43] S. C. Lu, "Regulation of hepatic glutathione synthesis: current concepts and controversies," *FASEB Journal*, vol. 13, no. 10, pp. 1169–1183, 1999.

Hindawi Publishing Corporation
Oxidative Medicine and Cellular Longevity
Volume 2013, Article ID 674593, 7 pages
http://dx.doi.org/10.1155/2013/674593

Research Article

Effects of Single Exposure of Sodium Fluoride on Lipid Peroxidation and Antioxidant Enzymes in Salivary Glands of Rats

Paula Mochidome Yamaguti, Alyne Simões, Emily Ganzerla, Douglas Nesadal Souza, Fernando Neves Nogueira, and José Nicolau

Departamento de Biomateriais e Biologia Oral, Faculdade de Odontologia, Universidade de São Paulo, 05508-000 São Paulo, SP, Brazil

Correspondence should be addressed to Alyne Simões; lysimoes@usp.br

Received 7 February 2013; Revised 3 April 2013; Accepted 4 April 2013

Academic Editor: Kota V. Ramana

Many studies suggest that fluoride exposure can inhibit the activity of various enzymes and can generate free radicals, which interfere with antioxidant defence mechanisms in living systems. To further the understanding of this issue, this present study examined the effects of low-dose fluoride treatment on the activity of enzymatic antioxidant superoxide dismutase (SOD) and catalase (CAT), as well as the levels of lipid peroxidation (LPO) in the parotid (PA) and submandibular (SM) salivary glands of rats. Rats were injected with a single dose of sodium fluoride (NaF) (15 mg F^-/kg b.w.) then euthanized at various time intervals up to 24 hours (h) following exposure. NaF exposure did not cause significant differences in SOD or CAT activity or LPO levels in PA glands compared to control. Conversely, SM glands presented increased SOD activity after 3 h and decreased SOD activity after 1, 12, and 24 h, while LPO was increased after 6, 12, and 24 h of the NaF injection. There were no significant differences in the CAT activity in the groups studied. Our results demonstrated that NaF intoxication caused oxidative stress in salivary glands few hours after administration. These changes were more pronounced in SM than in PA gland.

1. Introduction

Fluoride is widely regarded as the cornerstone of modern preventive dentistry. Because of its cariostatic properties, fluoride has been increasingly added to alternative delivery systems, such as toothpastes and mouth rinses, so that exposure of populations to fluoride other than through fluoridated water supplies and foodstuffs has become significant [1]. The widespread use of these fluoridated products, in addition to its ubiquitous presence in the environment, has renewed consideration of the margin which exists between safe and toxic levels of fluoride exposure [2, 3].

Although the most pronounced effects of fluoride intake are manifested in bones and teeth, it is also known to cross cell membranes by simple diffusion and enter soft tissues causing adverse effects on cell metabolism and function [1, 4–6]. In soft tissues, its concentration is proportional to the plasma concentration [7]. Salivary glands are important secretory organs, vital to various processes occurring in the oral cavity. Their secretory products have an utmost importance for several physiological functions, playing a critical role in oral and systemic health by monitoring, regulating, and maintaining the integrity of the oral hard and soft tissues [8]. The major salivary glands of both humans and rodents consist of three pairs of macroscopic glands: parotid (PA), submandibular (SM), and sublingual [9].

Studies with low doses of NaF administered to experimental animals have been shown to induce a number of alterations in the metabolism of their salivary glands. Some of these metabolic alterations include increases in glycogen content in SM glands [10] and higher levels of $3', 5'$cyclic AMP (cAMP) in PA and SM glands [11] as well as promoting the release of high molecular weight mucins from the SM gland [12]. Fluoride is also known to inhibit the activity of

many enzymes [13, 14]. Some of the effects reported arise indirectly because one pathway is inhibited by fluoride making more substrate available for other pathways which thus appear to be enhanced [14]. NaF in low concentrations can alter activities of some carbohydrate metabolizing enzymes such as phosphofructokinase-1, hexokinase, pyruvate kinase, glucose-6-phosphate dehydrogenase, and lactate dehydrogenase in SM glands of rats [15, 16] and promote the release of amylase secretion from PA glands of rats and humans [12].

Oxidative stress is biomolecular damage caused by the attack of reactive species (RS) upon the constituents of a living organism [17]. Among RS, reactive oxygen species (ROS) play a major part because they are highly reactive and formed by numerous enzymes [18]. The production of excessive amounts of ROS is toxic to the cell. The human body has different methods of reducing the impact of oxidative injury, using enzymatic or nonenzymatic defence systems to prevent oxidative stress damage or by repairing the damage after it has occurred [19]. The antioxidant defence systems such as antioxidant vitamins (vitamins A, C, and E), SOD, CAT, glutathione (GSH), and glutathione peroxidase (GSH-Px) protect the cells against LPO [20].

The problems associated with F exposure is that it amplifies the biochemical stress in the body by generating imbalance between ROS and antioxidants thereby inducing oxidative stress and inhibiting several groups of enzymes [13, 14, 21], including many whose action depends on divalent metals such as magnesium (enolase, phosphatases) or trivalent metals (catalase, peroxidase) [14]. These effects have been observed in several soft tissues and cells, such as brain [21–26], gastrocnemius muscle [26], kidney [21, 23–25, 27–29], liver [19, 21, 23–25, 28, 30–32], heart [21], nervous system [33], blood [5, 25, 28, 34, 35], and osteoblasts [36, 37].

However, to the best of our knowledge, no information exists concerning the relation between fluoride intake and oxidative stress in salivary glands. Therefore, the investigation reported herein was undertaken to evaluate the influence of a low dose of NaF over a time period of 24 h on some antioxidant enzymes and LPO in SM and PA salivary glands of rats.

2. Material and Methods

2.1. Chemicals and Reagents. Sodium fluoride (NaF) (CAS no. 7681-49-4), nicotinamide adenine dinucleotide phosphate, reduced form (NADPH) disodium salt, 2-mercaptoethanol, ethylene-diamine-tetra-acetic acid (EDTA), triethanolamine, diethanolamine, and trichloroacetic acid were purchased from Sigma Aldrich Co. (St. Louis, MO, USA). 2-Thiobarbituric acid was obtained from Merck KGaA (Darmstadt, Germany). All other chemical reagents were of highest pure analytical grade commercially available.

2.2. Ethical Aspects of Research. Experimental protocols and animal handling and care were conducted in compliance with the guidelines established by the Brazilian College of Animal Care (COBEA) and according to the standards of humane treatment for animals. This study was approved by the Bioethics Committee of Animals from School of Dentistry, University of São Paulo, approval number 01/06.

2.3. Experimental Design and Sample Preparation. One hundred two-month-old male rats of Wistar strain were used in the present investigation. Animals were obtained from the Department of Biomaterials and Oral Biochemistry, School of Dentistry (FOUSP), University of São Paulo, São Paulo, Brazil.

Rats were housed in solid bottomed polypropylene cages, acclimatized for 7 days to animal house conditions, and maintained locally with *ad libitum* commercially available rodent chow diet (Purina) and tap water. The fluoride concentration in the tap water of São Paulo is regulated by the city government at 0.7 ppm. Drugs were freshly prepared prior to administration. Prior to the treatment, all rats' body weights (b.w.) were obtained to minimize intergroup differences. Animals weighed between 220–270 g and, therefore, were randomly and equally ($n = 50$) stratified into two groups according to the treatment received, fluoride (F) and control (C). Fluoride treatment groups were intraperitoneally administered with a single injection of NaF solution (15 mg F^-/kg b.w.), and control rats received an equivalent dose of sodium chloride solution (0.9% NaCl). Each treatment group, F and C, was further divided into 5 subgroups according to the length of time after injection. The animals were euthanized 1, 3, 6, 12, and 24 h after injection, and SM and PA salivary glands were immediately excised, cleaned in isotonic solution, precooled in dry ice, and stored at −80°C until further processing. Tissues were minced and homogenized in a T-8 Ultra-Turrax homogenizer (IKA-Werke GMBH & CO.KG, Germany) at 10% (w/v) in an ice-cold 50 mM phosphate buffer solution (PBS), pH 7.0. To remove red blood cells, tissue samples were washed twice with 5 volumes of 0.9% NaCl solution. Fibrous material and other tissue debris were eliminated by centrifugation of the tissue homogenate at 1,540 ×g for 10 min at 4°C (Himac CF 15R, Hitachi, Japan), and the supernatants were used for all determinations.

2.4. Assay Procedures. All assays were monitored at 25°C in a model DU-800 spectrophotometer (Beckman, Fullerton, CA, USA).

Specific activity of CAT (EC 1.11.1.6) was determined by following the decomposition of hydrogen peroxide (H_2O_2) at 240 nm for 3 min and calculated using the molar extinction coefficient of 43.6 M cm^{-1}. One unit of activity is defined as the amount of the enzyme required to decompose 1 μmol of H_2O_2/min [38, 39].

Specific activity of total SOD (EC 1.15.1.1.) was determined measuring inhibition of superoxide-driven NADPH oxidation by mercaptoethanol in the presence of EDTA and manganese (II) chloride. Changes in the absorbance were measured at 340 nm. Percent inhibition was used as the index of SOD activity and calculated as (sample rate)/(control rate) × 100; one unit of SOD activity was defined as half-maximal inhibition [40, 41].

Malondialdehyde, the marker of extent lipid peroxidation, was estimated as thiobarbituric acid reactive substances

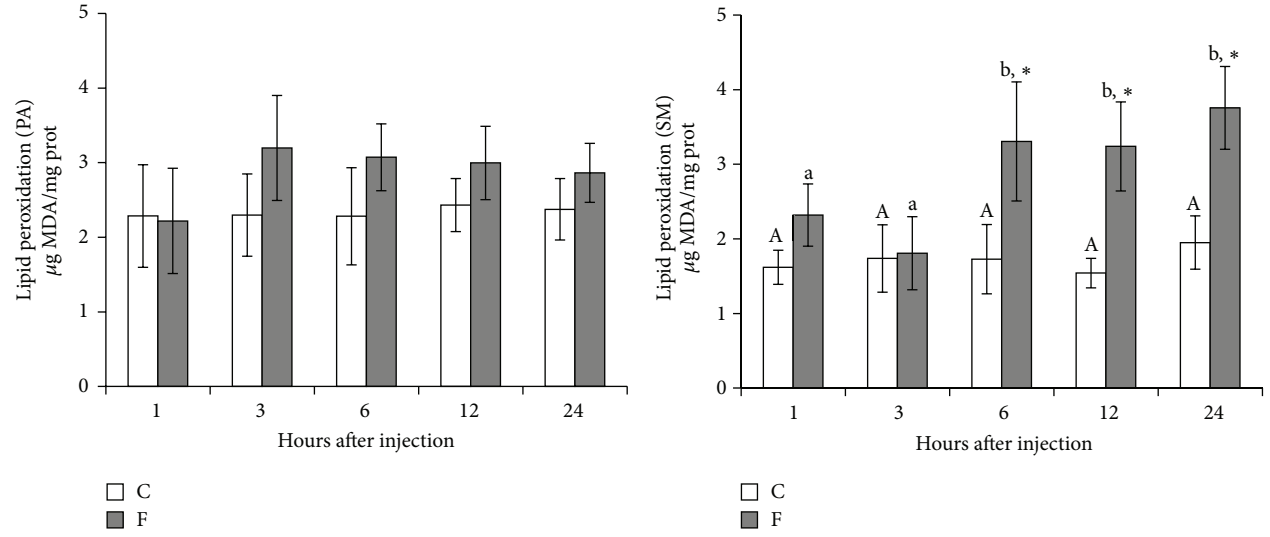

Figure 1: Levels of MDA in PA ($n = 6$) and SM ($n = 10$) glands of rats after treatment with a single IP injection of 15 mg F^-/kg b.w. in the experimental group (F) and with 0.9% NaCl in the control group (C). Rats were euthanized after 1, 3, 6, 12, and 24 h. No difference was observed in PA. $^*P < 0.05$ compared to the control group. Different letters show $P < 0.05$ for different time intervals in the same treatment group.

(TBARS) level in gland tissue by the method of Esterbauer and Cheeseman [42]. Samples were read at 532 nm, and the amount of TBARS was calculated using a molar extinction coefficient of 1.56×10^5 M/cm.

Protein content was determined by using Folin-phenol reagent with bovine serum albumin as standard by the method of Lowry et al. [43].

2.5. Statistical Analysis. All experiments were performed in duplicates, and the values are expressed as mean ± standard deviation (SD). All data were checked for normality and analyzed by one- (factor: treatment) or two-way (factors: treatment and time) analysis of variance (ANOVA). When significant main effects were detected in the outcome measures of the study (treatment × time), the means were subsequently analyzed by Tukey test for all pairwise comparisons. All statistical tests were performed using Minitab Statistical Software (PA, USA). Differences were considered statistically significant at $P < 0.05$.

3. Results

3.1. Effects of NaF on LPO of PA and SM Glands. Figure 1 shows the levels of MDA in PA ($n = 6$) and SM ($n = 10$) glands of rats, respectively, after injection of 15 mg F^-/kg b.w. Though the levels of MDA in PA glands were marginally higher in experimental groups (F), they were not statistically significant. In the SM glands, animals treated with fluoride presented higher levels of MDA production than the control group. The values were 91%, 110%, and 93% after 6, 12, and 24 h of the NaF injection, respectively ($P < 0.01$).

3.2. Specific Activity of CAT in PA and SM Glands after Treatment with Fluoride. Figure 2 presents the specific activity of CAT in PA ($n = 6$) and SM ($n = 10$) glands of rats, respectively, after injection of 15 mg F^-/kg b.w. Although, fluoride exposure promoted a very slight decrease in CAT activity of PA glands, no significant differences were observed in any time point within the studied groups. We observed a discrete increase trend in the activity of CAT in SM glands; however, it was also not significant ($P = 0.056$).

3.3. Total Activity of SOD in PA and SM Glands after Treatment with Fluoride. Figure 3 shows the total activity of SOD in PA ($n = 6$) and SM ($n = 10$) glands of rats, respectively, after injection of 15 mg F^-/kg b.w. Once again, fluoride treatment did not aggravate the activity of SOD in PA glands. As for SM glands, fluoride induced a different response. SM glands showed a significant reduction of SOD activity after 1 h (29%), 12 h (26%), and 24 h (40%) of NaF administration ($P < 0.05$). Conversely, a significantly increased activity of SOD (46%) ($P < 0.05$) was observed after 3 h.

4. Discussion

This study assessed the susceptibility of SM and PA salivary glands to oxidative stress and LPO induced by a single injection of a low concentration of fluoride over a period of 24 h. Injections of NaF (15 mg F^-/kg b.w.) resulted in very slight alterations in PA salivary glands of rats. SM glands presented an increase in SOD activity after 3 h and a decrease of its activity after 1, 12, and 24 h, while LPO was substantially increased after 6, 12, and 24 h. Another relevant observation

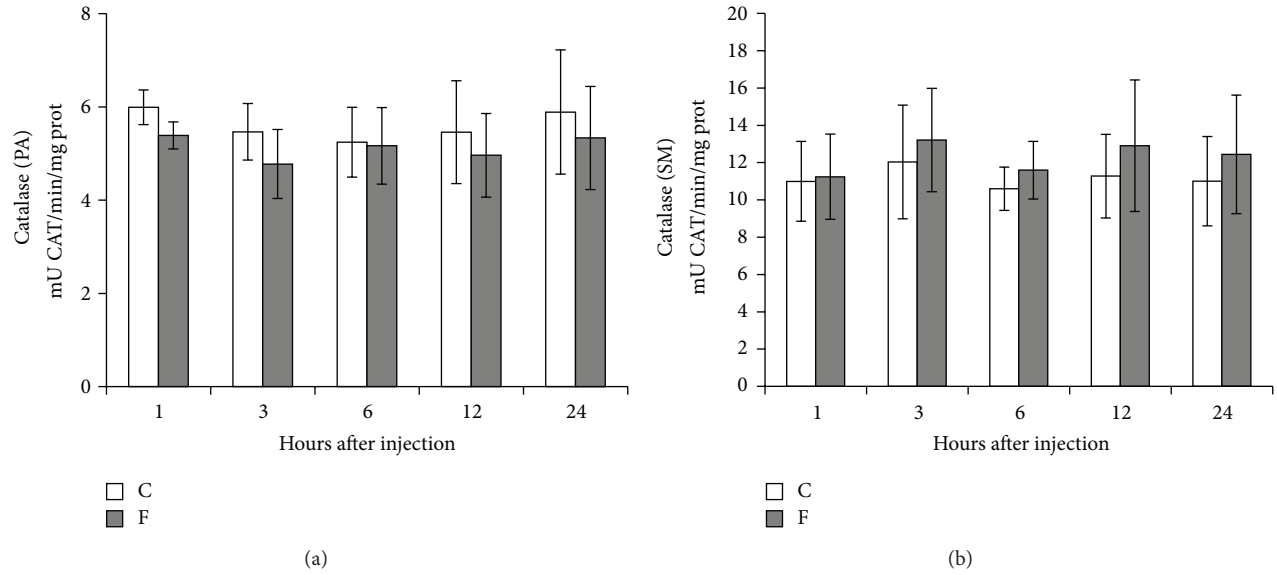

Figure 2: Specific activity of CAT in PA ($n = 6$) and SM ($n = 10$) glands of rats after treatment with a single IP injection of 15 mg F^-/kg b.w. in the experimental group (F) and with 0.9% NaCl in the control group (C). Rats were euthanized after 1, 3, 6, 12, and 24 h. No difference was observed in PA and SM.

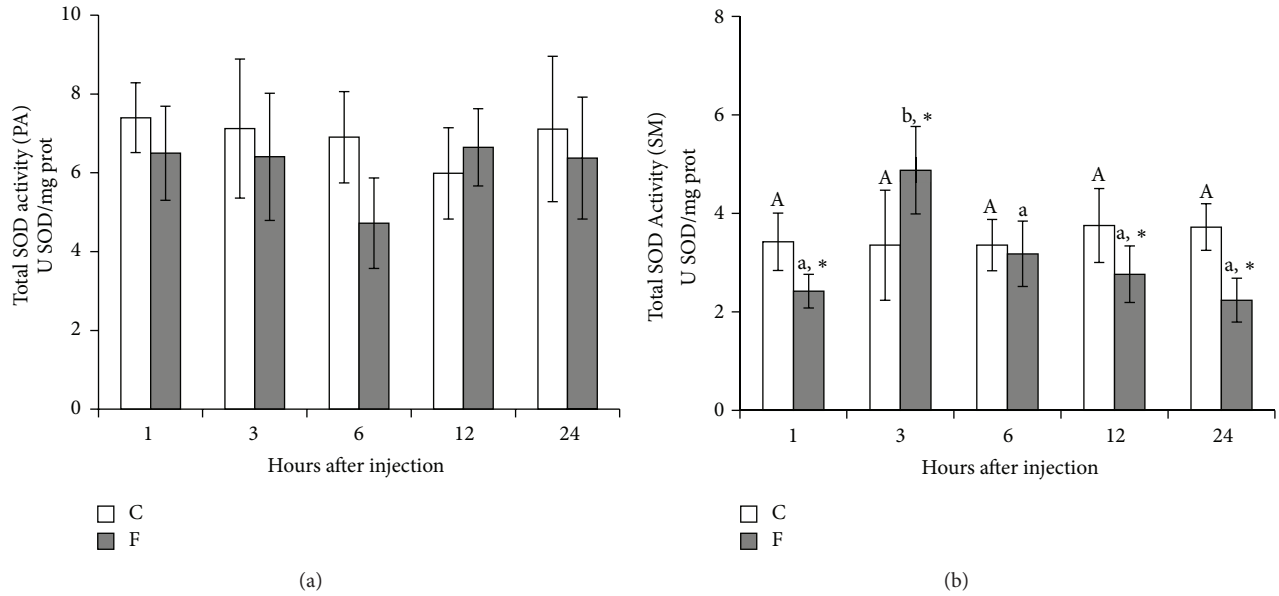

Figure 3: Total activity of SOD in PA ($n = 6$) and SM ($n = 10$) glands of rats after treatment with a single IP injection of 15 mg F^-/kg b.w. in the experimental group (F) and with 0.9% NaCl in the control group (C). Rats were euthanized after 1, 3, 6, 12, and 24 h. No difference was observed in PA. $^*P < 0.05$ compared to the control group. Different letters show $P < 0.05$ for different time intervals in the same treatment group.

in our study is that the time period after NaF injection did not influence PA gland response as it did on SM gland.

The mechanism by which fluoride produces its effects has still not been elucidated, and therefore, the manner in which whole body effects are produced is still unclear [4, 44, 45]. Many studies have proposed that fluoride in varying concentrations induces increased ROS generation, enhanced LPO, and impaired antioxidant enzyme defence system in blood and tissues of experimental animals by interfering with the major metabolic pathways of the living system [26, 28, 45–47].

Antioxidant protection of living organism consists of several levels of defensive response activity including enzymes, proteins, and low-molecular-mass agents [47]. The mitochondrial electron transport chain and a variety of cellular oxidases are the main source of ROS, which are continuously generated as by-products of various intracellular redox reactions. The primary defences against oxidative injury are

the antioxidant enzymes that control RS metabolism. One detoxifying enzyme that counteracts potentially deleterious-oxidizing agents is superoxide dismutase. SOD converts the dismutation of superoxide anions ($O_2^{\bullet-}$) to a less reactive nonradical specie, H_2O_2, in the presence of metal ions (copper and iron). It represents the primary line of ROS defence, as it prevents further generation of free radicals, by being highly efficient in catalytic removal of $O_2^{\bullet-}$ [17]. Published scientific literature reports that fluoride in varying concentrations impaired SOD activity in liver, kidney, brain, thyroid, and cultured cells [19, 26, 27, 29, 44, 45, 48], increased activity in osteoblasts [49] and effected no change in red blood cells [5]. In the SM gland particularly, treatment with fluoride decreased SOD activity after 1, 12, and 24 h and an increase after 3 h (Figure 3). This increase in SOD activity after 3 h of NaF administration may suggest an adaptive and transient response to fluoride intoxication [21]. The loss of SOD activity may be explained due to the fact that fluoride ions are among competitive inhibitors of SOD activity and the reaction rate for fluoride binding to the active site reaches an equilibrium within a very short period of time [50]. Alternately, it could be attributed to a direct action by fluoride on the enzyme leading to the diminished ability of the tissues to handle $O_2^{\bullet-}$ radicals [51].

CAT subsequently reduces the H_2O_2 produced by SOD to water. Catalase is a hemeprotein, which catalyses a dismutation reaction; one H_2O_2 is reduced to H_2O, and the other oxidized to ground-state O_2 [17]. Authors investigating the influence of fluoride on the activity of CAT reported contradictory results. Some studies have reported decreased [19, 22, 26–29], increased [21], and unchanged [45] CAT activity. Reddy et al. did not find any difference in the activity of CAT in red blood cells of fluoride-intoxicated rabbits [5]. In this investigation, although no changes were observed for the activity of CAT in both PA and SM glands over the studied intervals after fluoride treatment, we did observe a trend towards enhanced activity in SM glands of the experimental group (statistically insignificant, $P = 0.056$).

ROS react with antioxidants and attack redox-sensitive biomolecules. Reactions with these targets result in the cell damage frequently associated with oxidative stress [18]. They react with methylene groups of polyunsaturated fatty acids, initiating the peroxidation of membrane lipids and producing MDA as one of the end products [47]. MDA is considered to be the most significant indicator of membrane LPO arising from the interaction of reactive oxygen types with cellular membranes. Increased LPO from fluoride toxicity may be due to the generation of ROS by high levels of H_2O_2 being formed in cells by controlled pathways. H_2O_2 at high concentration is deleterious to cells, and its accumulation causes oxidation of cellular targets such as proteins, lipids, and DNA leading to mutagenesis and cell death [52]. Removal of H_2O_2 from cells is, therefore, necessary for protection against oxidative damage. In this study, the exposure to a low concentration of fluoride altered the MDA content in SM salivary glands. A marked increase in the concentration of MDA was observed in SM glands of the experimental animals after 6, 12, and 24 h. These data corroborate with many authors who have observed increased levels of MDA in different tissues and cells of fluoride-intoxicated animal [19, 21–24, 27–29, 31, 44, 45, 48, 53].

Extensive amounts of available information concerning the role of fluoride in oxidative stress are inconclusive and conflicting. Reddy et al. suggested that oxidative stress may not be directly related to fluoride toxicity but could be a secondary effect [5]. On the other hand, it is relevant to state that many other factors could have influenced the outcome response to fluoride exposure among these studies, such as diet, route of administration, gender, species, body weight and age of experimental animals, acid-base status, and fluoride compound [13]. Rats are more resistant to fluoride than sheep and rabbits [4]. Younger rats of both sexes are more resistant than older rats, with females being less resistant than males of the same age [14]. In our investigation, the dose of 15 mg F^-/kg b.w. is relatively low and corresponds to approximately 1/6 of the 24 hour median lethal dose (LD_{50}) for a rat intraperitoneally injected with NaF, which has been reported to range from 85.5 to 98.0 mg F^-/kg [13, 54]. Small amounts of fluoride have been shown to cause normal plasma fluoride levels to surge and peak to potentially harmful values [3]. It has been demonstrated that NaF at a concentration as low as 0.5 mg F^-/kg increases cAMP levels in PA gland of rats, altering salivary function [12]. IP injections of NaF (15 mg F^-/kg b.w) increased cAMP concentration in SM gland of rats after 30 and 60 min [55]. The same increased level of cAMP was observed for PA gland cells of rats incubated 0.01 mmol/L of NaF after 10 min [56]. Low concentrations stimulate LPO, and at high and very high concentrations may act as inhibitor of MDA generation [47]. Xu et al. reported that low concentrations of fluoride increased activity of antioxidant enzymes and enhanced LPO in osteoblasts of mice [49]. Moreover, the different responses found between SM and PA salivary glands could be possible due to metabolic differences between the two glands: PA gland metabolism is predominantly aerobic, and SM gland metabolism is predominantly anaerobic [57] in addition to distinct histological characteristics and secretion end products in each [58]. Nagler et al. reported that PA saliva secretion presents much higher levels of salivary molecular and enzymatic antioxidants parameters than SM/SL saliva [59], which corroborate with our findings, where PA salivary glands were more able to cope with oxidative stress induced by NaF exposure than SM gland.

In conclusion, the results observed in this present study have demonstrated that intraperitoneal administration of a low concentration dose of NaF caused impairments in the antioxidant defence system in the salivary glands of experimental animals. Specifically, SOD activity was decreased while LPO was increased in the first hours after intoxication. Also significant was that the oxidative stress induced by NaF intoxication was more pronounced in the SM gland than in the PA gland.

Funding

The authors would like to thank CAPES and FAPESP no. 2006/00998-8.

References

[1] D. Chachra, A. P. G. F. Vieira, and M. D. Grynpas, "Fluoride and mineralized tissues," *Critical Reviews in Biomedical Engineering*, vol. 36, no. 2-3, pp. 183–223, 2008.

[2] A. J. Dunipace, E. J. Brizendine, W. Zhang et al., "Effect of aging on animal response to chronic fluoride exposure," *Journal of Dental Research*, vol. 74, no. 1, pp. 358–368, 1995.

[3] G. E. Smith, "A surfeit of fluoride?" *Science Progress*, vol. 69, no. 275, pp. 429–442, 1985.

[4] P. A. Monsour and B. J. Kruger, "Effect of fluoride on soft tissues in vertebrates (a review)," *Fluoride*, vol. 18, no. 1, pp. 53–61, 1985.

[5] G. B. Reddy, A. L. Khandare, P. Y. Reddy, G. S. Rao, N. Balakrishna, and I. Srivalli, "Antioxidant defense system and lipid peroxidation in patients with skeletal fluorosis and in fluoride-intoxicated rabbits," *Toxicological Sciences*, vol. 72, no. 2, pp. 363–368, 2003.

[6] K. S. Pillai, A. T. Mathai, and P. B. Deshmukh, "Effect of subacute dosage of fluoride on male mice," *Toxicology Letters*, vol. 44, no. 1-2, pp. 21–29, 1988.

[7] G. M. Whitford, K. E. Reynolds, and D. H. Pashley, "Acute fluoride toxicity: influence of metabolic alkalosis," *Toxicology and Applied Pharmacology*, vol. 50, no. 1, pp. 31–39, 1979.

[8] J. Nicolau, *Fundamentos de Bioquímica Oral*, Fundamentos de Odontologia, Guanabara, 1st edition, 2009.

[9] O. Amano, K. Mizobe, Y. Bando et al., "Anatomy and histology of rodent and human major salivary glands: overview of the Japan salivary gland society-sponsored workshop," *Acta Histochemica et Cytochemica*, vol. 45, no. 5, pp. 241–250, 2012.

[10] J. Nicolau and D. M. Ribeiro, "Metabolism of glycogen in submandibular glands of rats. Alteration by NaF," *Journal de Biologie Buccale*, vol. 20, no. 2, pp. 97–102, 1992.

[11] D. W. Allmann, A. Miller, and H. S. Kleiner, "Effect of fluoridated water on 3′,5′ cyclic AMP levels in various rat tissues," *Journal of Dental Research*, vol. 57, no. 9-10, p. 881, 1978.

[12] D. W. Allmann and A. R. Shahed, "The effect of NaF on salivary gland function," *Deutsche Zahnarztliche Zeitschrift*, vol. 42, no. 10, supplement 1, pp. S95–S98, 1987.

[13] G. M. Whitford, "The metabolism and toxicity of fluoride," *Monographs in Oral Science*, vol. 16, pp. 1–153, 1996.

[14] H. C. S. Hodge, H. Joseph, and F. A. Smith, *Fluorine Chemistry*, vol. 4, Academic Press, New York, NY, USA, 1965.

[15] H. S. Kleiner, A. Miller, and D. W. Allmann, "Effect of dietary fluoride on rat tissue 3′,5′-cyclic AMP levels," *Journal of Dental Research*, vol. 58, no. 9, p. 1920, 1979.

[16] M. V. Da Motta, D. N. De Souza, and J. Nicolau, "Effects of subtoxic doses of fluoride on some enzymes of the glucose metabolism in submandibular salivary glands of fed and overnight-fasted rats," *Fluoride*, vol. 32, no. 1, pp. 20–26, 1999.

[17] B. Halliwell and J. M. Gutteridge, *Free Radicals in Biology and Medicine*, OUP Oxford, 2007.

[18] P. G. Winyard, C. J. Moody, and C. Jacob, "Oxidative activation of antioxidant defence," *Trends in Biochemical Sciences*, vol. 30, no. 8, pp. 453–461, 2005.

[19] S. M. Nabavi, S. F. Nabavi, S. Eslami et al., "In vivo protective effects of quercetin against sodium fluoride-induced oxidative stress in the hepatic tissue," *Food Chemistry*, vol. 132, no. 2, pp. 931–935, 2012.

[20] F. N. Nogueira, A. M. Carvalho, P. M. Yamaguti, and J. Nicolau, "Antioxidant parameters and lipid peroxidation in salivary glands of streptozotocin-induced diabetic rats," *Clinica Chimica Acta*, vol. 353, no. 1-2, pp. 133–139, 2005.

[21] P. M. Basha and N. S. Sujitha, "Combined influence of intermittent exercise and temperature stress on the modulation of fluoride toxicity," *Biological Trace Element Research*, vol. 148, no. 1, pp. 69–75, 2012.

[22] P. M. Basha, P. Rai, and S. Begum, "Evaluation of fluoride-induced oxidative stress in rat brain: a multigeneration study," *Biological Trace Element Research*, vol. 142, no. 3, pp. 623–637, 2011.

[23] I. Inkielewicz-Stepniak and W. Czarnowski, "Oxidative stress parameters in rats exposed to fluoride and caffeine," *Food and Chemical Toxicology*, vol. 48, no. 6, pp. 1607–1611, 2010.

[24] J. Krechniak and I. Inkielewicz, "Correlations between fluoride concentrations and free radical parameters in soft tissues of rats," *Fluoride*, vol. 38, no. 4, pp. 293–296, 2005.

[25] I. Inkielewicz and J. Krechniak, "Fluoride effects on glutathione peroxidase and lipid peroxidation in rats," *Fluoride*, vol. 37, no. 1, pp. 7–12, 2004.

[26] M. L. Vani and K. P. Reddy, "Effects of fluoride accumulation on some enzymes of brain and gastrocnemius muscle of mice," *Fluoride*, vol. 33, no. 1, pp. 17–26, 2000.

[27] I. Błaszczyk, E. Grucka-Mamczar, S. Kasperczyk, and E. Birkner, "Influence of fluoride on rat kidney antioxidant system: effects of methionine and vitamin E," *Biological Trace Element Research*, vol. 121, no. 1, pp. 51–59, 2008.

[28] D. Shanthakumari, S. Srinivasalu, and S. Subramanian, "Effect of fluoride intoxication on lipidperoxidation and antioxidant status in experimental rats," *Toxicology*, vol. 204, no. 2-3, pp. 219–228, 2004.

[29] S. M. Nabavi, S. Habtemariam, S. F. Nabavi et al., "Protective effect of gallic acid isolated from Peltiphyllum peltatum against sodium fluoride-induced oxidative stress in rat's kidney," *Molecular and Cellular Biochemistry*, vol. 372, no. 1-2, pp. 233–239, 2013.

[30] I. Błaszczyk, E. Birkner, and S. Kasperczyk, "Influence of methionine on toxicity of fluoride in the liver of rats," *Biological Trace Element Research*, vol. 139, no. 3, pp. 325–331, 2011.

[31] X. Y. Guo, G. F. Sun, and Y. C. Sun, "Oxidative stress from fluoride-induced hepatotoxicity in rats," *Fluoride*, vol. 36, no. 1, pp. 25–29, 2003.

[32] A. R. Shivashankara, Y. M. Shivarajashankara, P. G. Bhat, and S. Hanumanth Rao, "Lipid peroxidation and antioxidant defense systems in liver of rats in chronic fluoride toxicity," *Bulletin of Environmental Contamination and Toxicology*, vol. 68, no. 4, pp. 612–616, 2002.

[33] X. Shuhua, L. Ziyou, Y. Ling et al., "A role of fluoride on free radical generation and oxidative stress in BV-2 microglia cells," *Mediators of Inflammation*, vol. 2012, Article ID 102954, 8 pages, 2012.

[34] I. Błaszczyk, E. Grucka-Mamczar, S. Kasperczyk, and E. Birkner, "Influence of methionine upon the concentration of malondialdehyde in the tissues and blood of rats exposed to sodium fluoride," *Biological Trace Element Research*, vol. 129, no. 1–3, pp. 229–238, 2009.

[35] R. Ranjan, D. Swarup, and R. C. Patra, "Oxidative stress indices in erythrocytes, liver, and kidneys of fluoride-exposed rabbits," *Fluoride*, vol. 42, no. 2, pp. 88–93, 2009.

[36] Z. Wang, X. Yang, S. Yang et al., "Sodium fluoride suppress proliferation and induce apoptosis through decreased insulin-like growth factor-I expression and oxidative stress in primary cultured mouse osteoblasts," *Archives of Toxicology*, vol. 85, no. 11, pp. 1407–1417, 2011.

[37] H. Liu, J. C. Sun, Z. T. Zhao et al., "Fluoride-induced oxidative stress in three-dimensional culture of OS732 cells and rats," *Biological Trace Element Research*, vol. 143, no. 1, pp. 446–456, 2011.

[38] H. Aebi, "Catalase in vitro," *Methods in Enzymology C*, vol. 105, pp. 121–126, 1984.

[39] R. F. Beers and I. W. Sizer, "A spectrophotometric method for measuring the breakdown of hydrogen peroxide by catalase," *The Journal of Biological Chemistry*, vol. 195, no. 1, pp. 133–140, 1952.

[40] F. Paoletti and A. Mocali, "Chapter 18: determination of superoxide dismutase activity by purely chemical system based on NAD(P)H oxidation," in *Oxygen Radicals in Biological Systems Part B: Oxygen Radicals and Antioxidants*, pp. 209–220, Elsevier, 1990.

[41] F. Paoletti, D. Aldinucci, A. Mocali, and A. Caparrini, "A sensitive spectrophotometric method for the determination of superoxide dismutase activity in tissue extracts," *Analytical Biochemistry*, vol. 154, no. 2, pp. 536–541, 1986.

[42] H. Esterbauer and K. H. Cheeseman, "Determination of aldehydic lipid peroxidation products: malonaldehyde and 4-hydroxynonenal," *Methods in Enzymology*, vol. 186, pp. 407–421, 1990.

[43] O. H. Lowry, N. J. Rosebrough, A. L. Farr, and R. J. Randall, "Protein measurement with the Folin phenol reagent," *The Journal of Biological Chemistry*, vol. 193, no. 1, pp. 265–275, 1951.

[44] X. A. Zhan, Z. R. Xu, J. X. Li, and M. Wang, "Effects of fluorosis on lipid peroxidation and antioxidant systems in young pigs," *Fluoride*, vol. 38, no. 2, pp. 157–161, 2005.

[45] M. Mittal and S. J. S. Flora, "Effects of individual and combined exposure to sodium arsenite and sodium fluoride on tissue oxidative stress, arsenic and fluoride levels in male mice," *Chemico-Biological Interactions*, vol. 162, no. 2, pp. 128–139, 2006.

[46] R. Rzeuski, D. Chlubek, and Z. Machoy, "Interactions between fluoride and biological free radical reactions," *Fluoride*, vol. 31, no. 1, pp. 43–45, 1998.

[47] D. Chlubek, "Fluoride and oxidative stress," *Fluoride*, vol. 36, no. 4, pp. 217–228, 2003.

[48] M. Zhang, A. Wang, W. He et al., "Effects of fluoride on the expression of NCAM, oxidative stress, and apoptosis in primary cultured hippocampal neurons," *Toxicology*, vol. 236, no. 3, pp. 208–216, 2007.

[49] H. Xu, C. H. Wang, Z. T. Zhao, W. B. Zhang, and G. S. Li, "Role of oxidative stress in osteoblasts exposed to sodium fluoride," *Biological Trace Element Research*, vol. 123, no. 1–3, pp. 109–115, 2008.

[50] P. B. Lawson and M. H. Yu, "Fluoride inhibition of superoxide dismutase (SOD) from the earthworm Eisenia fetida," *Fluoride*, vol. 36, no. 3, pp. 143–151, 2003.

[51] D. Chlubek, E. Grucka-Mamczar, E. Birkner, R. Polaniak, B. Stawiarska-Pięta, and H. Duliban, "Activity of pancreatic antioxidative enzymes and malondialdehyde concentrations in rats with hyperglycemia caused by fluoride intoxication," *Journal of Trace Elements in Medicine and Biology*, vol. 17, no. 1, pp. 57–60, 2003.

[52] B. Halliwell, S. Chirico, M. A. Crawford, K. S. Bjerve, and K. F. Gey, "Lipid peroxidation: its mechanism, measurement, and significance," *American Journal of Clinical Nutrition*, vol. 57, supplement 5, pp. 715S–724S, 1993.

[53] Y. M. Shivarajashankara, A. R. Shivashankara, P. Gopalakrishna Bhat, and S. Hanumanth Rao, "Brain lipid peroxidation and antioxidant systems of young rats in chronic fluoride intoxication," *Fluoride*, vol. 35, no. 3, pp. 197–203, 2002.

[54] S. E. Gruninger, R. Clayton, S. B. Chang et al., "Acute oral toxicity of dentifrice fluorides in rats and mice," *Journal of Dental Research*, vol. 67, article 334, 1988.

[55] D. W. Allmann and H. S. Kleiner, "Effect of NaF on rat tissue cAMP levels in vivo," *Pharmacology and Therapeutics in Dentistry*, vol. 5, no. 3-4, pp. 73–78, 1980.

[56] A. R. Shahed and D. W. Allmann, "Effect of NaF on cAMP accumulation, cAMP-dependent protein kinase activity in, and amylase secretion from, rat parotid gland cells," *Journal of Dental Research*, vol. 67, no. 2, pp. 462–466, 1988.

[57] J. Nicolau and K. T. Sassaki, "Metabolism of carbohydrate in the major salivary glands of rats," *Archives of Oral Biology*, vol. 21, no. 11, pp. 659–661, 1976.

[58] L. C. P. M. Schenkels, E. C. I. Veerman, and A. V. N. Amerongen, "Biochemical composition of human saliva in relation to other mucosal fluids," *Critical Reviews in Oral Biology and Medicine*, vol. 6, no. 2, pp. 161–175, 1995.

[59] R. M. Nagler, I. Klein, N. Zarzhevsky, N. Drigues, and A. Z. Reznick, "Characterization of the differentiated antioxidant profile of human saliva," *Free Radical Biology and Medicine*, vol. 32, no. 3, pp. 268–277, 2002.

Hindawi Publishing Corporation
Oxidative Medicine and Cellular Longevity
Volume 2013, Article ID 904370, 8 pages
http://dx.doi.org/10.1155/2013/904370

Research Article

Ulinastatin Suppresses Burn-Induced Lipid Peroxidation and Reduces Fluid Requirements in a Swine Model

Hong-Min Luo,[1] Ming-Hua Du,[1] Zhi-Long Lin,[1] Quan Hu,[2] Lin Zhang,[3] Li Ma,[1] Huan Wang,[1] Yu Wen,[1] Yi Lv,[1] Hong-Yuan Lin,[4] Yu-Li Pi,[5] Sen Hu,[1] and Zhi-Yong Sheng[1]

[1] *Laboratory of Shock and Organ Dysfunction, Burns Institute, the First Hospital Affiliated to the People's Liberation Army General Hospital, 51 Fu Cheng Road, Beijing 100048, China*
[2] *Burns Institute, the First Hospital Affiliated to the People's Liberation Army General Hospital, 51 Fu Cheng Road, Beijing 100048, China*
[3] *Obstetrics and Gynecology Department, the First Hospital Affiliated to the People's Liberation Army General Hospital, 51 Fu Cheng Road, Beijing 100048, China*
[4] *Department of Critical Care Medicine, the First Hospital Affiliated to the People's Liberation Army General Hospital, 51 Fu Cheng Road, Beijing 100048, China*
[5] *Department of Ophthalmology, the First Hospital Affiliated to the People's Liberation Army General Hospital, 51 Fu Cheng Road, Beijing 100048, China*

Correspondence should be addressed to Sen Hu; hs82080@yahoo.com.cn and Zhi-Yong Sheng; shengzhy@cae.cn

Received 29 January 2013; Revised 6 April 2013; Accepted 8 April 2013

Academic Editor: Kota V. Ramana

Objective. Lipid peroxidation plays a critical role in burn-induced plasma leakage, and ulinastatin has been reported to reduce lipid peroxidation in various models. This study aims to examine whether ulinastatin reduces fluid requirements through inhibition of lipid peroxidation in a swine burn model. *Methods*. Forty miniature swine were subjected to 40% TBSA burns and were randomly allocated to the following four groups: immediate lactated Ringer's resuscitation (ILR), immediate LR containing ulinastatin (ILR/ULI), delayed LR resuscitation (DLR), and delayed LR containing ulinastatin (DLR/ULI). Hemodynamic variables, net fluid accumulation, and plasma thiobarbituric acid reactive substances (TBARS) concentrations were measured. Heart, liver, lung, skeletal muscle, and ileum were harvested at 48 hours after burn for evaluation of TBARS concentrations, activities of antioxidant enzymes, and tissue water content. *Results*. Ulinastatin significantly reduced pulmonary vascular permeability index (PVPI) and extravascular lung water index (ELWI), net fluid accumulation, and water content of heart, lung, and ileum in both immediate or delayed resuscitation groups. Furthermore, ulinastatin infusion significantly reduced plasma and tissue concentrations of TBARS in both immediate or delayed resuscitation groups. *Conclusions*. These results indicate that ulinastatin can reduce fluid requirements through inhibition of lipid peroxidation.

1. Introduction

Burn injury is one of the most severe forms of injuries that evokes both strong physical and emotional responses, producing considerable morbidity and mortality. Data supplied by the National Center for Injury Prevention and Control indicate that in 2010 there were 412,256 (133.53/100,000) nonfatal fire/burn injuries and 3,194 (1.03/100,000) fire/burn deaths in the United States [1, 2]. The cost of fire/burn injuries, including both medical costs and cost of lost productivity, is very high, costing a total of 7.546 billion dollars in 2000 [3]. Hypovolemic shock can develop rapidly after major burn injury, and current treatment for burn shock mainly focuses on maintaining a sufficient tissue perfusion with

early, adequate fluid resuscitation. Currently, the most wildly used formula of fluid resuscitation in burn injury is the Parkland formula, which advocates providing 4 mL of Ringer's lactate/kg/%TBSA (total body surface area) burned/24 hours after burn, with one-half of the fluid expected to be infused over the first 8 hours and the remaining infused over the next 16 hours [4]. However, burn shock can develop and progress despite fluid resuscitation because much of the infused fluid leaks into the extravascular space, and sometimes extensive fluid resuscitation can exacerbate the interstitial edema, producing life-threatening complication such as abdominal compartment syndrome [5, 6]. Furthermore, although an early, adequate fluid resuscitation is practically achievable under normal conditions, effective treatment is a challenging issue in mass casualty incidents caused by forces of nature or by accidental or intentional explosions and conflagrations, where the environmental conditions, the presence of mass casualties, and logistic constraints preclude the availability of intensive fluid resuscitation. Thus, the development of pharmacologic resuscitation strategies that could reduce the fluid requirements for burn injury would be beneficial both in civilian burns or in burn disasters.

Previous studies have indicated that the burn-induced hypovolemic shock is mainly due to the increase in total body capillary permeability and the subsequent plasma leakage [4, 7]. Previous studies also suggest that reactive oxygen species (ROS) contribute to the increased microvascular permeability, edema formation, and tissue damage after burn injury [8–12]. After major injury, the peripheral perfusion and oxygen are decreased; however, the restoration of oxygen delivery during aggressive fluid resuscitation will initiate a deleterious cascade of events that results in the burst of oxygen radicals and causes lipid peroxidation which influences numerous cellular functions [13]. Physiological functions of cell membranes change because lipid peroxidation modifies properties of the membrane such as membrane potential, fluidity, and permeability to different substance [14]. Increased plasma and tissue levels of lipid peroxidation products, such as malondialdehyde (MDA), have been well documented after thermal injury [13, 15–20]. In addition, the use of antioxidants has been found to be efficacious in reducing fluid requirements after burn injury [21–27].

Ulinastatin is a protease inhibitor obtained from human urine, and it has been reported to have free radical-scavenging properties in various models [28–30]. Our recent study also showed that ulinastatin attenuated vasopermeability both in vivo and in vitro [31]. The present study tested the hypothesis that ulinastatin would attenuate lipid peroxidation and tissue edema, thereby reducing fluid requirement after major burn injury in a swine model.

2. Materials and Methods

2.1. Swine Burn Model and Treatment. Forty female, inbred Chinese Wuzhishan miniature swine (4–6 months, 20–25 kg, purchased from the Institute of Animal Sciences, Chinese Academy of Agricultural Sciences, Beijing, China) were used. They were acclimatized in the animal quarter of our laboratory for two weeks. All the animals were fasted for 16 h, and water was withheld for 4 h before the surgery. Under anesthesia with intramuscular injection of ketamine (Gu-Tian Pharmacy, Fu Jian Province, China), animals were then instrumented with a thermodilution catheter of PICCO-PLUS monitor (Pulsion Co., Germany) in the aorta for the measurement of hemodynamic variables, and a vascular catheter was positioned in the superior vena cava for drawing blood samples and fluid infusion. After surgery, all animals were monitored for 1 hour to assure hemodynamic stabilization, and the baseline data were then recorded. The animals were then infused with 5 mg/kg of propofol to assure adequate anesthesia and were subjected to a 40% TBSA full-thickness flam burn injury. A urinary catheter was inserted in the bladder and connected to a commercial urine collection bag. Animals were given buprenorphine (10 micrograms/kg i.v., Sigma, St. Louis, MO) immediately after burn injury and every 12 hours thereafter for sedation and pain control. The animals were kept in special slings for monitoring. All animal experiments were approved by the Committee of Scientific Research of First Hospital Affiliated to General Hospital of PLA, China, and were conducted in accordance with the National Institute of Health Guide for the Care and Use of Laboratory Animals.

The injured animals were randomly allocated to the following four groups: immediate resuscitation with lactated Ringer's (ILR), immediate resuscitation with lactated Ringer's containing ulinastatin (ILR-ULI), delayed resuscitation with lactated Ringer's (DLR); delayed resuscitation with lactated Ringer's containing ulinastatin (DLR-ULI), and with 10 pigs in each group. For ILR and ILR-ULI groups, each pig was infused with 4 mL/kg lactated Ringer's alone or lactated Ringer's containing ulinastatin (80,000 U/kg) over 30 minutes immediately after burn injury, followed by continuous infusion of lactated Ringer's, with the infusion rate adjusted each hour to maintain a urine output of 1-2 mg/kg/h. For DLR and DLR-ULI groups, each swine was initially infused with 4 mL/kg or lactated Ringer's containing ulinastatin (80,000 U/kg) over 30 minutes at 6 hours after burn, followed by continuous infusion of lactated Ringer's, with the infusion rate adjusted each hour to maintain a urine output of 1-2 mg/kg/h. 24 hours after burn injury, a second dose of 40,000 U/kg ulinastatin was given simultaneously with continuous lactated Ringer's in ILR-ULI and DLR-ULI groups.

2.2. Experimental Measurements. Hemodynamics variables including mean arterial pressure (MAP), cardiac output (CO), pulmonary vascular permeability index (PVPI), and extravascular lung water index (ELWI) were measured using PICCO-PLUS monitor (Pulsion, Germany).

Net fluid accumulation was defined as cumulative infused fluid volume minus cumulative urine output and was measured hourly as previously described by Dubick et al. [24].

Blood samples were collected for determination of hematocrit and thiobarbituric acid reactive substances (TBARS) concentration. Hematocri was determined by the clinical laboratory in our hospital. TBARS were determined as an index of lipid peroxidation using a commercial kit (Nanjing Jiancheng Science and Technology Co., Ltd, Nanjing, China)

Table 1: Hemodynamic variables in MAP, CO, ELWT, and PVPI.

Variables	After injury (h)						
	0	6	12	18	24	36	48
MAP (mm Hg)							
Group ILR	90.5 ± 6.5	90.2 ± 5.8[c]	93.6 ± 6.3	91.2 ± 6.1	92.3 ± 6.5	92.6 ± 6.4	96.2 ± 4.9
Group ILR/ULI	89.3 ± 4.4	93.2 ± 6.4[d]	94.6 ± 5.5	94.2 ± 6.3	93.3 ± 5.2	90.1 ± 4.3	94.0 ± 3.3
Group DLR	91.1 ± 6.6	75.2 ± 3.4	89.2 ± 5.3	96.0 ± 6.2	92.0 ± 5.3	96.3 ± 6.9	93.8 ± 6.8
Group DLR/ULI	90.7 ± 5.3	73.2 ± 4.6	90.6 ± 4.5	91.0 ± 5.7	95.0 ± 5.9	95.1 ± 6.8	94.5 ± 5.5
CO ($L \cdot min^{-1}$)							
Group ILR	3.76 ± 0.43	3.66 ± 0.38[c]	3.39 ± 0.46[c]	3.61 ± 0.34[c]	3.88 ± 0.49[c]	3.78 ± 0.45	3.79 ± 0.47
Group ILR/ULI	3.69 ± 0.44	3.70 ± 0.39[d]	3.55 ± 0.36[d]	3.58 ± 0.35[d]	4.06 ± 0.69	3.87 ± 0.52	3.83 ± 0.57
Group DLR	3.89 ± 0.53	2.66 ± 0.35	2.87 ± 0.40	2.86 ± 0.35	3.07 ± 0.36	3.35 ± 0.45	3.69 ± 0.50
Group DLR/ULI	3.76 ± 0.45	2.70 ± 0.38	3.05 ± 0.28	3.18 ± 0.33[b]	3.66 ± 0.28[b]	3.67 ± 0.41	3.80 ± 0.49
ELWI ($mL \cdot kg^{-1}$)							
Group ILR	8.13 ± 0.64	11.17 ± 1.15[c]	11.65 ± 1.54	10.05 ± 1.09[c]	9.98 ± 0.87	9.56 ± 1.05	9.23 ± 0.56
Group ILR/ULI	8.02 ± 0.62	11.38 ± 1.24[d]	10.22 ± 0.98[a]	9.46 ± 1.07	9.23 ± 0.85[a]	8.76 ± 0.95[a]	8.48 ± 0.63[a]
Group DLR	8.15 ± 0.81	13.02 ± 0.86	12.55 ± 1.05	11.89 ± 1.12	10.26 ± 0.57	9.84 ± 0.67	9.68 ± 0.76
Group DLR/ULI	8.14 ± 0.69	13.26 ± 1.04	11.18 ± 0.78[b]	10.06 ± 0.75[b]	9.12 ± 0.60[b]	8.86 ± 0.54[b]	8.55 ± 0.57[b]
PVPI							
Group ILR	2.71 ± 0.26	3.31 ± 0.37[c]	3.78 ± 0.30	3.87 ± 0.37	3.82 ± 0.29	3.68 ± 0.35	3.25 ± 0.31
Group ILR/ULI	2.58 ± 0.25	3.28 ± 0.25[d]	3.32 ± 0.29[a]	3.13 ± 0.34[a]	3.01 ± 0.33[a]	2.98 ± 0.21[a]	2.90 ± 0.29[a]
Group DLR	2.57 ± 0.24	4.29 ± 0.51	3.99 ± 0.27	3.78 ± 0.32	3.67 ± 0.34	3.64 ± 0.18	3.44 ± 0.31
Group DLR/ULI	2.68 ± 0.18	4.11 ± 0.14	3.50 ± 0.26[b]	3.24 ± 0.11[b]	3.17 ± 0.29[b]	3.02 ± 0.35[b]	2.75 ± 0.23[b]

MAP: mean arterial pressure, CO: cardiac output, ELWI: extravascular lung water index, PVPI: pulmonary vascular permeability index. Data were expressed as mean ± SD. n = 7–10 per time point. [a]ULI versus ILR; [b]DLR/ULI versus DLR; [c]ILR versus DLR; and [d]ILR/ULI versus DLR/ULI at $P < 0.05$.

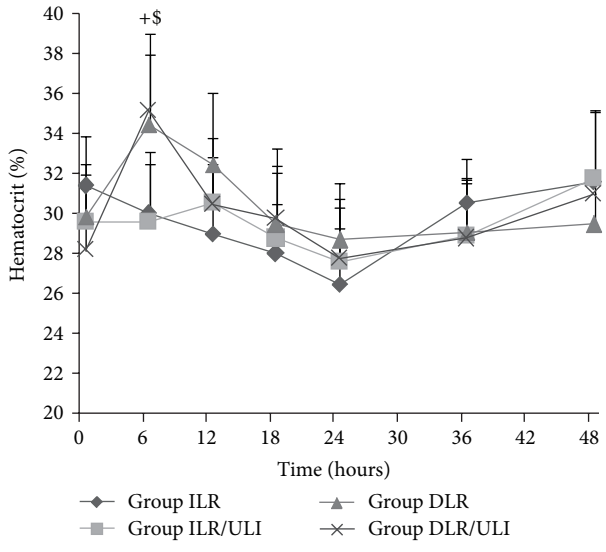

Figure 1: Hematocrit after thermal injury and fluid resuscitation in pigs. Data were expressed as mean ± SD. n = 7–10 per time point. [+]ILR versus DLR; [$]ILR/ULI versus DLR/ULI at $P < 0.05$.

according to manufacturer's instruction. At 48 hours after burn, pigs were euthanized, and heart, liver, lung, muscle and ileum were harvested for determining concentrations of TBARS, activities of antioxidant enzymes (catalase, copper-zinc, and manganese superoxide dismutase) using commercial kits (all purchased from Nanjing Jiancheng Science and Technology Co., Ltd, Nanjing, China). Water content rate of the harvested tissues was measured in percentage of dry/wet ratio as previously described [31].

2.3. Statistical Analysis. SPSS 13.0 statistical software was used, and all results were expressed as mean ± SD. One-way ANOVA was used for comparison among all groups, followed by the Student-Newman-Keuls (SNK) test for comparison between two groups. Differences were considered to be statistically significant when $P < 0.05$.

3. Results

3.1. Hemodynamic Variables. After thermal injury, no significant changes in MAP or CO in immediate resuscitation groups were observed (Table 1). MAP and CO were decreased in the delayed resuscitation groups before resuscitation is initiated. After resuscitation, the MAP and CO in both delayed resuscitation groups were gradually restored to near baseline levels; however, the CO was slightly higher in DLR-ULI group when compared to that of DLR group (Table 1). The PVPI and ELWI were increased after thermal injury despite resuscitation; however, ulinastatin significantly attenuated the increase in PVPI and ELWI both in immediate or delayed resuscitation groups (Table 1).

There were no significant changes in hematocrit in immediate resuscitation groups after thermal injury (Figure 1). In delayed resuscitation groups, hematocrit increased after burn injury due to loss of plasma volume, however, it was returned

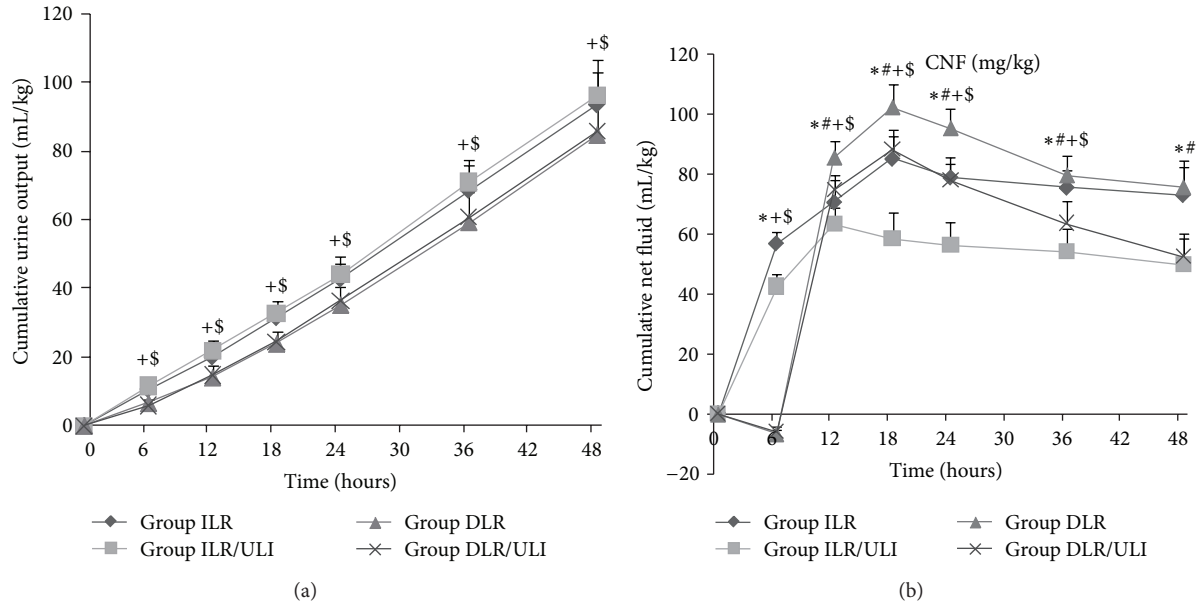

Figure 2: Accumulative urine output (a) and net fluid accumulation (b) after thermal injury and fluid resuscitation in pigs. Data were expressed as mean ± SD. $n = 7$–10 per time point. *ULI versus ILR; $^{\#}$DLR/ULI versus DLR; $^{+}$ILR versus DLR; and $^{\$}$ILR/ULI versus DLR/ULI at $P < 0.05$.

to near baseline levels after resuscitation, showing adequate restoration of plasma volume in both groups (Figure 1).

3.2. Effect of Ulinastatin on Net Fluid Accumulation. After thermal injury, pigs were given either immediate or delayed resuscitation with adjusted infusion rate to maintain urine output between 1 and 2 mL/kg/h. Burn injury resulted in a decrease in urine outputs in both delayed resuscitation groups before resuscitation; however, when resuscitation initiated, urine outputs were similar in all groups (Figure 2(a)). Resuscitation resulted in different extent of net fluid accumulation in all groups; however, ulinastatin significantly reduced net fluid accumulation both in immediate and delayed resuscitation groups (Figure 2(b)).

3.3. Effect of Ulinastatin on TBARS Concentrations and Antioxidant Enzymes Activities. Burn insult and resuscitation resulted in an increase in plasma TBARS concentrations, which was more prominent in delayed resuscitated animals early after burn (Figure 3). Ulinastatin significantly prevented the increase in plasma TBARS both in immediate and delayed resuscitation groups (Figure 3). The TBARS concentrations in different organs, especially in lung and liver tissues, were lower in ulinastatin-treated animals, although some of them did not reach statistical significance (Figure 4). However, activities of antioxidant enzymes (superoxide dismutase and catalase) in heart, liver, lung, skeletal muscle, and ileum were similar in all groups (Table 2).

3.4. Effect of Ulinastatin on Water Content in Different Organs. Ulinastatin significantly reduced the water content of heart, lung, and ileum in both immediate or delayed resuscitation groups (Figure 5). However, there was no significant difference among all groups in the water content of liver and skeletal muscle tissues (Figure 5).

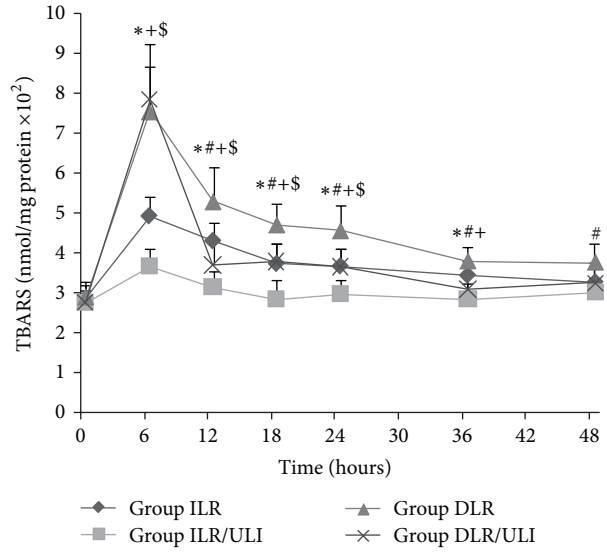

Figure 3: Plasma TBARS concentrations after thermal injury and fluid resuscitation in pigs. Data were expressed as mean ± SD. $n = 7$–10 per time point. *ULI versus ILR; $^{\#}$DLR/ULI versus DLR; $^{+}$ILR versus DLR; and $^{\$}$ILR/ULI versus DLR/ULI at $P < 0.05$.

4. Discussion

Hypovolemic shock is a key factor influencing the mortality rate during the early phase of major burn injury. Current

Table 2: Effect of ulinastatin on tissue antioxidant enzyme activities.

Variables	Group	Organs				
		Heart	Lung	Liver	Muscle	Ileum
Cu-Zn SOD[#]	ILR	3.4 ± 0.5	1.3 ± 0.2	16.3 ± 2.2	1.0 ± 0.2	3.2 ± 0.5
	ILR/ULI	3.5 ± 0.6	1.2 ± 0.2	17.3 ± 2.5	0.9 ± 0.1	3.1 ± 0.4
	DLR	3.8 ± 0.2	1.2 ± 0.3	17.6 ± 1.4	1.1 ± 0.2	2.9 ± 0.4
	DLR/ULI	3.2 ± 0.6	1.0 ± 0.3	16.8 ± 1.9	1.0 ± 0.1	3.0 ± 0.3
MnSOD[+]	ILR	7.9 ± 1.3	1.7 ± 0.3	6.6 ± 0.8	1.2 ± 0.1	2.2 ± 0.3
	ILR/ULI	8.6 ± 1.5	1.5 ± 0.3	6.8 ± 0.8	1.3 ± 0.3	2.1 ± 0.4
	DLR	8.4 ± 1.4	1.5 ± 0.2	6.3 ± 0.9	1.4 ± 0.2	2.2 ± 0.3
	DLR/ULI	8.3 ± 1.4	1.6 ± 0.4	6.6 ± 0.7	1.3 ± 0.2	2.4 ± 0.3
Catalase	ILR	42.6 ± 5.6	54.3 ± 6.2	485.2 ± 73.1	8.6 ± 1.1	34.0 ± 6.5
	ILR/ULI	46.6 ± 8.3	57.0 ± 7.5	428.8 ± 63.7	7.6 ± 1.4	37.4 ± 8.5
	DLR	47.3 ± 6.1	56.3 ± 4.6	523.5 ± 59.5	8.6 ± 1.3	32.5 ± 4.4
	DLR/ULI	42.6 ± 5.7	54.3 ± 6.2	489.3 ± 76.5	8.6 ± 1.4	32.6 ± 5.3

Data were expressed as mean ± SD of units per milligram of protein. n = 7–10 in each group.
[#]Copper zinc superoxide dismutase.
[+]Manganese superoxide dismutase.

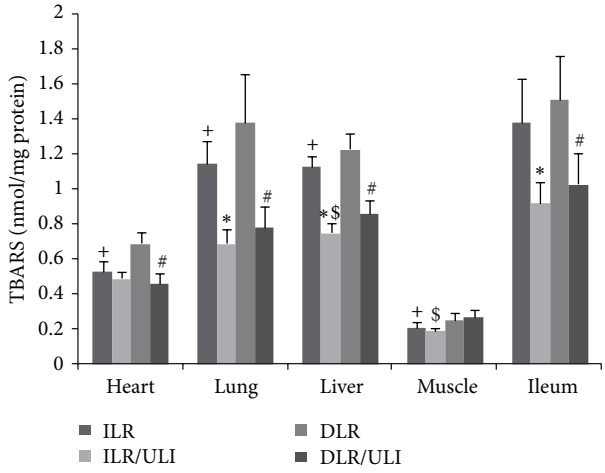

Figure 4: TBARS concentrations in heart, liver, lung, muscle, and ileum 48 hours after thermal injury in pigs. Data were expressed as mean ± SD. n = 7–10 in each group. [*]ULI versus ILR; [#]DLR/ULI versus DLR; [+]ILR versus DLR; and [$]ILR/ULI versus DLR/ULI at $P < 0.05$.

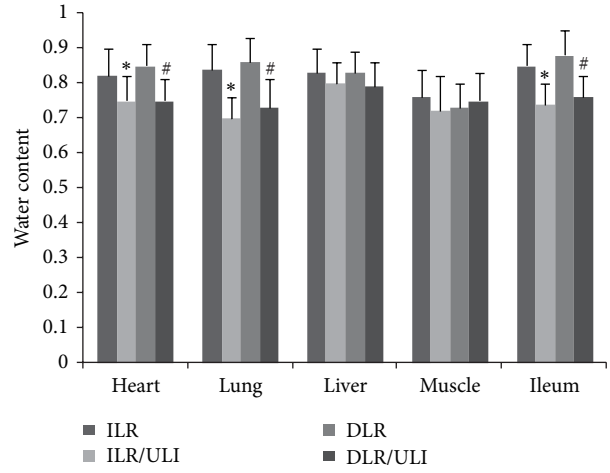

Figure 5: Water content in heart, liver, lung, muscle and ileum 48 hours after thermal injury in pigs. Data were expressed as mean ± SD. n = 7–10 in each group. [*]ULI versus ILR; [#]DLR/ULI versus DLR at $P < 0.05$.

efforts to improve burn shock outcome mainly focus on early and adequate fluid resuscitation. Intensive fluid resuscitation, however, may exacerbate interstitial edema and cause serious adverse events, such as abdominal compartment syndrome. Furthermore, intensive fluid resuscitation from burn shock is usually difficult in austere environments (battlefield, forest conflagration, or earthquake) due to the environmental conditions, the presence of mass casualties, and logistic constraints. Thus, pharmacologic agents that could reduce the fluid requirements for burn injury by attenuating plasma leakage would benefit casualties both in civilian burns or in burn disasters.

Emerging evidence suggests that lipid peroxidation after thermal injury plays a critical role in the increase in vascular permeability and the subsequent plasma leakage [4]. Ulinastatin is a protease inhibitor obtained from human urine, and it has been reported to reduce lipid peroxidation in various models [29, 32–35]. Our recent study also showed that ulinastatin attenuated vasopermeability both in vivo and in vitro [31]. However, it remains unknown whether ulinastatin treatment would reduce lipid peroxidation and fluid requirements in swine model of major burn injury.

In this study we adopted a swine model of 40% TBSA burn injury to investigate the effects of ulinastatin on lipid peroxidation and fluid requirements. We have shown that in this swine burn model, ulinastatin treatment attenuates lipid peroxidation, tissue edema, and net fluid accumulation and thereby reducing fluid requirements.

Ulinastatin is a relatively safe drug, and the dosages from 5,000 to 1,000,000 U/kg have been reported in different animal models [36–38]. In this study, we used a high dosage of ulinastatin (80,000 U/kg in the first 24 hours after burn and then another 40, 000 U/kg in the second 24 hours after burn) in order to obtain more significant protective effects.

We first evaluated the effects of ulinastatin on fluid requirements in burnt pigs followed by immediate resuscitation or delayed resuscitation in an adjusted rate according to urine output. The hemodynamic response to burn injury and resuscitation was similar to previous reports [24, 39, 40]. There was no significant changes in MAP and CO in immediate resuscitation groups. Although there was a reduction in MAP and CO in delayed resuscitation groups after burn injury, they were gradually restored to near baseline levels when resuscitation initiated. Similarly, hematocrit increased after burn injury due to loss of plasma volume, however, it was returned to near baseline levels after resuscitation in delayed resuscitation groups. These results suggest that adequate restoration of plasma volume was achieved in both resuscitation strategies. An increase in PVPI and ELWI was observed after thermal injury despite resuscitation, however, ulinastatin significantly attenuated the burn-induced increase in PVPI and ELWI both in immediate or delayed resuscitation groups. This suggests that ulinastatin could attenuate burn-induced lung injury and edema which was supported by other studies [41, 42]. PVPI and ELWI in DLR and DLR/ULI groups were significantly higher than those in ILR and ILR/ULI groups at 6 hours after injury when DLR and DLR/ULI groups were not given fluid resuscitation. It is possible that ELWI and PVPI are overestimated by PiCCO system because of hypovolemia which is one of the limitations of PiCCO system [43].

In this experiment, the urine output was maintained at 1-2 mL/kg/h by adjusting the infusion rate. Urine output was similar in animals treated with or without ulinastatin. However, ulinastatin significantly attenuated the net fluid accumulation in both immediate and delayed resuscitation groups. Furthermore, water content of heart, lung, and ileum was significantly reduced in ulinastatin-treated animals. These findings, together with previous studies by ours and others [31, 42], indicate that ulinastatin is able to attenuate the burn-induced increase in vascular permeability and plasma volume loss and thereby reducing fluid requirements.

Since free radical-induced lipid peroxidation is suggested to be implicated in burn-induced increase in vascular permeability and the subsequent plasma leakage [4], ulinastatin has been reported to reduce lipid peroxidation in various models, including burn models [29, 32–35, 44]. Thus, we further investigated whether the protective effects of ulinastatin on burn-induced increase in vascular permeability and plasma volume loss were associated with reduced lipid peroxidation. We measured the plasma and tissue concentrations of TBARS as an index of lipid peroxidation. In consistent with previous study [44], we found that burn insult that resulted in an increase in lipid peroxidation and ulinastatin administration effectively attenuated the burn-induced lipid peroxidation. We further measured the antioxidant enzymes activities in heart, liver, lung, muscle, and ileum harvested at 48 hours after burn. However, in contrast to previous investigation by Shimazaki et al. [44], no significant difference in antioxidant enzymes activities was observed among all groups. Differences between Shimazaki's results and ours could be due to differences in animals, tissues, or time of tissue harvest, and further study is needed to confirm the effects of ulinastatin on antioxidant enzymes activities.

5. Conclusions

In summary, ulinastatin, a protease inhibitor, attenuates burn-induced increase in vascular permeability and net fluid accumulation and has a therapeutic role in reducing fluid requirements of thermal injuries. These protective effects of ulinastatin may be mediated in part through the inhibition of burn-induced lipid peroxidation. This study offers a potential small-volume fluid resuscitation strategy in combating major burn injury.

Conflict of Interests

The authors declare that they have no conflict of interests.

Acknowledgments

The authors thank Hui-Ping Zhang for technical help. Our research was supported by (1) the National Basic Research Program of China (973 Program, Grant 2012CB518101), and (2) Techpool Research Fund no. 02100917, Techool Bio-Pharma Co., Ltd, China. The sponsors did not involve in the study design, in the collection, analysis and interpretation of data, in the writing of the paper, and in the decision to submit the paper for publication.

References

[1] WISQARS, *Overall Fire/Burn Nonfatal Injuries and Rates Per 100,000, 2010, United States, All Races, Both Sexes, All Ages, Disposition: All Cases*, Office of Statistics and Programming, National Center for Injury Prevention and Control, CDC.

[2] WISQARS, *Fire/Burn Deaths and Rates Per 100,000, 2010, United States, All Races, Both Sexes, All Ages*, Office of Statistics and Programming, National Center for Injury Prevention and Control, CDC.

[3] E. Finkelstein, P. S. Corso, and T. R. Miller, *The Incidence and Economic Burden of Injuries in the United States*, Oxford University Press, 2006.

[4] D. N. Herndon, *Total Burn Care*, Saunders Elsevier, 3rd edition, 2007.

[5] M. E. Ivy, P. P. Possenti, J. Kepros et al., "Abdominal compartment syndrome in patients with burns," *Journal of Burn Care and Rehabilitation*, vol. 20, no. 5, pp. 351–353, 1999.

[6] J. Oda, K. Yamashita, T. Inoue et al., "Resuscitation fluid volume and abdominal compartment syndrome in patients with major burns," *Burns*, vol. 32, no. 2, pp. 151–154, 2006.

[7] W. W. Monafo, "Initial management of burns," *New England Journal of Medicine*, vol. 335, no. 21, pp. 1581–1586, 1996.

[8] G. O. Till, J. R. Hatherill, and W. W. Tourtellotte, "Lipid peroxidation and acute lung injury after thermal trauma to skin.

Evidence of a role for hydroxyl radical," *American Journal of Pathology*, vol. 119, no. 3, pp. 376–384, 1985.

[9] Y. K. Youn, C. Lalonde, and R. Demling, "Oxidants and the pathophysiology of burn and smoke inhalation injury," *Free Radical Biology and Medicine*, vol. 12, no. 5, pp. 409–415, 1992.

[10] T. T. Nguyen, C. S. Cox, D. L. Traber et al., "Free radical activity and loss of plasma antioxidants, vitamin E, and sulfhydryl groups in patients with burns: the 1993 Moyer Award," *Journal of Burn Care and Rehabilitation*, vol. 14, no. 6, pp. 602–609, 1993.

[11] J. A. Leff, L. K. Burton, E. M. Berger, B. O. Anderson, C. P. Wilke, and J. E. Repine, "Increased serum catalase activity in rats subjected to thermal skin injury," *Inflammation*, vol. 17, no. 2, pp. 199–204, 1993.

[12] O. Cetinkale, A. Belce, D. Konukoglu, C. Senyuva, M. K. Gumustas, and T. Tas, "Evaluation of lipid peroxidation and total antioxidant status in plasma of rats following thermal injury," *Burns*, vol. 23, no. 2, pp. 114–116, 1997.

[13] J. W. Horton, "Free radicals and lipid peroxidation mediated injury in burn trauma: the role of antioxidant therapy," *Toxicology*, vol. 189, no. 1-2, pp. 75–88, 2003.

[14] H. Rauchova, M. Vokurkova, and J. Koudelova, "Hypoxia-induced lipid peroxidation in the brain during postnatal ontogenesis," *Physiological Research*, vol. 61, supplement 1, pp. S89–S101, 2012.

[15] R. H. Demling and C. Lalonde, "Systemic lipid peroxidation and inflammation induced by thermal injury persists into the post-resuscitation period," *Journal of Trauma*, vol. 30, no. 1, pp. 69–74, 1990.

[16] R. H. Demling and C. LaLonde, "Early postburn lipid peroxidation: effect of ibuprofen and allopurinol," *Surgery*, vol. 107, no. 1, pp. 85–93, 1990.

[17] R. Daryani, C. LaLonde, D. Zhu, M. Weidner, J. Knox, and R. H. Demling, "Effect of endotoxin and a burn injury on lung and liver lipid peroxidation and catalase activity," *Journal of Trauma*, vol. 30, no. 11, pp. 1330–1334, 1990.

[18] R. Demling, K. Ikegami, and C. Lalonde, "Increased lipid peroxidation and decreased antioxidant activity correspond with death after smoke exposure in the rat," *Journal of Burn Care and Rehabilitation*, vol. 16, no. 2 I, pp. 104–110, 1995.

[19] C. Lalonde, J. Knox, Y. K. Youn, and R. Demling, "Relationship between hepatic blood flow and tissue lipid peroxidation in the early postburn period," *Critical Care Medicine*, vol. 20, no. 6, pp. 789–796, 1992.

[20] G. Bekyarova, T. Yankova, I. Kozarev, and D. Yankov, "Reduced erythrocyte deformability related to activated lipid peroxidation during the early postburn period," *Burns*, vol. 22, no. 4, pp. 291–294, 1996.

[21] H. Tanaka, H. Matsuda, S. Shimazaki, M. Hanumadass, and T. Matsuda, "Reduced resuscitation fluid volume for second-degree burns with delayed initiation of ascorbic acid therapy," *Archives of Surgery*, vol. 132, no. 2, pp. 158–161, 1997.

[22] M. Sakurai, H. Tanaka, T. Matsuda, T. Goya, S. Shimazakidagger, and H. Matsuda, "Reduced resuscitation fluid volume for second-degree experimental burns with delayed initiation of vitamin C therapy (beginning 6 h after injury)," *Journal of Surgical Research*, vol. 73, no. 1, pp. 24–27, 1997.

[23] H. Tanaka, T. Lund, H. Wiig et al., "High dose vitamin C counteracts the negative interstitial fluid hydrostatic pressure and early edema generation in thermally injured rats," *Burns*, vol. 25, no. 7, pp. 569–574, 1999.

[24] M. A. Dubick, C. Williams, G. I. Elgjo, and G. C. Kramer, "High-dose vitamin C infusion reduces fluid requirements in the resuscitation of burn-injured sheep," *Shock*, vol. 24, no. 2, pp. 139–144, 2005.

[25] T. Matsuda, H. Tanaka, S. Williams, M. Hanumadass, H. Abcarian, and H. Reyes, "Reduced fluid volume requirement for resuscitation of third-degree burns with high-dose vitamin C," *Journal of Burn Care and Rehabilitation*, vol. 12, no. 6, pp. 525–532, 1991.

[26] T. Matsuda, H. Tanaka, S. Shimazaki et al., "High-dose vitamin C therapy for extensive deep dermal burns," *Burns*, vol. 18, no. 2, pp. 127–131, 1992.

[27] T. Matsuda, H. Tanaka, H. M. Reyes et al., "Antioxidant therapy using high dose vitamin C: reduction of postburn resuscitation fluid volume requirements," *World Journal of Surgery*, vol. 19, no. 2, pp. 287–291, 1995.

[28] Y. Koga, M. Fujita, R. Tsuruta et al., "Urinary trypsin inhibitor suppresses excessive superoxide anion radical generation in blood, oxidative stress, early inflammation, and endothelial injury in forebrain ischemia/reperfusion rats," *Neurological Research*, vol. 32, no. 9, pp. 925–932, 2010.

[29] R. Tanaka, M. Fujita, R. Tsuruta et al., "Urinary trypsin inhibitor suppresses excessive generation of superoxide anion radical, systemic inflammation, oxidative stress, and endothelial injury in endotoxemic rats," *Inflammation Research*, vol. 59, no. 8, pp. 597–606, 2010.

[30] Y. Kudo, T. Egashira, and Y. Yamanaka, "Protective effect of ulinastatin against liver injury caused by ischemia-reperfusion in rats," *Japanese Journal of Pharmacology*, vol. 60, no. 3, pp. 239–245, 1992.

[31] H. M. Luo, S. Hu, G. Y. Zhou et al., "The effects of ulinastatin on systemic inflammation, visceral vasopermeability and tissue water content in rats with scald injury," *Burns*, 2012.

[32] L. W. Zhou, Y. L. Wang, X. T. Yan, and X. H. He, "Urinary trypsin inhibitor treatment ameliorates acute lung and liver injury resulting from sepsis in a rat model," *Saudi Medical Journal*, vol. 29, no. 3, pp. 368–373, 2008.

[33] Y. Huang, K. Xie, J. Zhang, Y. Dang, and Z. Qiong, "Prospective clinical and experimental studies on the cardioprotective effect of ulinastatin following severe burns," *Burns*, vol. 34, no. 5, pp. 674–680, 2008.

[34] J. R. Yu, S. Yan, X. S. Liu et al., "Attenuation of graft ischemia-reperfusion injury by urinary trypsin inhibitor in mouse intestinal transplantation," *World Journal of Gastroenterology*, vol. 11, no. 11, pp. 1605–1609, 2005.

[35] T. Htwe, M. Suzuki, K. Ouchi, K. Fukuhara, and S. Matsuno, "Effects of urinastatin and free radical scavengers on hepatic lipid peroxidation in endotoxemia," *Journal of Surgical Research*, vol. 61, no. 1, pp. 206–214, 1996.

[36] F. Yamasaki, M. Ishibashi, M. Nakakuki, M. Watanabe, T. Shinkawa, and M. Mizota, "Protective action of ulinastatin against cisplatin nephrotoxicity in mice and its effect on the lysosomal fragility," *Nephron*, vol. 74, no. 1, pp. 158–167, 1996.

[37] Y. Z. Cao, Y. Y. Tu, X. Chen, B. L. Wang, Y. X. Zhong, and M. H. Liu, "Protective effect of Ulinastatin against murine models of sepsis: inhibition of TNF-α and IL-6 and augmentation of IL-10 and IL-13," *Experimental and Toxicologic Pathology*, vol. 64, no. 2, pp. 543–547, 2012.

[38] R. Koizumi, H. Kanai, A. Maezawa, T. Kanda, Y. Nojima, and T. Naruse, "Therapeutic effects of Ulinastatin on experimental crescentic glomerulonephritis in rats," *Nephron*, vol. 84, no. 4, pp. 347–353, 2000.

[39] T. Kuwa, B. S. Jordan, and L. C. Cancio, "Use of power Doppler ultrasound to monitor renal perfusion during burn shock," *Burns*, vol. 32, no. 6, pp. 706–713, 2006.

[40] T. Tadros, D. L. Traber, J. P. Heggers, and D. N. Herndon, "Angiotensin II inhibitor DuP753 attenuates burn- and endotoxin-induced gut ischemia, lipid peroxidation, mucosal permeability, and bacterial translocation," *Annals of Surgery*, vol. 231, no. 4, pp. 566–576, 2000.

[41] C. Gao, Y. Liu, L. Ma, and S. Wang, "Protective effects of ulinastatin on pulmonary damage in rats following scald injury," *Burns*, vol. 38, no. 7, pp. 1027–1034, 2012.

[42] Y. Fang, P. Xu, C. Gu et al., "Ulinastatin improves pulmonary function in severe burn-induced acute lung injury by attenuating inflammatory response," *The Journal of Trauma*, vol. 71, no. 5, pp. 1297–1230, 2011.

[43] N. R. Lange and D. P. Schuster, "The measurement of lung water," *Critical Care*, vol. 3, no. 2, pp. R19–R24, 1999.

[44] E. Shimazaki, H. Tanaka, S. Ohta, T. Yukioka, H. Matsuda, and S. Shimazaki, "Effects of the antiprotease ulinastatin on mortality and oxidant injury in scalded rats," *Archives of Surgery*, vol. 130, no. 9, pp. 994–997, 1995.

Hindawi Publishing Corporation
Oxidative Medicine and Cellular Longevity
Volume 2013, Article ID 285825, 11 pages
http://dx.doi.org/10.1155/2013/285825

Review Article

Plasma Lipoproteins as Mediators of the Oxidative Stress Induced by UV Light in Human Skin: A Review of Biochemical and Biophysical Studies on Mechanisms of Apolipoprotein Alteration, Lipid Peroxidation, and Associated Skin Cell Responses

Paulo Filipe,[1] Patrice Morlière,[2,3,4] João N. Silva,[1] Jean-Claude Mazière,[2,3,4] Larry K. Patterson,[3,5] João P. Freitas,[1] and R. Santus[3,6]

[1] *Faculdade de Medicina de Lisboa, Hospital de Santa Maria, Clínica Dermatologica Universitaria, Avenida Professor Egas Moniz, 1699 Lisboa Codex, Portugal*
[2] *INSERM, U1088, UFR de Pharmacie, 3 rue des Louvels, 80036 Amiens, France*
[3] *CHU Amiens, Pôle Biologie, Pharmacie et Santé des Populations, Centre de Biologie Humaine, Laboratoire de Biochimie, Avenue René Laennec, Salouël, 80054 Amiens, France*
[4] *UFR de Médecine et de Pharmacie, Université de Picardie Jules Verne, 3 rue des Louvels, 80036 Amiens, France*
[5] *Radiation Laboratory, University of Notre Dame, Notre Dame, IN 46556, USA*
[6] *Département RDDM, Muséum National d'Histoire Naturelle, 43 rue Cuvier, 75231 Paris, France*

Correspondence should be addressed to Patrice Morlière; morliere.patrice@chu-amiens.fr

Received 10 January 2013; Accepted 21 March 2013

Academic Editor: Kota V. Ramana

There are numerous studies concerning the effect of UVB light on skin cells but fewer on other skin components such as the interstitial fluid. This review highlights high-density lipoprotein (HDL) and low-density lipoprotein (LDL) as important targets of UVB in interstitial fluid. Tryptophan residues are the sole apolipoprotein residues absorbing solar UVB. The UVB-induced one-electron oxidation of Trp produces $^{\bullet}$Trp and $^{\bullet}O_2^-$ radicals which trigger lipid peroxidation. Immunoblots from buffered solutions or suction blister fluid reveal that propagation of photooxidative damage to other residues such as Tyr or disulfide bonds produces intra- and intermolecular bonds in apolipoproteins A-I, A-II, and B100. Partial repair of phenoxyl tyrosyl radicals (TyrO$^{\bullet}$) by α-tocopherol is observed with LDL and HDL on millisecond or second time scales, whereas limited repair of α-tocopherol by carotenoids occurs in only HDL. More effective repair of Tyr and α-tocopherol is observed with the flavonoid, quercetin, bound to serum albumin, but quercetin is less potent than new synthetic polyphenols in inhibiting LDL lipid peroxidation or restoring α-tocopherol. The systemic consequences of HDL and LDL oxidation and the activation and/or inhibition of signalling pathways by oxidized LDL and their ability to enhance transcription factor DNA binding activity are also reviewed.

1. Introduction

Human skin is chronically attacked by deleterious environmental agents such as ultraviolet (UV) light, ionizing radiation, and air pollutants, for example, ozone. These may generate free radicals and other reactive oxygen species (ROS), which—through processes of oxidative stress [1–3]—can aggravate or even cause many skin disorders including skin cancers, cutaneous autoimmune diseases, phototoxicity, and skin aging.

During the last three decades, the incidence of cutaneous cancers due to exaggerated exposure to solar UV radiation

has markedly increased as a result of outdoor occupations and sun-bathing habits. The spectral limit for the solar UV radiation reaching the Earth is ~295 nm. The biological effects of UV light have led photobiologists to separate the solar UV spectrum into two domains, namely, UVB (295–315 nm) and UVA (315–390 nm). While UVA mainly produces oxidative stress [3, 4], UVB is responsible for both direct photochemistry of molecules as well as development of oxidative stress. At the cellular level, the two major early events accompanying exposure to UVB light are the induction of DNA damage and lipid peroxidation [5, 6].

Our group—which involves collaboration among dermatologists, biochemists, chemists, and biophysicists from several countries—has spent more than 20 years investigating the molecular and cellular aspects of UV-induced photooxidative stress related to skin pathophysiology. This review deals with several aspects of our contribution to dermatological science and to the photobiology of skin.

A full comprehension of all mediators involved in the response of human skin to UV light requires that the molecular bases of the multifocal biological effects of the UV radiation be understood. Not only epidermal cells but also extracellular skin components have been considered in our studies. For example, we have been interested in the effect of UV light on some components of the interstitial fluid which feeds the dermis and epidermis, as this fluid plays an essential role in mediating the transport of nutrients, hormones, essential proteins, and lipids required for cell growth and differentiation. In addition to studies concerning the deleterious effects on cells and other components of the skin, preventive molecular strategies against oxidative stress have also been developed by searching for new families of antioxidants.

2. The Lipoproteins of the Interstitial Fluid: Neglected Mediators of the Action of the UV Radiation on Skin

Early on, it appeared to us that high-density lipoprotein (HDL) and low-density lipoprotein (LDL) are important UVB targets. First, it has been shown that oxidation of some amino acid residues of lipoproteins such as tyrosine (Tyr), tryptophan (Trp), and lysine (Lys) leads to apolipoprotein alterations and lipid peroxidation [7]. Secondly, thanks to their lipid core, lipoproteins have been shown to be natural carriers of the essential lipophilic antioxidants, α-tocopherol (αTocOH) and carotenoids (Car) [8], which can reduce UVB-induced oxidative damage in skin [9]. Lastly, apolipoproteins are known to contain tryptophan (Trp), the only aromatic residue absorbing solar UVB (but not UVA) susceptible to UVB-induced photooxidation with subsequent formation of reactive indolyl radicals and ROS as primary species [10].

HDL and LDL like most other macromolecular components of blood can cross vessel walls by a process resembling ultrafiltration. Thus, the interstitial fluid feeding epidermal cells can be considered as a serum ultrafiltrate. Therefore, the concentration of serum proteins in this ultrafiltrate is determined by their molecular size [11, 12]. That is, the smaller the lipoprotein size, the greater its concentration in the interstitial fluid as compared to that in serum. Thus, the concentration of apolipoprotein A-1 (apoA-I)—a principle constituent protein of HDL—is about 15 μM, whereas that of the LDL apolipoprotein B100 (apoB100) is on the order of 0.4 μM. Each of apoA-I and apoB100 contains 4 and 37 Trp residues, respectively. As the indole ring of Trp has appreciable molar extinction coefficients of 1500 M^{-1} cm^{-1} at 295 nm and even 510 M^{-1} cm^{-1} at 300 nm, one may conclude that the most significant fraction of UVB light absorbance by lipoproteins occurs in the 120 μM of HDL_3 Trp (HDL_3 has 2 apoA-I) compared to the 15 μM of LDL Trp. For comparison, the concentration of the single Trp of albumin in the interstitial fluid is about 160 μM. Consequently, in the ~50 μm thick layer of the epidermis reached by the UVB radiation, the Trp residues of lipoproteins absorb more than half the quantity of light absorbed by albumin. Thus, despite its large concentration, albumin cannot be considered as an effective sunscreen for the lipoproteins. All these data support the contention that lipoproteins must be considered as mediators in the overall effects of UVB on human skin through the specific or unspecific interaction of photochemically oxidized HDL and LDL with human skin cells.

3. The UVB Light Absorption by Trp Residues Is Responsible for Lipoprotein Lipid Peroxidation

Upon irradiation of aerated solutions of LDL and HDL_3 with UVB light, Trp residues of apoA-I and apoB100 are readily destroyed. The quantum yields of Trp photolysis are 5×10^{-4} and 2×10^{-3} for LDL and HDL_3, respectively. This Trp destruction is accompanied by formation of lipid peroxidation decomposition products as measured by the thiobarbituric acid assay (TBARS) and by the consumption of αTocOH and Car carried by the lipoproteins. On the other hand, neither Trp destruction nor antioxidant consumption is observed when solutions are irradiated with the UVA radiation [13]. From UVB radiation data in [14], demonstrating that the initial rate of Trp destruction and the corresponding TBARS production are both proportional to the lipoprotein concentration, it can be deduced that TBARS production is proportional to the initial rate of Trp photolysis (Figure 1). Furthermore, since a surfactant will disrupt the lipid molecular organization necessary to lipid peroxidation, 1% SDS was added to the lipoprotein solution before the irradiation in subsequent experiments. This addition did not alter the Trp destruction but suppressed the TBARS production [15]. As a consequence, it is likely that lipid peroxidation in lipoproteins results from the Trp photolysis. The fact that Car are not consumed under UVA irradiation of HDL and LDL solutions—despite strong absorbance in the UVA region—suggests that antioxidant consumption under UVB cannot be solely attributed to direct photobleaching. One must also consider their consumption while acting as inhibitors of ROS and of the "dark" radical chain reactions of the lipid peroxidation. Such chain reactions may be sustained by trace metal ions probably present in the lipoprotein

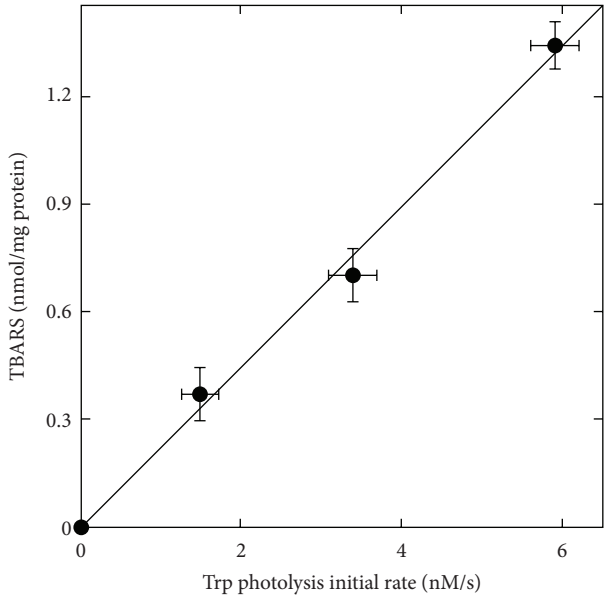

Figure 1: TBARS production as a function of the initial rate of Trp photolysis. TBARS expressed in nmol/mg of protein and the Trp photolysis initial rate expressed in nM/s have been determined with air-saturated pH 7 buffered solutions of HDL at concentrations up to 1 μM. The incident UVB light dose in these experiments was 6.7 J/min. Drawn from data in [14].

preparations. Accordingly, the strong enhancement of postirradiation damage at the apolipoprotein level by redox metal ions demonstrates a synergism between UVB-induced lipid photoperoxidation and autoperoxidation [13].

The primary process of Trp residue photolysis by UVB radiation in HDL and LDL is undoubtedly the one-electron oxidation (e.g., photoionization) of the indole ring with formation of a neutral Trp radical ($^{\bullet}$Trp) as well as a hydrated electron (e_{aq}) [10, 15]. In aerated solutions, e_{aq} is scavenged by O_2 at diffusion-controlled rate in competition with reactions involving endogenous electrophilic residues (i.e., in less than 200 ns) to produce the superoxide anion whose dismutation produces H_2O_2, making it a primary product of Trp photolysis [10, 16]. An additional demonstration of e_{aq} production in one-electron oxidation of Trp residues is the inhibition of 30% of the TBARS upon saturation of the lipoprotein solutions with a mixture of N_2O/O_2 (80/20 v/v). This transforms approximately 80% of the e_{aq} (hence of $^{\bullet}O_2^-$) into strongly oxidizing $^{\bullet}$OH radicals. The $^{\bullet}$OH radicals react nonspecifically with all constituents of HDL or LDL, not only unsaturated lipids but also most residues of apolipoproteins including Trp itself, and a 50% increase of the rate of Trp destruction is observed upon N_2O/O_2 saturation [14]. Interestingly, it may be noted that the same $^{\bullet}$Trp radical has been shown to be involved in the induction of lipid peroxidation, which occurs during the well-established process of Cu^{2+}-induced LDL autooxidation. The binding of the redox Cu^{2+} ions in the vicinity of 7 of the 37 apoB100 Trp residues in LDL probably catalyzes the Trp autooxidation [17].

4. Propagation of the Photooxidative Trp Damage to Other Apolipoprotein Sites

The major HDL fraction in human serum is that of HDL_3 composed of two main irregularly distributed proteins: apoA-I (MW: 28 kDa) and apolipoprotein A-II (apoA-II, MW: 17.4 kDa). The remaining proteins comprise less than 10% of the total protein content. On average, 75% of HDL_3 particles contain 2 apoA-I and 2 apoA-II, while the rest are devoid of apoA-II. The apoA-II is a dimer of 77 residues connected by a disulphide bond with no Trp, free Cys, His, or Arg.

It has been long known that free radical formation in proteins can induce their cleavage or cross-linking [18]. This rule applies to UVB irradiated lipoproteins as shown in Figure 2 which demonstrates that HDL apolipoproteins are strongly altered by such radiation. SDS-polyacrylamide gel electrophoresis and immunoblots with specific monoclonal antibodies reveal that the apolipoprotein alteration, which requires oxygen, occurs after a few minutes of irradiation at low absorbed light (compare lanes A and B in Figure 2). The dose rate was 0.4 J/min with an incident dose rate of 6.7 J/min before complete antioxidant consumption [15]. Self-aggregation of apolipoproteins is a consequence of UVB light absorption by apoA-I Trp residues as unirradiated samples do not form aggregates. Dimers of apoA-I or apoA-II and higher polymers of apoA-I or of both apolipoproteins are also observed. ApoA-II produces dimers although it cannot be directly altered by UVB [15]. Similarly, the formation of high molecular mass apoA-I-containing particles is observed during the Cu^{2+}-induced oxidation of dialyzed plasma as obtained with isolated HDL_3 [19]. Further, both protein modifications and TBARS formation are inhibited upon addition of either desferrioxamine (lanes C; Figure 2), a strong Fe(III) ion complexing agent, or of SDS before irradiation. These effects occurring after only limited Trp photolysis [13, 14] suggest that lipid peroxidation and Fenton-type reactions catalyzed by trace metal ions bound to the lipoproteins play a key role in these alterations. However, the incomplete inhibition of these alterations by desferrioxamine suggests other reaction pathways for the intra- and interapolipoprotein cross-linking. The light-induced polymer formation can result—at least in part—from the propagation of other primary species related to Trp residue photolysis as $^{\bullet}$Trp can oxidize intact Tyr residues in LDL [20] to produce the tyrosyl phenoxyl radical (TyrO$^{\bullet}$) through long range electron transfer reactions [21]. In HDL, Tyr 100 and Tyr 115 are at sites close to Trp 108 which appears to play a key role in these alternative pathways. Moreover, basic amino acids that react with e_{aq} and disulphide bond are split by e_{aq}, leading to additional radical formation. All these apolipoprotein radical species (noted as $^{\bullet}$apoA-I, $^{\bullet}$apoA-II, or $^{\bullet}$apoB100) can, in turn, contribute to cross-linking and/or polymer formation during Trp photolysis.

As oxidized lipoproteins cannot properly perform their biological functions [22], these results would only be of interest if they were obtained with absorbed light doses of physiological significance. The minimal erythemal doses (MED), that is, the minimum doses required to produce sunburn, for fair-skinned people are about 40 mJ/cm^2 at

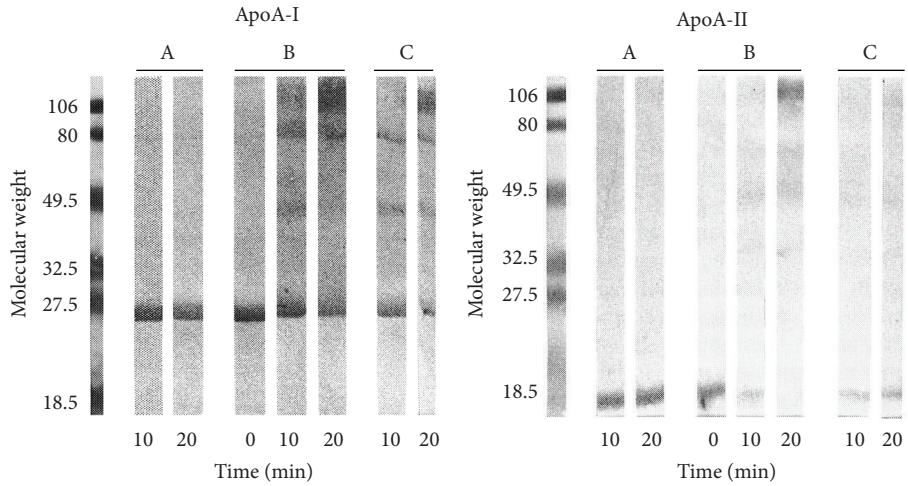

Figure 2: Immunoblots of air-saturated solutions of HDL with antibodies specific for apoA-I or apoA-II. Lanes A: unirradiated samples bubbled with air; lanes B: as in A but irradiated with 6.7 J/min of UVB during the indicated times; lanes C: same as B but the solutions contained 50 μM desferrioxamine, a strong Fe(III) complexing agent. Adapted from [15].

300 nm, 50 mJ/cm^2 at 304 nm, and 1000 mJ/cm^2 at 313 nm [23]. Since the *stratum corneum* transmits about 45% and 30% at 313 nm and 304 nm, respectively, the UVB absorbed in the ~50 μm of the epidermal layer [24] at 1 MED around 310 nm is about 50 J/cm^3. Thus, considering the light doses used in [15], for example, 0.1 to 0.2 J/cm^3, there is more than enough light at 1 MED to induce lipoprotein alterations in skin similar to those reported in this reference.

A convenient stratagem for gathering the interstitial fluid feeding the dermis and epidermis is to collect blister fluid (0.7 mL) from 2 cm diameter blisters formed by mild suction (−175 mm Hg). In our studies, the methodology followed to demonstrate the oxidative modifications of apolipoprotein by a UVB stress in neutral buffered aqueous solutions has been applied to the suction blister fluid gathered before irradiation [25]. The 8 Trp residues of the two apoA-I of the HDL_3 fraction and the 37 Trp residues of apoB100 absorb practically 80% as much light as absorbed by the single Trp residue of human serum albumin (HSA). Hence, the HDL and LDL of the suction blister fluid or of a "reconstituted fluid" based on protein concentrations reported in [11, 12] may be readily photooxidized. Such photooxidation leads to a UVB dose-dependent TBARS formation accompanying Trp loss. Furthermore, the same apolipoprotein alterations as those reported with buffered HDL and LDL solutions are observed with appropriate specific monoclonal antibodies as illustrated with apoB-100 of LDL (Figure 3(a)). Incidentally, marked photocleavage and photopolymer formation also occur in blister fluid HSA (Figure 3(b), lane 5) [25]. Although HSA functions as an antioxidant of lipoprotein autooxidation *in vitro* [26] and *in vivo* [27], it is not an effective antioxidant in the photooxidation of the suction blister fluid.

The TBARS formation as well as the structural modifications of apolipoproteins and HSA in the suction blister fluid are induced by UVB irradiation of skin at doses well below 1 MED (see Figure 3 legend). The detection of apoA-II polymers in Figure 3(b) (lanes 3 and 4) suggests again the intervention of radical lipid chain peroxidation reactions which propagate the initial photooxidative damage at the apoA-I level within the HDL particles present in the suction blister fluid. Accordingly, the formation of apoB100 polymers can be attributed to the same reaction sequence [25].

It is of note that, in contrast to buffered solutions of purified lipoproteins [13], irradiation of the suction blister fluid with the UVA radiation produces apoA-I polymers, demonstrating the presence of ROS-producing photosensitizers probably associated with nutrients such as flavins or resulting from nutrient metabolism products in the undialyzed blister fluid.

5. Time Course of the Repair of Apolipoprotein Photodamage by Antioxidants

As noted above, the marked consumption of αTocOH and Car at low absorbed doses of UVB irradiation cannot be attributed solely to their photobleaching. Although Car strongly absorb UVA (Figure 4), the consumption of Car is arrested immediately by removing the UVB radiation from a UVB + UVA light source. This consumption parallels an immediate production of TBARS [13, 14]. By contrast, time lags of at least 30 min are observed in the Cu^{2+}-catalyzed autooxidation of lipoproteins (Figure 4), before TBARS or conjugated diene production which parallels a marked consumption of carotenoids (see also [29]). The notable difference in behavior between the UVB-induced photooxidation and the Cu^{2+}-induced autoperoxidation suggests links between antioxidant consumption and the one-electron oxidation of Trp residues with UVB irradiation.

Given the pivotal role played by one-electron oxidation of Trp in the propagation of photooxidative damage to multiple sites of apoA-I, ApoA-II, and apoB100, it is essential to establish relationships between the initial Trp photoionization

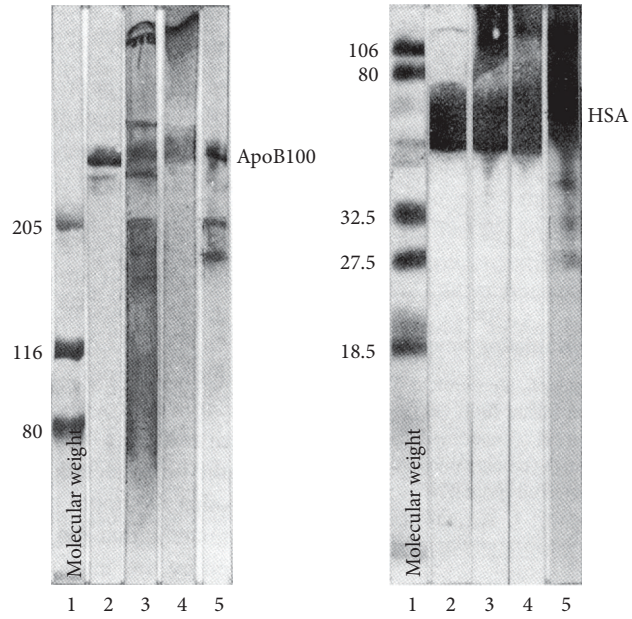

Figure 3: Immunoblots of apoB100 and albumin from air-saturated suction blister fluid before and after irradiation with UVB (absorbed light dose: 12 J/mL). (a) Unmodified apoB100 migration is indicated as apoB100. Lane 1: molecular weight standards; lane 2: unirradiated suction blister fluid (130 μg); lane 3: irradiated suction blister fluid; lane 4: reconstituted blister fluid; lane 5: isolated LDL as reference (prepared from human serum and irradiated). (b) same as (a) but with 20 μg of proteins. See [25] for full experimental details.

step and reactions which repair UVB-induced damage to apolipoproteins.

The investigation of kinetics in such reactions requires the production of $^{\bullet}$Trp concentrations much greater ($\sim \mu$M) than those obtained under steady-state irradiation ($\ll$pM) with incident light doses comparable to those used in [13, 15, 25]. In HDL and LDL aqueous solutions, micromolar $^{\bullet}$Trp concentrations can be produced rather selectively by pulse radiolysis [20], a fast kinetics spectroscopic technique involving radiolysis of water with a high energy electron pulse of a few nanosecond duration. Such electrons produce almost equal yields of $^{\bullet}$OH and e_{aq} as major radical species with H$^{\bullet}$ atoms as a minor component. Subsequently, $^{\bullet}$Trp radicals are formed within 50 μs by reaction of Trp residues with $^{\bullet}Br_2^-$ radical-anions. These radical-anions are selective, mild oxidants formed by scavenging the $^{\bullet}$OH radicals with Br^- anions. Most importantly, $^{\bullet}Br_2^-$ is the sole radical formed in N_2O-saturated solutions, while both $^{\bullet}Br_2^-$ and $^{\bullet}O_2^-$ radical-anions are simultaneously produced at almost equal yields in air- or O_2-saturated solutions.

Using the pulse radiolysis technique, the transient absorbance parameters, absorbance maximum (λ_{max}) as well as molar extinction coefficient (ε_{max}) at λ_{max}, of the $^{\bullet}$Trp, TyrO$^{\bullet}$, and α-tocopheroxyl (αTocO$^{\bullet}$) radicals have been measured in the UV-visible spectral regions. With these parameters kinetics of their formation and/or disappearance have been determined in lipoprotein aqueous solutions on time scales extending from microseconds to seconds. The λ_{max} characteristics for $^{\bullet}$Trp, TyrO$^{\bullet}$, and αTocO$^{\bullet}$ radicals are 520 nm, 410 nm, and 430 nm, respectively, while the corresponding ε_{max} are 1750 M^{-1} cm^{-1}, 2700 M^{-1} cm^{-1}, and 7100 M^{-1} cm^{-1}, respectively. The αTocO$^{\bullet}$ radical absorbance also presents a shoulder at 410 nm with ε_{max} = 4500 M^{-1} cm^{-1} [30]. This powerful tool allows one to elucidate and quantify unknown repair reaction pathways as well as to characterize the formation and decay of the various radical species in different lipoprotein microenvironments [20, 31]. Transient absorbance spectra presented in Figures 5(a) and 5(b) allow one to clearly identify the different steps of the repair reactions taking place in N_2O-saturated LDL and HDL solutions following oxidation with $^{\bullet}Br_2^-$ radical-anions. While the repair of $^{\bullet}$Trp by Tyr residues with formation of TyrO$^{\bullet}$ radicals takes place on a time scale of a few hundreds of μs [20], TyrO$^{\bullet}$ radicals are repaired by αTocOH on longer time scales with formation of the αTocO$^{\bullet}$. An unrepaired population of $^{\bullet}$Trp species remains stable for more than 2.5 s. For the repairable damage, the repair reaction can be schematized as

$$\alpha\text{TocOH} + \left(^{\bullet}\text{apoA-I}, {}^{\bullet}\text{apoA-II or } {}^{\bullet}\text{apoB100}\right) \longrightarrow \alpha\text{TocO}^{\bullet} + \left(\text{apoA-I, apoA-II or apoB100}\right) \quad (1)$$

Due to the extensive structural differences between their two apolipoproteins, there are notable disparities concerning the rates of repair in the two lipoprotein particles by αTocOH. In oxidized LDL, αTocO$^{\bullet}$ radicals formation is already completed after 2.5 ms with no indication of remaining TyrO$^{\bullet}$ transient absorbance (see Figure 5(b)). On the other hand,

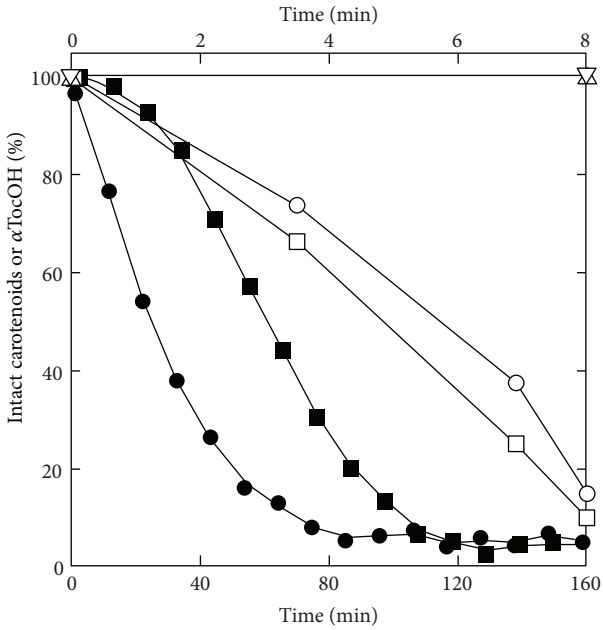

Figure 4: Time courses of Car and αTocOH consumption. Lower time scale: carotenoid consumption during Cu^{2+}-catalyzed oxidation of 240 nM of LDL in the absence (●) or presence (■) of 0.75 μM quercetin. Upper time scale: Car (□, △) or αTocOH (○, ▽) consumption under irradiation of 400 nM of LDL with UVB (□, ○) or UVA (△, ▽). Drawn from data in [14, 28].

the rate of repair by αTocOH is much slower in oxidized HDL (Figure 5(a)) where absorbance of TyrO$^\bullet$ radicals at their 410 nm maximum and that of the αTocO$^\bullet$ radicals at 430 nm are still visible 2.5 s after the radiolytic pulse [31].

An important structural feature should be noted. Each LDL particle contains several αTocOH molecules, whereas on average there is only one αTocOH molecule in each 3 to 5 HDL particles. This major discrepancy in the average number of αTocOH molecules in LDL and in HDL has two implications. First, there is a much greater intrinsic probability of TyrO$^\bullet$ radical repair in the LDL particles containing αTocOH, leading to a much faster reaction rate (1) as evidenced by the rapid disappearance of the TyrO$^\bullet$ radical absorbance over ~300 μs (Figure 5(b)). Secondly, the observation of TyrO$^\bullet$ transient absorbance at least 2.5 s after HDL oxidation by $^\bullet Br_2^-$ results from the absence of αTocOH in ~60% to 80% of the HDL particles, with no repair being possible in those particles devoid of αTocOH (Figure 5(a)). By analogy, it is reasonable to assume that the limited repair of the TyrO$^\bullet$ and $^\bullet$Trp radicals in the UVB-induced oxidation of HDL and LDL leads to the permanent damage evidenced by the immunoblots of Figures 2 and 3 and the oxidation of Trp residues (Figure 1). Furthermore, the time scale of the various repair reactions by αTocOH and Car described here after one-electron oxidation of Trp residues by $^\bullet Br_2^-$ is consistent with the kinetics of bleaching observed with UVB photooxidation.

Another interesting feature is revealed in Figure 5(b) by comparing transient spectra obtained 30 ms and 2.5 sec after oxidation by $^\bullet Br_2^-$ radical-anions. A bleaching is observed in the 440–510 nm region corresponding to Car absorption. Analyses of the kinetics of formation and decay of the αTocO$^\bullet$ radicals in HDL at 430 nm and of the Car consumption over a 2.5 s time scale (Figure 6) demonstrate a limited (2%) repair of αTocOH by Car according to the following reaction:

$$\alpha\text{TocO}^\bullet + \text{Car} \longrightarrow {}^\bullet\text{Car}^+ + \alpha\text{TocOH} \quad (2)$$

Interestingly, this partial "sparing effect" is only observed in HDL even though LDL contains 10 times more Car than HDL [31]. Comparative studies of LDL and HDL_3 by surface pressure measurements on monolayers [34] and by EPR with spin labeled fatty acids [35] have demonstrated that the smaller HDL particles (e.g., ~9 nm diameter versus 20 nm for LDL) with lower nonesterified cholesterol and less saturated phospholipid composition have a more fluid structure. As a result of increased fluidity and of the interpenetration of apoA-I within the particle, the full sequence of oxidation and repair reactions can occur.

6. Sensitivity of αTocO$^\bullet$ Radical Decay and Car Bleaching to the Presence of O_2

The effects of oxygen on radical reactions involved in the formation and repair of oxidative damage in apoA-I and apoA-II or apoB100 have been considered because of the obvious relevance to processes in the *in vivo* environment. The $^\bullet$Trp, TyrO$^\bullet$, and αTocO$^\bullet$ radicals are rather unreactive with oxygen itself. On the other hand, αTocO$^\bullet$ and $^\bullet$Trp, in the free form or in proteins, readily react with the $^\bullet O_2^-$ radical-anion. Additionally, αTocO$^\bullet$ can directly oxidize Car but not Trp or αTocOH itself (see [31] for key references). However, the complex lipoprotein structure and associated microenvironments modulate this reactivity. Surprisingly, $^\bullet$Trp radicals do not react with $^\bullet O_2^-$ in LDL or in HDL suggesting reduced accessibility of the pool of remaining long-lived $^\bullet$Trp radicals to $^\bullet O_2^-$ in both lipoproteins.

Figures 6(a) and 6(b) show that the αTocO$^\bullet$ radical yields resulting from repair of oxidative damage to apoA-I and apoA-II as well as to apoB100 are approximately half those measured under N_2O saturation; this is consistent with the expected yields of TyrO$^\bullet$ and $^\bullet$Trp radicals under O_2 saturation. They also show that at short times after the radiolytic pulse, a portion of αTocO$^\bullet$ radical in HDL disappears at an increased rate while the remainder—represented by at least 50% of the absorbance—is hardly affected by the presence of $^\bullet O_2^-$ radicals. Thus, from three categories of αTocO$^\bullet$ species identified in these lipoproteins, only two react with $^\bullet O_2^-$ presumably by the following repair reaction:

$$\alpha\text{TocO}^\bullet + {}^\bullet O_2^- + H^+ \longrightarrow \alpha\text{TocOH} + O_2 \quad (3)$$

which leads to partial αTocOH restoration. Carotenoid bleaching, accounting for partial αTocOH repair, is still observed with HDL (Figure 6(a)) but not with LDL in which the lack of Car bleaching rules out direct Car oxidation by $^\bullet O_2^-$ and, thus, penetration of $^\bullet O_2^-$ into the LDL lipid core.

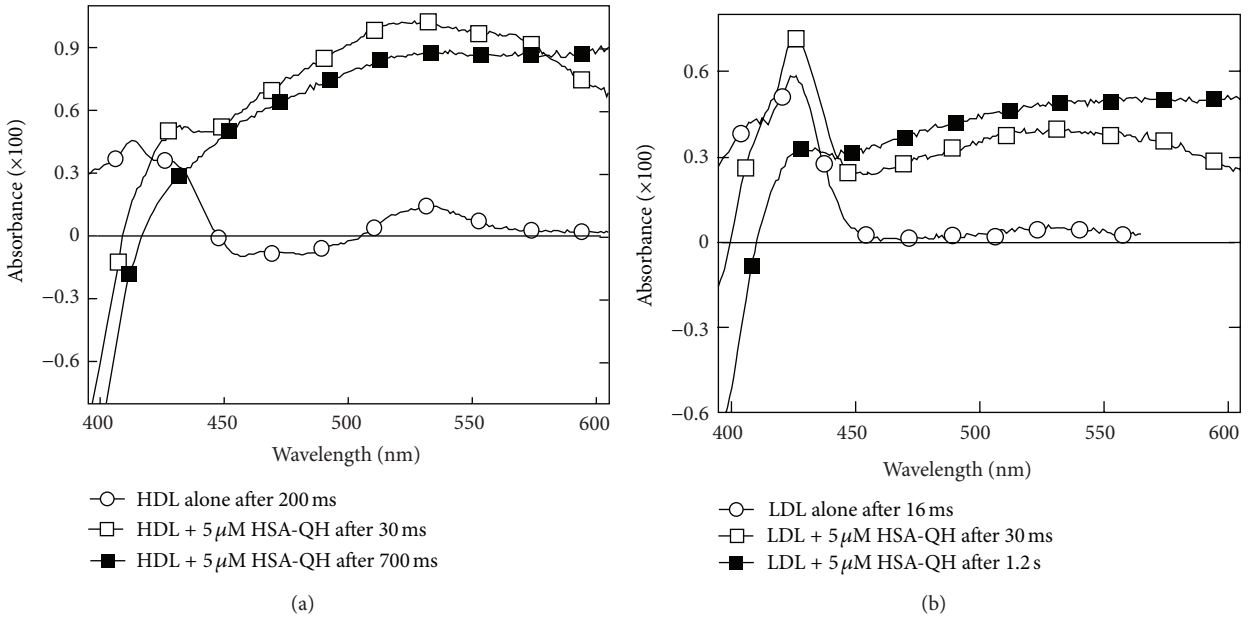

FIGURE 5: (a) Absorbance of apolipoprotein and quercetin radicals in HDL_3. (○) Transient absorbance spectra of 12.5 μM HDL_3 in N_2O saturated 10 mM pH 7 phosphate buffer containing 0.1 M KBr recorded 200 ms after oxidation with 3.2 μM of $^{\bullet}Br_2^-$ radical-anions. (□, ■) The same but solutions contained 18.75 μM HDL_3, 5 μM HSA, and 5 μM QH. Spectra were recorded at 30 ms (□) and 700 ms (■) after oxidation with 2.9 μM of $^{\bullet}Br_2^-$ radical-anions. (b) Absorbance of apoB100 and quercetin radicals in LDL. (○) Transient absorbance spectra of 1.6 μM LDL in N_2O saturated 10 mM, pH 7, recorded 16 ms after oxidation with 4.0 μM of $^{\bullet}Br_2^-$ radical-anions. (□, ■) The same but the solutions contained 2.4 μM LDL, 5 μM HSA, and 5 μM QH. Spectra were recorded at 30 ms (□) and 1.2 s (■) after oxidation with 3.2 μM of $^{\bullet}Br_2^-$ radical-anions. Redrawn from data in [32].

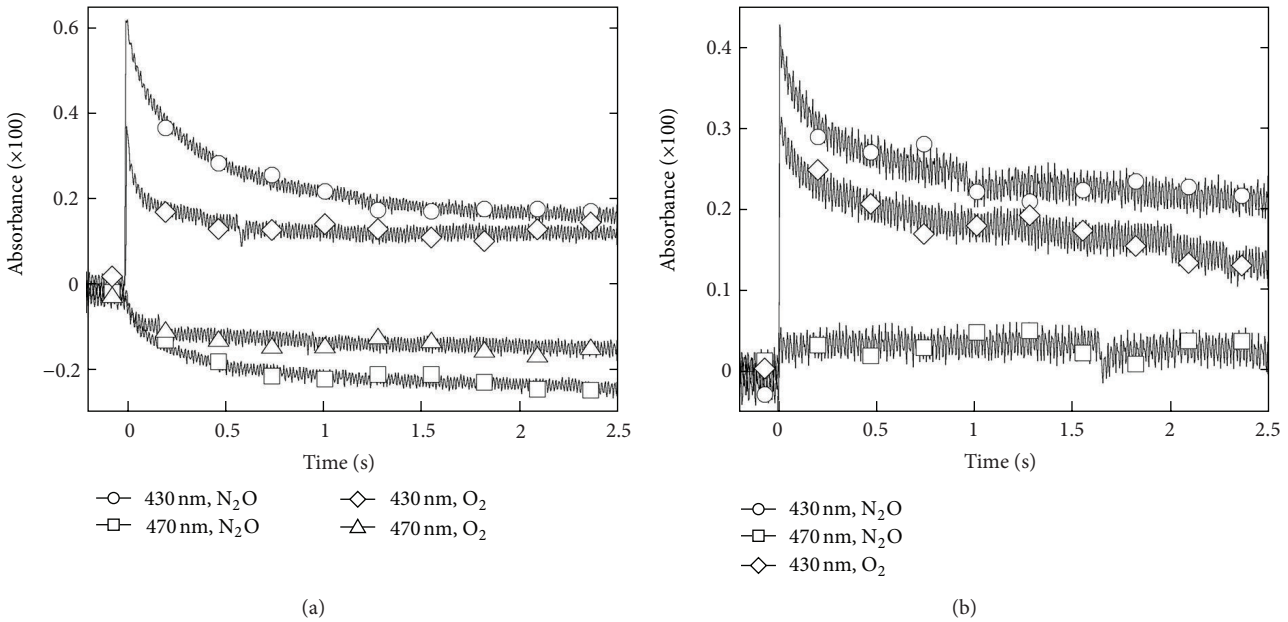

FIGURE 6: (a) Decay of transient absorbance of αTocO$^{\bullet}$ radicals at 430 nm (○, ◇) and bleaching of the carotenoid absorbance at 470 nm (□, △) after oxidation of 20 μM HDL by $^{\bullet}Br_2^-$ radical-anions in 10 mM pH 7 phosphate buffer. Solutions were saturated with N_2O (□, ○) and O_2 (◇, △). (b) Transient absorbance changes measured at 430 nm and 470 nm for solutions containing 1.6 μM LDL. In (a) and (b), $[^{\bullet}Br_2^-] = 3.0$ μM for N_2O-saturated solutions and $[^{\bullet}Br_2^-] = 5.0$ μM for O_2-saturated solutions (see [31] for full experimental details).

7. Polyphenols as Effective Antioxidants in Repair of Oxidative Damage to Apolipoproteins: Restoration of αTocOH by Albumin-Bound Quercetin

Given the particular role attributed to flavonoid-type antioxidants in the control of atherogenesis [36], it is of apparent interest to determine whether quercetin (QH)—when bound to its physiological carrier, HSA [37]—may supplement the incomplete repair of apolipoprotein damage in HDL_3 and LDL by endogenous αTocOH and may thus ameliorate the subsequent biological consequences of skin irradiation.

The transient absorbance spectra observed thirty milliseconds after the radiolytic pulse in N_2O-saturated solutions of HDL_3 and LDL containing 5 μM QH and 5 μM HSA are shown in Figures 5(a) and 5(b). In these figures, the transient absorbance spectrum of the $^{\bullet}Q$ radical, that is, the semioxidized QH molecule, appears as a very broad spectrum extending from the near UV to the far red. The formation of $^{\bullet}Q$ radicals also accounts for the bleaching of the QH absorption in the near UV region. Hence, kinetic analyses may be most conveniently performed in the red region at a wavelength with no contribution from the absorbance of the $TyrO^{\bullet}$, $^{\bullet}Trp$, and $\alpha TocO^{\bullet}$ radicals or from QH bleaching [38].

In the minor fraction of HDL_3 containing αTocOH, the semioxidized species, $TyrO^{\bullet}$ is repaired by endogenous αTocOH, generating $\alpha TocO^{\bullet}$ radicals. In addition, two populations representing 80% of $\alpha TocO^{\bullet}$ initially formed are repaired over a 3-second time scale by quercetin bound to HSA at physiologically relevant concentration. In contrast to the *intramolecular* repair reaction by the endogenous antioxidants leading to $\alpha TocO^{\bullet}$ or $^{\bullet}Car^{+}$ formation [31], the HSA-bound $^{\bullet}Q$ radicals are formed by *intermolecular* reaction implying collision between HSA and the lipoproteins.

In the major fraction of HDL_3 particles lacking αTocOH, both $TyrO^{\bullet}$ and $^{\bullet}Trp$ are repaired by free and HSA-bound quercetin. In LDL particles, all of which contain αTocOH, $\alpha TocO^{\bullet}$ radicals are formed on the millisecond time scale by the repair of $TyrO^{\bullet}$ radicals produced in apoB100. Subsequently, 75% of initial $\alpha TocO^{\bullet}$ are repaired by HSA-bound quercetin over a time interval of seconds. In summary, the following repair reactions have been demonstrated:

$$TyrO^{\bullet} + QH \longrightarrow Tyr + {}^{\bullet}Q \quad (4a)$$

$$\alpha TocO^{\bullet} + QH \longrightarrow \alpha TocOH + {}^{\bullet}Q \quad (4b)$$

$$^{\bullet}Trp + QH \longrightarrow Trp + {}^{\bullet}Q \quad (4c)$$

Once the major reactions have been characterized in deaerated solutions, the intervention of O_2 in these reactions can be analyzed. First, it should be noted that the $^{\bullet}O_2^{-}$ radical-anion can readily oxidize QH with high rate constant [32] according to

$$QH + {}^{\bullet}O_2^{-} + H^{+} \longrightarrow {}^{\bullet}Q + H_2O_2 \quad (5)$$

The transient absorbance spectra observed in O_2-saturated solutions of HDL_3 and LDL containing 5 μM QH and HSA are similar to those obtained in the absence of oxygen. In addition to the direct reduction of the $^{\bullet}O_2^{-}$ radicals (5), the reactions (4a), (4b), and (4c) observed in deaerated solutions also occur. The fraction of $\alpha TocO^{\bullet}$ radicals (more than 50%) not repaired by superoxide radical-anions can be repaired by HSA-bound quercetin with formation of $^{\bullet}Q$ but to a much lesser extent in LDL than in HDL [38].

The extensive repair of oxidative damage to lipoproteins by QH is particularly interesting as QH exists in plasma as conjugated derivatives with antioxidant activities comparable to or exceeding that of unconjugated QH [39].

Several recent studies suggest that newly synthesized flavones such as 3-alkyl-3′,4,5,7-tetrahydroxyflavones [28] or hydroxyl-2,3-diarylxanthones [40] are much more effective antioxidants than QH in the Cu^{2+}-induced LDL oxidation model [28] or in restoring αTocOH [40]. Because of their obvious relevance to dermatology and/or possible cosmetic applications, such new antioxidants merit further evaluation. Unfortunately, it should be recalled that antioxidants—for example, QH—may be either pro- or antioxidant under some experimental conditions in the Cu^{2+}-induced LDL oxidation model [29]. It is known that contrasting behaviours may be exhibited among the flavonoid molecules closely related to QH. For example, flavanol catechin, flavonol QH, and the flavones luteolin and rutin effectively protect human skin fibroblasts against the photooxidative stress induced by UVA alone or in the presence of a photosensitizer. By contrast, the isoflavones genistein can aggravate the photodamage [41]. Thus, the efficacy of antioxidants introduced by natural nutrition or supplementation is still under debate [42].

8. Putative Biological Consequences of UVB-Induced Lipoprotein Oxidation

The present review illustrates that photooxidation and autooxidation of serum lipoproteins share common mechanisms although they occur on quite different time scales. These involve the direct oxidation of Trp residues with propagation of damage to other residues such as Tyr and induction of lipid peroxidation leading to formation of multiple TBARS. These, in turn, can react with free amino groups of the apolipoproteins. For example, aldehydic end products of lipid peroxidation react with Lys residues responsible for LDL binding to their cell receptors. Furthermore, both oxidation modes lead to consumption of vitamin E and Car, the natural antioxidants that lipoproteins carry in human serum. A major difference between photo- and autooxidation is that HDL is strongly altered by light, owing to its large excess in the interstitial fluid as compared to LDL. As a result, this oxidized HDL cannot properly fulfil one of its most important functions, the protection of LDL from autooxidation [43]. Furthermore, the radical chain reactions of lipid peroxidation produce prostanoids with vasoconstrictive activity and platelet aggregation potency [44].

Beside systemic effects, lipoprotein oxidation induces or impairs numerous crucial cell physiological responses. For

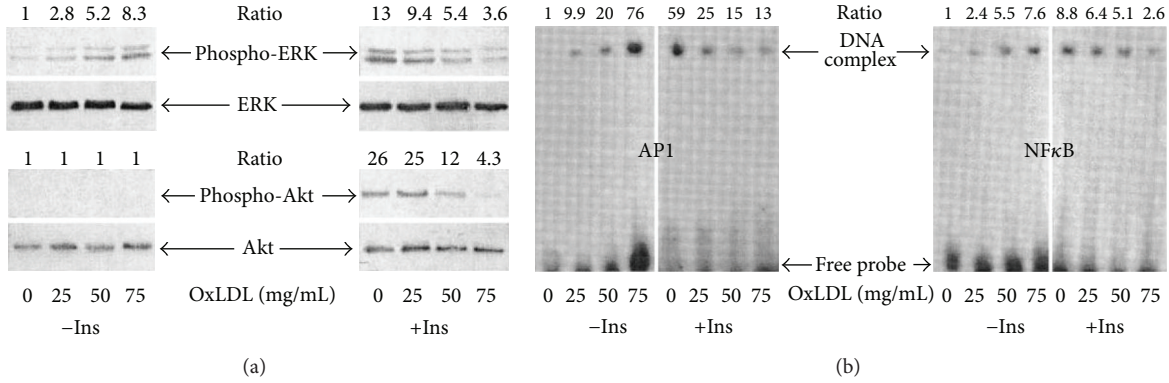

Figure 7: Immunoblots using specific antibodies for ERK, phospho-ERK, Akt, phospho-Akt, and electrophoretic mobility shift assays showing the concentration-dependent effect of oxidized LDL (oxLDL) in presence (Ins) or absence (−Ins) of insulin on signalling kinases ERK and Akt (A) and on transcription factors AP1 and NFκB (see full experimental details in [33]).

instance, we have shown that oxidation of HDL by various sources of oxidative stress decreases cholesterol efflux from human cultured fibroblasts. The reduced ability of HDL to remove intracellular cholesterol pools and to bind to their receptors has been attributed to apoA-I and apoA-II alterations involving Lys and Trp residues [45].

In the case of oxidized LDL—depending on the degree of alterations of the apoB100—either an imperfect recognition by its receptor or a direct scavenging by macrophages is observed. As a result, more or less oxidized LDL cannot precisely regulate cholesterol uptake and synthesis by cells [7, 22]. Additionally, it must be noted that irradiation of cultured human fibroblasts with UVA decreases the uptake and degradation of native LDL [46]. Most importantly, oxidized LDL (and presumably photooxidized HDL) inhibits cell migration [7]. These oxidized species are cytotoxic and can induce apoptosis of normal or tumour cells, probably by transferring radical damage from the lipoproteins to cell targets [47]. This ability to induce apoptosis is consistent with activation and/or inhibition of signalling pathways such as signalling kinases (PKC, MAPK) by oxidized lipoproteins or with the ability of oxidized lipoproteins to enhance the DNA binding activities of transcription factors such as NFκB, AP, and STAT1/3 (see [33] and references therein).

The inhibition of insulin (Ins) signalling by oxidized LDL in cultured human fibroblasts is an excellent system to illustrate these properties as these cells have a wide range of biological responses to this hormone [48]. As shown in Figure 7(a), oxidized LDL by itself increases phosphorylation of the signalling kinase ERK but not that of PKB/Akt. In addition, it stimulates the DNA binding activity of AP1 and NFκB transcription factors (Figure 7(b)). Furthermore, oxidized LDL prevents the activation of the Ins-signalling pathway by inhibiting the Ins-induced phosphorylation of ERK and PKB/Akt and the activation of AP1 and NFκB. All these altered signalling events are partially restored by αTocOH, demonstrating that the oxidative stress generated by oxidized LDL has a negative effect on the Ins-signalling pathway which is independent of the Ins-induced ROS formation [33].

9. Conclusions

The main reasons for the paucity of studies addressing the effects of UVB on the interstitial fluid—as compared to the innumerable ones on skin cells—are probably due to the difficulties in obtaining samples large enough through suction blister fluid collection compared to ready accessibility of skin cells. The analysis of the effects of UVB radiation on major lipoproteins (LDL, HDL) of the interstitial fluid, which bathes the epidermis, demonstrates that to achieve a full understanding of the skin aging process, this medium should not be ignored. Further, the need for such understanding is supported by data which have established the primary processes leading to αTocOH and Car consumption after propagation of initial radical damage from Trp residues to other apolipoprotein residues as well as to the lipid core. This review illustrates that, in addition to systemic effects, UVB-induced alterations of proteins of the interstitial fluid may make consequential contributions to inflammation and degenerative processes of skin exposed to UVB attack. Moreover, the local and systemic perturbations reported here concern normal skin. They may also contribute to the mechanism of action and long-term adverse effects observed with the UVB phototherapy of chronic inflammatory skin diseases such as psoriasis and atopic dermatitis [49, 50].

References

[1] J. H. Epstein, "Photocarcinogenesis, skin cancer, and aging," *Journal of the American Academy of Dermatology*, vol. 9, no. 4, pp. 487–502, 1983.

[2] J. Nishi, R. Ogura, M. Sugiyama, T. Hidaka, and M. Kohno, "Involvement of active oxygen in lipid peroxide radical reaction of epidermal homogenate following ultraviolet light exposure," *The Journal of Investigative Dermatology*, vol. 97, no. 1, pp. 115–119, 1991.

[3] R. M. Tyrrell, "UVA (320-380 nm) radiation as an oxidative stress," in *Oxidative Stress. Oxidants and Antioxidants*, H. Sies, Ed., pp. 57–83, Academic Press, London, UK, 1991.

[4] P. Morlière, A. Moysan, and I. Tirache, "Action spectrum for UV-induced lipid peroxidation in cultured human skin

fibroblasts," *Free Radical Biology and Medicine*, vol. 19, no. 3, pp. 365–371, 1995.

[5] K. Matsumoto, M. Sugiyama, and R. Ogura, "Non-dimer DNA damage in Chinese hamster V-79 cells exposed to ultraviolet-B light," *Photochemistry and Photobiology*, vol. 54, no. 3, pp. 389–392, 1991.

[6] Y. Shindo, E. Witt, D. Han, and L. Packer, "Dose-response effects of acute ultraviolet irradiation on antioxidants and molecular markers of oxidation in murine epidermis and dermis," *The Journal of Investigative Dermatology*, vol. 102, no. 4, pp. 470–475, 1994.

[7] U. P. Steinbrecher, H. Zhang, and M. Lougheed, "Role of oxidatively modified LDL in atherosclerosis," *Free Radical Biology and Medicine*, vol. 9, no. 2, pp. 155–168, 1990.

[8] L. K. Bjornson, H. J. Kayden, E. Miller, and A. N. Moshell, "The transport of α tocopherol and β carotene in human blood," *The Journal of Lipid Research*, vol. 17, no. 4, pp. 343–352, 1976.

[9] M. Lopez-Torres, J. J. Thiele, Y. Shindo, D. Han, and L. Packer, "Topical application of α-tocopherol modulates the antioxidant network and diminishes ultraviolet-induced oxidative damage in murine skin," *The British Journal of Dermatology*, vol. 138, no. 2, pp. 207–215, 1998.

[10] M. Bazin, L. K. Patterson, and R. Santus, "Direct observation of monophotonic photoionization in tryptophan excited by 300-nm radiation. A laser photolysis study," *The Journal of Physical Chemistry*, vol. 87, no. 2, pp. 189–190, 1983.

[11] B. J. Vermeer, F. C. Reman, and C. M. Van Gent, "The determination of lipids and proteins in suction blister fluid," *The Journal of Investigative Dermatology*, vol. 73, no. 4, pp. 303–305, 1979.

[12] B. Vessby, S. Gustafson, and M. J. Chapman, "Lipoprotein composition of human suction-blister interstitial fluid," *The Journal of Lipid Research*, vol. 28, no. 6, pp. 629–641, 1987.

[13] S. Salmon, J. C. Mazière, R. Santus, P. Morlière, and N. Bouchemal, "UVB-induced photoperoxidation of lipids of human low and high density lipoproteins. A possible role of tryptophan residues," *Photochemistry and Photobiology*, vol. 52, no. 3, pp. 541–545, 1990.

[14] S. Salmon, J. C. Mazière, R. Santus, and P. Morlière, "A mechanistic study of the interaction of UVB radiations with human serum lipoproteins," *Biochimica et Biophysica Acta*, vol. 1086, no. 3, pp. 1–6, 1991.

[15] S. Salmon, R. Santus, J. C. Mazière, M. Aubailly, and J. Haigle, "Modified apolipoprotein pattern after irradiation of human high-density lipoproteins by ultraviolet B," *Biochimica et Biophysica Acta*, vol. 1128, no. 2-3, pp. 167–173, 1992.

[16] P. Walrant, R. Santus, and L. I. Grossweiner, "Photosensitizing properties of N formylkynurenine," *Photochemistry and Photobiology*, vol. 22, no. 1-2, pp. 63–65, 1975.

[17] A. Gießauf, B. Van Wickern, T. Simat, H. Steinhart, and H. Esterbauer, "Formation of N-formylkynurenine suggests the involvement of apolipoprotein B-100 centered tryptophan radicals in the initiation of LDL lipid peroxidation," *FEBS Letters*, vol. 389, no. 2, pp. 136–140, 1996.

[18] J. V. Hunt and R. T. Dean, "Free radical-mediated degradation of proteins: the protective and deleterious effects of membranes," *Biochemical and Biophysical Research Communications*, vol. 162, no. 3, pp. 1076–1084, 1989.

[19] Z. Zawadzki, R. W. Milne, and Y. L. Marcel, "Cu^{2+}-mediated oxidation of dialyzed plasma: effects on low and high density lipoproteins and cholesteryl ester transfer protein," *The Journal of Lipid Research*, vol. 32, no. 2, pp. 243–250, 1991.

[20] P. Filipe, P. Morlière, L. K. Patterson et al., "Repair of amino acid radicals of apolipoprotein B100 of low-density lipoproteins by flavonoids. A pulse radiolysis study with quercetin and rutin," *Biochemistry*, vol. 41, no. 36, pp. 11057–11064, 2002.

[21] J. Butler, E. J. Land, W. A. Prütz, and A. J. Swallow, "Charge transfer between tryptophan and tyrosine in proteins," *Biochimica et Biophysica Acta*, vol. 705, no. 2, pp. 150–162, 1982.

[22] J. L. Witztum, "The oxidation hypothesis of atherosclerosis," *The Lancet*, vol. 344, no. 8925, pp. 793–795, 1994.

[23] J. A. Parrish, K. F. Jaenicke, and R. R. Anderson, "Erythema and melanogenesis action spectra of normal human skin," *Photochemistry and Photobiology*, vol. 36, no. 2, pp. 187–191, 1982.

[24] I. A. Magnus, *Dermatological Photobiology: Clinical and Experimental Aspects*, Blackwell Scientific Publications, Oxford, UK, 1976.

[25] S. Salmon, J. Haigle, M. Bazin, R. Santus, J. C. Mazière, and L. Dubertret, "Alteration of lipoproteins of suction blister fluid by UV radiation," *Journal of Photochemistry and Photobiology B*, vol. 33, no. 3, pp. 233–238, 1996.

[26] A. Dobrian, R. Mora, M. Simionescu, and N. Simionescu, "In vitro formation of oxidatively-modified and reassembled human low-density lipoproteins: antioxidant effect of albumin," *Biochimica et Biophysica Acta*, vol. 1169, no. 1, pp. 12–24, 1993.

[27] H. P. Deigner, E. Friedrich, H. Sinn, and H. A. Dresel, "Scavenging of lipid peroxidation products from oxidizing LDL by albumin alters the plasma half-life of a fraction of oxidised LDL particles," *Free Radical Research Communications*, vol. 16, no. 4, pp. 239–246, 1992.

[28] P. Filipe, A. M. S. Silva, R. S. G. R. Seixas et al., "The alkyl chain length of 3-alkyl-3′,4′,5,7-tetrahydroxyflavones modulates effective inhibition of oxidative damage in biological systems: illustration with LDL, red blood cells and human skin keratinocytes," *Biochemical Pharmacology*, vol. 77, no. 6, pp. 957–964, 2009.

[29] P. Filipe, J. Haigle, J. N. Silva et al., "Anti- and pro-oxidant effects of quercetin in copper-induced low density lipoprotein oxidation: quercetin as an effective antioxidant against pro-oxidant effects of urate," *European Journal of Biochemistry*, vol. 271, no. 10, pp. 1991–1999, 2004.

[30] D. Jore, L. K. Patterson, and C. Ferradini, "Pulse radiolytic study of α-tocopherol radical mechanisms in ethanolic solution," *Journal of Free Radicals in Biology and Medicine*, vol. 2, no. 5-6, pp. 405–410, 1986.

[31] A. Boullier, J. C. Mazière, P. Filipe et al., "Interplay of oxygen, vitamin E, and carotenoids in radical reactions following oxidation of Trp and Tyr residues in native HDL_3 apolipoproteins. Comparison with LDL. A time-resolved spectroscopic analysis," *Biochemistry*, vol. 46, no. 17, pp. 5226–5237, 2007.

[32] P. Filipe, P. Morlière, L. K. Patterson et al., "Mechanisms of flavonoid repair reactions with amino acid radicals in models of biological systems: a pulse radiolysis study in micelles and human serum albumin," *Biochimica et Biophysica Acta*, vol. 1572, no. 1, pp. 150–162, 2002.

[33] C. Mazière, P. Morlière, R. Santus et al., "Inhibition of insulin signaling by oxidized low density lipoprotein: protective effect of the antioxidant Vitamin E," *Atherosclerosis*, vol. 175, no. 1, pp. 23–30, 2004.

[34] J. A. Ibdah, S. Lund-Katz, and M. C. Phillips, "Molecular packing of high-density and low-density lipoprotein surface lipids and apolipoprotein A-I binding," *Biochemistry*, vol. 28, no. 3, pp. 1126–1133, 1989.

[35] C. Foucher, L. Lagrost, V. Maupoil, M. Le Meste, L. Rochette, and P. Gambert, "Alterations of lipoprotein fluidity by non-esterified fatty acids known to affect cholesteryl ester transfer protein activity: an electron spin resonance study," *European Journal of Biochemistry*, vol. 236, no. 2, pp. 436–442, 1996.

[36] C. V. De Whalley, S. M. Rankin, J. R. S. Hoult, W. Jessup, and D. S. Leake, "Flavonoids inhibit the oxidative modification of low density lipoproteins by macrophages," *Biochemical Pharmacology*, vol. 39, no. 11, pp. 1743–1750, 1990.

[37] D. W. Boulton, U. K. Walle, and T. Walle, "Extensive binding of the bioflavonoid quercetin to human plasma proteins," *Journal of Pharmacy and Pharmacology*, vol. 50, no. 2, pp. 243–249, 1998.

[38] P. Filipe, L. K. Patterson, D. M. Bartels et al., "Albumin-bound quercetin repairs vitamin E oxidized by apolipoprotein radicals in native HDL_3 and LDL," *Biochemistry*, vol. 46, no. 49, pp. 14305–14315, 2007.

[39] C. Manach, C. Morand, V. Crespy et al., "Quercetin is recovered in human plasma as conjugated derivatives which retain antioxidant properties," *FEBS Letters*, vol. 426, no. 3, pp. 331–336, 1998.

[40] P. Morlière, L. K. Patterson, C. M. M. Santos et al., "The dependence of a-tocopheroxyl radical reduction by hydroxy-2,3-diarylxanthones on structure and micro-environment," *Organic & Biomolecular Chemistry*, vol. 10, no. 10, pp. 2068–2076, 2012.

[41] P. Filipe, J. N. Silva, J. Haigle et al., "Contrasting action of flavonoids on phototoxic effects induced in human skin fibroblasts by UVA alone or UVA plus cyamemazine, a phototoxic neuroleptic," *Photochemical and Photobiological Sciences*, vol. 4, no. 5, pp. 420–428, 2005.

[42] J. Lademann, A. Patzelt, S. Schanzer et al., "Uptake of antioxidants by natural nutrition and supplementation: pros and cons from the dermatological point of view," *Skin Pharmacology and Physiology*, vol. 24, no. 5, pp. 269–273, 2011.

[43] S. Parthasarathy, J. Barnett, and L. G. Fong, "High-density lipoprotein inhibits the oxidative modification of low-density lipoprotein," *Biochimica et Biophysica Acta*, vol. 1044, no. 2, pp. 275–283, 1990.

[44] S. M. Lynch, J. D. Morrow, L. J. Roberts, and B. Frei, "Formation of non-cyclooxygenase-derived prostanoids (F2-isoprostanes) in plasma and low density lipoprotein exposed to oxidative stress in vitro," *Journal of Clinical Investigation*, vol. 93, no. 3, pp. 998–1004, 1994.

[45] S. Salmon, C. Mazière, M. Auclair, L. Theron, R. Santus, and J. C. Mazière, "Malondialdehyde-modification and copper-induced autooxidation of high-density lipoprotein decrease cholesterol efflux from human cultured fibroblasts," *Biochimica et Biophysica Acta*, vol. 1125, no. 2, pp. 230–235, 1992.

[46] M. Djavaheri-Mergny, J. C. Maziére, R. Santus et al., "Exposure to long wavelength ultraviolet radiation decreases processing of low density lipoprotein by cultured human fibroblasts," *Photochemistry and Photobiology*, vol. 57, no. 2, pp. 302–305, 1993.

[47] E. T. Fossel, C. L. Zanella, J. G. Fletcher, and K. K. S. Hui, "Cell death induced by peroxidized low-density lipoprotein: endopepsis," *Cancer Research*, vol. 54, no. 5, pp. 1240–1248, 1994.

[48] C. A. Conover, R. L. Hintz, and R. G. Rosenfeld, "Comparative effects of somatomedin C and insulin on the metabolism and growth of cultured human fibroblasts," *Journal of Cellular Physiology*, vol. 122, no. 1, pp. 133–141, 1985.

[49] I. Emerit, J. Antunes, J. M. Silva, J. Freitas, T. Pinheiro, and P. Filipe, "Clastogenic plasma factors in psoriasis—comparison of phototherapy and anti-TNF-α treatments," *Photochemistry and Photobiology*, vol. 87, no. 6, pp. 1427–1432, 2011.

[50] J. Krutmann, A. Morita, and J. H. Chung, "Sun exposure: what molecular photodermatology tells us about its good and bad sides," *The Journal of Investigative Dermatology*, vol. 132, no. 3, part 2, pp. 976–984, 2012.

Hindawi Publishing Corporation
Oxidative Medicine and Cellular Longevity
Volume 2013, Article ID 690545, 11 pages
http://dx.doi.org/10.1155/2013/690545

Review Article

Regulation of NF-κB-Induced Inflammatory Signaling by Lipid Peroxidation-Derived Aldehydes

Umesh C. S. Yadav and Kota V. Ramana

Department of Biochemistry and Molecular Biology, University of Texas Medical Branch, Galveston, TX 77555, USA

Correspondence should be addressed to Kota V. Ramana; kvramana@utmb.edu

Received 21 February 2013; Accepted 22 March 2013

Academic Editor: Sharad S. Singhal

Oxidative stress plays a critical role in the pathophysiology of a wide range of diseases including cancer. This view has broadened significantly with the recent discoveries that reactive oxygen species initiated lipid peroxidation leads to the formation of potentially toxic lipid aldehyde species such as 4-hydroxy-trans-2-nonenal (HNE), acrolein, and malondialdehyde which activate various signaling intermediates that regulate cellular activity and dysfunction via a process called redox signaling. The lipid aldehyde species formed during synchronized enzymatic pathways result in the posttranslational modification of proteins and DNA leading to cytotoxicity and genotoxicty. Among the lipid aldehyde species, HNE has been widely accepted as a most toxic and abundant lipid aldehyde generated during lipid peroxidation. HNE and its glutathione conjugates have been shown to regulate redox-sensitive transcription factors such as NF-κB and AP-1 via signaling through various protein kinase cascades. Activation of redox-sensitive transcription factors and their nuclear localization leads to transcriptional induction of several genes responsible for cell survival, differentiation, and death. In this review, we describe the mechanisms by which the lipid aldehydes transduce activation of NF-κB signaling pathways that may help to develop therapeutic strategies for the prevention of a number of inflammatory diseases.

1. Introduction

Lipid peroxidation-derived aldehydes (LDAs) have been implicated in a number of oxidative stress-induced inflammatory pathologies such as diabetes, metabolic syndrome, vascular and neural degeneration, liver and kidney toxicity, cancer, retinopathy of prematurity, aging, and ischemia [1–12]. LDAs such as malondialdehyde (MDA), 4-hydroxy-2-nonenal (HNE), and acrolein are generated upon degradation of lipid peroxides subsequent to free radical-induced peroxidation of membrane lipids, particularly the polyunsaturated fatty acids, in the biological membranes [13, 14]. Arachidonic acid present in the biological membranes is predominantly susceptible to free radical attacks due to the presence of unsaturated bonds and is the primary source of LDAs. LDAs are relatively more stable as compared to free radicals such as oxygen and hydroxyl free radicals and act as highly reactive electrophilic molecules [13]. Quantitatively, while HNE and MDA are the most abundant aldehydes formed subsequent to lipid peroxidation, acrolein is the most reactive one. However, LDAs in general, have a tendency to react readily with the nucleophiles including thiols and amines containing cellular macromolecules such as proteins, and nucleic acids leading to cellular damage and accumulation of chemically altered macromolecules [15, 16]. In various disease states conjugates of LDAs with proteins and nucleic acids have been identified; for example, HNE-protein adducts were detected in mitotic, necrotic, and apoptotic cells in brain tumor tissues [17]. LDAs can act as toxic secondary messengers to propagate redox signals leading to cellular and tissue injury [18–20].

HNE generated from the peroxidation of arachidonic acid is highly toxic and the most abundant LDA in the living tissue reaching a reported concentration of up to 10 nanomol/g tissue [13]. Its in-situ concentration plays a key role in the cell growth, death, and differentiation. HNE has been shown to exert marked biological effects by affecting and altering cellular signaling events, modifying and damaging protein and DNA, eventually leading to cytotoxicity and pathogenesis

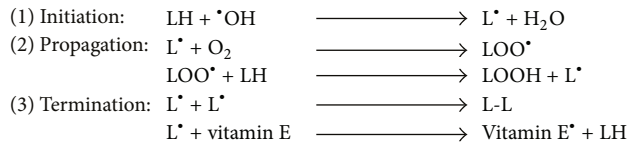

Figure 1: Three reaction steps in free radical initiated lipid (LH)—peroxidation leading to the formation of reactive lipid molecules ($LOO^{\cdot}$) that form lipid-derived aldehydes such as HNE, acrolein, MDA, and HHE.

[18, 19]. Similar effects have been reported for acrolein as well [21–23]. In this review, we have discussed the mechanism of production of LDAs and their roles in regulating the inflammatory signals that activate redox-sensitive transcription factors such as NF-κB.

2. Oxidative Stress and Lipid Peroxidation

In aerobes, varieties of highly reactive chemical entities are formed as the by-product of the oxygen utilization which is collectively termed as reactive oxygen species (ROS) [24, 25]. The ROS include superoxide anion (O_2^{-}), hydroxy radical ($OH^{\cdot}$), nitric oxide radical ($NO^{\cdot}$), and their by-products (e.g., hydrogen peroxide, H_2O_2). A constant flux of ROS caused by acute or chronic inflammatory diseases or environmental stresses leads to a state of moderately increased levels of intracellular ROS resulting in a condition referred to as oxidative stress [26]. The eukaryotic cells are evolutionarily evolved to modulate the oxidant levels in a highly efficient manner by maintaining sufficient antioxidant levels, induction of new gene expression and protein modification, and tightly regulating their redox status within a narrow range [27]. However, in the event of persistent exposure to the oxidants and other toxic agents, excessive ROS are produced that are capable of causing oxidative damage to biomacromolecules such as peroxidation of membrane lipids, oxidation of amino acid side chains (especially cysteine), formation of protein-protein cross-links, oxidation of polypeptide backbones resulting in protein fragmentation, DNA damage, and DNA strand breaks [28, 29]. Out of all these events, the formation of lipid peroxidation products is highly damaging because it leads to widespread free radical reactions besides compromising the membrane integrity leading to loss of cell function and eventually results in severe cytotoxicity that may either lead to uncontrolled cell growth (neoplasia) or cell death (apoptosis) [30, 31].

The process of lipid peroxidation includes several chemical reactions or steps such as initiation, propagation, and termination (Figure 1) [32]. The first step of lipid peroxidation that is, initiation, includes hydrogen atom abstraction by free radicals such as hydroxyl ($^{\cdot}OH$), alkoxyl ($RO^{\cdot}$), peroxyl ($ROO^{\cdot}$), and $HO_2^{\cdot}$. The initial reaction of $^{\cdot}OH$ with polyunsaturated fatty acids produces a lipid radical ($L^{\cdot}$), which in turn reacts with the molecular oxygen to form a lipid peroxyl radical ($LOO^{\cdot}$) in the propagation reaction. The $LOO^{\cdot}$ species then acquire a hydrogen atom from the neighboring fatty acid molecule and produce a lipid hydroperoxide (LOOH) and simultaneously generate a second lipid radical [32]. The LOOH can further be cleaved by reduced metals, such as Fe^{++}, forming a lipid alkoxyl radical ($LO^{\cdot}$). In addition, LOOH may also break down into the reactive aldehyde products or LDAs including MDA, HNE, ONE, 4-HHE, and acrolein in the presence of reduced metals or ascorbate [13, 33, 34]. A chain reaction sets in which both alkoxyl and peroxyl radicals stimulate lipid peroxidation by abstracting additional hydrogen atoms from neighboring lipid molecules [33–35]. This results in the disruption of major chunk of cell membrane lipids that disturbs the assembly of cell membrane causing alterations in membrane fluidity and permeability, alterations of ion transport, and suppression of metabolic processes [36]. The final and third step is the termination which involves the formation of a hydroperoxide which is achieved by reaction of a peroxyl radical with α-tocopherol, a lipophilic chain-breaking molecule found in the cell membrane. Termination could also be achieved when a lipid radical ($L^{\cdot}$) reacts with lipid peroxide ($LOO^{\cdot}$) or when two peroxide molecules combine together and result in nonreactive species LOOL or hydroxylated derivative (LOH), respectively, which are relatively stable. Some of the lipid peroxides could also react with the membrane proteins that result in the termination [37, 38]. The propagation reaction is self-sustaining and continues unabated until the substrate is consumed or the termination reaction sets in by antioxidants or free radical quenchers [38]. Thus, being a self-sustaining process, lipid peroxidation amplifies the effects of the original free radical and results in extensive tissue damage.

Lipid peroxidation, an indicator of oxidative stress in cells and tissues, is a well-defined mechanism of cell injury. Peroxidation of membrane lipids has been shown to generate toxic and unstable biomolecules such as reactive carbonyl compounds including LDAs. These highly reactive electrophiles readily react with cellular proteins and nucleic acids, and also activate signaling cascade molecules and activate transcription factors thus causing inflammation (Figure 2). The cells have elaborate mechanisms to handle the excessive levels of LDAs which include enzymes that detoxify the LDA by reducing them to respective alcohols, for example, aldose reductase (AR) and aldehyde reductase or by oxidizing them to acids, for example, aldehyde dehydrogenase. Most of the unsaturated LDAs such as HNE and acrolein are also metabolized through forming GS-LDAs. Some of the glutathione-S-transferase (GST) isozymes such as human GSTA4-4 and GST5-8 have been shown to significantly catalyze the conjugation of HNE. Several studies indicate that regulation of enzymatic activity of GSTs could modulate the cytotoxicity associated with the HNE [39–41]. Further, LDAs also readily react with cellular glutathione (GSH) forming GS-LDA conjugates which further get reduced into GS-lipid alcohols and transported out of the cells. Recently, our laboratory has extensively presented evidence that AR-catalyzed GS-LDAs could mediate the activation of redox-sensitive transcription factors.

3. NF-κB and Cell Signaling

NF-κB is a family of transcription factors that regulate expression of numerous genes and play important roles in immune

and stress responses, inflammation, and apoptosis [42–45]. There are five known proteins which come together as subunits to constitute the transcription factor NF-κB. These are subunits p50 (derived from p105), p52 (derived from p100), p65 (RelA), c-Rel, and RelB. These subunits, ubiquitously expressed in mammalian cells and highly conserved across the species, can either form homodimer or heterodimer to form biologically active molecule of NF-κB, which translocates to the nucleus upon phosphorylation and transcribes various genes [46]. Activation of NF-κB via canonical or noncanonical pathways is an important mechanism to regulate the body's immune and inflammatory responses [47]. Various pathogens, oxidants, cytokines, chemokines, and growth factors either via specific receptors or general oxidative stress induce the molecular signals that eventually lead to activation of a redox-sensitive transcription factor NF-κB [48]. Once activated either via canonical or noncanonical pathway, NF-κB enters nucleus where it binds to the kB DNA binding sequence and transcribes various genes for cytokines, chemokines, and other inflammatory markers. The expression of a large number of genes involved in apoptosis, cell growth, survival, differentiation, and immune response is regulated by NF-κB, which is associated with an array of diseases such as autoimmune, cancer, and inflammatory diseases.

4. Lipid Aldehydes in NF-κB Mediated Cell Signaling

Increasing evidences suggest that aldehyde molecules generated endogenously during ROS-induced process of lipid peroxidation are involved in most of the pathophysiological effects associated with oxidative stress in cells and tissues [49, 50]. Though previously held view implied that lipid peroxidation products only elicit damage, more recently evolved paradigm suggests that their impact could be more varied and dependent upon factors including the species, concentration and the protein targets involved [51–53]. Increasing number of studies now implicate LDAs in regulating oxidant-induced cellular signaling [54–56]. The lipid aldehydes regulate cellular functions by interacting with the specific proteins covalently and non-covalently [57–59]. For example, protein adducts are formed through the reaction of lipid aldehydes with nucleophilic protein constituents, including amino acid residues such as cysteine, lysine, and histidine, resulting in Schiff base formation [60, 61]. Michael addition is another mechanism of protein adduction, where thiolate groups of cysteine residues react with electrophilic carbons present in α-β unsaturated carbonyls. The most simple oxidation products containing this reactive group, resulting from β-scission, include 4-HNE and acrolein. Please refer to few reviews available on the covalent reactivity of α-β unsaturated carbonyls with cellular biomolecules [57–61] for detailed information.

LDAs have been shown to regulate various signaling pathways initiated by cytokines, chemokines, and growth factors. HNE has been shown to regulate many PKC isozymes depending upon its in situ concentration. For example, in rat

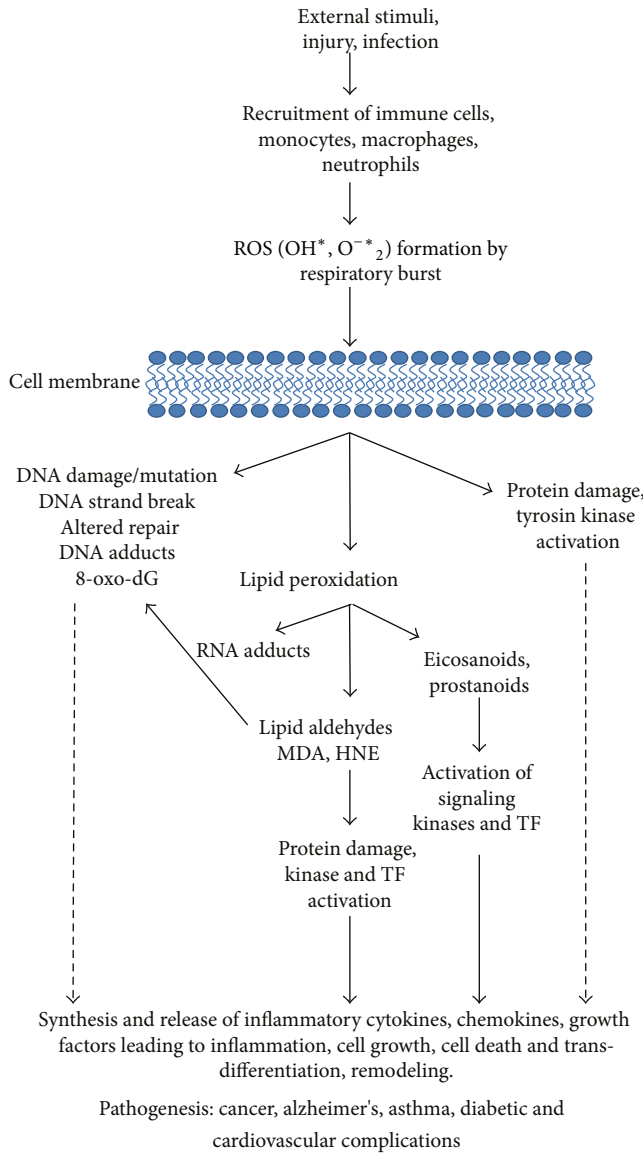

Figure 2: Contribution of lipid peroxidation-derived aldehydes in various disease complications.

hepatocytes low concentrations of HNE (0.1–1 uM) activate PKC beta1 and beta2 isozymes while higher concentrations of HNE (1–10 uM) inhibit PKC beta isozymes [62]. Further, PKC delta activity was inhibited by low concentrations of HNE (0.1 uM) and increased by high concentration of HNE (>1 uM; [63]). Although it is not clear how PKC isozymes are differentially regulated by HNE, it is possible that HNE could target upstream signals of PKC such as PLC and DAG which in turn may activate PKC isozymes. In addition to PKC, HNE can also regulate other kinases such as MAPK, ERK, and JNK indirectlyby activating upstream kinases or directly by interacting with kinase active domains. Parola et al. [64] indicated that HNE could directly form conjugate with JNK which is responsible for histone modification and subsequent nuclear translocation. On the other hand, Song et al. [65] reported that HNE could activate JNK via

activating an upstream kinase called stress-activated protein kinase kinase-1 (SPKK1). Similarly, HNE activates ERK via activating MEK1/2 and P38MAPK via activating MKK3/6 [66, 67]. However, it is not clear how HNE activates upstream kinases of ERK and MAPK. HNE could also activate receptor tyrosine kinases such as EGFR and PDGFR through direct conjugation [68].

The cell signaling pathways activated by LDAs include noncovalent mechanisms that involve binding to a protein receptor and covalent mechanisms that modify protein kinases directly. The direct interaction of LDAs with protein kinases such as SRC and PLC could change cellular calcium signaling and alter in-situ cation mobilization leading to activation of the caspases involved in cell death. Vatsyayan et al. [6] have shown that HNE besides being cytotoxic, at lower doses it triggers phosphorylation of epidermal growth factor receptor (EGFR) and activation of its downstream signaling components ERK1/2 and AKT which are known to be involved in cell proliferation. Similarly, Chaudhary et al. [69] concluded that HNE could evoke signaling for defense mechanisms to self-regulate its toxicity and simultaneously may affect multiple signaling pathways through its interactions with membrane receptors and transcription factors/repressors [57]. Dwivedi et al. [70] suggested that HNE has concentration-dependent opposing effects to cell death and growth. This report indicates that constitutive levels of HNE are needed for normal cell functions and low levels of HNE promote proliferative machinery while high levels promote apoptotic signaling. Further, they suggested that HNE can modulate ligand-independent signaling by membrane receptors such as EGFR or Fas (CD95) and may act as a sensor of external stimuli for eliciting stress-response, suggesting a key role of HNE in cellular signaling [70]. Furthermore, our laboratory has presented numerous evidences [71–73] that GS-LDAs when enzymatically reduced by AR, become important secondary messengers to activate signaling molecules that eventually leads to activation of NF-κB via yet unknown mechanism (Figure 3). The regulation of NF-κB activation is the key for LDAs to modulate various inflammatory pathologies. Since NF-κB transcribes various proinflammatory cytokines, growth factors, cell survival proteins, structural proteins, and apoptotic proteins, regulation of intracellular concentrations of LDAs could be novel strategy to prevent inflammatory complications. Indeed, recent studies indicate that enzymes that regulate LDAs generation or participate in their metabolism could actually prevent pathological effects of LDA-induced inflammatory complications [2–5, 73].

5. Activation of NF-κB under Oxidative Stress

Increased oxidative stress is a hallmark of inflammatory diseases such as those caused by infections, xenobiotics, environmental pollutants, and those of autoimmune etiology, and ROS is an essential mediator of intracellular signaling under a variety of conditions [74–79]. Several lines of evidence suggest that ROS mediates the activation of redox-sensitive transcription factors such as NF-κB and AP1, which in turn stimulate the expression of an array of inflammatory cytokines and chemokines genes [80, 81]. These evidences largely suggest the use of a variety of antioxidants that inhibit NF-κB activation and also antioxidant enzymes which are overexpressed as a counter mechanism to bring down the NF-κB activation. Excessive and unrestrained production of inflammatory mediators causes cytotoxicity in an autocrine and paracrine manner. Among various redox-sensitive transcription factors such as NF-κB, AP1, CREB, ERF2, NFAT, and ATF2 that are activated by increased ROS levels, NF-κB has been extensively studied and is implicated in many oxidative stress-induced inflammatory diseases [45–49]. Activation of NF-κB under oxidative stress has been noticed in a number of inflammatory complications. However, how exactly ROS activates various protein kinases upstream to NF-κB is not known clearly. In the preceding section, we presented evidence that suggests that ROS-generated HNE and other LDAs may directly or indirectly activate upstream kinases including tyrosine receptor kinases [6, 68].

We and others have also presented many evidences which implicate ROS-induced lipid peroxidation products such as lipid aldehydes in the activation of signaling cascade that eventually activates NF-κB [70, 73, 82, 83]. Indeed, ROS-induced lipid peroxidation has been proposed to be major contributor in the pathophysiology of many inflammatory disorders. HNE, generated by a number of oxidative stress conditions inducing etiologies including bacterial infection, xenobiotics, environmental pollutants, and autoimmune disorders, is one of the highly abundant and toxic lipid aldehydes [84]. Acrolein is another highly reactive species generated both exo- and endogenously. Depending upon their respective concentrations both HNE and acrolein elicit phenotypically varied outcomes. Both are known to activate various upstream kinases including MAPK and PKC [71, 82, 85–89], thus enzymes that either regulate or metabolize HNE could be mediators of oxidative stress signals. Modification of multiple cytoskeletal proteins and the activation of MAPKs and ROS-sensitive transcription factors by HNE metabolizing enzymes have been demonstrated by various investigators [71, 82]. Further, growth factors and cytokine-induced increased generation of ROS could be an essential step for cell growth because overexpression of antioxidants such as catalase and super oxide dismutase (SOD) or treatment with antioxidants such as N-acetylcysteine (NAC) are known to diminish growth factor and cytokine-stimulated cell growth or death [90, 91]. Many studies have indeed indicated that ROS themselves can act as toxic messengers that activate NF-κB and affect the cellular functions of growth factors, cytokines and other molecules [92, 93]. These evidences clearly indicate that various stimulants and oxidants activate redox-sensitive transcription factors including NF-κB by generating ROS which in turn generate other secondary messengers such as lipid aldehydes that phosphorylate upstream signaling kinases.

6. Modulation of Oxidative Stress and Lipid Aldehydes Signals by Antioxidants

In oxidative stress-induced inflammatory diseases, antioxidant status of the tissues undergoes severe alteration leaving

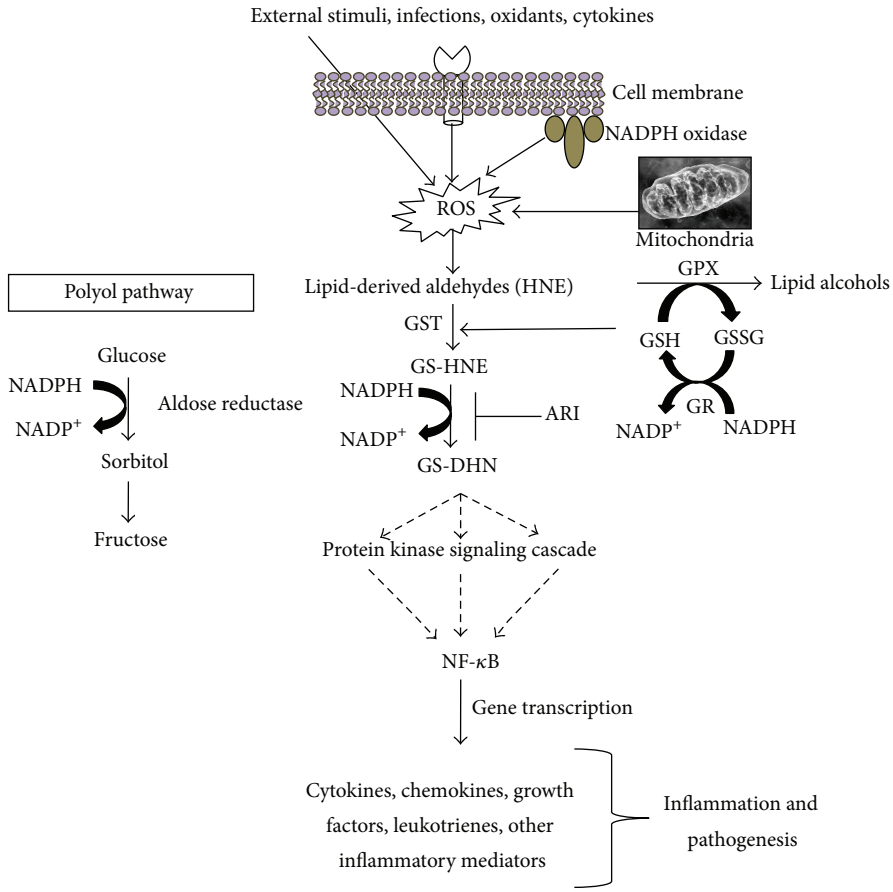

Figure 3: Regulation of lipid aldehyde-induced inflammatory signaling by aldose reductase.

the cells overexposed to oxidative free radicals. The lipid peroxidation caused by increased ROS continues unabated leading to generation of further more free radicals and in this way a vicious cycle continues which results in the establishment and progression of the disease [94]. The cells are endowed with antioxidant system which includes (a) SOD that catalyzes the breakdown of the superoxide anion into oxygen and hydrogen peroxide; (b) catalase, which catalyzes the conversion of hydrogen peroxide to water and oxygen, and (c) peroxiredoxin, which catalyzes the reduction of hydrogen peroxide, organic hydroperoxides, and peroxynitrate to tackle oxidative bouts [95, 96]. In addition, the cells also contain glutathione system which includes glutathione, glutathione reductase, glutathione peroxidases, and glutathione *S*-transferases, which maintains redox balance and protect from oxidative challenges [97, 98]. However, in the overwhelming oxidative stress these mechanisms become ineffective and cellular homeostasis disrupts [98]. Many investigators have demonstrated that supplementation of antioxidants in the experimental animal models of oxidative stress-generated inflammatory pathologies successfully blocks the inflammatory changes [98–100]. Many antioxidants that inhibit oxidative stress signaling pathways are known to be effective in halting the inflammation in experimental animal models. For example, Vitamin C and E, N-acetylcysteine (NAC), Lipoic acid, GSH, carotenoids and flavonoids from plants, and melatonins, have been shown to be effective in experimental models of many diseases including cardiovascular, neurodegenerative, infection, diabetic complications, autoimmune, and allergic complications. A number of antioxidants have undergone clinical trials [101–107] to prevent disease pathologies including cardiovascular and cancer. These antioxidants however have not been successfully translated for the clinical use because at the clinical doses they become prooxidants and result in serious side effects. This restricts the use of antioxidants as therapeutic drugs and leaves them as prophylactic or preventive drugs only. In this scenario, a new drug which can be both antioxidative as well as anti-inflammatory that could regulate both ROS, and LDAs-induced signals could be a better approach to prevent inflammatory complications. Our results from the use of AR inhibitors in different preclinical models indicate that AR inhibitors such as fidarestat could be such a drug that can be used in the amelioration of inflammatory diseases including cardiovascular, sepsis, infection and autoimmune-induced uveitis, allergic asthma, cancer and metastasis, and angiogenesis [73, 108]. These encouraging observations have helped us to develop a highly specific and potent AR inhibitor, fidarestat, which has been tested in the phase-iii clinical studies for diabetic neuropathy and found to be safe for

human use, as a potential antioxidative, anti-inflammatory, antiangiogenic, antimitogenic, and chemopreventive drug for preventing inflammatory diseases such as allergic asthma, colon cancer, and uveitis.

7. Role of AR in Mediation of Lipid Aldehydes Signals

It is well known that AR is overexpressed under oxidative stress initiated by various cytokines, growth factors, bacterial endotoxins such as lipopolysaccharides (LPS), and high glucose. Overexpression of AR increases the turnover of ROS-generated LDAs [73, 108]. The LDAs readily react with cellular GSH and form GSH-LDA conjugates which are excellent AR substrates [109, 110]. Since ROS is known to mediate and regulate intracellular signaling under diverse conditions, some of the effects of ROS can be mediated by ROS-derived LDAs and their GSH conjugates. We have systematically investigated the involvement of lipid aldehydes and their GSH conjugates in the mediation of signaling cascades that play important role in the pathophysiology of a number of diseases. The results from our studies indicate that reduction of LDAs and their GSH conjugates by AR is essential for transduction of cytotoxic signals [82–84]. This was firmly confirmed by various evidences including that AR has poor affinity for glucose (Km of 50–100 mM), and in normal conditions only a small percentage (3%) of glucose is metabolized by AR [111]. Further, the kinetic and structural properties of AR are unlike those of other glucose-metabolizing enzymes [112, 113]. The low Km for catalysis of carbohydrate reduction is probably due to high hydrophobicity of the substrate binding domain of AR which essentially prevents efficient reduction of glucose by AR and suggests that hydrophobic aldehydes could likely be the preferred substrates. Indeed, we have unequivocally demonstrated that AR efficiently catalyzes lipid aldehydes and their GSH conjugates [109, 110]. For example, recombinant human AR has been shown to catalyze the reduction of a large series of saturated and unsaturated aldehydes with 1000-fold higher efficiency when compared to glucose [109–112]. Medium- to long-chain (C-6 to C-18) aldehydes, which are generated during lipid peroxidation, are most efficiently catalyzed by AR [109]. In particular, the catalytic site of AR has more affinity towards GS-aldehyde conjugates than parent aldehydes. This is confirmed by site-directed mutagenesis studies showing that AR active site has amino acid residues which efficiently bind with glutathione moiety [109]. Further, molecular modeling of AR-GSH analog crystal structure confirmed that AR has a specific GS-aldehyde binding site at its catalytic site [112]. Thus, these observations firmly support that physiological role of AR could be the reduction of LDAs besides glucose metabolism in polyol pathway.

Since LDAs are known to modulate the cellular function by regulating the oxidative stress signals mediated by NF-κB and AP1 [114–118], we postulated that AR regulates cellular functions by modulating oxidative stress signals. Our claim is supported by the studies demonstrating that AR inhibition prevents HNE-, growth factor-, and cytokine-induced cytotoxicity in a variety of cultured cells [73, 108]. Further, our studies also demonstrated that inhibition of AR prevents endotoxin-, allergen-, cytokine-, and growth factor-induced activation of NF-κB signals (Figure 3). In all these conditions, increased ROS levels, lipid peroxidation, and subsequent formation of lipid aldehydes play a major role in disrupting the cellular homeostasis. Thus, our observations present a basis for the novel role of AR in the pathophysiology of various inflammatory disease processes mediated by LDAs.

Besides the novel role implicating AR in mediating signaling of the ROS-derived lipid aldehydes in inflammatory pathologies, the exact role of AR in the mediation of cellular signaling is not yet clear. How AR-catalyzed product of GS-LDAs activates PKC and PLC isozymes still needs to be investigated. Nevertheless, we have shown that AR-catalyzed reduced product of GS-DHN activates various kinases including PLC, PKC, and PI3K in cultured cells. Activation of these kinases eventually results in the activation of redox-sensitive transcription factors which transcribe various inflammatory genes responsible for disease progression. The involvement of AR-catalyzed reaction products in eliciting oxidative stress-induced cytotoxicity and inflammation is more obvious given the fact that inhibition of AR prevents the increased synthesis of inflammatory cytokines and chemokines by various oxidant stimuli such as LPS, cytokines, growth factors, and high glucose. This is further substantiated by our demonstration that HNE, GS-HNE, and AR-catalyzed reduced product of GS-LDAs, that is, GS-DHN promote, VSMC growth in vitro [71]. AR inhibition by pharmacological inhibitors or ablation by siRNA prevents HNE- and GS-HNE-induced VSMC proliferation but has no effect on the GS-DHN-induced changes. These studies thus suggest that the reduced forms of lipid-aldehyde glutathione conjugates (such as GS-DHN) could be involved in the oxidative stress-induced inflammatory signaling. Further studies are required to investigate the exact mechanism of GS-DHN-induced activation of upstream kinases that results in transcription of inflammatory genes. Nevertheless, our observations have opened up a new area of research in understanding the role of AR in the mediation of oxidative stress signaling in a number of inflammatory diseases.

8. Current and Future Developments

Oxidative stress-induced generation of lipid aldehydes has been observed in many inflammatory complications including cardiovascular disorders, bacterial sepsis, cancer, and asthma, which present enormous clinical challenges worldwide. Many researchers have presented the immense importance of this aspect of pathophysiology, and therefore there is an urgent need for development of new therapeutic strategies targeting the intervention in lipid aldehyde-mediated inflammatory signals in these diseases. However, a more precise elucidation of lipid aldehyde-induced inflammatory signaling is crucial for understanding the pathophysiology of multiple diseases including infections, atherosclerosis, autoimmune, and cancer. Based on these elucidations, a better therapeutic

intervention could be developed to contain the inflammatory responses in patients. Our extensive research during recent years has identified that oxidative stress-induced LDAs and their GS-conjugates catalyzed by AR play a major role in the mediation of NF-κB-induced inflammatory signals via PLC/PKC/IKK/MAPK pathways. We have demonstrated that in experimental animal models, inhibition of GS-LDA metabolizing enzymes, specifically AR, prevents inflammatory diseases such as uveitis, sepsis, colon cancer, atherosclerosis, and allergic asthma. These results have delineated a novel mechanism regulating inflammation and have laid foundation for future studies that could result in clinical application of AR inhibitors. Further, a better understanding of the role of AR-catalyzed LDAs and their GSH-conjugates in the signalosome and inflammasome signaling pathways will better reveal underlying pathophysiological events in various inflammatory diseases.

Abbreviations

AR:	Aldose reductase
ARI:	AR inhibitor
ROS:	Reactive oxygen species
LDAs:	Lipid peroxidation-derived aldehydes
MDA:	malondialdehyde
HNE:	4-hydroxynonenal
GSH:	Reduced glutathione
GS-LDAs:	Glutathione-lipid-derived aldehydes
GS-HNE:	Glutathione-HNE conjugate
GS-DHN:	Glutathione-1,4-dihydroxynonene conjugate
LPS:	Lipopolysacharides
NADPH:	Reduced nicotinamide adenine dinucleotide phosphate
PKC:	Protein kinase C
PLC:	Phospholipase C
MAPK:	Mitogen-activated protein kinase
NF-κB:	Nuclear factor kappa B
AP-1:	Activator protein 1
CREB:	cAMP response element-binding protein
VSMC:	Vascular smooth muscle cells
SOD:	Superoxide dismutase
NAC:	N-acetylcysteine
AMD:	Age-related macular degeneration
EGFR:	Epidermal growth factor receptor.

References

[1] N. J. Pillon, M. L. Croze, R. E. Vella, L. Soulère, M. Lagarde, and C. O. Soulage, "The lipid peroxidation by-product 4-hydroxy-2-nonenal (4-HNE) induces insulin resistance in skeletal muscle through both carbonyl and oxidative stress," *Endocrinology*, vol. 153, no. 5, pp. 2099–2111, 2012.

[2] M. P. Mattson, "Roles of the lipid peroxidation product 4-hydroxynonenal in obesity, the metabolic syndrome, and associated vascular and neurodegenerative disorders," *Experimental Gerontology*, vol. 44, no. 10, pp. 625–633, 2009.

[3] C. S. Kang, H. W. Kim, B. K. Kim et al., "Hepatotoxicity and nephrotoxicity produced by 4-hydroxy-2-nonenal (4-HNE) following 4-week oral administration to sprague-dawley rats," *Journal of Toxicology and Environmental Health A*, vol. 74, no. 12, pp. 779–789, 2011.

[4] P. Karihtala, S. Kauppila, U. Puistola, and A. Jukkola-Vuorinen, "Divergent behaviour of oxidative stress markers 8-hydroxydeoxyguanosine (8-OHdG) and 4-hydroxy-2-nonenal (HNE) in breast carcinogenesis," *Histopathology*, vol. 58, no. 6, pp. 854–862, 2011.

[5] K. Uno, K. Kato, G. Kusaka, N. Asano, K. Iijima, and T. Shimosegawa, "The balance between 4-hydroxynonenal and intrinsic glutathione/glutathione S-transferase A4 system may be critical for the epidermal growth factor receptor phosphorylation of human esophageal squamous cell carcinomas," *Molecular Carcinogenesis*, vol. 50, no. 10, pp. 781–790, 2011.

[6] R. Vatsyayan, P. Chaudhary, A. Sharma et al., "Role of 4-hydroxynonenal in epidermal growth factor receptor-mediated signaling in retinal pigment epithelial cells," *Experimental Eye Research*, vol. 92, no. 2, pp. 147–154, 2011.

[7] S. Qin and G. A. Rodrigues, "Differential roles of AMPKα1 and AMPKα2 in regulating 4-HNE-induced RPE cell death and permeability," *Experimental Eye Research*, vol. 91, no. 6, pp. 818–824, 2010.

[8] M. Singh, T. N. Dang, M. Arseneault, and C. Ramassamy, "Role of by-products of lipid oxidation in Alzheimer's disease brain: a focus on acrolein," *Journal of Alzheimer's Disease*, vol. 21, no. 3, pp. 741–756, 2010.

[9] D. A. Butterfield, M. L. Bader Lange, and R. Sultana, "Involvements of the lipid peroxidation product, HNE, in the pathogenesis and progression of Alzheimer's disease," *Biochimica et Biophysica Acta*, vol. 1801, no. 8, pp. 924–929, 2010.

[10] W. Völkel, T. Sicilia, A. Pähler et al., "Increased brain levels of 4-hydroxy-2-nonenal glutathione conjugates in severe Alzheimer's disease," *Neurochemistry International*, vol. 48, no. 8, pp. 679–686, 2006.

[11] M. Fukai, T. Hayashi, R. Yokota et al., "Lipid peroxidation during ischemia depends on ischemia time in warm ischemia and reperfusion of rat liver," *Free Radical Biology and Medicine*, vol. 38, no. 10, pp. 1372–1381, 2005.

[12] E. McCracken, D. I. Graham, M. Nilsen, J. Stewart, J. A. R. Nicoll, and K. Horsburgh, "4-hydroxynonenal immunoreactivity is increased in human hippocampus after global ischemia," *Brain Pathology*, vol. 11, no. 4, pp. 414–421, 2001.

[13] H. Esterbauer, R. J. Schaur, and H. Zollner, "Chemistry and biochemistry of 4-hydroxynonenal, malonaldehyde and related aldehydes," *Free Radical Biology and Medicine*, vol. 11, no. 1, pp. 81–128, 1991.

[14] A. Loidl-Stahlhofen, K. Hannemann, and G. Spiteller, "Generation of α-hydroxyaldehydic compounds in the course of lipid peroxidation," *Biochimica et Biophysica Acta*, vol. 1213, no. 2, pp. 140–148, 1994.

[15] R. M. LoPachin, T. Gavin, D. R. Petersen, and D. S. Barber, "Molecular mechanisms of 4-hydroxy-2-nonenal and acrolein toxicity: nucleophilic targets and adduct formation," *Chemical Research in Toxicology*, vol. 22, no. 9, pp. 1499–1508, 2009.

[16] A. T. Jacobs and L. J. Marnett, "Systems analysis of protein modification and cellular responses induced by electrophile stress," *Accounts of Chemical Research*, vol. 43, no. 5, pp. 673–683, 2010.

[17] G. Juric-Sekhar, K. Zarkovic, G. Waeg, A. Cipak, and N. Zarkovic, "Distribution of 4-hydroxynonenal-protein conjugates as a marker of lipid peroxidation and parameter of malignancy in astrocytic and ependymal tumors of the brain," *Tumori*, vol. 95, no. 6, pp. 762–768, 2009.

[18] U. C. S. Yadav, K. V. Ramana, Y. C. Awasthi, and S. K. Srivastava, "Glutathione level regulates HNE-induced genotoxicity in human erythroleukemia cells," *Toxicology and Applied Pharmacology*, vol. 227, no. 2, pp. 257–264, 2008.

[19] N. Zarković, K. Zarković, R. J. Schaur et al., "4-hydroxynonenal as a second messenger of free radicals and growth modifying factor," *Life Sciences*, vol. 65, no. 18-19, pp. 1901–1904, 1999.

[20] C. A. Thompson and P. C. Burcham, "Genome-wide transcriptional responses to acrolein," *Chemical Research in Toxicology*, vol. 21, no. 12, pp. 2245–2256, 2008.

[21] Y. S. Park and N. Taniguchi, "Acrolein induces inflammatory response underlying endothelial dysfunction: a risk factor for atherosclerosis," *Annals of the New York Academy of Sciences*, vol. 1126, pp. 185–189, 2008.

[22] C. C. Wu, C. W. Hsieh, P. H. Lai, J. B. Lin, Y. C. Liu, and B. S. Wung, "Upregulation of endothelial heme oxygenase-1 expression through the activation of the JNK pathway by sublethal concentrations of acrolein," *Toxicology and Applied Pharmacology*, vol. 214, no. 3, pp. 244–252, 2006.

[23] J. Roy, P. Pallepati, A. Bettaieb, A. Tanel, and D. A. Averill-Bates, "Acrolein induces a cellular stress response and triggers mitochondrial apoptosis in A549 cells," *Chemico-Biological Interactions*, vol. 181, no. 2, pp. 154–167, 2009.

[24] J. D. Lambeth, "NOX enzymes and the biology of reactive oxygen," *Nature Reviews Immunology*, vol. 4, no. 4, pp. 181–189, 2004.

[25] K. Bedard and K. H. Krause, "The NOX family of ROS-generating NADPH oxidases: physiology and pathophysiology," *Physiological Reviews*, vol. 87, no. 1, pp. 245–313, 2007.

[26] K. Datta, S. Sinha, and P. Chattopadhyay, "Reactive oxygen species in health and disease," *National Medical Journal of India*, vol. 13, no. 6, pp. 304–310, 2000.

[27] M. Valko, D. Leibfritz, J. Moncol, M. T. D. Cronin, M. Mazur, and J. Telser, "Free radicals and antioxidants in normal physiological functions and human disease," *International Journal of Biochemistry and Cell Biology*, vol. 39, no. 1, pp. 44–84, 2007.

[28] M. Vuillaume, "Reduced oxygen species, mutation, induction and cancer initiation," *Mutation Research*, vol. 186, no. 1, pp. 43–72, 1987.

[29] B. S. Berlett and E. R. Stadtman, "Protein oxidation in aging, disease, and oxidative stress," *Journal of Biological Chemistry*, vol. 272, no. 33, pp. 20313–20316, 1997.

[30] M. L. Circu and T. Y. Aw, "Reactive oxygen species, cellular redox systems, and apoptosis," *Free Radical Biology and Medicine*, vol. 48, no. 6, pp. 749–762, 2010.

[31] H. Bartsch and J. Nair, "Oxidative stress and lipid peroxidation-derived DNA-lesions in inflammation driven carcinogenesis," *Cancer Detection and Prevention*, vol. 28, no. 6, pp. 385–391, 2004.

[32] A. Catalá, "An overview of lipid peroxidation with emphasis in outer segments of photoreceptors and the chemiluminescence assay," *International Journal of Biochemistry and Cell Biology*, vol. 38, no. 9, pp. 1482–1495, 2006.

[33] M. Parola, G. Bellomo, G. Robino, G. Barrera, and M. U. Dianzani, "4-hydroxynonenal as a biological signal: molecular basis and pathophysiological implications," *Antioxidants and Redox Signaling*, vol. 1, no. 3, pp. 255–284, 1999.

[34] K. Uchida, "Current status of acrolein as a lipid peroxidation product," *Trends in Cardiovascular Medicine*, vol. 9, no. 5, pp. 109–113, 1999.

[35] G. R. Buettner, "The pecking order of free radicals and antioxidants: lipid peroxidation, α-tocopherol, and ascorbate," *Archives of Biochemistry and Biophysics*, vol. 300, no. 2, pp. 535–543, 1993.

[36] S. Nigam and T. Schewe, "Phospholipase A2s and lipid peroxidation," *Biochimica et Biophysica Acta*, vol. 1488, no. 1-2, pp. 167–181, 2000.

[37] H. Rubbo, S. Parthasarathy, S. Barnes, M. Kirk, B. Kalyanaraman, and B. A. Freeman, "Nitric oxide inhibition of lipoxygenase-dependent liposome and low- density lipoprotein oxidation: termination of radical chain propagation reactions and formation of nitrogen-containing oxidized lipid derivatives," *Archives of Biochemistry and Biophysics*, vol. 324, no. 1, pp. 15–25, 1995.

[38] S. Jongberg, C. U. Carlsen, and L. H. Skibsted, "Peptides as antioxidants and carbonyl quenchers in biological model systems," *Free Radical Research*, vol. 43, no. 10, pp. 932–942, 2009.

[39] R. Sharma, D. Brown, S. Awasthi et al., "Transfection with 4-hydroxynonenal-metabolizing glutathione S-transferase isozymes leads to phenotypic transformation and immortalization of adherent cells," *European Journal of Biochemistry*, vol. 271, no. 9, pp. 1690–1701, 2004.

[40] J. Z. Cheng, S. S. Singhal, A. Sharma et al., "Transfection of mGSTA4 in HL-60 cells protects against 4-hydroxynonenal-induced apoptosis by inhibiting JNK-mediated signaling," *Archives of Biochemistry and Biophysics*, vol. 392, no. 2, pp. 197–207, 2001.

[41] S. K. Srivastava, S. S. Singhal, S. Awasthi, S. Pikula, N. H. Ansari, and Y. C. Awasthi, "A glutathione S-transferases isozyme (bGST 5.8) involved in the metabolism of 4-hydroxy-2-trans-nonenal is localized in bovine lens epithelium," *Experimental Eye Research*, vol. 63, no. 3, pp. 329–337, 1996.

[42] M. Comporti, "Lipid peroxidation and cellular damage in toxic liver injury," *Laboratory Investigation*, vol. 53, no. 6, pp. 599–623, 1985.

[43] P. A. Baeuerle and T. Henkel, "Function and activation of NF-kappa B in the immune system," *Annual Review of Immunology*, vol. 12, pp. 141–179, 1994.

[44] P. A. Baeuerle and D. Baltimore, "Nf-κB: ten years after," *Cell*, vol. 87, no. 1, pp. 13–20, 1996.

[45] P. J. Barnes and M. Karin, "Nuclear factor-κB—a pivotal transcription factor in chronic inflammatory diseases," *New England Journal of Medicine*, vol. 336, no. 15, pp. 1066–1071, 1997.

[46] S. Ghosh, M. J. May, and E. B. Kopp, "NF-κB and Rel proteins: evolutionarily conserved mediators of immune responses," *Annual Review of Immunology*, vol. 16, pp. 225–260, 1998.

[47] W. C. Sha, "Regulation of immune responses by NF-κB/Rel transcription factors," *Journal of Experimental Medicine*, vol. 187, no. 2, pp. 143–146, 1998.

[48] M. Grossmann, Y. Nakamura, R. Grumont, and S. Gerondakis, "New insights into the roles of ReL/NF-κB transcription factors in immune function, hemopoiesis and human disease," *International Journal of Biochemistry and Cell Biology*, vol. 31, no. 10, pp. 1209–1219, 1999.

[49] G. Poli, F. Biasi, E. Chiaprotto, M. U. Dianzani, A. de Luca, and H. Esterbauer, "Lipid peroxidation in human diseases: evidence of red cell oxidative stress after circulatory shock," *Free Radical Biology and Medicine*, vol. 6, no. 2, pp. 167–170, 1989.

[50] M. Polak and Z. Zagórski, "Lipid peroxidation in diabetic retinopathy," *Annales Universitatis Mariae Curie-Sklodowska. Sectio D: Medicina*, vol. 59, no. 1, pp. 434–437, 2004.

[51] A. Higdon, A. R. Diers, J. Y. Oh, A. Landar, and V. M. Darley-Usmar, "Cell signalling by reactive lipid species: new concepts and molecular mechanisms," *Biochemical Journal*, vol. 442, no. 3, pp. 453–464, 2012.

[52] J. Ruef, M. Moser, C. Bode, W. Kübler, and M. S. Runge, "4-hydroxynonenal induces apoptosis, NF-κB-activation and formation of 8-isoprostane in vascular smooth muscle cells," *Basic Research in Cardiology*, vol. 96, no. 2, pp. 143–150, 2001.

[53] S. P. Faux and P. J. Howden, "Possible role of lipid peroxidation in the induction of NF-kappa B and AP-1 in RFL-6 cells by crocidolite asbestos: evidence following protection by vitamin E," *Environmental Health Perspectives*, vol. 105, 5, pp. 1127–1130, 1997.

[54] A. L. Levonen, A. Landar, A. Ramachandran et al., "Cellular mechanisms of redox cell signalling: role of cysteine modification in controlling antioxidant defences in response to electrophilic lipid oxidation products," *Biochemical Journal*, vol. 378, part 2, pp. 373–382, 2004.

[55] E. K. Ceaser, D. R. Moellering, S. Shiva et al., "Mechanisms of signal transduction mediated by oxidized lipids: the role of the electrophile-responsive proteome," *Biochemical Society Transactions*, vol. 32, part 1, pp. 151–155, 2004.

[56] J. W. Zmijewski, A. Landar, N. Watanabe, D. A. Dickinson, N. Noguchi, and V. M. Darley-Usmar, "Cell signalling by oxidized lipids and the role of reactive oxygen species in the endothelium," *Biochemical Society Transactions*, vol. 33, part 6, pp. 1385–1389, 2005.

[57] D. A. Dickinson, V. M. Darley-Usmar, and A. Landar, "The covalent advantage: a new paradigm for cell signaling by thiol reactive lipid oxidation products," in *Redox Proteomics: From Protein Modifications to Cellular Dysfunction and Diseases*, I. Dalle-Donne, A. Scalone, and D. A. Butterfield, Eds., pp. 345–367, John Wiley & Sons, Indianapolis, Ind, USA, 2006.

[58] K. Stamatakis and D. Pérez-Sala, "Prostanoids with cyclopentenone structure as tools for the characterization of electrophilic lipid-protein interactomes," *Annals of the New York Academy of Sciences*, vol. 1091, pp. 548–570, 2006.

[59] J. A. Doorn and D. R. Petersen, "Covalent modification of amino acid nucleophiles by the lipid peroxidation products 4-hydroxy-2-nonenal and 4-oxo-2-nonenal," *Chemical Research in Toxicology*, vol. 15, no. 11, pp. 1445–1450, 2002.

[60] K. Uchida, "4-hydroxy-2-nonenal: a product and mediator of oxidative stress," *Progress in Lipid Research*, vol. 42, no. 4, pp. 318–343, 2003.

[61] A. L. Isom, S. Barnes, L. Wilson, M. Kirk, L. Coward, and V. Darley-Usmar, "Modification of cytochrome c by 4-hydroxy-2-nonenal: evidence for histidine, lysine, and arginine-aldehyde adducts," *Journal of the American Society for Mass Spectrometry*, vol. 15, no. 8, pp. 1136–1147, 2004.

[62] E. Chiarpotto, C. Domenicotti, D. Paola et al., "Regulation of rat hepatocyte protein kinase C β isoenzymes by the lipid peroxidation product 4-hydroxy-2,3-nonenal: a signaling pathway to modulate vesicular transport of glycoproteins," *Hepatology*, vol. 29, no. 5, pp. 1565–1572, 1999.

[63] M. Nitti, C. Domenicotti, C. D'Abramo et al., "Activation of PKC-β isoforms mediates HNE-induced MCP-1 release by macrophages," *Biochemical and Biophysical Research Communications*, vol. 294, no. 3, pp. 547–552, 2002.

[64] M. Parola, G. Robino, F. Marra et al., "HNE interacts directly with JNK isoforms in human hepatic stellate cells," *Journal of Clinical Investigation*, vol. 102, no. 11, pp. 1942–1950, 1998.

[65] B. J. Song, Y. Soh, M. A. Bae, J. E. Pie, J. Wan, and K. S. Jeong, "Apoptosis of PC12 cells by 4-hydroxy-2-nonenal is mediated through selective activation of the c-Jun N-Terminal protein kinase pathway," *Chemico-Biological Interactions*, vol. 130–132, pp. 943–954, 2001.

[66] N. Shibata, Y. Kato, Y. Inose et al., "4-hydroxy-2-nonenal upregulates and phosphorylates cytosolic phospholipase A2 in cultured Ra2 microglial cells via MAPK pathways," *Neuropathology*, vol. 31, no. 2, pp. 122–128, 2011.

[67] S. J. Lee, C. E. Kim, M. R. Yun et al., "4-hydroxynonenal enhances MMP-9 production in murine macrophages via 5-lipoxygenase-mediated activation of ERK and p38 MAPK," *Toxicology and Applied Pharmacology*, vol. 242, no. 2, pp. 191–198, 2010.

[68] S. Saito, G. D. Frank, M. Mifune et al., "Ligand-independent trans-activation of the platelet-derived growth factor receptor by reactive oxygen species requires protein kinase C-δ and c-Src," *Journal of Biological Chemistry*, vol. 277, no. 47, pp. 44695–44700, 2002.

[69] P. Chaudhary, R. Sharma, A. Sharma et al., "Mechanisms of 4-hydroxy-2-nonenal induced pro- and anti-apoptotic signaling," *Biochemistry*, vol. 49, no. 29, pp. 6263–6275, 2010.

[70] S. Dwivedi, A. Sharma, B. Patrick, R. Sharma, and Y. C. Awasthi, "Role of 4-hydroxynonenal and its metabolites in signaling," *Redox Report*, vol. 12, no. 1-2, pp. 4–10, 2007.

[71] K. V. Ramana, A. Bhatnagar, S. Srivastava et al., "Mitogenic responses of vascular smooth muscle cells to lipid peroxidation-derived aldehyde 4-hydroxy-trans-2-nonenal (HNE): role of aldose reductase-catalyzed reduction of the HNE-glutathione conjugates in regulating cell growth," *Journal of Biological Chemistry*, vol. 281, no. 26, pp. 17652–17660, 2006.

[72] K. V. Ramana, M. S. Willis, M. D. White et al., "Endotoxin-induced cardiomyopathy and systemic inflammation in mice is prevented by aldose reductase inhibition," *Circulation*, vol. 114, no. 17, pp. 1838–1846, 2006.

[73] K. V. Ramana, "Aldose reductase: new insights for an old enzyme," *BioMolecular Concepts*, vol. 2, no. 1-2, pp. 103–114, 2011.

[74] H. J. Forman, M. Maiorino, and F. Ursini, "Signaling functions of reactive oxygen species," *Biochemistry*, vol. 49, no. 5, pp. 835–842, 2010.

[75] J. Segovia, A. Sabbah, V. Mgbemena et al., "TLR2/MyD88/NF-κB pathway, reactive oxygen species, potassium efflux activates NLRP3/ASC inflammasome during respiratory syncytial virus infection," *PLoS One*, vol. 7, no. 1, Article ID e29695, 2012.

[76] S. Mena, A. Ortega, and J. M. Estrela, "Oxidative stress in environmental-induced carcinogenesis," *Mutation Research*, vol. 674, no. 1-2, pp. 36–44, 2009.

[77] A. Auerbach and M. L. Hernandez, "The effect of environmental oxidative stress on airway inflammation," *Current Opinion in Allergy and Clinical Immunology*, vol. 12, no. 2, pp. 133–139, 2012.

[78] K. J. Chuang, C. C. Chan, T. C. Su, C. T. Lee, and C. S. Tang, "The effect of urban air pollution on inflammation, oxidative stress, coagulation, and autonomic dysfunction in young adults," *American Journal of Respiratory and Critical Care Medicine*, vol. 176, no. 4, pp. 370–376, 2007.

[79] E. Profumo, B. Buttari, and R. Riganò, "Oxidative stress in cardiovascular inflammation: its involvement in autoimmune responses," *International Journal of Inflammation*, vol. 2011, Article ID 295705, 6 pages, 2011.

[80] V. J. Thannickal and B. L. Fanburg, "Reactive oxygen species in cell signaling," *American Journal of Physiology—Lung Cellular and Molecular Physiology*, vol. 279, no. 6, pp. L1005–L1028, 2000.

[81] P. D. Ray, B. W. Huang, and Y. Tsuji, "Reactive oxygen species (ROS) homeostasis and redox regulation in cellular signaling," *Cellular Signalling*, vol. 24, no. 5, pp. 981–990, 2012.

[82] K. V. Ramana, A. A. Fadl, R. Tammali, A. B. M. Reddy, A. K. Chopra, and S. K. Srivastava, "Aldose reductase mediates the lipopolysaccharide-induced release of inflammatory mediators in RAW264.7 murine macrophages," *Journal of Biological Chemistry*, vol. 281, no. 44, pp. 33019–33029, 2006.

[83] R. Tammali, K. V. Ramana, S. S. Singhal, S. Awasthi, and S. K. Srivastava, "Aldose reductase regulates growth factor-induced cyclooxygenase-2 expression and prostaglandin E2 production in human colon cancer cells," *Cancer Research*, vol. 66, no. 19, pp. 9705–9713, 2006.

[84] S. K. Srivastava, U. C. Yadav, A. B. Reddy et al., "Aldose reductase inhibition suppresses oxidative stress-induced inflammatory disorders," *Chemico-Biological Interactions*, vol. 191, no. 1–3, pp. 330–338, 2011.

[85] S. J. Lee, C. E. Kim, K. W. Seo, and C. D. Kim, "HNE-induced 5-LO expression is regulated by NF-κB/ERK and Sp1/p38 MAPK pathways via EGF receptor in murine macrophages," *Cardiovascular Research*, vol. 88, no. 2, pp. 352–359, 2010.

[86] S. J. Lee, K. W. Seo, M. R. Yun et al., "4-hydroxynonenal enhances MMP-2 production in vascular smooth muscle cells via mitochondrial ROS-mediated activation of the Akt/NF-κB signaling pathways," *Free Radical Biology and Medicine*, vol. 45, no. 10, pp. 1487–1492, 2008.

[87] H. Zhang and H. J. Forman, "Acrolein induces heme oxygenase-1 through PKC-δ and PI3K in human bronchial epithelial cells," *American Journal of Respiratory Cell and Molecular Biology*, vol. 38, no. 4, pp. 483–490, 2008.

[88] A. Tanel and D. A. Averill-Bates, "P38 and ERK mitogen-activated protein kinases mediate acrolein-induced apoptosis in Chinese hamster ovary cells," *Cellular Signalling*, vol. 19, no. 5, pp. 968–977, 2007.

[89] H. Zhang and H. J. Forman, "Signaling pathways involved in phase II gene induction by α, B-unsaturated aldehydes," *Toxicology and Industrial Health*, vol. 25, no. 4-5, pp. 269–278, 2009.

[90] Y. Q. Fu, F. Fang, Z. Y. Lu, F. W. Kuang, and F. Xu, "N-acetylcysteine protects alveolar epithelial cells from hydrogen peroxideinduced apoptosis through scavenging reactive oxygen species and suppressing c-Jun N-terminal kinase," *Experimental Lung Research*, vol. 36, no. 6, pp. 352–361, 2010.

[91] S. Umar, J. Zargan, K. Umar, S. Ahmad, C. K. Katiyar, and H. A. Khan, "Modulation of the oxidative stress and inflammatory cytokine response by thymoquinone in the collagen induced arthritis in Wistar rats," *Chemico-Biological Interactions*, vol. 197, no. 1, pp. 40–46, 2012.

[92] J. M. Müller, R. A. Rupec, and P. A. Baeuerle, "Study of gene regulation by NF-κB and AP-1 in response to reactive oxygen intermediates," *Methods*, vol. 11, no. 3, pp. 301–312, 1997.

[93] M. Meyer, H. L. Pahl, and P. A. Baeuerle, "Regulation of the transcription factors NF-κB and AP-1 by redox changes," *Chemico-Biological Interactions*, vol. 91, no. 2-3, pp. 91–100, 1994.

[94] H. Bartsch and J. Nair, "Chronic inflammation and oxidative stress in the genesis and perpetuation of cancer: role of lipid peroxidation, DNA damage, and repair," *Langenbeck's Archives of Surgery*, vol. 391, no. 5, pp. 499–510, 2006.

[95] P. Amstad and P. Cerutti, "Genetic modulation of the cellular antioxidant defense capacity," *Environmental Health Perspectives*, vol. 88, pp. 77–82, 1990.

[96] P. Cerutti, R. Ghosh, Y. Oya, and P. Amstad, "The role of the cellular antioxidant defense in oxidant carcinogenesis," *Environmental Health Perspectives*, vol. 102, no. 10, pp. 123–129, 1994.

[97] J. H. Limón-Pacheco and M. E. Gonsebatt, "The glutathione system and its regulation by neurohormone melatonin in the central nervous system," *Central Nervous System Agents in Medicinal Chemistry*, vol. 10, no. 4, pp. 287–297, 2010.

[98] N. Ballatori, S. M. Krance, S. Notenboom, S. Shi, K. Tieu, and C. L. Hammond, "Glutathione dysregulation and the etiology and progression of human diseases," *Biological Chemistry*, vol. 390, no. 3, pp. 191–214, 2009.

[99] M. Valko, D. Leibfritz, J. Moncol, M. T. D. Cronin, M. Mazur, and J. Telser, "Free radicals and antioxidants in normal physiological functions and human disease," *International Journal of Biochemistry and Cell Biology*, vol. 39, no. 1, pp. 44–84, 2007.

[100] N. Tailor and M. Sharma, "Antioxidant hybrid compounds: a promising therapeutic intervention in oxidative stress induced diseases," *Mini-Reviews in Medicinal Chemistry*, vol. 13, no. 2, pp. 280–297, 2013.

[101] M. H. Hopkins, V. Fedirko, D. P. Jones, P. D. Terry, and R. M. Bostick, "Antioxidant micronutrients and biomarkers of oxidative stress and inflammation in colorectal adenoma patients: results from a randomized, controlled clinical trial," *Cancer Epidemiology Biomarkers and Prevention*, vol. 19, no. 3, pp. 850–858, 2010.

[102] Z. Mazloom, N. Hejazi, M. H. Dabbaghmanesh, H. R. Tabatabaei, A. Ahmadi, and H. Ansar, "Effect of vitamin C supplementation on postprandial oxidative stress and lipid profile in type 2 diabetic patients," *Pakistan Journal of Biological Sciences*, vol. 14, no. 19, pp. 900–904, 2011.

[103] M. Goodman, R. M. Bostick, O. Kucuk, and D. P. Jones, "Clinical trials of antioxidants as cancer prevention agents: past, present, and future," *Free Radical Biology and Medicine*, vol. 51, no. 5, pp. 1068–1084, 2011.

[104] E. C. Ienco, A. LoGerfo, C. Carlesi et al., "Oxidative stress treatment for clinical trials in neurodegenerative diseases," *Journal of Alzheimer's Disease*, vol. 24, no. 2, pp. 111–126, 2011.

[105] E. R. Greenberg, J. A. Baron, T. D. Tosteson et al., "A clinical trial of antioxidant vitamins to prevent colorectal adenoma," *New England Journal of Medicine*, vol. 331, no. 3, pp. 141–147, 1994.

[106] M. C. Mathew, A. M. Ervin, J. Tao, and R. M. Davis, "Antioxidant vitamin supplementation for preventing and slowing the progression of age-related cataract," *Cochrane Database of Systematic Reviews*, vol. 6, Article ID CD004567, 2012.

[107] U. C. S. Yadav, N. M. Kalariya, and K. V. Ramana, "Emerging role of antioxidants in the protection of uveitis complications," *Current Medicinal Chemistry*, vol. 18, no. 6, pp. 931–942, 2011.

[108] S. K. Srivastava, K. V. Ramana, and A. Bhatnagar, "Role of aldose reductase and oxidative damage in diabetes and the consequent potential for therapeutic options," *Endocrine Reviews*, vol. 26, no. 3, pp. 380–392, 2005.

[109] K. V. Ramana, B. L. Dixit, S. Srivastava, G. K. Balendiran, S. K. Srivastava, and A. Bhatnagar, "Selective recognition of glutathiolated aldehydes by aldose reductase," *Biochemistry*, vol. 39, no. 40, pp. 12172–12180, 2000.

[110] B. L. Dixit, G. K. Balendiran, S. J. Watowich et al., "Kinetic and structural characterization of the glutathione-binding site of aldose reductase," *Journal of Biological Chemistry*, vol. 275, no. 28, pp. 21587–21595, 2000.

[111] A. D. Morrison, R. S. Clements Jr., S. B. Travis, F. Oski, and A. I. Winegrad, "Glucose utilization by the polyol pathway

in human erythrocytes," *Biochemical and Biophysical Research Communications*, vol. 40, no. 1, pp. 199–205, 1970.

[112] R. Singh, M. A. White, K. V. Ramana et al., "Structure of a glutathione conjugate bound to the active site of aldose reductase," *Proteins*, vol. 64, no. 1, pp. 101–110, 2006.

[113] K. V. Ramana, B. L. Dixit, S. Srivastava et al., "Characterization of the glutathione binding site of aldose reductase," *Chemico-Biological Interactions*, vol. 130–132, pp. 537–548, 2001.

[114] H. J. Forman, "Reactive oxygen species and α,β-unsaturated aldehydes as second messengers in signal transduction," *Annals of the New York Academy of Sciences*, vol. 1203, pp. 35–44, 2010.

[115] H. J. Forman, J. M. Fukuto, T. Miller, H. Zhang, A. Rinna, and S. Levy, "The chemistry of cell signaling by reactive oxygen and nitrogen species and 4-hydroxynonenal," *Archives of Biochemistry and Biophysics*, vol. 477, no. 2, pp. 183–195, 2008.

[116] K. Uchida, "Lipid peroxidation and redox-sensitive signaling pathways," *Current Atherosclerosis Reports*, vol. 9, no. 3, pp. 216–221, 2007.

[117] K. Uchida, "Role of reactive aldehyde in cardiovascular diseases," *Free Radical Biology and Medicine*, vol. 28, no. 12, pp. 1685–1696, 2000.

[118] O. Kutuk and H. Basaga, "Apoptosis signalling by 4-hy- droxynonenal: a role for JNK-c-Jun/AP-1 pathway," *Redox Report*, vol. 12, no. 1-2, pp. 30–34, 2007.

Hindawi Publishing Corporation
Oxidative Medicine and Cellular Longevity
Volume 2013, Article ID 516051, 12 pages
http://dx.doi.org/10.1155/2013/516051

Research Article

Oxidative Stress and Mitogen-Activated Protein Kinase Pathways Involved in Cadmium-Induced BRL 3A Cell Apoptosis

Zhang Yiran, Jiang Chenyang, Wang Jiajing, Yuan Yan, Gu Jianhong, Bian Jianchun, Liu Xuezhong, and Liu Zongping

College of Veterinary Medicine, Yangzhou University, Yangzhou 225009, Jiangsu, China

Correspondence should be addressed to Liu Zongping; liuzongping@yzu.edu.cn

Received 18 December 2012; Accepted 25 February 2013

Academic Editor: Kota V. Ramana

In this study, BRL 3A cells were treated with different Cd concentrations (0, 10, 20, and 40 μmol/L) for 12 h and preincubated with or without N-acetyl-L-cysteine (NAC) (2 mmol/L) for 30 min, and cells were treated with Cd (0 and 20 μmol/L), pretreated with p38 inhibitor (SB203580), JNK (c-Jun NH2-terminal kinases) inhibitor (SP600125), and extracellular signal-regulated kinase (ERK) inhibitor (U0126) for 30 min, and then treated with 20 μmol/L Cd for 12 h. Cd decreased cell viability, SOD, and GSH-Px activity in a concentration-dependent manner. Increased MDA level, ROS generation, nuclear condensation, shrinkage, and fragmentation in cell morphology were inhibited by NAC. Cd-induced apoptosis was attenuated by pretreatment with SB203580, SP600125, and U0126. The results of western blot showed that NAC preincubation affected Cd-activated MAPK pathways, p38 and ERK phosphorylation. Cd treatment elevated the mRNA levels of Bax and decreased the mRNA levels of Bcl-2, respectively. The same effect was found in their protein expression levels. These results suggest that oxidative stress and MAPK pathways participate in Cd-induced apoptosis and that the balance between pro- and antiapoptotic genes (Bax and Bcl-2) is important in Cd-induced apoptosis.

1. Introduction

Cadmium (Cd) is one of the most toxic environmental and industrial pollutants. Acute or chronic exposure to this pollutant induces disturbances in several organs and tissues [1]. Occupational and environmental Cd pollution originates from mining, metallurgical industries, and manufacturers of nickel-Cd batteries, pigments, and plastic stabilizers. Important sources of human intoxication include cigarette smoke as well as food, water, and air contaminations. At the cellular level, Cd affects proliferation and differentiation. It also causes apoptosis. The International Agency for Research on Cancer has already classified Cd as a carcinogen [2].

Numerous studies revealed that Cd is a powerful inducer of oxidative stress [3], causing oxidative toxicity in broiler chicken, bone tissue, silver catfish, primary rat proximal tubular cells, and so on [4–9]. Cd decreases cell viability via a reactive oxygen species- (ROS-) mediated mechanism [10] and causes apoptosis through oxidative stress [8]. N-acetyl-L-cysteine (NAC) is a free radical scavenger used to determine the involvement of ROS in Cd-induced apoptosis and to suppress the renal proximal tubular damage caused by prolonged Cd exposure. Thus, oxidative stress has a critical function in Cd-induced toxicity [11]. However, the contributions of oxidative stress and apoptotic mechanisms to Cd-induced toxicity warrant further investigation.

In the pathways of oxidative stress-mediated apoptosis, mitogen-activated protein kinases (MAPKs) are given more attention in apoptosis. MAPKs, including extracellular signal-regulated kinases (ERKs), stress-activated protein kinases (c-Jun NH2-terminal kinases or JNK), and p38 MAPK, belong to a family of ser/thr protein kinases that mediate numerous complex cellular programs, such as cell proliferation, differentiation, and cell death in response to different stimuli [12–14]. ERK, which is activated by growth factors, is important for cell survival such as proliferation,

differentiation, and development. By contrast, JNK and p38 MAPK are involved in apoptosis by promoting cell death rate [15, 16]. Several studies demonstrated that Cd activates MAPKs in neuronal cells [17, 18], immature hippocampus [19], and human retinal pigment epithelial cells [20]. Cd activates p38 MAPK and JNK in C6 rat glioma cells [21]. Yang et al. [22] suggested that Cd induces the apoptosis of the anterior pituitary both *in vivo* and *in vitro*. ERK and p38 MAPK pathways were found to be involved in the aforementioned processes. Similarly, Haase et al. [23] reported that monocytes/macrophages treated with Cd stimulate ERK and p38 MAPK phosphorylation. U-937 promonocytic cells treated with 200 μmol/L $CdCl_2$ for 2 h induce apoptosis, rapid p38 MAPK phosphorylation, and late ERK phosphorylation [24]. These reports suggest that the members of the MAPK family are activated by Cd exposure according to cell type, Cd concentration, and Cd exposure duration. The possible function of MAPK activation in Cd-induced apoptosis was determined using MAPK inhibitors, such as p38 (SB203580), ERK (U0126), and JNK (SP600125). However, the mechanism by which Cd activates the family members of MAPKs in BRL 3A cell line and whether Cd targets other signaling pathways responsible for BRL 3A cell survival remain unknown.

The protein and mRNA expression levels of Bcl-2 family members, such as Bax and Bcl-2, were investigated in Cd-induced apoptosis. Apoptotic-related proteins are members of the Bcl-2 family. These proteins regulate mitochondrial outer membrane permeabilization and can be either proapoptotic (Bax, Bak, and Bad) or antiapoptotic (Bcl-2, Bcl-xL, and Bcl-w). Bax regulates the mitochondrial pathway by triggering the release of apoptotic factors, such as cytochrome c (cyt c), from the mitochondria subsequent to the death signal [25]. Bcl-2 is an anti-apoptotic protein that regulates cell apoptosis by controlling mitochondrial membrane permeability and inhibits caspase activity either by preventing the release of cyt c from the mitochondria into the cytosol or by binding to the apoptosis-activating factor damage [26, 27]. Given the importance of Bcl-2 family members in apoptosis, the regulation of Bax and Bcl-2 in Cd-induced apoptosis is necessary to be determined.

Based on these considerations, this study investigated whether Cd can induce apoptosis. The effects of Cd on BRL 3A cells and the possible functions of oxidative stress, MAPK pathways, and Bcl-2 family members on Cd hepatotoxicity were also determined. We used BRL 3A cells to observe the effect of Cd and to explore the possible function of oxidative stress, MAPK pathways, and Bcl-2 family members on apoptosis induced by different concentrations of Cd and NAC.

2. Materials and Methods

2.1. Materials. Cadmium acetate ($CdAC_2$), 2-,7-dichlorofluorescein diacetate (DCFH-DA), penicillin, streptomycin, and Hoechst 33258 kit were purchased from Sigma-Aldrich (St. Louis, MO, USA). Fluorescein isothiocyanate (FITC) Annexin V apoptosis detection kits were purchased from BD Biosciences Pharmingen (San Diego, CA, USA). Dulbecco's modified Eagle's medium (DMEM) and fetal bovine serum (FBS) were obtained from Gibco Laboratories (Grand Island, NY, USA). 3-(4,5-Dimethylthiazol-2-yl)-2,5-diphenyl-tetrazolium bromide (MTT) and trypsin were from Amresco Inc. (Solon, OH, USA). Malondialdehyde (MDA), superoxide dismutase (SOD), and glutathione peroxidase (GSH-Px) kits were purchased from Jiancheng Bioengineering Institute (Nanjing, China). A bicinchoninic acid (BCA) protein assay kit was provided by Beyotime Institute of Biotechnology (Jiangsu, China). Antibodies antirat JNK, P-JNK, ERK, P-ERK, p38, P-p38, Bax, Bcl-2, β-actin, and horseradish peroxidase- (HRP-) conjugated goat antirabbit IgG were obtained from Cell Signaling Technology, Inc. (Danvers, MA, USA). Radio-immunoprecipitation assay (RIPA) lysis buffer was from Solarbio China, Inc. (Beijing, China). Kodak X-ray film was purchased from Eastman Kodak Co. (Rochester, NY, USA). Cell culture plates were obtained from Corning Inc. (Corning, NY, USA). PrimerScript RT reagent Kit and SYBR Premix Ex Taq were from TaKaRa Bio Inc. (Shiga, Japan). Nitrocellulose (NC) filter membrane was from Pall Gelman Sciences (Port Washington, NY, USA). Enhanced chemiluminescence (ECL) detection kit was from ECL Millipore Ltd. (Burlington, MA, USA). Other reagents used were available locally and of analytical grade.

2.2. Cell Culture and Treatments. BRL 3A-immortalized rat hepatocytes were used between passages 10 and 20 (Cell of Chinese Academy of Science, Shanghai, China). BRL 3A cells were cultured in DMEM culture medium (Gibco, USA) supplemented with 100 U/mL penicillin, 100 μg/mL streptomycin, and 10% FBS. The cells were incubated at 37°C under a humid 5% CO_2 atmosphere (Thermo, USA).

BRL 3A cells were seeded at a density of 2×10^5 cells/mL in 6- or 96-well plates. CdAC2 was dissolved in distilled-deionized water as stock solution and diluted with nonserum culture medium to different concentrations before being added to the cell culture.

2.3. Cell Viability Assay. BRL 3A cells were treated with 0, 10, 20, and 40 μmol/L Cd for 12 h. In the other two experiments, the cells were preincubated with 2 mmol/L NAC for 30 min and then incubated with 20 μmol/L Cd for 12 h. Cell viability was evaluated by MTT assay. After the incubation period, the cells were incubated with MTT at a final concentration of 0.5 mg/mL for 4 h at 37°C prior to discarding the medium. Then, 150 μL of DMSO was added to each well, and the plate was stirred thoroughly for 10 min on a shaker. The optical density (OD) of each well was measured at 490 nm with a sunrise-basic ELISA Reader (Tecan, Austria). Cell viability was expressed as the proportion of OD to the control.

2.4. Cell Morphological Analysis. BRL 3A cells were treated with 0, 10, 20, and 40 μmol/L Cd for 12 h. In the other two experiments, the cells were incubated with 2 mmol/L NAC for 12 h and pre-incubated with 2 mmol/L NAC for 30 min, followed by incubation with 20 μmol/L Cd for 12 h. After the treatment, images were taken with an inverted phase-contrast microscope (Leica, Germany) equipped with a Quick Imaging system.

2.5. Hoechst 33258 Staining. Nuclear morphology was analyzed using Hoechst 33258. BRL 3A cells were treated with 0, 10, 20, and 40 μmol/L Cd for 12 h. In the other two experiments, the cells were incubated with 2 mmol/L NAC for 12 h and pre-incubated with 2 mmol/L NAC for 30 min, followed by incubation with 20 μmol/L Cd for 12 h. The culture medium was removed after the treatment. The cells were washed twice with phosphate-buffered saline (PBS) and fixed in 4% formaldehyde at 4°C for 10 min. The fixed cells were washed, stained with 5 μg/mL Hoechst 33258 at room temperature for 15 min in the dark, and then washed twice with PBS. Cell nuclear morphology was observed under a camera-equipped fluorescence light microscope using the filter of 450 nm to 490 nm.

2.6. Determination of Apoptosis. BRL 3A cells were seeded into six-well plates. Apoptosis was tested using an apoptosis detection kit according to the manufacturer's instructions. BRL 3A cells were treated with 0 and 20 μmol/L Cd for 12 h. In the other three experiments, the cells were pre-incubated with 10 μmol/L SB203580, SP600125, and U0126 for 30 min, followed by incubation with 20 μmol/L Cd for 12 h. After treatment, BRL 3A cells were collected and suspended in 100 μL of binding buffer containing 5 μL of FITC Annexin V and 5 μL of propidium iodide (PI) dye solution. After incubation in the dark at 25°C for 15 min, 400 μL of binding buffer was added. Then, the cells were analyzed by a FACSAria flow cytometer (Becton-Dickinson, San Jose, CA, USA) at excitation and emission wavelengths of 488 and 605 nm, respectively. A minimum of 10,000 cells per sample were registered. Quadrants were positioned on Annexin V/PI dot plots. Living (Annexin V−/PI−), early apoptotic (Annexin V+/PI−), late apoptotic (Annexin V+/PI+), and necrotic (Annexin V−/PI+) cells were distinguished. Therefore, the total apoptotic proportion included the percentage of cells with fluorescence Annexin V+/PI− and Annexin V+/PI+ [28].

Each independent experiment needed to set another three samples: unstained cells, FITC Annexin V only, and PI only. Each experiment was repeated at least three times.

2.7. ROS Determination. The intracellular ROS levels were measured using the stable nonfluorescent molecule DCFH-DA. This molecule passively diffuses into cells, where the acetate can be cleaved by intracellular esterases to produce a polar diol that is retained well within the cells. Relative ROS production was expressed as a change in fluorescence compared with the fluorescence of the corresponding control.

BRL 3A cells were treated with 0, 10, 20, and 40 μmol/L Cd for 12 h. In the other two experiments, the cells were incubated with 2 mmol/L NAC for 12 h and pre-incubated with 2 mmol/L NAC for 30 min, followed by incubation with 20 μmol/L Cd for 12 h. After the treatment, the cells were collected, incubated with 20 μmol/L DCFH-DA at 37°C for 20 min in the dark, and then washed twice with PBS. The cells were analyzed in a FACSAria flow cytometer (Becton-Dickinson, USA) at excitation and emission wavelengths of 488 and 525 nm, respectively.

2.8. Measurement of SOD Activity, GSH-Px Activity, and MDA Level. As a breakdown product of the oxidative degradation of cell membrane lipids, MDA is generally considered as an indicator of lipid peroxidation. Lipid peroxidation was evaluated by measuring MDA concentrations through spectrophotometry of the color produced during the reaction of thiobarbituric acid with MDA. MDA concentrations expressed in nmol/mg protein were calculated from the absorbance of thiobarbituric acid reactive substances at 532 nm. SOD is a superoxide scavenger. Total SOD activity was determined from the inhibition rate of the superoxide radical-dependent cyt c reduction. In the assay, the xanthine-xanthine oxidase system was used as the source of superoxide ions, and the absorbance was determined at 550 nm. The values were expressed as U/mg protein. GSH-Px activity was assessed according to the kit's instruction via the reaction $H_2O_2 + 2GSH \rightarrow 2H_2O + GSSG$ (oxidized glutathione). The absorbance was determined at 412 nm, and the enzyme activity was expressed as U/mg protein [28, 29].

BRL 3A cells were treated with 0, 10, 20, and 40 μmol/L Cd for 12 h. In the other two experiments, the cells were incubated with 2 mmol/L NAC for 12 h and pre-incubated with 2 mmol/L NAC for 30 min, followed by incubation with 20 μmol/L Cd for 12 h. The treated cells were pelleted and lysed in 200 μL of cell lysis solution (containing 0.1 M Tris-HCl and 0.1% Triton-100) to evaluate lipid peroxidation following the protocol of SOD, GSH-Px, and MDA assay kits.

2.9. Western Blot Analysis. BRL 3A cells were treated with 0, 10, 20, and 40 μmol/L Cd for 12 h. In the other two experiments, the cells were incubated with 2 mmol/L NAC for 12 h and pre-incubated with 2 mmol/L NAC for 30 min, followed by incubation with 20 μmol/L Cd for 12 h (only in the ERK- and P38-related groups). After the treatment, the cells were washed twice with cold PBS, extracted into RIPA lysis buffer on ice for 30 min, and then sonicated at 3 W for 15 s. The cell lysates were centrifuged at 12,000 g for 10 min at 4°C. The protein content was determined using a BCA protein assay kit. Lysate aliquots were diluted with 6× sodium dodecyl sulfate (SDS) sample buffer and boiled for 10 min. A total of 30 μg of protein from each treatment was separated by 12% SDS-polyacrylamide gel and then electrophoretically transferred onto NC membranes (Poll, USA). After being blocked at room temperature for 2 h with 5% nonfat milk in TBS with 0.1% Tween-20 (TBST), the membranes were incubated overnight at 4°C with the corresponding primary antibodies: rabbit anti-rat antibody (JNK, P-JNK, ERK, P-ERK, p38, P-p38, Bax, and Bcl-2) in 1 : 1000 and rabbit anti-rat β-actin antibody in 1 : 5000. After being washed with TBST (6 × 5 min), the membranes were incubated with HRP-conjugated goat anti-rabbit IgG (at a dilution of 1 : 5000) at room temperature for 2 h. After additional washes, the membranes were visualized using an ECL detection kit according to the manufacturer's instructions and then exposed to X-ray film. The volumes of the bands were determined by standard scanning densitometry with normalization of densitometry measures to β-actin.

2.10. Quantitative Real-Time Polymerase Chain Reaction (PCR) of Bax and Bcl-2. BRL 3A cells were treated with 0, 10, 20, and 40 μmol/L Cd for 12 h. After the treatment, RNA was extracted from BRL 3A cells using the AXYPrep multisource total RNA miniprep kit (Axygen, USA) according to the manufacturer's instructions. The OD ratios (OD260/OD280) of the samples were assessed between 1.8 and 2.0. For cDNA synthesis, 900 ng of total RNA was reverse transcribed to complementary DNA using a PrimerScript RT reagent kit with a gDNA eraser. After the RT reaction, each sample was conducted in triplicate, and each reaction mixture was prepared using the SYBR Premix Ex Taq in a total volume of 20 μL. In a 96-well plate, cDNA fragments of Bax, Bcl-2, and β-actin were amplified separately by PCR in triplicate using an ABI PRISM7500 Sequence Detection System (Applied Biosystems, USA). The reaction conditions were as follows: 95°C for 2 min; 95°C for 5 s; 40 cycles of 95°C for 5 s, 59°C for 34 s, and 95°C for 15 s; 60°C for 1 min; and 95°C for 15 s. Relative quantification of gene expression within each reaction was calculated with the $2^{-\Delta\Delta Ct}$ method according to the manufacturer's instructions (ABI PRISM 7500 Sequence Detection System, Applied Biosystems, USA).

The primer sequences (Table 1) were designed according to cDNA sequences from Gene Bank. All primers were synthesized by Invitrogen China, Inc. (Shanghai, China).

2.11. Statistical Analysis. Results were represented statistically as means ± SD. Significance was assessed by one-way ANOVA following appropriate transformation to normalized data and equalized variance where necessary. Statistical analysis was performed using SPSS statistics 17.0 (SPSS Inc., USA); $P < 0.05$ and $P < 0.01$ were considered to indicate significance and high significance, respectively. All assays were performed in triplicate.

3. Results

3.1. Cell Viability. To determine the appropriate concentration of Cd for the mechanism studies, we measured the effect of Cd exposure on cell viability. As shown in Figure 1, Cd (0 μmol/L to 40 μmol/L) decreased cell viability in a concentration-dependent manner. The cell viability of the 20 μmol/L Cd group was approximately 50% of that of the control. Therefore, 20 μmol/L of Cd was used in the experiments of inhibitory effects. NAC (2 mmol/L) alone did not obviously alter cell viability compared with the control. However, preincubation with 2 mmol/L NAC for 30 min attenuated the reduction in cell viability induced by 20 μmol/L Cd compared with the 20 μmol/L Cd group.

3.2. Effects of Cd on Cell Morphology. Phase-contrast microscopic observations after exposure to increasing Cd concentrations (10 μmol/L to 40 μmol/L) revealed morphological changes showing cytoplasmic shrinkage, rounding, and loss of cell integrity. NAC (2 mmol/L) alone had no significant effect on cell morphology compared with the control. Pre-incubation with 2 mmol/L NAC for 30 min could attenuate cytotoxicity to maintain cell integrity induced by 20 μmol/L Cd compared with the 20 μmol/L Cd group.

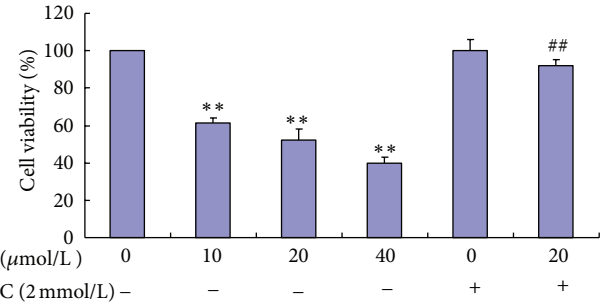

Figure 1: Cell viability of BRL 3A cells treated with Cd and NAC. Cells were treated with 0 μmol/L to 40 μmol/L Cd and pre-treated with or without 2 mmol/L NAC for 12 h. Data are presented as mean ± SD of three independent experiments performed in triplicate. Significant difference: $^{*}P < 0.05$, $^{**}P < 0.01$, compared with the control. $^{\#}P < 0.05$, $^{\#\#}P < 0.01$, compared with the 20 μmol/L Cd group.

Following detection of apoptosis-related proteins and genes, BRL 3A cell apoptosis was observed after Hoechst 33258 staining. Significant morphological changes were observed in the cells exposed to 10 μmol/L to 40 μmol/L Cd for 12 h. The cells of the control group appeared normal with round and homogenous nuclei, whereas those treated with 10 μmol/L to 40 μmol/L Cd exhibited typical apoptotic features, such as plasma membrane blebbing, cell shrinkage, fragmentation, and nuclear chromatin condensation. The fluorescence intensity of cell staining with Hoechst 33258 indicated that the untreated cells displayed evenly dispersed chromatin structures. However, the cells treated with NAC (2 mmol/L) alone showed no significant changes compared with the control cells. Pre-incubation with 2 mmol/L NAC could attenuate changes, such as abnormal nuclear contents (Figure 2).

3.3. Effects of Cd on Cell Apoptosis. The involvement of MAPK signaling in Cd-induced apoptosis was investigated. Flow cytometry was used to distinguish the effects of MAPK inhibitors in apoptosis and necrosis after double staining with Annexin V-FITC and PI. Pre-incubation with 10 μmol/L SB203580, SP600125, and U0126 for 30 min before treatment with 20 μmol/L Cd significantly decreased cell apoptotic rates to 10.47%, 14.43%, and 11.47%, respectively, in BRL 3A cells compared with the corresponding rate of 20.6% in the 20 μmol/L Cd control group (Figure 3).

3.4. Effects of Cd on ROS Generation. ROS generation was expressed as the measured fluorescence intensity in analyzed cells. Representative results of ROS are shown in Figure 4. Cd (10 μmol/L to 40 μmol/L) increased the level of ROS production in a concentration-dependent manner, whereas pre-incubation with 2 mmol/L NAC significantly reduced ROS generation induced by 20 μmol/L Cd.

3.5. Effects of Cd on SOD Activity, GSH-Px Activity, and MDA Level. To assess the intracellular oxidant and antioxidant status, SOD activity, GSH-Px activity, and MDA level were

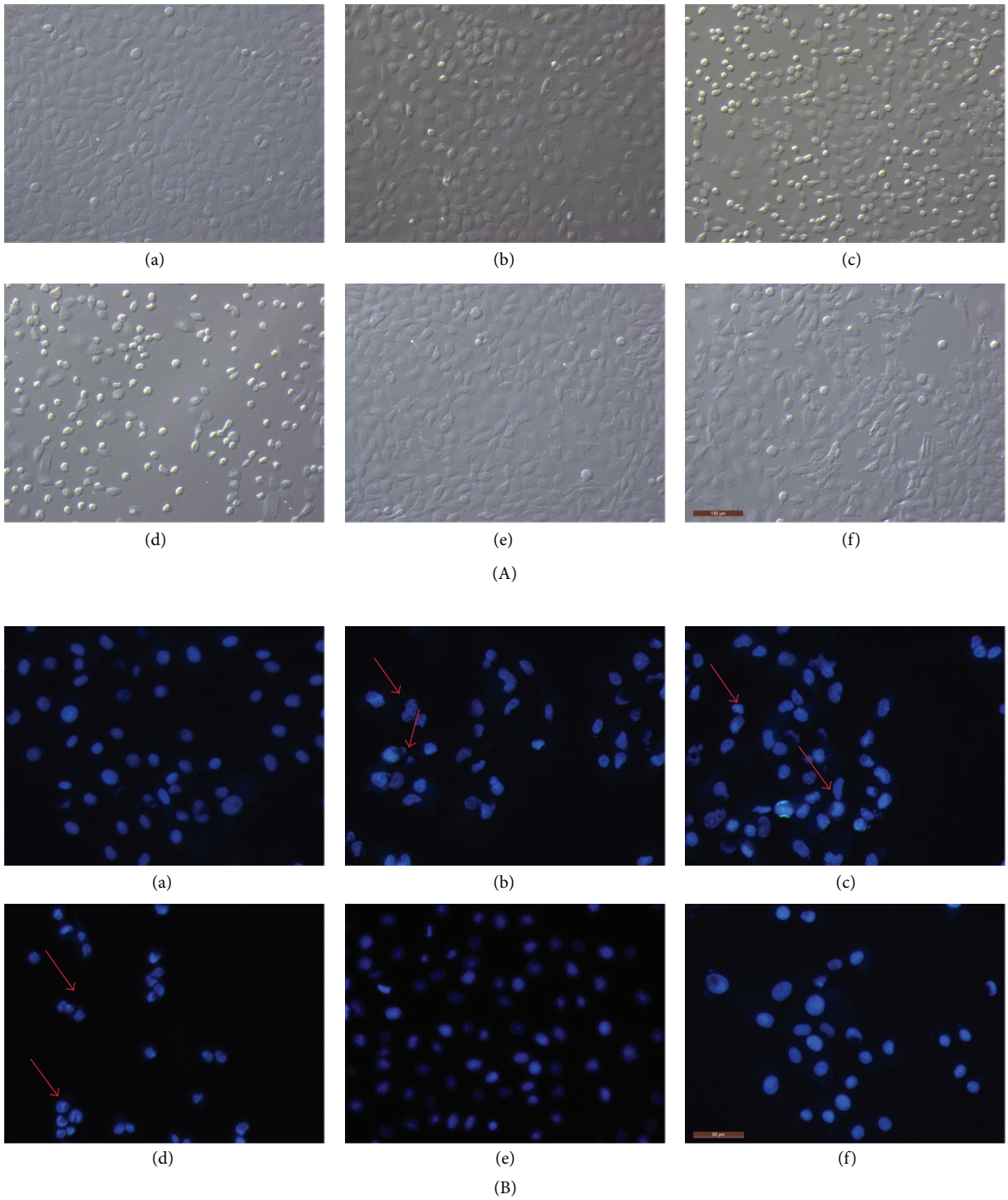

Figure 2: Cd and NAC induce morphological changes in BRL 3A cells. Cultured cells were exposed to 0, 10, 20, and 40 μmol/L Cd for 12 h (a, b, c, and d). In the other experiment, the cells were pre-incubated with 2 mmol/L NAC for 30 min and incubated with 20 μmol/L Cd or only incubated with 2 mmol/L NAC for 12 h (f and e). (A) After the treatment, images were taken with an Olympus inverted phase-contrast microscope. (B) Thereafter, the cells were fixed, stained with Hoechst 33258, and then observed under a fluorescence microscope. Arrows indicate morphological changes (blebbing cells, chromatin condensation, or fragmentation) in the nuclei of BRL 3A cells. Scale bar: 100 μm.

evaluated in BRL 3A cells (Figure 5). The MDA levels in the groups treated with 20 μmol/L to 40 μmol/L Cd were remarkably higher than those in the control group. Cd (20 μmol/L to 40 μmol/L) significantly decreased SOD activity. Compared with the 20 μmol/L Cd group, SOD activity significantly increased in the group pre-incubated with 2 mmol/L NAC. The GSH-Px activity in the groups treated with 10 μmol/L to 40 μmol/L Cd was significantly lower than that in the control

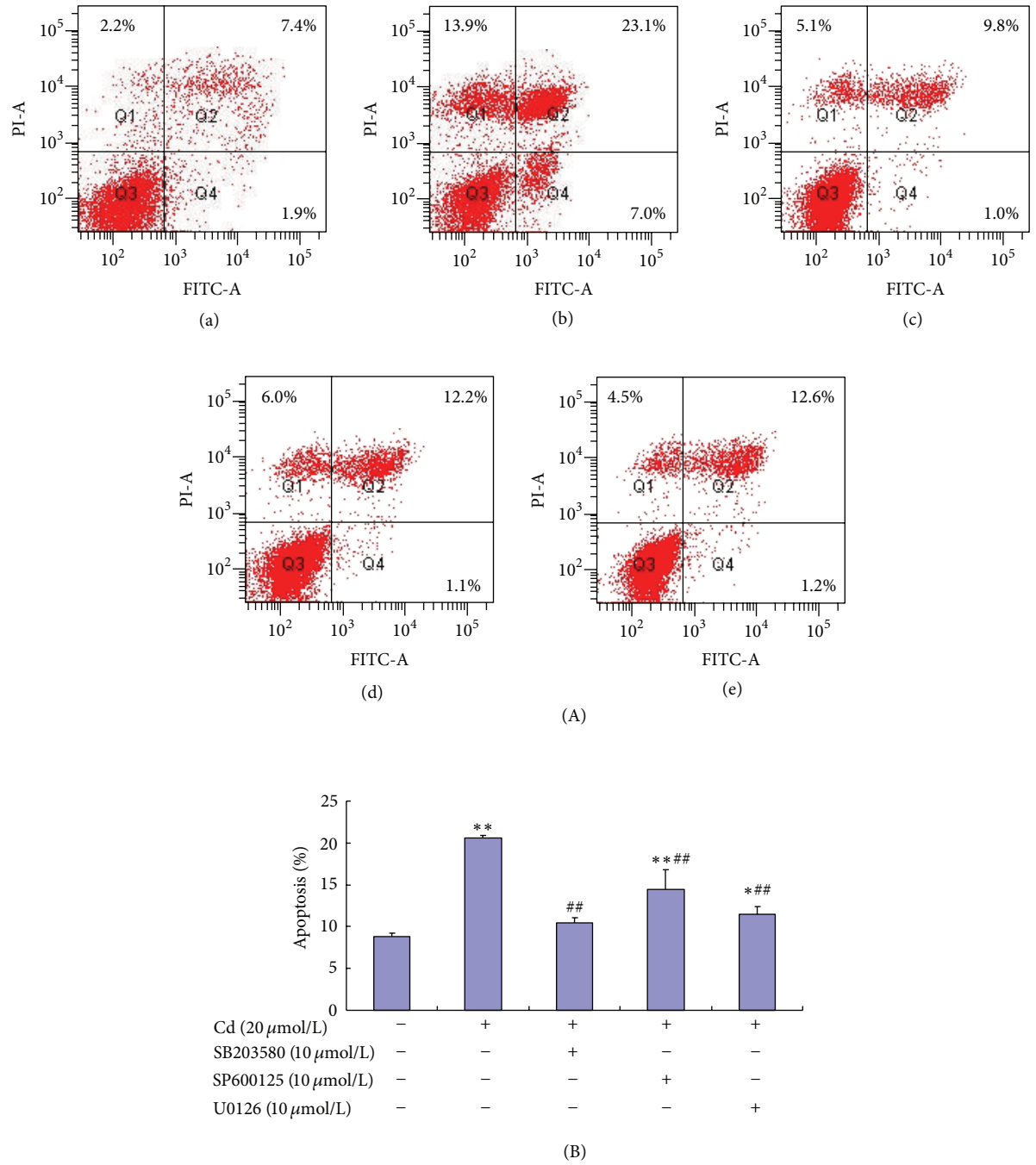

Figure 3: Flow cytometric analysis of BRL 3A cells after treatment with Cd and MAKP inhibitors. Cellular apoptosis was tested using an apoptosis detection kit. (A) BRL 3A cells were treated with 0 and 20 μmol/L Cd for 12 h (a and b). In the other three experiments, the cells were pre-incubated with 10 μmol/L SB203580, SP600125, and U0126 for 30 min, followed by incubation with 20 μmol/L Cd for 12 h (c, d, and e). (B) The apoptotic percentage shows that 10 μmol/L p38 inhibitor (SB203580), JNK inhibitor (SP600125), and ERK inhibitor (U0126) can reduce cell apoptosis significantly. Data are presented as mean ± SD of three independent experiments performed in triplicate. Significant difference: $^{*}P < 0.05$, $^{**}P < 0.01$, compared with the control. $^{\#}P < 0.05$, $^{\#\#}P < 0.01$, compared with the 20 μmol/L Cd group.

group. The GSH-Px activity in the cells pre-incubated with 2 mmol/L NAC was significantly higher than that in the cells treated with 20 μmol/L Cd alone.

3.6. Effects of Cd on Protein Expression of p38, ERK, and JNK. Immunoblot analyses were performed with antibodies to determine the effects of Cd on the phosphorylation of MAPKs. The effects of Cd exposure on protein expression were also observed. Western blot analysis showed that the treatment of BRL 3A cells with Cd for 12 h caused some changes. Robust phosphorylation of p38 and JNK (1/2) was observed in the groups treated with 10 μmol/L to 40 μmol/L

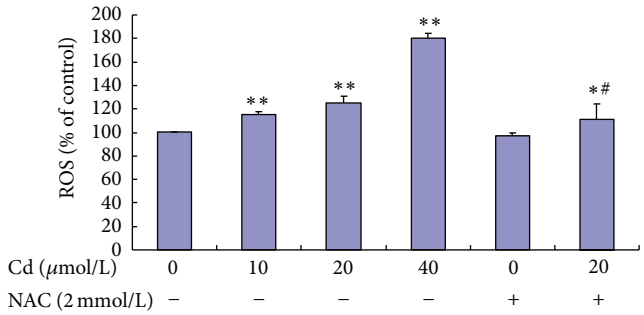

Figure 4: Effect of Cd and NAC on ROS generation of BRL 3A cells. Cultured cells were exposed to 0 μmol/L to 40 μmol/L Cd and pretreated with or without 2 mmol/L NAC for 12 h. Data are presented as mean ± SD of three independent experiments performed in triplicate. Significant difference: $^{*}P < 0.05$, $^{**}P < 0.01$, compared with the control. $^{\#}P < 0.05$, $^{\#\#}P < 0.01$, compared with the 20 μmol/L Cd group.

Table 1: The primers for real-time PCR.

Gene	Primers (5′-3′)
Bax	Sense: TTGTTACAGGGTTTCATCCAGG
	Antisense: GTGTCCACGTCAGCAATCATC
Bcl-2	Sense: GGGAGCGTCAACAGGGAG
	Antisense: AGCCAGGAGAAATCAAACAGA
β-Actin	Sense: CGTTGACATCCGTAAAGAC
	Antisense: TGGAAGGTGGAGTGAG

Cd, whereas decreased phosphorylation of ERK was found in the groups treated with 10 μmol/L to 20 μmol/L Cd. Meanwhile, 40 μmol/L Cd did not significantly alter the phosphorylation of 44 kD ERK but significantly elevated the phosphorylation of 42 kD ERK. ERK phosphorylation could be increased and p38 phosphorylation could be inhibited by NAC pre-incubation compared with the 20 μmol/L Cd group.

A significant increase in Bax protein level was found in the groups treated with 10 μmol/L to 40 μmol/L Cd. A significant reduction in Bcl-2 protein level was observed in the groups treated with 10 μmol/L to 40 μmol/L Cd. The data shown (Figure 6) are expressed as percentage of the control (considered as 100%).

3.7. Effects of Cd on the mRNA Levels of Bax and Bcl-2. Transcriptional changes in Bax and Bcl-2 were observed in the Cd-treated BRL 3A cells. The Bax mRNA level was significantly elevated in the groups treated with 10 μmol/L to 40 μmol/L Cd, with the peak found in the 10 μmol/L Cd group. The Bcl-2 mRNA level in the groups treated with 10 μmol/L to 40 μmol/L Cd significantly decreased. Figure 7 shows the relative quantification of gene expression levels by real-time PCR in relation to β-actin.

4. Discussion

In the present study, Cd was demonstrated to be toxic to BRL 3A cells, resulting in decreased cell viability and increased oxidative stress. Furthermore, MAPK pathways and Bax gene family have critical functions in Cd-induced apoptosis. The antioxidant NAC attenuated most of these changes. Thus, ROS elevation is an early event in Cd-induced apoptosis.

In this study, 10 μmol/L to 40 μmol/L Cd significantly decreased cellular viability. This finding may be attributed to apoptotic cell death. Chen et al. [17] reported that neuronal cell apoptosis is induced by 10 μmol/L Cd, whereas Iryo [30] observed apoptosis in CCRF-CEM cells treated with 5 μmol/L Cd. Exposure to 5 μmol/L Cd decreases granulosa cell number and viability and causes chromatin condensation and DNA fragmentation [28]. Thus, Cd at doses higher than 5 μmol/L is harmful to cells *in vitro* possibly because of apoptosis induction.

Apoptosis is a major mode of elimination of damaged cells in Cd toxicity and precedes necrosis [31]. In the present study, morphological observations and flow cytometric assessment showed that Cd induced the apoptosis of BRL 3A cells. This observation is compatible with the report of Coonse et al. [32], who proved the occurrence of apoptosis after Cd treatment of the human osteoblast-like cell line Saos-2. In addition, morphological and biochemical analyses revealed that Cd induces the apoptosis of murine fibroblasts [33].

The mechanisms of Cd toxicity have been suggested to interfere with cell adhesion and signaling, oxidative stress, apoptosis, genotoxicity, and cell cycle disturbance [34]. Although the overall effect of Cd on any cell or tissue is likely to be due to a synergism of several mechanisms, only one mechanism possibly dominates in a specific cell type [28]. In these studies, the toxic manifestations induced by Cd were associated with oxidative stresses, including lipid peroxidation and ROS production. Previous studies found that oxidative stress can be induced by Cd. Moreover, Cd-induced apoptosis is mediated by oxidative stress in LLC-PK1 [11]. Aydin et al. [31] demonstrated that Cd induces oxidative stress, resulting in oxidative deterioration of biological macromolecules. Cd possibly affects bone tissues through disorders in its oxidative/antioxidative balance, resulting in oxidative stress [5]. ROS reportedly possess important functions in the initiation of apoptosis. Bertin and averbeck [2] confirmed that Cd can provoke ROS generation. NAC is an antioxidant and ROS scavenger that can effectively block the Cd-induced activation of ERK, JNK, and p38 signaling network, prevent Cd-induced cell death, and significantly reduce Cd-induced toxicity in human lens epithelial cells and human retinal pigment epithelial cells [17, 20, 35]. These findings demonstrate the association between apoptosis and intracellular ROS. Similarly, Chen showed that Cd induces ROS generation, leading to apoptosis of PC12 and SH-SY5Y cells. Pretreatment with NAC scavenged Cd-induced ROS and prevented cell death, suggesting that Cd-induced apoptosis is caused by ROS generation. Thus, antioxidants can be exploited for the prevention of Cd-induced diseases [17]. The present study showed that Cd elevated ROS generation and NAC antagonized Cd-induced ROS. As ROS scavengers, SOD and GSH-Px were depleted. As a lipid peroxidation product, MDA accumulated in BRL 3A cells exposed to Cd. NAC elevated the activities of SOD and GSH-Px. The

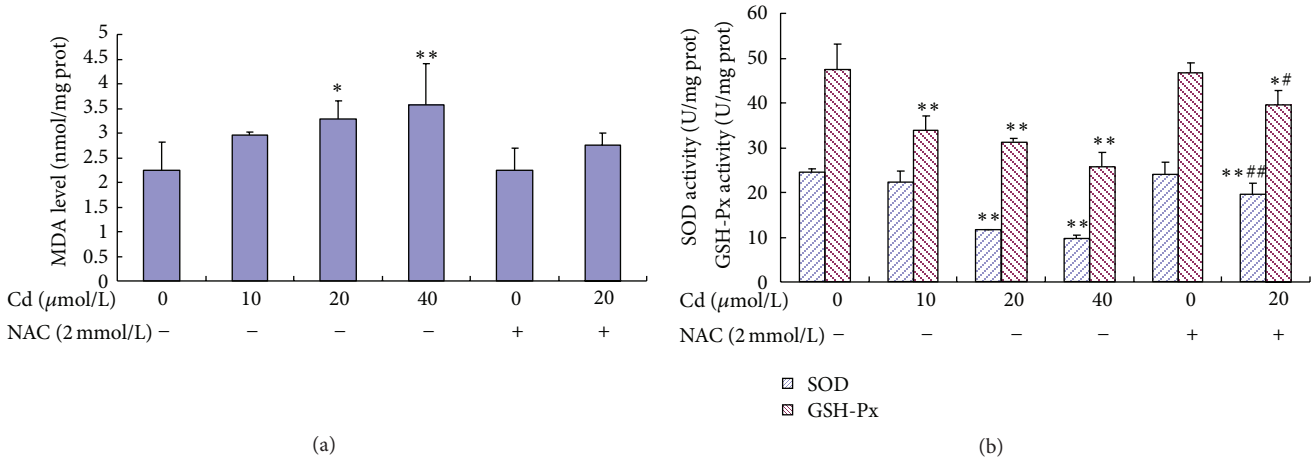

Figure 5: Effect of Cd and NAC on MDA level (A), SOD activity, and GSH-Px activity (B) in BRL 3A cells. Cells were treated with 0 μmol/L to 40 μmol/L Cd and pre-treated with or without 2 mmol/L NAC for 12 h. Data are presented as mean ± SD of three independent experiments performed in triplicate. Significant difference: $^{*}P < 0.05$, $^{**}P < 0.01$, compared with the control. $^{\#}P < 0.05$, $^{\#\#}P < 0.01$, compared with the 20 μmol/L Cd group.

results of the present study are in accordance with previous reports, suggesting that oxidative stress has a major function in BRL 3A cells exposed to Cd. The toxic influence of Cd is most likely due to the formation of excess free radicals that cause oxidative stress, resulting in cell damage. Similarly, Cd can inhibit SOD and GSH-Px in human embryonic kidney cells, suggesting enhanced ROS levels [36]. Cd treatment significantly increased MDA level and decreased GSH-Px and SOD activities in granulosa cells from chicken ovarian follicles [28]. Cd exposure increases MDA content and reduces GSH-Px and SOD activities in the frontal cortex and hippocampus [37]. Moreover, exposure of yeast cells to Cd increases MDA level. By contrast, SOD and GSH-Px activities were also high in Cd-exposed cells [7]. The present study found that NAC cannot block MDA. These discrepancies may be dependent on cell type, stimulus, Cd concentration, and Cd exposure duration.

MAPKs are important signal enzymes in controlling cell survival, proliferation, and differentiation. They are also involved in many facets of cellular regulation. ERK, which is currently believed to be activated by growth factors, is necessary for cell proliferation, differentiation, and development. By contrast, JNK and p38 are involved in apoptosis by promoting cell death rate [15, 16]. Previous studies demonstrated that the activation of MAPK pathways is responsible for Cd-induced apoptosis in various cells. Cd was reported to activate MAPKs in human retinal pigment epithelial cells [20] and human lens epithelial cells [35]. Several studies noted that Cd activates the MAPKs in neuronal cells [17, 18]. The present results showed that treating BRL 3A cells with 10 μmol/L to 40 μmol/L Cd for 12 h resulted in the robust phosphorylation of p38 and JNK (1/2). Meanwhile, p38 phosphorylation was inhibited by NAC preincubation compared with the 20 μmol/L Cd group. The present findings indicated that Cd induced the apoptosis of BRL 3A cells at least partially by activating p38 and JNK (1/2) and that p38 phosphorylation can be inhibited by NAC pre-incubation. Thus, p38 and JNK (1/2) both participate in Cd-induced apoptosis. In addition, oxidative stress might lay upstream of p38, indicating a key function in its activation. Cd at 10 and 20 μmol/L decreased the phosphorylation of ERK. Conversely, 40 μmol/L Cd did not significantly alter the phosphorylation of 44 kD ERK but significantly elevated the phosphorylation of 42 kD ERK. ERK phosphorylation was increased by NAC pre-incubation, which is contradicting to previous findings. ERK is involved in the regulation of proliferation and apoptosis in several cells [38]. ERK has also been associated with two apparently opposing processes. The involvement of ERK in cell proliferation has been extensively described, as well as its function in postmitotic cells undergoing differentiation. Depending on the cell type and stimulus, ERK also acts as a negative regulator of cell proliferation and induces apoptosis when its activity is highly increased [38, 39]. Analysis of these apparent discrepancies led to a more precise understanding of the multiple functions and regulations of ERK [40]. The present results showed no significant change between the control and 40 μmol/L Cd groups in the phosphorylation of 44 kD ERK. By contrast, the phosphorylation of 42 kD ERK increased significantly. These results suggest that low Cd concentrations result in an unconventional ERK phosphorylation, which in turn leads to apoptosis signaling. High Cd concentrations can activate ERK phosphorylation. This claim is in accordance with the theory that the final cellular outcome of activated ERK is dependent on the cell type, the stimulus that induces ERK, and the duration of ERK activation [41].

To investigate the relationship between MAPK phosphorylation and apoptosis, BRL 3A cells were pretreated with SB203580, SP600125, and U0126 for 30 min before treatment with 20 μmol/L Cd. Pretreatment with these inhibitors significantly blocked Cd-induced apoptosis, indicating that p38, ERK, and JNK are involved in BRL 3A cells exposed to Cd

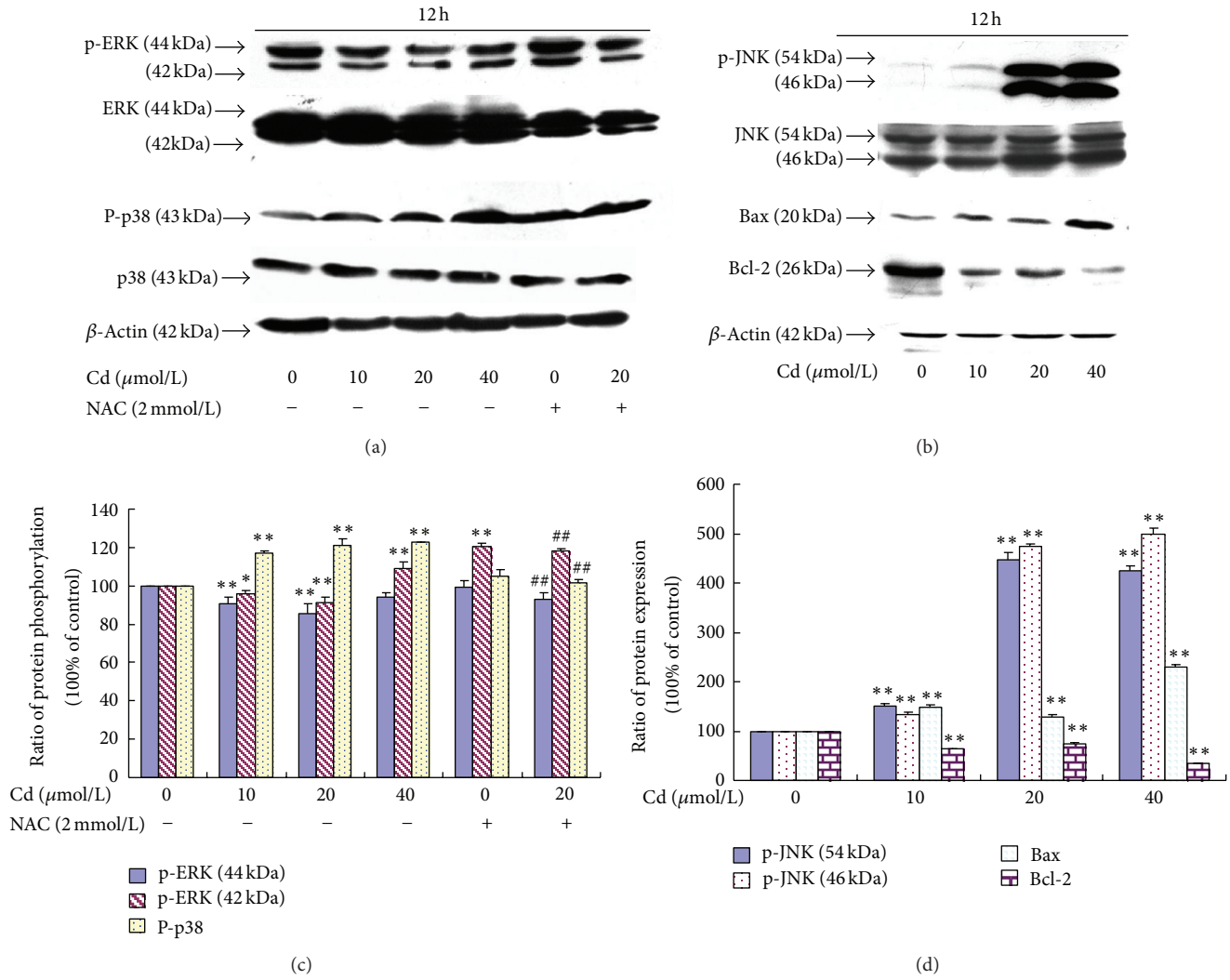

Figure 6: (a) Effect of Cd and NAC on ERK and p38 phosphorylation of BRL 3A cells. (b) Effect of Cd on the JNK phosphorylation and Bax and Bcl-2 protein expression levels of BRL 3A cells. (c) Quantitative analysis of the immunoreactive phosphorylated ERK and p38 proteins in treated BRL 3A cells. (d) Quantitative analysis of the immunoreactive phosphorylated JNK, Bax, and Bcl-2 proteins in Cd-treated BRL 3A cells. Each value is expressed as the phospho/total MAPK percentage of phosphorylation and the ratio of OD in Bax and Bcl-2 with respect to β-actin. Significant difference: $^{*}P < 0.05$, $^{**}P < 0.01$, compared with the control. $^{\#}P < 0.05$, $^{\#\#}P < 0.01$, compared with the 20 μmol/L Cd group.

and that MAPK pathways are the downstream pathways of oxidative stress in apoptosis. Similarly, in human promonocytic cells, the p38-specific inhibitor SB203580 can attenuate apoptosis [24]. In PC12 and SH-SY5Y cells, inhibition of ERK (U0126) and JNK (SP600125), but not p38 (SB203580), partially protects the cells from Cd-induced apoptosis. In CCRF-CEM cells, treatment with the ERK inhibitor U0126 suppresses Cd-induced ERK activation and apoptosis, whereas the inhibition of p38 activity with SB203580 cannot protect cells from apoptosis [30]. By contrast, SB202190 is a p38 inhibitor that decreases the cytotoxicity and apoptosis induced by high Cd concentrations [42]. In summary, some MAPK inhibitors suppress cell death and apoptosis depending on the concentrations of Cd and inhibitors. This finding indicates that JNK, ERK, and p38 independently participate in Cd-induced cell death and apoptosis. These results strongly suggest that MAPKs have different functions in Cd-exposed BRL 3A cells and that MAPK inhibitors can prevent Cd-induced toxicity, even though other signaling pathways are involved in the Cd-induced toxicity. Three major apoptosis pathways are involved in mammalian cells: mitochondria-, death receptor-, and endoplasmic reticulum-mediated apoptosis. Several studies showed cell apoptosis via mitochondria, death receptor, and endoplasmic reticulum pathways during Cd exposure. Coutant et al. [43] suggested that Cd-induced apoptosis can occur in the Boleth cell line through caspase-dependent and -independent pathways. Cd-induced apoptosis was investigated in LLC-PK1 cells via ROS- and mitochondria-linked signal pathways [11]. Endoplasmic reticulum (ER) stress signaling and mitochondrial pathways

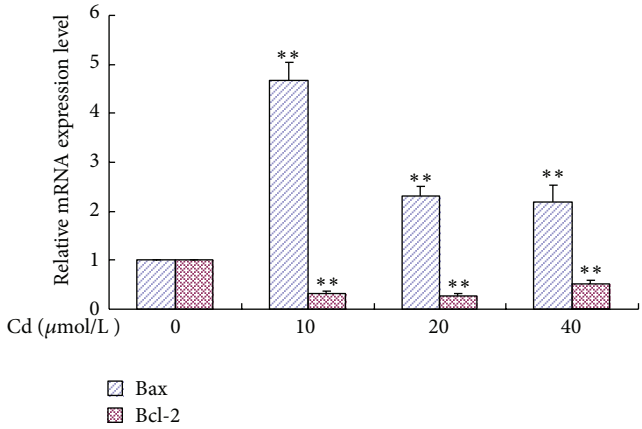

Figure 7: Relative quantification of Bax and Bcl-2 gene expression levels by real-time PCR in relation to β-actin. Cells were treated with 0 μmol/L to 40 μmol/L for 12 h. Data are presented as mean ± SD of three independent experiments performed in triplicate. Significant difference: $^{*}P < 0.05$, $^{**}P < 0.01$, compared with the control; $^{\#}P < 0.05$, $^{\#\#}P < 0.01$, compared with the 20 μmol/L Cd group.

mediate Cd-induced testicular germ cell apoptosis [44]. Cd can induce apoptosis via the mitochondrial pathway in human embryonic kidney cells [36]. Apoptosis is usually controlled by the coeffects of different signal pathways rather than any single pathway. Thus, *in vitro* studies on the mitochondrial, death receptor, and ER pathways in Cd-exposed BRL 3A cells should be prioritized in the future.

The Bcl-2 family members were found to play important roles in regulating mitochondrial-mediated apoptosis. The Bcl-2 family is divided into two groups based on function. Members of the first group, such as Bcl-2 and Bcl-xL, have anti-apoptotic activity and protect cells from death. By contrast, Bax, Bad, and Bid, as members of the second group, show pro-apoptotic activity [45]. In addition, Bcl-2 was observed to promote cell survival by preserving the integrity of the external mitochondrial membrane, which prevents the release of cyt C from the mitochondria, inducing cell death [26]. Bax is a 21 kDa protein that promotes mitochondrial membrane permeability, leading to apoptotic cell death [46]. The present study showed an increase in Bax and a decrease in Bcl-2 in protein expression and mRNA level. Similarly, Zhou et al. [11] revealed that Bcl-2 protein expression can decrease significantly and Bax protein expression can increase as early as 12 h after exposure to Cd in LLC-PK1 cells. Cd induces apoptosis by provoking higher Bax expression and inhibiting Bcl-2 expression in granulosa cells from chicken ovarian follicles [28]. These results suggest that the up- or downregulation of Bax and Bcl-2 by Cd accounts for its pro- or anti-apoptotic effect on BRL 3A cells *in vitro*.

5. Conclusion

Cd can enhance oxidative stress and induce MAPK pathway activation. Inhibition of p38, JNK, and ERK protected the cells from Cd-induced apoptosis. The apoptosis of BRL 3A cells was also associated with the Bcl-2 family. This study partly elucidates the hepatotoxic mechanism of *in vitro* exposure to Cd and offers opportunities for the development of therapeutic agents for Cd-induced hepatic diseases.

Conflict of Interests

The authors declare that there is no conflict of interests.

Acknowledgments

This work was supported by grants of the National Natural Science Foundation of China (nos. 31101866, 31172373) and a Project Funded by the Priority Academic Program Development of Jiangsu Higher Education Institutions (PAPD).

References

[1] M. Méndez-Armenta and C. Ríos, "Cadmium neurotoxicity," *Environmental Toxicology and Pharmacology*, vol. 23, no. 3, pp. 350–358, 2007.

[2] G. Bertin and D. Averbeck, "Cadmium: cellular effects, modifications of biomolecules, modulation of DNA repair and genotoxic consequences (a review)," *Biochimie*, vol. 88, no. 11, pp. 1549–1559, 2006.

[3] J. Thompson, T. Doi, E. Power, I. Balasubramanian, P. Puri, and J. Bannigan, "Evidence against a direct role for oxidative stress in cadmium-induced axial malformation in the chick embryo," *Toxicology and Applied Pharmacology*, vol. 243, no. 3, pp. 390–398, 2010.

[4] K. Bharavi, A. G. Reddy, G. S. Rao, A. R. Reddy, and S. V. R. Rao, "Reversal of cadmium-induced oxidative stress in chicken by herbal adaptogens *Withania somnifera* and *Ocimum sanctum*," *Toxicology International*, vol. 17, no. 2, pp. 59–63, 2010.

[5] M. M. Brzóska, J. Rogalska, and E. Kupraszewicz, "The involvement of oxidative stress in the mechanisms of damaging cadmium action in bone tissue: a study in a rat model of moderate and relatively high human exposure," *Toxicology and Applied Pharmacology*, vol. 250, no. 3, pp. 327–335, 2011.

[6] A. Pretto, V. L. Loro, B. Baldisserotto et al., "Effects of water cadmium concentrations on bioaccumulation and various oxidative stress parameters in Rhamdia quelen," *Archives of Environmental Contamination and Toxicology*, vol. 60, no. 2, pp. 309–318, 2011.

[7] K. Muthukumar and V. Nachiappan, "Cadmium-induced oxidative stress in Saccharomyces cerevisiae," *Indian Journal of Biochemistry and Biophysics*, vol. 47, no. 6, pp. 383–387, 2010.

[8] G. Swapna, A. G. Reddy, and A. R. Reddy, "Cadmium-induced oxidative stress and evaluation of *Embilica officinalis* and stressroak in broilers," *Toxicology International*, vol. 17, no. 2, pp. 49–51, 2010.

[9] A. Cuypers, M. Plusquin, T. Remans et al., "Cadmium stress: an oxidative challenge," *BioMetals*, vol. 23, no. 5, pp. 927–940, 2010.

[10] Y. J. Lee, G. J. Lee, B. J. Baek et al., "Cadmium-induced upregulation of aldo-keto reductase 1C3 expression in human nasal septum carcinoma RPMI-2650 cells: involvement of reactive oxygen species and phosphatidylinositol 3-kinase/Akt," *Environmental Toxicology and Pharmacology*, vol. 31, no. 3, pp. 469–478, 2011.

[11] Y. J. Zhou, S. P. Zhang, C. W. Liu, and Y. Q. Cai, "The protection of selenium on ROS mediated-apoptosis by mitochondria dysfunction in cadmium-induced LLC-PK_1 cells," *Toxicology in Vitro*, vol. 23, no. 2, pp. 288–294, 2009.

[12] L. A. Tibbles and J. R. Woodgett, "The stress-activated protein kinase pathways," *Cellular and Molecular Life Sciences*, vol. 55, no. 10, pp. 1230–1254, 1999.

[13] S. T. Zheng, Q. Huo, A. Tuerxun et al., "The expression and activation of ERK/MAPK pathway in human esophageal cancer cell line EC9706," *Molecular Biology Reports*, vol. 38, no. 2, pp. 865–872, 2011.

[14] H. Zheng, S. Xue, F. Lian, and Y. Y. Wang, "A novel promising therapy for vein graft restenosis: overexpressed Nogo-B induces vascular smooth muscle cell apoptosis by activation of the JNK/p38 MAPK signaling pathway," *Medical Hypotheses*, vol. 77, no. 2, pp. 278–281, 2011.

[15] P. Rockwell, J. Martinez, L. Papa, and E. Gomes, "Redox regulates COX-2 upregulation and cell death in the neuronal response to cadmium," *Cellular Signalling*, vol. 16, no. 3, pp. 343–353, 2004.

[16] T. Wada and J. M. Penninger, "Mitogen-activated protein kinases in apoptosis regulation," *Oncogene*, vol. 23, no. 16, pp. 2838–2849, 2004.

[17] L. Chen, L. Liu, and S. Huang, "Cadmium activates the mitogen-activated protein kinase (MAPK) pathway via induction of reactive oxygen species and inhibition of protein phosphatases 2A and 5," *Free Radical Biology and Medicine*, vol. 45, no. 7, pp. 1035–1044, 2008.

[18] S. D. Kim, C. K. Moon, S. Y. Eun, P. D. Ryu, and S. A. Jo, "Identification of ASK1, MKK4, JNK, c-Jun, and caspase-3 as a signaling cascade involved in cadmium-induced neuronal cell apoptosis," *Biochemical and Biophysical Research Communications*, vol. 328, no. 1, pp. 326–334, 2005.

[19] A. P. Rigon, F. M. Cordova, C. S. Oliveira et al., "Neurotoxicity of cadmium on immature hippocampus and a neuroprotective role for $p38^{MAPK}$," *NeuroToxicology*, vol. 29, no. 4, pp. 727–734, 2008.

[20] N. M. Kalariya, N. K. Wills, K. V. Ramana, S. K. Srivastava, and F. J. G. M. van Kuijk, "Cadmium-induced apoptotic death of human retinal pigment epithelial cells is mediated by MAPK pathway," *Experimental Eye Research*, vol. 89, no. 4, pp. 494–502, 2009.

[21] S. M. Kim, J. G. Park, W. K. Baek et al., "Cadmium specifically induces MKP-1 expression via the glutathione depletion-mediated p38 MAPK activation in C6 glioma cells," *Neuroscience Letters*, vol. 440, no. 3, pp. 289–293, 2008.

[22] X. F. Yang, W. Zhu, Q. Wei, and Z. N. Lin, "Effect on apoptosis of anterior pituitary induced by cadmium chloride and its relations with p38 MAPK & ERK1/2 passway," *Wei Sheng Yan Jiu*, vol. 34, no. 6, pp. 681–684, 2005.

[23] H. Haase, J. L. Ober-Blöbaum, G. Engelhardt, S. Hebel, and L. Rink, "Cadmium ions induce monocytic production of tumor necrosis factor-alpha by inhibiting mitogen activated protein kinase dephosphorylation," *Toxicology Letters*, vol. 198, no. 2, pp. 152–158, 2010.

[24] A. Galán, M. L. García-Bermejo, A. Troyano et al., "Stimulation of p38 mitogen-activated protein kinase is an early regulatory event for the cadmium-induced apoptosis in human promonocytic cells," *The Journal of Biological Chemistry*, vol. 275, no. 15, pp. 11418–11424, 2000.

[25] Y. T. Hsu, K. G. Wolter, and R. J. Youle, "Cytosol-to-membrane redistribution of Bax and Bcl-X_L during apoptosis," *Proceedings of the National Academy of Sciences of the United States of America*, vol. 94, no. 8, pp. 3668–3672, 1997.

[26] S. Desagher and J. C. Martinou, "Mitochondria as the central control point of apoptosis," *Trends in Cell Biology*, vol. 10, no. 9, pp. 369–377, 2000.

[27] A. J. Bruce-Keller, J. G. Begley, W. Fu et al., "Bcl-2 protects isolated plasma and mitochondrial membranes against lipid peroxidation induced by hydrogen peroxide and amyloid β-peptide," *Journal of Neurochemistry*, vol. 70, no. 1, pp. 31–39, 1998.

[28] Y. Jia, J. Lin, Y. Mi, and C. Zhang, "Quercetin attenuates cadmium-induced oxidative damage and apoptosis in granulosa cells from chicken ovarian follicles," *Reproductive Toxicology*, vol. 31, no. 4, pp. 477–485, 2011.

[29] Y. Mi and C. Zhang, "Toxic and hormonal effects of polychlorinated biphenyls on cultured testicular germ cells of embryonic chickens," *Toxicology Letters*, vol. 155, no. 2, pp. 297–305, 2005.

[30] Y. Iryo, M. Matsuoka, B. Wispriyono, T. Sugiura, and H. Igisu, "Involvement of the extracellular signal-regulated protein kinase (ERK) pathway in the induction of apoptosis by cadmium chloride in CCRF-CEM cells," *Biochemical Pharmacology*, vol. 60, no. 12, pp. 1875–1882, 2000.

[31] H. H. Aydin, H. A. Celik, R. Deveci et al., "Characterization of the cellular response during apoptosis induction in cadmium-treated Hep G2 human hepatoma cells," *Biological Trace Element Research*, vol. 95, no. 2, pp. 139–153, 2003.

[32] K. G. Coonse, A. J. Coonts, E. V. Morrison, and S. J. Heggland, "Cadmium induces apoptosis in the human osteoblast-like cell line Saos-2," *Journal of Toxicology and Environmental Health A*, vol. 70, no. 7, pp. 575–581, 2007.

[33] M. Biagioli, W. Wätjen, D. Beyersmann et al., "Cadmium-induced apoptosis in murine fibroblasts is suppressed by Bcl-2," *Archives of Toxicology*, vol. 75, no. 6, pp. 313–320, 2001.

[34] F. Thévenod, "Cadmium and cellular signaling cascades: to be or not to be?" *Toxicology and Applied Pharmacology*, vol. 238, no. 3, pp. 221–239, 2009.

[35] N. M. Kalariya, B. Nair, D. K. Kalariya, N. K. Wills, and F. J. G. M. van Kuijk, "Cadmium-induced induction of cell death in human lens epithelial cells: implications to smoking associated cataractogenesis," *Toxicology Letters*, vol. 198, no. 1, pp. 56–62, 2010.

[36] W. P. Mao, N. N. Zhang, F. Y. Zhou et al., "Cadmium directly induced mitochondrial dysfunction of human embryonic kidney cells," *Human and Experimental Toxicology*, vol. 30, no. 8, pp. 920–929, 2011.

[37] S. Amara, T. Douki, C. Garrel et al., "Effects of static magnetic field and cadmium on oxidative stress and DNA damage in rat cortex brain and hippocampus," *Toxicology and Industrial Health*, vol. 27, no. 2, pp. 99–106, 2011.

[38] K. Nakata, Y. Suzuki, T. Inoue, C. Ra, H. Yakura, and K. Mizuno, "Deficiency of SHP1 leads to sustained and increased ERK activation in mast cells, thereby inhibiting IL-3-dependent proliferation and cell death," *Molecular Immunology*, vol. 48, no. 4, pp. 472–480, 2011.

[39] S. Subramaniam and K. Unsicker, "ERK and cell death: ERK1/2 in neuronal death," *FEBS Journal*, vol. 277, no. 1, pp. 22–29, 2010.

[40] P. Martin and P. Pognonec, "ERK and cell death: cadmium toxicity, sustained ERK activation and cell death," *FEBS Journal*, vol. 277, no. 1, pp. 39–46, 2010.

[41] S. Subramaniam and K. Unsicker, "Extracellular signal-regulated kinase as an inducer of non-apoptotic neuronal death," *Neuroscience*, vol. 138, no. 4, pp. 1055–1065, 2006.

[42] S. M. Chuang, I. C. Wang, and J. L. Yang, "Roles of JNK, p38 and ERK mitogen-activated protein kinases in the growth inhibition and apoptosis induced by cadmium," *Carcinogenesis*, vol. 21, no. 7, pp. 1423–1432, 2000.

[43] A. Coutant, J. Lebeau, N. Bidon-Wagner, C. Levalois, B. Lectard, and S. Chevillard, "Cadmium-induced apoptosis in lymphoblastoid cell line: involvement of caspase-dependent and -independent pathways," *Biochimie*, vol. 88, no. 11, pp. 1815–1822, 2006.

[44] Y. L. Ji, H. Wang, X. F. Zhao et al., "Crosstalk between endoplasmic reticulum stress and mitochondrial pathway mediates cadmium-induced germ cell apoptosis in testes," *Toxicological Sciences*, vol. 124, no. 2, pp. 446–459, 2011.

[45] J. M. Adams and S. Cory, "The Bcl-2 protein family: arbiters of cell survival," *Science*, vol. 281, no. 5381, pp. 1322–1326, 1998.

[46] K. G. Wolter, Y. T. Hsu, C. L. Smith, A. Nechushtan, X. G. Xi, and R. J. Youle, "Movement of Bax from the cytosol to mitochondria during apoptosis," *Journal of Cell Biology*, vol. 139, no. 5, pp. 1281–1292, 1997.

Hindawi Publishing Corporation
Oxidative Medicine and Cellular Longevity
Volume 2013, Article ID 513742, 9 pages
http://dx.doi.org/10.1155/2013/513742

Clinical Study

The Effect of High-Dose Insulin Analog Initiation Therapy on Lipid Peroxidation Products and Oxidative Stress Markers in Type 2 Diabetic Patients

Hazal Tuzcu,[1] Ibrahim Aslan,[2] and Mutay Aslan[1]

[1] *Department of Medical Biochemistry, Akdeniz University Medical School, 07070 Antalya, Turkey*
[2] *Endocrinology Clinic, Antalya Research and Education Hospital, 07100 Antalya, Turkey*

Correspondence should be addressed to Mutay Aslan; mutayaslan@akdeniz.edu.tr

Received 29 December 2012; Revised 16 February 2013; Accepted 18 February 2013

Academic Editor: Kota V. Ramana

Effect of high-dose insulin analog initiation therapy was evaluated on lipid peroxidation and oxidative stress markers in type 2 diabetes mellitus (T2DM). Twenty-four T2DM patients with HbA1c levels above 10% despite ongoing therapy with sulphonylurea and metformin were selected. Former treatment regimen was continued for the first day followed by substitution of sulphonylurea therapy with different insulin analogs. Glycemic profiles were determined over 72 hours by Continuous Glucose Monitoring System (CGMS), and blood/urine samples were collected at 24 and 72 hours. Insulin analog plus metformin treatment significantly reduced glucose variability. Plasma and urine lipid peroxidation were markedly decreased following insulin analog plus metformin treatment. No correlation existed between glucose variability and levels of plasma and urine oxidative stress markers. Likewise, changes in mean blood glucose from baseline to end point showed no significant correlation with changes in markers of oxidative stress. On the contrary, decreased levels of oxidative stress markers following treatment with insulin analogs were significantly correlated with mean blood glucose levels. In conclusion, insulin plus metformin resulted in a significant reduction in oxidative stress markers compared with oral hypoglycemic agents alone. Data from this study suggests that insulin analogs irrespective of changes in blood glucose exert inhibitory effects on free radical formation.

1. Introduction

Intensive treatment of diabetes leads to a reduction in plasma levels of glycosylated hemoglobin (HbA1c), which is associated with a significant decrease in the development and progression of vascular and neurologic complications [1, 2]. At present, measurement of HbA1c level is considered the gold standard for assessing long-term glycemic control and is regarded as a key therapeutic target for the prevention of diabetes-related complications [3]. Although HbA1c level is a measure of metabolic control and the effectiveness of therapeutic interventions directed to control hyperglycemia, it does not reveal any information on the extent and frequency of blood glucose excursions [3]. In this regard, it is important to note that recent studies show that glycemic instability may present additional risk to the development of complications over that predicted by the mean glucose value alone [4]. This being the case, HbA1c level may not always be the most clinically useful glycemic indicator of the risk for complications. Patients with similar mean glucose or HbA1c values can have different glycemic profiles, with differences both in the number and duration of glucose excursions [5]. It is therefore unknown whether two individuals with the same mean blood glucose (MBG) but extremes of glucose variability might have the same or different level of risk for complications.

Postprandial hyperglycemia may be a risk factor for cardiovascular disease in individuals with diabetes [6]. Endothelial dysfunction is one of the first stages, and one of the earliest markers, in the development of cardiovascular disease [7]. The possible deleterious roles of either postprandial hyperglycemia or glycemic variability were assessed via different markers of oxidative stress, and it was demonstrated that postprandial hyperglycemia independently induced

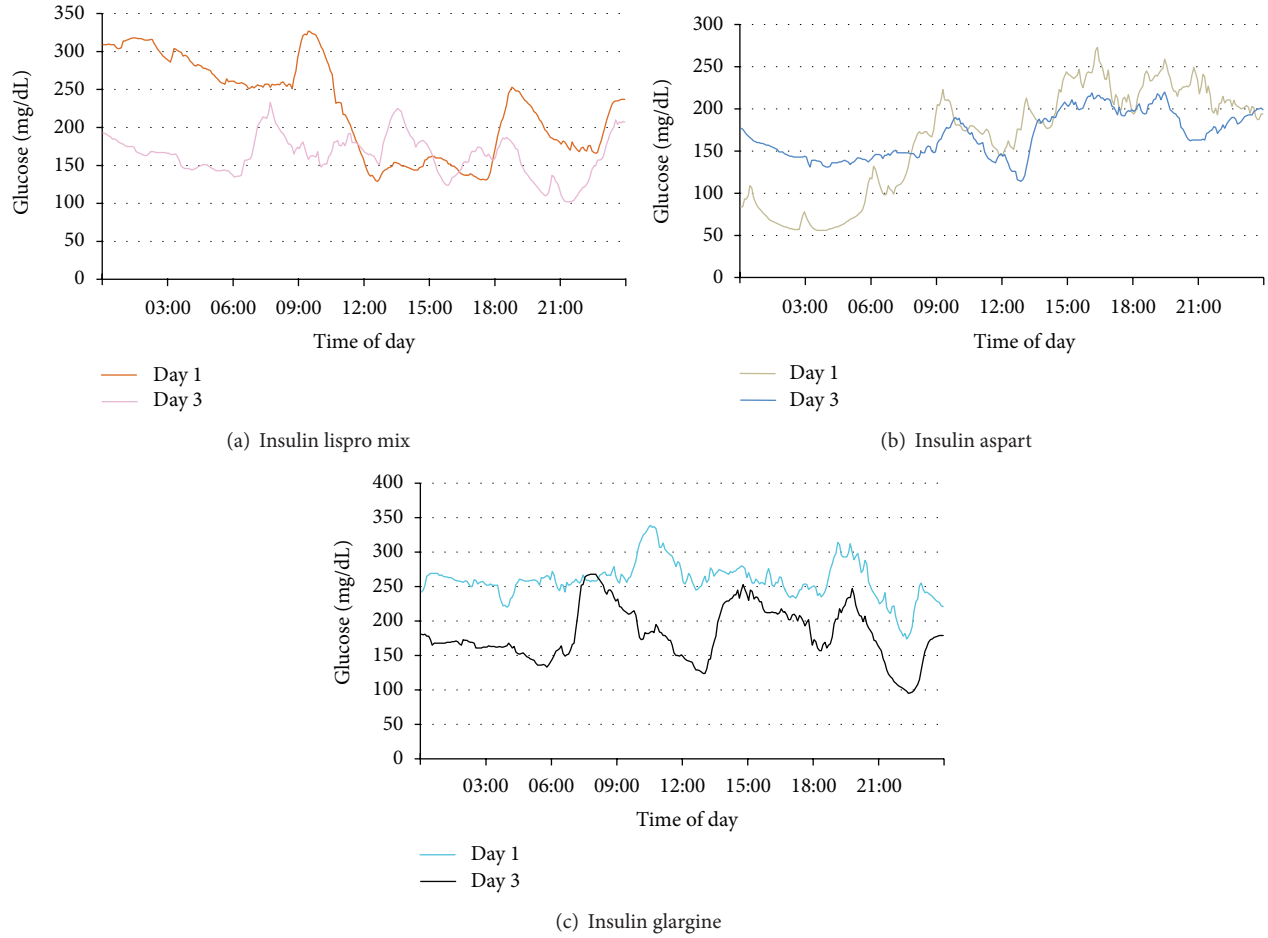

Figure 1: Representative micrographs of CGMS data from each experimental group. (a) Biphasic insulin lispro group, (b) biphasic insulin aspart group, and (c) insulin glargine group.

endothelial dysfunction, through oxidative stress [8]. The fact that postprandial hyperglycemia induces oxidative stress is of particular significance. Recent studies demonstrated that hyperglycemia-induced overproduction of superoxide by the mitochondrial electron-transport chain and hyperglycemia-driven reactive oxygen species production enhanced four mechanisms of tissue damage via the polyol pathway, the hexosamine pathway, protein kinase C (PKC) activation, and formation of advanced glycation end-products (AGEs) [9].

With the apparent evidence that glycemic variability may be related to the pathogenesis of complications in diabetes [4] and in view of the need to reduce glycemic variability in order to achieve desired levels of control [10], it is important to have simple, clinically meaningful estimates of glycemic variability. MiniMed was the first commercial glucose sensor with FDA approval of the Continuous Glucose Monitoring System (CGMS) and includes a 3-day sensor and the necessary hardware to record the sensor current data and blood glucose measurements used for sensor calibration. Daily glycemic profiles can be recorded for 72 hours by CGMS, and intraday glycemic variability can be determined by the standard deviation (SD) around the mean glucose values. The recorded information is processed and analyzed retrospectively, which provides insights to improve insulin therapy [11].

This study applied continuous glucose monitoring technology to investigate the effect of high-dose insulin analog initiation therapy on glycemic variability and on formation of oxidative stress as determined from plasma and urine 8-iso prostaglandin F2α (8-iso PGF2α), plasma protein carbonyl, and nitrotyrosine levels. Plasma nitrite and nitrate levels were also determined to assess nitric oxide production.

2. Patients and Methods

2.1. Determination of Patient Groups. The study group included 24 patients who were admitted to Antalya Research and Education Hospital, Endocrinology Clinic, with a diagnosis of type 2 diabetes mellitus (DM). HbA1c levels in all patients were above 10% despite ongoing therapy with sulphonylurea and metformin. Patients enrolled in the study were divided into three groups according to the given insulin treatment. Former treatment regimen was continued for the first day followed by substitution of sulphonylurea therapy with different insulin analogs. Group 1 ($N = 8$) received 0.4 U/kg/day lispro mix (50% insulin lispro protamine and

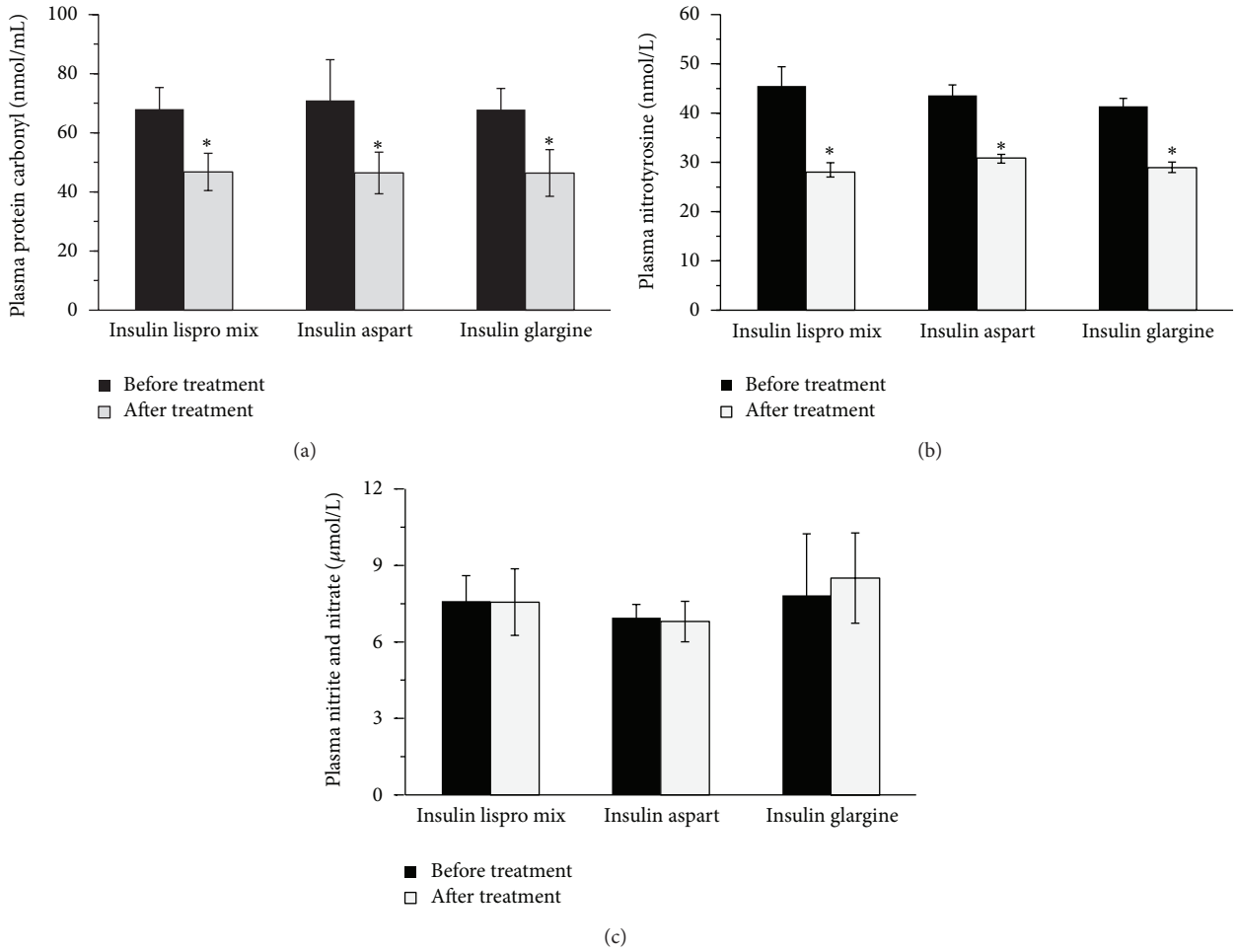

Figure 2: (a) Plasma protein carbonyl levels in experimental groups. $^{*}P < 0.001$ compared to pretreatment. (b) Plasma nitrotyrosine levels in experimental groups. $^{*}P < 0.001$ compared to pretreatment. (c) Plasma nitrite/nitrate levels in experimental groups.

50% insulin lispro) subcutaneously (SC) in three equal doses plus 2000 mg/day oral metformin; Group 2 ($N = 8$) received 0.4 U/kg/day insulin aspart (30% insulin aspart and 70% protamine insulin aspart) SC in two equal doses plus 2000 mg/day oral metformin; Group 3 ($N = 8$) received 0.4 U/kg/day insulin glargine SC in one dose plus 2000 mg/day oral metformin. The given insulin treatments were in accordance with American Association of Clinical Endocrinologists (AACE) Diabetes Mellitus guidelines [12]. All patients gave written informed consent prior to entry. This study was approved by the Institutional Review Board of Akdeniz University School of Medicine and was performed in accordance with the Declaration of Helsinki.

2.2. Continuous Glucose Monitoring. All patients were equipped with CGMS (Medtronic MiniMed, USA) and were monitored for 72 consecutive hours after admission. A CGMS sensor was inserted into the subcutaneous abdominal fat tissue and calibrated according to the standard Medtronic MiniMed operating guidelines. During CGMS monitoring, blood glucose levels were checked via a glucometer (Accu-Check Go, Roche Co.) 4 times per day and the data was entered into the CGMS. After monitoring for 72 hours, the recorded data were downloaded into a personal computer for the analysis of the glucose profile. After downloading the recorded data, MBG levels and the SD around the mean glucose values, assessing glycemic variability, were analyzed from the data.

2.3. Laboratory Measurements. Blood and urine samples were obtained from all patients at 24 and 72 hours. HbA1c levels were determined by Abbott ARCHITECT c16000 System (Abbott Diagnostic, Abbott Park, IL, USA) via immunoturbidimetric method.

2.4. Measurement of Plasma Protein Carbonyl Levels. Plasma protein-bound carbonyls were measured via a protein carbonyl assay kit (Cat. no.1005020 Cayman Chemical, Ann Arbor, MI, USA). The utilized method was based on the covalent reaction of the carbonylated protein side chain with 2,4 dinitrophenylhydrazine (DNPH) and detection of the produced protein hydrazone at an absorbance of 370 nm. The results were calculated using the extinction coefficient of

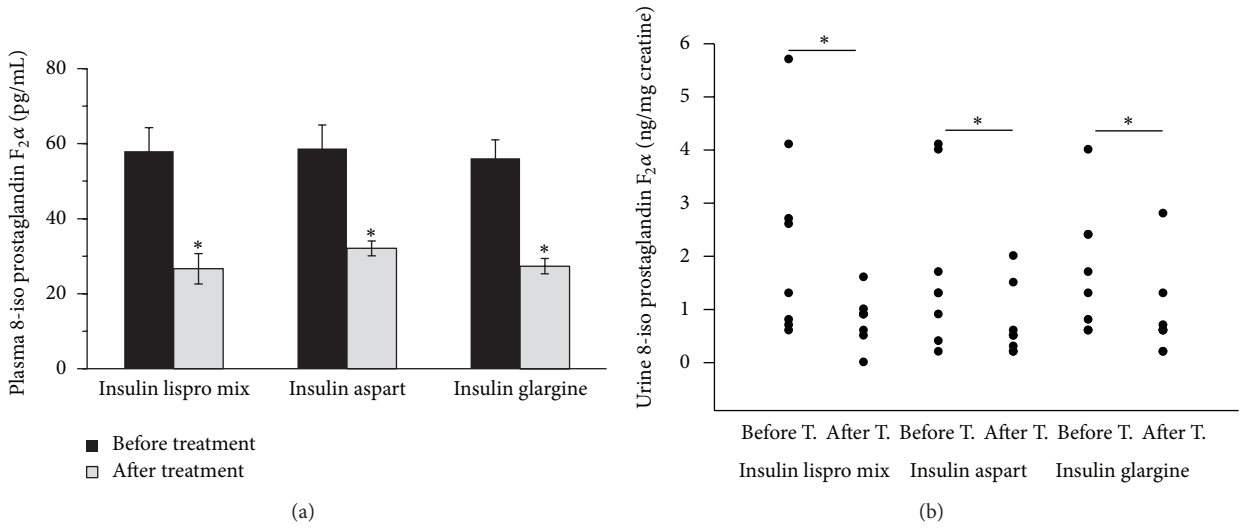

FIGURE 3: (a) Plasma-free 8-iso prostaglandin F2α levels in experimental groups. $^{*}P < 0.001$ compared to pretreatment. (b) Urine 8-iso prostaglandin F2α levels in experimental groups.$^{*}P < 0.01$ compared to pretreatment.

22 mM^{-1} cm^{-1} for aliphatic hydrazones and were expressed as nmol/mL. As written in the instruction manual of the assay kit, typically human plasma has a protein carbonyl content of 35–280 nmol/mL. The intra- and interassay coefficients of variation (CV) for protein carbonyl measurements are 4.7% and 8.5%, respectively.

2.5. Measurement of Plasma Nitrotyrosine Levels. Plasma nitrotyrosine content was measured via ELISA using a commercial kit (Cat. no.STA-305, Cell Biolabs, Inc. San Diego, CA, USA). Antigen captured by a solid phase monoclonal antibody (nitrated keyhole limpet hemocyanin raised in mouse) was detected with a biotin-labeled goat polyclonal antinitrotyrosine. A streptavidin peroxidase conjugate was then added to bind the biotinylated antibody. A TMB substrate was added and the yellow product was measured at 450 nm. A standard curve of absorbance values of known nitrotyrosine standards was plotted as a function of the logarithm of nitrotyrosine standard concentrations using the GraphPad Prism Software program for windows version 5,03. (GraphPad Software Inc). Nitrotyrosine concentrations in the samples were calculated from their corresponding absorbance values via the standard curve. The reported range of plasma nitrotyrosine levels in healthy human population determined via this assay kit is 20–148 nmol/L [13].

2.6. Measurement of Plasma Nitrite/Nitrate Levels. Plasma samples were transferred to an ultrafiltration unit and centrifuged through a 10-kDa molecular mass cut-off filter (Amicon, Millipore Corporation, Bedford, MA, USA) for 1 hr to remove proteins. Analyses were performed in duplicate via the Griess reaction using a colorimetric assay kit (Cayman Chemical, Cat. no.780001, Ann Arbor, MI, USA). The reported ranges of plasma nitrite/nitrate levels in healthy human population determined via this assay kit are 2–20 μM [13]. The intra- and interassay coefficients of variation (CV) for nitrite/nitrate measurements are 2.7% and 3.4%, respectively.

2.7. Measurement of Plasma-Free 8-iso Prostaglandin F2α. Plasma-free 8-iso PGF2α levels were determined by enzyme immunoassay (EIA) using 8-iso PGF2α EIA kit (Cayman Chemical, Cat. no.516351, Ann Arbor, MI, USA). Purification and extraction of plasma samples were performed before assay. Purification was done by 8-iso PGF2α affinity purification kit (Cayman Chemical, Cat. no.10368, Ann Arbor, MI, USA). The elution solution was evaporated to dryness by vacuum centrifugation via Savant DNA 120 speed vac concentrator (Thermo Scientific, IL, USA) and reconstituted with EIA buffer. As written in the instruction manual of the assay kit, plasma from human volunteers contains 40–100 pg/mL of 8-iso PGF2α. The interassay CV is 16.4% and 15.5% and intra-assay CV is 11.7% and 7.2% for 8-iso PGF2α measurements of 200 pg/mL and 12.8 pg/mL, respectively.

2.8. Measurement of Urine 8-iso Prostaglandin F2α. Urine-free 8-iso PGF2α levels were determined by enzyme immunoassay (EIA) using 8-iso PGF2α EIA kit (Cayman Chemical, Cat. no.516351, Ann Arbor, MI, USA). Isoprostane concentrations are expressed as nanograms per milligram of urine creatinine. As written in the instruction manual of the assay kit, normal human urinary levels of 8-iso PGF2α range from 10 to 50 ng/mmol creatinine. Urine creatinine levels were determined by colorimetric reaction (Jaffe reaction) of creatinine with alkaline picrate measured kinetically at 490 nm via commercial assay kit (Biolabo Reagents, Maizy, France).

2.9. Statistical Analysis. Statistical analysis was performed by using SigmaStat statistical software version 2.0. Statistical analysis for each measurement is given in the result section.

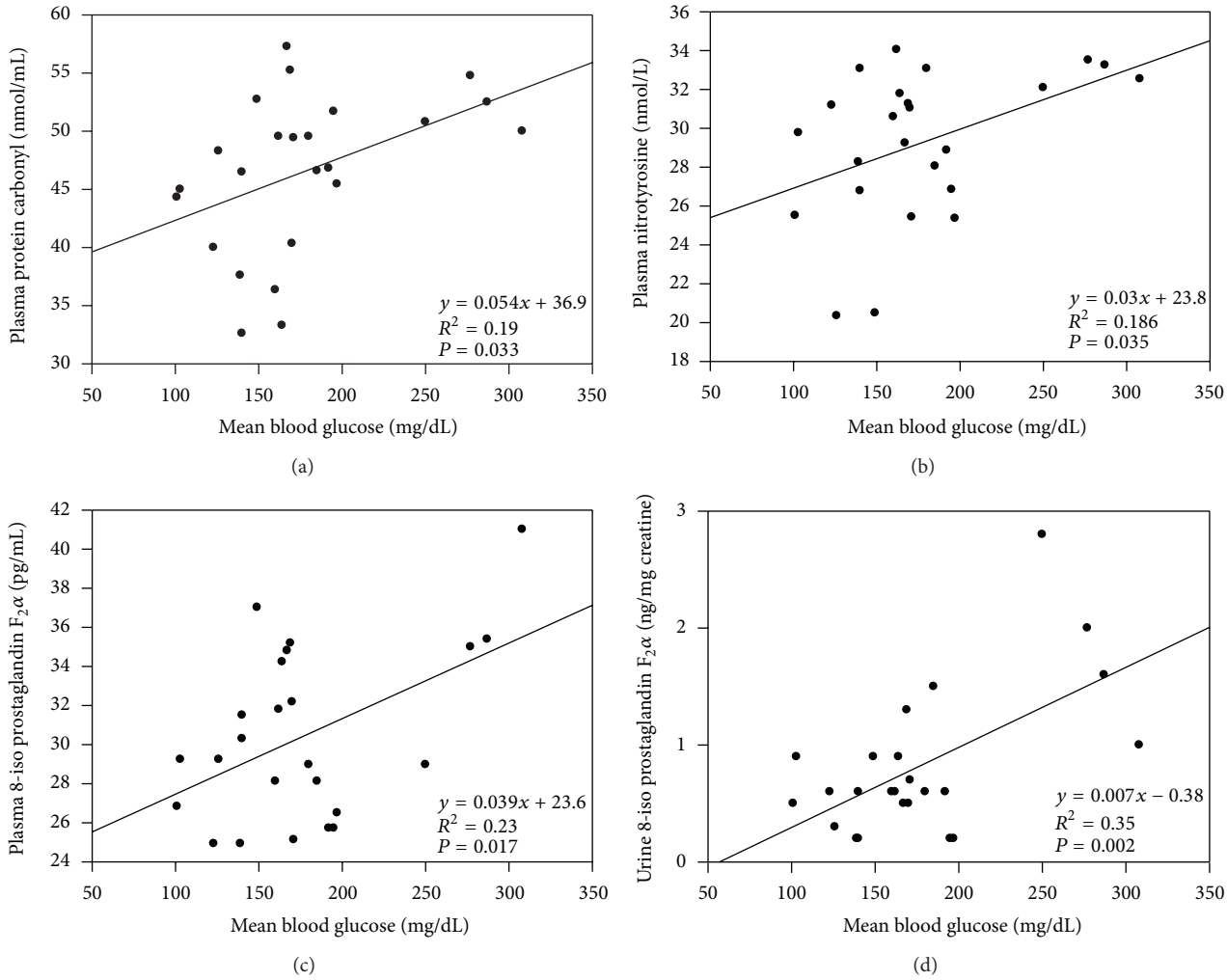

Figure 4: Scatter plots and correlation coefficients between mean blood glucose and oxidative stress markers following high-dose insulin analog therapy. (a) The correlation between mean blood glucose and plasma protein carbonyl levels, (b) the correlation between blood glucose and plasma nitrotyrosine levels, (c) the correlation between mean blood glucose and plasma-free 8-iso prostaglandin F2α levels, and (d) the correlation between mean blood glucose and urine 8-iso prostaglandin F2α levels.

3. Results

3.1. Patient Characteristics of Experimental Groups. Patient characteristics of experimental groups are given in Table 1.

3.2. CGMS Data of Experimental Groups. CGMS data of experimental groups are given in Table 2. A representative graph of CGMS results from each group is given in Figure 1. Mean blood glucose and SD around the mean glucose values after treatment with insulin analog plus metformin were significantly lower compared to those before treatment levels in all experimental groups. No significant difference was observed among different insulin analog treatments with respect to MBG and SD around the mean glucose values. Statistical analysis for MBG and SD levels was performed by two-way analysis of variance, and all pairwise multiple comparisons were done via Tukey test.

3.3. Plasma Protein Carbonyl Levels. Plasma protein carbonyl levels in treatment groups are given in Figure 2(a). Levels of plasma protein carbonyl (mean ± SD) were significantly ($P < 0.001$) decreased after treatment with insulin analog plus metformin (biphasic insulin lispro ($N = 8$), 46.78 ± 6.29; biphasic insulin aspart ($N = 8$), 46.42 ± 7.04; insulin glargine ($N = 8$), 46.39 ± 7.89 nmol/mL) compared to those before treatment levels in all experimental groups (biphasic insulin lispro ($N = 8$), 68.01 ± 7.34; biphasic insulin aspart ($N = 8$), 70.94 ± 13.79; insulin glargine ($N = 8$), 67.84 ± 7.20 nmol/mL). No significant difference was observed among different insulin analog treatments with respect to plasma protein carbonyl levels. Statistical

Table 1: Patient characteristics of experimental groups.

Group	Age (years)	Gender (female/male)	HbA1c (%)
Insulin lispro mix ($n = 8$)	54.25 ± 16.10	4/4	11.94 ± 3.08
Insulin aspart ($n = 8$)	46.5 ± 9.7	4/4	11.91 ± 1.99
Insulin glargine ($n = 8$)	52.25 ± 6.48	3/5	11.48 ± 1.85

Data are mean ± SD. SD: standard deviation; HbA1c : hemoglobin A1c.

analysis for plasma protein carbonyl levels was performed by two-way analysis of variance and all pairwise multiple comparisons were done via Tukey test. The correlation of plasma protein carbonyl levels with mean blood glucose values and SD around the mean glucose values following treatment with insulin analogs was evaluated by linear regression analysis. A significant correlation was observed between protein carbonyl levels and mean blood glucose values ($r = 0.435$, $P = 0.033$) (Figure 4(a)). Although levels of plasma protein carbonyl were significantly decreased after treatment with insulin analogs, no significant correlation was observed between glucose variability and plasma protein carbonyl levels ($r = 0.055$, $P = 0.79$). Likewise, changes in mean blood glucose from baseline to end point showed no significant correlation with changes in plasma protein carbonyl levels ($r = 0.032$, $P = 0.882$).

3.4. Plasma Nitrotyrosine Levels. Plasma nitrotyrosine levels are given in Figure 2(b). Plasma nitrotyrosine levels (mean ± SEM) were significantly ($P < 0.001$) decreased after treatment with insulin analog plus metformin (biphasic insulin lispro ($N = 8$), 28.01 ± 1.91; biphasic insulin aspart ($N = 8$), 30.86 ± 0.76; insulin glargine ($N = 8$), 28.93 ± 1.11 nmol/L) compared to those before treatment levels in all experimental groups (biphasic insulin lispro ($N = 8$), 45.11 ± 3.88; biphasic insulin aspart ($N = 8$), 43.61 ± 2.11; insulin glargine ($N = 8$), 41.36 ± 1.63 nmol/L). No significant difference was observed among different insulin analog treatments regarding plasma nitrotyrosine levels. Statistical analysis for plasma nitrotyrosine levels was performed by two-way analysis of variance and all pairwise multiple comparisons were done via Tukey test. The correlation of protein nitrotyrosine levels with mean blood glucose values and SD around the mean glucose values following treatment with insulin analogs was evaluated by linear regression analysis. A significant correlation was observed between nitrotyrosine levels and mean blood glucose values ($r = 0.431$, $P = 0.035$) (Figure 4(b)). Although levels of plasma nitrotyrosine were significantly decreased after treatment with insulin analogs, no significant correlation was observed between glucose variability and plasma nitrotyrosine levels ($r = 0.10$, $P = 0.63$). Likewise, changes in mean blood glucose from baseline to end point showed no significant correlation with changes in plasma nitrotyrosine levels ($r = 0.066$, $P = 0.761$).

3.5. Plasma Nitrite/Nitrate Levels. Plasma nitrite/nitrate levels are given in Figure 2(c). No significant difference was observed in nitrite/nitrate levels (mean ± SEM) after treatment with insulin analog plus metformin (biphasic insulin lispro ($N = 8$), 7.56 ± 1.3; biphasic insulin aspart ($N = 8$), 6.8 ± 0.79; insulin glargine ($N = 8$), 8.5 ± 1.77 μmol/L) compared to those before treatment levels in all experimental groups (biphasic insulin lispro ($N = 8$), 7.6 ± 0.99; biphasic insulin aspart ($N = 8$), 6.95 ± 0.52; insulin glargine ($N = 8$), 7.83 ± 2.4 μmol/L). No significant difference was observed among different insulin analog treatments with regard to plasma nitrate/nitrite levels. Statistical analysis for plasma nitrite/nitrate levels was performed by two-way analysis of variance and all pairwise multiple comparisons were done via Tukey test.

3.6. Plasma-Free 8-iso Prostaglandin F2α. Measured plasma-free 8-iso PGF2α levels are shown in Figure 3(a). Plasma-free 8-iso PGF2α levels (mean ± SEM) were significantly higher ($P < 0.001$) before treatment with insulin analogs plus metformin (biphasic insulin lispro ($N = 8$), 57.98 ± 6.3; biphasic insulin aspart ($N = 8$), 58.73 ± 6.23; insulin glargine ($N = 8$), 56.11 ± 4.89 pg/mL) compared to those after treatment levels (biphasic insulin lispro ($N = 8$), 26.67 ± 4.04; biphasic insulin aspart ($N = 8$), 32.10 ± 1.97; insulin glargine ($N = 8$), 27.36 ± 2.02 pg/mL). No significant difference was observed among different insulin analog treatments with respect to plasma-free 8-iso PGF2α levels. Statistical analysis for plasma-free 8-iso PGF2α was performed by two-way analysis of variance and all pairwise multiple comparisons were done via Tukey test. The correlation of plasma-free 8-iso PGF2α levels with mean blood glucose values and SD around the mean glucose values following treatment with insulin analogs was evaluated by linear regression analysis. A significant correlation was observed between plasma-free 8-iso PGF2α levels and mean blood glucose values ($r = 0.481$, $P = 0.017$) (Figure 4(c)). Although levels of plasma-free 8-iso PGF2α were significantly decreased after treatment with insulin analogs no significant correlation was observed between glucose variability and plasma-free 8-iso PGF2α levels ($r = 0.06$, $P = 0.77$). Likewise, changes in mean blood glucose from baseline to end point showed no significant correlation with changes in plasma-free 8-iso PGF2α levels ($r = 0.045$, $P = 0.834$).

3.7. Urine 8-iso Prostaglandin F2α. Urine 8-iso PGF2α levels are shown in Figure 3(b). Urine 8-iso PGF2α levels (mean ± SD) were significantly higher ($P < 0.01$) before treatment with insulin analogs plus metformin (biphasic insulin lispro ($N = 8$), 2.31 ± 1.84; biphasic insulin aspart ($N = 8$), 1.76 ± 1.51; insulin glargine ($N = 8$), 1.72 ± 1.17 ng/mg creatinine) compared to those after treatment levels (biphasic insulin lispro ($N = 8$), 0.81 ± 0.46; biphasic insulin aspart ($N = 8$), 0.71 ± 0.66; insulin glargine ($N = 8$), 0.87 ± 0.86 ng/mg creatinine). No significant difference was observed among different insulin analog treatments with respect to urine-free 8-iso PGF2α levels. Statistical analysis for urine 8-iso PGF2α levels was performed by two-way analysis of variance

Table 2: CGMS data of experimental groups.

Group	Mean blood glucose (mg/dL) before treatment	SD (mg/dL) before treatment	Mean blood glucose (mg/dl) after treatment	SD (mg/dL) after treatment
Insulin lispro mix ($n = 8$)	227.00 ± 65.91	67.25 ± 28.53	183.25 ± 77.09[a]	39.38 ± 16.99[b]
Insulin aspart ($n = 8$)	187.75 ± 51.17	45.88 ± 17.06	165.88 ± 50.08[a]	32.50 ± 14.35[b]
Insulin glargine ($n = 8$)	231.63 ± 30.87	38.75 ± 10.59	182.75 ± 32.85[a]	32.25 ± 9.50[b]

Data are mean ± SD. SD: standard deviation; [a]$P < 0.05$ compared to mean blood glucose before treatment within the same group; [b]$P < 0.01$ compared to SD before treatment within the same group.

and all pairwise multiple comparisons were done via Tukey test. The correlation of urine-free 8-iso PGF2α levels with mean glucose values and SD around the mean blood glucose values following treatment with insulin analogs was evaluated by linear regression analysis. A significant correlation was observed between urine-free 8-iso PGF2α levels and mean blood glucose values ($r = 0.593$, $P = 0.002$) (Figure 4(d)). Although levels of urine-free 8-iso PGF2α were significantly decreased after treatment with insulin analogs, no significant correlation was observed between glucose variability and urine-free 8-iso PGF2α levels ($r = 0.22$, $P = 0.3$). Likewise, changes in mean blood glucose from baseline to end point showed no significant correlation with changes in urine-free 8-iso PGF2α levels ($r = 0.165$, $P = 0.441$).

4. Discussion

The role of glycemic variability, assessed by using CGMS, in the formation of oxidative stress has been investigated in different studies. Mean amplitude of glycemic excursions and 24 h urinary excretion rates of 8-iso-PGF2α were calculated to determine glucose variability and oxidative stress, respectively. One study was performed in 21 type 2 diabetes patients and reported a strong correlation between glucose variability and oxidative stress [14]. Two other studies performed on 25 type 1 and 24 type 2 diabetic patients could not confirm a strong correlation between glucose variability and oxidative stress [15, 16]. To our knowledge, this is the first study to apply CGMS technology to investigate the effect of high-dose insulin analog initiation therapy on glycemic variability and on oxidative stress as determined from plasma and urine 8-iso PGF2α, plasma protein carbonyl, and nitrotyrosine levels.

Previous studies have reported increased levels of carbonyl groups in plasma proteins of type 2 diabetes mellitus subjects [17], while more recent studies have investigated the role of glycemic control in plasma protein oxidation. In one study, HbA1c levels were used as an index of glycemic control, and plasma carbonyl levels were measured in 17 patients with HbA1c >7% (poor glycemic control) and in 23 patients with HbA1c <7% (good glycemic control). A significant increase was reported in protein carbonyl levels in the poor glycemic control group [18]. In two similar studies, it was shown that type 2 diabetic patients with retinopathy and nephropathy had higher plasma levels of protein carbonyls as compared to type 2 diabetic patients without these complications [19, 20]. In a recent article, it was reported that elevated levels of carbonyl compounds correlated with insulin resistance in type 2 diabetes [21]. In support of previous studies, our data has shown that better glycemic control through initiation of high-dose insulin analog therapy resulted in decreased plasma protein carbonyl formation in type 2 diabetic patients. Although levels of plasma protein carbonyl were significantly decreased after treatment with insulin analogs, a significant correlation was not observed between SD around the mean glucose values and plasma protein carbonyl levels.

Previous studies have shown a significant increase in plasma nitrotyrosine levels in type 2 diabetic patients [22] and a significant correlation of nitrotyrosine values with plasma glucose concentrations ($r = 0.38$, $P < 0.02$) [23]. The role of hyperglycemia in postprandial nitrotyrosine generation was also investigated in 23 type 2 diabetic patients and 15 healthy subjects. Fasting nitrotyrosine was significantly increased in diabetic patients and was further increased during meal tests compared to controls. As compared with regular insulin, aspart administration significantly reduced the area under the curve of both glycemia and nitrotyrosine levels [24]. To our knowledge, this is the first study evaluating the effect of different insulin analogs on nitrotyrosine formation in type 2 diabetes. The observed decrease of plasma nitrotyrosine levels following high-dose insulin analog initiation therapy is in agreement with previous studies that show a significant correlation between nitrotyrosine levels and increased plasma glucose [23, 24]. The significant decrease of nitrotyrosine levels observed 48 hours after the initiation of insulin therapy supports the concept of increased transport of nitrated proteins across vascular endothelium [25]. Although we observed that plasma nitrotyrosine levels were significantly decreased after treatment with insulin analogs, we could not find a significant correlation between SD around the mean glucose values and plasma nitrotyrosine levels.

Plasma and urine 8-iso PGF2α levels were significantly decreased following insulin analog initiation therapy. This observation is in accordance with the reported literature, which shows a link between glucose fluctuations and increased plasma and urine 8-iso PGF2α [14, 26]. In an observational study, 60 patients with type 2 diabetes were treated by oral hypoglycaemic agents alone, and 31 patients with type 2 diabetes were treated with insulin plus oral hypoglycaemic agents. Oxidative stress was estimated in these patients from 24 h urinary excretion rates of 8-iso PGF2α, and mean amplitude of glycemic excursions was estimated by CGMS. The 24 h excretion rate of 8-iso PGF2α was much higher ($P < 0.001$) in type 2 diabetic patients treated with oral hypoglycaemic agents alone than in type 2 diabetes group treated with insulin [27]. In a cross-sectional study recruiting type 2 diabetic patients, 17 patients were

treated with basal bolus-insulin therapy, and 20 patients were treated with twice daily injection of premixed insulin analog therapy. No significant difference was observed in urinary 8-iso PGF2α levels in the two patient groups, and it was suggested that premixed insulin analog therapy was equivalent to basal bolus-insulin therapy in terms of glycemic fluctuations and oxidative stress [28]. A recent observational study was performed on 122 persons with type 2 diabetes, 61 were treated with oral hypoglycaemic agents alone, and 61 were treated with a combination of oral hypoglycaemic agents and insulin at either a low dose (<0.40 unit/kg/day) or high dose (≥0.40 unit/kg/day). The 24-h excretion rates of 8-iso PGF2α were much lower in patients receiving combination of oral hypoglycemic agents and insulin at a low dose [29]. A recent study also examined the relation between glycemic variability and oxidative stress in a cohort of type 2 diabetic patients treated with oral hypoglycemic agents. Twenty-four patients with type 2 diabetes underwent 48 hours of continuous glucose monitoring, and two consecutive 24-hour urine samples were collected for the determination of 8-iso PGF2α using high-performance liquid chromatography tandem mass spectrometry. Standard deviation and mean amplitude of glycemic excursions were calculated as markers of glycemic variability. Regression analysis showed no relevant relationship between glucose variability and 8-iso PGF2α excretions in patients enrolled in the study [16]. In our study, we also observed no significant correlation of urine-free 8-iso PGF2α levels with SD around the mean glucose values, evaluated by linear regression analysis.

There are discrepancies among studies that have measured plasma nitrite/nitrate levels in type 2 diabetic patients. Some reports show increased levels of nitrite/nitrate in type 2 diabetic patients compared to healthy control subjects [30] while some studies show no difference among the two groups [31]. We observed no significant difference in nitrite/nitrate levels after treatment with insulin analogs plus metformin compared to those before treatment levels. Our observation is in agreement with a study which shows that metabolic control does not affect plasma levels of nitrate and nitrite in type 2 diabetic patients [32].

5. Conclusions

We have observed that treatment with insulin analog plus metformin resulted in a significant reduction in glycemic variability and oxidative stress as compared to oral hypoglycemic agents alone. The decrease in levels of oxidative stress markers, including plasma and urine 8-iso PGF2α, plasma protein carbonyl, and nitrotyrosine, following treatment with insulin analogs was significantly correlated with mean blood glucose levels. No significant correlation existed between glucose variability, determined by SD, and levels of plasma and urine oxidative stress markers. Likewise, changes in mean blood glucose from baseline to end point showed no significant correlation with changes in markers of oxidative stress. Data from this study suggests that treatment with insulin analogs, regardless of blood glucose changes, exerts inhibitory effects on free radical formation.

Conflict of Interests

All authors declare that they have no financial, consulting, and personal relationships with other people or organizations that could influence the presented work.

Acknowledgment

This work was supported by a Grant (no: 2010.02.0122.013) from Akdeniz University Research Foundation.

References

[1] UK Prospective Diabetes Study (UKPDS) Group, "Intensive blood-glucose control with sulphonylureas or insulin compared with conventional treatment and risk of complications in patients with type 2 diabetes (UKPDS 33)," *Lancet*, vol. 352, no. 9131, pp. 837–853, 1998.

[2] The Diabetes Control and Complications Trial Research Group, "The effect of intensive treatment of diabetes on the development and progression of long-term complications in insulin-dependent diabetes mellitus," *The New England Journal of Medicine*, vol. 329, pp. 977–986, 1993.

[3] A. Ceriello, M. Hanefeld, L. Leiter et al., "Postprandial glucose regulation and diabetic complications," *Archives of Internal Medicine*, vol. 164, no. 19, pp. 2090–2095, 2004.

[4] A. Ceriello, K. Esposito, L. Piconi et al., "Oscillating glucose is more deleterious to endothelial function and oxidative stress than mean glucose in normal and type 2 diabetic patients," *Diabetes*, vol. 57, no. 5, pp. 1349–1354, 2008.

[5] M. Brownlee and I. B. Hirsch, "Glycemic variability: a hemoglobin A1c-independent risk factor for diabetic complications," *Journal of the American Medical Association*, vol. 295, no. 14, pp. 1707–1708, 2006.

[6] J. L. Chiasson, R. G. Josse, R. Gomis, M. Hanefeld, A. Karasik, and M. Laakso, "Acarbose Treatment and the Risk of Cardiovascular Disease and Hypertension in Patients with Impaired Glucose Tolerance: The STOP-NIDDM Trial," *Journal of the American Medical Association*, vol. 290, no. 4, pp. 486–494, 2003.

[7] R. De Caterina, "Endothelial dysfunctions: common denominators in vascular disease," *Current Opinion in Lipidology*, vol. 11, no. 1, pp. 9–23, 2000.

[8] A. Ceriello, C. Taboga, L. Tonutti et al., "Evidence for an independent and cumulative effect of postprandial hypertriglyceridemia and hyperglycemia on endothelial dysfunction and oxidative stress generation: effects of short- and long-term simvastatin treatment," *Circulation*, vol. 106, no. 10, pp. 1211–1218, 2002.

[9] M. Brownlee, "Biochemistry and molecular cell biology of diabetic complications," *Nature*, vol. 414, no. 6865, pp. 813–820, 2001.

[10] D. Rodbard, "Optimizing display, analysis, interpretation and utility of self-monitoring of blood glucose (SMBG) data for management of patients with diabetes," *Journal of Diabetes Science and Technology*, vol. 1, pp. 62–71, 2007.

[11] G. McGarraugh, "The chemistry of commercial continuous glucose monitors," *Diabetes technology & therapeutics*, vol. 11, pp. S17–S24, 2009.

[12] H. W. Rodbard, L. Blonde, S. S. Braithwaite et al., "American association of clinical endocrinologists medical guidelines for

clinical practice for the management of diabetes mellitus," *Endocrine Practice*, vol. 13, no. 1, pp. 1–68, 2007.

[13] A. Kupesiz, G. Celmeli, S. Dogan, B. Antmen, and M. Aslan, "The effect of hemolysis on plasma oxidation and nitration in patients with sickle cell disease," *Free Radical Research*, vol. 46, pp. 883–890, 2012.

[14] L. Monnier, E. Mas, C. Ginet et al., "Activation of oxidative stress by acute glucose fluctuations compared with sustained chronic hyperglycemia in patients with type 2 diabetes," *Journal of the American Medical Association*, vol. 295, no. 14, pp. 1681–1687, 2006.

[15] I. M. E. Wentholt, W. Kulik, R. P. J. Michels, J. B. L. Hoekstra, and J. H. DeVries, "Glucose fluctuations and activation of oxidative stress in patients with type 1 diabetes," *Diabetologia*, vol. 51, no. 1, pp. 183–190, 2008.

[16] S. E. Siegelaar, T. Barwari, W. Kulik, J. B. Hoekstra, and H. J. DeVries, "No relevant relationship between glucose variability and oxidative stress in well-regulated type 2 diabetes patients," *Journal of diabetes science and technology*, vol. 5, no. 1, pp. 86–92, 2011.

[17] P. Odetti, S. Garibaldi, G. Noberasco et al., "Levels of carbonyl groups in plasma proteins of type 2 diabetes mellitus subjects," *Acta Diabetologica*, vol. 36, no. 4, pp. 179–183, 1999.

[18] U. Çakatay, "Protein oxidation parameters in type 2 diabetic patients with good and poor glycaemic control," *Diabetes and Metabolism*, vol. 31, no. 6, pp. 551–557, 2005.

[19] H. Z. Pan, H. Zhang, D. Chang, H. Li, and H. Sui, "The change of oxidative stress products in diabetes mellitus and diabetic retinopathy," *British Journal of Ophthalmology*, vol. 92, no. 4, pp. 548–551, 2008.

[20] H. Z. Pan, L. Zhang, M. Y. Guo et al., "The oxidative stress status in diabetes mellitus and diabetic nephropathy," *Acta Diabetologica*, vol. 47, no. 1, pp. S71–S76, 2010.

[21] P. Sarkar, K. Kar, M. C. Mondal, I. Chakraborty, and M. Kar, "Elevated level of carbonyl compounds correlates with insulin resistance in type 2 diabetes," *Annals of the Academy of Medicine Singapore*, vol. 39, no. 12, pp. 909–912, 2010.

[22] E. C. Pereira, S. Ferderbar, M. C. Bertolami et al., "Biomarkers of oxidative stress and endothelial dysfunction in glucose intolerance and diabetes mellitus," *Clinical Biochemistry*, vol. 41, no. 18, pp. 1454–1460, 2008.

[23] A. Ceriello, F. Mercuri, L. Quagliaro et al., "Detection of nitrotyrosine in the diabetic plasma: evidence of oxidative stress," *Diabetologia*, vol. 44, no. 7, pp. 834–838, 2001.

[24] A. Ceriello, L. Quagliaro, B. Catone et al., "Role of hyperglycemia in nitrotyrosine postprandial generation," *Diabetes Care*, vol. 25, no. 8, pp. 1439–1443, 2002.

[25] D. Predescu, S. Predescu, and A. B. Malik, "Transport of nitrated albumin across continuous vascular endothelium," *Proceedings of the National Academy of Sciences of the United States of America*, vol. 99, no. 21, pp. 13932–13937, 2002.

[26] F. Zheng, W. Lu, C. Jia, H. Li, Z. Wang, and W. Jia, "Relationships between glucose excursion and the activation of oxidative stress in patients with newly diagnosed type 2 diabetes or impaired glucose regulation," *Endocrine*, vol. 37, no. 1, pp. 201–208, 2010.

[27] L. Monnier, C. Colette, E. Mas et al., "Regulation of oxidative stress by glycaemic control: Evidence for an independent inhibitory effect of insulin therapy," *Diabetologia*, vol. 53, no. 3, pp. 562–571, 2010.

[28] M. Sakamoto, G. Inoue, K. Tsuyusaki et al., "Comparison of oxidative stress markers in type 2 diabetes: Basal bolus therapy versus twice daily premixed insulin analogs," *Internal Medicine*, vol. 49, no. 5, pp. 355–359, 2010.

[29] L. Monnier, C. Colette, F. Michel, J. P. Cristol, and D. R. Owens, "Insulin therapy has a complex relationship with measure of oxidative stress in type 2 diabetes: a case for further study," *Diabetes/Metabolism Research and Reviews*, vol. 27, no. 4, pp. 348–353, 2011.

[30] S. F. Nunes, I. V. Figueiredo, P. J. Soares, N. E. Costa, M. C. Lopes, and M. M. Caramona, "Semicarbazide-sensitive amine oxidase activity and total nitrite and nitrate concentrations in serum: Novel biochemical markers for type 2 diabetes?" *Acta Diabetologica*, vol. 46, no. 2, pp. 135–140, 2009.

[31] M. Catalano, G. Carzaniga, E. Perilli et al., "Basal nitric oxide production is not reduced in patients with noninsulin-dependent diabetes mellitus," *Vascular Medicine*, vol. 2, no. 4, pp. 302–305, 1997.

[32] F. Francesconi, R. Mingardi, S. DeKreutzenberg, and A. Avogaro, "Effect of metabolic control on nitrite and nitrate metabolism in type 2 diabetic patients," *Clinical and Experimental Pharmacology and Physiology*, vol. 28, no. 7, pp. 518–521, 2001.

Hindawi Publishing Corporation
Oxidative Medicine and Cellular Longevity
Volume 2013, Article ID 438321, 8 pages
http://dx.doi.org/10.1155/2013/438321

Clinical Study

Effects of Open versus Laparoscopic Nephrectomy Techniques on Oxidative Stress Markers in Patients with Renal Cell Carcinoma

Celestyna Mila-Kierzenkowska,[1] Alina Woźniak,[1] Tomasz Drewa,[2] Bartosz Woźniak,[3] Michał Szpinda,[4] Ewa Krzyżyńska-Malinowska,[1] and Paweł Rajewski[5]

[1] *The Chair of Medical Biology, Collegium Medicum of Nicolaus Copernicus University, Karłowicza 24, 85-092 Bydgoszcz, Poland*
[2] *Department of Tissue Engineering, Collegium Medicum of Nicolaus Copernicus University, Karłowicza 24, 85-092 Bydgoszcz, Poland*
[3] *Department of Neurosurgery, Stanisław Staszic Specialist Hospital, Rydygiera 1, 64-920 Piła, Poland*
[4] *Department of Normal Anatomy, Collegium Medicum of Nicolaus Copernicus University, Karłowicza 24, 85-092 Bydgoszcz, Poland*
[5] *Department of Nephrology and Internal Medicine, City Hospital, Szpitalna 19, 85-826 Bydgoszcz, Poland*

Correspondence should be addressed to Celestyna Mila-Kierzenkowska; celestyna@o2.pl

Received 19 December 2012; Accepted 14 January 2013

Academic Editor: Kota V. Ramana

The aim of the study was to determine the concentration of lipid peroxidation products, the activity of selected antioxidant and lysosomal enzymes, and protease inhibitor in patients with renal cell carcinoma who underwent radical nephrectomy. The studied group included 44 patients: 21 of them underwent open surgery, while 23 underwent laparoscopy. Blood samples were collected three times: before treatment and 12 hours and five days after nephrectomy. In blood of participants, the concentration of thiobarbituric acid reactive substances (TBARS), the activity of catalase (CAT), superoxide dismutase (SOD) and glutathione peroxidase (GPx), and the activity of acid phosphatase (AcP), arylsulfatase (ASA), cathepsin D (CTSD), and α_1-antitrypsin (AAT) were assayed. No statistically significant differences in investigated parameters were found between studied groups. Moreover, TBARS concentration and CAT, SOD, and GPx activity were not altered in the course of both types of surgery. Five days after both open and laparoscopic nephrectomy techniques, AAT activity was higher than its activity 12 hours after the procedure. The obtained results suggest that laparoscopy may be used for nephrectomy as effectively as open surgery without creating greater oxidative stress. Reduced period of convalescence at patients treated with laparoscopy may be due to less severe response of acute-phase proteins.

1. Introduction

Renal cell carcinoma (RCC) is the most common kidney cancer that arises from the cells of the renal tubule [1]. Despite of the fact that renal cell carcinoma is relatively rare compared with other cancers, its incidence is still increasing [2]. Cigarette smoking, obesity, hypertension, and/or related medications have been implicated as risk factors [3]. For localized RCC, the radical nephrectomy remains the mainstay of surgical treatment, however, techniques are being modified [4]. Since its introduction, laparoscopic radical nephrectomy has been established as a standard care for the surgical management of localized renal cell carcinoma [5, 6]. Laparoscopic surgery seems to have considerable advantages over open surgery, such as decreased blood loss, decreased postoperative pain, and less morbidity, as well as shorter hospital stay [7–9]. However, laparoscopy requires special skills using unfamiliar devices, and there is a limited pool of urologist, trained in laparoscopy [6, 9]. Moreover, the induction of pneumoperitoneum during laparoscopy procedure has several local and systemic effects [10]. Still very little is known about the effect of different nephrectomy techniques on antioxidant-oxidant balance and inflammatory markers in patients with RCC.

An imbalance between the production of reactive oxygen species (ROS) and an ability of human system to detoxify

them or easily repair the resulting damage of ROS may cause oxidative stress. The most often investigated process involved in reactive oxygen species generation in cells is lipid peroxidation. Lipid peroxidation products, such as thiobarbituric acid reactive substances (TBARS), change the capacity of biological membranes [11]. The final result of structural disorders of cellular constituents caused by ROS is the change of their function and even cell death [12]. Yet, human organism is endowed with a complex arsenal of antioxidant defense mechanisms protecting them from an increased ROS formation and their reactions with cell compounds. One of the defense mechanisms is based on antioxidant enzyme activity and includes superoxide dismutase (SOD), catalase (CAT), and glutathione peroxidase (GPx) [13]. Oxidative stress may also lead to some disturbances in lysosomal membranes, hence, provoking some changes in activity of lysosomal enzymes in blood serum. These enzymes are involved in housekeeping tasks such as turnover of intracellular proteins, antigen presentation, and bone remodeling, but they are also known to be found outside lysosomes in certain pathological conditions and participate in numerous diseases [14].

The aim of this study was to determine the effect of two different nephrectomy techniques on the concentration of lipid peroxidation products, the activity of main antioxidant enzymes, and the activity of selected lysosomal enzymes as well as protease inhibitor in patients with renal cell carcinoma who underwent open surgery and laparoscopy.

2. Materials and Methods

The study was conducted on the group of patients attending the Department of Urology of the Jan Biziel Regional Hospital in Bydgoszcz. The inclusion criteria were patients ≥18 years of age who underwent radical nephrectomy for localized renal cell carcinoma and agreed to voluntary participation in experiment. Patients suffering from any other disease were excluded from the study as the treatment may have an impact on antioxidants level in blood. Exclusion criteria were also cigarettes smoking and use of supplement of diet containing antioxidants. Blood samples were obtained from a total number of 44 subjects (24 men and 20 women) aged between 30 and 76 years. All of the patients underwent radical nephrectomy; however, two different techniques were used, and hence, the subjects were divided into two groups. The first group consists of 21 persons treated with open surgery, while the other included 23 subjects treated with laparoscopy.

Blood samples were collected from the basilic vein before nephrectomy and 12 hours and five days after both open surgery and laparoscopy. The Local Bioethical Committee at Collegium Medicum of the Nicolaus Copernicus University in Toruń agreement was obtained, and all subjects had given their written informed consent.

Thiobarbituric acid reactive substances level was determined in blood plasma and erythrocytes according to Buege and Aust [15] method in the Esterbauer and Cheesman modification [16]. The method involves creation of coloured complex between lipid peroxidation products and thiobarbituric acid at the temperature of 100°C and in acidic environment. The maximum absorption of that complex occurs at a wavelength of 532 nm. The main product of lipid peroxidation reacting with thiobarbituric acid is malondialdehyde (MDA), and, therefore, the level of TBARS in plasma was expressed as nmol of MDA/mL and in the erythrocytes as nmol of MDA/gHb.

The activity of antioxidant enzymes was measured in erythrocytes. Beers and Sizer [17] method was used to assay catalase activity. This method is based on measurement of absorbance decrease of hydrogen peroxide, which is decomposed by catalase, measured at a wavelength of 240 nm. CAT activity was expressed as 10^4 IU/gHb. Superoxide dismutase activity was performed by Misra and Fridovich method [18]. This procedure is based on SOD impeding the reaction of autooxidation of adrenaline to adrenochrome in an alkaline environment. SOD activity was expressed as U/gHb. Glutathione peroxidase activity was determined according to Paglia and Valentine [19] by a method based on the measurement of changes in absorbance at a wavelength of 340 nm, caused by oxidation of reduced nicotinamide adenine dinucleotide phosphate (NADPH). NADPH is a coenzyme of reduction of glutathione disulfide. The obtained oxidized glutathione is a product of reaction catalysed by glutathione peroxidase. Activity of GPx was expressed as U/gHb.

The activity of lysosomal enzymes and protease inhibitor was measured in the blood serum. The activity of acid phosphatase was determined by means of Bessey's method [20]. The activity measure was the quantity of p-nitrophenol generated during enzymatic hydrolysis of 4-nitrophenylphosphate disodium salt used as a substrate. Roy's method modified by Błeszyński [21] was used to assay arylsulfatase activity. The substrate employed here was 4-nitrocatechol sulfate (4-NCS), and the measure recorded was the quantity of 4-nitrocatechol released during enzymatic hydrolysis. Cathepsin D activity was determined using the Anson method [22] based on measurement of tyrosine quantity released during hydrolysis of haemoglobin by CTSD. The activity of α_1-antitrypsin was determined according to Eriksson [23]. This procedure relies on the evaluation of the level of trypsin inhibited by AAT present in 1 mL of blood serum.

All results were statistically analysed by means of factorial repeated-measures ANOVA test with post hoc analysis (Tukey's range test). Before running ANOVA, model assumptions were also tested (Shapiro-Wilk test for normality and Box's Test for homogeneity of covariance). The correlation coefficients (r) between parameters for an evaluation of relationships were also estimated. Changes with a level of significance $P < 0.05$ were regarded as statistically significant.

3. Results

The concentration of TBARS both in blood plasma and in erythrocytes of patients with renal cell carcinoma after nephrectomy was not altered in patients who underwent either open or laparoscopic surgery as compared to the value before the surgical treatment (Table 1). There were also no statistically significant differences in thiobarbituric acid reactive substances concentration between the two groups of RCC patients. However, some increasing tendency in TBARS levels

Table 1: Lipid peroxidation products level and antioxidant enzymes activity in patients with renal cell carcinoma before and after radical nephrectomy by open surgery and laparoscopy.

	Open radical nephrectomy ($n = 21$)		
	Before surgery	12 hours after surgery	5 days after surgery
$TBARS_{plasma}$ (nmol MDA/mL)	0.51 ± 0.14	0.53 ± 0.12	0.55 ± 0.14
$TBARS_{erythrocytes}$ (nmol MDA/gHb)	37.6 ± 13.2	39.0 ± 18.2	38.6 ± 14.5
CAT (10^4 IU/gHb)	61.4 ± 18.6	67.2 ± 27.0	61.4 ± 19.6
SOD (U/gHb)	1167.6 ± 345.4	1132.5 ± 193.3	1110.3 ± 222.9
GPx (U/gHb)	9.0 ± 3.7	8.8 ± 3.2	7.8 ± 3.5
	Laparoscopic radical nephrectomy ($n = 23$)		
	Before laparoscopy	12 hours after laparoscopy	5 days after laparoscopy
$TBARS_{plasma}$ (nmol MDA/mL)	0.45 ± 0.11	0.56 ± 0.13	0.56 ± 0.18
$TBARS_{erythrocytes}$ (nmol MDA/gHb)	32.6 ± 19.2	40.1 ± 12.6	35.4 ± 12.9
CAT (10^4 IU/gHb)	74.7 ± 32.3	55.8 ± 15.9	61.3 ± 17.3
SOD (U/gHb)	1161.0 ± 298.2	1060.3 ± 135.1	1011.7 ± 131.3
GPx (U/gHb)	6.9 ± 3.9	9.9 ± 3.1	6.5 ± 2.9

No statistically significant differences between open surgery and laparoscopy.
TBARS: thiobarbituric acid reactive substances; CAT: catalase; SOD: superoxide dismutase; GPx: glutathione peroxidase.

was noticed 12 hours and 5 days after the surgery as compared to the value before the intervention.

Considering the activity of catalase, superoxide dismutase, and glutathione peroxidase in investigated groups of patients, no statistically significant changes were found as a result of radical nephrectomy. There were also no statistically significant differences between patients undergoing open surgery versus laparoscopy (Table 1). Yet, some statistically significant correlations between studied antioxidant enzymes were found. Before the treatment, there was a positive correlation ($r = 0.52$, $P < 0.05$) between CAT and SOD activity in group of patients treated with open surgery and negative correlation ($r = -0.63$, $P < 0.01$) between CAT activity and TBARS level in erythrocytes in patients before laparoscopy. In patients treated with laparoscopy 12 hours after the nephrectomy, positive correlation ($r = 0.50$, $P < 0.05$) was revealed between CAT and GPx activity.

No statistically significant differences were found in activity of investigated lysosomal enzymes and protease inhibitor between the patients treated with open surgery as compared to patients who were subjected to laparoscopy. However, some changes in their activity were found as a consequence of surgical treatment. The pattern of changes was similar in both groups of patients, but some differences were noticed. The activity of arylsulfatase decreased after the nephrectomy in comparison to the value before the intervention (Table 2). In patients treated with open surgery, it decreased by about 26% ($P < 0.05$) 12 hours and by about 22% ($P < 0.05$) 5 days after the nephrectomy. In subjects who underwent laparoscopy, it decreased even much more, by about 37% ($P < 0.001$) and 45% ($P < 0.001$) 12 hours and 5 days after nephrectomy, respectively. In turn, CTSD activity in both statistically significant groups increased as a result of surgical treatment (Table 2). At patients treated with open surgery, CTSD activity 12 hours after the procedure was 77% higher ($P < 0.05$), while 5 days after surgery 89% higher ($P < 0.01$) than before the treatment. Twelve hours and 5 days after laparoscopy, CTSD activity was 61% ($P < 0.01$) and 55% higher ($P < 0.05$), respectively. Comparing the activity of protease inhibitor in the course of treatment, its activity 12 hours after both techniques of nephrectomy decreased, but this was statistically insignificant. Five days after the treatment, AAT activity statistically significantly increased as compared to the value 12 hours after the treatment (Table 2). At patients subjected to open surgery, AAT activity was then 84% higher ($P < 0.001$), while at subjects treated with laparoscopy, it was 51% higher ($P < 0.05$). There were no statistically significant changes in AcP activity after open surgery or laparoscopy (Table 2).

Considering correlation coefficients between all studied lysosomal enzymes and protease inhibitor, positive correlation was revealed between ASA and AcP activity ($r = 0.49$, $P < 0.05$) and between ASA and AAT activity ($r = 0.66$, $P < 0.01$) and negative correlation between CTSD and ASA activity ($r = -0.78$, $P < 0.001$) at patients treated with open surgery 5 days after the treatment. At patients subjected to laparoscopy, negative correlation between CTSD and ASA activity was found both 12 hours ($r = -0.62$, $P < 0.05$) and 5 days after ($r = -0.81$, $P < 0.001$) the nephrectomy.

Moreover, in the presented study, some correlations were found between parameters of oxidative stress and lysosomal enzymes. Twelve hours after the open surgery, negative correlation (Figure 1) was observed between SOD and CTSD activity ($r = -0.45$, $P < 0.05$), while 12 hours after the laparoscopy, negative correlation (Figures 2 and 3) was revealed between SOD and CTSD activity ($r = -0.52$, $P < 0.05$) as well as between GPx and CTSD activity ($r = -0.51$, $P < 0.05$). Five days after the surgical treatment at patients subjected to open surgery, statistically significant negative correlation (Figure 4) was observed between SOD and CTSD activity ($r = -0.49$, $P < 0.05$). In a group of patients who underwent laparoscopy, 5 days after the intervention, statistically significant negative correlation (Figure 5) was

Table 2: Lysosomal enzymes and protease inhibitor activity in patients with renal cell carcinoma before and after radical nephrectomy by open surgery and laparoscopy.

	Open radical nephrectomy ($n = 21$)		
	Before surgery	12 hours after surgery	5 days after surgery
AcP (10^{-2} nM p-nitrophenol/mg protein/min)	1.87 ± 0.78	2.46 ± 0.89	2.22 ± 0.99
ASA (10^{-3} nM NCS/mg protein/min)	2.13 ± 0.46	1.58 ± 0.59[a]	1.66 ± 0.68[a]
CTSD (10^{-2} nM tyrosine/mg protein/min)	2.31 ± 1.19	4.10 ± 1.82[a]	4.37 ± 2.17[aa]
AAT (mg trypsin/mL serum)	0.62 ± 0.2	0.43 ± 0.2	0.79 ± 0.2[bbb]
	Laparoscopic radical nephrectomy ($n = 23$)		
	Before laparoscopy	12 hours after laparoscopy	5 days after laparoscopy
AcP (10^{-2} nM p-nitrophenol/mg protein/min)	2.07 ± 0.86	1.62 ± 0.79	1.61 ± 0.58
ASA (10^{-3} nM NCS/mg protein/min)	2.22 ± 0.36	1.40 ± 0.72[ccc]	1.23 ± 0.51[ccc]
CTSD (10^{-2} nM tyrosine/mg protein/min)	2.81 ± 0.97	4.53 ± 2.01[cc]	4.35 ± 2.10[c]
AAT (mg trypsin/mL serum)	0.61 ± 0.2	0.49 ± 0.2	0.74 ± 0.3[d]

No statistically significant differences between open surgery and laparoscopy.
Statistically significant differences: versus before open surgery: [a]$P < 0.05$, [aa]$P < 0.01$; versus 12 hours after open surgery: [bbb]$P < 0.001$; versus before laparoscopy: [c]$P < 0.05$ and [cc]$P < 0.01$ and [ccc]$P < 0.001$; versus 12 hours after laparoscopy: [d]$P < 0.05$.
AcP: acid phosphatase; AAT: α_1-antitrypsin; ASA: arylsulphatase; CTSD: cathepsin D.

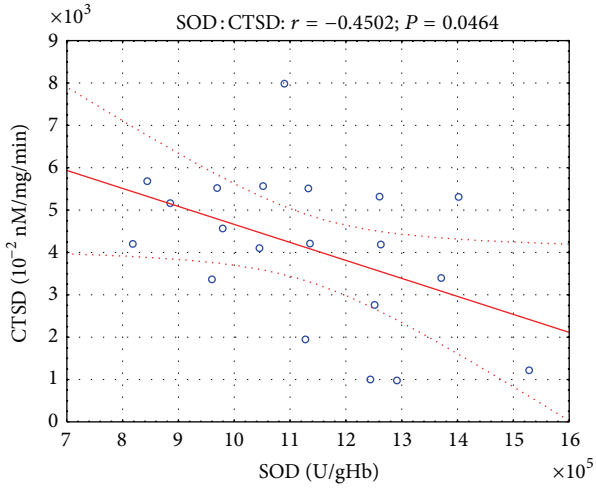

Figure 1: Linear regression of superoxide dismutase (SOD) activity versus cathepsin D (CTSD) activity, at patients with renal cell carcinoma, 12 hours after open surgery nephrectomy.

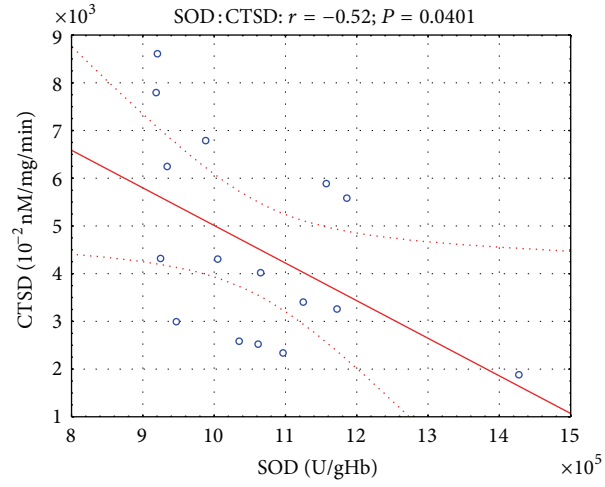

Figure 2: Linear regression of superoxide dismutase (SOD) activity versus cathepsin D (CTSD) activity, at patients with renal cell carcinoma, 12 hours after laparoscopic nephrectomy.

observed between CAT and CTSD activity ($r = -0.65$, $P < 0.05$), as well as positive correlation between SOD and ASA activity ($r = 0.69$, $P < 0.01$). Moreover, positive correlation between $TBARS_{plasma}$ level and AAT activity ($r = 0.59$, $P < 0.05$) was found.

4. Discussion

Laparoscopic surgery has become one of the most important and popular technique in general surgery and is the procedure of choice for almost all types of abdominal operations, because of its advantages over open surgery [10]. Although it is technically demanding, laparoscopy provides RCC patients improved quality of life during recovery period with decreased analgetic requirements, fewer complications, and more rapid convalescence [24, 25]. However, there are some reports about higher in-hospital mortality and more common failure to rescue after laparoscopy probably due to poor experience of surgeons and hospitals [24, 25]. Despite all the advantages, laparoscopic surgery can have several local and systemic consequences related to the induction of pneumoperitoneum used to facilitate the visual field.

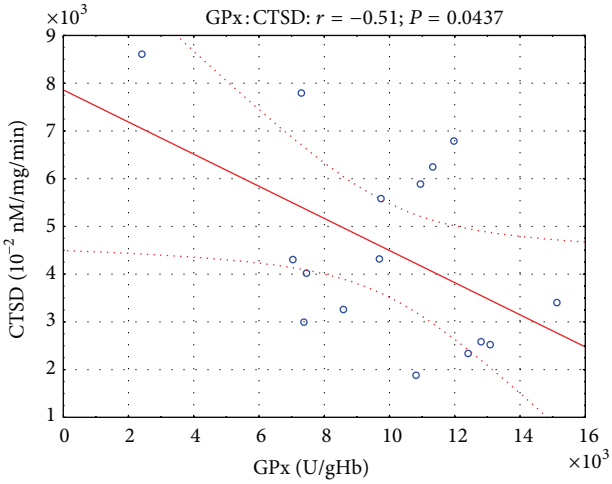

Figure 3: Linear regression of glutathione peroxidase (GPx) activity versus cathepsin D (CTSD) activity, at patients with renal cell carcinoma, 12 hours after laparoscopic nephrectomy.

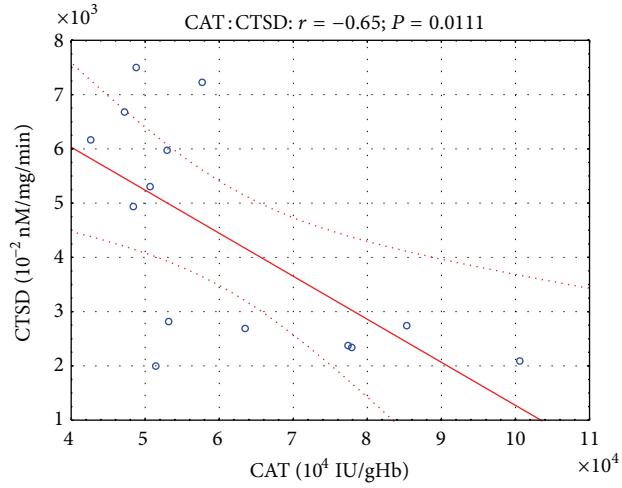

Figure 5: Linear regression of catalase (CAT) activity versus cathepsin D (CTSD) activity, at patients with renal cell carcinoma, 5 days after laparoscopic nephrectomy.

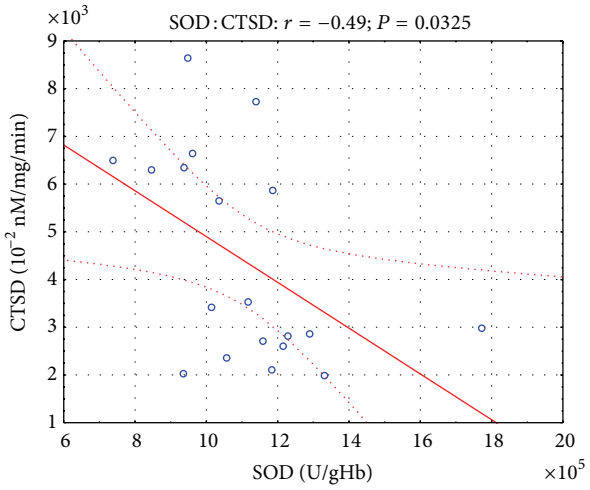

Figure 4: Linear regression of superoxide dismutase (SOD) activity versus cathepsin D (CTSD) activity, at patients with renal cell carcinoma, 5 days after open surgery nephrectomy.

Insufflation of carbon dioxide into peritoneal cavity leads to alterations in acid-base balance, blood gases, and cardiovascular and pulmonary physiology [26] and causes reversible renal dysfunction [27, 28]. The effects of pneumoperitoneum depend on many factors like the pressure level and gas used [29]. For example, helium seems to limit postoperative oxidative response following laparoscopy as higher MDA and carbonyl responses and sulfydryl consumption were revealed after CO_2 insufflation compared with helium [30].

Recently, some clinical and experimental studies demonstrate that creating a pneumoperitoneum results in oxidative stress. Laparoscopy may among others alter the production of reactive oxygen species because of the effect of carbon dioxide on peroxynitrite metabolism [31]. Oxidative stress during surgical injury is also due to ischemia/reperfusion injury. During laparoscopy, increase of intra-abdominal pressure caused by pneumoperitoneum may cause splanchnic ischemia followed by reperfusion due to deflation [32]. An increase in lipid peroxidation products during the immediate postoperative period and postoperative decrease in endogenous antioxidants after laparoscopy, but not after open cholecystectomy, were shown by Glantzounis et al. [32]. The authors suggest that free radicals are generated at the end of laparoscopic procedure, possibly as a result of ischemia-reperfusion phenomenon induced by pneumoperitoneum. Increased oxidative stress due to pneumoperitoneum was also observed during laparoscopic donor nephrectomy, both in donor and remaining kidneys [25].

In our study, no statistically significant changes in the level of lipid peroxidation products and the activity of antioxidant enzymes were revealed both 12 hours and 5 days after open surgery or laparoscopy. There were also no differences in parameters of oxidative stress between patients treated with different nephrectomy techniques. The literature data about the effect of open and laparoscopic surgery techniques on parameters of oxidative stress are unequivocal. Gianotti et al. [33] demonstrated that both laparoscopy and open colon surgery may cause oxidative damage during mesentery traction and immediately after the end of operation. Bukan et al. [34] showed that both open and laparoscopic cholecystectomy techniques caused an increased oxidative stress; however, laparoscopy induces less significantly oxidative stress than open surgery. The others concluded that cholecystectomy, either open or laparoscopic, caused only moderate oxidative stress [31]. SOD activity and total antioxidant status was not changed after both procedures, while endogenous lipid peroxide level was higher onday 7 after intervention. Moreover, they found that the level of oxidized low density lipoproteins was higher after surgery, but only after open cholecystectomy. On the other hand, comparing open donor nephrectomy, laparoscopic donor nephrectomy,

and retroperitoneoscopic donor nephrectomy, no differences were detected in oxidative stress markers in renal tissue samples [35].

Despite the lack of changes in oxidative stress markers after the surgical treatment, some statistically significant changes in ASA activity in serum of RCC patients after nephrectomy were found. However, it is known that this enzyme is a member of family of sulfatases activated by the oxidation of cysteine to formylglycine [36]. In turn, formylglycine-generating enzyme is inhibited by oxidation of its cysteine due to increased ROS generation [37]. Hence, it is possible that decrease in ASA activity observed in our study after nephrectomy is a consequence of presence of limiting factor for its activity related to increased generation of reactive oxygen species after the surgical treatment.

Comparing open and laparoscopic nephrectomy techniques no statistically significant differences were found in cathepsin D activity; yet, after both procedures, its activity increased relevantly. Among the lysosomal hydrolases, cathepsins play major role in cellular proteolysis [38]. Originally, cathepsins were believed to participate exclusively in terminal protein degradation during necrotic and autophagic death. Nowadays, it is well established that those enzymes execute numerous specific functions participating in important physiological processes [39]. The increase in CTSD activity in blood serum is probably due to its release into cytosol after labilization of lysosomal membrane. Although the mechanism of lysosomal membrane destabilization is still poorly understood, the list of agents able to destabilize the membrane is very comprehensive and includes reactive oxygen species, which disturb the membranes by peroxidation of their lipids [40]. No significant statistically changes in antioxidant enzymes activity and lipid peroxidation level as a result of radical nephrectomy were found in this paper, but some statistically significant negative correlations between antioxidant enzymes and cathepsin D activity were revealed after surgical treatment in both groups of patients. This may suggest insufficient antioxidant defense after the surgery, which may lead to some oxidative damage, like lysosomes disruption. The confirmation of increased level of reactive oxygen species generation after the nephrectomy may be the increasing tendency in TBARS levels observed in this paper. Accumulating data suggest that ROSs not only act as damaging entitles, but also may carry important beneficial functions [41]. Reactive oxygen species occurring after the surgery may play a possible role in the healing of laparotomic wound [31].

The main way in which cathepsins activity is regulated is by interaction with their endogenous protease inhibitors [42]. In human plasma, serine protease inhibitors represent about 10% of the total protein, of which 70% is α_1-antitrypsin [43]. AAT is nowadays considered as one of the acute-phase proteins as its normal plasma level increases 3-to 5-fold under variety of physiological and pathological conditions like stress, infections, and inflammation [44]. In present study, 12 hours after nephrectomy, the activity of α_1-antitrypsin statistically insignificantly decreased, but 5 days after the procedure, its activity was higher than before treatment and 12 hours after the treatment. An increasing amount of evidences suggest that AAT possesses not only the ability to inhibit proteases, but also to exert anti-inflammatory and tissue protective effects independent of protease inhibition [45]. AAT in concert with other proteins is probably involved in protecting extracellular spaces from protein misfolding and precipitation especially under stress conditions [46]. Despite the fact that there were no statistically significant differences between patients from both studied groups, it can be noticed that the rise of AAT activity was higher after open surgery, which may suggest more intense inflammatory reaction than after laparoscopic procedure. Those results are in agreement with some research which compared inflammatory response in open and laparoscopic cholecystectomy techniques [47–49]. They found more significant increase in acute-phase inflammatory markers, such as α_1-antitrypsin, after open surgery than after laparoscopy. They postulate that laparoscopic cholecystectomy, which is related to less tissue damage, provokes less intense stress response. Gál et al. [50] also showed that both open and laparoscopic procedures induced changes of acute-phase proteins level, free radical mediated reactions, and neutrophil functions. However, laparoscopy induces a significantly less intense response in these parameters. Considering the inflammatory response after open versus laparoscopic nephrectomy techniques, less intense surgical trauma-induced immune dysfunction was found after laparoscopy [51].

5. Conclusions

Our study demonstrates that neither open nor laparoscopic radical nephrectomy has effect on postoperative level of lipid peroxidation products and on activity of antioxidant enzymes in blood of RCC patients, and both techniques may cause only moderate changes in oxidant-antioxidant balance. Therefore, we believe that laparoscopy may be used for radical nephrectomy as effectively as open surgery without creating oxidative stress. Moreover, we have observed that the response of α_1-antitrypsin is more severe after open surgery than after laparoscopy in studied RCC patients. The attenuation of acute-phase response may explain the reduced period of convalescence at patients treated with laparoscopy.

Conflict of Interests

The authors declare they haveno conflict of interests.

References

[1] L. Hanak, O. Slaby, L. Lauerova, L. Kren, R. Nenutil, and J. Michalek, "Expression pattern of HLA class I antigens in renal cell carcinoma and primary cell line cultures: methodological implications for immunotherapy," *Medical Science Monitor*, vol. 15, no. 12, pp. CR638–CR643, 2009.

[2] B. J. Drucker, "Renal cell carcinoma: current status and future prospects," *Cancer Treatment Reviews*, vol. 31, no. 7, pp. 536–545, 2005.

[3] R. Dhôte, M. Pellicer-Coeuret, N. Thiounn, B. Debré, and G. Vidal-Trecan, "Risk factors for adult renal cell carcinoma: a systematic review and implications for prevention," *BJU International*, vol. 86, no. 1, pp. 20–27, 2000.

[4] R. J. Motzer, D. M. Nanus, P. Russo, and W. J. Berg, "Renal cell carcinoma," *Current Problems in Cancer*, vol. 21, no. 4, pp. 191–232, 1997.

[5] C. Tait, S. Tandon, L. Baker, C. Goodman, N. Townell, and G. Nabi, "Long-term oncologic outcomes of laparoscopic radical nephrectomy for kidney cancer resection: Dundee cohort and metaanalysis of observational studies," *Surgical Endoscopy*, vol. 25, no. 10, pp. 3154–3161, 2011.

[6] S. P. Stroup, K. L. Palazzi, D. C. Chang, N. T. Ward, and J. K. Parsons, "Inpatient safety trends in laparoscopic and open nephrectomy for renal tumours," *BJU International*, vol. 110, no. 11, pp. 1808–1813, 2012.

[7] N. Albqami and G. Janetschek, "Indications and contraindications for the use of laparoscopic surgery for renal cell carcinoma," *Nature Clinical Practice Urology*, vol. 3, no. 1, pp. 32–37, 2006.

[8] L. M. Siani, F. Ferranti, M. Benedetti, A. De Carlo, and A. Quintiliani, "Laparoscopic versus open radical nephrectomy in T1-T2 renal carcinoma: personal 5-year experience about the oncologic outcome," *Minerva Chirurgica*, vol. 66, no. 4, pp. 317–321, 2011.

[9] M. Tokunaga, M. Okajima, H. Egi et al., "The importance of stressing the use of laparoscopic instruments in the initial training for laparoscopic surgery using box trainers: a randomized control study," *The Journal of Surgical Research*, vol. 174, no. 1, pp. 90–97, 2012.

[10] G. K. Glantzounis, I. Tsimaris, A. D. Tselepis, C. Thomas, D. A. Galaris, and E. C. Tsimoyiannis, "Alterations in plasma oxidative stress markers after laparoscopic operations of the upper and lower abdomen," *Angiology*, vol. 56, no. 4, pp. 459–465, 2005.

[11] C. Mila-Kierzenkowska, A. Woźniak, B. Woźniak et al., "Whole-body cryostimulation in kayaker women: a study of the effect of cryogenic temperatures on oxidative stress after the exercise," *Journal of Sports Medicine and Physical Fitness*, vol. 49, no. 2, pp. 201–207, 2009.

[12] E. Cadenas, "Mechanisms of oxygen activation and reactive oxygen species detoxification," in *Oxidative Stress and Antoxidative Defenses in Biology*, S. Ahmad, Ed., pp. 1–60, Chapman & Hall, New York, NY, USA, 1995.

[13] C. Mila-Kierzenkowska, K. Kędziora-Kornatowska, A. Woźniak et al., "The effect of brachytherapy on antioxidant status and lipid peroxidation in patients with cancer of the uterine cervix," *Cellular and Molecular Biology Letters*, vol. 9, no. 3, pp. 511–518, 2004.

[14] A. Piwowar, M. Knapik-Kordecka, I. Fus, and M. Warwas, "Urinary activities of cathepsin B, N-acetyl-β-D-glucosaminidase, and albuminuria in patients with type 2 diabetes mellitus," *Medical Science Monitor*, vol. 12, no. 5, pp. CR210–CR214, 2006.

[15] J. A. Buege and S. D. Aust, "Microsomal lipid peroxidation," *Methods in Enzymology*, vol. 52, pp. 302–310, 1978.

[16] H. Esterbauer and K. H. Cheeseman, "Determination of aldehydic lipid peroxidation products: malonaldehyde and 4-hydroxynonenal," in *Methods in Enzymology*, L. Packer and A. N. Glazer, Eds., pp. 407–421, Academic Press, New York, NY, USA, 1990.

[17] R. F. Beers and I. W. Sizer, "A spectrophotometric method for measuring the breakdown of hydrogen peroxide by catalase," *The Journal of biological chemistry*, vol. 195, no. 1, pp. 133–140, 1952.

[18] H. P. Misra and I. Fridovich, "The role of superoxide anion in the autoxidation of epinephrine and a simple assay for superoxide dismutase," *Journal of Biological Chemistry*, vol. 247, no. 10, pp. 3170–3175, 1972.

[19] D. E. Paglia and W. N. Valentine, "Studies on the quantitative and qualitativecharacterization of erythrocyte glutatione peroxidase," *Journal of Laboratory and Clinical Medicine*, vol. 70, pp. 158–169, 1967.

[20] J. Krawczyński, *Diagnostyka Enzymologiczna w Medycynie Praktycznej*, PZWL, Warszawa, Poland, 1972.

[21] W. Błeszyński and L. M. Działoszyński, "Purification of soluble arylsulphatase from ox brain," *Biochemical Journal*, vol. 97, pp. 360–364, 1965.

[22] S. C. Colowick and N. C. Kaplan, *Methods in Enzymology*, vol. 2, Academic Press, New York, NY, USA, 1955.

[23] S. Eriksson, "Studies in alpha 1-antitrypsin deficiency," *Acta Medica Scandinavica*, vol. 432, pp. 1–85, 1965.

[24] H. J. Tan, J. S. Wolf Jr., Z. Ye, J. T. Wei, and D. C. Miller, "Population-level comparative effectiveness of laparoscopic versus open radical nephrectomy for patients with kidney," *Cancer*, vol. 117, no. 18, pp. 4184–4193, 2011.

[25] H. J. Tan, J. S. Wolf Jr., Z. Ye, J. T. Wei, and D. C. Miller, "Complications and failure to rescue after laparoscopic versus open radical nephrectomy," *The Journal of Urology*, vol. 186, no. 4, pp. 1254–1260, 2011.

[26] D. B. Safran and R. Orlando, "Physiologic effects of pneumoperitoneum," *American Journal of Surgery*, vol. 167, no. 2, pp. 281–286, 1994.

[27] A. W. Chiu, L. S. Chang, D. H. Birkett, and R. K. Babayan, "The impact of pneumoperitoneum, pneumoretroperitoneum, and gasless laparoscopy on the systemic and renal hemodynamics," *Journal of the American College of Surgeons*, vol. 181, no. 5, pp. 397–406, 1995.

[28] C. Güler, M. Sade, and Z. Kirkali, "Renal effects of carbon dioxide insufflation in rabbit pneumoretroperitoneum model," *Journal of Endourology*, vol. 12, no. 4, pp. 367–370, 1998.

[29] S. Yilmaz, C. Polat, A. Kahraman et al., "The comparison of the oxidative stress effects of different gases and intra-abdominal pressures in an experimental rat model," *Journal of Laparoendoscopic and Advanced Surgical Techniques Part A*, vol. 14, no. 3, pp. 165–168, 2004.

[30] M. McHoney, S. Eaton, A. Wade et al., "Inflammatory response in children after laparoscopic vs open Nissen fundoplication: randomized controlled trial," *Journal of Pediatric Surgery*, vol. 40, no. 6, pp. 908–914, 2005.

[31] I. Stipancic, N. Zarkovic, D. Servis, S. Sabolović, F. Tatzber, and Z. Busic, "Oxidative stress markers after laparoscopic and open cholecystectomy," *Journal of Laparoendoscopic and Advanced Surgical Techniques Part A*, vol. 15, no. 4, pp. 347–352, 2005.

[32] G. K. Glantzounis, A. D. Tselepis, A. P. Tambaki et al., "Laparoscopic surgery-induced changes in oxidative stress markers in human plasma," *Surgical Endoscopy*, vol. 15, no. 11, pp. 1315–1319, 2001.

[33] L. Gianotti, L. Nespoli, S. Rocchetti, A. Vignali, A. Nespoli, and M. Braga, "Gut oxygenation and oxidative damage during and after laparoscopic and open left-sided colon resection: a prospective, randomized, controlled trail," *Surgical Endoscopy*, vol. 25, no. 6, pp. 1835–1843, 2011.

[34] M. H. Bukan, N. Bukan, N. Kaymakciouglu, and T. Tufan, "Effects of open vs. laparoscopic cholecystectomy on oxidative stress," *Tohoku Journal of Experimental Medicine*, vol. 202, no. 1, pp. 51–56, 2004.

[35] M. Demirbas, M. Samli, Y. Aksoy, C. Guler, A. Kilinc, and C. Dincel, "Comparison of changes in tissue oxidative-stress markers in experimental model of open, laparoscopic, and retroperitoneoscopic donor nephrectomy," *Journal of Endourology*, vol. 18, no. 1, pp. 105–108, 2004.

[36] M. P. Cosma, S. Pepe, I. Annunziata et al., "The multiple sulfatase deficiency gene encodes an essential and limiting factor for the activity of sulfatases," *Cell*, vol. 113, no. 4, pp. 445–456, 2003.

[37] T. Dierks, A. Dickmanns, A. Preusser-Kunze et al., "Molecular basis for multiple sulfatase deficiency and mechanism for formylglycine generation of the human formylglycine-generating enzyme," *Cell*, vol. 121, no. 4, pp. 541–552, 2005.

[38] V. Turk, V. Stoka, O. Vasiljeva et al., "Cysteine cathepsins: from structure, function and regulation to new frontiers," *Biochimica et Biophysica Acta*, vol. 1824, no. 1, pp. 68–88, 2012.

[39] C. Mila-Kierzenkowska, A. Woźniak, T. Boraczyński, A. Jurecka, B. Augustyńska, and B. Woźniak, "The effect of whole-body cryostimulation on the activity of lysosomal enzymes in kayaker women after intense exercise," *Journal of Thermal Biology*, vol. 36, no. 1, pp. 29–33, 2011.

[40] U. Repnik, V. Stoka, V. Turk, and B. Turk, "Lysosomes and lysosomal cathepsins in cell death," *Biochimica et Biophysica Acta*, vol. 1824, no. 1, pp. 22–33, 2012.

[41] M. Gago-Dominguez, J. E. Castelao, M. C. Pike, A. Sevanian, and R. W. Haile, "Role of lipid peroxidation in the epidemiology and prevention of breast cancer," *Cancer Epidemiology Biomarkers and Prevention*, vol. 14, no. 12, pp. 2829–2839, 2005.

[42] V. Turk, B. Turk, G. Gunčar, D. Turk, and J. Kos, "Lysosomal cathepsins: structure, role in antigen processing and presentation, and cancer," *Advances in Enzyme Regulation*, vol. 42, pp. 285–303, 2002.

[43] F. Zsila, "Inhibition of heat- and chemical-induced aggregation of various proteins reveals chaperone-like activity of the acute-phase component and serine protease inhibitor human α_1-antitrypsin," *Biochemical and Biophysical Research Communications*, vol. 393, no. 2, pp. 242–247, 2010.

[44] O. Pos, M. E. Van der Stelt, G. J. Wolbink, M. W. N. Nijsten, G. L. Van der Tempel, and W. Van Dijk, "Changes in the serum concentration and the glycosylation of human α_1-acid glycoprotein and α1-protease inhibitor in severely burned persons: relation to interleukin-6 levels," *Clinical and Experimental Immunology*, vol. 82, no. 3, pp. 579–582, 1990.

[45] E. C. Lewis, "Expanding the clinical indications for α_1-antitrypsin therapy," *Molecular Medicine*, vol. 18, no. 9, pp. 957–970, 2012.

[46] S. Süer Gökmen, C. Kazezoğlu, B. Sunar et al., "Relationship between serum sialic acids, sialic acid-rich inflammation-sensitive proteins and cell damage in patients with acute myocardial infarction," *Clinical Chemistry and Laboratory Medicine*, vol. 44, no. 2, pp. 199–200, 2006.

[47] R. Gürlich, P. Maruna, J. Lindner, and F. Fidler, "Evaluation of laparoscopic and laparotomy cholecystectomy by comparing the dynamics of acute phase proteins," *Rozhledy v Chirurgii*, vol. 73, no. 5, pp. 214–217, 1994.

[48] S. Demirer, K. Karadayi, S. Şimşek, N. Erverdi, and C. Bumin, "Comparison of postoperative acute-phase reactants in patients who underwent laparoscopic v open cholecystectomy: a randomized study," *Journal of Laparoendoscopic and Advanced Surgical Techniques Part A*, vol. 10, no. 5, pp. 249–252, 2000.

[49] G. di Vita, C. Sciumè, S. Milano et al., "Inflammatory response in open and laparoscopic cholecystectomy," *Annali Italiani di Chirurgia*, vol. 72, no. 6, pp. 669–673, 2001.

[50] I. Gál, E. Röth, J. Lantos, G. Varga, T. J. Mohamed, and J. Nagy, "Surgical trauma induced by laparoscopic cholecystectomy," *Orvosi Hetilap*, vol. 139, no. 13, pp. 739–746, 1998.

[51] A. Aminsharifi, M. Salehipoor, and H. Arasteh, "Systemic immunologic and inflammatory response after laparoscopic versus open nephrectomy: a prospective cohort trail," *Journal of Endourology*, vol. 26, no. 9, pp. 1231–1236, 2012.